

8-2011

CONJUGATED POLYMERS AND INTER- CHROMOPHORE INTERACTIONS: SYNTHESIS, PHOTOPHYSICAL CHARACTERIZATION AND APPLICATION

Anshuman Mangalum
Clemson University, anshumm@clemson.edu

Follow this and additional works at: https://tigerprints.clemson.edu/all_dissertations

 Part of the [Organic Chemistry Commons](#)

Recommended Citation

Mangalum, Anshuman, "CONJUGATED POLYMERS AND INTER-CHROMOPHORE INTERACTIONS: SYNTHESIS, PHOTOPHYSICAL CHARACTERIZATION AND APPLICATION" (2011). *All Dissertations*. 787.
https://tigerprints.clemson.edu/all_dissertations/787

This Dissertation is brought to you for free and open access by the Dissertations at TigerPrints. It has been accepted for inclusion in All Dissertations by an authorized administrator of TigerPrints. For more information, please contact kokeefe@clemson.edu.

CONJUGATED POLYMERS AND INTER-CHROMOPHORE INTERACTIONS:
SYNTHESIS, PHOTOPHYSICAL CHARACTERIZATION AND APPLICATION

A Dissertation
Presented to
the Graduate School of
Clemson University

In Partial Fulfillment
of the Requirements for the Degree
Doctor of Philosophy
Chemistry

by
Anshuman Mangalum
August 2010

Accepted by:
Dr. Rhett C. Smith, Committee Chair
Dr. Gautam Bhattacharyya
Dr. Jason McNeil
Dr. Andrew G. Tennyson

ABSTRACT

Ever since the discovery of conducting polymers (**CPs**) in the late 1970s, organic conjugated materials and polymers is one of the most popular and fascinating research area among the scientists due to the remarkably unique properties and broad range of applications of **CPs**, notably organic photovoltaic (**OPVs**), organic or polymer based light emitting devices (**OLEDs / PLEDs**), field effect transistors (**FETs**), nonlinear optical (**NLO**) devices and sensor for biologically relevant analytes, metal ions and anions. Optical properties of these materials depend on intra / interchromophoric interaction, geometry and relative orientation in space. Detailed study of such materials can also help us to understand various intriguing properties of conducting polymers such as charge carrier mobility, quantum yield, and how the excited states transfer energy.

The primary focus of my research is to develop novel materials which can be employed as sensors for biological relevant molecules and ions and the synthesis of novel scaffolded chromophores to investigate the interchromophoric interactions and to tune their photophysical properties.

The basic introduction of conducting polymers and its applications are described in chapter one followed by the detailed study of *m*-xylene and *m*-terphenyl based phosphate and pyrophosphate anions sensors in chapter two and three. Also polymer supported *m*-xylene based materials were studied for catalytic decomposition of phosphoesters in chapter two.

Synthesis and photophysical characterization of π -conjugated cruciforms is reported in chapters four and five. Chapter four accounts for the synthesis of 1,3-

bis(dimethylaminomethyl)phenyl based cruciform receptors as metal ion sensor whereas chapter five describes the synthesis and photophysical characterization of five phosphorous-containing cruciform derivatives.

Synthesis of novel *m*-terphenyl based halogenated oxacyclophane scaffolds for covalent attachment of chromophores using C-C coupling reaction is reported in chapter six to study the controlled interchain interaction for both monomer and polymers.

DEDICATION

To my family and friends who believe in me.

ACKNOWLEDGMENTS

First and foremost I would like to thank my advisor Dr. Rhett C. Smith for giving me an opportunity to work under his supervision. The continuous encouragement and flawless guidance I got from him throughout my Ph.D., made it possible for me to finish this work.

I would also like to thank Smith group, (former and present group members), *esp* Dr. Brad P. Morgan, Susan He and Ellie Tennyson for providing helpful and productive work environment.

I would like to express my sincerer gratitude to my committee members Dr. Gautam Bhattacharyya, Dr. Jason McNeill and Dr. Andrew Tennyson for taking time to serve on my Ph.D. committee.

Finally, I would like to thank Clemson university and chemistry department for providing me an opportunity to study here.

TABLE OF CONTENTS

	Page
TITLE PAGE	i
ABSTRACT	ii
DEDICATION	iv
ACKNOWLEDGMENTS	v
LIST OF TABLES	xii
LIST OF FIGURES	xiii
LIST OF SCHEMES.....	xvii
CHAPTER	
I. GENERAL INTRODUCTION.....	1
1.1 π -Conjugated System.....	3
1.1.1 Poly(<i>p</i> -phenylenevinylene) (PPVs)	5
1.1.2 Poly(phenyleneethynylene) (PPEs)	9
1.2 Applications	15
1.2.1 Sensor.....	15
1.2.2 Organic light emitting diodes (OLEDs).....	18
1.2.3 Organic photovoltaics (OPVs).....	21
1.3 Scaffolds and shielding	25
1.4 Proposed work	28
1.5 References.....	29
II. POLYGLYCEROL-BOUND PHOSPHOTRIESTERASE ENZYME MODEL COMPLEXES FOR DETECTION AND HYDROLYSIS OF PHOSPHORUS SPECIES IN AQUEOUS SOLUTION.....	36
2.1 Introduction.....	36
2.2 Synthesis and characterizatio.....	41
2.2.1 Synthetic characterization.....	41
2.2.2 Transmission electron microscopy (TEM) characterization.....	42
2.3 Photophysical studies and calculation	44
2.3.1 Catalysis of phosphorus species.....	44

2.3.2 Detection of phosphorus species.....	44
2.4 Conclusion	50
2.5 Experimental section.....	51
2.6 References.....	58
Appendices.....	65
Appendix 2 A.....	66
Appendix 2 B	84
III. DIZINC PHOSPHOHYDROLASE MODEL BUILT ON A <i>m</i> -TERPHENYL SCAFFOLD AND ITS USE IN INDICATOR DISPLACEMENT ASSAYS FOR PYROPHOSPHATE UNDER PHYSIOLOGICAL CONDITION	110
3.1 Introduction.....	110
3.2 Synthesis and characterization.....	114
3.3 Photophysical studies and calculations	115
3.4 Conclusion	122
3.5 Experimental section.....	123
3.6 References.....	128
Appendices.....	136
Appendix 3 A.....	137
Appendix 3 B	140
IV. METAL ION DETECTION BY LUMINESCENT 1,3- BIS(DIMETHYLAMINOMETHYL) PHENYL RECEPTOR-MODIFIED CHROMOPHORES AND CRUCIFORMS	149
4.1 Introduction.....	149
4.2 Synthesis and characterization.....	154
4.3 Density functional theory (DFT) calculations	158
4.4 Photophysical studies and calculations	160
4.5 Conclusion	166
4.6 Experimental section.....	167
4.7 References.....	185
Appendices.....	190
Appendix 4 A.....	191
V. BIFUNCTIONAL CROSS-CONJUGATED LIGHT-HARVESTING PHOSPHINES AND PHOSPHINE DERIVATIVES: PHOSPHA- CRUCIFORMS.....	237
5.1 Introduction.....	237
5.2 Synthesis and characterization	242

Table of Contents (Continued)

	Page
5.2.1 Synthetic characterization.....	242
5.2.2 Density functional theory (DFT) calculations	243
5.3 Photophysical studies and calculations.....	246
5.4 Conclusion	250
5.5 Experimental section.....	251
5.6 References.....	259
Appendices.....	268
Appendix 5 A.....	269
VI. INTERCHROMOPHORIC ORIENTATION SCAFFOLDING BY <i>m</i> - TERPHENYL OXACYCLOPHANES	285
6.1 Introduction.....	285
6.1.1 Scaffolds for chromophores.....	286
6.2 Synthesis and characterization.....	291
6.2.1 X-ray characterization.....	299
6.2.2 Density functional theory (DFT) calculations	311
6.3 Photophysical studies and calculations.....	313
6.4 Conclusion	328
6.5 Experimental section.....	329
6.6 References.....	358
Appendices.....	365
Appendix 6 A.....	366
VII THE FINALE AND SCOPE	428
BIBLIOGRAPHY.....	431

LIST OF ABBREVAITIONS

λ_{em}	wavelength of emission
λ_{em}	wavelength if maximum absorbance
Φ	quantum yield
BHJ	bulk hetrojunction
Bipy	2,2'-bipyridyl
CDCl ₃	chloroform-d ₁
CH ₃ CN	acetonitrile
CMP	conducting metallopolymer
CP	conducting polymer
CuI	copper iodide
DCM	dichloromethane
DFT	density functional calculation
DMF	N,N-dimethylformamide
DMSO-d ₆	dimethylsulfoxide-d ₆
EL	electroluminescence
ESC	esculetin
FRET	fluorescence resonance energy transfer
HCl	hydrochloric acid
HEPES	2-[4-(2-hydroxyethyl)piperazin-1-yl]ethanesulfonic acid
HOMO	highest occupied molecular orbital

IDA	indicator displacement assay
IRS	indicator spacer receptor
ITO	indium tin oxide
k_d	dissociation constant
LUMO	lowest unoccupied molecular orbital
MDMO-PPV	poly[2-methoxy-5-(3,7-dimethyloctyloxy)-1,4-phenylen]-alt-(vinylene)
MEH-PPV	poly[2-methoxy-5-(2'-ethyl-hexyloxy)-1,4-phenylenevinylene]
MeOH	methanol
<i>n</i> -BuLi	<i>n</i> -butyllithium
NLO	nonlinear optics
NMR	nuclear magnetic resonance
NO	nitric oxide
NPP	4-nitrophenyl phosphate
OLED	organic light emitting diode
OPV	organic photovoltaics
ORTEP	oak ridge thermal ellipsoid plot
PA	polyacetylene
P3HT	poly(3-hexylthiophene)
PCBM	[6,6]-phenyl-C ₆₁ -butyric acid methyl ester
PCE	power conversion efficiency
PET	photoinduced electron transfer

Pi	phosphate
PG	poly glycerol
PL	photoluminescence
PPE	poly(<i>p</i> -phenyleneethynylene)
PPi	pyrophosphate
ppm	parts per million
PPV	poly(<i>p</i> -phenylenevinylene)
PTEase	phosphotriesterase
TBAF	tetrabutylammoniumfluoride
TEM	transmission electron microscopy
THF	tetrahydrofuran
TLC	thin layer chromatography
TMS	tetramethylsilane
TMSA	trimethylsilylacetylene
Tos-PG	tosylated polyglycerol
UV-vis	ultra-violet visible

LIST OF TABLES

Table	Page
2.1	Dissociation constants (K_d in μM) for the binding of indicators to the dizinc complexes..... 48
3.1	Absorption data and photos demonstrating the range of colorimetric responses observed in free, bound and pyrophosphate-displaced states.... 116
4.1	Selected photophysical properties of A – E and effect of metal ion binding on photoluminescence properties 162
5.1	Select properties of 8 – 13 and model M1 248
6.1	Refinement detail for 6 300
6.2	Refinement detail for 7 302
6.3	Refinement detail for 13 304
6.4	Refinement detail for CP1 306
6.5	Refinement detail for CP2 308
6.6	Refinement detail for CP2b 310
6.7	Photophysical data for oxacyclophane materials and various upper and lower π -system models 313
6.8	Photophysical data for oxacyclophanes π -conjugated materials 14, 15, CP1a, CP2a, CP1b, CP2b, CP1c and CP2c 319
6.9	Select photophysical data for cross linked and model polymers for solution and film..... 323

LIST OF FIGURES

Figure		Page
1.1	Schematic representation of trans-polyacetylene.....	1
1.2	Examples of very commonly used conducting polymers	2
1.3	Schematic representation of conjugated polymers (A and B) and C shows the empty π -orbital on polymeric backbone	3
1.4	Commonly used monomeric units in literature.....	4
1.5	Schematic representation of conducting metallopolymers (CMPs).....	5
1.6	General representation of Wittig reaction.....	6
1.7	Structure of phenylenevinylene dimer	7
1.8	Copolymer synthesized by Liu <i>et al.</i> , using CN substituted phenylenevinylene chromophore	8
1.9	PPV based conducting polymers used as sensors	9
1.10	General Sonogashira coupling reaction and its catalytic cycle.....	10
1.11	Few examples of PPE polymer known in literature.....	12
1.12	Novel compounds synthesized by Zhang <i>et al</i>	13
1.13	Pt containing organometallic PPEs synthesized by vanKoten <i>et al</i>	14
1.14	Schematic representation of Indicator-Spacer-Receptor (IRS) approach....	16
1.15	Schematic representation of Indicator Displacement Assay approach (IDA)	16
1.16	Examples of fluorescent based conducting polymer sensors.....	18
1.17	Schematic representation of LED device	19
1.18	PPV based conducting polymer used for EL layer in LED based device ..	20

List of Figures (Continued)

Figure	Page
1.19	Flowchart distribution showing contribution of energy source to the total production 21
1.20	Schematic representation of functioning of OPVs 23
1.21	Scaffolds used in literature for chromophore appendage 26
1.22	Sterically shielded conjugated materials used for various applications..... 27
2.1	Five of the seven globally stockpiled chemical warfare agents are simple phosphoesters 36
2.2	General form of binucleating ligands whose bimetallic complexes are useful for inorganic phosphate detection and can catalytically hydrolyze phosphoester 37
2.3	Representation of the structure of 7-PG and 8-PG 39
2.4	TEM image of 8-PG 43
2.5	Structures of commercially available complexometric indicators used in the current study..... 46
2.6	Titration of MX with Zn_2 - 8-PG , followed by UV-vis spectroscopy..... 47
3.1	Schematic representation of indicator displacement assay 110
3.2	Binucleating ligand (L1 and L3) and complexometric indicators tested for displacement of inorganic phosphates..... 112
3.3	Changes in emission intensity of ESC-Zn₂L2 as PPi were added..... 118
3.4	Calibration curve for (PPi) measured via displacement of PV measured by ratiometric absorption spectroscopy (A) and displacement of ESC measured by increase in emission intensity of PL spectra 120
4.1	Structure of the 1,3-bis(dimethylaminomethyl)phenyl substituted chromophores 150

List of Figures (Continued)

Figure	Page
4.2	Some cruciforms that have been used as fluorescent sensors..... 152
4.3	DFT calculation o compounds A – E 159
4.4	Absorption and emission spectra for A – E 161
4.5	Metal ion response of compounds A – E 163
5.1	Phosphorus containing small molecule chromophores and π -conjugated polymers known in literature..... 239
5.2	Cross conjugated materials such as cruciforms known in literature 240
5.3	DFT calculation of compounds 8, 9 and 10 245
5.4	Absorption and photoluminescence spectra for compounds 8 – 12 and M1 247
6.1	Generalized representation of cyclophane 287
6.2	Representative <i>m</i> -terphenyl and <i>m</i> -xylyl cyclophanes 288
6.3	Representation of [2,2]paracyclophane and chromophore derivatized paracyclophane 289
6.4	Inclusion of [2,2]paracyclophane in polymeric system..... 289
6.5	Un scaffolded model compounds for photophysical comparison..... 293
6.6	ORTEP drawing (50% probability ellipsoids) of the compound 6 299
6.7	ORTEP drawing (50% probability ellipsoids) of the compound 7 301
6.8	ORTEP drawing (50% probability ellipsoids) of the compound 13 303
6.9	ORTEP drawing (50% probability ellipsoids) of the compound CP1 305
6.10	ORTEP drawing (50% probability ellipsoids) of the compound CP2 307

List of Figures (Continued)

Figure	Page
6.11 ORTEP drawing (50% probability ellipsoids) of the compound CP2b	309
6.12 DFT calculation of OC1 and OC2	311
6.13 Space filling models of OC1 and OC2	312
6.14 Absorption and emission spectra of OC1 and OC2	314
6.15 Absorption and emission spectra of M1 , M2 and M4	316
6.16 Absorption and emission spectra of 14 , 15 , 16 , CP1a , CP1b , CP2b CP1c and CP2c	320
6.17 Absorption and emission spectra of CLa1 , CLa3 , CLa5 , MPa1 MPa3 and MPa5	325
6.18 Absorption and emission spectra of CLb1 , CLb3 , CLb5 , MPb1 MPb3 and MPb5	327

LIST OF SCHEMES

Scheme	Page
2.1 Preparation of 7 and 8	41
3.1 Preparation of L2	114
4.1 Preparation of A , B and C	154
4.2 Preparation of D and E	155
5.1 Preparation of 8	242
5.2 Preparation of 9 – 13 and structure of phosphorus free model M1	242
6.1 Preparation of compound 5	292
6.2 Preparation of 6 , 7 and OCs	293
6.3 Preparation of 14 and 15	294
6.4 Preparation of CP1 and CP2	295
6.5 Synthetic scheme for covalent attachment of chromophores on CP1 and CP2	296
6.6 Synthetic scheme for 1,2-cross linked polymers and linear model polymers.....	298
6.7 Synthetic scheme for 1,2-cross linked polymers and linear model polymers.....	298

CHAPTER ONE

GENERAL INTRODUCTION

Since 2000, when the prestigious Nobel Prize committee rewarded the groundbreaking efforts of Alan MacDiarmid,¹ Hideki Shirakawa² and Alan J. Heeger³ in the area of conducting polymers, there began a new era of lightweight electro-active organic plastics materials; these materials actually revolutionized this field with their enormous potential applications and its remarkable properties.

Actually, the first step leading to this historic event in the field of science occurred in the late 70s when serendipitous discovery of chemical doping of polyacetylene (**PA**; **Figure 1.1**) with oxidizing agents like Br₂ resulted in ten million fold increase in the conductivity and since then this branch of science has grown vigorously.⁴

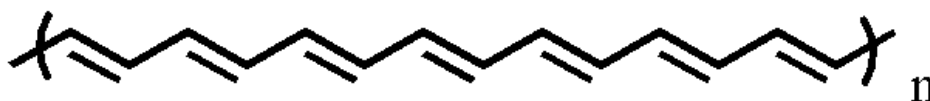


Figure 1.1 Schematic representation of trans-polyacetylene (**PA**).

Earlier then, polymers and conjugated systems were well known for their dormant character and used as in various insulation applications such as insulators for metallic conductors, photoresists and incapsulation layers in electronic and plastic industries.^{5, 6} However insolubility and unprocessibility were major drawbacks for such systems at that time which impeded the development and usage of these materials in mass scale.⁶ But

this breakthrough in the field of conducting polymer completely changed the application and usage of these materials and provided a new dimension in this area which allows us to synthesize new organic materials which can not only possess electrical and optical properties comparable to metals such as copper but also have mechanical properties like polymers.⁵⁻⁷

The quest to develop cheap, soluble in common organic solvents and easily processable materials such as **MEH-PPV** and **P3HT** (**Figure 1.2**)⁶ attracted numerous research groups and in the past 25 years due the persistent endeavor of various people all around the world unveiled the chemical and physical properties of such materials in detail which helped to address several unanswered questions.

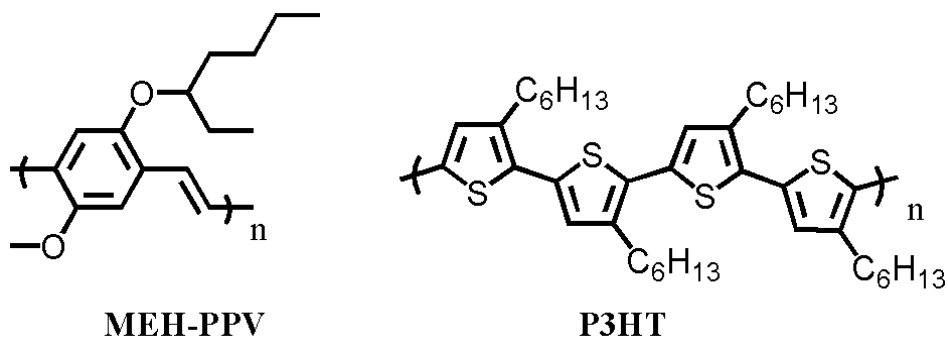


Figure 1.2 Examples of very commonly used conducting polymers.

Conducting polymer has emerged as field with variety of practical applications in our day -to -day life such as in organic light emitting diodes (**OLEDs**),⁸ photovoltaics (**PVs**),⁹ sensors for biological relevant molecules and ions,¹⁰ molecular electronics and photoactuators,¹¹ thin film transistors,¹² etc.

1.1 π -Conjugated Systems

Conjugated materials are made up of alternating repeating unit of single and double or triple bond with extended π - π interactions (**Figure 1.3; A, B**) where the benzene ring in red (**Figure 1.3; B**) is a spacer and variable and the R- groups act as solubilizing agent which can be either aliphatic or alkyloxy chain. They are also known as organic semiconductor as their empty π -molecular orbital can delocalize over the π -backbone (**Figure 1.3; C**). One of the most unique features of these conducting polymers is their dual nature where they can possess properties of both metal (conductivity) and polymers (processibility). Additionally, their response towards electronic excitation is non-linear and so their emission can be either radiative or nonradiative which can be used in either **OLEDs** or photovoltaic (**PV**) devices.^{13, 14}

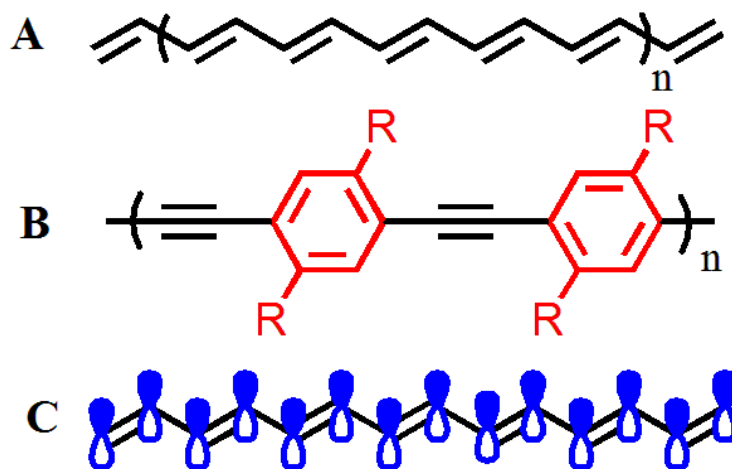


Figure 1.3 Schematic representation of conjugated polymers (**A** and **B**) and **C** shows the empty π -orbital on polymeric backbone.

Extended conjugated π -electron systems (conducting polymers, **CPs**) have drawn attention to the researchers due to its extensive usage in numerous applications such as optical, electronic, optoelectronic, chemical sensing (chemo- and biosensing) and magnetic materials.^{15, 16} Functional building blocks, spacer connecting the monomers, effective conjugation length, molecular geometry and spatial orientation of the conjugated π -electron system are responsible for their unique electronic and optoelectronic properties. Also their highest occupied molecular orbital (**HOMO**) and lowest unoccupied molecular orbital (**LUMO**) energy levels can be adjusted by selectively picking up the suitable functional group for the polymer backbone. Hence it is extremely important to synthesize and investigate such compounds in order to improve their electronic and optoelectronic properties.^{17, 18} **Figure 1.4** shows a few widely used monomer units known in literature for conjugated polymers.

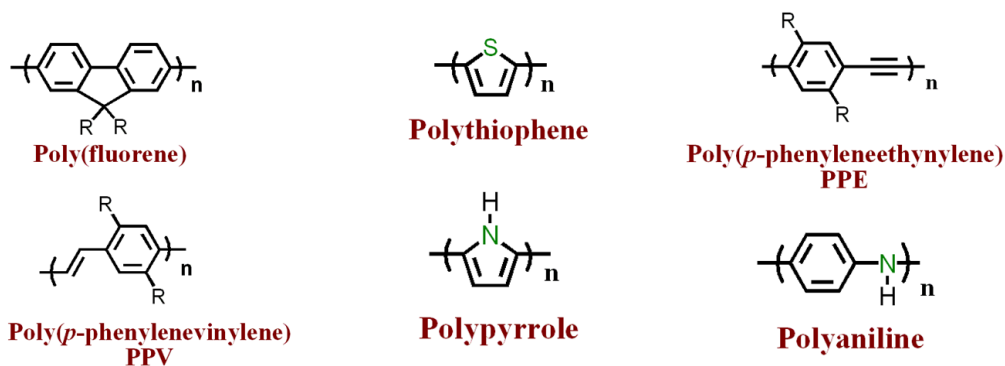


Figure 1.4 Commonly used monomeric units in literature.⁷

Metallopolymers are a special class of conducting polymer wherein metals can be incorporated either directly or indirectly into the π -backbone. In some cases, such as systems like bipyridyl substituted conducting metallopolymers (**CMs**) are very well

studied for sensing transition metals due to the strong binding affinity of bipyridyl unit for transition metals and electronic perturbation around π -backbone due to this binding will produce huge detectable optical signal.¹⁹ In addition to that, **CMPs** like Pt-Acetylide **CMPs** are well known for the study of emission from triplet excited state. Heavy metals such as Pt favors the forbidden intersystem crossing (singlet to triplet state) and spin-orbital coupling which leads to emission from a triplet state leading to phosphorescence (Figure 1.5).²⁰

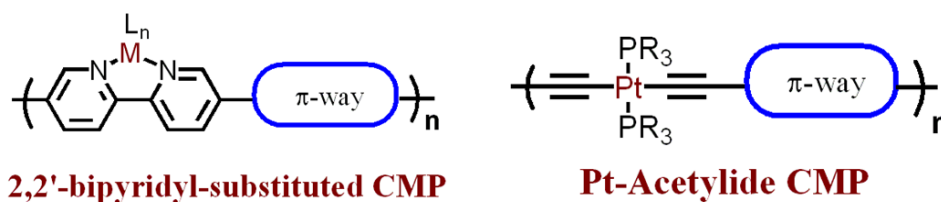


Figure 1.5 Schematic representation of conducting metallopolymer (CMPs).

Few classes of conducting polymer such as **PPV** and **PPE**; very commonly used in literature as in electronic and photonic devices (**OLEDs**, **PVs** and **Sensors**) are discussed in detail (*vide infra*).

1.1.1 Poly(*p*-phenylenevinylene)s (PPVs)

One of the most important class of such conjugated system is poly(*p*-phenylenevinylene)s (**PPVs**), which was first introduced in light-emitting device (**LED**) by Burroughes *et al.* in 1990. In this study, they used simplest analogue of **PPVs** poly(1,4-phenylenevinylene) polymer which is bright yellow powder and insoluble in common organic solvents which makes it hard to process to transparent thin films for electroluminescent device.¹³ Chemical structure of such compounds can be easily

modified in order to tune their optoelectronic properties because such properties are related to the electronic structure of the compounds; addition of functional groups can also be employed to make these polymers processable, a prime requirement for device fabrication.

There are various routes reported in the literature for the synthesis of **PPVs** such as C-C coupling reactions (Wittig, Heck, Gilch *etc.*)²¹ or electrochemical polymerization *etc.* however, Wittig or modified Wittig reactions are the simplest and easiest methods to prepare **PPVs** in bulk where a carbonyl carbon (ketone or aldehyde) can be reacted with an ylide in presence of base in polar aprotic solvent to form a C=C bond. A wide variety of substitution is possible on carbonyl or ylide compounds which provide a broad range of variations to synthetic chemist (**Figure 1.6**).^{19, 21}

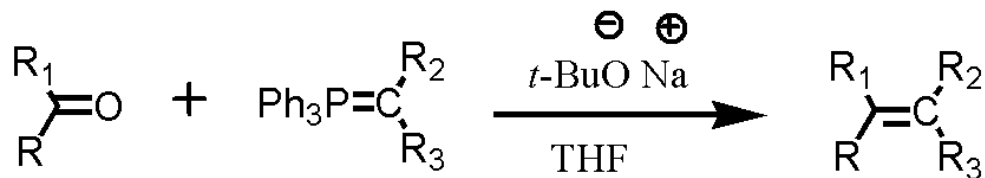


Figure 1.6 General representation of Wittig reaction.

To optimize and tune the optical properties of processable π -conjugated materials Wu *et al.* in 2001, synthesized phenylenevinylene dimers with different substitution by using standard *bis*-Wittig reaction in order to study the effect of substitution on the optical properties of such compounds (**Figure 1.7**). On the basis of such substitutions, he concluded that R groups with more electron donacity produce a greater red shift in the UV-vis spectra of the dimmers.²²

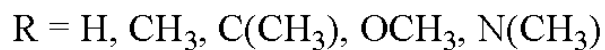
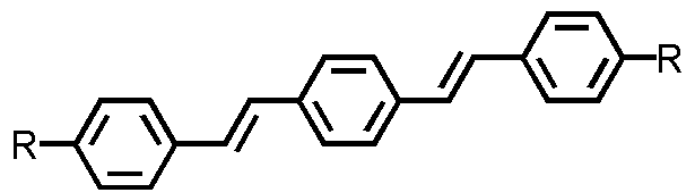


Figure 1.7 Structure of phenylene vinylene dimer.

Electroluminescence (**EL**) study of such compounds can be done by injecting electrons through cathode to the conduction band and insertion of holes through anode (indium tin oxide; **ITO**) to their valence band of the conducting polymer which leads to excitation of the molecule and finally getting back to the ground state by emitting light. Prerequisite to achieve high efficiency of such optical device, we need to inject balanced charge and also mobility of the holes and electron should be similar.¹⁷

In most cases, electron transport is hindered by the impurities and defects present in the molecules.¹⁷ Hence charge is carried mostly by holes in such emissive polymer since they have higher mobility and smaller injection barrier. Also, most conjugated polymers have low electron affinity as they are already electron rich.²³

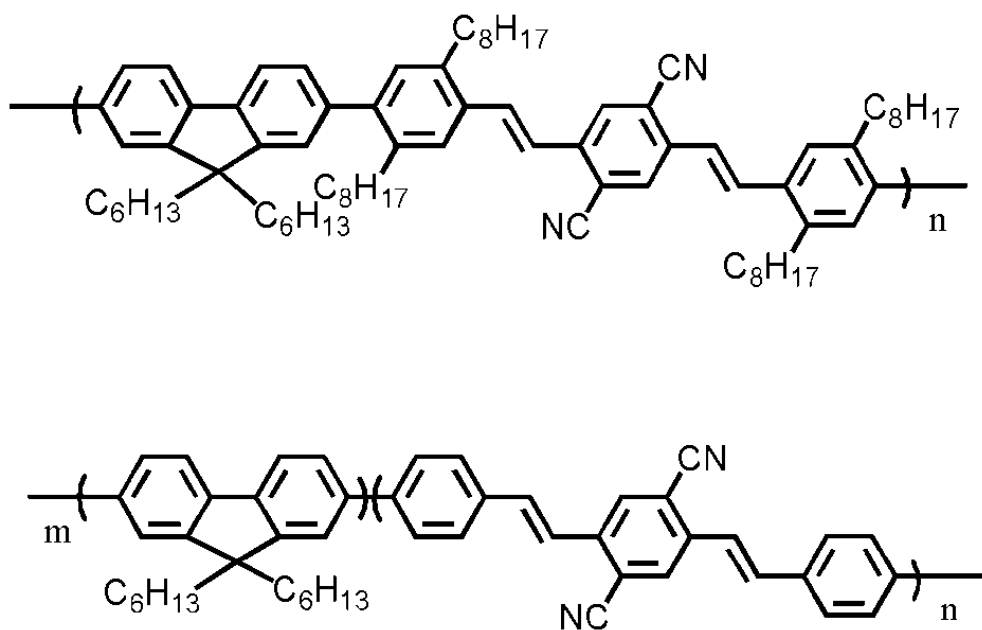


Figure 1.8 Copolymers synthesized by Liu *et al.* using CN substituted phenylenevinylene chromophore.

Liu *et al.* tried to overcome this limitation by synthesizing polymers with relatively higher electron affinities. By altering the back bone of such polymers they were able to tune the **HOMO** and **LOMO** energy levels and its optoelectronic properties which leads to the change in their charge transport properties (**Figure 1.8**).¹⁷

PPV based conducting polymers are also well utilized as sensors for biologically relevant molecules and ions. Smith *et al.* studied 2,2'-bipyridyl comprised **PPV** conducting polymers as fluorescent nitric oxide sensor (**Figure 1.9; A**).

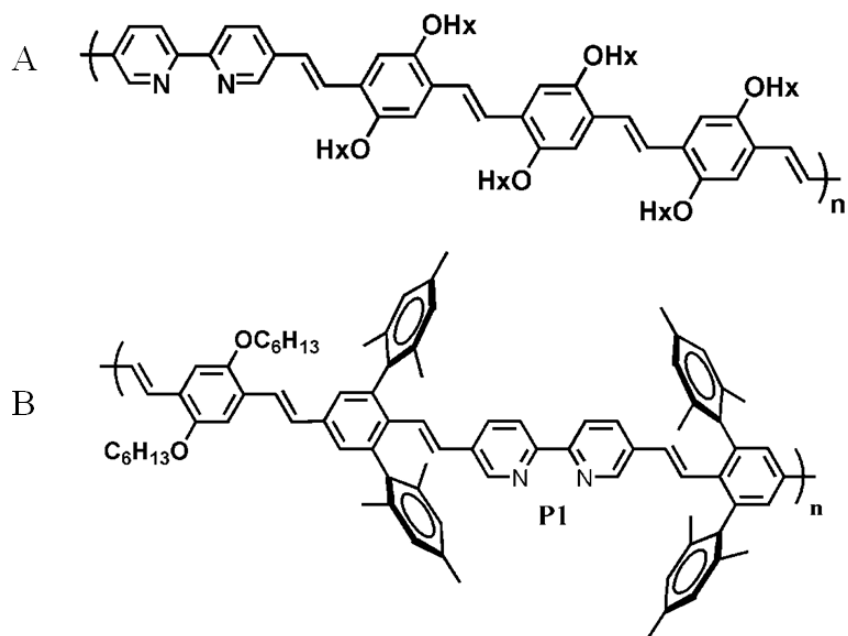


Figure 1.9 PPV based conducting polymers used as sensors.

He *et al.* incorporated bulky mesityl side chain into the **PPV** polymer in order to study the controlled inter chain interactions in conducting polymers (**Figure 1.9; B**) which inhibits the coordinative cross linkage at the metal center and 1:1 interaction of metal and binding site can be achieved (Bipy in this case), a very useful finding in the field of **PPV** based sensors.²⁴

1.1.2 Poly(phenyleneethynylene) (PPEs)

Poly(phenyleneethynylene) (**PPE**) is an another important class of conjugated π -system and can be easily synthesized via Heck-Cassar-Sonogashira-Hagihara reaction which involve Pd catalyzed cross coupling reaction between terminal alkynes and aromatic halide (mainly bromo and iodo) in the presence of amine as a solvent. By

utilizing this reaction we can easily connect sp and sp^2 hybridized carbon. **Figure 1.10** shows the catalytic cycle and mechanism for this coupling reaction.¹⁴

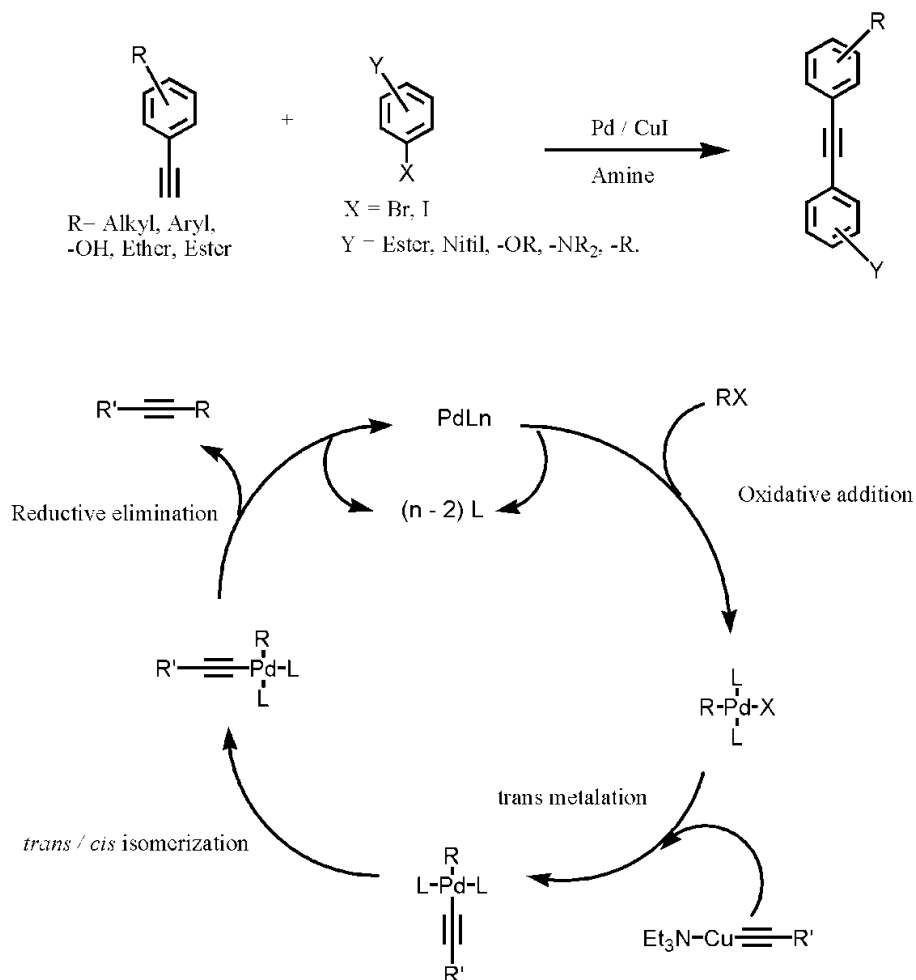


Figure 1.10 General Sonogashira coupling reaction and its catalytic cycle.¹⁴

Possible variation for Sonogashira reaction

A) Halides

The most suitable precursor for this reaction is either bromo or iodo aromatic halides. This reaction usually occurs at high temperature except for iodo aromatic halides,

which react relatively faster than bromo analogs and require milder conditions in order to prevent cross coupling or any other side products. The oxidative addition in case of iodo is faster than bromo because this step is both thermodynamically and kinetically favoured.¹⁴

B) Substituted aromatic halide

$\text{Pd}(\text{PPh}_3)_4$, the active catalyst in this case is an electron rich species so an aromatic halide having an electron withdrawing substituent on it will speed up the first step *i.e.* oxidative addition especially the *ortho*- or *para*- substituted functional groups and eventually ameliorate the yield of the reaction.¹⁴

C) Amines and cosolvent

Suitable choice of amine and cosolvent has an enormous effect on the reaction especially on yield. There is no such bright-line rule but a few of the amines prominently used for this reaction such as diisopropylamine, triethylamine, piperidine, pyrrolidine and morpholine. This reaction works best at elevated temperature since we are using $\text{Pd}(0)(\text{PPh}_3)_4$. Piperidine is more useful amine for reactions involving aromatic iodides, but triethylamine is a better choice for aromatic bromides. The reaction works best in concentrated solutions to enhance the coupling rate. Cosolvents such as toluene, THF, diethyl ether, chloroform or dichloromethane can be used accordingly to the solubility of reactants and product.¹⁴

D) Catalysts and cocatalyst

Catalyst (Pd complex) and co-catalyst (CuI) are used up to 5 mol % for this reaction depending upon the reactivity of the haloarene used. If the haloarene is quite

reactive then we can use small amount of these catalysts; conversely, if the haloarene is not especially reactive, heating the reaction can also help in initiating the reaction. One of the major drawbacks of this reaction is its low yield due to the formation of side products such as diyne because of the coordination of Pd²⁺ complex with the alkyne and can give rise to the formation of diyne as a side product. Hence researchers started modifying the reactants in order to enhance the yield like Heitz *et al.* who reduced (*in situ*) the Pd complex from its +2 oxidation state to 0 oxidation state. There are many more different modified Pd complex used for this reaction. CuI is used as cocatalyst, which enhances the acidity of terminal alkyne in order to increase its reactivity.¹⁴

Some of the poly(phenyleneethynylene) (**PPEs**) polymers synthesized are shown in **Figure 1.11**.

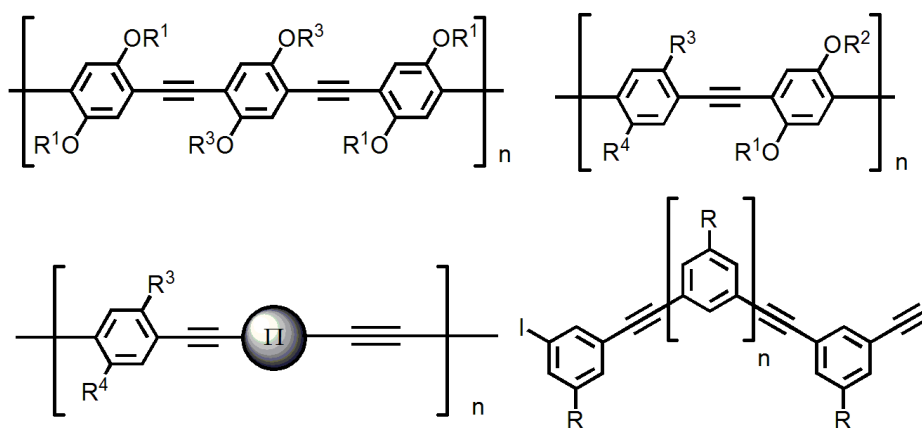


Figure 1.11 Few examples of PPE polymer known in literature.¹⁴

Researchers are also interested in introducing metals into the conjugated π -system in order to study its effect on the optical and electronic properties. Zhang *et al.*

synthesized novel ferrocenyl containing conjugated molecules where ferrocene and phenothiazine monomers were connected with ethynylene linker (**Figure 1.12**).¹⁸

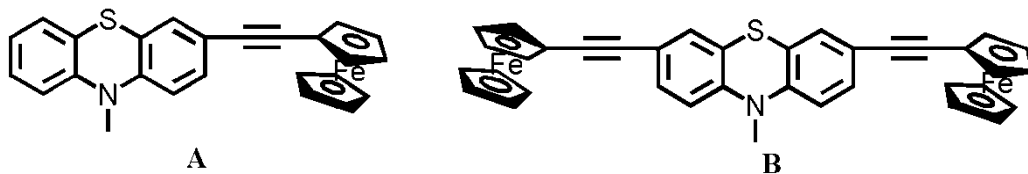


Figure 1.12 Novel compound synthesized by Zhang *et. al.*

Compound **B**, (**Figure 1.12**) due to better coplanarity and more conjugated subunits has a large effective conjugation length, which leads to different electronic properties from compound **A** and small **HOMO – LUMO** band gap (E_g) lead researchers to conclude that these properties depend on structural and conjugative effects of the molecules.¹⁸

Second order non-linear optical properties of any compound depend on both donor and acceptor functional groups attached to it. Hence connecting them through a suitable π -conjugated spacer will allow us to have a better electronic response within the system. Since only few electrons are involved in such process; hence, bi- and oligometallic complexes gained importance in past few years due to the dual nature of transition metals (donor and acceptor moiety). Such organometallic polymeric complexes can be very well used for optical devices.²⁵

Research groups like vanKoten *et al.* worked extensively on the synthesis and electrochemical properties of **PPV** organometallic polymers. They are the first group to develop a stepwise synthesis of a directional polymeric complex along the polymeric

chain. Until then, only symmetric, non-directional organometallic polymers were known. These polymers have a metal ion bridged with an alkyne through hydrogen bonding in order to prepare rigid multimetallic complexes such as the NCN-platinum complex shown in figure 4.6; **A**. The compound was highly insoluble in common organic solvents and hence has possibility to improve the solubility and chain length of such compounds.^{26, 27}

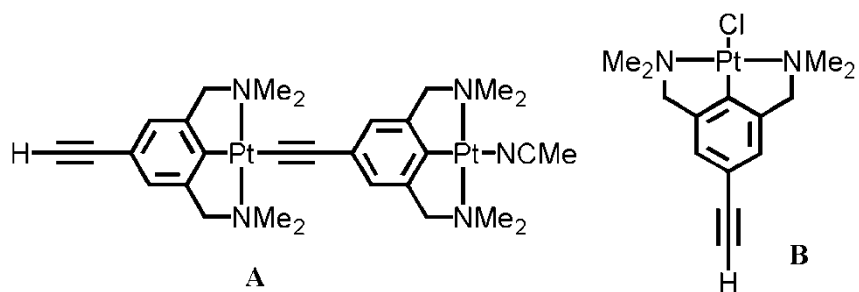


Figure 1.13 Pt containing organometallic **PPEs** synthesized by the vanKoten *et al.*

A simple condensation reaction, through platinum acetylide bond (**Figure 1.13; B**) yields the platinum containing polymer. These kinds of complexes can attain high stability due to the chelating ligands present; the simple metal oxidation also allows us to synthesize various derivatives.²⁷

1.2 Applications

1.2.1 Sensor

Good chemosensors consist of both binding (receptor) and signaling site (indicator) where a signaling site can be a chromophores or fluorophores.²⁸ Upon binding with an analyte, the electronic properties of the receptor is perturbed and generates an optical signal due to photoinduced electron transfer (**PET**), fluorescence resonance energy transfer (**FRET**) or possibly due to changes in ionic strength or pH; the signal can be detected through different techniques. We can also calculate the binding constant of receptor and analyte using these techniques. Changes in the optical properties such as absorption or emission spectra of the signaling site in presence of analyte are the easiest and most convenient means of chemical detection.²⁸ The binding affinity of the analyte to the receptor relative to the affinity for other species is responsible for sensitivity and selectivity for the analyte.²⁹ Therefore the more binding affinity of the analyte, the more selective the sensor will be.

There are different approaches such as indicator-spacer-receptor (**ISR**) and indicator displacement assay (**IDA**) used for the chemosensing. **ISR**; where receptor and indicator are connected to each other through a spacer and binding of analyte to receptor induces detectable changes in their fluorescence or absorbance profile which can further be used for calculating binding constants. The major disadvantage involved in **ISR** is the tedious synthesis of sensing materials (**Figure 1.14**).³⁰

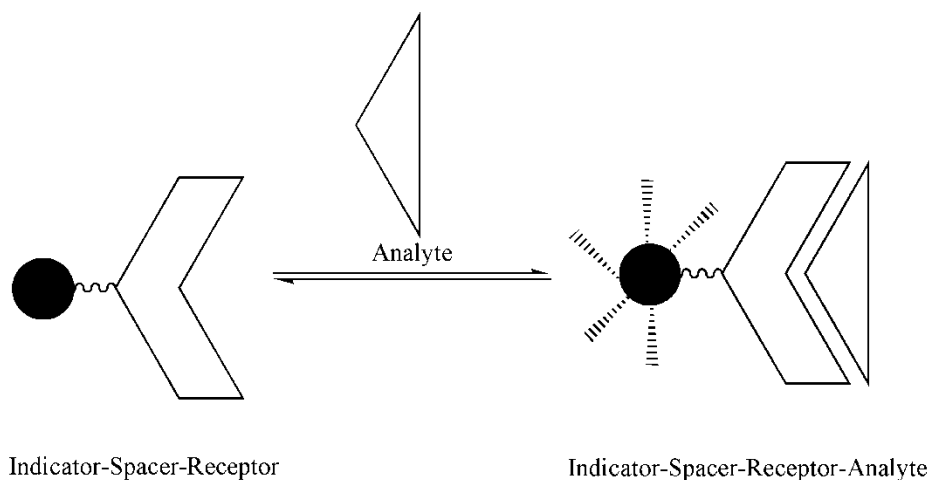


Figure 1.14 Schematic representation of Indicator-Spacer-Receptor (ISR) approach.

IDA comes into existence which is based on interactions like H-bonding, electrostatic or metal complexation for the attachment of receptor and indicator or analyte. There are various factors which contribute to the better guest and host interaction such as geometry of the analyte, charge, hydrophobicity and solvent.³⁰ For **IDA**, binding affinity for receptor to analyte and binding of receptor to indicator should be comparable so that when analyte comes in contact with receptor-indicator system it can displace the indicator from the receptor which in turn gives a signal (**Figure 1.15**).³¹

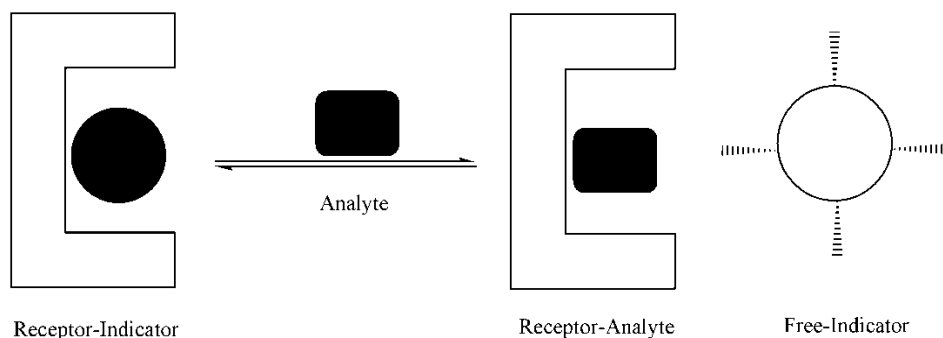


Figure 1.15 Schematic representation of Indicator Displacement Assay approach (IDA).

IDA requires less tedious synthetic steps than **IRS** since there is no covalent bonding involved between receptor and indicator or analyte, thereby allowing the repeated use of a single receptor for different indicators. Also as compared to **IRS**, this approach works in both organic and aqueous solvent systems. One of the major demerits of **IDA** is that they do not work well with tissue or cell imaging since it is hard to differentiate between free and bound indicator in the solution.³¹

IDAs are in general of three types differentiated on the basis of the kind of indicator used. The colorimetric **IDA (C-IDA)** are those where colorimetric indicators are used, fluorescent **IDA (F-IDA)** in which fluorescent indicators are used and metal complexing indicator (**M-IDA**) where metal is involved.³⁰ **M-IDA** can also work in highly polar solvents and has a high affinity for the analyte, as shown by Fabbrizzi *et al.*³² All kinds of biologically relevant molecules or ions (anions and cations) can be studied by utilizing **IDA** sensor. Researchers are increasingly interested with anions as they play vital role in the numerous biological processes such as DNA regulation, protein synthesis, bioenergetics, different metabolic process, etc.³³

Some of the fluorescent conjugated polymer based sensors reported in the literature are listed in **Figure 1.16**. These kinds of model are very successful for sensing application for various molecules or ions. Swager *et al.* reported a crown ether based PPE (**A**)³⁴ conducting polymer for potassium metal ion sensor, whereas Bazan *et al.* reported a polyfluorene based cationic conjugated polymer (**B**)³⁵ for DNA sensor. Bunz and coworkers synthesized a water soluble anionic **PPE** based polymer (**C**)³⁶ that they studied for as lead ion sensor.

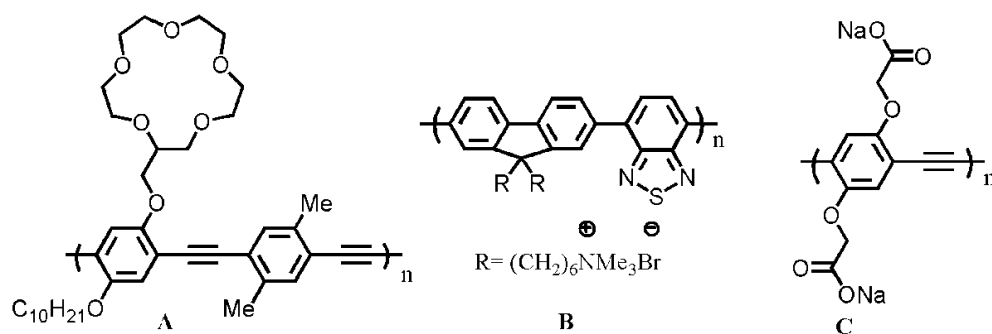


Figure 1.16 Examples of fluorescent based conducting polymer sensors.

This study shows that the conducting polymeric system provides a model where simple modifications of building blocks or solubilizing groups (R) allows researchers to probe a wide range of analyte from cations to anions to biological relevant molecules.

1.2.2 Organic Light Emitting Diodes (OLEDs)

Electroluminescence (**EL**) is a phenomenon that generates light by passing electricity through materials like conducting polymers. A schematic representation of an **LED** device is illustrated in **Figure 1.17**. A typical electroluminescence device mainly consists of an electrode, cathode, conducting polymer and transparent substrate such as glass on which device can be fabricated. Due to the high work function, transparent indium tin oxide (**ITO**) layer is a good candidate for anode from where holes can be injected. The cathode can be made from low work function metals like Al, Ca or Mg deposited by simple thermal evaporation of metal. At least one transparent electrode is required to facilitate the removal of generated light between the diode; usually ITO is deposited on glass surface. In between the cathode and anode electrode, a thin layer of conducting polymer deposited to act as a charge carrier.^{8, 13, 23}

Once the device is setup, holes can be injected at the anode, which leads to removal of electrons from the **HOMO** energy level and generates a positively charged carrier. Electrons can also be injected from the cathode, thereby producing a negatively charged species. After applying current to the device, charge tends to travel towards the opposite electrode via conducting polymer and combination of the opposite charged species produces light via fluorescence or phosphorescence.^{8, 13, 23}

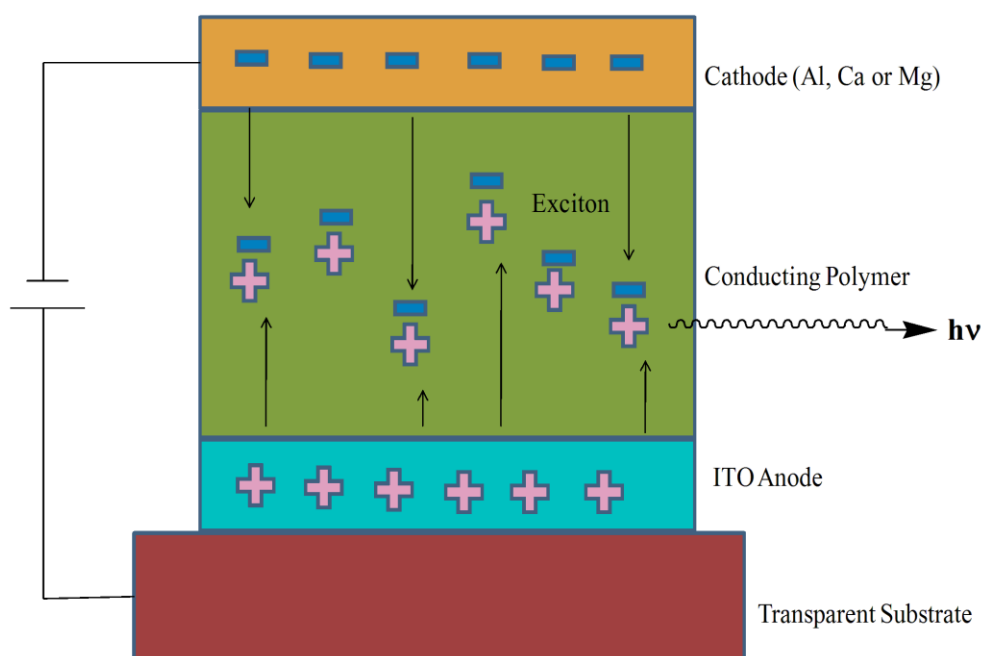


Figure 1.17 Schematic representation of an **LED** device.²¹

Earlier, it was the inorganic semiconductors such as GaAs that were used in **OLEDs** device. A cheap, efficient and easily prepared alternative for these semiconductor layers led scientists to semiconducting polymer; the important feature of these materials is their high photoluminescence quantum yield, ability to carry charge and tunable optical properties makes them a better candidate for **EL** devices.^{8, 13, 23}

In recent years, conducting polymers have proved themselves as an integral and essential component in electroluminescent devices such as **OLEDs**. The very first electroluminescence (**EL**) was observed in 1963 by Pope *et al.* from anthracene crystals. Almost after 20 years, Tang and coworkers observed the first **EL** from the multilayer organic films which offered a huge thrust in the field of organic **EL** industry.⁸

Finally, in 1990, Burroughes and coworker reported their work in *Nature* where they synthesized and studied the optical properties of poly(*p*-phenylenevinylene) and successfully fabricated it as an active electroluminescent material on **OLED** device and exhibited the possible usage of conducting polymers in **OLEDs**. Author found quantum yield (Φ) of their **PPV** device $\sim 0.05\%$ and attributed this low value to the bad interface of polymer and thin metal which leads to overheating at the surface. They reported the quantum yield (Φ) of $\sim 8\%$ for their **PPV** polymers and this low photoluminescence is due to nonradiative decay from the excited state which might be because of the defects present in the polymer.¹³ A few of the conducting polymers successfully fabricated on the device are shown in **Figure 1.18**.^{8, 23}

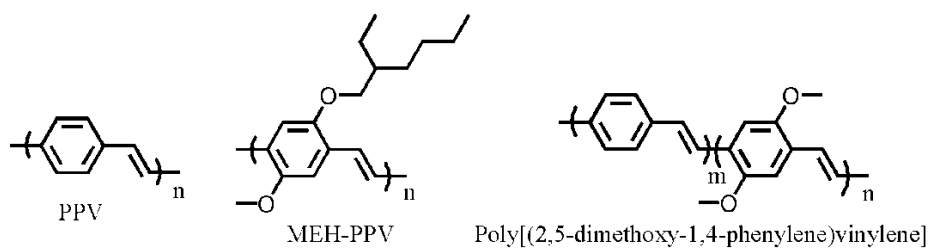


Figure 1.18 PPV based conducting polymer used for **EL** layer in **LED** based device.

A major drawback of using conducting polymers on devices is the photooxidation via atmospheric moisture and oxygen generating carbonyl groups on the polymeric

backbone due to the presence of defects which eventually degrade the polymer. Also degradation facilitates nonradiative emission which eventually reduces the efficiency of the **LED** devices.²¹ To enhance the efficiency, reliability and life time of such device, it is crucial to synthesize defect free and highly emissive (over a broad range of wavelength) conducting polymer.

1.2.3 Organic Photovoltaics (OPVs)

In this era, when our energy resources are depleting at an alarming rate, the need for new energy sources is very much apparent in order to reduce our dependence on vanishing fossil fuel energy source. Sunlight, wind, rain, tides, geothermal heat, biomass and biofuels are few very commonly used renewable energy sources know to human race but, unfortunately, the majority of our energy usage is fulfilled from fossil fuels and nuclear power plants and only a small portion comes from abundant renewable energy sources and relatively very small portion comes from solar energy (**Figure 1.19**).³⁷

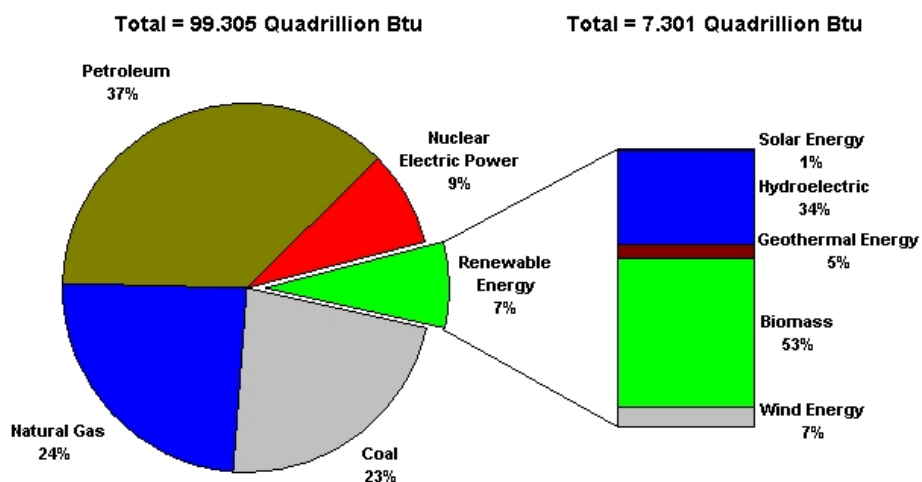


Figure 1.1.9 Flowchart distribution showing contribution of energy source to the total production.

If we can harness this uninterrupted energy source towards a pragmatic application, it has potential to solve our energy problems and here comes the role of photovoltaic which converts solar radiation to electrical energy which is fastest growing technology now days. Several materials used in **PVs** are complexes made up of silicon, cadmium, tellurium, copper, indium and selenium³⁸ but now scientists hope that these inorganic materials can be replaced by conducting polymers commonly known as organic photovoltaics (**OPVs**) due to their tunable optical properties, charge conductivity and processability.

Similar to **LEDs**, **OPVs** are also consists of cathode and anode electrodes and a layer of conducting polymer. Here, the electroluminescent layer can be a monolayer like in Schottky type or double layer like in *pn*-heterojunction cell where *p*-type are electron-donating and *n*-type are electron accepting conjugated materials. Schematic representation of functioning of organic photovoltaics is shown in **Figure 1.20**.^{39, 40}

Initially, the donor conjugated π -system absorbs a photon, which leads to excitation of electrons from **HOMO** to **LUMO** energy level which eventually diffuses to the donor-acceptor (D-A) junction. Relaxation of the exciton from **LUMO** of donor to the **LUMO** energy level of the acceptor occurs via charge transfer. This charge transfer creates two free charges (positive on donor and negative on acceptor conjugated system) which in the presence of applied potential travel to their respective electrodes and in this process current is generated. The short life time of excitons allows them to travel only short distance; hence relaxation often occurs before reaching the donor-acceptor interface

and diminishes the efficiency of the device, thereby leading to the blending of the donor and acceptor substrate known as the bulk heterojunction (**BHJ**).^{39, 40}

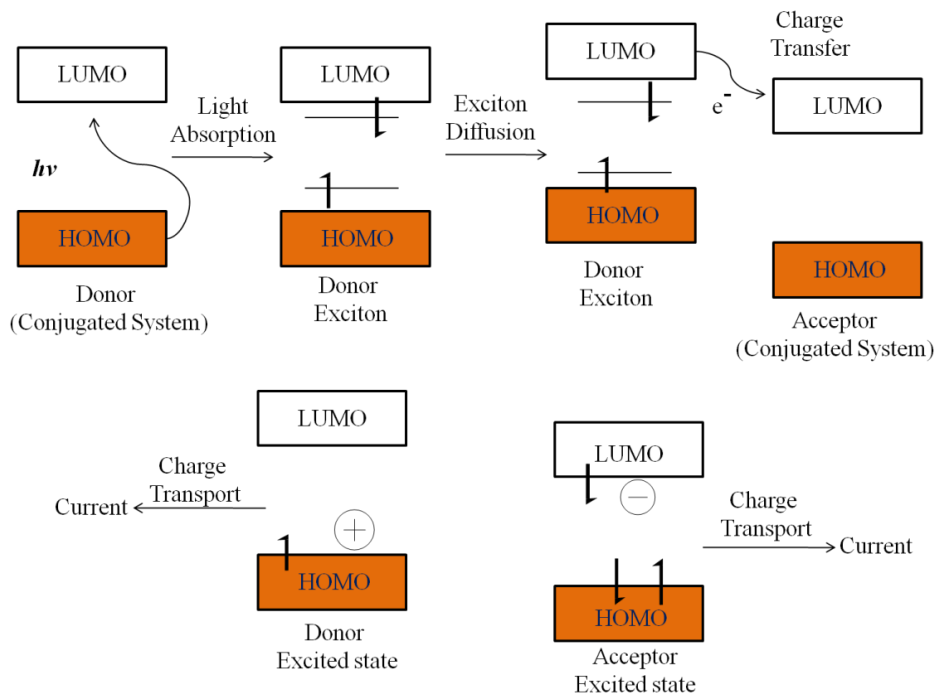


Figure 1.20 Schematic representation of functioning of **OPVs**.

C_{60} derivatives are the best electron acceptor (*n*-type) material used in **OPVs** mainly because of several unique properties such as low lying **LUMO** energy level which facilitates the electron transfer from **LUMO** of excited donor material; C_{60} can very well stabilize negative charge and can acquire up to 6 electrons and most importantly it facilitates the electron transfer process.³⁹ Insolubility of C_{60} in common organic solvent and tendency to crystallize makes it almost impossible to use in devices; scientists therefore turned to functionalization of C_{60} and to date [6,6]-phenyl- C_{61} -butyric acid methyl ester (**PCBM**) and C_{70} PCBM (**PC₇₁BM**) are the best *n*-type material used for **OPVs**.⁴¹

Conducting polymers (electron rich) are the best candidate for *p*-type material for **OPVs**. Poly(3-hexylthiophene) (**P3HT**) and (poly[2-methoxy-5-(3,7-dimethyloctyloxy)-1,4-phenylene]-*alt*-(vinylene) (**MDMO-PPV**) are the two best *p*-type material used for such devices. So far, scientists achieved only 5% of the power conversion efficiency (**PCE**) for **OPVs** device. Based on rational theoretical calculations, scientists have shown that 10% of **PCE** is quite achievable with suitable conducting polymer in hand. Apart from the basic requirement for the conducting polymers such as cost effective, light-weight, easy to process and can be fabricated onto device, they must possess high absorptivity, good positive charge carrier and also suitable band gap which can facilitate the most important step in **OPVs** device, charge transfer from donor to acceptor material. This requirement to have suitable pair of donor and acceptor molecule provides a great deal of challenge for synthetic chemist.^{39, 40}

1.3 Scaffolds and steric shielding

So far, conjugated π -systems have successfully proved their potential usefulness in various photonic and electronic devices and very well replaced the much used traditional inorganic complexes for electroluminescent purpose but there is always a possibility to improve; in this case, the efficiency of these **EL** devices is prime candidate for improvement. Efficiency of the device depends on various factors such as optimal photophysical properties of conjugated system, charge conduction and processability to useful structures.

Optical and electronic properties of such materials depend on numerous factors such as inter- and intra-chromophoric interaction, geometry and its orientation in space. Questions about charge carrier mobility, quantum yield, and how the excited states transfer energy, can also be addressed by detailed study of such materials.^{42, 43} In order to gain a better understanding about the functioning of such devices and their development, it is important to understand these interactions among π -conjugating materials. Hence, synthesizing scaffolds followed by covalently attaching chromophores on them in different spatial orientation is an important field of research.

There are numerous scaffolds reported in the literature (**Figure 1.21**) serving as a platform to hold chromophores at appropriate distance and orientation. Among all, [2,2] paracyclophane is one of most studied scaffold used for this appending chromophores especially where two aryl rings engage in face-to-face, π -stacking which make it appropriate for interchromophoric interaction. Bazan and coworkers utilize it for attaching various kinds of chromophores on it (donor and acceptor chromophores).⁴³

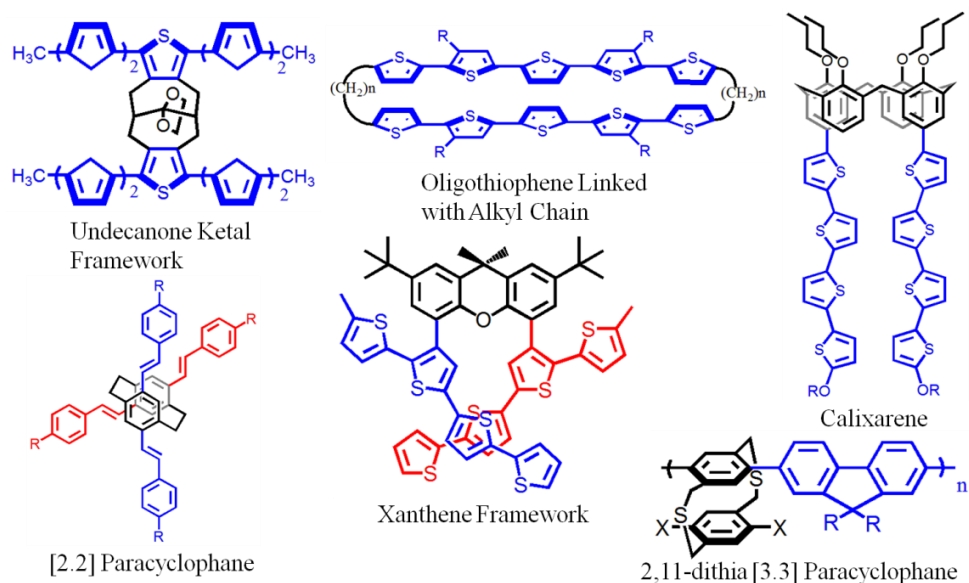


Figure 1.21 Scaffolds used in literature for chromophore appendage.

Novel scaffolds can be synthesized in order to attach chromophores at appropriate orientation and to control interchain interactions of conjugated polymers (**Figure 1.21**) for example Collard and coworkers synthesized undecanone ketal framework which allowed them to attach oligothiophene chains to study controlled inter chain interaction.⁴⁴ Sakai *et al.* connected two oligothiophene chains by single bonds (alkyl chain). Their model not only allowed them to study the inter chain interaction between two chromophore chains but also allowed them to modify the distance between them by using different alkyl chain.⁴⁵ Also calixarene and xanthene or dithiaparacyclophane based scaffolds reported by Swager and Wang *et al.* respectively, also very well suited to studying these properties.^{11, 46, 47} Also in some cases (dithia-paracyclophane), postpolymerization modification is possible which allowed us to optimize their photophysical properties accordingly.

Various research groups have used steric shielding as a tool to study controlled inter chain interactions successfully by employing sterically encumbered groups on either one or both side of polymer chain (**Figure 1.22**).

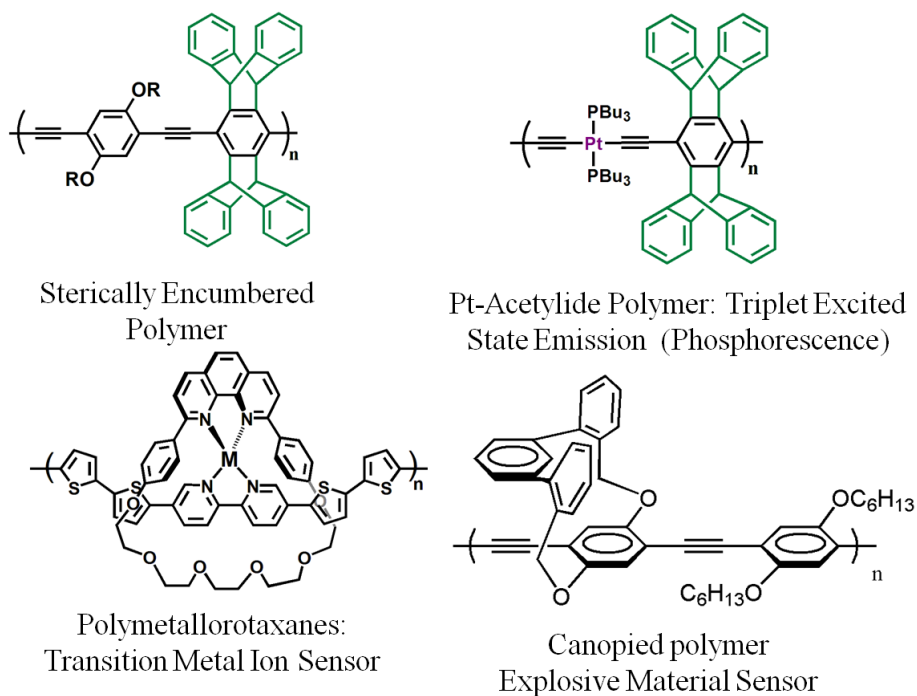


Figure 1.22 Sterically shielded conjugated materials used for various applications.

Steric shielding also controls the π - π stacking and improves the solubility of conjugated materials in common organic solvents.⁴⁸ Schanze *et al.* reported a sterically encumbered Pt-acetylide polymer to study triplet excited state emission.⁴⁹ Various groups utilized this tool for sensing various biologically relevant molecules and ions such as Morgan⁵⁰ *et al.* (canopied polymer) or Swager¹⁹ *et al.* (polymetallorotaxane).

1.4 Proposed Work

The purpose of the current research is generally divided into two areas: (1) developing novel materials which can be utilized as sensor and (2) synthesis of novel scaffolds where chromophores can be appended to study the interchromophoric interactions in order to tune their photophysical properties.

Chapters two and three describe the synthesis of *m*-xylene and *m*-terphenyl based materials used for detection of phosphate and pyrophosphate anions using the indicator displacement assay (**IDA**) approach; this work is especially important as most of the known chemical warfare agents are phosphoester derivative. Also, an *m*-xylene based material (Chapter 2) was tethered to polymer support (polyglycerol) in order to provide high surface area for decomposition of phosphoester.

Chapters four and five describe the synthesis and photophysical characterization of π -conjugated cruciforms. A series of 1,3-bis(dimethylaminomethyl)phenyl based receptors (Chapter 4) were synthesized and studied for metal ion detection whereas Chapter 5 describes the synthesis and photophysical study of five phosphorous based cruciforms

Chapter six describes the synthesis of various halogenated oxacyclophane scaffolds which allows us to attach various chromophores on to it using C-C coupling reactions known in the literature to study the controlled inter chain interaction. This section also contains detailed photophysical study of monomer as well as polymers.

1.5 References

1. MacDiarmid, A. G., "Synthetic Metals": A Novel Role for Organic Polymers (Nobel Lecture). *Angewandte Chemie International Edition* **2001**, 40, (14), 2581-2590.
2. Shirakawa, H., The Discovery of Polyacetylene Film: The Dawning of an Era of Conducting Polymers (Nobel Lecture). *Angewandte Chemie International Edition* **2001**, 40, (14), 2574-2580.
3. Heeger, A. J., Semiconducting and Metallic Polymers: The Fourth Generation of Polymeric Materials (Nobel Lecture). *Angewandte Chemie International Edition* **2001**, 40, (14), 2591-2611.
4. Shirakawa, H.; Louis, E. J.; MacDiarmid, A. G.; Chiang, C. K.; Heeger, A. J., Synthesis of electrically conducting organic polymers: halogen derivatives of polyacetylene, (CH)_x. *Journal of the Chemical Society, Chemical Communications* **1977**, (16), 578-80.
5. Shirakawa, H.; MacDiarmid, A.; Heeger, A. J., Twenty-five years of conducting polymers. *Chemical Communications* **2003**, (1), 1-4.
6. de Boer, B.; Facchetti, A., Semiconducting Polymeric Materials. *Polymer Reviews* **2008**, 48, (3), 423 - 431.
7. Patil, A. O.; Heeger, A. J.; Wudl, F., Optical properties of conducting polymers. **1988**, 88, (1), 183-200.
8. Friend, R. H.; Gymer, R. W.; Holmes, A. B.; Burroughes, J. H.; Marks, R. N.; Taliani, C.; Bradley, D. D. C.; Dos Santos, D. A.; Bredas, J. L.; Logdlund, M.;

- Salaneck, W. R., Electroluminescence in conjugated polymers. *Nature (London)* **1999**, 397, (6715), 121-128.
9. Brabec, C. J.; Sariciftci, N. S.; Hummelen, J. C., Plastic solar cells. *Advanced Functional Materials* **2001**, 11, (1), 15-26.
10. Thomas, S. W., III; Joly, G. D.; Swager, T. M., Chemical Sensors Based on Amplifying Fluorescent Conjugated Polymers. *Chemical Reviews (Washington, DC, United States)* **2007**, 107, (4), 1339-1386.
11. Takita, R.; Song, C.; Swager, T. M., π -Dimer Formation in an Oligothiophene Tweezer Molecule. *Org. Lett.* **2008**, 10, 5003-5005.
12. Murphy, A. R.; Frechet, J. M. J., Organic Semiconducting Oligomers for Use in Thin Film Transistors. **2007**, 107, (4), 1066-1096.
13. Burroughes, J. H.; Bradley, D. D. C.; Brown, A. R.; Marks, R. N.; Mackay, K.; Friend, R. H.; Burns, P. L.; Holmes, A. B., Light-emitting diodes based on conjugated polymers. *Nature (London, United Kingdom)* **1990**, 347, (6293), 539-41.
14. Bunz, U. H. F., Poly(aryleneethynylene)s: Syntheses, Properties, Structures, and Applications. *Chemical Reviews (Washington, D. C.)* **2000**, 100, (4), 1605-1644.
15. Carroll, R. L.; Christopher, B. G., The Genesis of Molecular Electronics. *Angewandte Chemie International Edition* **2002**, 41, (23), 4378-4400.
16. Elangovan, A.; Kao, K.-M.; Yang, S.-W.; Chen, Y.-L.; Ho, T.-I.; Su, Y. O., Synthesis, Electronic Properties, and Electrochemiluminescence of Donor-Substituted Phenylethynylantrons. **2005**, 70, (11), 4460-4469.

17. Liu, M. S.; Jiang, X.; Liu, S.; Herguth, P.; Jen, A., K.-Y., Effect of Cyano Substituents on Electron Affinity and Electron-Transporting Properties of Conjugated Polymers. *Macromolecules* **2002**, 35, (9), 3532-3538.
18. Zhang, W.-W.; Yu, Y.-G.; Lu, Z.-D.; Mao, W.-L.; Li, Y.-Z.; Meng, Q.-J., Ferrocene^η-Phenothiazine Conjugated Molecules: Synthesis, Structural Characterization, Electronic Properties, and DFT-TDDFT Computational Study. *Organometallics* **2007**, 26, (4), 865-873.
19. Zhu, S. S.; Carroll, P. J.; Swager, T. M., Conducting Polymetalloporotaxanes: A Supramolecular Approach to Transition Metal Ion Sensors. *Journal of the American Chemical Society* **1996**, 118, (36), 8713-8714.
20. Wilson, J. S.; Chawdhury, N.; Al-Mandhary, M. R.; Younus, M.; Khan, M. S.; Raithby, P. R.; Kohler, A.; Friend, R. H., The energy gap law for triplet states in Pt-containing conjugated polymers and monomers. *J Am Chem Soc FIELD Full Journal Title: Journal of the American Chemical Society* **2001**, 123, (38), 9412-7.
21. Grimsdale Andrew, C.; Chan, K. L.; Martin, R. E.; Jokisz, P. G.; Holmes Andrew, B., Synthesis of Light-Emitting Conjugated Polymers for Applications in Electroluminescent Devices. *Chemical Reviews (Washington, D. C.)* **2009**, 109, (3), 897-1091.
22. Wu, F.; Tian, W.; Sun, J.; Shen, J.; Pan, X.; Su, Z., Study on the electronic structure of phenylene vinylene dimers with different substituents. *Materials Science & Engineering, B: Solid-State Materials for Advanced Technology* **2001**, 85, (2-3), 165-168.

23. Kraft, A.; Grimsdale, A. C.; Holmes, A. B., Electroluminescent Conjugated Polymers-Seeing Polymers in a New Light. *Angew. Chem. Int. Ed* **1998**, 37, 402-428.
24. He, S.; Dennis, A. E.; Smith, R. C., Steric Coordination Control of Interchain Interactions in Conducting Metallopolymers. *Macromolecular Rapid Communications* **2009**, 30, 2079-2083.
25. Back, S.; Lutz, M.; Spek, A. L.; Lang, H.; Koten, G. v., Preparation and electrochemical behaviour of dinuclear platinum complexes containing NCN ligands (NCN=[C₆H₃(Me₂NCH₂)_{2-2,6}]-). The crystal structure of [C₆H₃(Me₂NCH₂)_{2-1,3}-(C[6-point triple bond; length half of m-dash]C)-5]₂. *Journal of Organometallic Chemistry* **2001**, 620, (1-2), 227-234.
26. James, S. L.; Verspui, G.; Spek, A. L.; van Koten, G., Organometallic polymers: an infinite organoplatinum chain in the solid state formed by (CCHClPt) hydrogen bonds. *Chemical Communications (Cambridge)* **1996**, (11), 1309-1310.
27. Back, S.; Albrecht, M.; Spek, A. L.; Rheinwald, G.; Lang, H.; Koten, G. v., Toward Organometallic Polymers with High Directionality Containing Bis-ortho-Chelating Ligands. *Organometallics* **2001**, 20, (5), 1024-1027.
28. Wiskur, S. L.; Ait-Haddou, H.; Lavigne, J. J.; Anslyn, E. V., Teaching old indicators new tricks. *Accounts of Chemical Research* **2001**, 34, (12), 963-972.
29. Knapton, D.; Burnworth, M.; Rowan, S. J.; Weder, C., Fluorescent organometallic sensors for the detection of chemical-warfare-agent mimics. *Angewandte Chemie, International Edition in English* **2006**, 45, (35), 5825-5829.

30. Nguyen, B. T.; Anslyn, E. V., Indicator-displacement assays. *Coordination Chemistry Reviews* **2006**, 250, (23+24), 3118-3127.
31. Nguyen, B. T.; Wiskur, S. L.; Anslyn, E. V., Using Indicator-Displacement Assays in Test Strips and To Follow Reaction Kinetics. *Organic Letters* **2004**, 6, (15), 2499-2501.
32. Fabbrizzi, L.; Licchelli, M.; Taglietti, A., The design of fluorescent sensors for anions: taking profit from the metal-ligand interaction and exploiting two distinct paradigms. *Dalton Transactions* **2003**, (18), 3471-3479.
33. Lipscomb, W. N.; Strater, N., Recent Advances in Zinc Enzymology. *Chemical Reviews (Washington, D. C.)* **1996**, 96, (7), 2375-2434.
34. Kim, J.; McQuade, D. T.; McHugh, S. K.; Swager, T. M., Ion-specific aggregation in conjugated polymers: highly sensitive and selective fluorescent ion chemosensors. *Angewandte Chemie, International Edition* **2000**, 39, (21), 3868-3872.
35. Liu, B.; Bazan Guillermo, C., Synthesis of cationic conjugated polymers for use in label-free DNA microarrays. *Nature Protocols* **2006**, 1, (4), 1698-1702.
36. Kim, I.-B.; Dunkhorst, A.; Gilbert, J.; Bunz Uwe, H. F., Sensing of Lead Ions by a Carboxylate-Substituted PPE: Multivalency Effects. *Macromolecules* **2005**, 38, (11), 4560-4562.
37. http://www.eia.doe.gov/cneaf/alternate/page/renew_energy_consump/images/fig1_09_small.jpg, (retrieved July 3, 2010).
38. Jacobson, M. Z., Review of solutions to global warming, air pollution, and energy security *Energy & Environmental Science* **2009**, 2, (2), 148-173.

39. Cheng, Y.-J.; Yang, S.-H.; Hsu, C.-S., Synthesis of Conjugated Polymers for Organic Solar Cell Applications. *Chemical Reviews (Washington, D. C.)* **2009**, 109, (11), 5868-5923.
40. Shirota, Y.; Kageyama, H., Charge Carrier Transporting Molecular Materials and Their Applications in Devices. *Chemical Reviews (Washington, D. C.)* **2007**, 107, (4), 953-1010.
41. Sariciftci, N. S.; Smilowitz, L.; Heeger Alan, J.; Wudl, F., Photoinduced Electron Transfer from a Conducting Polymer to Buckminsterfullerene *Science* **1992**, 258, (5087), 1474-1476.
42. Smith, R. C., Covalently Scaffolded Inter-p-System Orientations in p-Conjugated Polymers and Small Molecule Models. *Macromolecular Rapid Communications* **2009**, 30, 2067-2078.
43. Bazan, G. C., Novel Organic Materials through Control of Multichromophore Interactions. *Journal of Organic Chemistry* **2007**, 72, 8615-8635.
44. Knoblock, K. M.; Silvestri, C. J.; Collard, D. M., Stacked conjugated oligomers as molecular models to examine interchain interactions in conjugated materials. *J Am Chem Soc* **2006**, 128, (42), 13680-1.
45. Sakai, T.; Satou, T.; Kaikawa, T.; Takimiya, K.; Otsubo, T.; Aso, Y., Syntheses, Structures, Spectroscopic Properties, and pi-Dimeric Interactions of [n.n]Quinquethiophenophanes. *J. Am. Chem. Soc.* **2005**, 127, (22), 8082-8089.
46. Song, C.; Swager, T. M., π -Dimer Formation as the Driving Force for Calix[4]arene-Based Molecular Actuators. *Org. Lett.* **2008**, 10, 3575-3578.

47. Wang, W.; Xu, J.; Lai, Y.-H., Alternating Conjugated and Transannular Chromophores: Tunable Property of Fluorene-Paracyclophane Copolymers via Transannular p-p Interaction. *Organic Letters* **2003**, 5, (16), 2765-2768.
48. Zhu, Z.; Swager, T. M., Conjugated Polymers Containing 2,3-Dialkoxybenzene and Iptycene Building Blocks. *Organic Letters* **2001**, 3, (22), 3471-3474.
49. Zhao, X.; Cardolaccia, T.; Farley, R. T.; Abboud, K. A.; Schanze, K. S., A platinum acetylide polymer with sterically demanding substituents: Effect of aggregation on the triplet excited state. *Inorganic Chemistry* **2005**, 44, (8), 2619-2627.
50. Morgan, B. P.; Gilliard, R. J.; Loungani, R. S.; Smith, R. C., Poly(*p*-phenylene ethynylene) Incorporating Sterically Enshrouding *m*-Terphenyl Oxacyclophane Canopies. *Macromolecular Rapid Communications* **2009**, 30, 1399-1405.

CHAPTER TWO

POLYGLYCEROL-BOUND PHOSPHOTRIESTERASE ENZYME MODEL COMPLEXES FOR DETECTION AND HYDROLYSIS OF PHOSPHORUS SPECIES IN AQUEOUS SOLUTION[#]

2.1 Introduction

The nerve agents of chemical warfare, as well as many widely-used commercial pesticides, are phosphoesters. Some of these neurotoxic compounds, including G and V agents (Figure 2.1) are among the most toxic synthetic materials ever isolated.

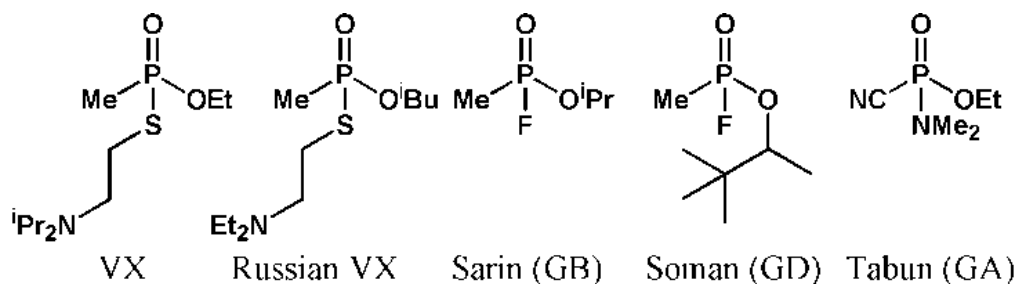


Figure 2.1 Five of the seven globally stockpiled chemical warfare agents are simple phosphoesters.

The simple structure and availability of starting materials make these agents attractive weapons for terrorism, as exemplified by the use of sarin (**GB**) in attacks on

[#] Adapted from Mangalum, A.; Smith, R. C. *Tetrahedron*, **2009**, *65*, 4298-4303, with permission.

subway trains in Japan in 1995.¹ Recent increases in awareness regarding terrorist threats and the environmental impact of pesticides highlight the desire to detect^{2,3} and degrade^{4,5} organophosphorus toxins.

Phosphotriesterase (**PTEase**) is a bacterial dizinc hydrolase enzyme capable of hydrolyzing phosphoesters.⁶ The active site of PTEase features two zinc ions held at a distance of ~ 3.4 Å.⁷ One actively explored area of research is thus to prepare small molecule bimetallic models of PTEase that can catalytically hydrolyze phosphoesters to biologically innocuous phosphates. Di(2-picolylaminomethyl)xylyl scaffolded ligands shown in **Figure 2.2 (R-PTE-X)** support dizinc complexes with M–M distances similar to that in the native PTEase active site.

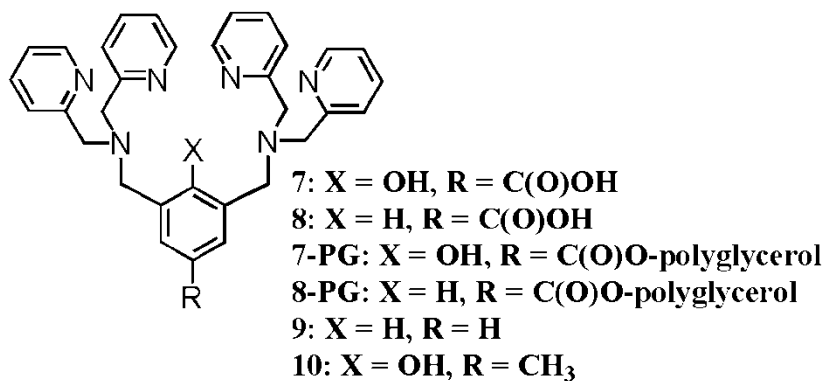


Figure 2.2 General form of binucleating ligands whose bimetallic complexes are useful for inorganic phosphate detection and can catalytically hydrolyze phosphoesters.

Complexes of **R-PTE-X** ligands have thus been utilized in a variety of sensing and catalytic applications under physiological conditions.⁸⁻¹⁷ An IR-dye modified variation has been applied to image phosphate production resulting from bacterial

infection in live mice, unequivocally demonstrating the stability of this binucleating scaffold for extended periods in biological milieu.¹⁸

Our work with PTEase model-based detection⁸ has focused on the indicator displacement assay sensing mechanism.¹⁹ In this strategy an optical (colorimetric or fluorescent) signal transduction event is effected by displacement of an indicator from a receptor upon exposure to an analyte. Sensitivity is attained when the analyte binds significantly more strongly to the receptor than does the displaceable indicator.

This strategy is attractive because a variety of commercial indicators can be utilized, providing various response wavelengths and binding affinities with a single receptor, and the simple visual colorimetric detection provided by this strategy is desirable for field use. Related bioorganic model-based indicator displacement assays for nerve agents operate via metal ion displacement from fluorogenic ligands in response to neutral nerve agent simulants²⁰ or anionic partial hydrolysis products of G agents.²¹

Another of our interests is to tether PTEase models to polymeric supports for catalytic applications. Covalent linkage or physical encapsulation of native phosphohydrolase enzymes to polymers and foams have already shown promise for decontamination.^{22, 23} Covalent linkage is preferred because it prevents catalyst leaching from the polymer, thus increasing shelf life of the material. Model complexes should be an affordable alternative to isolated enzymes and may be more robust components of decontamination solutions. The polymer support we selected

for this initial study is a biocompatible water-soluble hyperbranched polyglycerol (Figure 2.3).

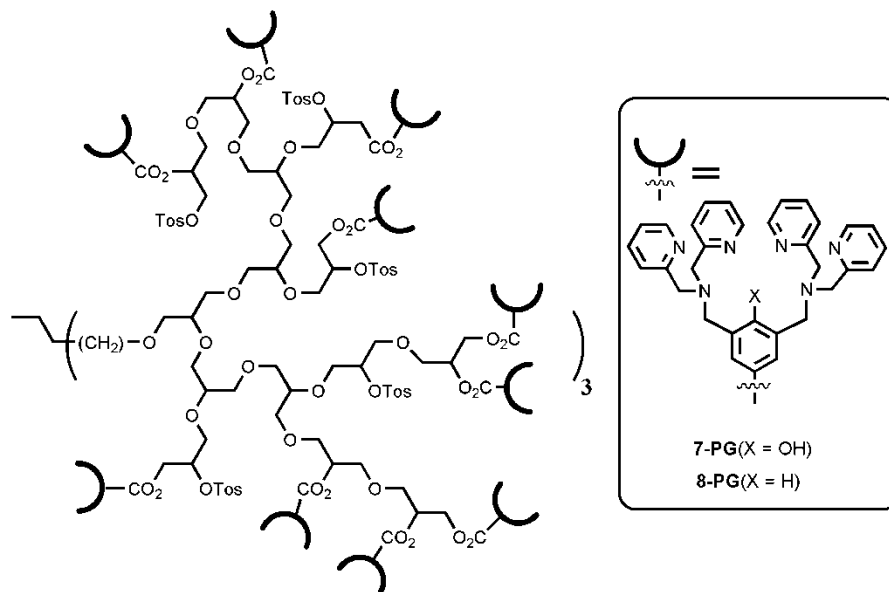


Figure 2.3 Representation of the structure of **7-PG** and **8-PG**. Note that the size of PG branches varies, and this is only one possible representation demonstrating the global structure of the PG.

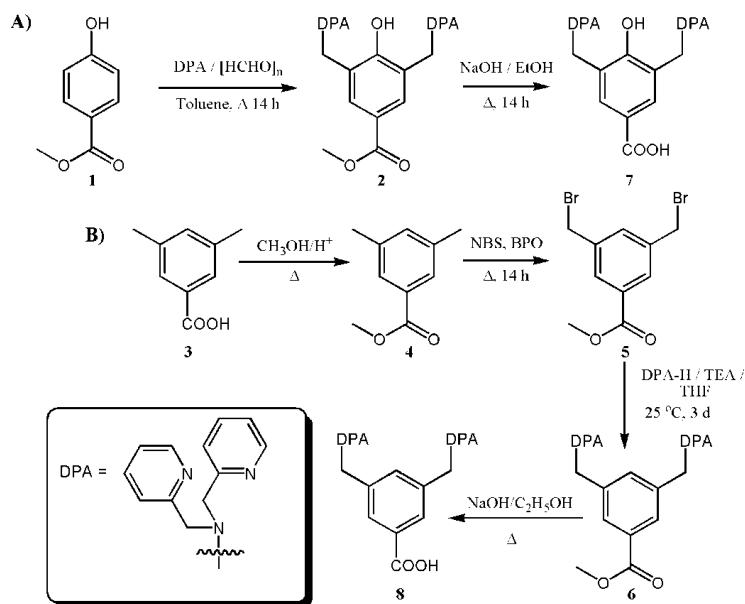
In selecting a polymer support for a decontamination catalyst, biocompatibility and high surface area for functionalization are advantageous. Dendrimers are promising chaperones for drug targeting / delivery and their high surface area and potential for supporting cooperative effects have been exploited for catalytic applications.²⁴⁻²⁷ The often time-consuming synthesis of dendrimers, however, is the most auspicious hindrance to their widespread application.

Hyperbranched polymers, however, can be prepared more efficiently and retain the high surface area typical of dendrimers.²⁸⁻³⁰ Biocompatible hyperbranched polymers are thus privileged scaffolds for high activity bioremediation and decontamination technologies.

For organophosphorus neurotoxins, polymers such as polyglycerol, which can efficiently permeate and solubilize agents from thickened chemical agent mixtures often used in warfare contexts (where poly(ethyleneglycol) is a preferred thickener),³¹ are of particular relevance in a practical sense.⁴ Polyglycerol is approved in the United States and Europe for use in pharmaceuticals,³²⁻³⁴ cosmetics,^{35, 36} and even as food additives,^{37, 38} making it a safe candidate for protective creams. The bioavailability of polyglycerol^{32, 33} also suggests its potential as a carrier support to deliver OP-decontaminating agents in prophylactic medical treatment. The polymeric support also facilitates catalyst recyclability and use in continuous membrane reactors for water treatment.

Herein we describe the preparation of hyperbranched polyglycerol modified by two dinucleating PTE model ligand scaffolds. We demonstrate that their Co(III) complexes efficiently hydrolyze a phosphoester model compound, and that their Zn(II) complexes are useful receptors for indicator displacement assays for phosphate / pyrophosphate. Both hydrolysis and detection experiments were carried out under ambient conditions in aqueous solution buffered at physiological pH (7.4).

2.2 Synthesis and Characterization



Scheme 2.1 Preparation of **7** (A) and **8** (B). Synthetic details are provided in the experimental section.

2.2.1 Synthetic Characterization

The hyperbranched PG support ($M_n = 3700$, PDI = 1.2) was prepared via a literature protocol³⁹ involving anionic polymerization of glycidol from a trimethylolpropane core. In order to facilitate attachment of PTE models, the PG was reacted with tosyl chloride in the presence of pyridine to give tosylated polyglycerol (**Tos-PG**).⁴⁰

The small molecule carboxylate-derivatized binucleating ligand moieties required for condensation with **Tos-PG** were readily prepared via the sequence shown in **Scheme 2.1**. Simple S_N2 reaction of **7** and **8** with **PG-Tos** yields **7-PG** and **8-PG**

(**Figure 2.3**; the size of PG branches will vary and the structure shown is a simplified representation). The approach selected to tether enzyme model complexes to the polymers was inspired by a reported route to hyperbranched PGs derivatized with α,α' -diamino-*m*-xylene-based pincer ligands in which highly efficient complex loading was accomplished, leading to active complexes for Pd-catalyzed C–C bond forming reactions.⁴⁰⁻⁴²

In the current system, the efficiency of substituting **7** or **8** for tosylate units was readily gauged by integration of well-resolved proton NMR resonances at ~2.3 ppm (tosyl methyl group) and ~8.5 ppm (pyridyl subunit). Unfortunately, a relatively low loading efficiency (36% and 25% of tosyl groups substituted in **7-PG** and **8-PG** respectively) was observed, despite repeated efforts to improve this step. The low efficiency is presumably a result of the fairly voluminous carboxylates lacking sufficient access to some potential substitution sites due to crowding by the hyperbranched support.

2.2.2. Transmission Electron Microscopy (TEM) Characterization

Upon dispersion in a solvent such as THF, hyperbranched polyglycerol-supported transition metal complexes have been shown to form micellar structures that can be fractionated by size exclusion chromatography to produce uniformly sized nanostructures.⁴⁰ Although preparing nanostructures is not the primary goal of the current study, we were interested in whether **7-PG** and **8-PG** form structures similar to those reported previously.

We thus conducted a transmission electron microscopy (**TEM**) study on a sample cast from a (nonfractionated) dispersion of **8-PG** in THF. The **TEM** images (i.e., **Figure 2.4**) revealed that irregularly-shaped particles, similar in size to those previously reported,⁴⁰ were observed.

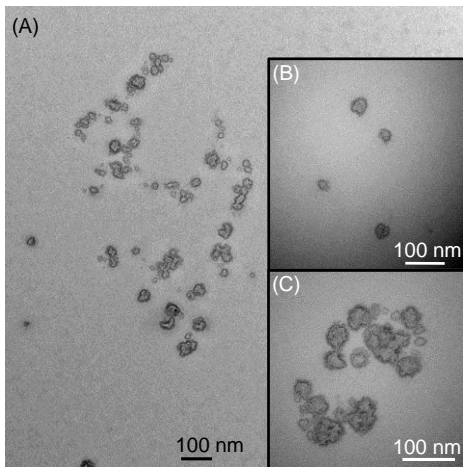


Figure 2.4 TEM image of **8-PG** (A). Insets show a set of variously-sized particles (B) and an agglomeration of smaller particles that make up larger features (C).

The particles ranged in size from about 15 - 35 nm (**Figure 2.4B**), and close inspection reveals that the apparent larger features visible in **Figure 2.4A** are actually clusters of the smaller particles (**Figure 2.4C**). The formation of micellar or reverse micellar nanostructures is of particular interest because catalysis can be enhanced within micellar structures or at their surface, depending on the substrate and solvent system employed. Catalyst recovery could also be affected by nanofiltration, ultracentrifugation or membrane techniques for particles in this size regime. These avenues are worth pursuing in more detail once optimized materials are accomplished.

2.3 Photophysical Studies and Calculations

2.3.1 Catalysis of Phosphorus Species

In order to test the viability of the PG-supported complexes to hydrolyze phosphoesters, the hydrolysis rate of 4-nitrophenylphosphate (**NPP**) was examined in the presence of **7-PG** and **8-PG** Co(III) complexes. NPP is a convenient and often-used substrate for such studies because the formation of its hydrolysis product, 4-nitrophenolate, is easily followed by UV-vis spectroscopy.^{43, 44}

By following NPP hydrolysis by absorption spectroscopy, employing solutions with varying substrate and catalyst concentrations as previously reported,⁴⁴ we determined the rate constants for NPP hydrolysis in HEPES (0.1 M, pH = 7.4) with the Co(III) complexes of **8-PG** ($6.2 \times 10^{-4} \text{ s}^{-1}$) and **7-PG** ($4.8 \times 10^{-4} \text{ s}^{-1}$).

These values indicate an approximate five orders of magnitude enhancement in hydrolysis rate for either of the PG-bound Co(III) complexes versus the uncatalyzed hydrolysis rate of $2 \times 10^{-9} \text{ s}^{-1}$.⁴⁵ Although higher activity would likely be necessary for practical application requiring hydrolysis of more challenging substrates, these preliminary complexes show promise for extension to additional polymer-bound complexes.

2.3.2 Detection of Phosphorus Species

Another interesting application of polymer bound enzyme models is their ability to act as selective receptors for the detection of biological species. In this case, the Zn(II) complexes (**Zn₂-7-PG** and **Zn₂-8-PG**) were employed rather than the

Co(III) complexes used in hydrolysis studies, because Zn(II) has greater ligand lability and thus favors reversible binding that is desirable for sensors.

Building on our work with related dizinc complexes,⁸ we tested the polymer-bound analogues as macromolecular receptors of polymeric indicator displacement assays (**IDAs**) for inorganic phosphate detection. The first step in this direction was to determine how Zn₂-**8-PG** complexes influence the absorption spectra of commercially available complexometric indicators upon binding, and whether the indicators are successfully displaced by various analytes. A large color change between the complex-bound and free (analyte - displaced) indicator states is desired because this would facilitate detection of small quantities of analyte. On the basis of our previous study,⁸ we selected six dyes (**Figure 2.5**) as indicators capable of potentially large color changes.

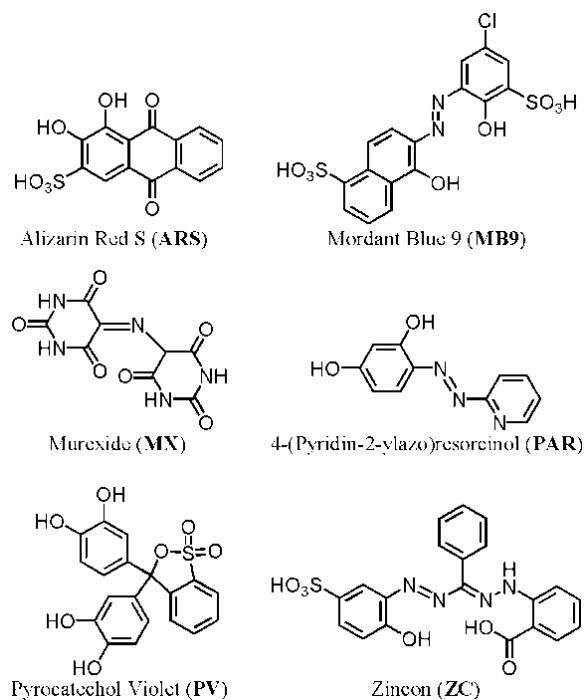


Figure 2.5 Structures of commercially available complexometric indicators used in the current study. Only one protonation state / resonance structure is shown in each case.

As an example of how dramatically spectral properties can change upon complexation, data from a titration of **MX** with Zn_2 -**8-PG** and subsequent displacement of the indicator by addition of pyrophosphate are shown in **Figure 2.6** (similar data for the remaining dyes are provided in the **appendix 2 B**).

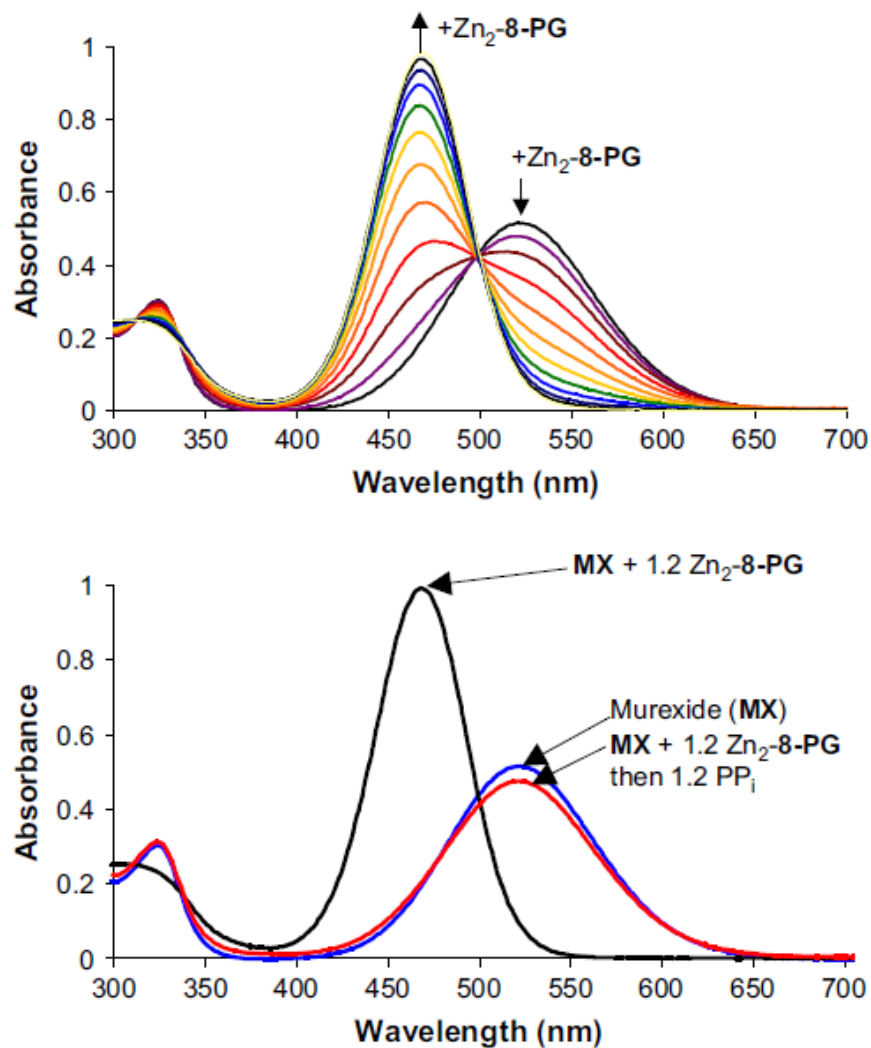


Figure 2.6 Upper chart: Changes in absorption spectra of murexide (5.0×10^{-5} M) as up to one equiv of Zn₂-8-PG is added to the solution. The first trace is murexide alone, and each subsequent trace represents addition of 0.1 equiv of Zn₂-8-PG. Lower chart: Absorption spectra for Murexide alone (blue trace), the same solution immediately after addition of 1.2 equiv Zn₂-8-PG (black trace), and subsequently 1.2 equiv pyrophosphate (PP_i, red trace). All solutions were in 0.1 M HEPES buffer at a pH of 7.4. Spectra are corrected for dilution factors.

Data from absorption spectroscopic titrations were used to extract dissociation constants (K_d) for the indicators (**Table 2.1**). **Table 2.1** also provides K_d values for the indicators with dizinc complexes of nonpolymer-bound ligands **9** and **10** (**Figure 2.2**) for comparison. Because the polymer-bound variations are in significantly altered environments in terms of both polarity and sterics, it is not surprising that there is a marked change in the dissociation constants for indicators bound to Zn_2 -**7-PG** and Zn_2 -**8-PG** complexes versus the small molecule analogues.

Table 2.1 Dissociation constants (K_d , in μM) for the binding of indicators to the dizinc complexes of the listed ligands, determined from absorption spectroscopic data (in 0.1 M HEPES buffer at pH 7.4). Structures and abbreviations for indicators are provided in **Figure 2.5**, and absorption spectra are provided in the **appendix 2 B**.

Dissociation Constants (K_d , μM)				
Indicator	8-PG	7-PG	9	10
ARS	60	42	63	280
MB9	NA ^a	29	NA ^a	5.1
MX	83	350	640	21
PAR	3.4	48	28	18
PV	110	160	98	30
ZC	68	59	480	2.9

^a Spectroscopic data could not be adequately fit using this model.

These changes in binding constant are accompanied by concomitant changes in how effectively inorganic phosphate anions displace the indicators to produce colorimetric responses. Though *m*-xylylene-supported bis(di(2-picolyamine)) dizinc complexes are useful phosphate (P_i) sensors,⁹⁻¹⁶ there is some evidence that pyrophosphate (PP_i) can bind more strongly, at least in some cases.^{8, 46}

Furthermore, selectivity can be acquired simply by judicious selection of the indicator to be displaced by the analyte (i.e., by selecting an indicator with an appropriate K_d).⁴⁶ The polymer-bound analogues behave similarly: when dizinc complex is the receptor, any of the indicators shown in **Figure 2.5** are selective for inorganic phosphates (P_i or PP_i) over all other common anions screened. No notable change in absorbance was observed in response to F^- , Cl^- , Br^- , I^- , AcO^- or HSO_4^- (all in 0.1 M HEPES, pH = 7.4).

An even greater specificity can be attained when the most weakly binding indicators are employed. Specifically, we found that PP_i can be selectively detected versus P_i at the same concentration when **MX** or **PV** is used as the indicator (The response using **MX** is shown in **Figure 2.6**; other absorption spectra are shown in the **appendix 2 B**). It is noteworthy that the best receptor-indicator pairs for the polyglycerol differ from those for small molecule analogues,⁸ emphasizing the importance of independent K_d measurements and indicator displacement trials in the course of polymer-bound sensor development.

2.4 Conclusion

We have prepared artificial enzyme modified, water-soluble hyperbranched polyglycerols. The Co(III) complexes of these materials catalyze the hydrolysis of a phosphoester model substrate in neutral aqueous buffer, with a rate enhancement of five orders of magnitude versus the uncatalyzed reaction. Zinc(II) complexes of PG-bound enzyme models are highly selective receptors for inorganic phosphates over other common anions.

There are significant differences in binding constants between the polyglycerol-supported enzyme models and their small molecule analogues. Caution should thus be exercised when attempting to extend data from small molecule model systems to polymer-bound analogues, especially in IDA studies where relative binding strengths dictate the selectivity of the receptor-indicator pairs for a given analyte. Additional polymer supported PTEase model-derivatized hyperbranched polymers are currently being prepared for optimization in our laboratory to improve upon the strategies reported herein.

2.5 Experimental Section

Reagents and General Methods

All reagents were obtained from Aldrich Chemical Co., TCI America, Alfa Aesar, Mallinckrodt, or MP Biomedicals, LLC and used as received. Hyperbranched polyglycerol (**PG**)³⁹ and tosylated polyglycerol (**Tos-PG**)⁴⁰ were prepared as previously described. Proton and carbon – 13 NMR spectra were recorded on a Bruker Avance 300 spectrometer and chemical shifts are reported in parts per million (δ ppm). Proton NMR was internally referenced to tetramethylsilane (δ 0.0) or residual solvent signal, carbon - 13 NMR chemical shifts were reported relative to the residual solvent peak. Compounds **4** and **5** were prepared as previously reported.⁴⁷

TEM imaging was performed using a Hitachi H-7600 variable kV TEM with acceleration voltage of 120 kV. The sample was prepared on formvar coated copper grids by drop-casting, and samples were dried in an oven overnight.

General Spectroscopic Methods

Absorption spectra were recorded on a Varian Cary 50 Bio UV-vis spectrophotometer. Samples for all absorbance spectra used 0.1 M *N*-2-hydroxyethylpiperazine-*N'*-2-ethanesulfonic acid (HEPES) buffer at pH 7.4 as solvent in spectrosil quartz cuvettes having a path length of 1 cm. Indicator displacement assay protocols,⁸ kinetic analyses,⁴⁴ and dissociation constant determinations (modified Benesi-Hildebrand method)⁴⁸ have been described previously. All absorption spectra for titrations and Benesi-Hildebrand plots used are provided in the **Appendix 2 B**.

Synthesis of polyglycerol (PG)

In a two-neck round bottom flask, trimethylolpropane (200 mg, 1.5 mmol) was taken and 0.1 mL of MeONa (25 % methanol solution) was added into it. Resulting mixture was stirred for overnight. Excess methanol was removed under vacuum and 3 mL of toluene was added. The resulting solution was heated at 90 °C under argon with a distillation head in place for the removal of ether. A solution of 24 mL of ether and glycidol (5.7 g, 76.9 mmol) was prepared and added portion wise into the flask over 12 h. (0.5 mL were added every 15 min). After complete addition, the sticky residue was dissolved in 25 mL of methanol. This solution was passed through cationic resin (Dowex ® HCR-W2; Na⁺, previously neutralized by adding 0.1 N HCl of 50 mL). To this solution, 270 mL of acetone was added and the solution was left over night to allow precipitation. Viscous oil at the bottom of flask was observed. Acetone was decanted off and the oil was dissolved in methanol. Methanol was further removed under reduced pressure. Colorless viscous oil was dried on vacuum at 80 °C. (1.9 g). ¹H NMR (300 MHz, CD₃OD): δ = 0.90 (s, 3H; CH₃), 1.40 (s, 2H; CH₂), 3.40 – 3.90 (b, polyether), 4.00 (s, 40H; OH). ¹³C NMR (75.4 MHz, CD₃OD): = 61.0, 63.5, 69.0, 70.5, 72.0, 78.5, 80.0.

Synthesis of tosylated polyglycerol (Tos-PG)

Polyglycerol (0.5 g, 6.8 mmol) was dissolved in 10 mL of pyridine in a round bottom flask. In another flask, *p*-toluenesulphonic acid (2.6 g, 13.6 mmol) was dissolved in 15 mL of pyridine at 50 °C and added dropwise to the polyglycerol solution. The reaction was stirred for 3 h followed by removal of pyridine under reduced pressure. The resultant residue was dissolved in DMSO and passed through anionic resin (details

below) to remove pyridinium chloride (8 times, 20 cm, dropwise). DMSO was removed by rotary evaporation. (4.7 g). ^1H NMR (300 MHz, DMSO): $\delta = 2.25$ (s, 3H; CH_3 of tosyl group), 3.35 – 3.70 (b, 22H; polyether), 7.15 (s, 2H; Aromatic), 7.49 (s, 2H; Aromatic).

Procedure to prepare anionic resin

Cationic exchange resin (Dowex $\text{\textcircled{R}}$ HCR-W2; Na^+) was washed with concentrated NaOH solution (8×50 mL), followed by water (3×50 mL).

Synthesis of methyl (3,5 dimethyl) benzoate (4)

3,5-dimethyl benzoic acid (2.0 g, 13.3 mmol) was dissolved in 30 mL of ethanol and 4 drops of H_2SO_4 was added. The reaction mixture was refluxed overnight. Methanol was removed under reduced pressure and 50 mL of dichloromethane was added. The solution was washed with saturated NaHCO_3 (aq) (3×50 mL). The organic layer was dried over Na_2SO_4 and volatiles were removed under reduced pressure. The compound was recovered as a white solid. (1.8 g, 84.8 %) ^1H NMR (300 MHz, CDCl_3): $\delta = 2.38$ (d, 6H; $J = 0.6$, $2 \times \text{CH}_3$), 3.92 (s, 3H; OCH_3), 7.21 (t, 1H; $J = 0.6$ Hz, Aromatic). 7.67 (q, 2H; $J_1 = 1.5$, $J_2 = 0.6$, Aromatic). ^{13}C NMR (75.4 MHz, CDCl_3): = 21.2, 52.0, 127.3, 130.0, 134.6, 138.0, 167.5.

Synthesis of methyl 3,5-bis(bromomethyl)benzoate (5)

To a round bottom flask were added methyl (3,5-dimethyl) benzoate (1.9 g, 11.6 mmol), *N*-bromosuccinimide (4.4 g, 24.7 mmol), benzoylperoxy anhydride (BPO) (0.4 g, 1.1 mmol) and 70 mL chloroform. The reaction mixture was refluxed overnight. After cooling to room temperature, the reaction mixture was washed with water (3×50 mL).

The organic layer was collected and volatiles were removed under reduced pressure. The residue was dissolved in mixture of hot 20 mL of hexane and 3 mL of dichloromethane. While cooling white crystalline solid precipitated out. (1.0 g, 27.7 %). ^1H NMR (300 MHz, CDCl_3): δ = 3.95 (s, 3H; OCH_3), 4.50 (s, 4H; $2 \times \text{CH}_2$), 7.65 (s, 1H; Aromatic), 8.02 (s, 2H; Aromatic).

Synthesis of methyl 3,5-bis[(bis(2-pyridylmethyl) amino)methyl]benzoate (6)

Solution of methyl 3,5-bis(bromomethyl)benzoate (1.0 g, 3.1 mmol) in 5 mL of dry THF was stirred to 0 °C under inert nitrogen atmosphere. Separately, a solution of triethylamine (1.3 g, 12.9 mmol) and DPA (1.3 g, 6.5 mmol) was prepared and then added dropwise to the reaction mixture. The reaction was allowed to warm at room temperature after complete addition and the reaction mixture was stirred for 3 days. The triethylammonium bromide was filtered off and volatiles were removed under reduced pressure, leaving behind red oil. Dichloromethane (50 mL) was added and solution was washed by saturated Na_2CO_3 (aq) (3×50 mL). The organic layer was collected, dried over Na_2SO_4 , and volatiles were removed under reduced pressure, yielding viscous red oil. (1.3 g, 72.0 %). ^1H NMR (300 MHz, CDCl_3): δ = 3.74 (s, 4H; C- CH_2), 3.82 (s, 8H; N- CH_2), 3.93 (s, 3H; OCH_3), 7.15 (b, 4H; pyridyl), 7.6 (m, 8H, pyridyl), 7.75 (s, 1H; Aromatic), 7.95 (d, 2H; $J=1.5$, Aromatic), 8.52 (m, 4H; pyridyl). ^{13}C NMR (75.4 MHz, CDCl_3): = 58.2, 60.1, 67.9, 122.0, 122.8, 128.8, 130.2, 133.8, 136.5, 139.7, 148.9, 159.5, 167.2. HRMS (FAB, m/z): calcd for $\text{C}_{34}\text{H}_{34}\text{N}_6\text{O}_2$ 558.2743; found 558.2749. This material was hydrolyzed to form the acid without further purification.

Synthesis of 3,5-bis[(bis(2-pyridylmethyl) amino)methyl]-benzoic acid (8)

Methyl 3,5-bis[(bis(2-pyridylmethyl) amino)methyl]benzoate (0.5 g, 0.9 mmol) was dissolved in 60 mL of ethanol and ~1.2 g of NaOH was added into the reaction mixture. After addition, the solution was refluxed overnight. Volatiles were removed followed by addition of water into it and subsequently extracted with dichloromethane (3 × 30 mL). The organic layer was dried over Na₂SO₄, and volatiles were removed under reduced pressure to give a yellow solid. (0.4 g, 80 %). ¹H NMR (300 MHz, CDCl₃): δ = 3.32 (s, 4H; C-CH₂), 3.52 (s, 8H; N-CH₂), 6.84 (t, 4H; *J* = 6, pyridyl), 7.19 - 7.38 (m, 8H, pyridyl), 7.79 (s, 2H; Aromatic), 8.38 (d, 4H; *J* = 4.5, pyridyl). ¹³C NMR (75.4 MHz, CDCl₃): δ = 58.9, 59.9, 121.9, 122.9, 129.3, 131.0, 136.4, 137.4, 138.3, 149.0, 159.2, 173.8. HRMS (FAB, m/z): calcd for C₃₃H₃₃N₆O₂ 545.2665; found 545.2674.

Synthesis of Methyl 3,5-bis[(bis(2-pyridylmethyl) amino)methyl]-4-hydroxybenzoate (2)

Methyl-4-hydroxy-benzoate (1.0 g, 6.6 mmol) was taken in a round bottom flask. DPA (3.9 g, 19.6 mmol), paraformaldehyde (0.6 g, 20.0 mmol) and 40 mL toluene were then added into it. After addition, the reaction mixture was refluxed overnight. After cooling to room temperature, toluene was removed under reduced pressure and the residue was dissolved in CH₂Cl₂. The resultant solution was washed with saturated Na₂CO₃ (4 × 50 mL). The organics were dried over Na₂SO₄ and then volatiles were removed by rotary evaporation. The desired product was obtained as viscous red oil. (2.6 g, 69.0 %). ¹H NMR (300 MHz, CDCl₃): δ = 3.84 (s, 4H; C-CH₂), 3.87 (s, 3H; OCH₃), 3.90 (s, 8H; N-CH₂), 7.15 (m, 4H; pyridyl), 7.50 (d, 4H, *J* = 7.8; pyridyl), 7.63 (m, 4H, pyridyl), 7.96 (s, 2H; Aromatic), 8.53 (dd, 4H, *J*₁ = 0.9, *J*₂ = 5.7; pyridyl). HRMS (FAB,

m/z): calcd for C₃₄H₃₄N₆O₃ 574.2692; found 574.2700. This material was hydrolyzed to form the acid without further purification.

Synthesis of 3,5-bis[(bis(2-pyridylmethyl) amino)methyl]-4-hydroxybenzoic acid (7)

Compound methyl-3,5-bis[(bis(2-pyridylmethyl)amino)methyl]-4-hydroxybenzoate (0.2 g, 0.3 mmol) was dissolved in 10 mL of ethanol and ~1.2 g of NaOH was added into the reaction mixture. After addition, solution was refluxed overnight. Volatiles were removed followed by addition of water into it and subsequently solution was extracted with dichloromethane (3 × 30 mL). Organic layer was dried over Na₂SO₄, and volatiles were removed under reduced pressure. (0.09 g, 26.30 %). ¹H NMR (300 MHz, DMSO): δ = 3.41 (s, 4H; C-CH₂), 3.62 (s, 8H; N-CH₂), 7.17 (m, 4H; pyridyl), 7.51 (d, 4H; *J* = 7.8, pyridyl), 7.66 (m, 6H; Aromatic and Pyridyl), 8.45 (d, 4H; *J* = 4.2, pyridyl). HRMS (FAB, m/z): calcd for C₃₃H₃₃N₆O₃ 561.2614; found 561.2623.

Synthesis of 8-PG

In a 25 mL round bottom flask compound 3,5-bis[(bis(2-pyridylmethyl) amino)methyl]-benzoic acid (23 mg, 0.04 mmol) and tosylated polyglycerol (100 mg) was taken. 5 mL of DMF was added into it and reaction mixture was stirred for 2 days at 70 °C. Salt was filtered and DMF was removed under reduced pressure. Residue left was co-evaporated with toluene (3 × 10 mL), yielding a dark orange color solid. (50 mg). ¹H NMR (300 MHz, DMSO): δ = 2.29 (s, 8H; Tos-CH₃), 3.34 (b, 31H; polyether), 3.63 (s, 4H; C-CH₂), 3.70 (s, 8H; N-CH₂), 7.10 (m, 6H; 2 × Aromatic H - Tosyl), 7.26 (m, 4H; pyridyl), 7.48 (dd, 6H; *J*₁ = 8.1, *J*₂ = 1.8, 2 × Aromatic H - Tosyl), 7.58 (d, 4H; *J* = 7.8, pyridyl), 7.75 (m, 6H; Aromatic and pyridyl), 8.49 (dd, 4H; *J*₁ = 2.4, *J*₂ = 0.9, pyridyl). ¹³C

NMR (75.4 MHz, DMSO): = 21.3, 21.5, 58.2, 59.6, 122.6, 122.7, 125.8, 126.0, 128.5, 128.7, 128.9, 129.4, 137.0, 138.0, 146.3, 149.3, 159.7.

Synthesis of 7-PG

In a 25 mL round bottom flask compound 3,5-bis[(bis(2-pyridylmethyl)amino)methyl]-4-hydroxybenzoic acid (60 mg, 0.1 mmol) and tosylated polyglycerol (260 mg) was taken. 5 mL of DMF was added into it and reaction mixture was stirred for 2 days at 70 °C. Salt was filtered and DMF was removed under reduced pressure. Residue left was co-evaporated with toluene (3 × 10 mL), yielding a dark yellow color solid. (90 mg). ¹H NMR (300 MHz, DMSO): δ = 2.29 (s, 12H; Tos-CH₃), 3.34 - 3.83(b, 52H; Polyether, C-CH₂, N-CH₂), 7.10 (m, 8H; 2 × Aromatic H - Tosyl), 7.35 (m, 4H; pyridyl), 7.48 (m, 11H; 2 × Aromatic H - Tosyl), 7.67 -7.82 (m, 9H; 2 × Aromatic and 2 × pyridyl), 8.49 (dd, 4H; pyridyl). ¹³C NMR (75.4 MHz, DMSO): = 21.2, 54.5, 59.3, 122.3, 122.4, 122.7, 123.1, 125.0, 128.5, 137.2, 138.0, 146.3, 149.2, 149.2, 159.0.

2.6 References

1. Croddy, E., "Urban terrorism: Chemical warfare in Japan". *Jane's Intelligence Rev.* **1995**, 7, 520-523.
2. Burnworth, M.; Rowan, S. J.; Weder, C., Fluorescent sensors for the detection of chemical warfare agents. *Chemistry--A European Journal* **2007**, 13, (28), 7828-7836.
3. Royo, S.; Martínez-Mañez, R.; Sancenón, F.; Costero, A. M.; Parra, M.; Gil, S., Chromogenic and fluorogenic reagents for chemical warfare nerve agents detection. *Chemical Communications* **2007**, 4839 - 4847.
4. Yang, Y.-C.; Baker, J. A.; Ward, J. R., Decontamination of Chemical Warfare Agents. *Chem. Rev.* **1992**, 92, 1729-1743.
5. Yang, Y.-C., Chemical Detoxification of Nerve Agent VX. *Acc. Chem. Res.* **1999**, 32, 109-115.
6. Weston, J., Mode of Action of Bi- and Trinuclear Zinc Hydrolases and Their Synthetic Analogues. *Chemical Reviews (Washington, DC, United States)* **2005**, 105, (6), 2151-2174.
7. Benning, M. M.; Shim, H.; Raushel, F. M.; Holden, H. M., *Biochemistry* **2001**, 40, 2712.
8. Morgan, B. P.; He, S.; Smith, R. C., Dizinc Enzyme Model / Complexometric Indicator Pairs in Indicator Displacement Assays for Inorganic Phosphates under Physiological Conditions. *Inorganic Chemistry* **2007**, 46, 9262-9266.

9. Leevy, W. M.; Johnson, J. R.; Lakshmi, C.; Morris, J.; Marquez, M.; Smith, B. D., Selective recognition of bacterial membranes by zinc(II)-coordination complexes. *Chemical Communications (Cambridge, United Kingdom)* **2006**, (15), 1595-1597.
10. Hanshaw, R. G.; Lakshmi, C.; Lambert, T. N.; Johnson, J. R.; Smith, B. D., Fluorescent detection of apoptotic cells by using zinc coordination complexes with a selective affinity for membrane surfaces enriched with phosphatidylserine. *ChemBioChem* **2005**, 6, (12), 2214-2220.
11. Hanshaw, R. G.; Smith, B. D., New reagents for phosphatidylserine recognition and detection of apoptosis. *Bioorganic & Medicinal Chemistry* **2005**, 13, (17), 5035-5042.
12. Lee, H. N.; Swamy, K. M. K.; Kim, S. K.; Kwon, J.-Y.; Kim, Y.; Kim, S.-J.; Yoon, Y. J.; Yoon, J., Simple but Effective Way to Sense Pyrophosphate and Inorganic Phosphate by Fluorescence Changes. *Organic Letters* **2007**, 9, (2), 243-246.
13. Jang, Y. J.; Jun, E. J.; Lee, Y. J.; Kim, Y. S.; Kim, J. S.; Yoon, J., Highly Effective Fluorescent and Colorimetric Sensors for Pyrophosphate over H₂PO₄⁻ in 100% Aqueous Solution. *Journal of Organic Chemistry* **2005**, 70, (23), 9603-9606.
14. Shiraishi, H.; Jikido, R.; Matsufuji, K.; Nakanishi, T.; Shiga, T.; Ohba, M.; Sakai, K.; Kitagawa, H.; Okawa, H., Dinuclear Mn(II), Ni(II), and Zn(II) complexes bridged by bis(p-nitrophenyl) phosphate ion: Relevance to bimetallic phosphodiesterase. *Bulletin of the Chemical Society of Japan* **2005**, 78, (6), 1072-1076.
15. Matsufuji, K.; Shiraishi, H.; Miyasato, Y.; Shiga, T.; Ohba, M.; Yokoyama, T.; Okawa, H., m-Hydroxo-m-phenolato dinuclear zinc(II) and nickel(II) complexes derived from dinucleating compartmental ligands of "end-off" type: synthesis,

- structures, and properties. *Bulletin of the Chemical Society of Japan* **2005**, 78, (5), 851-858.
16. Adams, H.; Bradshaw, D.; Fenton, D. E., Dinuclear nickel(II) and zinc(II) complexes of 2,6-bis[*bis*(2-pyridylmethyl)amino]methyl]-4-methylphenol. *Inorganica Chimica Acta* **2002**, 332, 195-200.
17. O'Neil, E. J.; Smith, B. D., Anion recognition using dimetallic coordination complexes. *Coordination Chemistry Reviews* **2006**, 250, (23+24), 3068-3080.
18. Leevy, W. M.; Gammon, S. T.; Jiang, H.; Johnson, J. R.; Maxwell, D. J.; Jackson, E. N.; Marquez, M.; Piwnica-Worms, D.; Smith, B. D., Optical Imaging of Bacterial Infection in Living Mice Using a Fluorescent Near-Infrared Molecular Probe. *Journal of the American Chemical Society* **2006**, 128, (51), 16476-16477.
19. Nguyen, B. T.; Anslyn, E. V., Indicator-displacement assays. *Coordination Chemistry Reviews* **2006**, 250, (23+24), 3118-3127.
20. Knapton, D.; Burnworth, M.; Rowan, S. J.; Weder, C., Fluorescent organometallic sensors for the detection of chemical-warfare-agent mimics. *Angewandte Chemie, International Edition in English* **2006**, 45, (35), 5825-5829.
21. He, S.; Iacono, S. T.; Budy, S. M.; Dennis, A. E.; Smith, D. W., Jr.; Smith, R. C., Photoluminescence and ion sensing properties of a bipyridyl chromophore-modified semifluorinated polymer and its metallopolymer derivatives. *J. Mater. Chem.* **2008**, 18, (17), 1970-1976.
22. LeJeune, K. E.; Wild, J. R.; Russell, A. J., Nerve agents degraded by enzymic foams. *Nature (London)* **1998**, 395, (6697), 27-28.

23. Lejeune, K. E.; Mesiano, A. J.; Bower, S. B.; Grimsley, J. K.; Wild, J. R.; Russell, A. J., Dramatically stabilized phosphotriesterase-polymers for nerve agent degradation. *Biotechnology and Bioengineering* **1997**, 54, (2), 105-114.
24. Hovestad, N. J.; Eggeling, E. B.; Heidbuchel, H. J.; Jastrzebski, J. T. B. H.; Kragl, U.; Keim, W.; Vogt, D.; Van Koten, G., Selective hydrovinylation of styrene in a membrane reactor: use of carbosilane dendrimers with hemilabile P,O ligands. *Angewandte Chemie, International Edition* **1999**, 38, (11), 1655-1658.
25. Bosman, A. W.; Janssen, H. M.; Meijer, E. W., About Dendrimers: Structure, Physical Properties, and Applications. *Chemical Reviews (Washington, D. C.)* **1999**, 99, (7), 1665-1688.
26. Gorman, C., Metallodendrimers. Structural diversity and functional behavior. *Advanced Materials (Weinheim, Germany)* **1998**, 10, (4), 295-309.
27. Zeng, F.; Zimmerman, S. C., Dendrimers in supramolecular chemistry: from molecular recognition to self-assembly. *Chemical Reviews (Washington, D. C.)* **1997**, 97, (5), 1681-1712.
28. Tomalia, D. A.; Durst, H. D., Genealogically directed synthesis: starburst/cascade dendrimers and hyperbranched structures. *Topics in Current Chemistry* **1993**, 165, (Supramolecular Chemistry I), 193-313.
29. Sunder, A.; Heinemann, J.; Frey, H., Controlling the growth of polymer trees: concepts and perspectives for hyperbranched polymers. *Chemistry--A European Journal* **2000**, 6, (14), 2499-2506.

30. Huck, W. T. S.; Snellink-Ruel, B. H. M.; Lichtenbelt, J. W. T.; van Veggel, F. C. J. M.; Reinhoudt, D. N., Self-assembly of hyperbranched spheres; correlation between monomeric synthon and sphere size. *Chemical Communications (Cambridge)* **1997**, (1), 9-10.
31. Teta, N. L.; Brown, D.; Glass, M. Enzyme-containing polymeric sensors. 6913928, 2005.
32. Tao, K. W. C.; Yu, P.; Roberts, R. L. High molecular weight, lipophilic, orally ingestible bioactive agents in formulations having improved bioavailability. 2003013566, 2003.
33. Patel, M. V.; Chen, F.-J. Pharmaceutical compositions and methods for improved delivery of hydrophobic therapeutic agents. 2000050007, 2000.
34. Akiyama, Y.; Nagahara, N.; Kitano, M.; Nakao, M. Gastrointestinal mucosa-adherent pharmaceutical composition. 9842311, 1998.
35. Guillou, V.; Morançais, J.-L. Foaming cosmetic cream for cleansing skin and hair. 1166747, 2002.
36. Valenty, V. B. Thickening agents for nitrocellulose-free aqueous nail polish compositions with good adhesion. 5747018, 1998.
37. Cain, F. W.; McNeill, G. P.; Tongue, T. Structured particulate systems for food items with improved mouthfeel and homogeneity. 1249180, 2002.
38. Vulfson, E. N.; Law, B. A. Modified food products and beverages, and additives for food and beverages. 2000041491, 2000.

39. Sunder, A.; Mulhaupt, R. Method for producing highly branched glycidol-based polyols. 99-EP9773 2000037532, 19991210., 2000.
40. Stiriba, S.-E.; Slagt, M. Q.; Kautz, H.; Gebbink, R. J. M. K.; Thomann, R.; Frey, H.; Van Koten, G., Synthesis and supramolecular association of immobilized NCN-pincer platinum(II) complexes on hyperbranched polyglycerol supports. *Chemistry--A European Journal* **2004**, 10, (5), 1267-1273.
41. Slagt, M. Q.; Stiriba, S.-E.; Kautz, H.; Gebbink, R. J. M. K.; Frey, H.; Van Koten, G., Optically Active Hyperbranched Polyglycerol as Scaffold for Covalent and Noncovalent Immobilization of Platinum(II) NCN-Pincer Complexes. Catalytic Application and Recovery. *Organometallics* **2004**, 23, (7), 1525-1532.
42. Slagt, M. Q.; Stiriba, S.-E.; Klein Gebbink, R. J. M.; Kautz, H.; Frey, H.; van Koten, G., Encapsulation of Hydrophilic Pincer-Platinum(II) Complexes in Amphiphilic Hyperbranched Polyglycerol Nanocapsules. *Macromolecules* **2002**, 35, (15), 5734-5737.
43. Breslow, R.; Singh, S., Phosphate ester cleavage catalyzed by bifunctional zinc complexes: comments on the "p-nitrophenyl ester syndrome". *Bioorganic Chemistry* **1988**, 16, (4), 408-17.
44. Seo, J. S.; Sung, N.-D.; Hynes, R. C.; Chin, J., Structure and Reactivity of a Dinuclear Cobalt(III) Complex with a Bridging Phosphate Monoester. *Inorganic Chemistry* **1996**, 35, (26), 7472-7473.
45. Kirby, A. J.; Jencks, W. P., *J. Am. Chem. Soc.* **1965**, 87, 3209.

46. Fabbrizzi, L.; Marcotte, N.; Stomeo, F.; Taglietti, A., Pyrophosphate detection in water by fluorescence competition assays: inducing selectivity through the choice of the indicator. *Angewandte Chemie, International Edition* **2002**, 41, (20), 3811-3814.
47. Kristina Kurz; Gobel, M. W., Hydrolytical cleavage of TAR-RNA, the trans-activation responsive region of HIV-1, by a bis(guanidinium) catalyst attached to arginine. *Helv. Chim. Acta* **1996**, 79, 1967-1979.
48. Hammond, P. R., The effect of experimental errors on Benesi-Hildebrand plots and on the inherent accuracy of the equation. *Journal of the Chemical Society* **1964**, (Jan.), 479-84.

APPENDICES

Appendix 2 A

NMR Spectra

Polyglycerol (PG)

Structure:

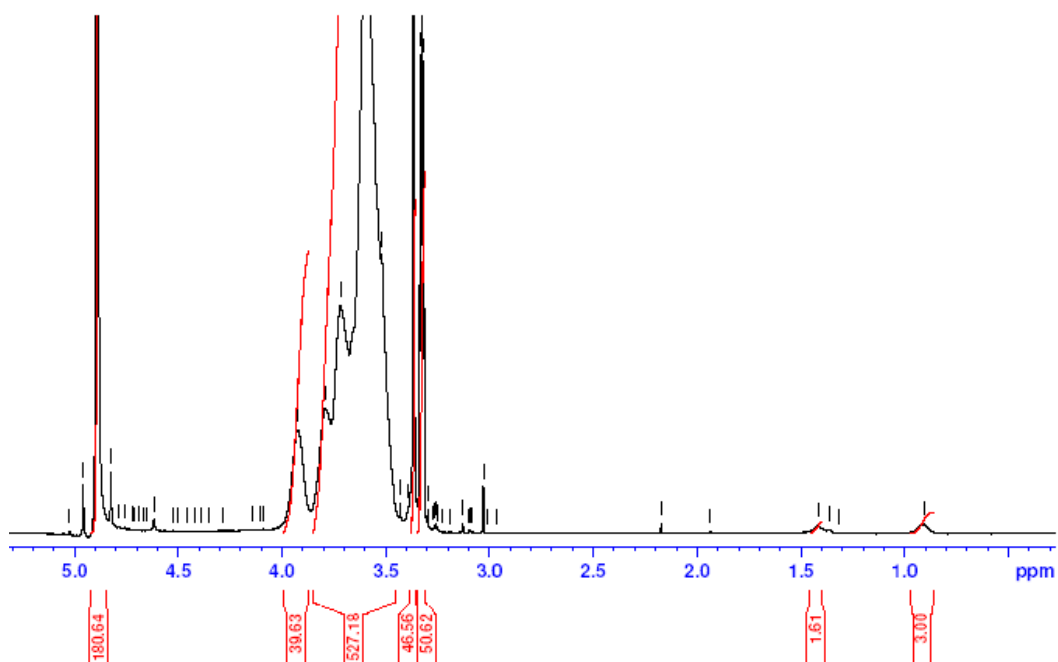
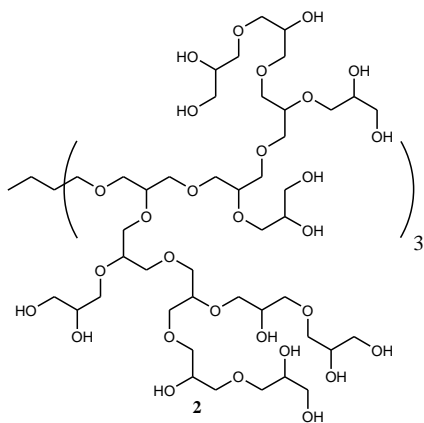


Figure 2 A.1 ¹H NMR (300 MHz, CDCl₃) of PG.

Polyglycerol (PG)

Structure:

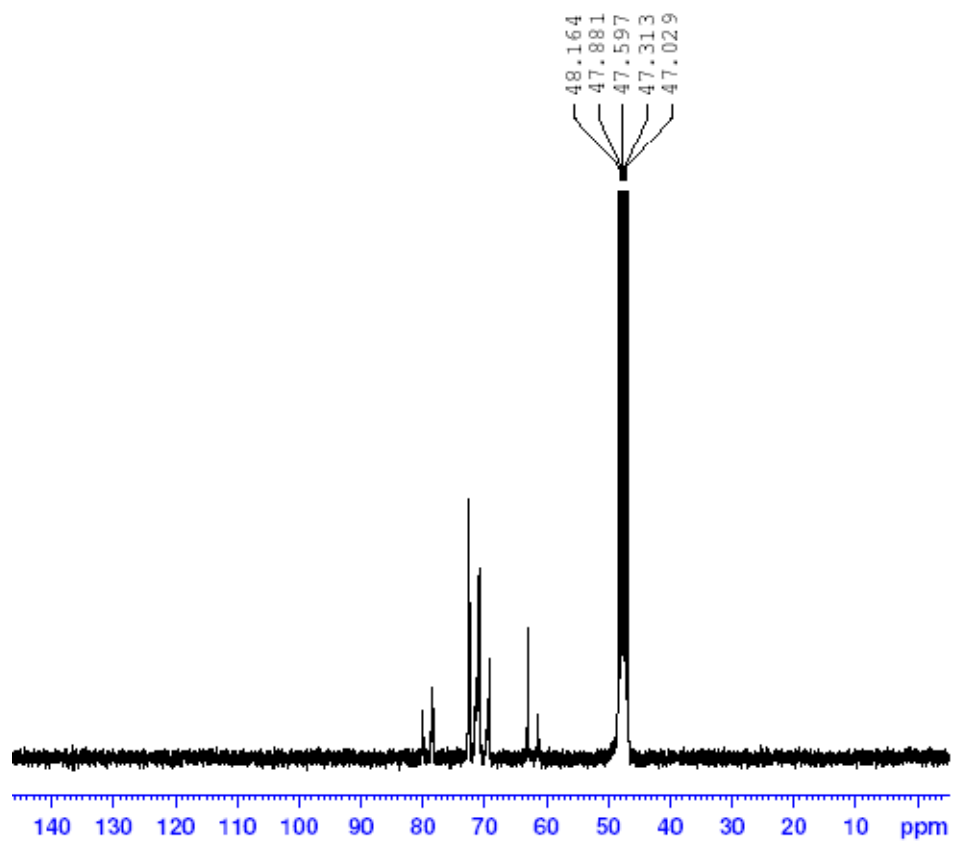
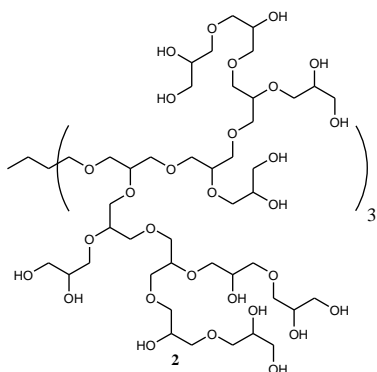


Figure 2 A.2 ^{13}C NMR (75 MHz, CDCl_3) of PG.

Tosylated polyglycerol (**Tos-PG**)

Structure:

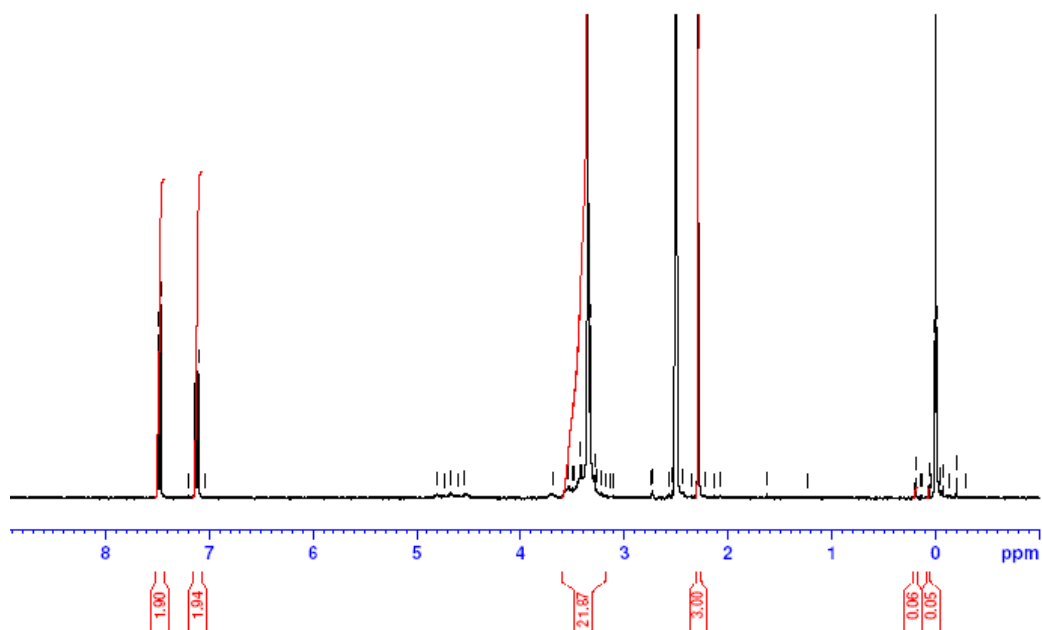
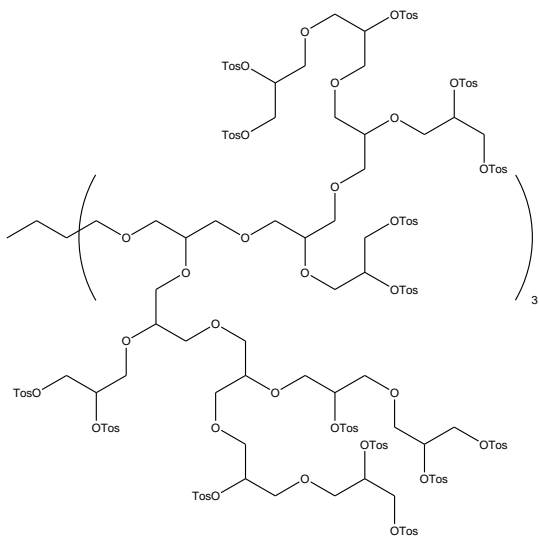


Figure 2 A.3 ^1H NMR (300 MHz, CDCl_3) of **Tos-PG**.

Methyl (3,5 dimethyl) benzoate (**4**)

Structure:

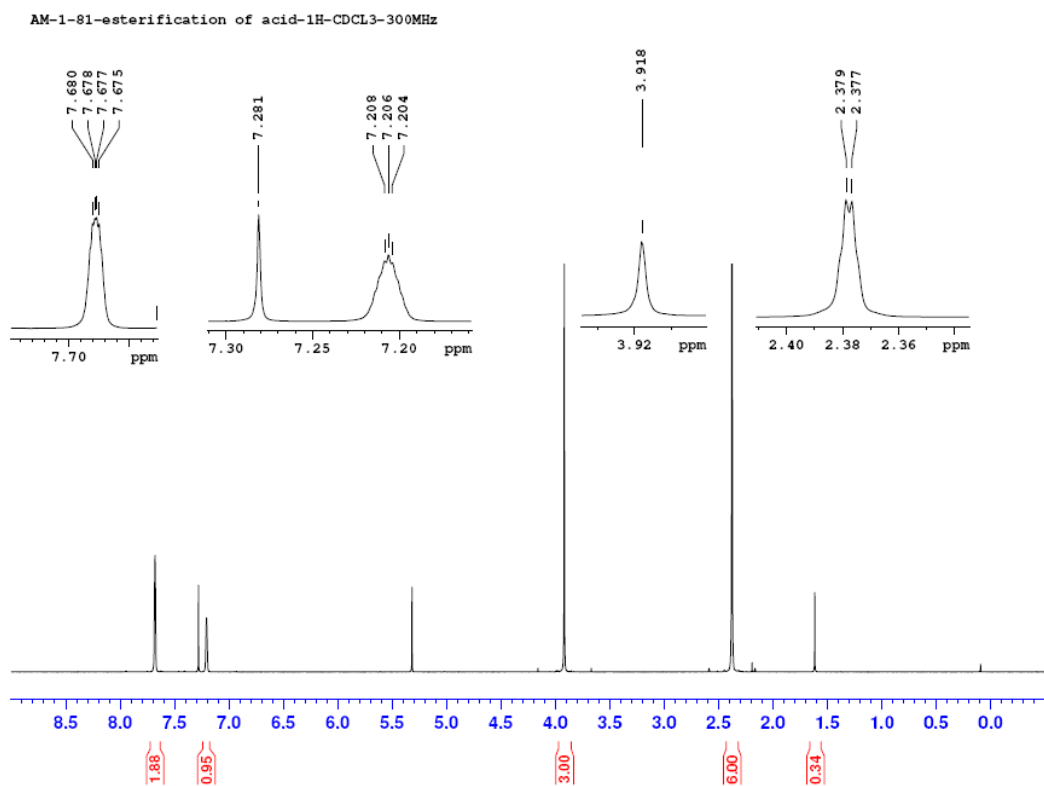
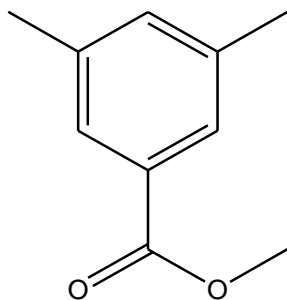


Figure 2 A.4 ¹H NMR (300 MHz, CDCl₃) of **4**.

Methyl (3,5 dimethyl) benzoate (**4**)

Structure:

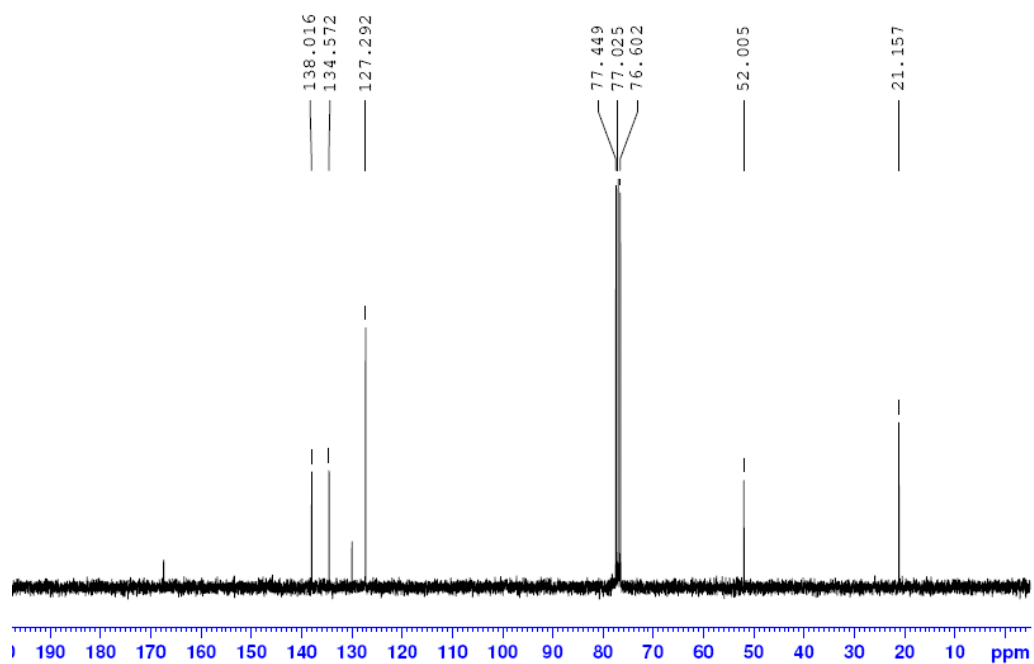
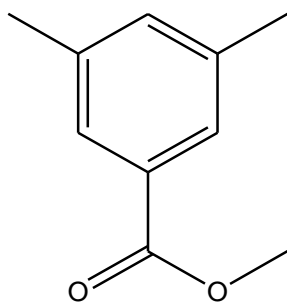


Figure 2 A.5 ^{13}C NMR (75 MHz, CDCl_3) of **4**.

Methyl 3,5-bis(bromomethyl)-benzoate (**5**)

Structure:

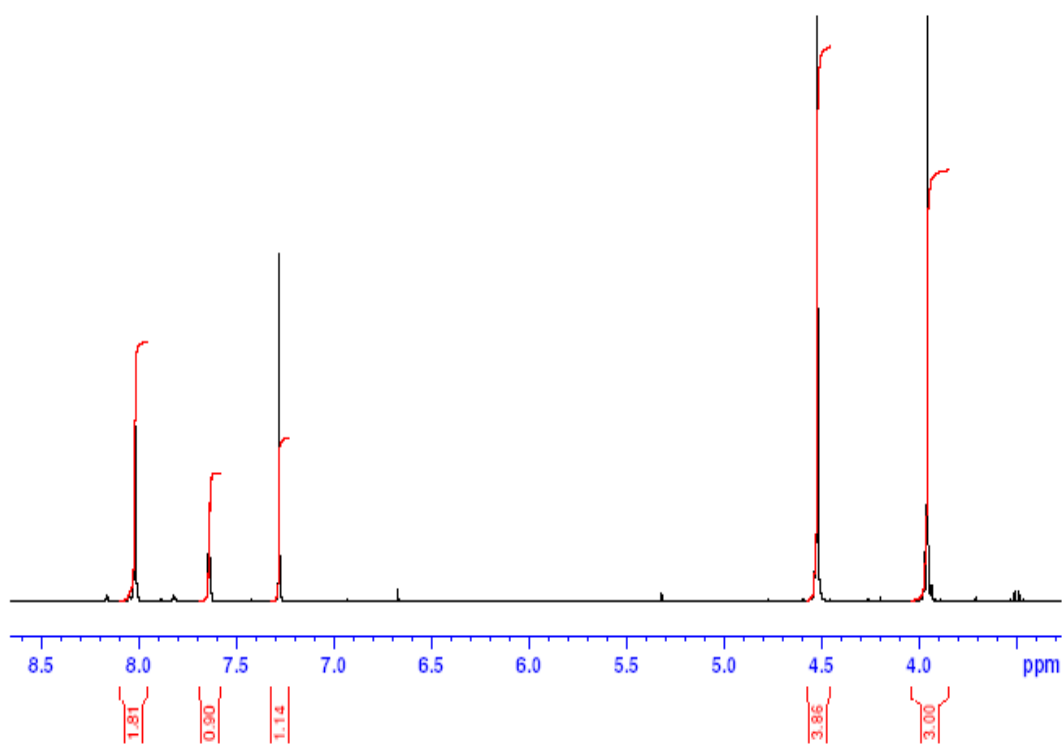
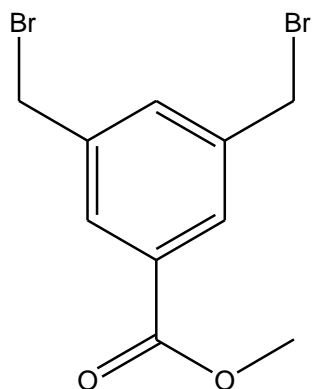


Figure 2 A.6 ^1H NMR (300 MHz, CDCl_3) of **5**.

Methyl 3,5-bis[(bis(2-pyridylmethyl) amino)methyl]-benzoate (**6**)

Structure:

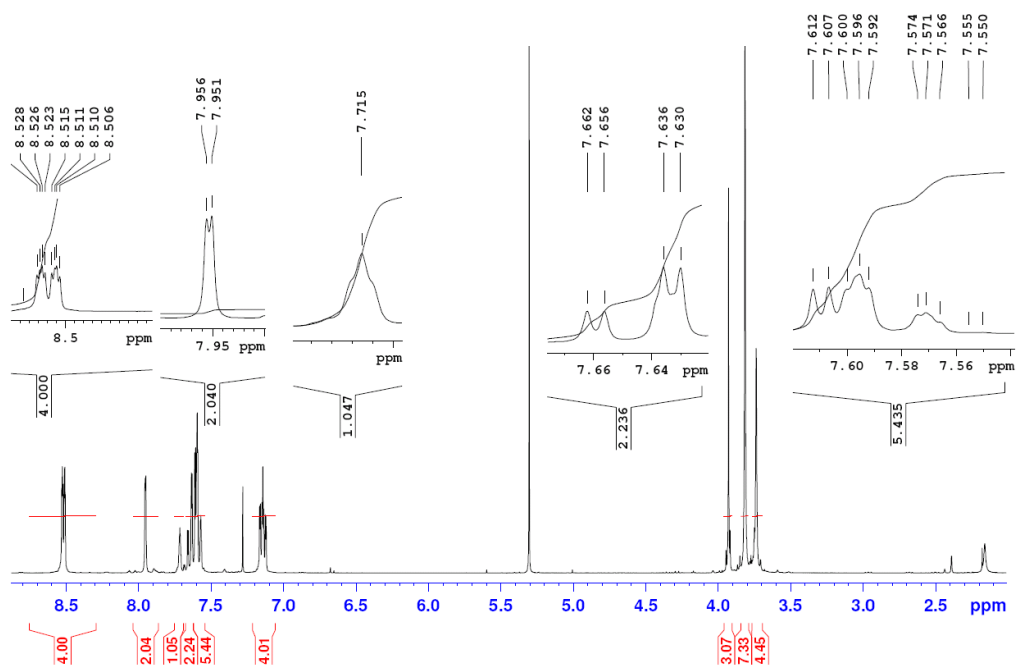
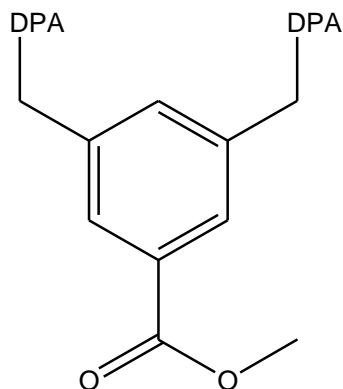


Figure 2 A.7 ^1H NMR (300 MHz, CDCl_3) of **6**.

Methyl 3,5-bis[(bis(2-pyridylmethyl) amino)methyl]-benzoate (**6**)

Structure:

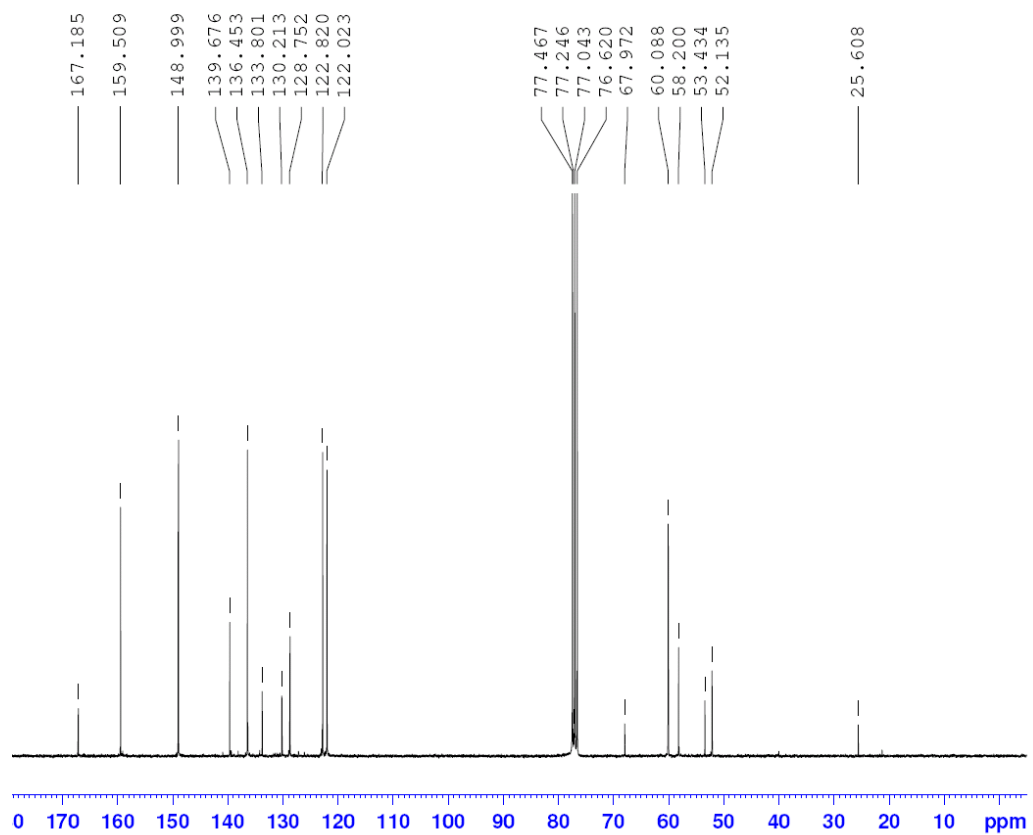
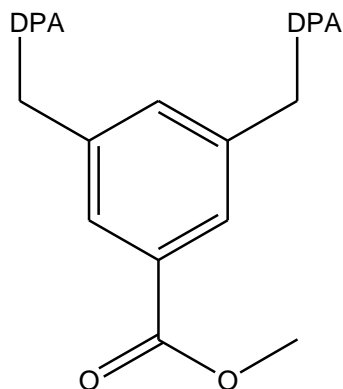


Figure 2 A.8 ^{13}C NMR (75 MHz, CDCl_3) of **6**.

3,5-bis[(bis(2-pyridylmethyl) amino)methyl]-benzoic acid (**8**)

Structure:

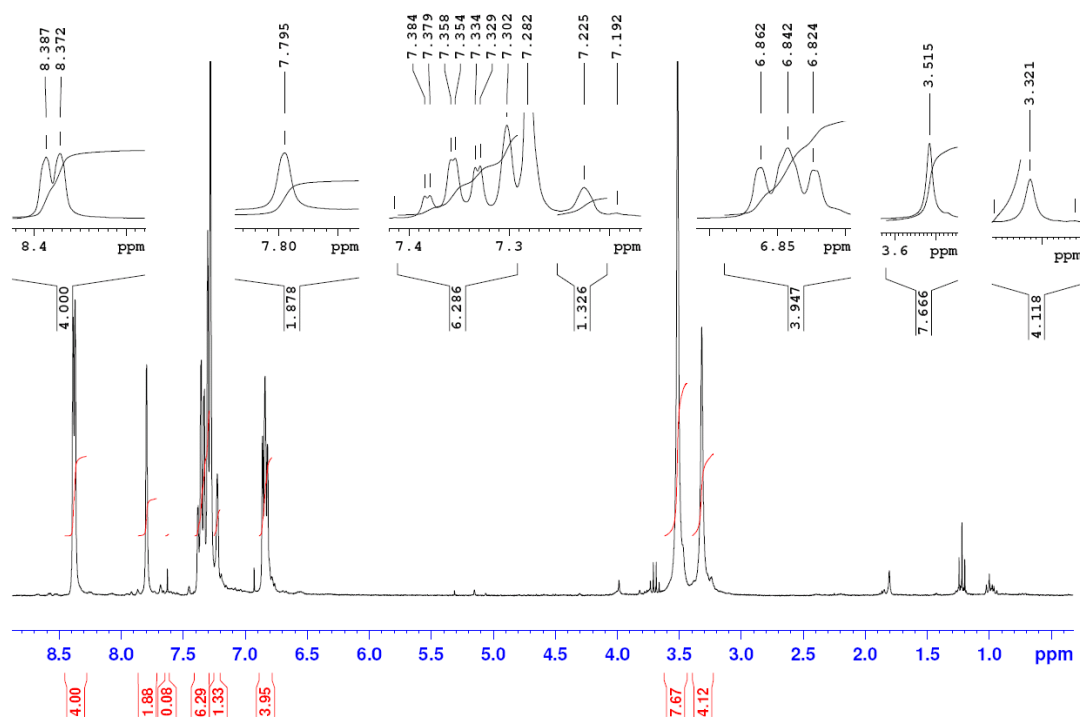
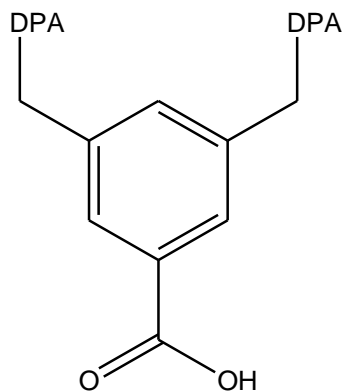


Figure 2 A.9 ^1H NMR (300 MHz, CDCl_3) of **8**.

3,5-bis[(bis(2-pyridylmethyl) amino)methyl]-benzoic acid (**8**)

Structure:

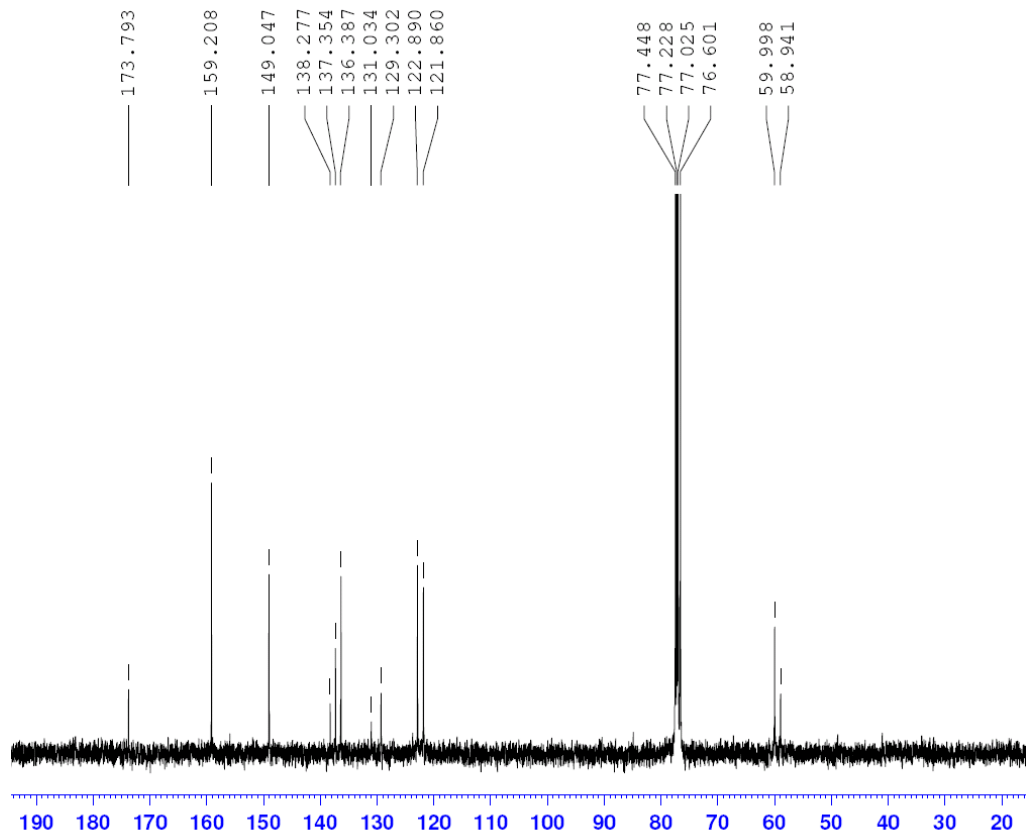
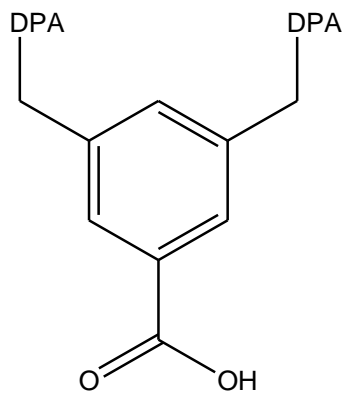


Figure 2 A.10 ^{13}C NMR (75 MHz, CDCl_3) of **8**.

Methyl 3,5-bis[(bis(2-pyridylmethyl) amino)methyl]-4-hydroxybenzoate (**2**)

Structure:

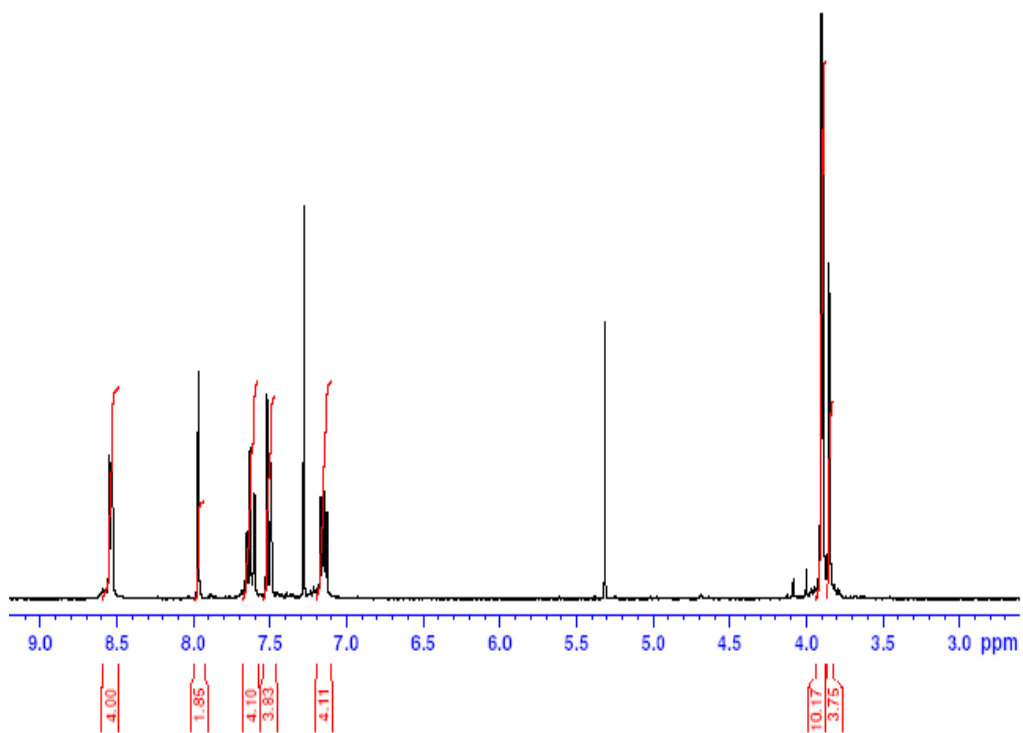
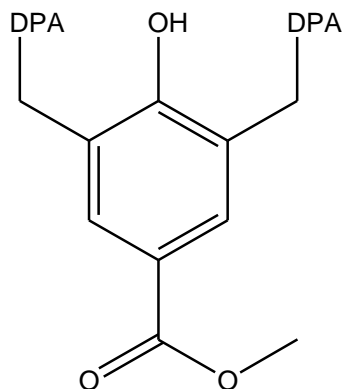


Figure 2 A.11 ^1H NMR (300 MHz, CDCl_3) of **2**.

Methyl 3,5-bis[(bis(2-pyridylmethyl) amino)methyl]-4-hydroxybenzoate (**2**)

Structure:

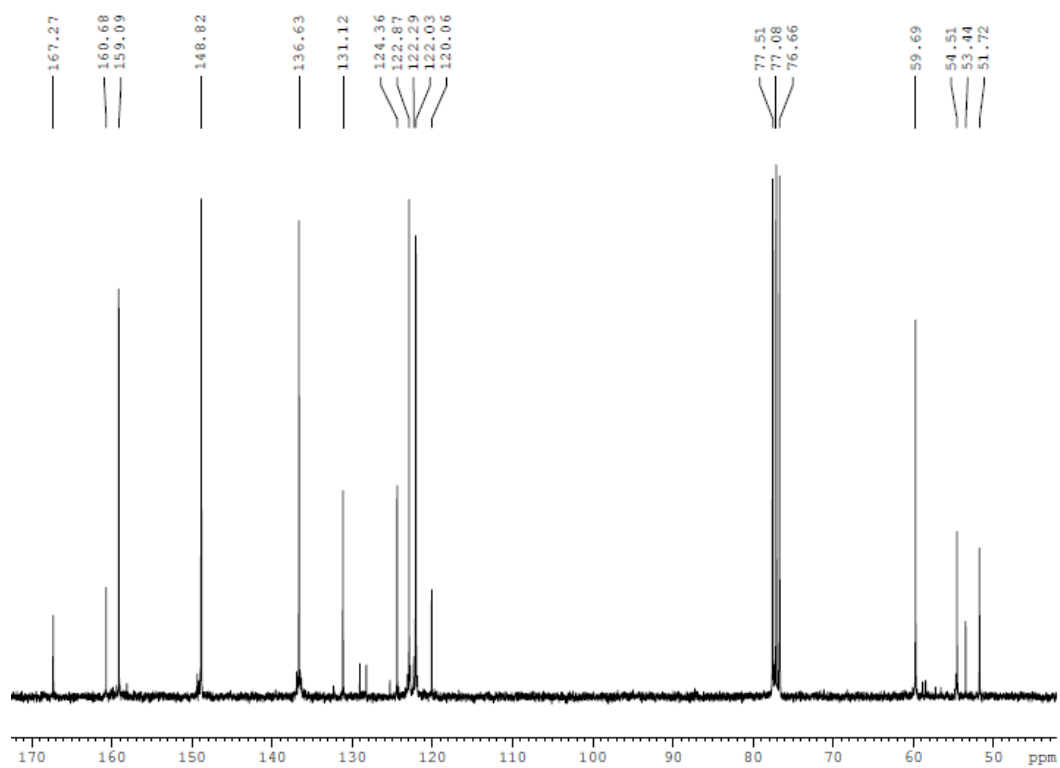
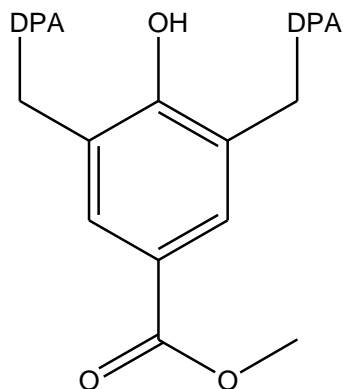


Figure 2 A.12 ^{13}C NMR (75 MHz, CDCl_3) of **2**.

3,5-bis[(bis(2-pyridylmethyl) amino)methyl]-4-hydroxybenzoic acid (**7**)

Structure:

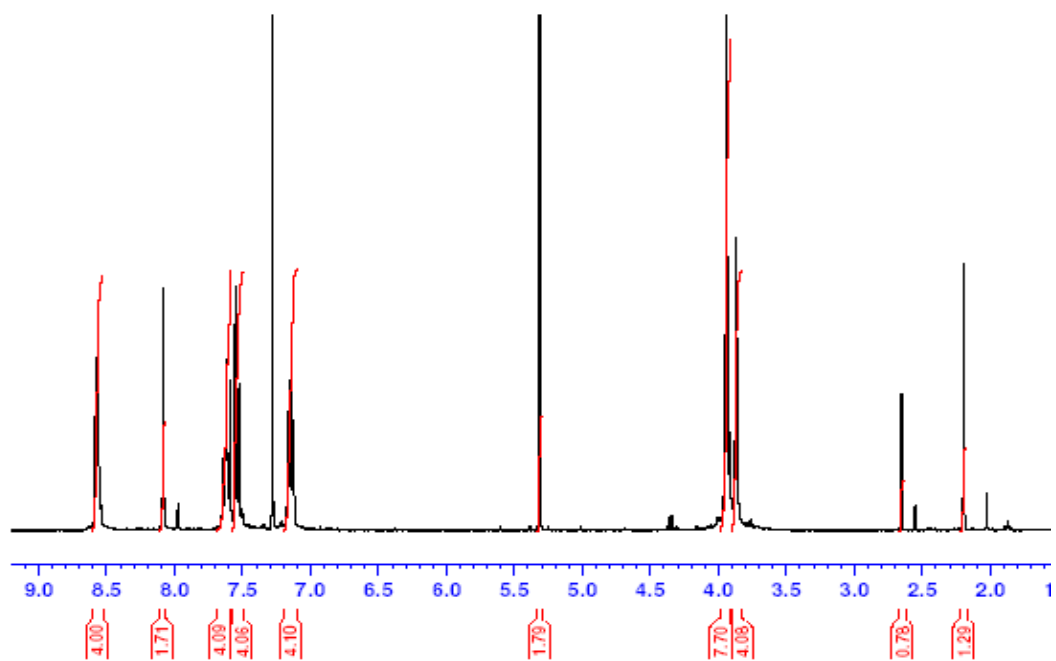
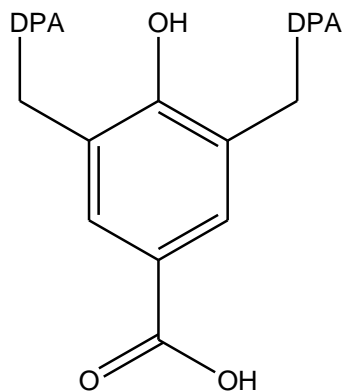


Figure 2 A.13 ^1H NMR (300 MHz, CDCl_3) of **7**.

7-PG

Structure

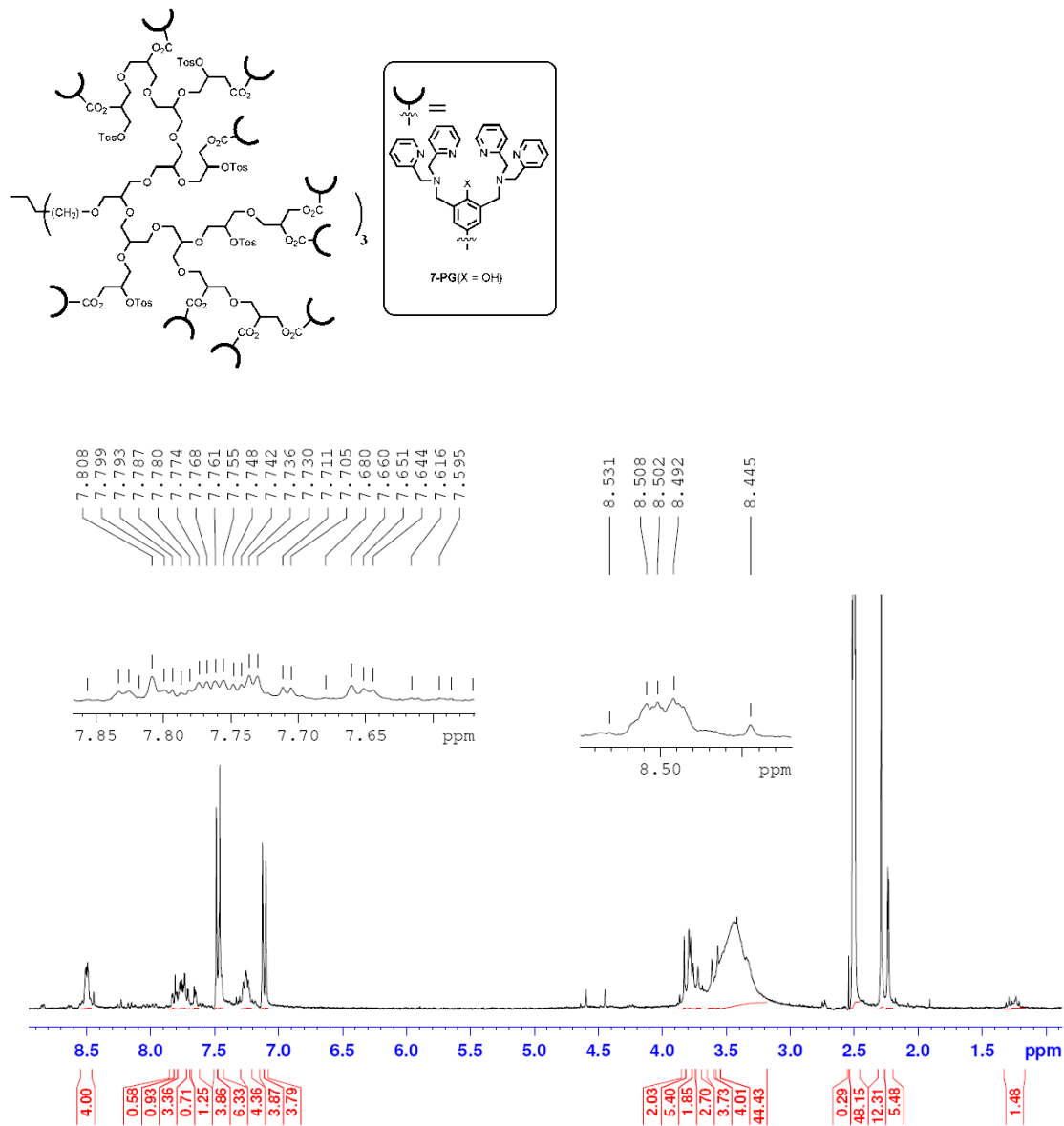


Figure 2 A 14 ^1H NMR (300 MHz, DMSO-d_6) of 7-PG.

7-PG

Structure

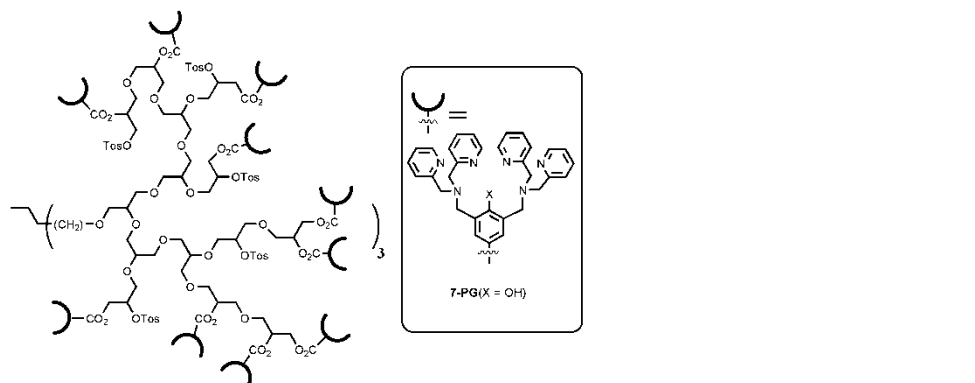


Figure 2 A ^{13}C NMR (75 MHz, DMSO-d₆) of 7-PG.

8-PG

Structure

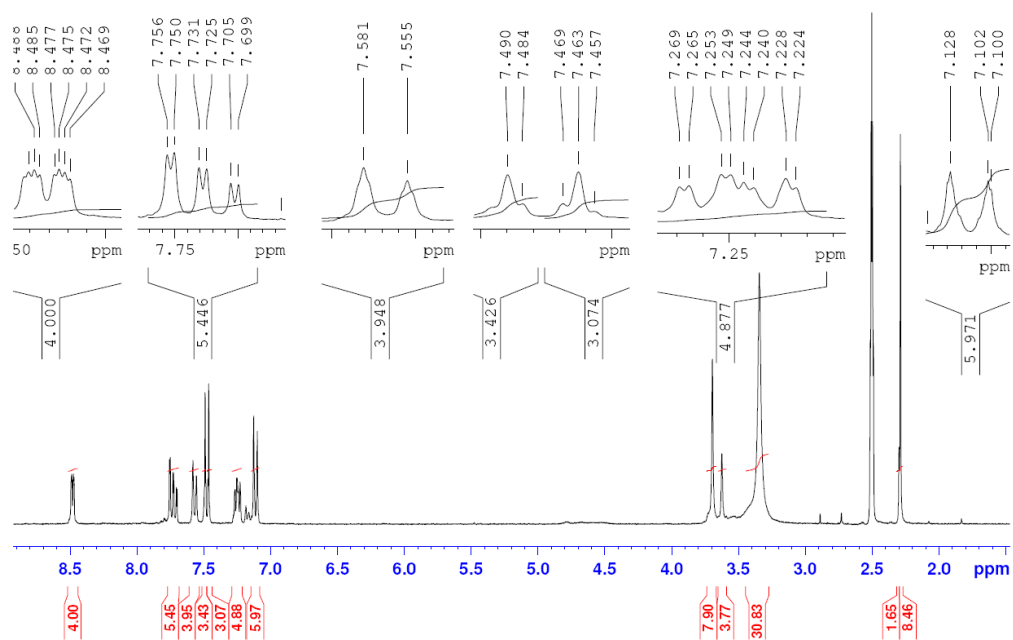
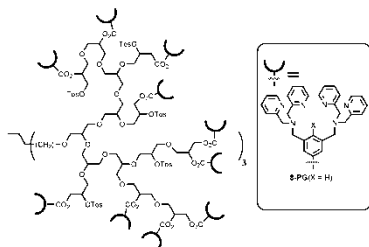


Figure 2 A 16 ¹H NMR (300 MHz, DMSO-d₆) of 8-PG.

8-PG

Structure

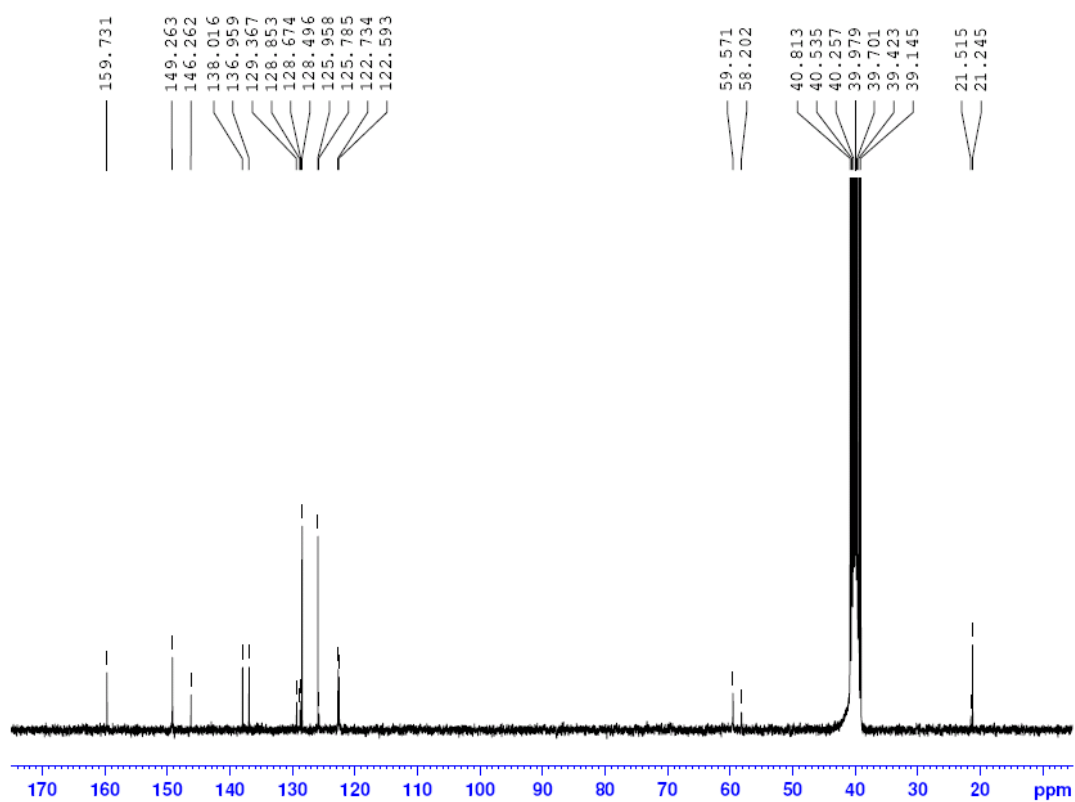
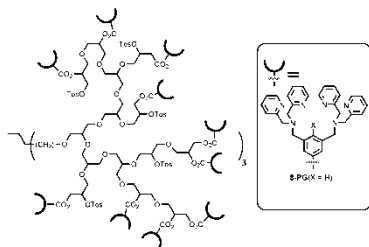
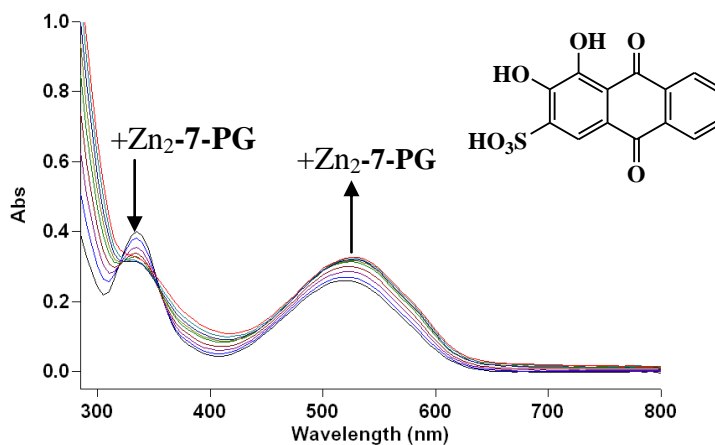


Figure 2 A 17 ^{13}C NMR (75 MHz, DMSO- d_6) of 8-PG.

Appendix 2 B

UV-vis Spectra

(A)



(B)

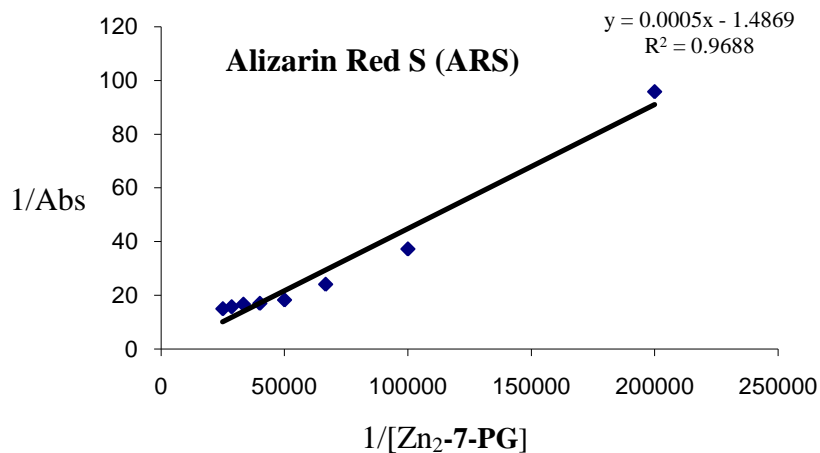
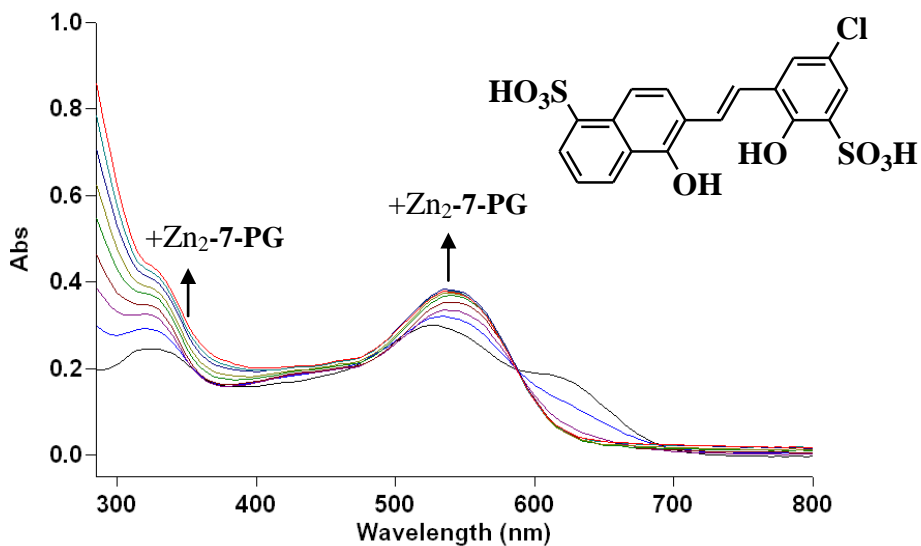


Figure 2 B 1 Titration of Alizarin Red S (ARS). (A) Structure of the indicator superimposed on UV-vis spectra collected as the indicator was titrated with Zn₂-7-PG, and (B) Benesi-Hildebrand plot of spectral data points (blue diamonds) and the linear fit (black line) used to calculate K_d . The equation and R^2 value for the linear fit are displayed in the upper right hand corner of the plot. This variation of the classic Benesi-Hildebrand method is based on a treatment described in reference 48 (note that slope does not equal K_d directly).

(A)



(B)

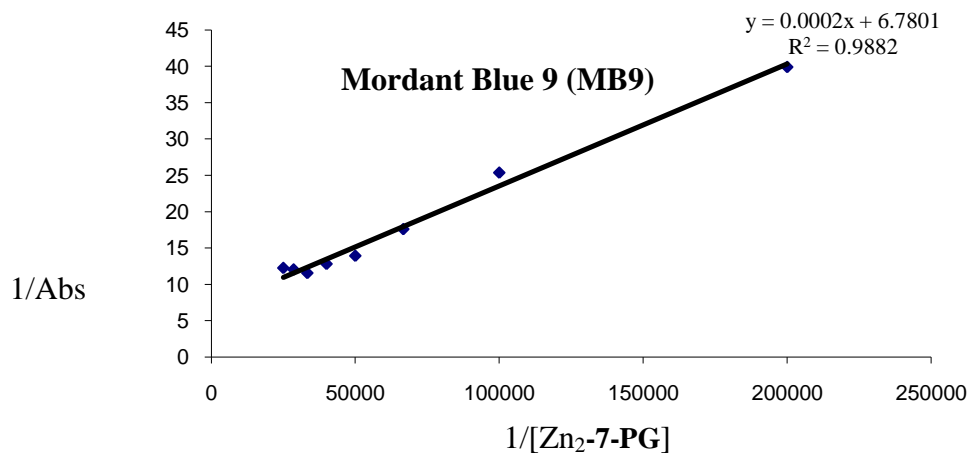
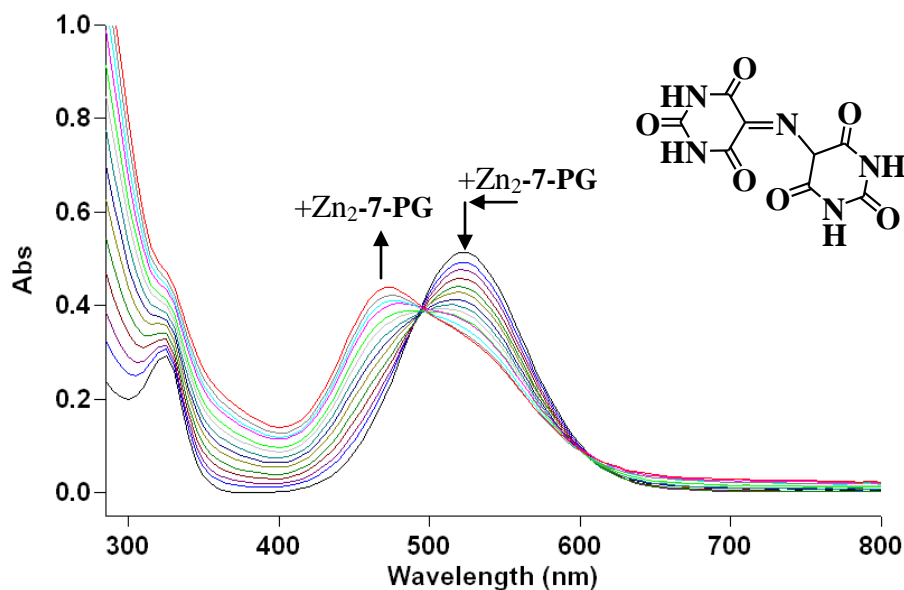


Figure 2 B 2 Titration of Mordant Blue 9 (MB9). (A) Structure of the indicator superimposed on UV-vis spectra collected as the indicator was titrated with Zn₂-7-PG, and (B) Benesi-Hildebrand plot of spectral data points (blue diamonds) and the linear fit (black line) used to calculate K_d . The equation and R^2 value for the linear fit are displayed in the upper right hand corner of the plot.

(A)



(B)

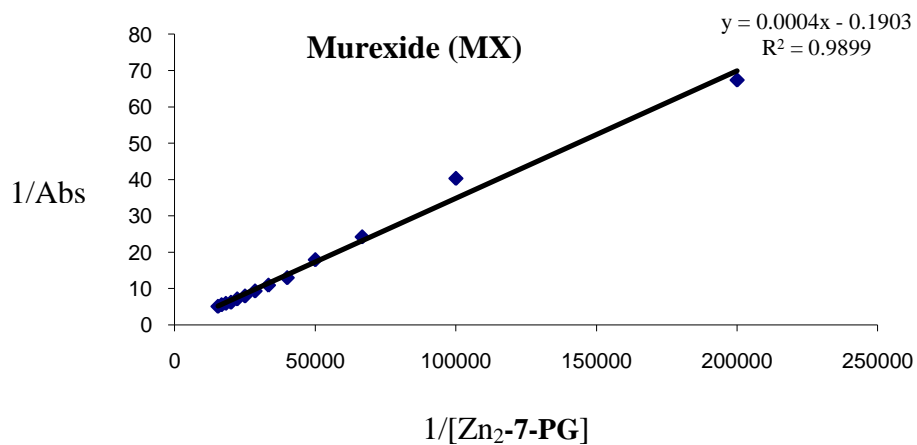


Figure 2 B 3 Titration of Murexide (MX). (A) Structure of the indicator superimposed on UV-vis spectra collected as the indicator was titrated with Zn₂-7-PG, and (B) Benesi-Hildebrand plot of spectral data points (blue diamonds) and the linear fit (black line) used to calculate K_d . The equation and R^2 value for the linear fit are displayed in the upper right hand corner of the plot.

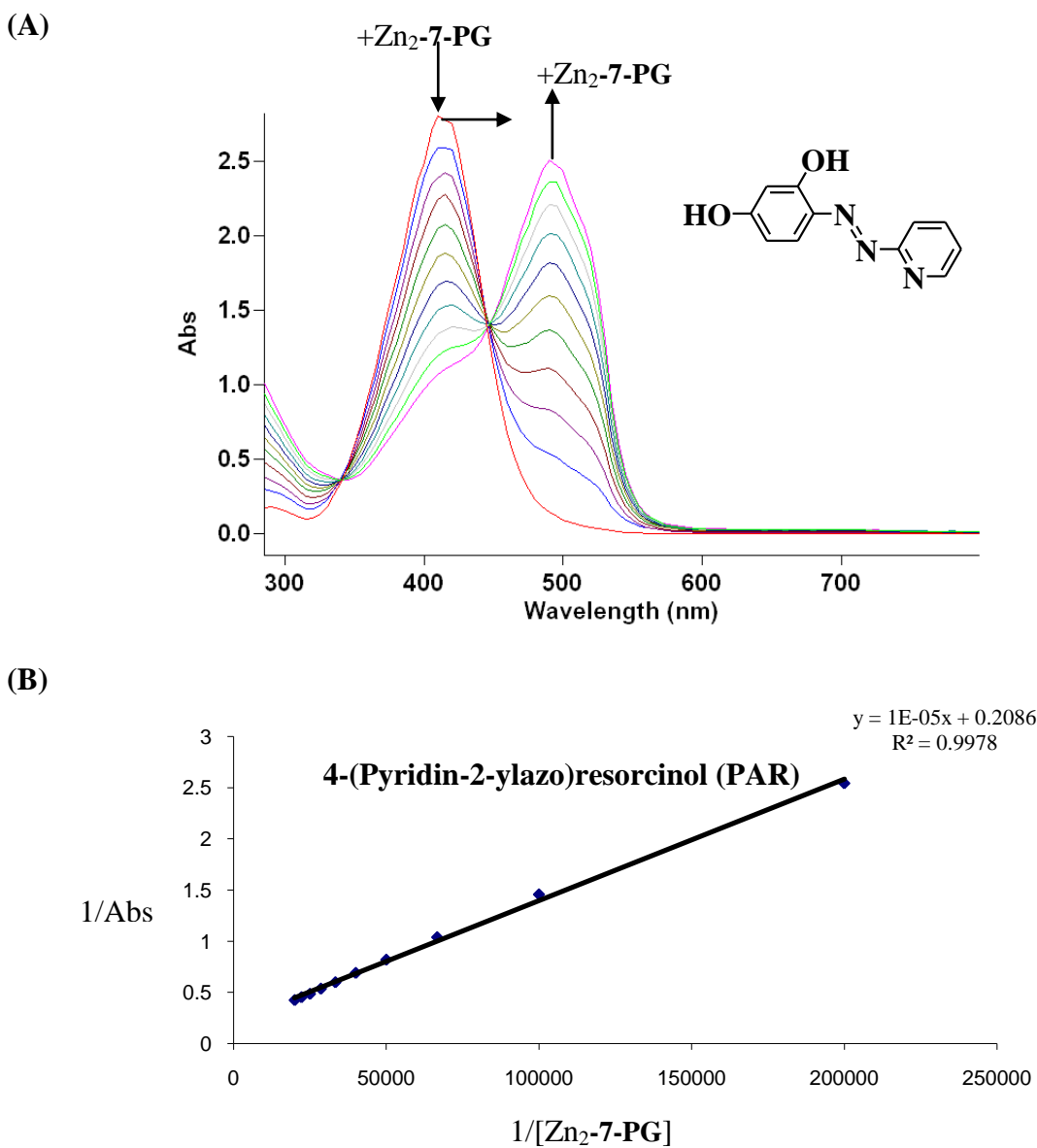
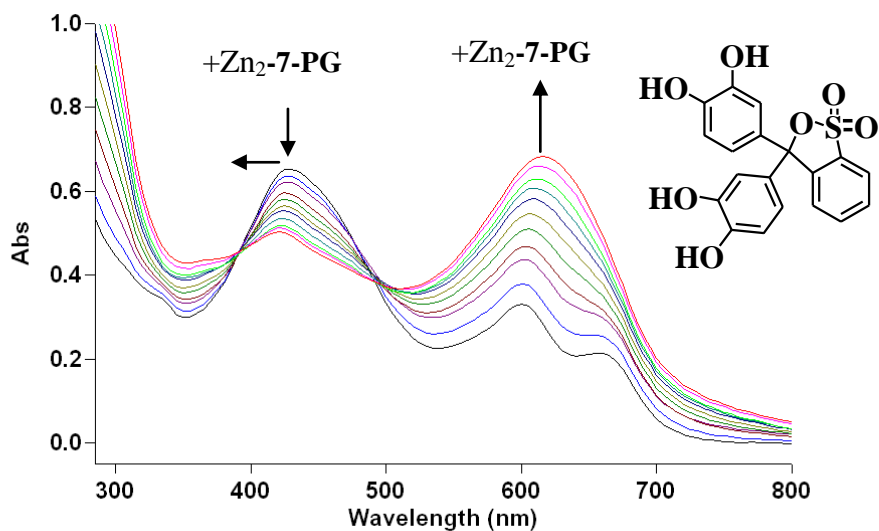


Figure B 4 Titration of 4-(Pyridin-2-ylazo)resorcinol (**PAR**). (A) Structure of the indicator superimposed on UV-vis spectra collected as the indicator was titrated with Zn_2 -**7-PG**, and (B) Benesi-Hildebrand plot of spectral data points (blue diamonds) and the linear fit (black line) used to calculate K_d . The equation and R^2 value for the linear fit are displayed in the upper right hand corner of the plot.

(A)



(B)

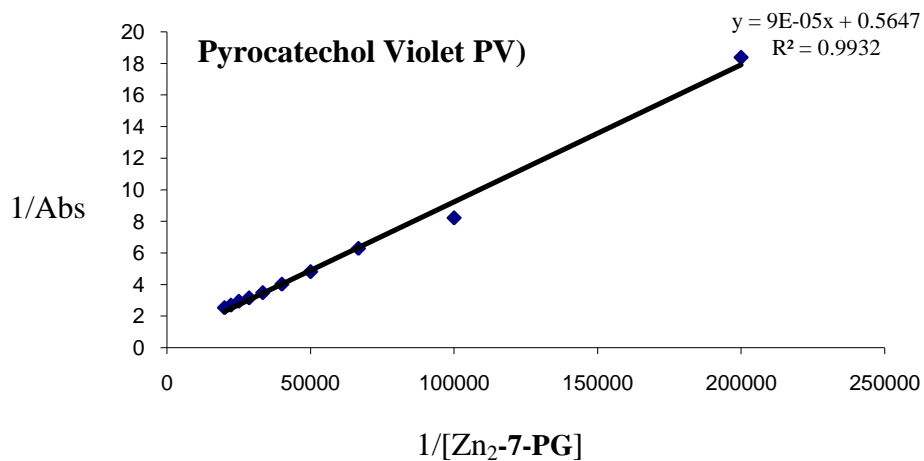
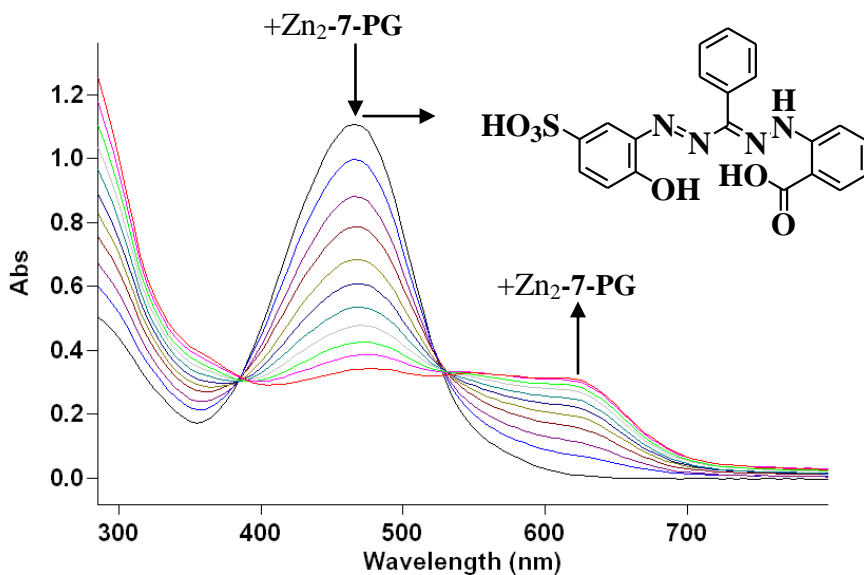


Figure 2 B 5 Titration of Pyrocatechol Violet(PV). (A) Structure of the indicator superimposed on UV-vis spectra collected as the indicator was titrated with Zn₂-7-PG, and (B) Benesi-Hildebrand plot of spectral data points (blue diamonds) and the linear fit (black line) used to calculate K_d . The equation and R^2 value for the linear fit are displayed in the upper right hand corner of the plot.

(A)



(B)

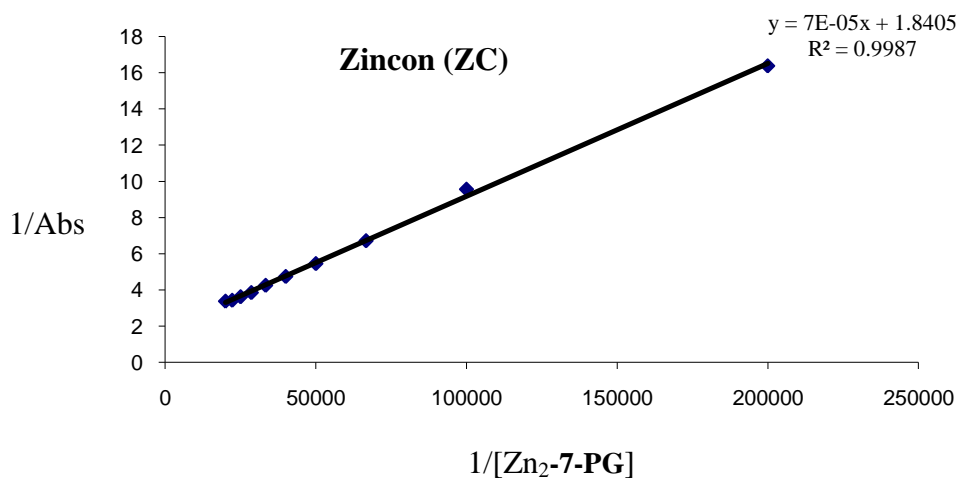
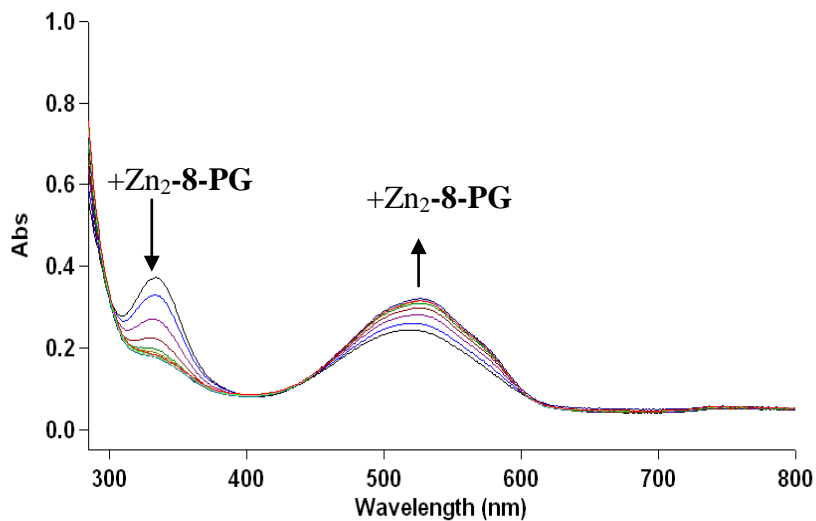


Figure 2 B 6 Titration of Zincon (ZC). (A) Structure of the indicator superimposed on UV-vis spectra collected as the indicator was titrated with Zn₂-7-PG, and (B) Benesi-Hildebrand plot of spectral data points (blue diamonds) and the linear fit (black line) used to calculate K_d . The equation and R^2 value for the linear fit are displayed in the upper right hand corner of the plot.

(A)



(B)

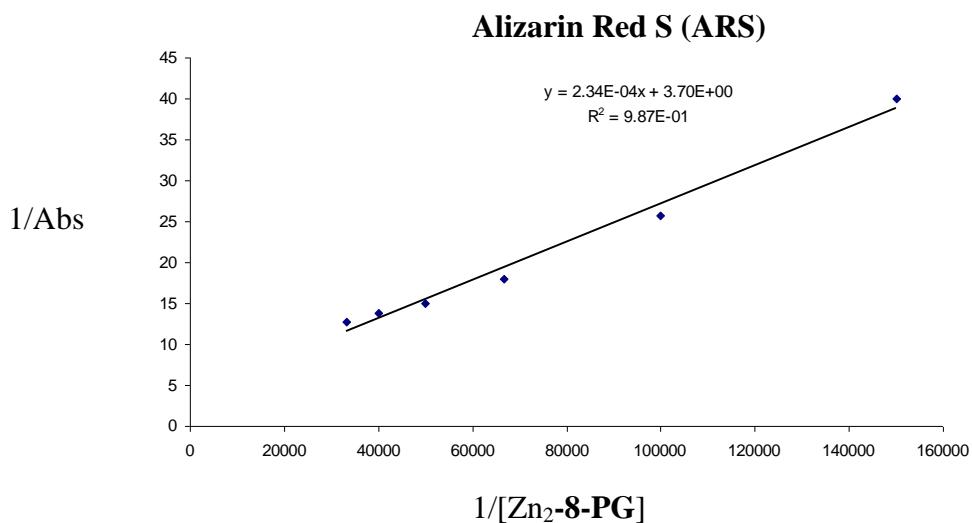


Figure 2.B.7 Titration of Alizarin Red S (ARS). (A) Structure of the indicator superimposed on UV-vis spectra collected as the indicator was titrated with Zn₂-8-PG, and (B) Benesi-Hildebrand plot of spectral data points (blue diamonds) and the linear fit (black line) used to calculate K_d . The equation and R^2 value for the linear fit are displayed in the upper right hand corner of the plot.

(A)

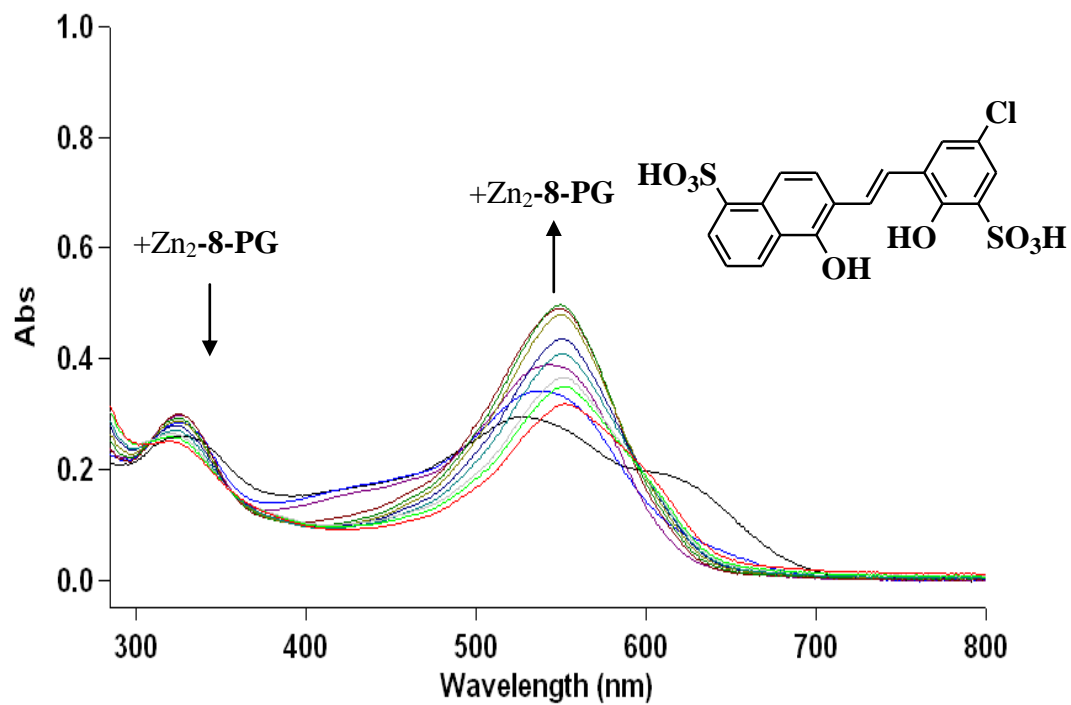
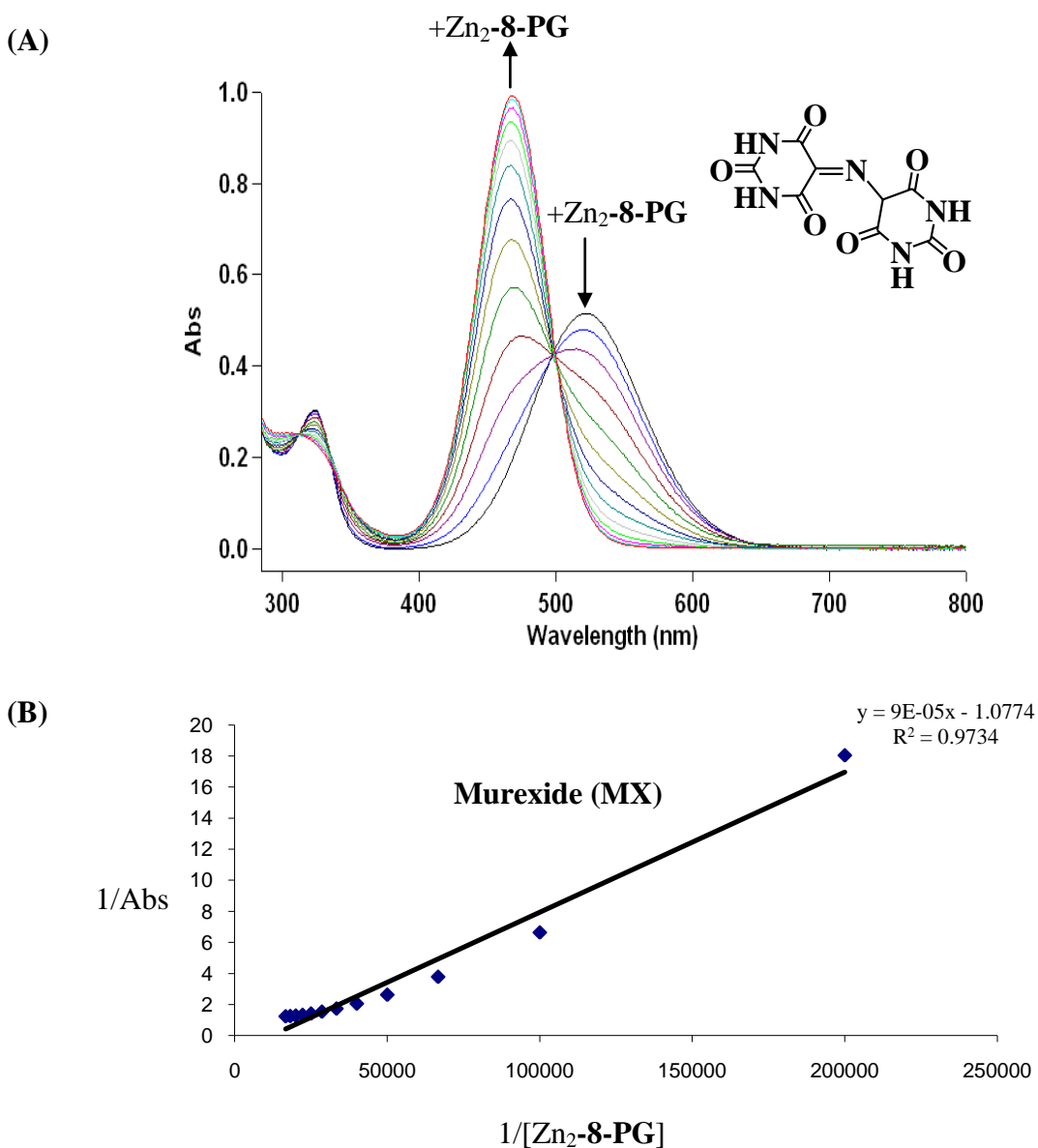


Figure 2 B 8 Titration of Mordant Blue 9 (MB9). (A) Structure of the indicator superimposed on UV-vis spectra collected as the indicator was titrated with Zn₂-8-PG. Titration data could not be fit using this treatment of the Benesi-Hildebrand method, probably due to formation of 1:1 and 2:1 complexes.



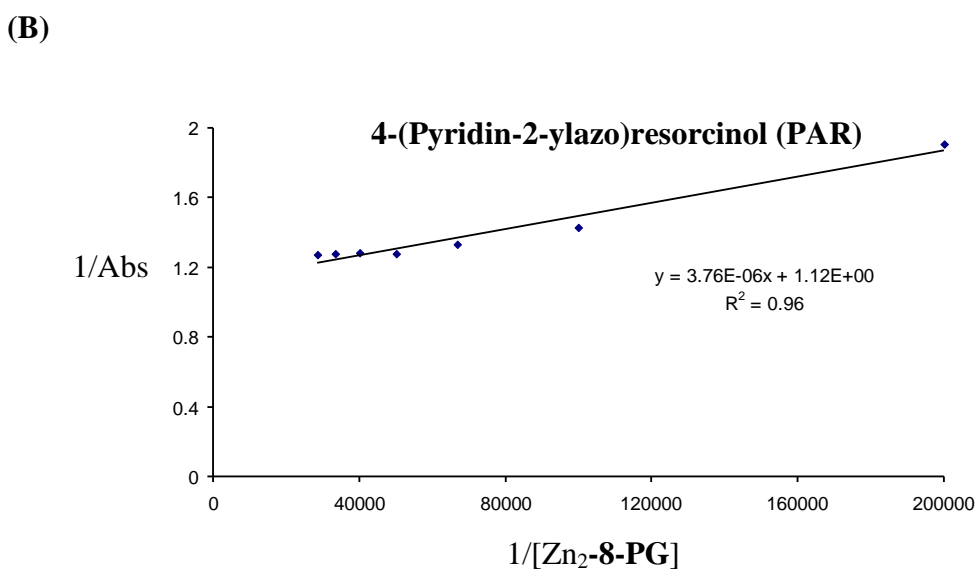
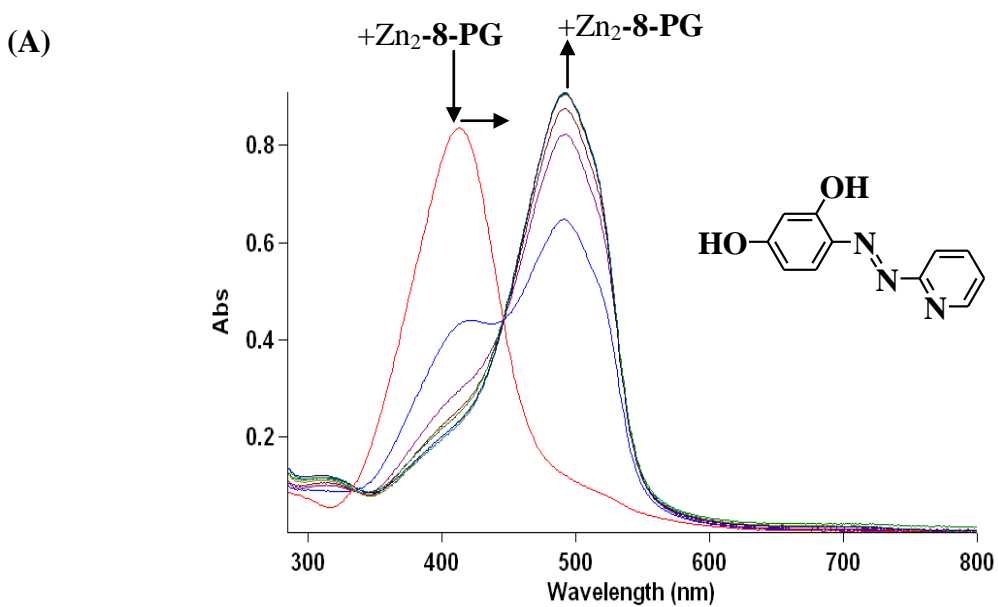


Figure 2 B 10 Titration of 4-(Pyridin-2-ylazo)resorcinol (PAR). (A) Structure of the indicator superimposed on UV-vis spectra collected as the indicator was titrated with Zn_2 -8-PG, and (B) Benesi-Hildebrand plot of spectral data points (blue diamonds) and the linear fit (black line) used to calculate K_d . The equation and R^2 value for the linear fit are displayed in the upper right hand corner of the plot.

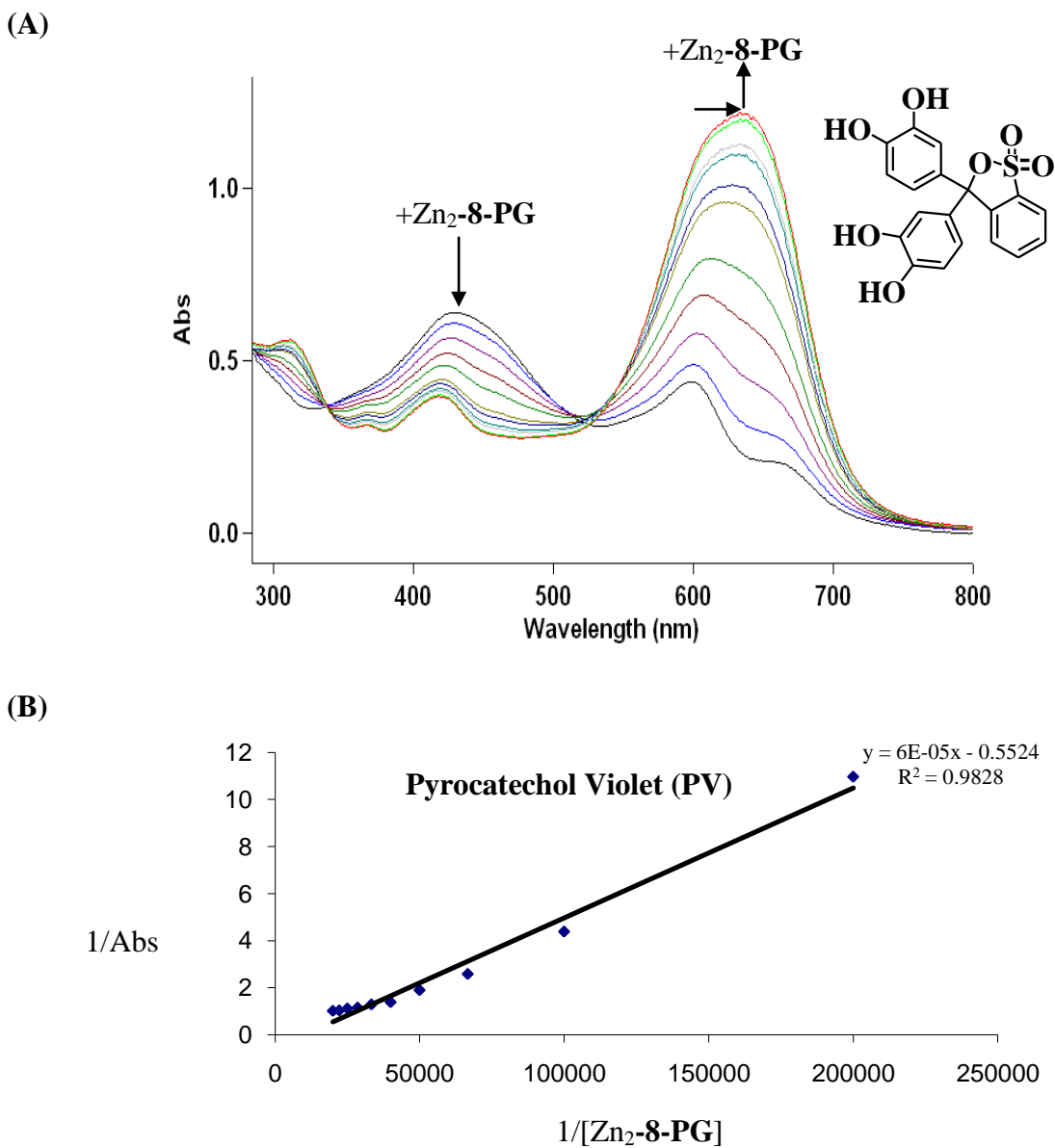


Figure 2 B 11 Titration of Pyrocatechol Violet(PV). (A) Structure of the indicator superimposed on UV-vis spectra collected as the indicator was titrated with Zn_2 -8-PG, and (B) Benesi-Hildebrand plot of spectral data points (blue diamonds) and the linear fit (black line) used to calculate K_d . The equation and R^2 value for the linear fit are displayed in the upper right hand corner of the plot.

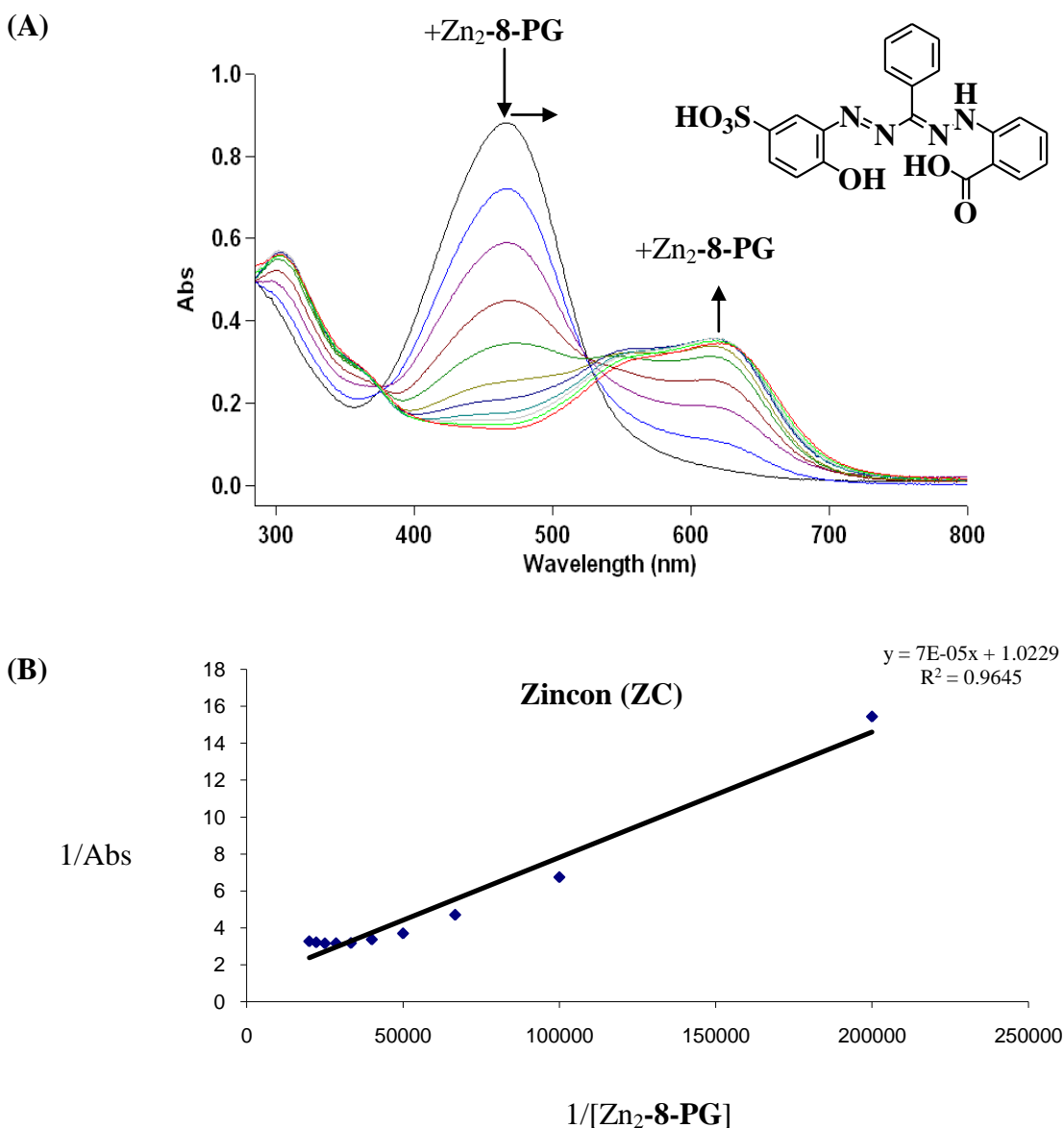


Figure 2 B 12 Titration of Zincon (ZC). (A) Structure of the indicator superimposed on UV-vis spectra collected as the indicator was titrated with Zn_2 -8-PG, and (B) Benesi-Hildebrand plot of spectral data points (blue diamonds) and the linear fit (black line) used to calculate K_d . The equation and R^2 value for the linear fit are displayed in the upper right hand corner of the plot.

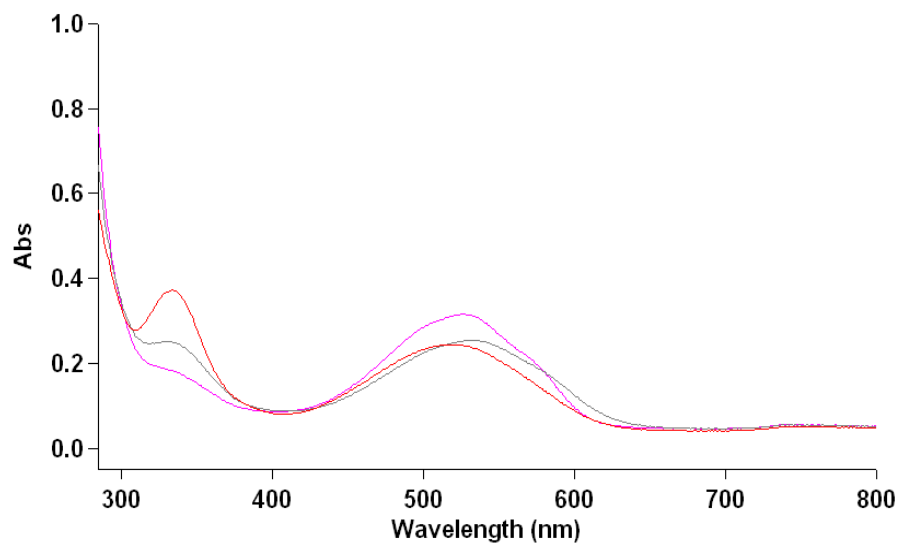
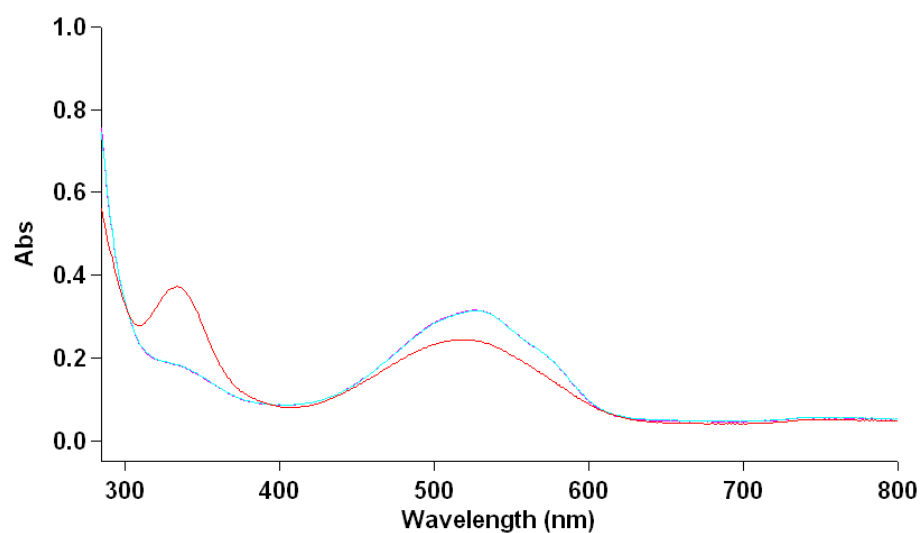


Figure 2 B 13 Phosphate (top) and pyrophosphate (bottom) displacement tests for Alizarin Red S (**ARS**). The red trace corresponds to the indicator alone, the blue trace corresponds to the (indicator)-Zn₂-**8-PG** complex, and the purple trace corresponds to (indicator)-Zn₂-**8-PG** complex plus the anion.

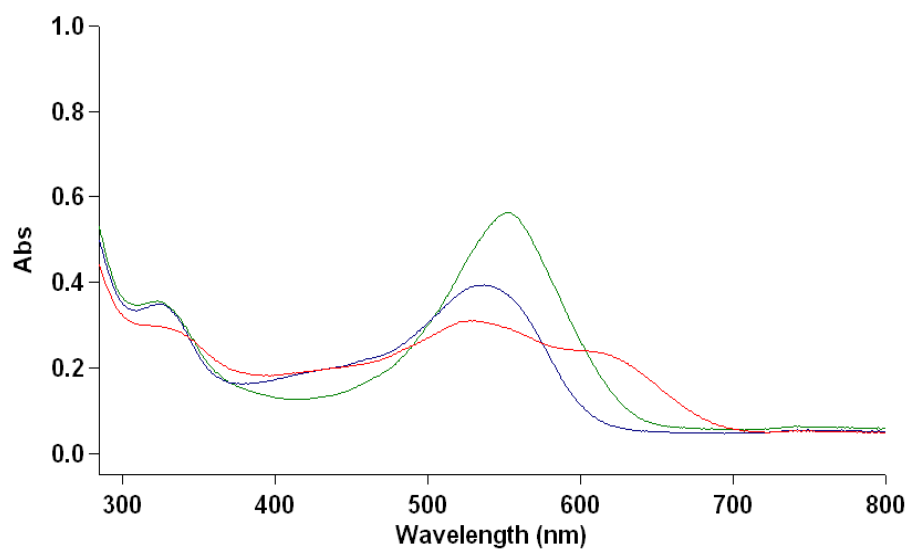
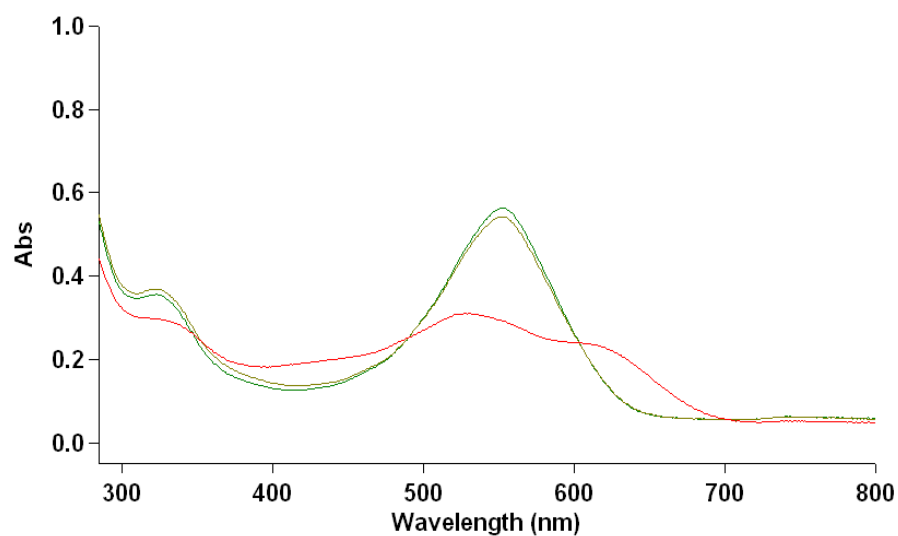


Figure 2 B 14 Phosphate (top) and pyrophosphate (bottom) displacement tests for Mordant Blue 9 (**MB9**). The red trace corresponds to the indicator alone, the green trace corresponds to the (indicator)-Zn₂-**8-PG** complex, and the blue trace corresponds to (indicator)-Zn₂-**8-PG** complex plus the anion.

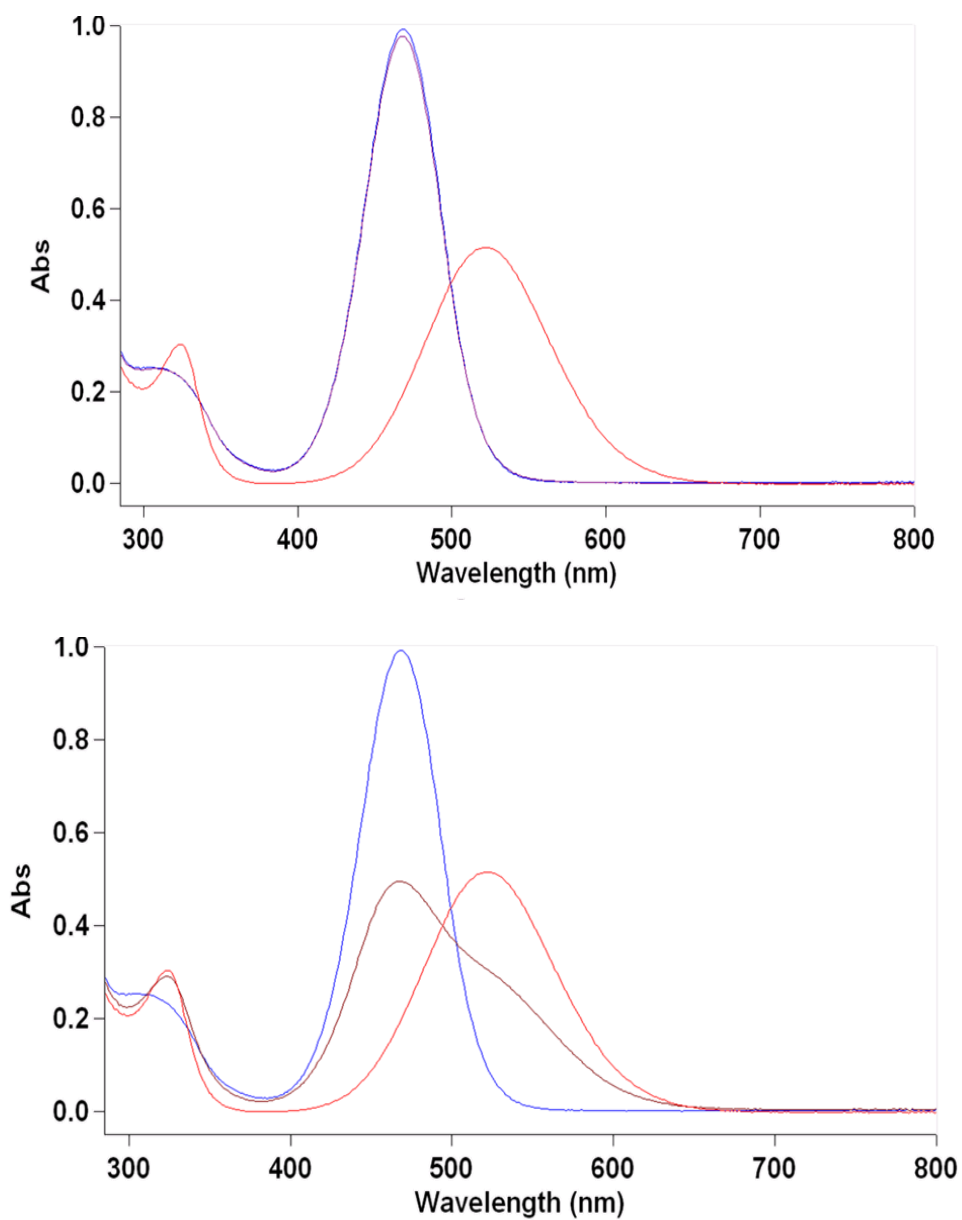


Figure 2 B 15 Phosphate (top) and pyrophosphate (bottom) displacement tests for Murexide (**MX**). The red trace corresponds to the indicator alone, the blue trace corresponds to the (indicator)- Zn_2 -**8-PG** complex, and the purple trace corresponds to (indicator)- Zn_2 -**8-PG** complex plus the anion.

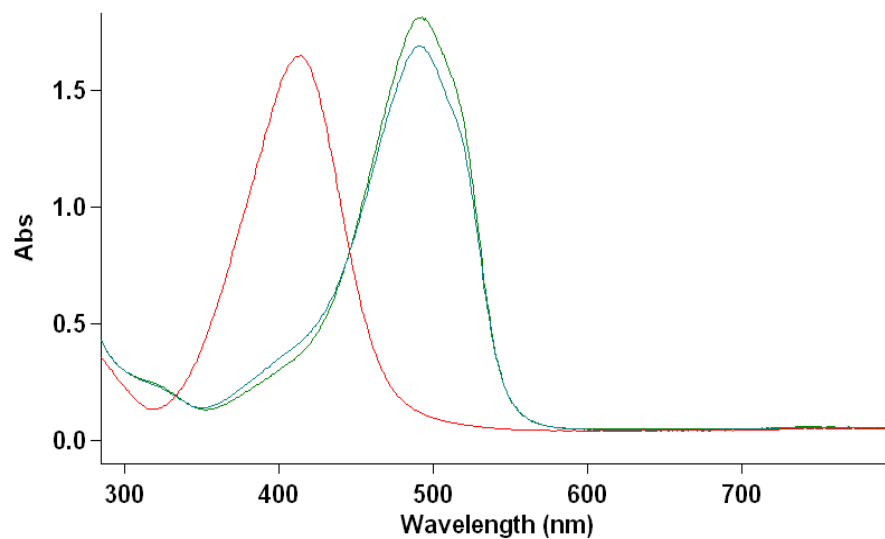
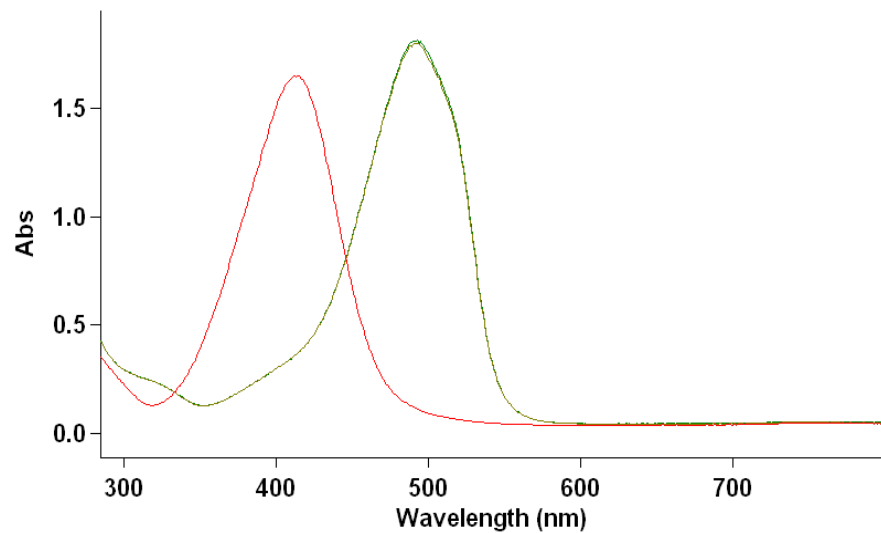


Figure 2 B 16 Phosphate (top) and pyrophosphate (bottom) displacement tests for 4-(Pyridin-2-ylazo)resorcinol (**PAR**). The red trace corresponds to the indicator alone, the green trace corresponds to the (indicator)-Zn₂-**8-PG** complex, and the blue trace corresponds to (indicator)-Zn₂-**8-PG** complex plus the anion.

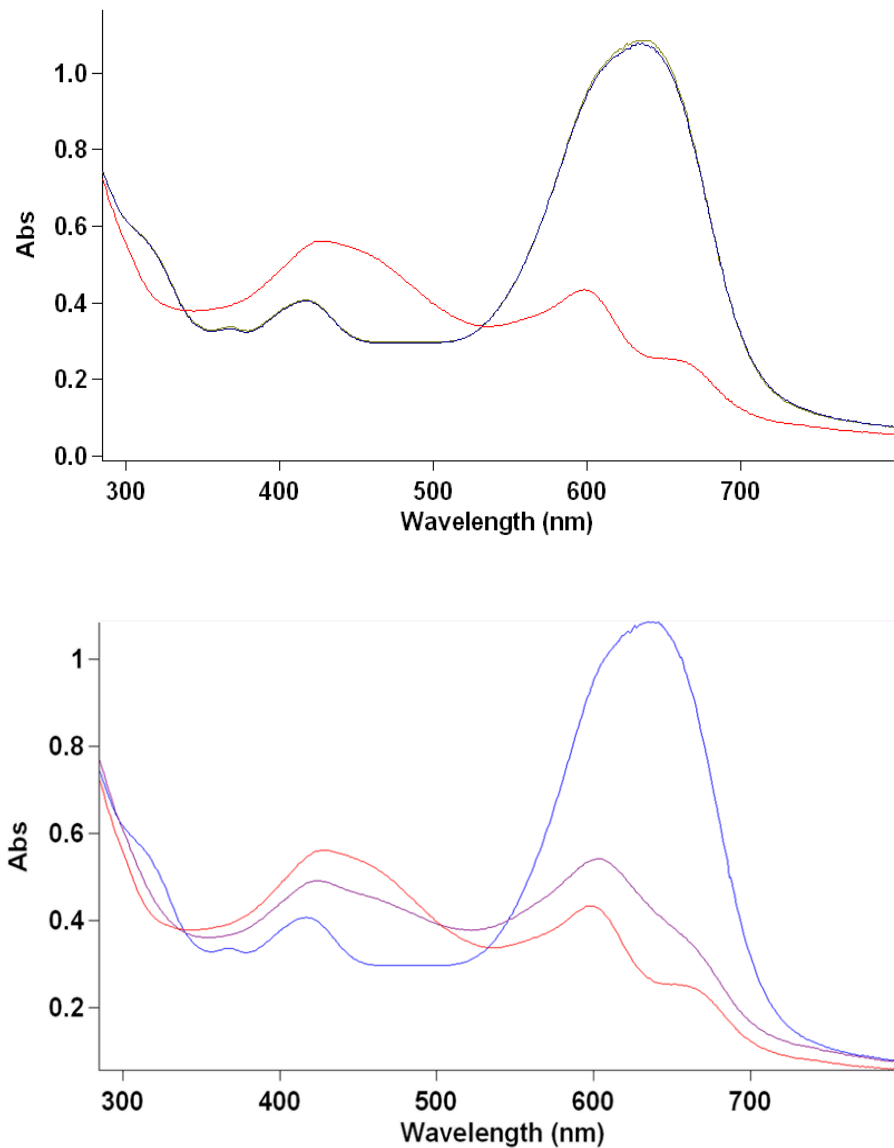


Figure 2 B 17 Phosphate (top) and pyrophosphate (bottom) displacement tests for Pyrocatechol Violet (**PV**). The red trace corresponds to the indicator alone, the blue trace corresponds to the (indicator)-Zn₂-**8-PG** complex, and the purple trace corresponds to (indicator)-Zn₂-**8-PG** complex plus the anion.

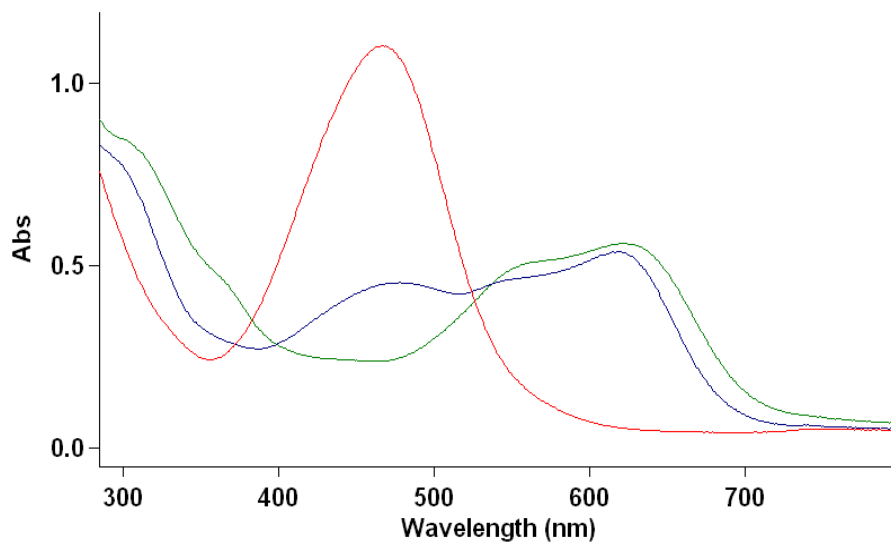
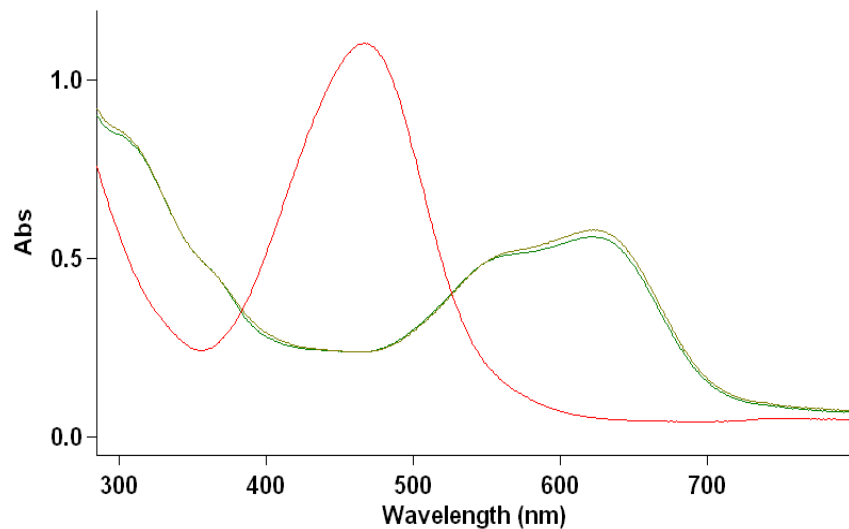


Figure 2 B 18 Phosphate (top) and pyrophosphate (bottom) displacement tests for Zincon (**ZC**). The red trace corresponds to the indicator alone, the green trace corresponds to the (indicator)-Zn₂-8-PG complex, and the blue trace corresponds to (indicator)-Zn₂-8-PG complex plus the anion.

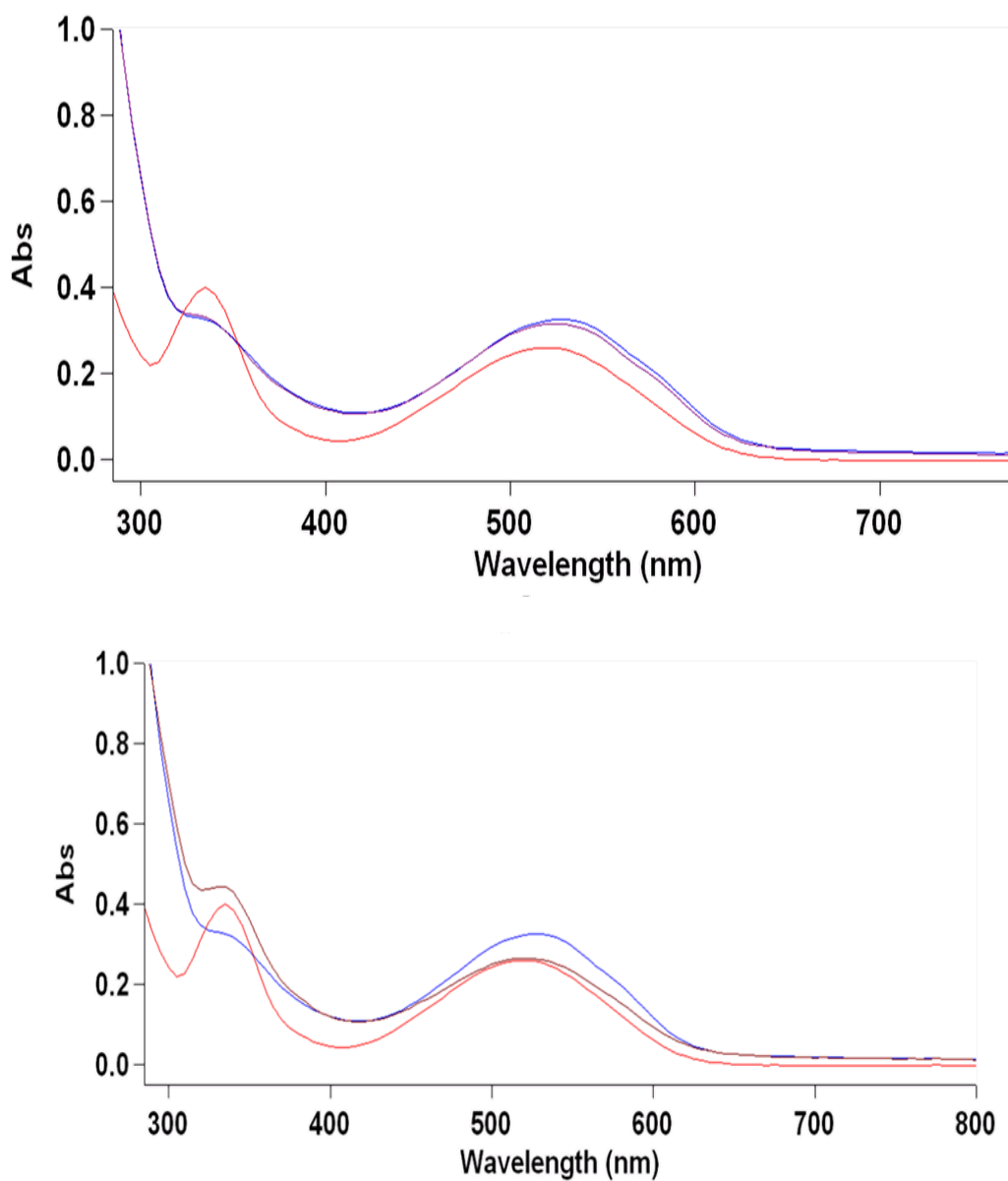


Figure 2 B 19 Phosphate (top) and pyrophosphate (bottom) displacement tests for Alizarin Red S (**ARS**). The red trace corresponds to the indicator alone, the blue trace corresponds to the (indicator)-Zn₂-7-PG complex, and the purple trace corresponds to (indicator)-Zn₂-7-PG complex plus the anion.

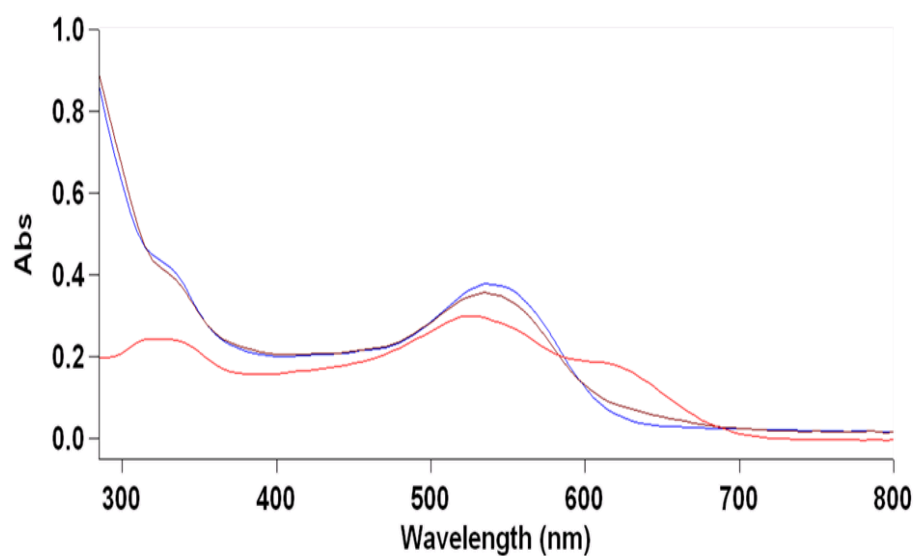
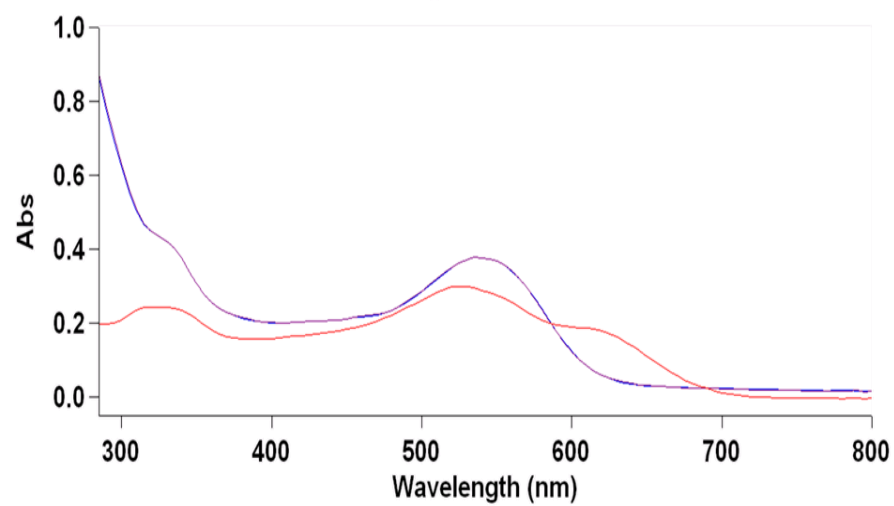


Figure 2 B 20 Phosphate (top) and pyrophosphate (bottom) displacement tests for Mordant Blue 9 (**MB9**). The red trace corresponds to the indicator alone, the blue trace corresponds to the (indicator)- Zn_2 -**7-PG** complex, and the purple trace corresponds to (indicator)- Zn_2 -**7-PG** complex plus the anion.

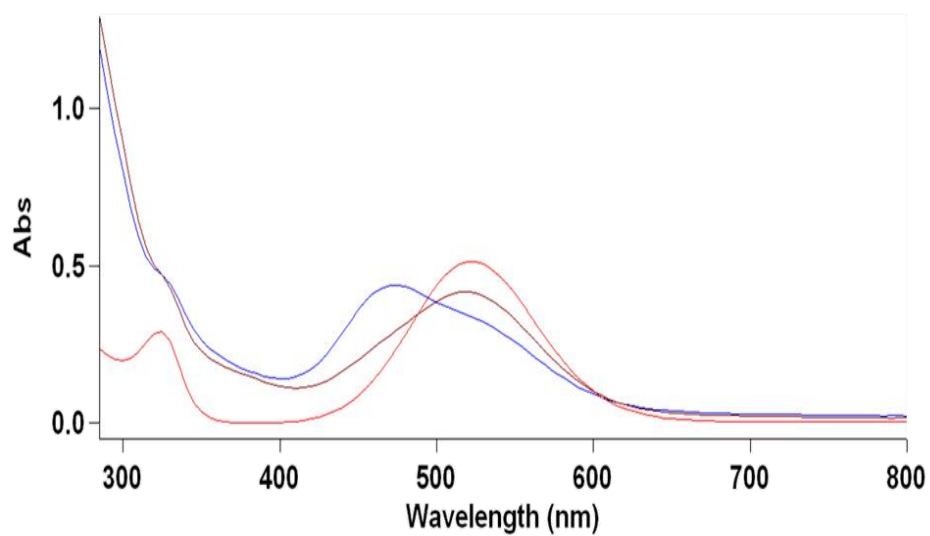
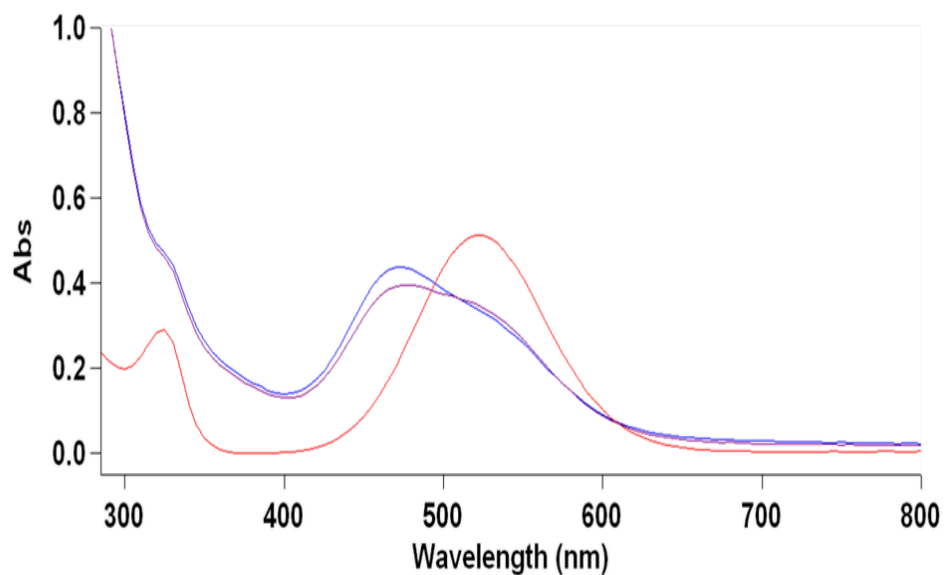


Figure 2 B 21 Phosphate (top) and pyrophosphate (bottom) displacement tests for Murexide (**MX**). The red trace corresponds to the indicator alone, the blue trace corresponds to the (indicator)- Zn_2 -**7-PG** complex, and the purple trace corresponds to (indicator)- Zn_2 -**7-PG** complex plus the anion.

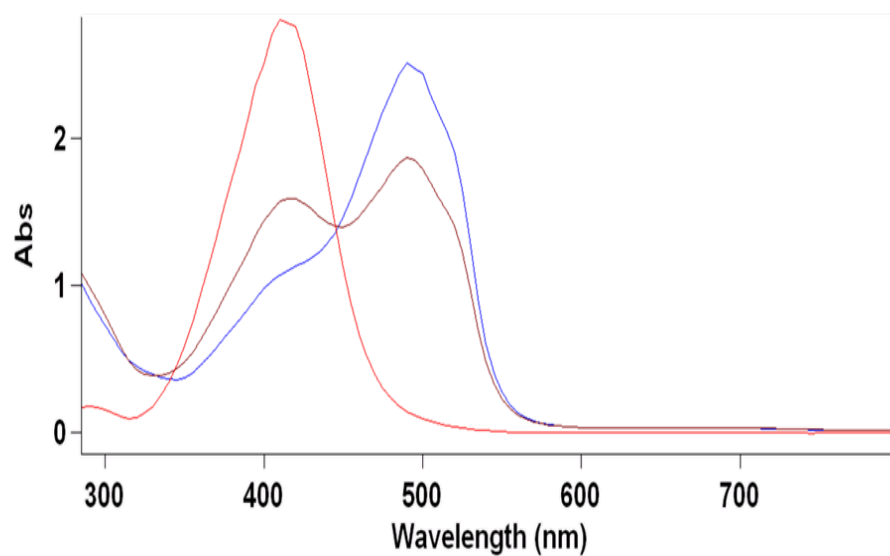
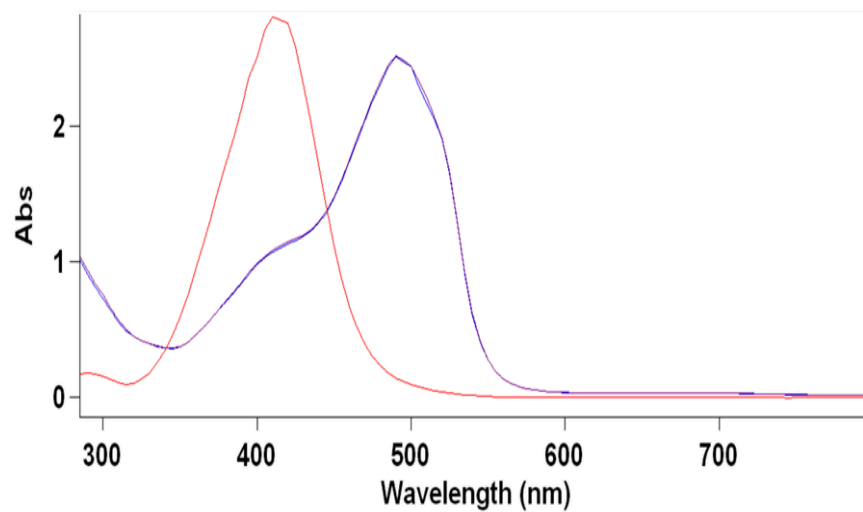


Figure 2 B 22 Phosphate (top) and pyrophosphate (bottom) displacement tests for 4-(Pyridin-2-ylazo)resorcinol (**PAR**). The red trace corresponds to the indicator alone, the blue trace corresponds to the (indicator)-Zn₂-**7-PG** complex, and the purple trace corresponds to (indicator)-Zn₂-**7-PG** complex plus the anion.

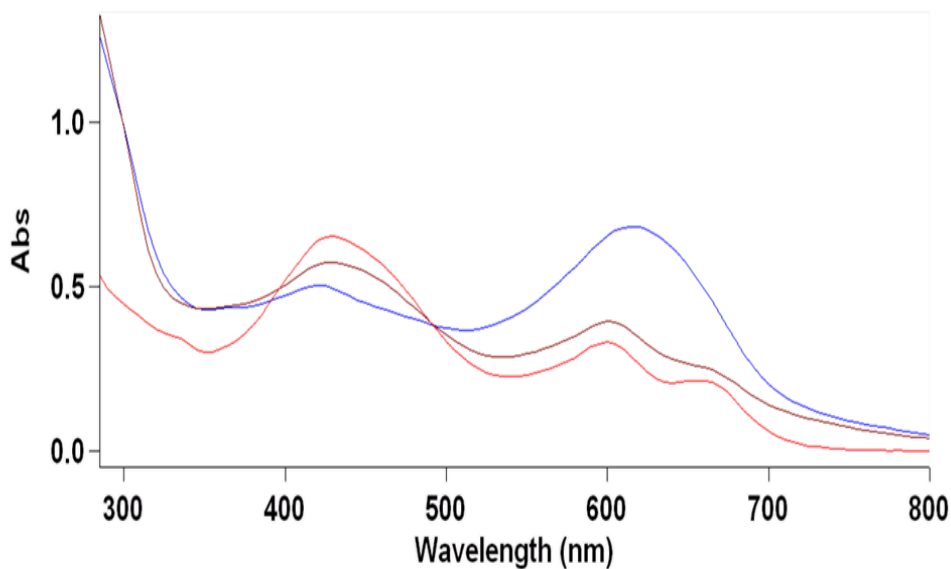
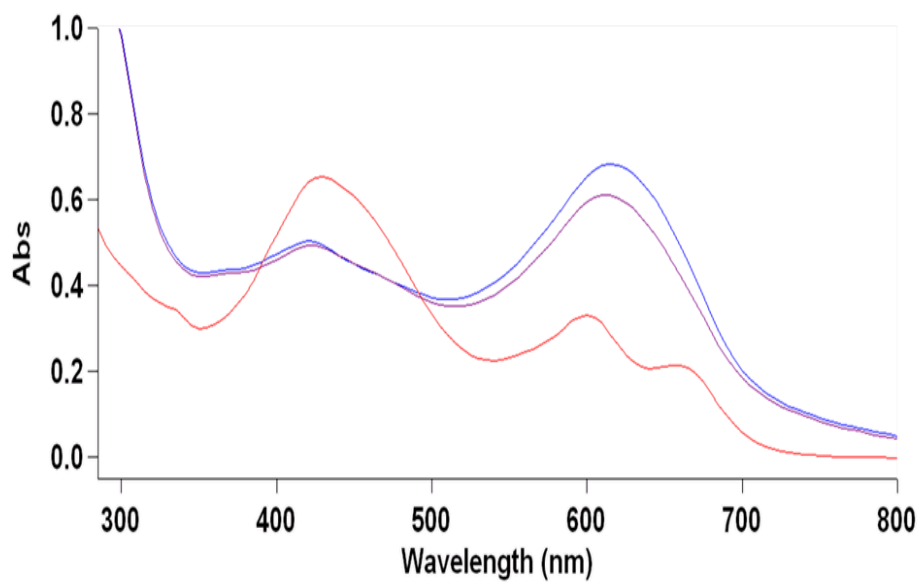


Figure 2 B 23 Phosphate (top) and pyrophosphate (bottom) displacement tests for Pyrocatechol Violet (**PV**). The red trace corresponds to the indicator alone, the blue trace corresponds to the (indicator)- Zn_2 -**7-PG** complex, and the purple trace corresponds to (indicator)- Zn_2 -**7-PG** complex plus the anion.

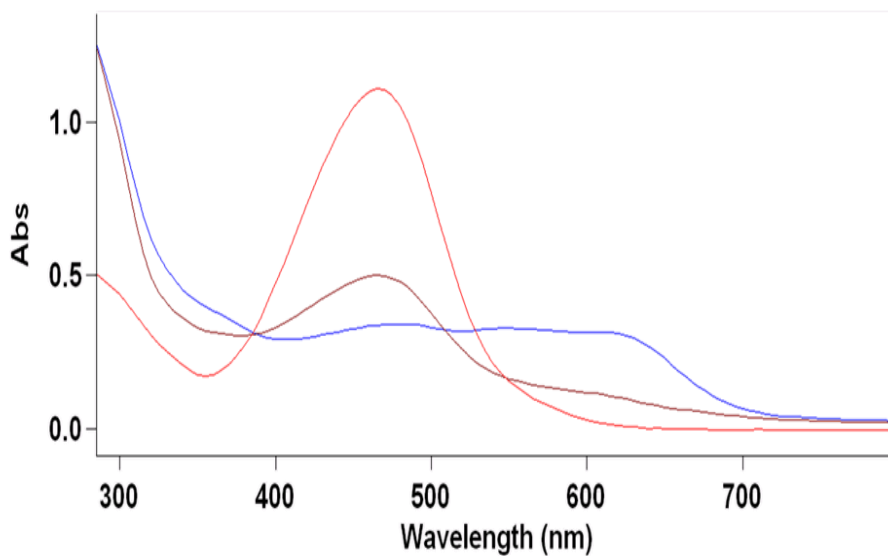
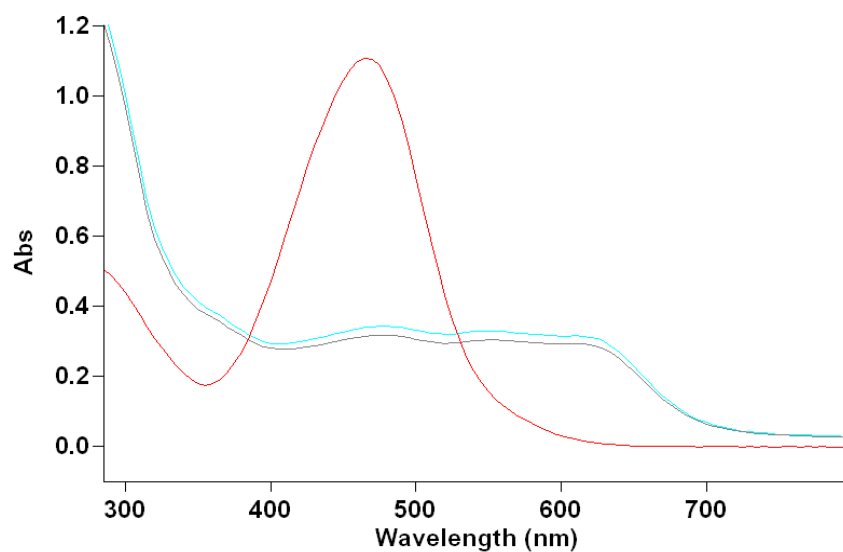


Figure 2 B 24 Phosphate (top) and pyrophosphate (bottom) displacement tests for Zincon (**ZC**). The red trace corresponds to the indicator alone, the blue trace corresponds to the (indicator)-Zn₂-**7-PG** complex, and the purple trace corresponds to (indicator)-Zn₂-**7-PG** complex plus the anion.

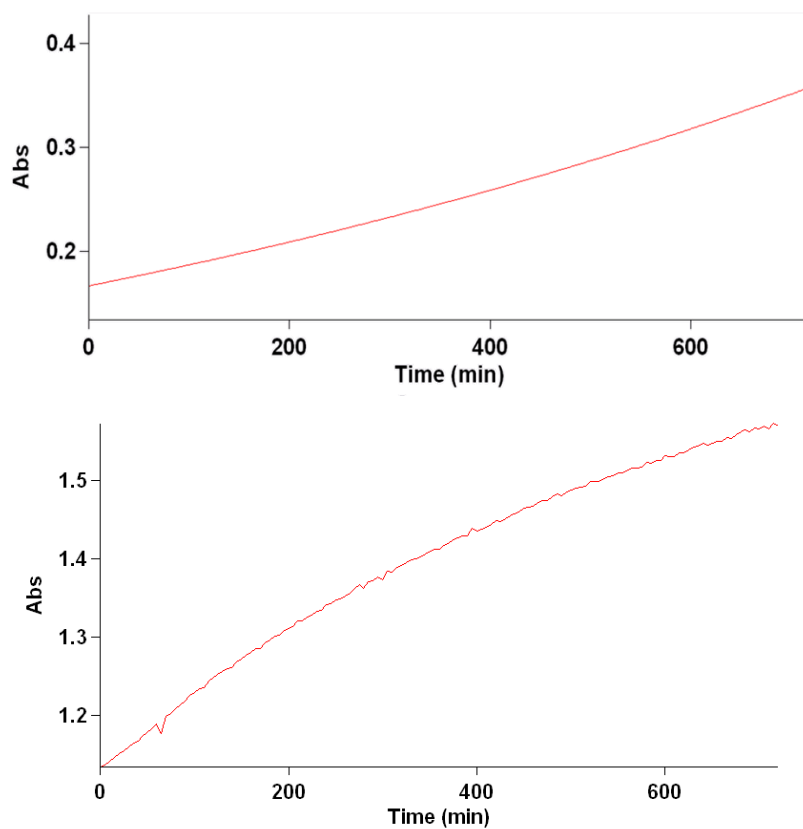


Figure 2 B 25 Time versus absorption profile for hydrolysis of NPP by Co₂-**8-PG** (top) and by Co₂-**7-PG** (bottom) indicating the change in absorbance at 420 nm over time (t = 0 corresponds to the point at which the NPP was added to the preformed Co(III) complex). Data were fit to the linear region at low conversion. Spectroscopic details and concentrations are provided in the Experimental section of the manuscript.

CHAPTER THREE

DIZINC PHOSPHOHYDROLASE MODEL BUILT ON A *m*-TERPHENYL SCAFFOLD AND ITS USE IN INDICATOR DISPLACEMENT ASSAYS FOR PYROPHOSPHATE UNDER PHYSIOLOGICAL CONDITIONS[#]

3.1 Introduction

The indicator displacement assay (**IDA**, **Figure 3.1**) strategy is a simple and increasingly popular approach to colorimetric and fluorescent chemosensing.^{1, 2} Early IDAs were developed to recognize a variety of anions,³⁻¹⁶ including inorganic phosphates,^{15, 17} and have even been adapted to challenging problems such as nitric oxide (**NO**) genesis by living cells¹⁸⁻²⁰ and nerve agent detection.²¹

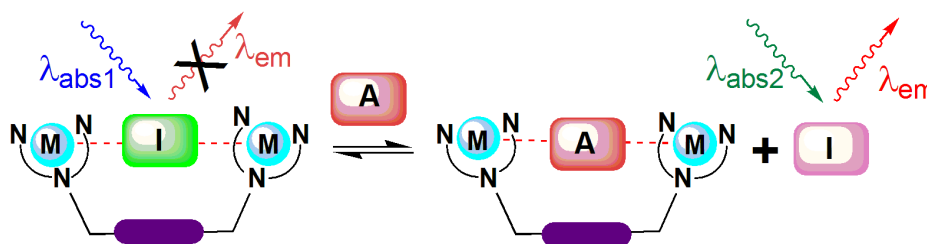


Figure 3.1 General indicator displacement assay strategy in which the receptor is a bimetallic complex (I = indicator, A = analyte). This representation assumes indicator emission enhancement upon displacement.

[#] Adapted from Coggins, M. K.; Parker, A. M.; Mangalum, A.; Galdamez, G. A.; Smith, R. C. *Eur. J. Org. Chem.*, 2009, 343-348, with permission.

The interplay between IDA receptor, indicator, target analyte, and potentially interfering species in the sample must be carefully controlled in order to achieve desired sensitivity and selectivity. Numerous multipodal and compartmental complexes have served as IDA receptors.²²⁻²⁶ The design of such receptors can be inspired by enzyme active sites known to bind target analytes.

Dizinc phosphohydrolase models, for example, are attractive candidates for detection of inorganic phosphates or phosphorylated bio-molecules such as proteins or phospholipids, which are important biological contributors in metabolic and signaling pathways.²⁷ Pyrophosphate (PP_i) is of particular interest to us because synovial fluid (PP_i) is a diagnostic marker used to differentiate osteoarthritic conditions wherein calcium pyrophosphate depositions form between joints,²⁸ and because there are already numerous phosphate (P_i) sensors relative to PP_i sensors.²⁹

Our previous work on IDAs^{30, 31} included a study³⁰ which built on extensive work by others who established *m*-xylylene scaffolded dizinc complexes as preeminent receptors for phosphate under physiologic conditions.^{16, 22, 32, 33} Zn₂L1 (the product of Zn²⁺ addition to aqueous L1, **Figure 3.2**), for example, has a Zn–Zn distance (3.0 Å)³⁴ somewhat less than that in phosphotriesterase (3.5 Å), which binds with high specificity to P_i derivatives,³⁵ whereas Zn₂L1 and related complexes bind both P_i and PP_i.^{36, 37}

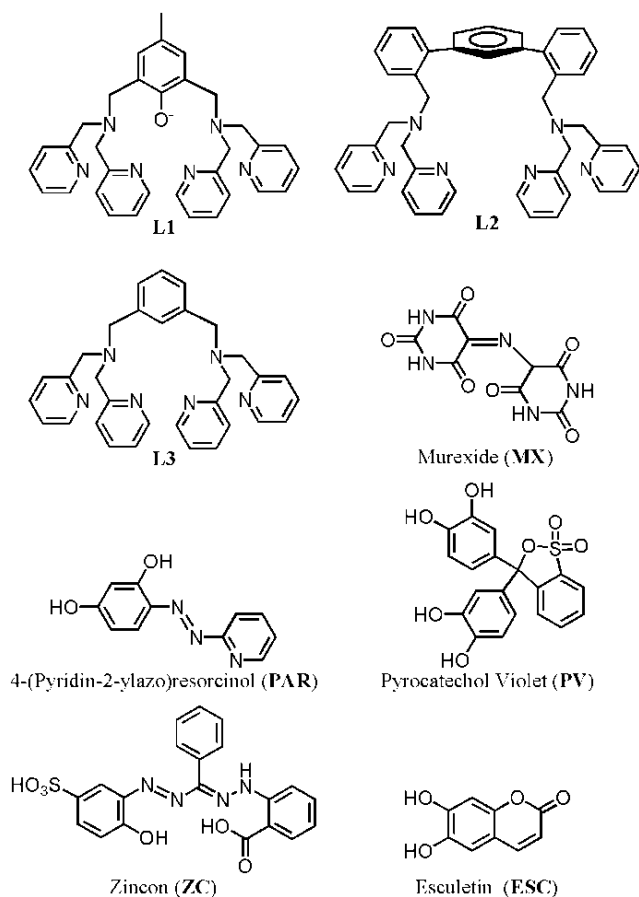


Figure 3.2 Binucleating ligands (**L1** - **L3**) and complexometric indicators tested for displacement by inorganic phosphates. Only one protonation state / resonance structure is provided for each.

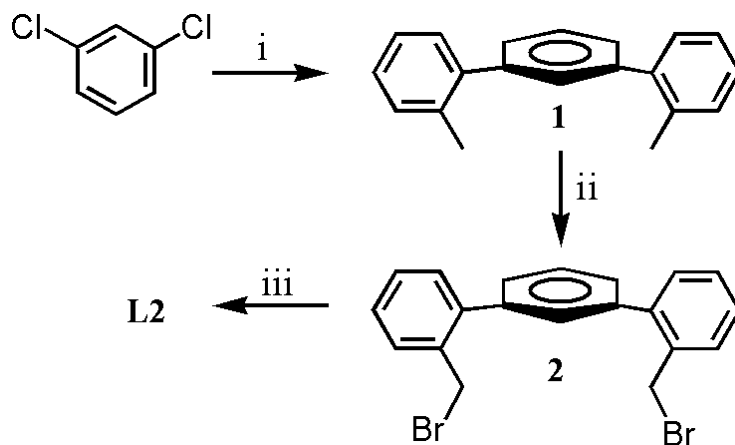
We tested $\text{Zn}_2\text{L1}$ as an IDA receptor with various commercial indicators, but the similar binding affinity of P_i and PP_i to $\text{Zn}_2\text{L1}$ made their differentiation difficult.³⁰ The Zn–Zn distance should play a key role in analyte preference. The dependence of phosphoester hydrolysis activity on Zn–Zn distance in phosphohydrolase models has been studied employing, for example, xylyl, naphthyl, anthryl, and biphenyl spacers between Zn-chelating moieties.³⁸

Although these spacers have provided some functional models, an emerging theme in bimetallic enzyme modeling has been to position metals within a steric pocket to exert control over metal-substrate interactions. This same strategy could prove useful for developing sensors as well, because steric coordination control may alter analyte selectivity and affinity. Notable bulky ligands for enzyme modeling include *m*-terphenyl carboxylates, particularly for diiron and dicopper enzyme models.³⁹⁻⁴²

This established success of *m*-terphenyl scaffolds for supporting bimetallic model complexes led us to explore translocation of the metal ligating units from their typical position on the central aryl ring onto the flanking rings, i.e. at the benzylic sites of **1** (**Scheme 3.1**). This substitution pattern could provide useful dinucleating ligands for a variety of enzyme models for both catalytic and chemosensor applications.

Herein we discuss a dizinc complex of one such *m*-terphenyl scaffolded ligand (**L2**, **Figure 3.2**) and report its utility as the receptor component of IDAs that are selective for PP_i at physiological pH. Binding and selectivity of **L2** complexes are compared with those of two related dinucleating ligands (**L1** and **L3**) that have been used in indicator displacement assays in biological contexts.

3.2 Synthesis and Characterization



Scheme 3.1 Preparation of **L2**: i. 1) 1.1 equiv *n*BuLi, -78 °C; 2) 3.5 equiv 2-tolylmagnesium bromide, Δ ; 3) H^+ . ii. *N*-bromosuccinimide, benzoyl peroxide, $CHCl_3$, Δ . iii. bis(2-picolyl)amine, triethylamine, THF.

There is only one example of a *m*-terphenyl scaffold supporting a bimetallic complex in which ligands are only present on the flanking aryl rings (rather than on the central ring), a bimetallic palladium complex with a Pd–Pd distance of 3.6 Å.⁴³ Molecular modeling, however, suggested that such a scaffold is capable of supporting M–M distances relevant for bimetallic enzyme modeling (typically 3–5 Å).⁴⁴



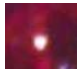
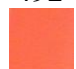


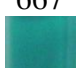


We therefore sought to incorporate ligands for binding biologically relevant metals, particularly zinc, onto the *m*-terphenyl scaffold. The bis(2-picolyl)amino unit was selected for our initial study on the basis of its strong affinity for Zn^{2+} and its widespread use in previous models.²² Ligand **L2** was readily prepared (**Scheme 3.1**) from known precursor **2**⁴⁵ in one step via a procedure analogous to that used to prepare **L1**.⁴⁶

3.3 Photophysical Studies and Calculations

The Zn₂L₂ complex used in absorption spectroscopic studies was prepared *in situ* in HEPES buffer (10 mM, pH 7.4), following the procedure reported for L₁.³⁰ The binding strength and optical changes of commercial indicators (**Figure 3.2**) upon binding to Zn₂L₂ were probed to reveal any differences from *m*-xylylene scaffolded analogues. Data from absorption spectroscopic titrations were used to calculate dissociation constants (K_d , **Table 3.1**) via a modification of the Benesi-Hildebrand method (Benesi-Hildebrand plots are provided in the **Appendix 3 B**).⁴⁷

Binding data for several indicators with Zn₂L₂, as well as for *m*-xylylene-based Zn₂L₁ (which has a bridging phenolate) and Zn₂L₃ (lacking a bridging ligand) are provided in **Table 3.1**. It is worth noting that the measured affinity of indicators for Zn²⁺ complexes is several orders of magnitude lower than that of Zn²⁺ for a dipicolylamine receptor,⁴⁸⁻⁵⁰ precluding the possibility that the indicators may be demetallating the receptor. Despite anticipated differences in *average* Zn–Zn distances, a similar range of K_d values were found for all three complexes (**Table 3.1**). The similarities are presumably due to the flexibility of the L₂ and L₃ scaffolds, which allows access to a range of Zn–Zn distances in order to optimize binding interactions with a particular indicator. Competitive binding analysis of absorption data from titration of indicator - Zn₂L₂ complexes with P_i and PP_i revealed K_d for P_i (3.1×10^{-5} M) and PP_i (2.4×10^{-6} M) on approximately the same order of magnitude as those reported for Zn₂L₁ complexes (9.1×10^{-6} M and 1.5×10^{-6} M for P_i and PP_i, respectively).⁵¹

Table 3.1 Absorption data and photos demonstrating the range of colorimetric responses observed in free, bound and pyrophosphate-displaced states. λ_{free} is the absorption maximum for the indicator alone and $\lambda_{\text{Zn}_2\text{L}_2}$ is the absorption maximum for the indicator when bound to the Zn_2L_2 complex. The photos under each absorption wavelength are of the color observed in the cuvettes by eye at 5×10^{-5} M indicator concentration. All data are for solutions in 1 mM HEPES buffer at pH = 7.4. Absorption spectra for these experiments are provided in the **appendix 3 B**.

Indicator	K_d μM	$\Delta\lambda$ nm	λ_{free} nm	λ_{bound} nm	Displacement ^a		PPi Slectivity	
					Pi	PPi	L1	L2
ARS	50	20	517 	537 	Y	Y 		
BPR	990	36	554 	590 	N	Y	X	X
MB9	85	25	527 	552 	Y 	N	X	
MX	28	58	552 	464 	Y	Y 		
PAR	13	81	414 	492 	N	Y 		X
PV	99	229	438 	667 	N	Y 		X
ZC	200	96	465 	561 	N	Y 	X	X

^a Y = yes, N = no. Indicator is considered to be displaced when there is >50% return in absorbance at λ_{bound} to the absorbance at that wavelength for the unbound form.

It is notable that although PP_i is bound equally well by both dizinc species, $\text{Zn}_2\mathbf{L2}$ binds P_i three times less strongly than does $\text{Zn}_2\mathbf{L1}$. The reduced affinity of $\text{Zn}_2\mathbf{L2}$ for P_i presumably stems from the larger Zn–Zn separation accessible using the *m*-terphenyl scaffold versus that provided by the *m*-xylylene spacer and anchoring of zinc centers by the μ -phenolate in $\mathbf{L1}$.

The enhanced preference for binding PP_i over P_i suggested that IDAs with improved selectivity for PP_i should be possible using $\mathbf{L2}$. Four commercial complexometric indicators previously shown³⁰ to exhibit notable differences in their absorption spectra between free and dizinc-bound states were tested (**Table 3.1**). All of these indicators provide IDAs selective for PP_i over P_i and other simple anions (no displacement of indicator is observed upon addition of excess F^- , Cl^- , Br^- , I^- , AcO^- , NO_3^- , CO_3^{2-} and HSO_4^-).

The zinc centers in $\text{Zn}_2\mathbf{L2}$ are not anchored by an intramolecular bridging ligand (cf. $\mathbf{L1}$), so the ability of $\text{Zn}_2\mathbf{L2}$ to expand and accommodate a larger anion such as triphosphate may be envisioned. Addition of one equiv of triphosphate, however, did not significantly displace any of the indicators. Because biological or environmental assays are targeted end uses of these IDAs, other potentially interfering bipodal biological anions were also tested.

Bio-molecules such as glutamate and aspartate are the most obvious candidates for testing in this regard due to their similarity in size (i.e., distance between anionic atoms) to PP_i and previous reports that these anions can displace indicators from bimetallic receptors.¹¹ None of the indicators were displaced from $\text{Zn}_2\mathbf{L2}$ to any

appreciable extent by glutamate or aspartate, indicating that Zn_2L2 maintains selectivity for phosphates over carboxylates, a property previously noted for xylylene-bridged dizinc analogues.³²

Although colorimetric assays are convenient for assessing analyte presence visually, fluorescent sensors exhibiting emission enhancement in response to analytes are considerably more sensitive and thus preferred for biological studies. Esculetin (**ESC**, **Figure 3.2**), a catechol-derivatized fluorescent indicator previously used in IDAs,¹⁹ was thus tested for detection of PP_i by fluorescence spectroscopy. Esculetin is effectively bound by Zn_2L2 ($K_d = 3.85 \times 10^{-5}$ M), and the **ESC- Zn_2L2** complex is only 25% as emissive as free esculetin.

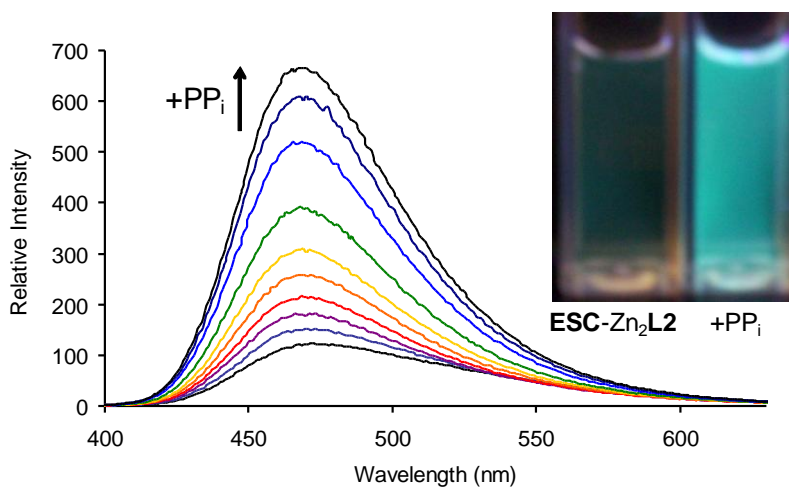
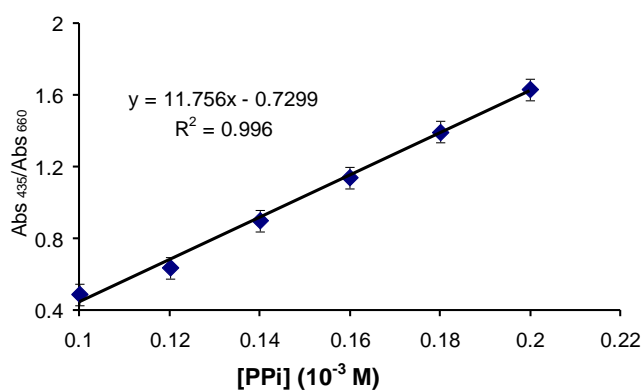


Figure 3.3 Change in emission intensity of **ESC- Zn_2L2** (2.5×10^{-5} M in pH 7.4 HEPES) as up to 1.5 equiv PP_i were added ($\lambda_{ex} = 380$ nm). The inset demonstrates the visual change in emission ($\lambda_{ex} = 365$ nm).

Near full restoration of emission to that of the free indicator was achieved upon addition of 1.5 equiv PP_i (**Figure 3.3**) corresponding to a 4.1-fold emission enhancement. The fluorescent turn-on IDA using **ESC-Zn₂L2** has a modest sensitivity limit (based on 5% increase in integrated emission) estimated at 2.5×10^{-6} M.

(A)



(B)

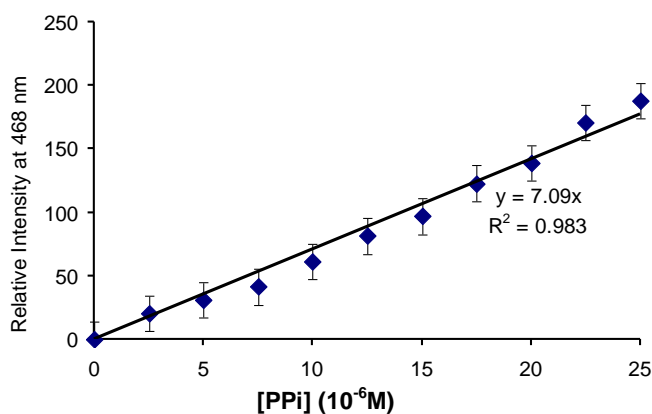


Figure 3.4 Calibration curves for (PP_i) measured via displacement of pyrocatechol violet measured by ratiometric absorption spectroscopy **(A)** and displacement of esculetin measured by increase in emission intensity of fluorescence spectra **(B)** in HEPES buffer (pH = 7.4). In both graphs, diamonds with error bars are original data points and the black line is a linear fit of the data. Equations of linear fits and corresponding R² values are also provided on each graph. Error bars represent error associated with absorption (a) and fluorescence intensity readings (b)

This is, however, within the level required for detection of biologically relevant (PP_i) found in synovial fluid (8.6×10^{-6} M to 15.9×10^{-6} M), which is elevated to higher

concentrations in arthritis patients.^{28, 52} Because clinical methods for measuring synovial (PP_i) rely most commonly on radiological methods and may not readily differentiate phosphate from pyrophosphate,^{28, 53} a sensitive fluorescence assay could eventually prove more economical and convenient for some practical applications.

Once PP_i selectivity was confirmed in the presence of 5 equiv P_i per PP_i in solution, the viability of the Zn₂L2 IDA for providing quantitative data on (PP_i) was examined. Calibration curves constructed from absorption (**Figure 3.4a**) and fluorescence (**Figure 3.4b**) spectral data indicate a linear response as a function of (PP_i) in HEPES buffer at physiological pH. The operational range obtainable from absorption (on the order of 10⁻⁴ M) versus fluorescence (on the order of 10⁻⁶ M) data emphasizes the approximate two orders of magnitude greater sensitivity of the later method; however, both techniques appear well suited for quantitative measurements.

3.4 Conclusion

To summarize, a binucleating ligand utilizing a *m*-terphenyl scaffold has been prepared. The dizinc complex of this ligand is a suitable receptor for PP_i at physiologic pH, affording improved selectivity over P_i in IDAs versus related systems. IDAs that employ ratiometric absorption changes and fluorescence emission enhancement have both been developed and provide linear responses to pyrophosphate at physiological pH. Although tests reported herein have been *ex vivo*, the fluorescence assay provides sensitivity appropriate for monitoring biologically relevant pyrophosphate concentrations. Efforts are underway to elaborate the *m*-terphenyl scaffold for additional applications in chemosensing and enzyme modeling.

3.5 Experimental Section

Reagents and General Methods

All reagents were obtained from Aldrich Chemical Co., TCI America, Alfa Aesar, Fischer Scientific, Mallinckrodt, Baker and Adamson, or MP Biomedicals, LLC and used as received. Solvents were purified by passage through alumina columns under a N₂ atmosphere using an MBraun solvent purification system. Literature procedures were employed for the preparation of 2,2''-dimethyl-*m*-terphenyl (**1**)⁵⁴ and 2,2''-Bis(bromomethyl)-1,1':3',1''-terphenyl (**2**).⁴⁵ All proton and carbon-13 NMR spectra were obtained using a Bruker Avance 300 spectrometer with operational parameters set at 300 MHz for ¹H nuclei and 75 MHz for carbon-13 nuclei. All spectra were collected at 20 °C and referenced to either tetramethylsilane (0 ppm) as an internal standard or the residual solvent peak.

General Spectroscopic Methods

Corning CHEK-MITE pH 25 sensor interfaced with a symphony Ag / AgCl pH electrode was used for measuring the pH of HEPES buffer, which was calibrated to the target pH value of 7.4 by the addition of NaOH (aq). All absorption and fluorescence spectra were collected at 20 °C using a Cary 50 spectrophotometer for absorbance, and a Cary Eclipse fluorescence spectrophotometer for photoluminescence. Samples were prepared in poly(methylmethacrylate) cuvettes (1.0 cm path lengths) from Starna Cells, Inc.

Absorption spectroscopic titration of indicators with Zn₂L2

Indicator stock solutions (50 mL, 5×10^{-5} M) were individually prepared in a buffered solution of HEPES (10 mM, pH 7.4) and used for all titration experiments. A solution of Zn₂L2 (1.5 mM, 10 mL) was prepared in 1:4 acetonitrile / HEPES (10 mM, pH 7.4) and utilized for all titration experiments. For delineation of respective spectral responses from each indicator due to the introduction of Zn₂L2, 3 mL of the stock indicator solution was added to a cuvette and the resulting spectrum was recorded in the absence of Zn₂L2. Subsequently, the indicator solution was titrated *in situ* with 10 μ L aliquots (0.10 equiv) of the Zn₂L2 solution; individual spectra were recorded following the addition of each Zn₂L2 aliquot until a total of at least 10 aliquots (1 equiv) had been added. Titrations were performed in identical fashions for all indicators under consideration. Resulting Absorption titration spectra for each indicator are provided in the **appendix 3 B**.

Determination of indicator / Zn₂L2 dissociation constants

Spectral data were used to estimate dissociation constants via a variation of the Benesi-Hildebrand method prescribed by Hammond.⁴⁷ Plots of $(\Delta\text{Abs})^{-1}$ versus $[\text{Zn}_2\text{L}_2]^{-1}$ were constructed for each series of indicator / receptor complex titration data, followed by a regression analysis of the data by a linear fit function. Benesi-Hildebrand plots, along with the corresponding linear regression functions and coefficients of determination (R^2), are provided in the **appendix 3 B**.

Absorption spectroscopic titration of indicator / Zn₂L2 complex with phosphorous-containing analyte

Indicator (5×10^{-5} M) and Zn_2L_2 (1.5 mM) solutions were used for indicator displacement assay titrations. Solutions of sodium hydrogen phosphate (1.5 mM, 5 mL) and sodium pyrophosphate decahydrate (1.5 mM, 5 mL) were prepared in HEPES buffer (10 mM, pH 7.4). Initially 3 mL of an indicator solution and 100 μ L of the Zn_2L_2 solution (1:1 stoichiometric equivalence) were added to a cuvette, followed by recording of the respective spectrum. For determination of the ability of the selected anion (phosphate or pyrophosphate) to displace the indicator from the indicator / Zn_2L_2 complex and concomitantly form an anion / Zn_2L_2 complex, the indicator / Zn_2L_2 solution was titrated *in situ* with 10 μ L aliquots (0.100 equiv relative to both the indicator and Zn_2L_2) aliquots of the anion solution. Individual spectra were recorded following the addition of each anion aliquot until a total of 20 aliquots had been added to the indicator solution (resulting in a 2:1:1 anion:indicator: Zn_2L_2 stoichiometry). Titrations were iterated in the same manner for all indicator / analyte combinations. Absorption spectra resulting from the titration of each indicator- Zn_2L_2 complex with PP_i are provided in the **appendix 3 B**.

Response of indicator- Zn_2L_2 to other anions

Indicator- Zn_2L_2 solutions were prepared as described above for absorption spectroscopic studies, and up to 10 equiv of NaF, NaCl, NaBr, NaI, NaO_2CCH_3 , NaP_3H_{10} , Na_2SO_4 , $NaNO_3$, Na_2CO_3 sodium glutamate or sodium aspartate was added to each cuvette, followed by collection of an absorption spectrum. None of these samples exhibited significant changes in absorption spectra.

Fluorescence titration of indicator- Zn_2L_2 complex with phosphorous-containing analyte

Fluorescence experiments were executed in a manner similar to that described above for absorption spectroscopic experiments, with the exception that initial indicator concentrations of 2.5×10^{-5} M were used.

Synthesis of 2,2''-Bis[(2,2'-dipicolylamino)methyl]-1,1':3',1''-terphenyl (L2)

A stirred solution of **2** (0.630 g, 1.51 mmol) was initially prepared in THF (10 mL, anhydrous) and allowed to cool to 0 °C in an ice water bath under N₂. Separately, a solution of triethylamine (0.460 g, 4.56 mmol) and di(2-picolyl)amine (0.600 g, 3.01 mmol) was prepared in anhydrous THF (5 mL). The solution containing triethylamine and di(2-picolyl)amine was added dropwise *via* syringe to the stirring 2,2''-Bis(bromomethyl)-1,1':3',1''-terphenyl solution, resulting in an orange mixture. The solution was removed from the ice water bath and allowed to slowly warm to room temperature where it was permitted to continue stirring under N₂ and ambient temperature for approximately 48 h, over which time the solution turned from orange to brown. The solution was filtered to remove precipitated triethylammonium bromide, and the filtrate was concentrated *in vacuo* to yield dark brown oil. About 50 mL of methylene chloride was added and the organics washed with sat'd NaHCO₃ (aq) (50 mL × 3). The organic layer was collected, dried over Na₂SO₄ and concentrated under reduced pressure to yield a red oil. Approximately 10 mL of acetone and two drops of concentrated HCl were added to the crude product. The solution was allowed to stand at room temperature for 12 h, over which time a white microcrystalline solid formed. The solid was collected by filtration, rinsed with acetone, and dried *in vacuo* to yield the target compound (0.270 g, 51%) as a hygroscopic off-white powder. ¹H NMR (300 MHz, CDCl₃): δ 8.47 (d, 4H;

$J = 7$ Hz), 7.81 (d, 2H; $J = 7$ Hz), 7.56 - 7.08 (m, 22H), 3.76 (s, 8H), 3.72 (s, 4H). ^{13}C NMR (CDCl_3): δ 159.7, 148.9, 142.3, 141.2, 136.4, 136.3, 130.3, 129.6, 127.9, 127.8, 127.5, 126.8, 122.6, 121.8, 60.1, 56.0. Anal. Calcd. for $\text{C}_{44}\text{H}_{41}\text{N}_6\text{O}$ (**L2**· H_2O): C, 79.85 H, 6.24. N, 12.70; Found: C, 79.96 H, 5.96. N, 12.58. m.p. 122-126° C.

3.6 References

1. Nguyen, B. T.; Anslyn, E. V., Indicator-displacement assays. *Coordination Chemistry Reviews* **2006**, 250, (23+24), 3118-3127.
2. Wiskur, S. L.; Ait-Haddou, H.; Lavigne, J. J.; Anslyn, E. V., Teaching old indicators new tricks. *Accounts of Chemical Research* **2001**, 34, (12), 963-972.
3. Folmer-Andersen, J. F.; Lynch, V. M.; Anslyn, E. V., \"Naked-eye\" detection of histidine by regulation of CuII coordination modes. *Chemistry--A European Journal* **2005**, 11, (18), 5319-5326.
4. Aiet-Haddou, H.; Wiskur, S. L.; Lynch, V. M.; Anslyn, E. V., Achieving large color changes in response to the presence of amino acids: a molecular sensing ensemble with selectivity for aspartate. *Journal of the American Chemical Society* **2001**, 123, (45), 11296-11297.
5. Wiskur, S. L.; Lavigne, J. J.; Metzger, A.; Tobey, S. L.; Lynch, V.; Anslyn, E. V., Thermodynamic analysis of receptors based on guanidinium/boronic acid groups for the complexation of carboxylates, α -hydroxycarboxylates, and diols: Driving force for binding and cooperativity. *Chemistry--A European Journal* **2004**, 10, (15), 3792-3804.
6. Lavigne, J. J.; Anslyn, E. V., Teaching old indicators new tricks: a colorimetric chemosensing ensemble for tartrate/malate in beverages. *Angewandte Chemie, International Edition* **1999**, 38, (24), 3666-3669.

7. Wiskur, S. L.; Anslyn, E. V., Using a Synthetic Receptor to Create an Optical-Sensing Ensemble for a Class of Analytes: A Colorimetric Assay for the Aging of Scotch. *Journal of the American Chemical Society* **2001**, 123, (41), 10109-10110.
8. McCleskey, S. C.; Floriano, P. N.; Wiskur, S. L.; Anslyn, E. V.; McDevitt, J. T., Citrate and calcium determination in flavored vodkas using artificial neural networks. *Tetrahedron* **2003**, 59, (50), 10089-10092.
9. Piatek, A. M.; Bomble, Y. J.; Wiskur, S. L.; Anslyn, E. V., Threshold detection using indicator-displacement assays: An application in the analysis of malate in Pinot Noir grapes. *Journal of the American Chemical Society* **2004**, 126, (19), 6072-6077.
10. Nguyen, B. T.; Wiskur, S. L.; Anslyn, E. V., Using Indicator-Displacement Assays in Test Strips and To Follow Reaction Kinetics. *Organic Letters* **2004**, 6, (15), 2499-2501.
11. Bonizzoni, M.; Fabbrizzi, L.; Piovani, G.; Taglietti, A., Fluorescent detection of glutamate with a dicopper(II) polyamine cage. *Tetrahedron* **2004**, 60, (49), 11159-11162.
12. Fabbrizzi, L.; Foti, F.; Taglietti, A., Metal-Containing Trifurcate Receptor that Recognizes and Senses Citrate in Water. *Organic Letters* **2005**, 7, (13), 2603-2606.
13. Hortala, M. A.; Fabbrizzi, L.; Marcotte, N.; Stomeo, F.; Taglietti, A., Designing the selectivity of the fluorescent detection of amino acids: A chemosensing ensemble for histidine. *Journal of the American Chemical Society* **2003**, 125, (1), 20-21.
14. Boiocchi, M.; Bonizzoni, M.; Fabbrizzi, L.; Piovani, G.; Taglietti, A., A dimetallic cage with a long ellipsoidal cavity for the fluorescent detection of dicarboxylate

- anions in water. *Angewandte Chemie, International Edition* **2004**, 43, (29), 3847-3852.
15. Fabbrizzi, L.; Marcotte, N.; Stomeo, F.; Taglietti, A., Pyrophosphate detection in water by fluorescence competition assays: inducing selectivity through the choice of the indicator. *Angewandte Chemie, International Edition* **2002**, 41, (20), 3811-3814.
16. Fabbrizzi, L.; Licchelli, M.; Taglietti, A., The design of fluorescent sensors for anions: taking profit from the metal-ligand interaction and exploiting two distinct paradigms. *Dalton Transactions* **2003**, (18), 3471-3479.
17. Tobey, S. L.; Anslyn, E. V., Determination of inorganic phosphate in serum and saliva using a synthetic receptor. *Organic Letters* **2003**, 5, (12), 2029-2031.
18. Lim, M. H.; Lippard, S. J., Fluorescence-Based Nitric Oxide Detection by Ruthenium Porphyrin Fluorophore Complexes. *Inorganic Chemistry* **2004**, 43, (20), 6366-6370.
19. Hilderbrand, S. A.; Lim, M. H.; Lippard, S. J., Dirhodium tetracarboxylate scaffolds as reversible fluorescence-based nitric oxide sensors. *Journal of the American Chemical Society* **2004**, 126, (15), 4972-4978.
20. Lim, M. H.; Xu, D.; Lippard, S. J., Visualization of nitric oxide in living cells by a copper-based fluorescent probe. *Nature Chemical Biology* **2006**, 2, (7), 375-380.
21. Knapton, D.; Burnworth, M.; Rowan, S. J.; Weder, C., Fluorescent organometallic sensors for the detection of chemical-warfare-agent mimics. *Angewandte Chemie, International Edition in English* **2006**, 45, (35), 5825-5829.
22. O'Neil, E. J.; Smith, B. D., Anion recognition using dimetallic coordination complexes. *Coordination Chemistry Reviews* **2006**, 250, (23+24), 3068-3080.

23. Amendola, V.; Bonizzoni, M.; Esteban-Gomez, D.; Fabbrizzi, L.; Licchelli, M.; Sancenon, F.; Taglietti, A., Some guidelines for the design of anion receptors. *Coordination Chemistry Reviews* **2006**, 250, (11+12), 1451-1470.
24. Anslyn, E. V., Supramolecular analytical chemistry. *Journal of Organic Chemistry* **2007**, 72, (3), 687-699.
25. Dai, Z.; Canary, J. W., Tailoring tripodal ligands for zinc sensing. *New J. Chem.* **2007**, 31, (10), 1708-1718.
26. Zhang, L.; Clark, R. J.; Zhu, L., A heteroditopic fluoroionophoric platform for constructing fluorescent probes with large dynamic ranges for zinc ions. *Chem. Eur. J.* **2008**, 14, (9), 2894-2903.
27. Horton, H. R.; Moran, L. A.; Scrimgeour, K. G.; Perry, M. D.; Rawn, J. D., *Principles of Biochemistry*. 4 ed.; Pearson Prentice Hall, : Upper Saddle River, NJ, 2006; 'Vol.' p.
28. Rosenthal, A. K., Update in calcium deposition diseases. *Current Opinion in Rheumatology* **2007**, 19, (2), 158-162.
29. S. K. Kim, D. H. Lee, J.-I. Hong, J. Yoon, *Acc. Chem. Res.*, 21 October 2008 (10.1021/accchemres/ar800003f). In ed.; 'Ed.'^'Eds.' 'Vol.' p^pp.
30. Morgan, B. P.; He, S.; Smith, R. C., Dizinc Enzyme Model / Complexometric Indicator Pairs in Indicator Displacement Assays for Inorganic Phosphates under Physiological Conditions. *Inorganic Chemistry* **2007**, 46, 9262-9266.
31. He, S.; Iacono, S. T.; Budy, S. M.; Dennis, A. E.; Smith, D. W., Jr.; Smith, R. C., Photoluminescence and ion sensing properties of a bipyridyl chromophore-modified

- semifluorinated polymer and its metallopolymer derivatives. *J. Mater. Chem.* **2008**, 18, (17), 1970-1976.
32. Han, M. S.; Kim, D. H., Naked-eye detection of phosphate ions in water at physiological pH. A remarkably selective and easy-to-assemble colorimetric phosphate-sensing probe. *Angewandte Chemie, International Edition* **2002**, 41, (20), 3809-3811.
33. Leevy, W. M.; Gammon, S. T.; Jiang, H.; Johnson, J. R.; Maxwell, D. J.; Jackson, E. N.; Marquez, M.; Piwnica-Worms, D.; Smith, B. D., Optical Imaging of Bacterial Infection in Living Mice Using a Fluorescent Near-Infrared Molecular Probe. *Journal of the American Chemical Society* **2006**, 128, (51), 16476-16477.
34. Matsufuji, K.; Shiraishi, H.; Miyasato, Y.; Shiga, T.; Ohba, M.; Yokoyama, T.; Okawa, H., m-Hydroxo-m-phenolato dinuclear zinc(II) and nickel(II) complexes derived from dinucleating compartmental ligands of "end-off" type: synthesis, structures, and properties. *Bulletin of the Chemical Society of Japan* **2005**, 78, (5), 851-858.
35. Benning, M. M.; Shim, H.; Raushel, F. M.; Holden, H. M., *Biochemistry* **2001**, 40, 2712.
36. Fry, F. H.; Spiccia, L.; Jensen, P.; Moubaraki, B.; Murray, K. S.; Tiekink, E. R. T., Binuclear Copper(II) Complexes of Xylyl-Bridged Bis(1,4,7-triazacyclononane) Ligands. *Inorg. Chem.* **2003**, 42, 5594-5603.

37. Lee, D. H.; Im, J. H.; Son, S. U.; Chung, Y. K.; Hong, J.-I., An azophenol-based chromogenic pyrophosphate sensor in water. *Journal of the American Chemical Society* **2003**, 125, (26), 7752-7753.
38. Bauer-Siebenlist, B.; Meyer, F.; Farkas, E.; Vidovic, D.; Dechert, S., Effect of Zn...Zn separation on the hydrolytic activity of model dizinc phosphodiesterases. *Chemistry--A European Journal* **2005**, 11, (15), 4349-4360.
39. Tshuva, E. Y.; Lippard, S. J., Synthetic Models for Non-Heme Carboxylate-Bridged Diiron Metalloproteins: Strategies and Tactics. *Chemical Reviews (Washington, DC, United States)* **2004**, 104, (2), 987-1011.
40. Lewis, E. A.; Tolman, W. B., Reactivity of Dioxygen-Copper Systems. *Chemical Reviews (Washington, DC, United States)* **2004**, 104, (2), 1047-1076.
41. Que, L., Jr.; Tolman, W. B., Bis(m-oxo)dimetal "diamond" cores in copper and iron complexes relevant to biocatalysis. *Angewandte Chemie, International Edition* **2002**, 41, (7), 1114-1137.
42. Tolman, W. B.; Que, L., Jr., Sterically hindered benzoates: a synthetic strategy for modeling dioxygen activation at diiron active sites in proteins. *Journal of the Chemical Society, Dalton Transactions* **2002**, (5), 653-660.
43. Smith, R. C.; Protasiewicz, J. D., A Trans-Spanning Diphosphine Ligand Based on a m-Terphenyl Scaffold and Its Palladium and Nickel Complexes. *Organometallics* **2004**, 23, (18), 4215-4222.
44. Lippard, S. J.; Berg, J. M., *Principles of Bioinorganic Chemistry*. ed.; University Science Books: Mill Valley, CA, 1994; 'Vol.' p 450.

45. Vinod, T. K.; Hart, H., Cupped azacyclophanes based on a m-terphenyl framework: conformational features of their N-tosylamide precursors. *Journal of Organic Chemistry* **1990**, *55*, (20), 5461-6.
46. Suzuki, M.; Kanatomi, H.; Murase, I., Synthesis and properties of a binuclear cobalt(II) oxygen adduct with 2,6-bis[bis(2-pyridylmethyl)aminomethyl]-4-methylphenol. *Chemistry Letters* **1981**, (12), 1745-8.
47. Hammond, P. R., The effect of experimental errors on Benesi-Hildebrand plots and on the inherent accuracy of the equation. *Journal of the Chemical Society* **1964**, (Jan.), 479-84.
48. Nolan, E. M.; Ryu, J. W.; Jaworski, J.; Feazell, R. P.; Sheng, M.; Lippard, S. J., Zinspy Sensors with Enhanced Dynamic Range for Imaging Neuronal Cell Zinc Uptake and Mobilization. *Journal of the American Chemical Society* **2006**, *128*, (48), 15517-15528.
49. Walkup, G. K.; Burdette, S. C.; Lippard, S. J.; Tsien, R. Y., A New Cell-Permeable Fluorescent Probe for Zn²⁺. *Journal of the American Chemical Society* **2000**, *122*, (23), 5644-5645.
50. Burdette, S. C.; Walkup, G. K.; Spingler, B.; Tsien, R. Y.; Lippard, S. J., Fluorescent Sensors for Zn²⁺ Based on a Fluorescein Platform: Synthesis, Properties and Intracellular Distribution. *Journal of the American Chemical Society* **2001**, *123*, (32), 7831-7841.

51. Hanshaw, R. G.; Hilkert, S. M.; Jiang, H.; Smith, B. D., An indicator displacement system for fluorescent detection of phosphate oxyanions under physiological conditions. *Tetrahedron Letters* **2004**, 45, (47), 8721-8724.
52. Patrick, M.; Hamilton, E.; Hornby, J.; Doherty, M., Synovial fluid pyrophosphate and nucleoside triphosphate pyrophosphatase: comparison between normal and diseased and between inflamed and non-inflamed joints. *Ann. Rheum. Dis.* **1991**, 50, (4), 214-8.
53. McCarty, D. J.; Solomon, S. D.; Warnock, M. L.; Paloyan, E., Inorganic pyrophosphate concentrations in the synovial fluid of arthritic patients. *J. Lab. Clin. Med.* **1971**, 78, (2), 216-29.
54. Saednya, A.; Hart, H., Two efficient routes to meta-terphenyls from 1,3-dichlorobenzenes. *Synthesis* **1996**, (12), 1455-1458.

APPENDICES

Appendix 3 A

NMR Spectra

2,2''-Bis[(2,2'-dipicolylamino)methyl]-1,1':3',1''-terphenyl (**L2**)

Structure:

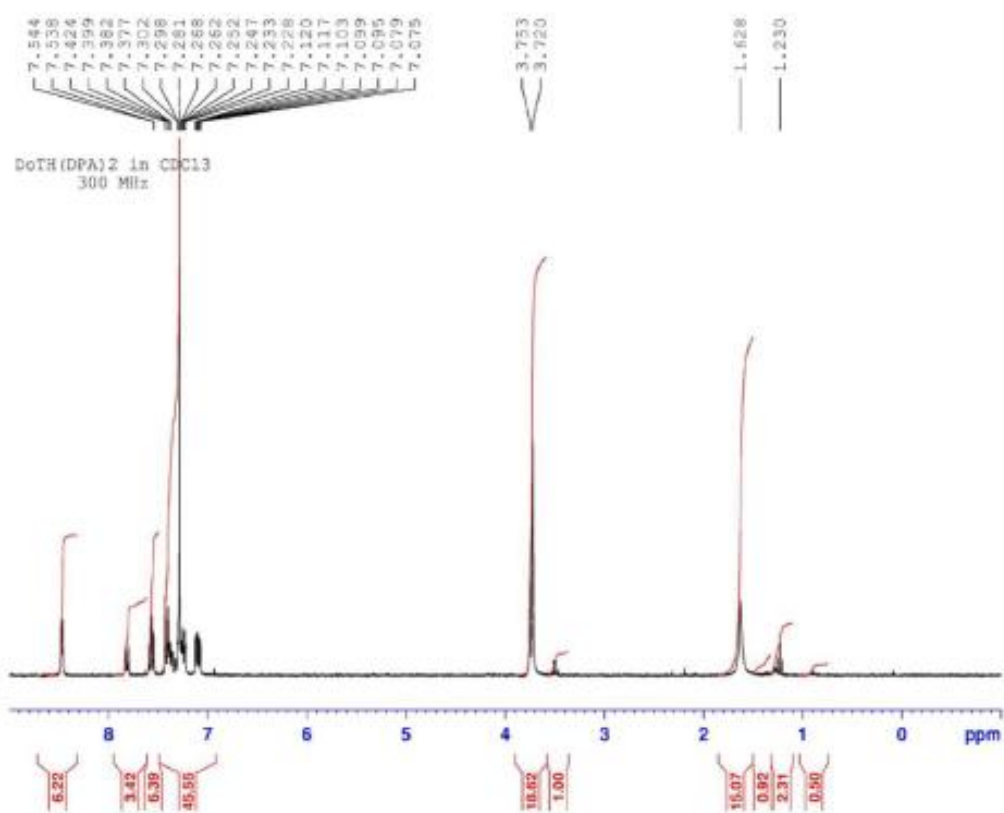
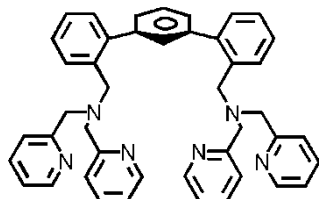


Figure 3 A.1 ^1H NMR (300 MHz, CDCl_3) of **L2**.

2,2''-Bis[(2,2'-dipicolylamino)methyl]-1,1':3',1''-terphenyl (**L2**)

Structure:

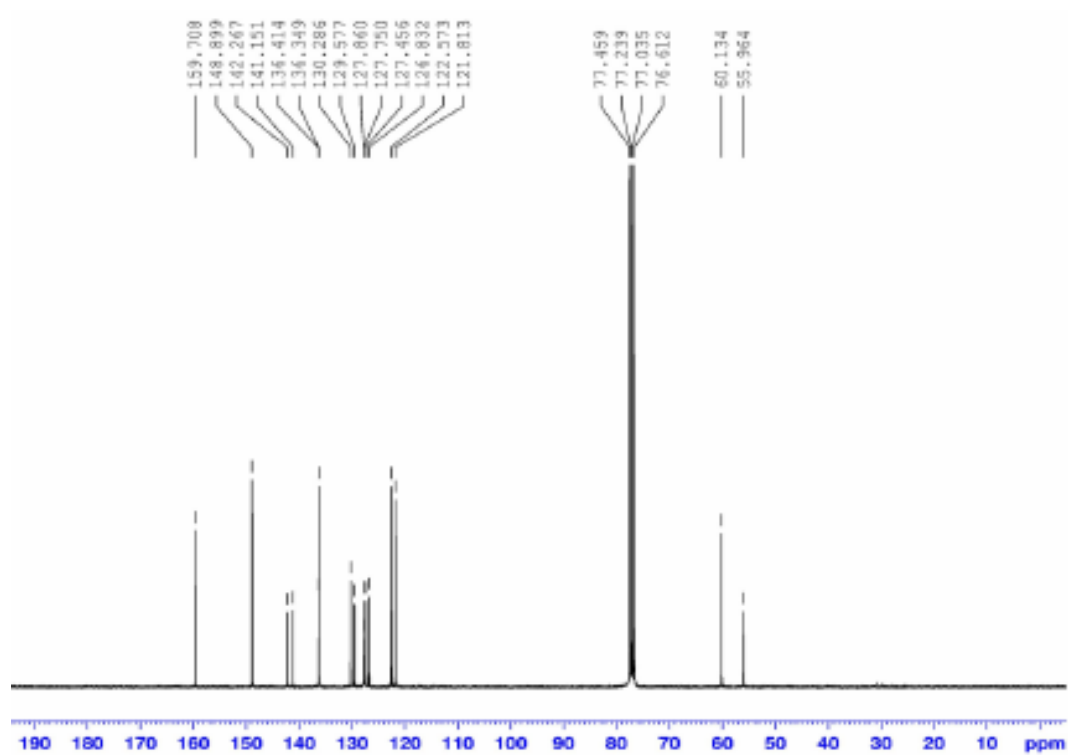
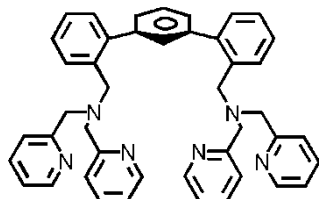


Figure 3 A.2 ^{13}C NMR (75 MHz, CDCl_3) of **L2**.

Appendix 3 B

UV-vis and Photoluminescence Spectra

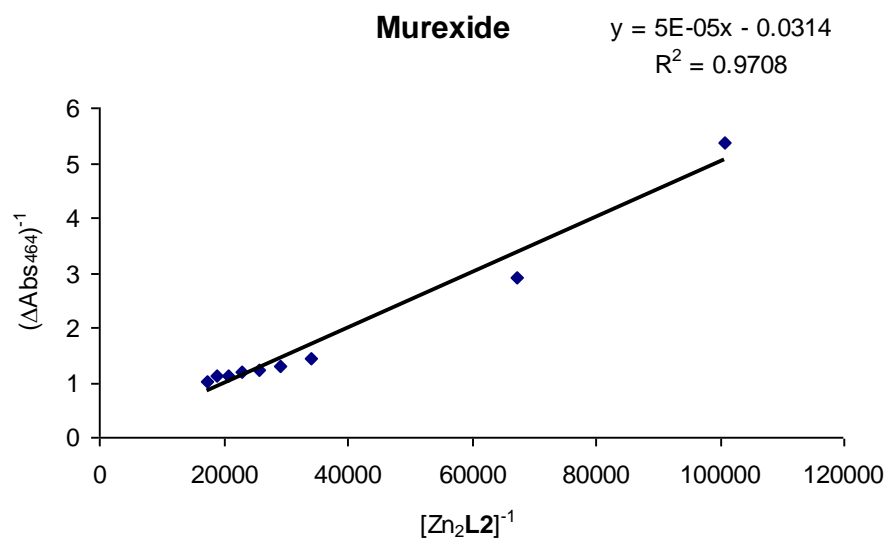
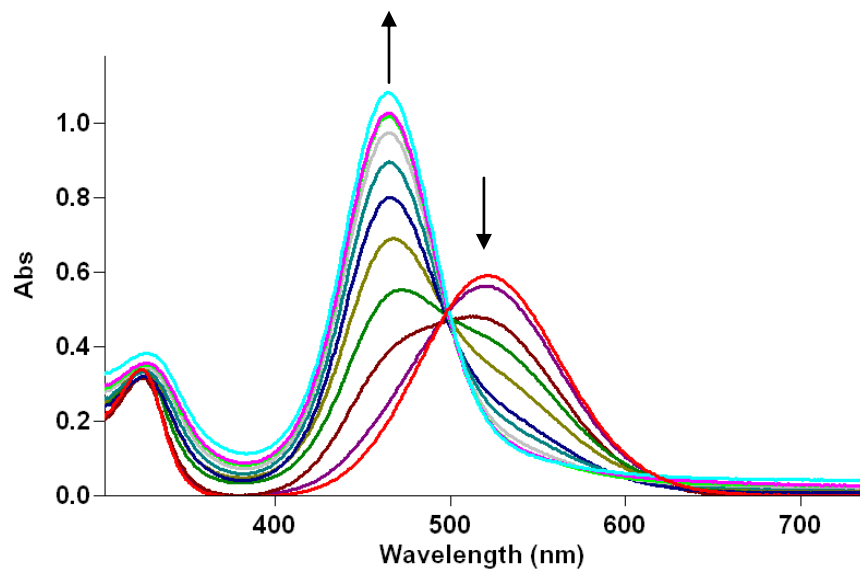


Figure 3 B.1 Titration of Murexide (**MX**) with Zn_2L_2 (top). Arrows designate the direction of change upon addition of Zn_2L_2 to the **MX** solution. Benesi-Hildebrand plot (bottom) of spectral data points (blue diamonds) and the linear regression function (black line) used for calculation of the dissociation constant respective to **MX** and Zn_2L_2 .

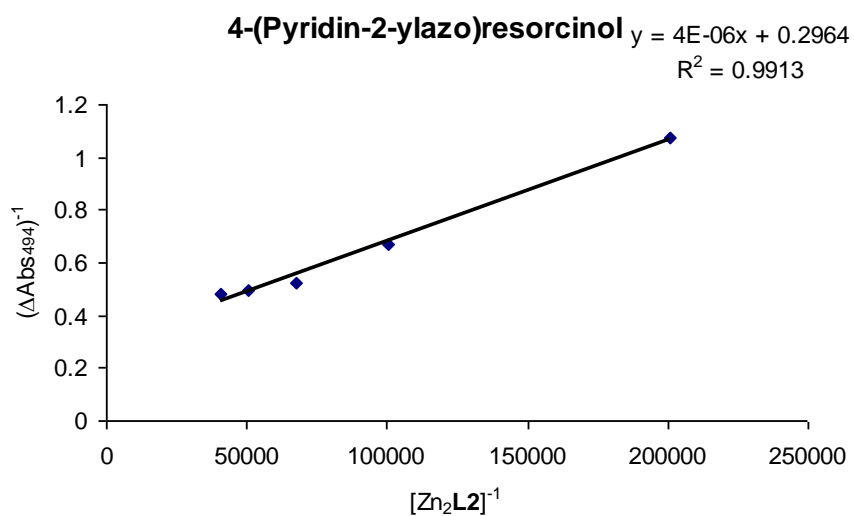
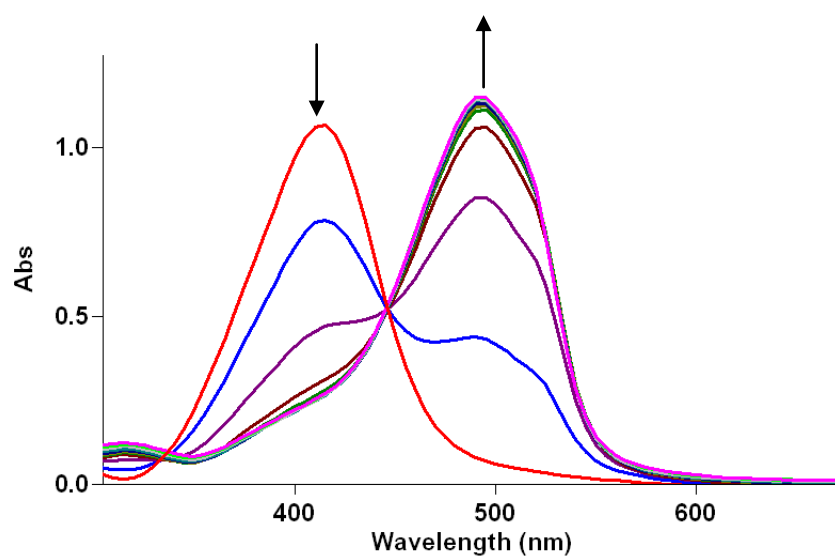


Figure 3 B.2 Titration of 4-(Pyridin-2-ylazo)resorcinol (**PAR**) with Zn_2L_2 (top). Arrows designate the direction of change upon addition of Zn_2L_2 to the **PAR** solution. Benesi-Hildebrand plot (bottom) of spectral data points (blue diamonds) and the linear regression function (black line) used for calculation of the dissociation constant respective to **PAR** and Zn_2L_2 .

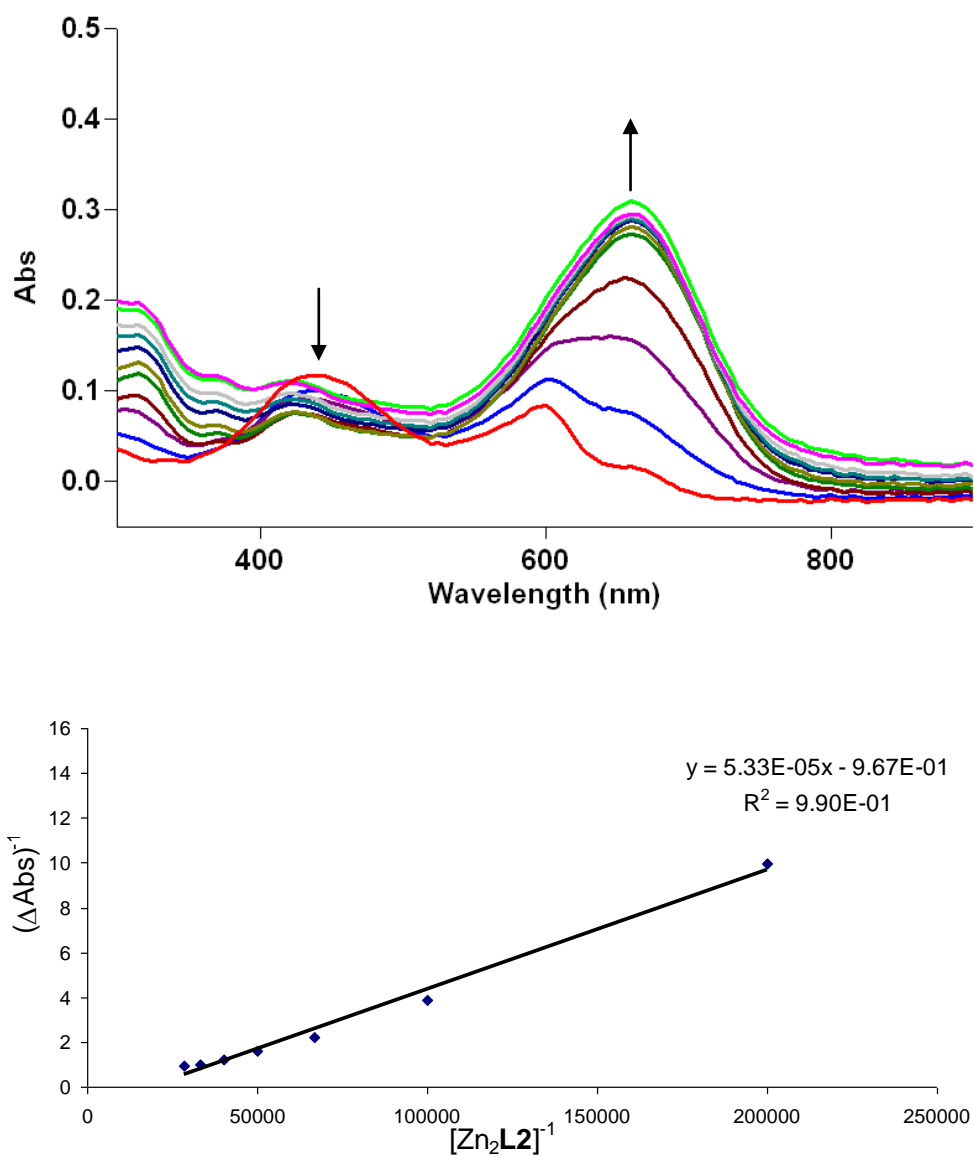
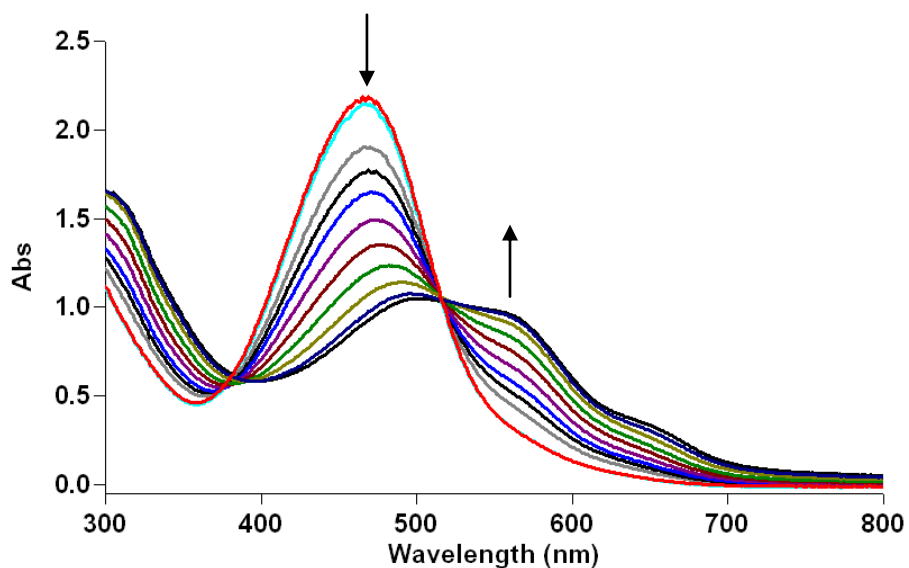


Figure 3 B.3 Titration of Pyrocatechol Violet (**PV**) with Zn_2L_2 (top). Arrows designate the direction of change upon addition of Zn_2L_2 to the **PV** solution. Benesi-Hildebrand plot (bottom) of spectral data points (blue diamonds) and the linear regression function (black line) used for calculation of the dissociation constant respective to **PV** and Zn_2L_2 .



Zincon

$$y = 8E-05x - 0.144$$

$$R^2 = 0.9902$$

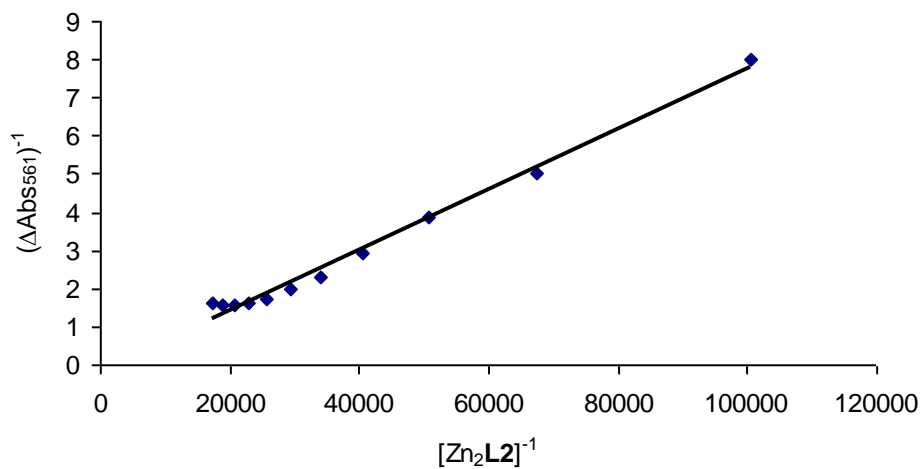


Figure 3 B.4 Titration of Zincon (**ZC**) with Zn_2L_2 (top). Arrows designate the direction of change upon addition of Zn_2L_2 to the **ZC** solution. Benesi-Hildebrand plot (bottom) of spectral data points (blue diamonds) and the linear regression function (black line) used for calculation of the dissociation constant respective to **ZC** and Zn_2L_2 .

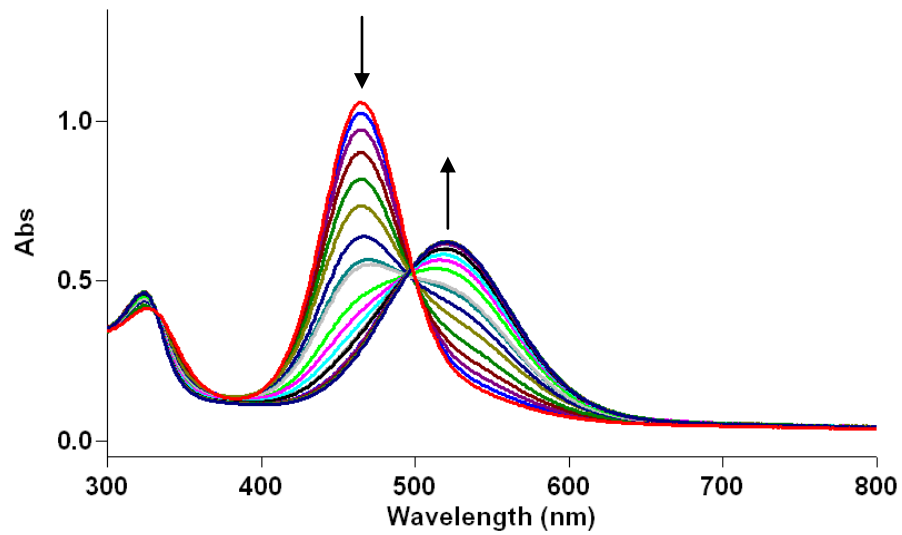


Figure 3 B.5 Titration of **MX/Zn₂L₂** with pyrophosphate. Arrows designate the direction of change upon addition of pyrophosphate to the solution.

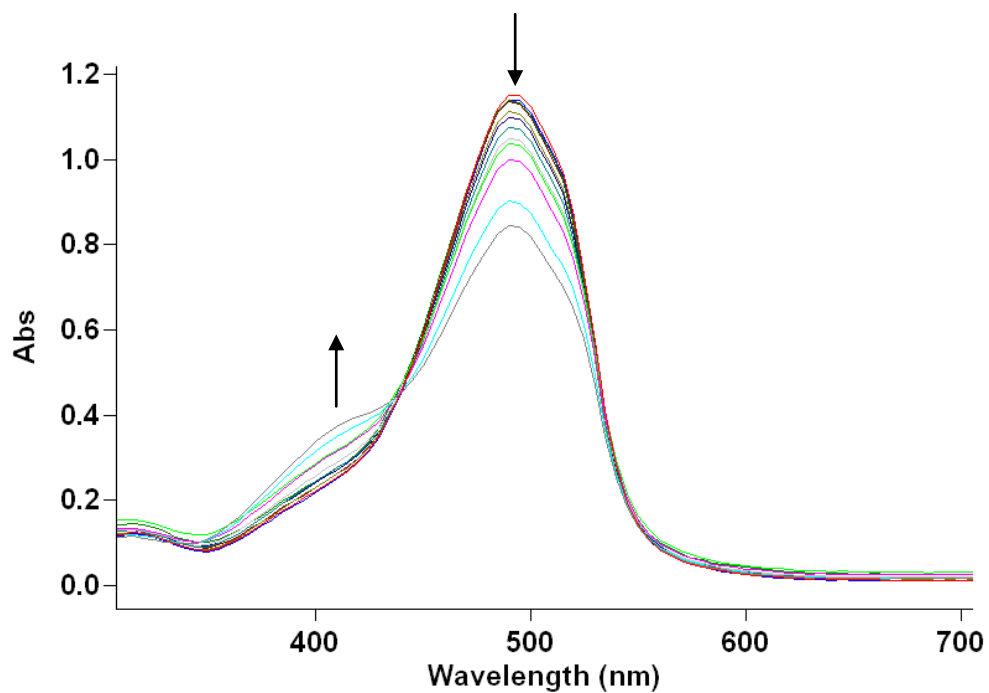


Figure 3 B.6 Titration of **PAR/Zn₂L₂** with pyrophosphate. Arrows designate the direction of change upon addition of pyrophosphate to the solution.

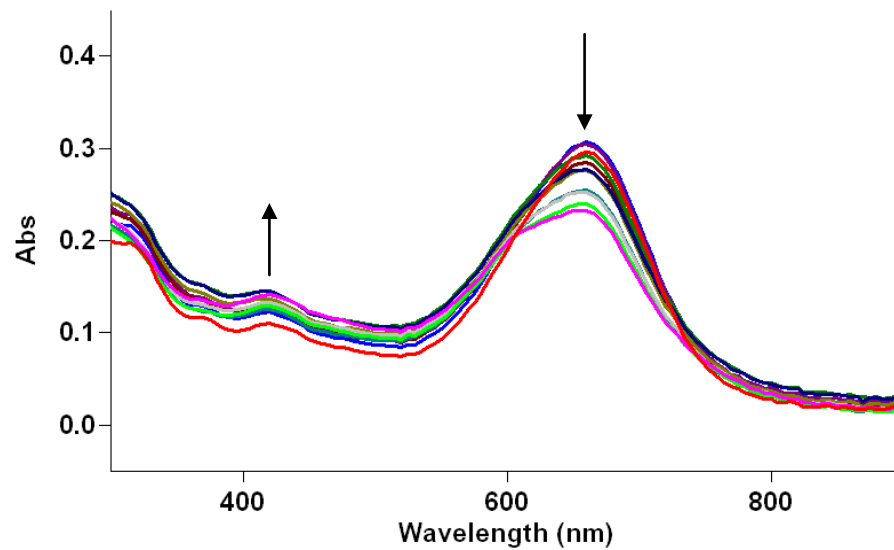


Figure 3 B.7 Titration of **PV/Zn₂L₂** with pyrophosphate. Arrows designate the direction of change upon addition of pyrophosphate to the solution.

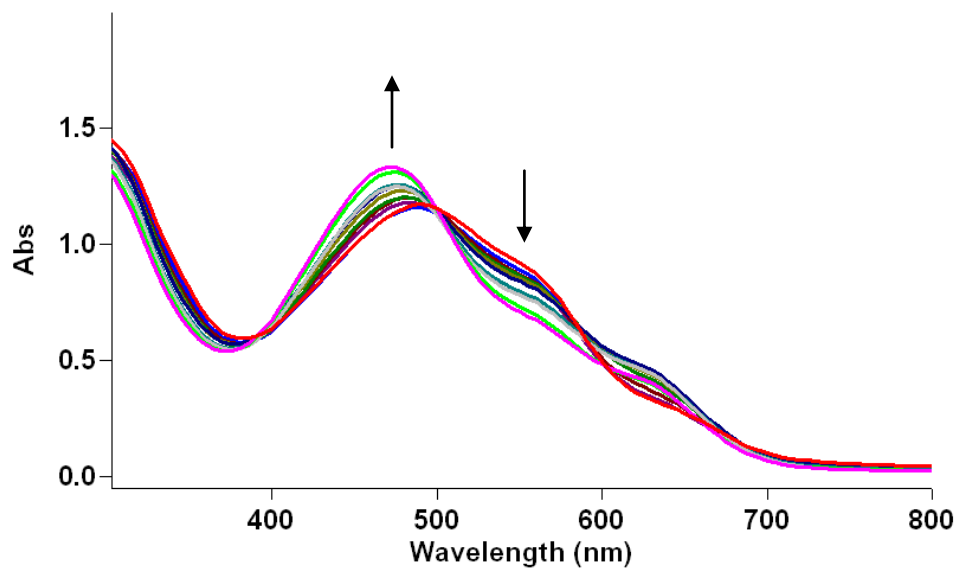


Figure 3 B.8 Titration of **ZC/Zn₂L₂** with pyrophosphate. Arrows designate the direction of change upon addition of pyrophosphate to the solution.

CHAPTER FOUR

METAL ION DETECTION BY LUMINESCENT 1,3-BIS(DIMETHYLAMINO METHYL) PHENYL RECEPTOR-MODIFIED CHROMOPHORES AND CRUCIFORMS

4.1 Introduction

The interaction of metal ions with ligand-modified chromophores / fluorophores can be exploited for the formation of well-ordered, optically active coordination polymers or for spectroscopic metal ion detection. In the field of metal ion sensing, fluorophores are often modified with specialized multidentate ligands that selectively bind a target ion by specific binding site size / shape and electronics.¹⁻¹⁵ For example, 2,2'-bis(2-picolyl)amino derivatives are often used for Zn²⁺ sensors,⁶⁻¹² and bis(2-aminophenoxy)ethane-*N,N,N',N'*-tetraacetic acid (**BAPTA**) is used in popular commercial Ca²⁺ biosensors.¹³⁻¹⁵

The multi-step syntheses often required to prepare such ligand-fluorophore constructs slows sensor development and increases the cost of chemosensors. We recently reported our efforts to prepare selective sensors featuring simpler, more promiscuous ligand motifs such as 2,2'-bipyridyl (**bipy**).¹⁶ In that example, a 1:1 ligand-metal binding was mediated by strategic placement of sterically encumbered substituents, and selectivity for Zn²⁺ was derived from its closed-shell d¹⁰ electronic configuration.

In the current study, we continue to explore the potential utility of simpler ligand sets for metal ion sensing by preparing several 1,3-bis(dimethylaminomethyl)phenyl-modified chromophores / fluorophores (**Figure 4.1**). Dimethylaminomethyl substituents were selected to be weakly metal-binding moieties that are synthetically trivial to incorporate into various platforms. These units are also attractive because they do not exhibit an elaborate predefined binding pocket or ligand set designed for a specific metal ion. It is important to note that the amino group is insulated from the π -system by an intervening methylene, such that the N lone pair cannot participate directly with the chromophore π -system via n- π interactions.

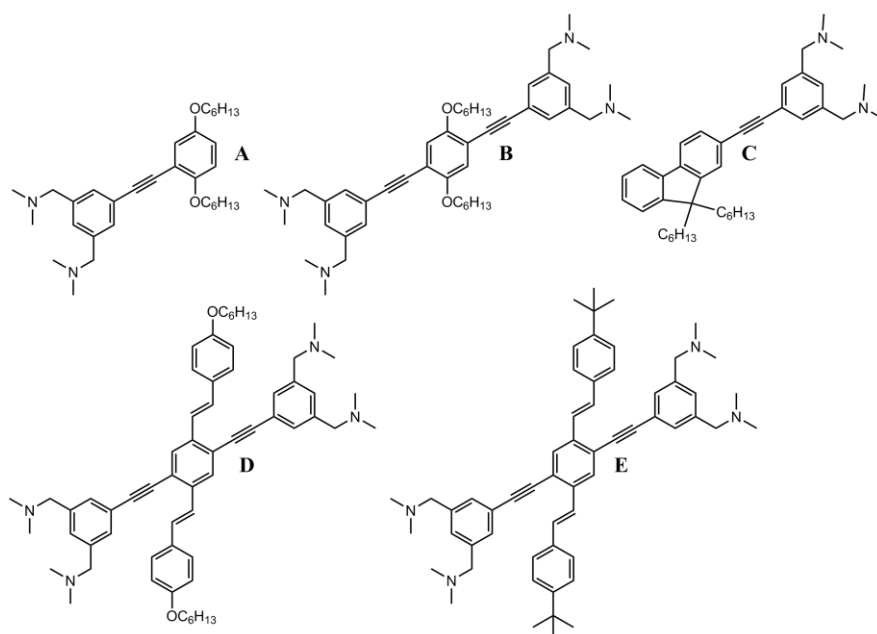


Figure 4.1 Structures of the 1,3-bis(dimethylaminomethyl)phenyl-substituted chromophores studied herein.

Ratiometric fluorescence sensors could thus be accomplished through the inductive perturbation of the π -system rather than quenching, which is often observed when a metal ion coordinates an atom that forms a part of the π -system. Selectivity for metal ions may be accomplished if different metal ions perturb the N lone pairs to different extents relative to the appended π -system and will depend on the relative energies of the π , π^* and nonbonding nitrogen lone pair orbital. Turn-on fluorescent sensors, for example, could be accomplished when the orbitals are of appropriate energies for a photoinduced electron transfer (**PET**)-type mechanism.

Because our group's main interests lie in π -conjugated polymer (**CP**) based sensors, chromophores representing small sections of common **CPs** were selected for initial screening (**Figure 4.1**). Both the conjugation length and the electronic properties of the chromophores were varied in order to access a wider range of π -system energies.

Compound **A** is a short π -system with electron-releasing hexyloxy substituents, while the other short π -system in **C** is more electron deficient. Compound **B** was designed as an analogue of **A** with a longer effective conjugation length and an additional metal binding arm. Compounds **D**, with electron-releasing hexyloxy groups, and less electron-rich **E** are examples of cross-conjugated molecules sometimes called cruciforms. Of particular importance for sensing are the Bunz-type cruciforms comprising a 1,4-distyrylbenzene branch whose π -system overlaps that of a 1,4-di(2-arylethynyl)benzene at a shared central aryl ring (**Figure 4.2**).¹⁷

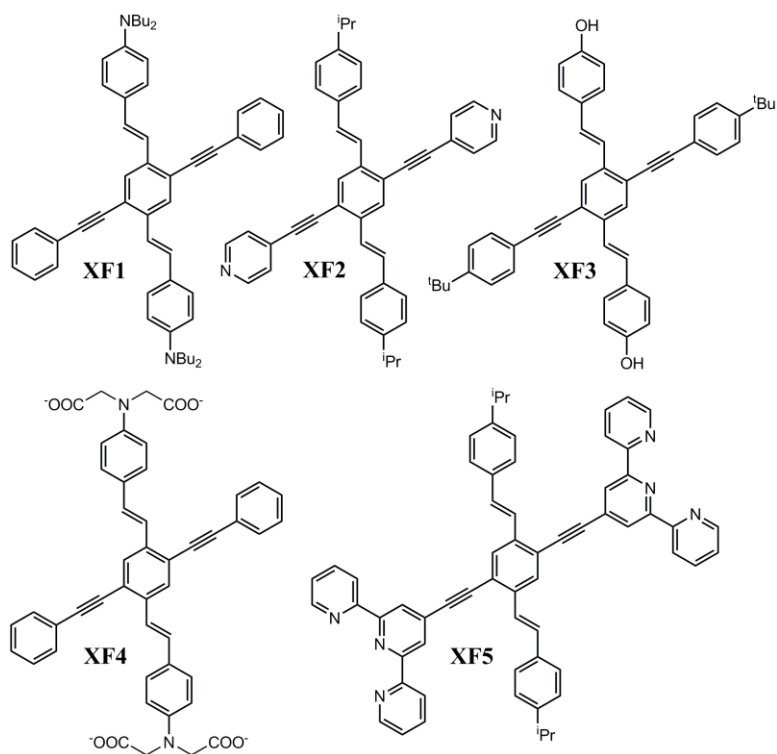
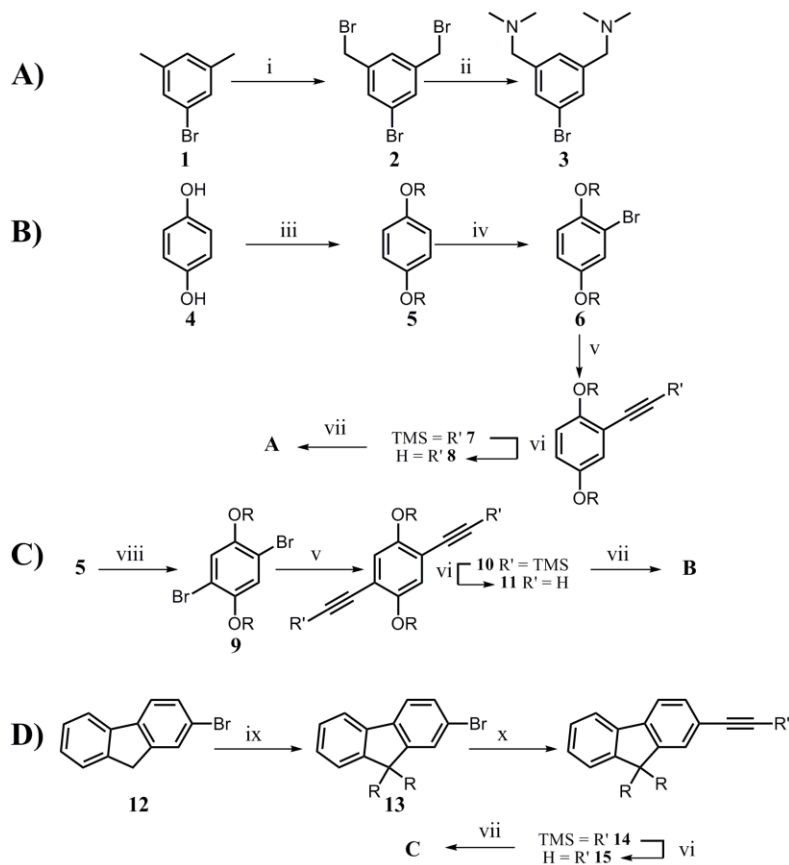


Figure 4.2 Some cruciforms that have been used as fluorescent sensors.

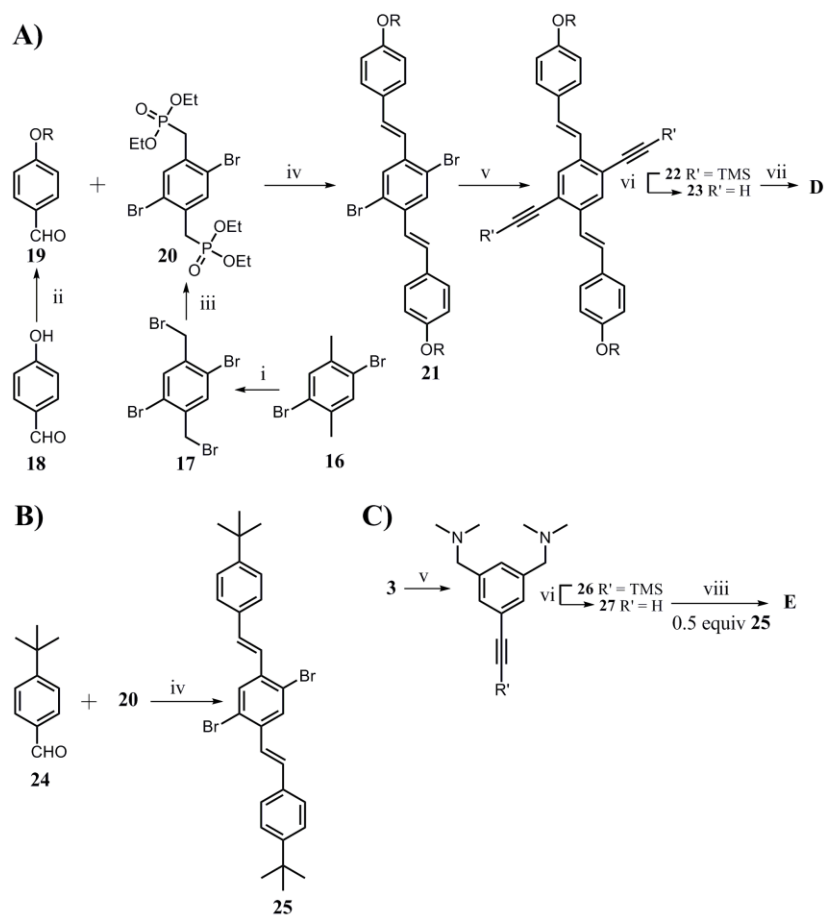
The presence of two cross-conjugated π -systems in such molecules can lead to geometrically separate HOMO and LUMO and consequent possibility for intramolecular charge transfer bands in the absorption spectra. Bunz's group has demonstrated how the unique nature of these π -systems makes them outstanding candidates for metal ion sensing when modified with ligands. The two cruciforms are of interest in the current context primarily for comparison to the metal-ion sensing ability of compound **B**, which has a similar π -system to the ethynylene-containing cruciform branches, and to accomplish ratiometric fluorescence signal transduction.

The current work describes the synthesis of dimethylaminomethyl-derivatized cruciforms **D** and **E** and of single-branch compounds **A** - **C** with accompanying photophysical characterization, metal ion response studies and density functional theory (**DFT**) calculations. Ratiometric and fluorescence intensity enhancement (**'turn-on'**) sensors for Zn^{2+} and Cu^{2+} are discussed.

4.2 Synthesis and Characterization



Scheme 4.1 Preparation of compound **A**, **B** and **C**. A) Preparation of **3**: i. *N*-bromosuccinimide, benzoyl peroxide, CHCl_3 , Δ . ii. Dimethylamine, THF. B) Preparation of **A**: iii. Hexylbromide, K_2CO_3 , CH_3CN , Δ . iv. 1.1 equiv Br_2 , CHCl_3 . v. Trimethylsilylacetylene, $\text{Pd}(\text{PPh}_3)_4$, CuI, triethylamine, toluene, 85°C . vi. NaOH (20% aq.), THF, MeOH. vii. **3**, $\text{Pd}(\text{PPh}_3)_4$, CuI, triethylamine, DMF, 85°C . C) Preparation of **B**: viii. 2.2 equiv Br_2 , CH_2Cl_2 . D) Preparation of **C**: ix. Hexylbromide, KOH, DMSO, Δ . x. Trimethylsilylacetylene, $\text{Pd}(\text{PPh}_3)_4$, CuI, diisopropylamine, 85°C . R = *n*-hexyl in all cases.



Scheme 4.2 Preparation of compound **D** and **E**. A) Preparation of **D**: i. *N*-bromosuccinimide, benzoyl peroxide, CHCl_3 , Δ . ii. Hexylbromide, K_2CO_3 , CH_3CN , Δ . iii. Triethylphosphite, 90°C , Δ . iv. Potassium *t*-butoxide, THF. v. Trimethylsilylacetylene, $\text{Pd}(\text{PPh}_3)_4$, CuI, triethylamine, toluene, 85°C . vi. TBAF, THF. vii. **3**, $\text{Pd}(\text{PPh}_3)_4$, CuI, triethylamine, DMF, 85°C . B-C) Preparation of **E**: viii. **25**, $\text{Pd}(\text{PPh}_3)_4$, CuI, triethylamine, DMF, 85°C .

The synthesis of compound **A** proceeded as shown in **Scheme 4.1A - B**. Commercial 5-bromo-*m*-xylene (**1**) underwent two-fold benzylic bromination to yield **2**

(27%). Condensation of **2**¹⁸ with aqueous dimethylamine provided key intermediate **3** (50%),¹⁸ which eventually served as the ligand-appended subunit for all compounds **A** - **E**. The first step in preparing the second fragment of **A** was condensation of hydroquinone (**4**) with 1-bromohexane to give **5** (60%).¹⁹ Although the next intermediate, **6**, was previously prepared from 1,4-dibromo-2,5-dihexyloxybenzene via single lithium-halogen exchange at low temperature followed by acid workup,²⁰ we found that **6** was more conveniently prepared in 33% yield by slow addition (over 12 h via syringe pump) of a solution of bromine in chloroform to **5** at room temperature. This route eliminates a step, and does not require dry ice cooling or use of a pyrophoric organolithium reagent. Sonogashira-Miyaura type coupling of trimethylsilylacetylene (**TMSA**) and **6** provided **7** (86%) that was deprotected by NaOH in water / THF / methanol (1:2:1) to give **8** (80%). Finally, compound **A** was prepared in 46% yield by Sonogashira-Miyaura type coupling of **3** and **8**.

Compound **B** was prepared by the sequence shown in **Scheme 4.1C**. Bromination of **5** gave **9** (80%),¹⁹ which readily underwent double Sonogashira-Miyaura coupling with **TMSA** to give **10** (68%) that was subsequently deprotected by NaOH in water / THF to give **11** (90%).²¹ Sonogashira-Miyaura coupling of **11** and **3** provided **B** (46%).

The first step in the preparation of fluorene derivative **C** (**Scheme 4.1D**) was alkylation of commercial 2-bromofluorene with 1-bromohexane in DMSO with KOH acting as the base to yield **13** (71%).²² Sonogashira-Miyaura coupling of **13** and **TMSA** gave **14** (64%) that was subsequently deprotected by NaOH in water /

methanol / THF (1:2:1) yielding **15** (95%).²² Finally, Sonogashira-Miyaura coupling of **15** and **3** produced **C** (46%) as a yellow oil.

Cruciform **D** was prepared as outlined in **Scheme 4.2A**. Two-fold benzylic bromination of 2,5-dibromo-*p*-xylene (**16**) gave **17** (56%)²³ that was then subjected to a Michaelis-Arbuzov reaction with triethylphosphite to give Horner-Wittig precursor **20** (95%).²⁴ Condensation of 1-bromohexane with 4-hydroxybenzaldehyde (**18**) gave **19** (96%),²⁵ the aldehyde required for Horner-Wittig condensation with **20** in the presence of KO^tBu to install the first π -system in **21** (54%). The Horner variation of the classic Wittig condensation was selected to favour the desired all-*E* isomeric olefins,²⁶ as confirmed by the diagnostic coupling constant between olefinic protons in the ¹H NMR spectrum.²⁷ Sonogashira-Miyaura coupling of **21** and TMSA gave **22** (48%), which was readily deprotected by tetrabutylammonium fluoride (**TBAF**) to yield **23** (88%). Sonogashira-Miyaura coupling of **22** and **3** gave target **D** (86%) as a fluorescent, pale yellow solid.

The second cruciform, **E**, was prepared in a manner analogous to that used to prepare **D**, but employing 4-*t*-butyl benzaldehyde (**24**) in place of **19** (**Scheme 4.2B - C**). Proton and carbon-13 NMR spectra for all non-commercial materials **1-27** and **A-E** are provided in the **appendix 4 A**.

4.3 Density Functional Theory (DFT) Calculations

The ground state HOMO and LUMO distributions for **A - E**, as determined by DFT calculations at the B3LYP/6-31G(d) level are shown in **Figure 4.3**. Because these are ground state calculations and are not time dependent, the most notable inference from these calculations is the geometric separation of the HOMO and LUMO in cruciforms **D** and **E**. In both cases, the HOMO is localized to large extent on the distyrylbenzene branches, whereas the LUMO is spread more equally over both branches of the cross-conjugated core. It is also noteworthy that in all of the neutral ground state molecules **A - E** the HOMO and LUMO are π and π^* in nature, respectively. The n-type nitrogen lone pair contributes primarily to the HOMO-1 (not shown in **Figure 4.3**) in the neutral ground state.

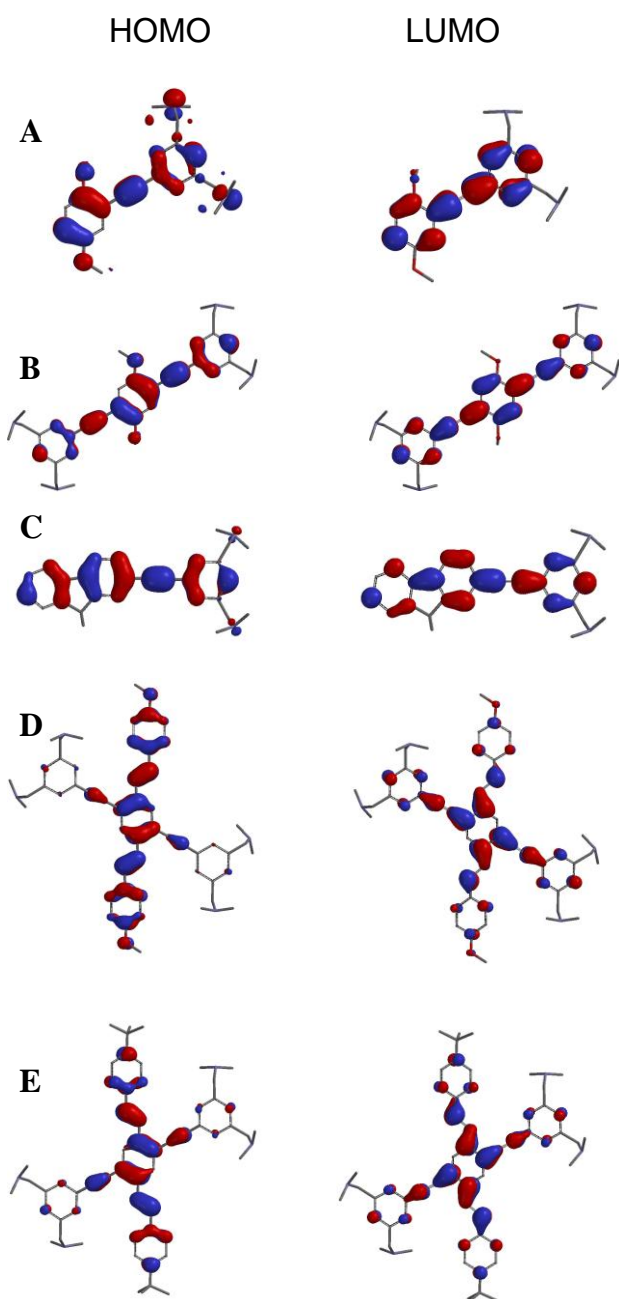


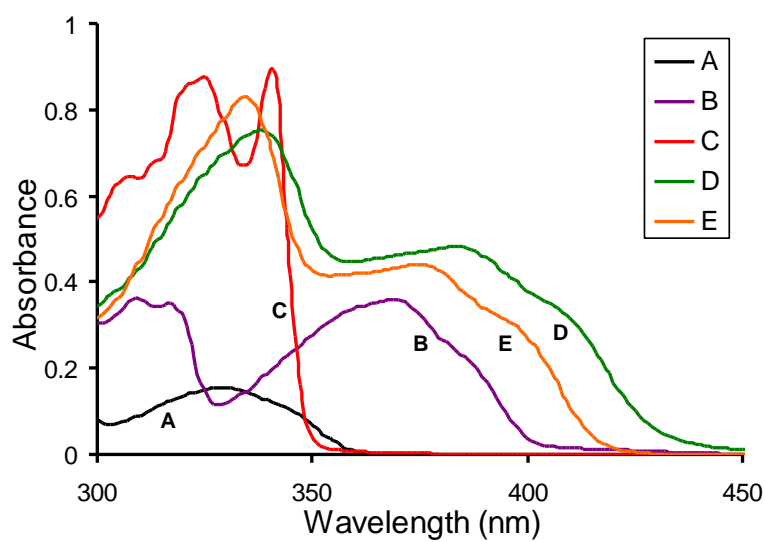
Figure 4.3 HOMO and LUMO parameters from DFT calculations (B3LYP-6-31G* level) for compounds **A** - **E**. Hexyl groups were truncated to methyl groups for the calculations.

4.4 Photophysical Studies and Calculations

The absorption and photoluminescence spectra of **A** - **E** are provided in **Figure 4.4**, with select photophysical properties summarized in **Table 4.1**. Probes **A** - **E** have a good range of emission wavelengths; strong emission anywhere from ~350 - 500 nm is obtainable by judicious selection of one of these probes. Access to probes with specific emission wavelengths is of interest for multidye fluorescence microscopy experiments, in which each dye can be observed separately if emission maxima are well-separated.

The dyes also have excellent molar absorptivities (ϵ , **Table 4.1**) on the order of $10^4 - 10^5 \text{ M}^{-1}\text{cm}^{-1}$. High molar absorptivity is a prerequisite for biosensing and environmental monitoring because it allows smaller amounts of dye to be used while retaining visual observability. Compounds **A**, **B**, **D** and **E** also have very high photoluminescence quantum yields (Φ , **Table 4.1**) of 0.48 - 0.64 in THF solution. Fluorene derivative **C**, on the other hand, has a rather low Φ of 0.075.

(A)



(B)

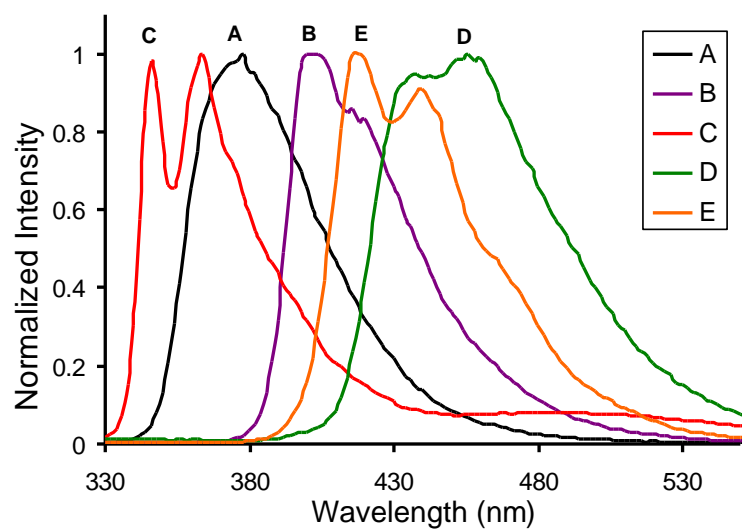


Figure 4.4 Absorption (A) and normalized fluorescence (B) spectra for A - E.

Table 4.1 Selected photophysical properties of **A - E** and effect of metal ion binding on photoluminescence properties.

	Metal – Free Chromophores				Metal Ion Response					
	Absorption		Fluorescence		Cu ²⁺			Zn ²⁺		
	λ_{abs}	log ϵ	λ_{em}	Φ	λ_{em}	$\Delta\lambda_{\text{em}}$	I/I ₀	λ_{em}	$\Delta\lambda_{\text{em}}$	I/I ₀
A	329	4.56	352	0.48	411	59	0.84	410	58	0.42
B	370	4.72	400	0.58	423	23	2.0	411	11	1.6
C	341	5.02	362	0.075	373	11	9.2	373	11	8.6
D	383	5.24	454	0.57	475	21	0.77	473	19	0.84
E	375	5.19	416	0.64	451	35	0.84	443	27	0.85

Once the beneficial photophysical properties of **A - E** had been established, a range of metal ions were screened as potential analytes for detection by photoluminescence spectroscopy in THF. Metal salts used for ion screening were Co(NO₃)₂·6H₂O, NiSO₄·6H₂O, Cu(ClO₄)₂·6H₂O, Zn(ClO₄)₂·6H₂O, Cd(ClO₄)₂·6H₂O, K(PF₆), Na(PF₆), Mg(SO₄), CaCl₂, Eu(NO₃)₃, [Cu(NCMe)₄][BF₄] and Hg(O₂CCF₃)₂. Of these metal ions, only Zn²⁺ and Cu²⁺ elicited notable photoluminescence changes in any of the molecules. Changes in emission intensity and maxima upon exposure to these ions are summarized in **Table 4.1**. The photoluminescence spectra shown in **Figure 4.5** demonstrate the progressive changes observed as up to one equiv of metal ion is added to **A - E**.

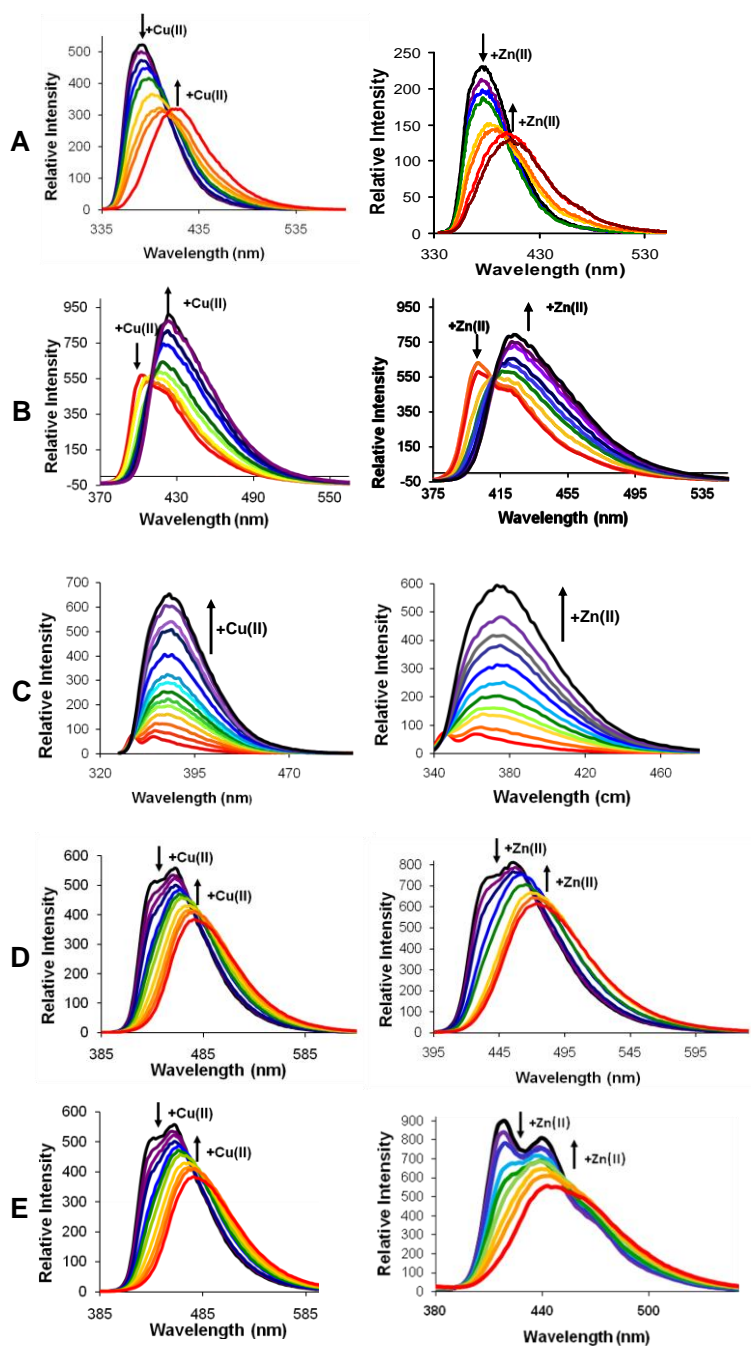


Figure 4.5 Metal ion response of compounds A - E.

Unfortunately, all of the molecules exhibited similar responses to both Zn^{2+} and Cu^{2+} , so these sensing platforms are not able to differentiate between the two ions under

the conditions employed. Interestingly, however, three distinct types of photoluminescence signal transduction were observed across the series.

The first signal transduction type, exemplified by **A**, **D**, and **E**, was a ratiometric response with concomitant emission quenching. Significant shifts in photoluminescence maxima ($\Delta\lambda_{em}$) to the red were achieved for **A**, **D** and **E** ($\Delta\lambda_{em} = 51, 21,$ and 35 nm, respectively), despite the fact that the N lone pairs with which the metal ions interact are insulated from the chromophore subunit by a methylene spacer. It can be inferred that the origin of the shift, then, is predominantly inductive in nature. Similar red-shifting of photoluminescence maxima was observed in phosphorus-derivatised cruciforms when appended substituents become more electron withdrawing.²⁸

A second type of signal transduction is a red-shifting ratiometric response similar to that observed for **A**, **D** and **E**, but with attendant emission enhancement. This dual ratiometric / turn-on type response was only exhibited by **B**. The $\Delta\lambda_{em}$ of **B** (21 nm) is similar to that of **D** (23 nm), which also features electron donating alkoxy groups and a longer effective conjugation length than in alkoxy-substituted **A**. This qualitative observation makes sense in light of the relationship between metal-chromophore orbital energy matching and photophysical response of metal complexes of ligands appended to π -conjugated scaffolds.²⁹

Compound **C** is unique among the molecules screened in that it features the least electron rich π -system, utilizing a fluorenyl moiety rather than ethynylaryl or styryl π -system constituents. This is also the only molecule screened that exhibits a notable emission enhancement without a large red shift in emission maximum upon metal

binding. An approximate 9-fold increase in integrated emission intensity was observed upon binding either Zn^{2+} or Cu^{2+} . A photoinduced electron transfer (PET) mechanism, similar to that exhibited by other amine-based Zn sensors,⁶⁻¹² is likely responsible for the turn-on response of **C**.

4.5 Conclusion

We have synthesized a series of easily-prepared materials **A - E** derivatized with a robust ligating unit. Several chromophore subunits of contemporary interest have been incorporated into these molecules, including phenylenevinylene, phenylene ethynylene and fluorene moieties. Cross-conjugated cruciforms, a class of materials of escalating importance in chemical sensing, have also been examined.

All of these molecules show a photoluminescence response to Zn^{2+} or Cu^{2+} over other common metal ions screened, although these two ions could not be differentiated from one another. Despite the inability of **A - E** to differentiate between Zn^{2+} and Cu^{2+} , the simple ligating units and modular approach to sensor assembly described herein should be attractive to others wishing to produce metal ion responsive materials. This simple strategy has also yielded materials capable of commercially viable ratiometric shifts in photoluminescence and emission turn-on magnitudes. The incorporation of other simplified ligand units into small molecules and extension to π -conjugated polymer analogues are currently being pursued in our laboratory.

4.6 Experimental Section

Reagents and General Methods

Reagents and solvents for extractions and chromatography were used as received from Acros, Aldrich Chemical Co., TCI America, or Alfa Aesar. Compound **2**, **3**, **26** and **27**;¹⁸ **5** and **9**;¹⁹ **6**;²⁰ **10** and **11**;²¹ **13**, **14** and **15**;²² **17**;²³ **19**;²⁵ **20**;²⁴ and [Pd(PPh₃)₄]³⁰ were prepared as previously reported. Synthetic avenues are summarized in **Schemes 4.1** and **4.2**. All solvents for reactions were purified by passage through alumina columns under a N₂ atmosphere employing an MBraun solvent purification system. All the air sensitive reactions were performed in an MBraun dry box or using standard Schlenk techniques under a N₂ atmosphere. Proton, carbon-13 and phosphorous-31 NMR spectra were acquired on a Bruker Avance 300 spectrometer operating at 300, 75 and 121 MHz, respectively. All spectra were collected at 25 °C and referenced to trimethylsilane or residual solvent peak for proton and carbon-13, and to external 85% phosphoric acid for phosphorus-31.

General Spectroscopic Methods

Absorption spectra were recorded on a Varian Cary 50 Bio UV-vis spectrophotometer. Photoluminescence (**PL**) spectra were recorded using a Varian Eclipse spectrofluorimeter. Samples for all absorption and photoluminescence spectra were prepared in HPLC grade tetrahydrofuran further purified in a MBraun Solvent Purification System. Absorption and photoluminescence spectra were recorded on samples in spectrosil quartz cuvettes (Starna Cells, Inc.) having a path length of 1 cm. Quantum yield (Φ) for all compounds were calculated relative to quinine bisulfate in 0.1

M H₂SO₄ (aq) ($\Phi = 0.546$).³¹ Metal salts used for ion screening were Co(NO₃)₂·6H₂O, NiSO₄·6H₂O, Cu(ClO₄)₂·6H₂O, Zn(ClO₄)₂·6H₂O, Cd(ClO₄)₂·6H₂O, K(PF₆), Na(PF₆), Mg(SO₄), CaCl₂, Eu(NO₃)₃, [Cu(NCMe)₄][BF₄] and Hg(O₂CCF₃)₂.

CAUTION: perchlorate salts are potentially explosive and should only be handled in small quantities by trained personnel familiar with their hazards.

Absorption spectroscopic titrations with metal ions

A 3.0 mL aliquot of the compound of interest in THF (1.0×10^{-5} M for **A**, **B** and **D**; 1.6×10^{-5} M for **C**; 6.1×10^{-6} for **E**) was added to a cuvette. Aliquots of metal ion solution were added to the solutions and changes were followed by collecting an absorption spectrum after each addition.

Photoluminescence spectroscopy titrations with metal ions

As for absorption titration, but using solutions diluted by 10-fold and following titrations by photoluminescence spectroscopy with $\lambda_{\text{ex}} = \lambda_{\text{max}}$

Synthesis of 3,5-bis(bromomethyl)-bromobenzene (2)

A sample of 5-bromo-*m*-xylene **1** (20.00 g, 105.8 mmol), N-bromosuccinamide (41.50 g, 233.0 mmol) and benzoylperoxide (BPO) (2.470 g, 10.20 mmol) were dissolved in chloroform (600 mL) and refluxed overnight. After cooling to room temperature, reaction mixture was extracted with water (3×100 mL) and organic layer was removed under reduced pressure. White crystalline solid was precipitated out while keeping the yellow oil residue on room temperature. Remaining oil was decanted out; 5 mL of methanol was added into it and left for recrystallization. White solid was washed with methanol (3×5 mL) (10 g, 27%). Observed Melting point 97.5 °C; Literature melting

point 95-98 °C. ¹H NMR (300 MHz, CDCl₃): δ = 4.426 (s, 4H; CH₂), 7.359 (s, 1H; Aromatic), 7.495 (d, 2H; *J* = 1.5 Hz, Aromatic).

Synthesis of 3,5-bis[(dimethylamino) methyl] bromobenzene (3)

A sample of 3,5-bis(bromomethyl)-bromobenzene **2** (5.00 g, 14.5 mmol) was dissolved in THF (20 mL) and dimethyl amine (6.60 g, 145 mmol) was added into it. Reaction mixture was stirred at room temperature for 2 d. Dimethylammonium bromide salt was filtered off and volatiles were removed under reduced pressure, yielding colorless oil. Dichloromethane (50 mL) was added and solution was washed by saturated aq. Na₂CO₃ (3 × 50 mL). Organic layer was collected, dried over Na₂SO₄ and removed under reduced pressure, yielding a viscous colorless oil (2.00 g, 50.0%). ¹H NMR (300 MHz, CDCl₃): δ = 2.245 (s, 12H; N-CH₃), 3.385 (s, 4H; N-CH₂), 7.191 (s, 1H; Aromatic), 7.382 (d, 2H; *J* = 1.2, Aromatic).

Synthesis of 1,4-bis(hexyloxy) benzene (5)

Hydroquinone **4** (25.0 g, 227 mmol) was dissolved in acetonitrile (300 mL) and K₂CO₃ (80.5 g, 582 mmol) was added into it. Hexylbromide (112 g, 681 mmol) was added dropwise to the heated solution and refluxed overnight. While the reaction was hot, K₂CO₃ was filtered off and volatiles were removed under reduced pressure. Residue was dissolved in minimum amount of DCM and added dropwise into 400 mL of methanol and left for recrystallization. Solid was filtered off and recrystallized again yielding pure off white solid flakes (38 g, 60%). ¹H NMR (300 MHz, CDCl₃): δ = 0.946 (t, 6H; *J* = 6.9 Hz, 2 × CH₃), 1.514 - 1.323 (m, 12H; 6 × CH₂), 1.818 (q, 4H; *J* = 6.6 Hz, 2 × CH₂), 3.941 (t, 4H; *J* = 6.6 Hz, 2 × O-CH₂), 6.840 (s, 4H; Aromatic).

Synthesis of 2-Bromo-1,4-bis(hexyloxy) benzene (6)

A sample of 1,4-bis(hexyloxy) benzene **5** (10 g, 36 mmol) was dissolved in CHCl₃ (120 mL) and 2 mL bromine (6.3 g, 39.6 mmol) in CHCl₃ (8 mL) was added dropwise into it through syringe pump for 12 h at room temperature. Reaction mixture was quenched with saturated Na₂SO₃ solution followed by extraction with H₂O (4 × 100 mL). Organic layer was collected, dried over Na₂SO₄ and removed under reduced pressure, yielding viscous oil. Column chromatography was done in pure hexane to purify the crude (4.2 g, 33%). ¹H NMR (300 MHz, CDCl₃): δ = 0.93 (t, 6H; *J* = 7.0 Hz, 2 × CH₃), 1.54 - 1.32 (m, 12H; 6 × CH₂), 1.87 – 1.72 (m, 4H; 2 × CH₂), 3.90 (t, 2H; *J* = 6.0 Hz, O-CH₂), 3.97 (t, 2H; *J* = 6.0 Hz, O-CH₂), 6.86 – 6.78 (m, 2H; Aromatic), 7.13 (d, 1H; *J* = 2.0 Hz, Aromatic). ¹³C NMR (75 MHz, CDCl₃): δ = 14.0, 22.6, 25.6, 29.2, 29.2, 31.5, 31.5, 68.8, 70.2, 112.7, 114.3, 114.7, 119.4, 149.7, 153.5.

Synthesis of (2-(2,5-bis(hexyloxy) phenyl)ethynyl) trimethylsilane (7)

Under nitrogen, compound **6** (2.0 g, 5.6 mmol) was dissolved in toluene (20 mL) followed by addition of [Pd(PPh₃)₄] (0.036 g, 0.30 mmol) and copper iodide (0.064 mg, 0.30 mmol). Trimethylsilylacetylene (1.1 g, 11 mmol) was dissolved in triethylamine (20 mL) separately and added dropwise into the reaction mixture and stirred for 48 h at 85 °C. The reaction mixture was passed through silica, followed by washing with ether (70 mL). The organic layer was extracted with sat'd aqueous sodium bicarbonate (4 × 100 mL), dried over sodium sulfate, and all volatiles were removed under reduced pressure. The residue was triturated with 20 mL pentane, and the pentane-soluble fraction was concentrated under reduced pressure, yielding **7** as a light yellow viscous oil (1.8 g,

86%). ^1H NMR (300 MHz, CDCl_3): δ = 0.27 (s, 9H; $3 \times \text{Si-CH}_3$), 0.90 – 0.95 (m, 6H; $2 \times \text{CH}_3$), 1.57 – 1.32 (m, 12H; $6 \times \text{CH}_2$), 1.86 – 1.71 (m, 4H; $2 \times \text{CH}_2$), 3.97 (t, 2H; J = 6.0 Hz, O- CH_2), 3.90 (t, 2H; J = 6.0 Hz, O- CH_2), 6.85 – 6.76 (m, 2H; Aromatic), 6.98 (d, 1H; J = 3.0 Hz, Aromatic). ^{13}C NMR (75 MHz, CDCl_3): δ = 0.0, 14.0, 14.0, 22.6, 22.6, 25.7, 25.7, 29.2, 29.4, 31.5, 31.6, 68.6, 69.6, 98.1, 101.4, 113.3, 114.0, 116.9, 118.6, 152.6, 154.6.

Synthesis of 2-ethynyl-1,4-bis(hexyloxy) benzene (8)

Compound **7** (0.3 g, 0.8 mmol), was dissolved in THF (20 mL) followed by addition of methanol (10 mL) and 20% aqueous NaOH solution (10 mL) and stirred for 2 h at room temperature. Ether (30 mL) was added into it, and extracted with water (4×50 mL). Organic layer was dried over sodium sulfate and removed under reduced pressure, yielding viscous oil (0.19 g, 80%). ^1H NMR (300 MHz, CDCl_3): δ = 0.92 (t, 6H; J = 6.0 Hz, $2 \times \text{CH}_3$), 1.52 – 1.32 (m, 12H; $6 \times \text{CH}_2$), 1.84 – 1.72 (m, 4H; $2 \times \text{CH}_2$), 3.26 (s, 1H; $\text{C}\equiv\text{CH}$), 3.91 (t, 2H; J = 6.0 Hz, O- CH_2), 4.00 (t, 2H; J = 6.0 Hz, O- CH_2), 6.89 – 6.80 (m, 2H; Aromatic), 7.01 (d, 1H; J = 3.0 Hz, Aromatic). ^{13}C NMR (75 MHz, CDCl_3): δ = 14.0, 22.6, 25.6, 25.7, 29.2, 29.2, 31.5, 68.7, 69.7, 80.1, 80.7, 112.3, 113.9, 117.0, 119.2, 152.6, 154.6.

Synthesis of Compound A

Under nitrogen, compound **3** (0.57 g, 2.1 mmol) was dissolved in *N,N*-dimethylformamide (DMF, 40 mL) followed by addition of $[\text{Pd}(\text{PPh}_3)_4]$ (0.13 g, 0.13 mmol) and copper iodide (0.024 g, 0.13 mmol). Compound **8** (0.70 g, 2.3 mmol) was dissolved in triethylamine (20 mL) separately and added dropwise to the reaction mixture

and stirred for 48 h at 85 °C. Reaction mixture was passed through silica, followed by washing with ether (20 mL). Organic layer was extracted with sat'd sodium bicarbonate solution (4 × 100 mL) followed by extraction with 50% aqueous HCl solution (3 × 50 mL) and finally aqueous layer was neutralized with NaOH pellets. This aqueous layer was extracted with ether (3 × 30 mL). Organic layer was dried over sodium sulfate and removed under reduced pressure. Column chromatography eluting with pentane through basic alumina (previously treated with triethylamine in ether then dried) afforded the product as a brown oil (0.12 g, 46%). ¹H NMR (300 MHz, CDCl₃): δ = 0.90 (m, 6H; 2 × CH₃), 1.59 – 1.33 (m, 12H; 6 × CH₂), 1.87 – 1.75 (m, 4H; 2 × CH₂), 2.26 (s, 12H; 4 × N-CH₃), 3.42 (s, 4H; 2 × N-CH₂), 3.93 (t, 2H; *J* = 6.0 Hz, O-CH₂), 4.03 (t, 2H; *J* = 6.0 Hz, O-CH₂), 6.84 (t, 2H; *J* = 3.0 Hz, Aromatic), 7.02 (m, 1H; Aromatic), 7.27 (s, 1H; Aromatic), 7.40 (d, 2H; *J* = 3.0 Hz, Aromatic). ¹³C NMR (75 MHz, CDCl₃): δ = 14.0, 14.0, 22.6, 22.6, 25.7, 25.8, 29.2, 29.4, 31.5, 31.6, 45.3, 63.9, 68.7, 69.8, 85.7, 93.3, 113.7, 114.2, 116.5, 118.3, 123.3, 129.6, 130.9, 139.1, 152.8, 154.0. HRMS (M+H)⁺: calc'd for C₃₂H₄₉O₂N₂: 493.3794; found, 493.3790.

Synthesis of 2,5-dibromo-1,4-bis(hexyloxy) benzene (9)

Compound **5** (20.0 g, 72.0 mmol) was dissolved in DCM (150 mL) and reaction mixture was cooled to 0 °C. Br₂ (25.4 g, 158 mmol) was added dropwise into it and stirred overnight at room temperature. Excess of bromine was quenched with saturated Na₂SO₃ solution followed by extraction with H₂O (4 × 100 mL). Organic layer was collected, dried over Na₂SO₄ and removed under reduced pressure, yielding off white solid (28 g, 89%). ¹H NMR (300 MHz, CDCl₃): δ = 0.926 (t, 6H; *J* = 6.9 Hz, 2 × CH₃),

1.550 - 1.332 (m, 12H; 6 × CH₂), 1.820 (q, 4H; *J* = 6.9 Hz, 2 × CH₂), 3.965 (t, 4H; *J* = 6.6 Hz, 2 × O-CH₂), 7.104 (s, 2H; Aromatic). ¹³C NMR (75 MHz, CDCl₃): δ = 14.0, 22.5, 25.6, 29.0, 31.4, 70.3, 111.1, 118.4, 150.0.

Synthesis of 1,4-bis(hexyloxy)-2,5-bis(2-(trimethylsilyl)ethynyl) benzene (10)

Under nitrogen, compound **9** (2.0 g, 4.6 mmol) was dissolved in toluene (20 mL) followed by addition of tetrakis(triphenylphosphine) palladium(0) (0.58 g, 0.60 mmol) and copper iodide (0.10 g, 0.60 mmol). Trimethylsilylacetylene (1.8 g, 18 mmol) was dissolved in triethylamine (20 mL) separately and added dropwise into the reaction mixture and stirred for 48 h at 85 °C. Reaction mixture was passed through silica, followed by washing with ether (50 mL). Organic layer was extracted with sat. sodium bicarbonate solution (4 × 100 mL), dried over sodium sulfate and removed under reduced pressure. Residue was washed with methanol (20 mL), yielding a dark brown solid (1.5 g, 68%). ¹H NMR (300 MHz, CDCl₃): δ = 0.27 (s, 18H; 6 × Si-CH₃), 0.93 (t, 6H; *J* = 9.0 Hz, 2 × CH₃), 1.55 – 1.33 (m, 12H; 6 × CH₂), 1.80 (q, 4H; *J* = 6.0 Hz, 2 × CH₂), 3.96 (t, 4H; *J* = 6.0 Hz, 2 × O-CH₂), 6.91 (s, 2H; Aromatic). ¹³C NMR (75 MHz, CDCl₃): δ = 0.0, 14.0, 22.6, 25.7, 29.2, 31.6, 69.4, 100.0, 101.0, 113.9, 117.1, 153.9. Small resonances attributable to residual triphenylphosphine oxide were observed in the NMR spectra (Figures S14-15); these impurities were removed (by methanol rinse) after deprotection to form compound **11** (*vide infra*).

Synthesis of 1,4-diethynyl-2,5-bis(hexyloxy) benzene (11)

Compound **10** (1.9 g, 4.1 mmol), was dissolved in THF (100 mL) followed by the addition of methanol (40 mL) and 20 % aqueous NaOH solution (20 mL) and stirred for 2

h at room temperature. Ether (50 mL) was added into it, and reaction mixture was extracted with water (4 × 50 mL). Organic layer was collected, dried over sodium sulfate and removed under reduced pressure. Methanol (20 mL) was added into crude residue and stirred for 20 min. Solid ppt. was filtered and washed with methanol, yielding off white solid (1.2 g, 90%). ¹H NMR (300 MHz, CDCl₃): δ = 0.93 (t, 6H; *J* = 6.0 Hz, 2 × CH₃), 1.51 – 1.33 (m, 12H; 6 × CH₂), 1.82 (q, 4H; *J* = 6.0 Hz, 2 × CH₂), 3.35 (s, 2H; C≡CH), 3.99 (t, 2H; *J* = 6.0 Hz, 2 × O-CH₂), 6.97 (s, 2H; Aromatic). ¹³C NMR (75 MHz, CDCl₃): δ = 14.0, 22.5, 25.5, 29.0, 31.5, 69.6, 79.7, 82.4, 113.2, 117.7, 154.0.

Synthesis of Compound B

Under nitrogen, compound **3** (0.91 g, 3.3 mmol) was dissolved in DMF (40 mL) followed by the addition of [Pd(PPh₃)₄] (0.19 g, 0.20 mmol) and copper iodide (0.034 g, 0.20 mmol). Compound **11** (0.50 g, 1.5 mmol) was dissolved in triethylamine (20 mL) separately and added dropwise to the reaction mixture and stirred for 48 h at 85 °C. Reaction mixture was passed through silica followed by washing with ether (20 mL). Organic layer was extracted with sat'd sodium bicarbonate solution (4 × 100 mL) followed by extraction with 50% aqueous HCl solution (3 × 50 mL) and finally aqueous layer was neutralized with NaOH pellets. This aqueous layer was extracted with ether (3 × 30 mL). Organic layer was collected, dried over sodium sulfate and all volatiles were removed under reduced pressure. Residue was dissolved in minimum amount of pentane and allowed to stand at room temperature overnight, leading to the formation of yellow crystals. The solid was collected by filtration and dried to afford **B** (0.46 g, 46%). ¹H NMR (300 MHz, CDCl₃): δ = 0.92 (t, 6H; *J* = 6.0 Hz, 2 × CH₃), 1.63 – 1.37 (m, 12H; 6 ×

CH₂), 1.88 (q, 4H; $J = 6.0$ Hz, $2 \times$ CH₂), 2.27 (s, 24H; $8 \times$ N-CH₃), 3.43 (s, 8H; $4 \times$ N-CH₂), 4.05 (t, 4H; $J = 6.0$ Hz, $2 \times$ O-CH₂), 7.02 (s, 2H; Aromatic), 7.41 (d, 4H; $J = 3.0$ Hz, Aromatic). ¹³C NMR (75 MHz, CDCl₃): $\delta = 14.1, 22.6, 25.8, 29.3, 31.6, 45.4, 63.9, 69.6, 85.8, 94.9, 114.0, 117.1, 123.2, 129.8, 130.9, 139.2, 153.5$. HRMS (M+H)⁺: calc'd for C₄₆H₆₇O₂N₄: 707.5264; found, 707.5259.

Synthesis of 2-bromo-9,9-dihexyl-9-H-fluorene (13)

Compound **12** (6.80 g, 27.8 mmol) was dissolved in DMSO (20 mL) and KOH (15.6 g, 278 mmol) was added into it. Hexylbromide (11.0 g, 66.8 mmol) was added dropwise to the heated solution and refluxed overnight. Reaction mixture was dissolved in water (400 mL) and extracted with ethyl acetate (3×50 mL). Organic layer was collected, dried over sodium sulfate and removed under reduced pressure yielding yellow color oil. Column chromatography, in pure hexane, was done on this compound yielding light yellow color oil (8.2 g, 71%). ¹H NMR (300 MHz, CDCl₃): $\delta = 0.61$ (b, 6H; $2 \times$ CH₃), 1.12 – 0.74 (m, 16H; $8 \times$ CH₂), 1.96, (b, 4H; $2 \times$ CH₂), 7.34 (m, 3H; Aromatic), 7.47 (m, 2H; Aromatic), 7.56 (m, 1H; Aromatic), 7.69 (m, 1H; Aromatic). ¹³C NMR (75 MHz, CDCl₃): $\delta = 14.0, 22.6, 23.7, 29.7, 31.5, 40.3, 55.4, 119.7, 121.0, 121.0, 122.8, 126.1, 126.9, 127.5, 129.9, 140.0, 140.1, 150.3, 153.0$.

Synthesis of (2-(9,9-dihexyl-9-H-fluorene-2-yl) ethynyl)trimethylsilane (14)

Under nitrogen, compound **13** (2.0 g, 4.8 mmol) was dissolved in diisopropylamine (70 mL) followed by addition of tetrakis(triphenylphosphine) palladium(0) (0.32 g, 0.30 mmol) and copper iodide (0.057 g, 0.30 mmol). Trimethylsilyl acetylene (1.0 g, 9.7 mmol) was added into the reaction mixture dropwise and stirred at

room temperature for 2 h and then heated at 85 °C for 48 h. Reaction mixture was passed through silica, followed by washing with ether (50 mL). Organic layer was extracted with sat. sodium bicarbonate solution (4 × 100 mL), dried over sodium sulfate and removed under reduced pressure. Column chromatography, in pure hexane, was done on this compound yielding light yellow color oil (1.4 g, 64%). ¹H NMR (300 MHz, CDCl₃): δ = 0.31 (s, 9H; 3 × Si-CH₃), 0.59 (b, 6H; 2 × CH₃), 0.76 – 1.16 (m, 16H; 8 × CH₂), 1.96 (t, 4H; *J* = 8.8 Hz, 2 × CH₂), 7.37 – 7.33 (m, 3H; Aromatic), 7.49 – 7.45 (m, 2H; Aromatic), 7.72 – 7.62 (m, 2H; Aromatic). ¹³C NMR (75 MHz, CDCl₃): δ = 0.1, 14.0, 22.6, 23.7, 29.7, 31.5, 40.4, 53.4, 55.1, 93.8, 106.3, 119.5, 120.0, 121.2, 122.9, 126.2, 126.8, 127.5, 131.1, 140.4, 141.7, 150.6, 151.0.

Synthesis of 2-ethynyl-9,9-dihexyl-9-H-fluorene (15)

Compound **14** (0.70 g, 1.6 mmol), was dissolved in THF (60 mL) followed by addition of methanol (30 mL) and 20 % aqueous NaOH solution (30 mL) and stirred for 2 h at room temperature. Ether (50 mL) was added into it, and reaction mixture was extracted with water (4 × 50 mL). Organic layer was collected, dried over sodium sulfate and removed under reduced pressure, yielding light yellow color oil (0.58 g, 95%). ¹H NMR (300 MHz, CDCl₃): δ = 0.55 – 0.65 (m, 4H; 2 × CH₃), 0.76 – 1.16 (m, 18H; 8 × CH₂ and 2H from CH₃), 1.94 – 1.99 (m, 4H; 2 × CH₂), 3.16 (s, 1H; C≡CH), 7.36 – 7.34 (m, 3H; Aromatic), 7.51 – 7.48 (m, 2H; Aromatic), 7.72 – 7.65 (m, 2H; Aromatic). ¹³C NMR (75 MHz, CDCl₃): δ = 14.0, 22.6, 23.7, 29.7, 31.5, 40.3, 55.1, 68.0, 84.8, 119.6, 120.1, 120.1, 122.9, 126.5, 126.9, 127.6, 131.1, 140.2, 141.9, 150.7, 151.0.

Synthesis of Compound C

Under nitrogen, compound **3** (0.40 g, 1.5 mmol) was dissolved in DMF (40 mL) followed by addition of [Pd(PPh₃)₄] (0.11 g, 0.10 mmol) and copper iodide (0.019 g, 0.10 mmol). Compound **15** (0.60 g, 1.7 mmol) was dissolved in triethylamine (20 mL) separately and added into the reaction mixture dropwise and stirred for 48 h at 85 °C. Reaction mixture was passed through silica, followed by washing with ether (20 mL). Organic layer was extracted with sat'd sodium bicarbonate solution (4 × 100 mL) followed by extraction with 50% aqueous HCl solution (3 × 50 mL) and finally aqueous layer was neutralized with NaOH pellets. This aqueous layer was extracted with ether (3 × 30 mL). Organic layer was collected, dried over sodium sulfate and all volatiles were removed under reduced pressure. Column chromatography was done in pure pentane over basic alumina (previously treated with triethylamine in ether then dried) in order to get desired dark yellow colour oil (0.42 g, 46%). ¹H NMR (300 MHz, CDCl₃): δ = 0.81 - 0.61 (m, 10H; 2 × CH₃ and 2 × CH₂), 1.15 – 1.03 (m, 12H; 6 × CH₂), 1.98 (t, 4H; *J* = 9.0 Hz, 2 × CH₂), 2.28 (s, 12H; 4 × N-CH₃), 3.44 (s, 4H; 2 × N-CH₂), 7.27 (s, 1H; Aromatic), 7.39 – 7.34 (m, 3H; Aromatic), 7.46 (d, 2H; *J* = 3.0 Hz, Aromatic), 7.52 – 7.49 (m, 2H; Aromatic), 7.73 – 7.67 (m, 2H; Aromatic). ¹³C NMR (75 MHz, CDCl₃): δ = 14.0, 22.6, 23.7, 29.7, 31.5, 40.4, 45.4, 55.1, 64.0, 89.5, 90.4, 119.6, 119.9, 121.5, 122.9, 123.2, 126.0, 126.8, 127.5, 129.7, 130.5, 130.9, 139.3, 140.4, 141.4, 150.7, 151.1. HRMS (M+H)⁺: calc'd for C₃₉H₅₃N₂: 549.4209; found, 549.4200.

Synthesis of Compound 17

Compound **16** (10 g, 0.038 mol), *N*-bromosuccinimide (15 g, 0.084 mol) and azobisisobutyronitrile (AIBN) (1.3 g, 0.0076 mol) were dissolved in CCl₄ (250 mL)

refluxed for 8 h. After cooling to room temperature, reaction mixture was washed with water (3×100 mL). Organic layer was collected, dried over sodium sulfate and removed under reduced pressure. Residue was recrystallized in ethanol yielding white crystalline solid (9.0 g, 56%). ^1H NMR (300 MHz, CDCl_3): $\delta = 4.53$ (s, 4H; $2 \times \text{CH}_2$), 7.68 (s, 2H; Aromatic).

Synthesis of 4-hexyloxybenzaldehyde (19)

Compound **18** (5.0 g, 41 mmol) was dissolved in acetonitrile (70 mL) and K_2CO_3 (11 g, 82 mmol) was added into it. Hexylbromide (8.3 g, 51 mmol) was added dropwise to the heated solution and refluxed overnight. H_2O (200 mL) was added into the reaction mixture and extracted with ether (3×50 mL). Organic layer was collected, dried over sodium sulfate and removed under reduced pressure (8.1 g, 96%). ^1H NMR (300 MHz, CDCl_3): $\delta = 0.952 - 0.896$ (b, 3H; CH_3), 1.562 - 1.330 (m, 6H; $3 \times \text{CH}_2$), 1.832 (q, 2H; $J = 6.0$ Hz, CH_2), 4.056 (t, 2H; $J = 6.6$ Hz, $2 \times \text{O-CH}_2$), 7.030 (dd, 2H; $J_1 = 8.7$ Hz, $J_2 = 1.8$ Hz, Aromatic), 7.858 (dd, 2H; $J_1 = 8.7$ Hz, $J_2 = 1.8$ Hz, Aromatic), 9.890 (s, 1H; CHO).

Synthesis of Compound 20

Compound **17** (6.20 g, 14.7 mmol) and triethylphosphite (12.2 g, 73.5 mmol) were heated up to 90°C for 3 h under nitrogen atmosphere. After completion, reaction mixture was vacuum distilled to remove excess triethylphosphite. Residue was triturated with pentane (10 ml) yielding white solid (7.6 g, 95%). ^1H NMR (300 MHz, CDCl_3): $\delta = 1.28$ (t, 12H; $J = 9.0$ Hz, $4 \times \text{CH}_3$), 3.36 (dd, 4H; $J_1 = 30.0$ Hz, $J_2 = 6.0$ Hz, $2 \times (\text{O})\text{PCH}_2$), 4.10 (m, 8H; $4 \times \text{CH}_2$), 7.65 (d, 2H; $J = 3.0$ Hz, Aromatic). ^{31}P NMR (121 MHz, CDCl_3): $\delta = 24.7$. This product was contaminated with a small amount of

nonvolatile P-containing impurities present in the triethylphosphite starting material (See **appendix 4 A**); we elected to remove the impurities by aqueous extraction following the next step.

Synthesis of Compound 21

Under nitrogen, compound **20** (3.5 g, 6.5 mmol) and 4-hexyloxy benzaldehyde (2.7 g, 13 mmol) were dissolved in dry THF (50 mL). Potassium *t*-butoxide (1.6 g, 14 mmol) was dissolved in dry THF separately and added dropwise to the reaction mixture and stirred overnight at room temperature. Methanol (100 mL) was added into the reaction mixture and all the volatiles were removed under reduced pressure. Residue was dissolved into CH₂Cl₂ (150 mL) and extracted with water (3 × 100 mL). Organic layer was collected, dried over sodium sulfate and removed under reduced pressure, yielding yellow solid. Crude solid was recrystallized in pure hexane (4.5 g, 54%). ¹H NMR (300 MHz, CDCl₃): δ = 0.94 (b, 6H; 2 × CH₃), 1.52 – 1.34 (m, 12H; 6 × CH₂), 1.82 (q, 4H; *J* = 6.0 Hz, 2 × CH₂), 4.01 (t, 4H; *J* = 6.0 Hz, 2 × O-CH₂), 6.92 (d, 4H; *J* = 9.0 Hz, Aromatic), 7.02 (d, 2H; *J* = 18 Hz, HC=CH), 7.24 (d, 2H; *J* = 18 Hz, HC=CH), 7.50 (d, 4H; *J* = 9.0 Hz, Aromatic), 7.86 (s, 2H, Aromatic). ¹³C NMR (75 MHz, CDCl₃): δ = 14.0, 22.6, 25.7, 29.2, 31.6, 68.1, 114.8, 122.8, 123.5, 128.3, 129.3, 130.0, 131.7, 137.8, 159.5. MALDI: calc'd for C₃₄H₄₀Br₂O₂: 638.1; found, 637.9.

Synthesis of Compound 22

Under nitrogen, compound **21** (2.0 g, 3.1 mmol) was dissolved in toluene (20 mL) followed by the addition of [Pd(PPh₃)₄] (0.40 g, 0.4 mmol) and copper iodide (0.070 mg, 0.4 mmol). Trimethylsilylacetylene (1.2 g, 12 mmol) was dissolved in triethylamine (30

mL) separately and added dropwise to the reaction mixture and stirred for 48 h at 85 °C. Ether (100 mL) was added to the reaction mixture and organic layer was extracted with sat'd sodium bicarbonate solution (4 × 150 mL), dried over sodium sulfate and removed under reduced pressure. Residue was dissolved in ether and passed through silica followed by washing with CHCl₃ (2 × 50 mL). Organic layer was collected and removed under reduced pressure, yielding light yellow solid (1.1 g, 48%). ¹H NMR (300 MHz, CDCl₃): δ = 0.34 (s, 18H; 6 × Si-CH₃), 0.94 (t, 6H; *J* = 9.0 Hz, 2 × CH₃), 1.52 – 1.34 (m, 12H; 6 × CH₂), 1.82 (q, 4H; *J* = 6.0 Hz, 2 × CH₂), 4.01 (t, 4H; *J* = 6.0 Hz, 2 × O-CH₂), 6.92 (d, 4H; *J* = 9.0 Hz, Aromatic), 7.17 (d, 2H; *J* = 18 Hz, HC=CH), 7.4-7.6 (m, 6H; Aromatic and HC=CH), 7.79 (s, 2H; Aromatic). ¹³C NMR (75 MHz, CDCl₃): δ = 0.0, 14.1, 22.6, 25.7, 29.2, 31.6, 68.1, 100.7, 103.4, 114.8, 121.9, 123.3, 127.9, 128.4, 129.9, 130.0, 137.6, 159.2. MALDI: calc'd for C₄₄H₅₈O₂Si₂: 674.4; found, 674.3.

Synthesis of Compound 23

Compound **22** (0.50 g, 0.70 mmol), was dissolved in THF (30 mL) followed by addition of tetrabutylammonium fluoride trihydrate (2.2 g, 7.0 mmol) and stirred for 2 h at room temperature. Volatiles were removed under reduced pressure and ether (30 mL) was added into the residue followed by extraction with sat'd bicarbonate solution (4 × 50 mL). Organic layer was collected, dried over sodium sulfate and removed under reduced pressure, yielding yellow colour solid (0.35 g, 88%). ¹H NMR (300 MHz, CDCl₃): δ = 0.93 (t, 6H; *J* = 9.0 Hz, 2 × CH₃), 1.52 – 1.34 (m, 12H; 6 × CH₂), 1.82 (q, 4H; *J* = 6.0 Hz, 2 × CH₂), 3.47 (s, 2H; C≡CH), 4.01 (t, 4H; *J* = 6.0 Hz, 2 × O-CH₂), 6.92 (d, 4H; *J* = 9.0 Hz, Aromatic), 7.15 (d, 2H; *J* = 15 Hz, HC=CH), 7.44 (d, 2H; *J* = 15 Hz, HC=CH), 7.50

(d, 4H; $J = 9$ Hz, Aromatic), 7.84 (s, 2H; Aromatic). MALDI: calc'd for $C_{38}H_{42}O_2$: 530.3; found, 530.4.

Synthesis of Compound D

Under nitrogen, compound **3** (0.28 g, 0.80 mmol) was dissolved in DMF (40 mL) followed by addition of $[Pd(PPh_3)_4]$ (0.11 g, 0.10 mmol) and copper iodide (19 mg, 0.10 mmol). Compound **23** (0.20 g, 0.40 mmol) was dissolved in triethylamine (20 mL) separately and added dropwise to the reaction mixture and stirred for 48 h at 85 °C. Reaction mixture was passed through silica, followed by washing with ether (40 mL). Organic layer was extracted with sat'd sodium bicarbonate solution (4×100 mL) and followed by extraction with 50% aqueous HCl solution (3×50 mL) and finally aqueous layer was neutralized with NaOH pellets. This aqueous layer was extracted with ether (3×30 mL). Organic layer was collected, dried over sodium sulfate and removed under reduced pressure. Residue was dissolved in minimum amount of pentane and left for recrystallization. Solid precipitate was filtered as pale yellow solid (0.30 g, 86%). 1H NMR (300 MHz, $CDCl_3$): $\delta = 0.90 - 0.96$ (b, 6H; $2 \times CH_3$), 1.52 – 1.34 (m, 12H; $6 \times CH_2$), 1.82 (t, 4H; $J = 9.0$ Hz, $2 \times CH_2$), 2.30 (s, 24H; $8 \times N-CH_3$), 3.47 (s, 8H; $4 \times N-CH_2$), 4.01 (t, 4H; $J = 9.0$ Hz, $2 \times O-CH_2$), 6.94 (d, 4H; $J = 9.0$ Hz, Aromatic), 7.24 (d, 2H; $J = 15$ Hz, HC=CH), 7.32 (s, 2H; Aromatic), 7.58 – 7.49 (m, 10H; Aromatic), 7.88 (s, 2H; Aromatic). ^{13}C NMR (75 MHz, $CDCl_3$): $\delta = 14.1, 22.6, 25.7, 29.2, 31.6, 45.5, 64.0, 68.1, 87.9, 95.5, 114.8, 122.0, 123.0, 123.5, 128.1, 128.6, 129.9, 130.1, 130.9, 137.3, 139.4, 159.2$. HRMS ($M+H$)⁺: calc'd for $C_{62}H_{79}O_2N_4$: 911.6203; found, 911.6195.

Synthesis of Compound 25

Under nitrogen, compound **20** (5.70 g, 10.6 mmol) and 4-*t*-butylbenzaldehyde **24** (3.45 g, 21.3 mmol) were dissolved in dry THF (50 mL). Potassium *t*-butoxide (2.62 g, 23.4 mmol) was dissolved in dry THF separately and added dropwise to the reaction mixture and stirred overnight at room temperature. Methanol (100 mL) was added into the reaction mixture and all the volatiles were removed under reduced pressure. Residue was dissolved into CH₂Cl₂ (150 mL) and extracted with water (3 × 100 mL). Organic layer was collected, dried over sodium sulfate and removed under reduced pressure, yielding light yellow solid (3.5 g, 60%). ¹H NMR (300 MHz, CDCl₃): δ = 1.38 (s, 18H; 6 × CH₃), 7.09 (d, 2H; *J* = 16 Hz, HC=CH), 7.39 (d, 2H; *J* = 16 Hz, HC=CH), 7.46 (d, 4H; *J* = 8.4 Hz, Aromatic), 7.54 (d, 4H; *J* = 8.4 Hz, Aromatic), 7.89 (s, 2H; Aromatic). ¹³C NMR (75 MHz, CDCl₃): δ = 31.2, 34.7, 123.0, 125.1, 125.7, 126.7, 130.2, 131.9, 133.9, 137.3, 151.7. MALDI: calc'd for C₃₀H₃₂Br₂: 550.1; found, 550.2.

Synthesis of 3,5-bis[(dimethylamino) methyl] phenyl trimethylsilyl acetylene (26)

Under nitrogen, compound **3** (2.0 g, 7.4 mmol) was dissolved in toluene (10 mL) followed by addition of tetrakis(triphenylphosphine) palladium(0) (0.50 g, 0.50 mmol) and copper iodide (85 mg, 0.50 mmol). Trimethylsilylacetylene (1.8 g, 18 mmol) was dissolved in triethylamine (15 mL) separately and added dropwise to the reaction mixture and stirred for 24 h at 85 °C. Ether (20 mL) was added into the reaction mixture and extracted with sat. sodium bicarbonate solution (4 × 50 mL). Organic layer was collected, dried over sodium sulfate and removed under reduced pressure. Residue was triturated with hexane (20 mL) and hexane layer was removed under reduced pressure, yielding

yellow viscous oil (1.3 g, 62%). ^1H NMR (300 MHz, CDCl_3): δ = 0.251 (s, 9H; Si- CH_3), 2.241 (s, 12H; N- CH_3), 3.385 (s, 4H; N- CH_2), 7.237 (s, 1H; Aromatic), 7.352 (d, 2H; J = 1.2 Hz, Aromatic). ^{13}C NMR (75 MHz, CDCl_3): δ = 0.0, 45.4, 63.9, 94.0, 105.2, 122.9, 130.0, 131.3, 139.2.

Synthesis of 3,5-bis[(dimethylamino)methyl]phenylacetylene (27)

Compound **26** (0.60 g, 2.1 mmol) was dissolved in THF (20 mL) followed by addition of tetrabutylammonium fluoride trihydrate (5.4 g, 21 mmol) and stirred for 2 h at room temperature. Volatiles were removed under reduced pressure and dissolved in ether (30 mL). Solution was extracted with sat. bicarbonate solution (4×50 mL). Organic layer was collected, dried over sodium sulfate and removed under reduced pressure, yielding brown viscous oil (0.2 g crude). ^1H NMR (300 MHz, CDCl_3): δ = 2.25 (s, 12H; N- CH_3), 3.05 (s, 1H; $\text{C}\equiv\text{CH}$), 3.40 (s, 4H; N- CH_2), 7.37 (m, 3H; aromatic). ^{13}C NMR (75 MHz, CDCl_3): δ = 45.3, 63.8, 76.8, 83.7, 121.8, 130.6, 131.4, 139.1.

Synthesis of Compound E

Under nitrogen, compound **25** was dissolved in DMF (20 mL) followed by the addition of $[\text{Pd}(\text{PPh}_3)_4]$ (44 mg, 0.040 mmol) and copper iodide (3.2 mg, 0.010 mmol). Compound **27** was dissolved in triethylamine (20 mL) separately and added dropwise in the reaction mixture and stirred for 48 h at 85 °C. Ether (20 mL) was added into the reaction mixture and washed with sat'd sodium bicarbonate solution (4×50 mL). Organic layer was collected, dried over sodium sulfate and removed under reduced pressure. Ether (20 mL) was added into the residue and washed with concentrated 25% aq. H_2SO_4 solution (v:v) (2×25 mL). Aqueous layer was collected and neutralized by

adding NaOH pallet (pH ~ 10). Aqueous layer was extracted with ether (3 × 20 mL). Organic layer was collected, dried over sodium sulfate and removed under reduced pressure, yielding pale yellow solid. Finally compound was purified over preparative TLC (CH₂Cl₂ / Methanol, 200:1). (0.020 g, 10%) ¹H NMR (300 MHz, CDCl₃): δ = 1.37 (s, 18H; C-CH₃), 2.23 (s, 24H; N-CH₃), 3.51 (s, 8H; N-CH₂), 7.25-7.33 (m, putatively 4H, aromatic, but overlaps CHCl₃), 7.40-7.45 (m, 4H; Aromatic), 7.51 (s, 4H; Aromatic), 7.58 (d, 4H; *J* = 8.4 Hz, Aromatic), 7.66 (d, 2H; *J* = 16 Hz, HC=CH), 7.91 (s, 2H; Aromatic). ¹³C NMR (75 MHz, CDCl₃): δ = 31.3, 34.7, 45.3, 63.8, 76.6, 87.9, 95.5, 122.2, 123.0, 125.0, 125.7, 126.6, 128.7, 130.3, 130.4, 131.1, 134.6, 137.4, 138.9, 151.2. HRMS (M+H)⁺: calc'd for C₅₈H₇₁N₄: 823.5679; found, 823.5684.

4.7 References

1. Zuccherro, A. J.; Wilson, J. N.; Bunz, U. H. F., Cruciforms as functional fluorophores: Response to protons and selected metal ions. *Journal of the American Chemical Society* **2006**, 128, (36), 11872-11881.
2. Wilson, J. N.; Bunz, U. H. F., Switching of Intramolecular Charge Transfer in Cruciforms: Metal Ion Sensing. *Journal of the American Chemical Society* **2005**, 127, (12), 4124-4125.
3. Cody, J.; Fahrni, C. J., Fluorescence sensing based on cation-induced conformational switching: copper-selective modulation of the photoinduced intramolecular charge transfer of a donor-acceptor biphenyl fluorophore. *Tetrahedron* **2004**, 60, (49), 11099-11107.
4. Henary, M. M.; Wu, Y.; Fahrni, C. J., Zinc(II)-selective ratiometric fluorescent sensors based on inhibition of excited-state intramolecular proton transfer. *Chemistry-A European Journal* **2004**, 10, (12), 3015-3025.
5. Fahrni, C. J.; O'Halloran, T. V., Aqueous Coordination Chemistry of Quinoline-Based Fluorescence Probes for the Biological Chemistry of Zinc. *Journal of the American Chemical Society* **1999**, 121, (49), 11448-11458.
6. Superior examples include Strem Chemicals' Zinpyr-1 (cat. no. 07-0314) and Zinpyr-4 (07-0312).
7. Nolan, E. M.; Ryu, J. W.; Jaworski, J.; Feazell, R. P.; Sheng, M.; Lippard, S. J., Zinspy Sensors with Enhanced Dynamic Range for Imaging Neuronal Cell Zinc

- Uptake and Mobilization. *Journal of the American Chemical Society* **2006**, 128, (48), 15517-15528.
8. Goldsmith, C. R.; Jaworski, J.; Sheng, M.; Lippard, S. J., Selective Labeling of Extracellular Proteins Containing Polyhistidine Sequences by a Fluorescein-Nitrilotriacetic Acid Conjugate. *Journal of the American Chemical Society* **2006**, 128, (2), 418-419.
 9. Nolan, E. M.; Jaworski, J.; Okamoto, K.; Hayashi, Y.; Sheng, M.; Lippard, S. J., QZ1 and QZ2: Rapid, Reversible Quinoline-Derivatized Fluoresceins for Sensing Biological Zn(II). *Journal of the American Chemical Society* **2005**, 127, (48), 16812-16823.
 10. Chang, C. J.; Jaworski, J.; Nolan, E. M.; Sheng, M.; Lippard, S. J., A tautomeric zinc sensor for ratiometric fluorescence imaging: Application to nitric oxide-induced release of intracellular zinc. *Proceedings of the National Academy of Sciences of the United States of America* **2004**, 101, (5), 1129-1134.
 11. Burdette, S. C.; Frederickson, C. J.; Bu, W.; Lippard, S. J., ZP4, an improved neuronal Zn²⁺ sensor of the zinpyr family. *Journal of the American Chemical Society* **2003**, 125, (7), 1778-1787.
 12. Walkup, G. K.; Burdette, S. C.; Lippard, S. J.; Tsien, R. Y., A New Cell-Permeable Fluorescent Probe for Zn²⁺. *Journal of the American Chemical Society* **2000**, 122, (23), 5644-5645.

13. Zacharias, D. A.; Baird, G. S.; Tsien, R. Y., Recent advances in technology for measuring and manipulating cell signals. *Current Opinion in Neurobiology* **2000**, 10, (3), 416-421.
14. Zhang, J.; Campbell, R. E.; Ting, A. Y.; Tsien, R. Y., Creating New Fluorescent Probes for Cell Biology. *Nature Reviews Molecular Cell Biology* **2002**, 3, (12), 906-918.
15. Tsien, R. Y., *Biochemistry* **1980**, 19, 2396.
16. Dennis, A. E.; Smith, R. C., "Turn-On" Fluorescent Sensor for the Selective Detection of Zinc Ion by a Sterically-Encumbered Bipyridyl-Based Receptor *Chemical Communications* **2007**, (44), 4641-4643.
17. Zuccherro, A. J.; McGrier, P. L.; Bunz, U. H. F., Cross-Conjugated Cruciform Fluorophores. *Acc. Chem. Res.* **2010**, 43, (3), 397-408.
18. Steenwinkel, P.; James, L. S.; Grove, D. M.; Veldman, N.; Spek, A. L.; van Koten, G., New ruthenium(II) complexes of functionalized monoanionic aryldiamine N,C,N'-terdentate ligands: syntheses of $[\text{Ru}^{\text{II}}\{2,6\text{-(Me}_2\text{NCH}_2\text{)}_2\text{-4-RC}_6\text{H}_2\}\text{(terpy)}]^+\text{Cl}^-$; X-ray structure of a dimeric organolithium compound, $[\text{Li}\{2,6\text{-(Me}_2\text{NCH}_2\text{)}_2\text{-4-Ph-C}_6\text{H}_2\}]_2$. *Chemistry--A European Journal* **1996**, 2, (11), 1440-1445.
19. Miyakoshi, R.; Shimono, K.; Yokoyama, A.; Yokozawa, T., Catalyst-Transfer Polycondensation for the Synthesis of Poly(p-phenylene) with Controlled Molecular Weight and Low Polydispersity. *J. Am. Chem. Soc.* **2006**, 128, 16012-16013.
20. Wu, C.-J. J.; Xue, C.; Kuo, Y.-M.; Luo, F.-T., Preparation and photoluminescence of p-terphenyl derivatives containing cyano groups. *Tetrahedron* **2005**, 61, 4735-4741.

21. Zhou, C.-Z.; Liu, T.; Xu, J.-M.; Chen, Z.-K., Synthesis, Characterization, and Physical Properties of Monodisperse Oligo(p-phenyleneethynylene)s. *Macromolecules* **2003**, 36, 1457-1464.
22. Li Liu; Wong, W.-Y.; Lam, Y.-W.; Tam, W.-Y., Exploring a series of monoethynylfluorenes as alkynylating reagents for mercuric ion: Synthesis, spectroscopy, photophysics and potential use in mercury speciation. *Inorganica Chimica Acta* **2007**, 360, 109-121.
23. Bonifacio, M. C.; Robertson, C. R.; Jung, J.-Y.; King, B. T., Polycyclic Aromatic Hydrocarbons by Ring-Closing Metathesis. *J. Org. Chem* **2005**, 70, 8522-8526.
24. Blum, J.; Zimmerman, M., Photocyclization of Substituted 1,4-Distyrylbenzenes to Dibenzo[*a,h*] Anthracenes. *Tetrahedron* **1972**, 28, 275-280.
25. Eggers, K.; Fyles, T. M.; Montoya-Pelaez, P. J., Synthesis and Characterization of Photoswitchable Lipids Containing Hemithioindigo Chromophores. *J. Org. Chem* **2001**, 66, 2966-2977.
26. Vedejs, E.; Peterson, M. J., *Top. Stereochem.* **1994**, 21, 1-157.
27. Crews, P.; Rodriguez, J.; Jaspars, M., *Organic Structure Analysis*. 2 ed.; Oxford University Press: New York, 2010.
28. Mangalum, A.; Smith, R. C., Bifunctional cross-conjugated luminescent phosphines and phosphine derivatives: phospho-cruciforms. *Dalton Trans.* **2010**, 39, 5145-5151.
29. Holliday, B. J.; Swager, T. M., Conducting metallopolymers: the roles of molecular architecture and redox matching. *Chem. Commun.* **2005**, (1), 23-36.
30. Coulson, D. R., *Inorganic Synthesis*. ed.; 1990; 'Vol.' 28, p 107-109.

31. Tennyson, E. G.; Smith, R. C., Visible-Absorbing Phosphines as Functional Elements of Luminescent Metallopolymers. *Inorg. Chem.* **2009**, 48, 11483-11485.

APPENDICES

Appendix 4 A

NMR Spectra

3,5-bis(bromomethyl)-bromobenzene (**2**)

Structure

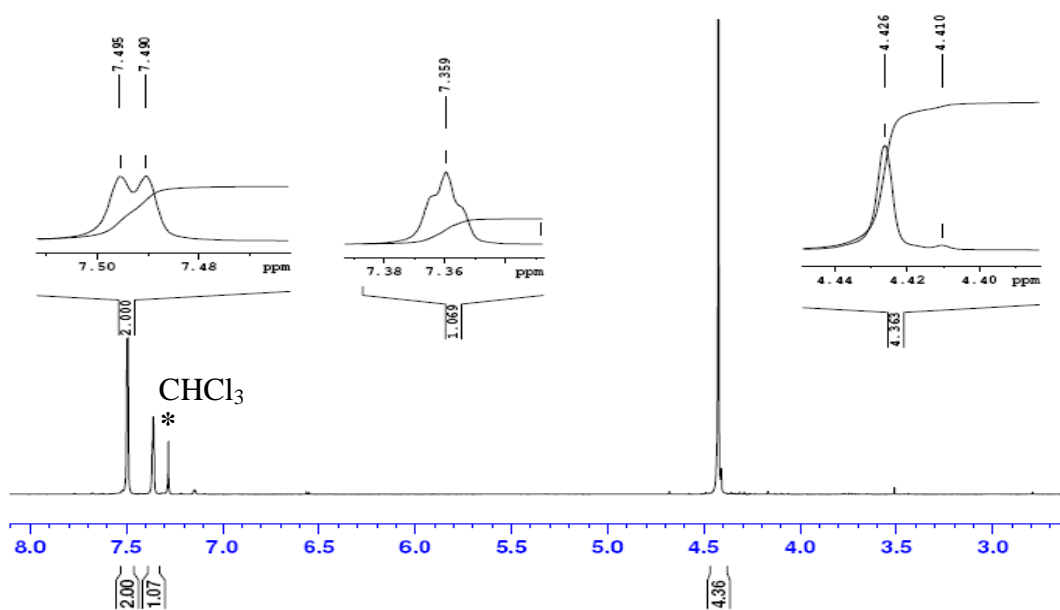
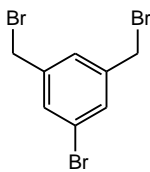


Figure 4 A.1 ^1H NMR (300 MHz, CDCl_3) of **2**.

3,5-bis[(dimethylamino) methyl] bromobenzene (**3**)

Structure

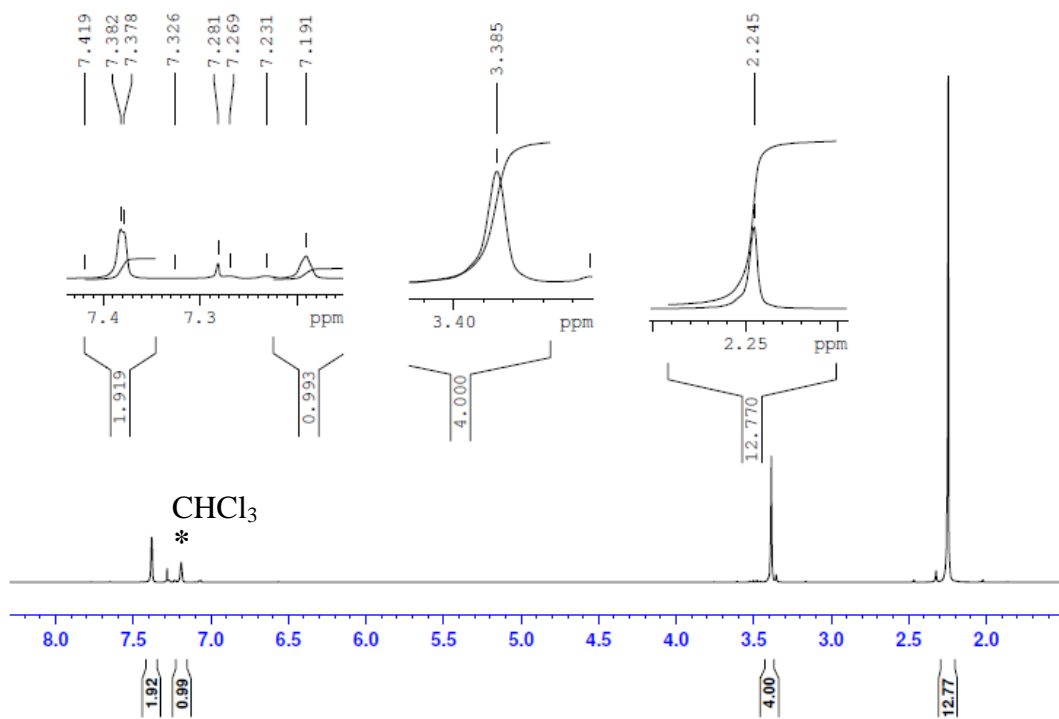
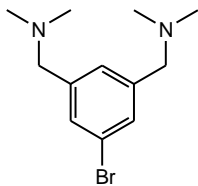


Figure 4 A.2 ¹H NMR (300 MHz, CDCl₃) of **3**.

1,4-bis(hexyloxy) benzene (**5**)

Structure

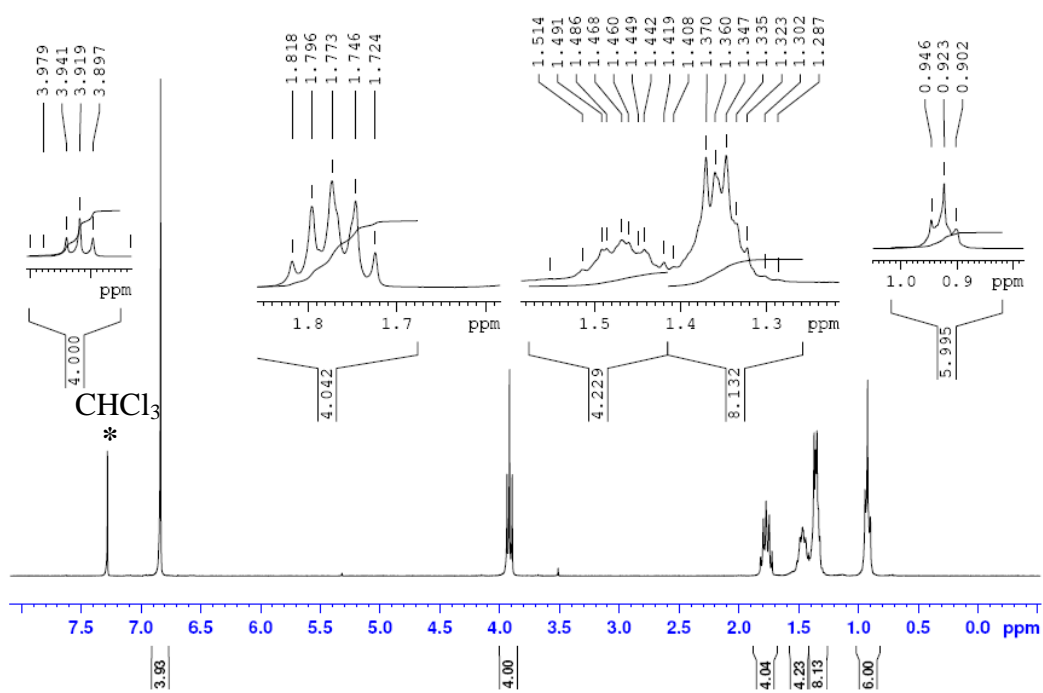
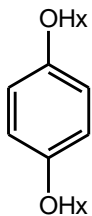


Figure 4 A.3 ¹H NMR (300 MHz, CDCl₃) of **5**.

2-Bromo-1,4-bis(hexyloxy) benzene (**6**)

Structure

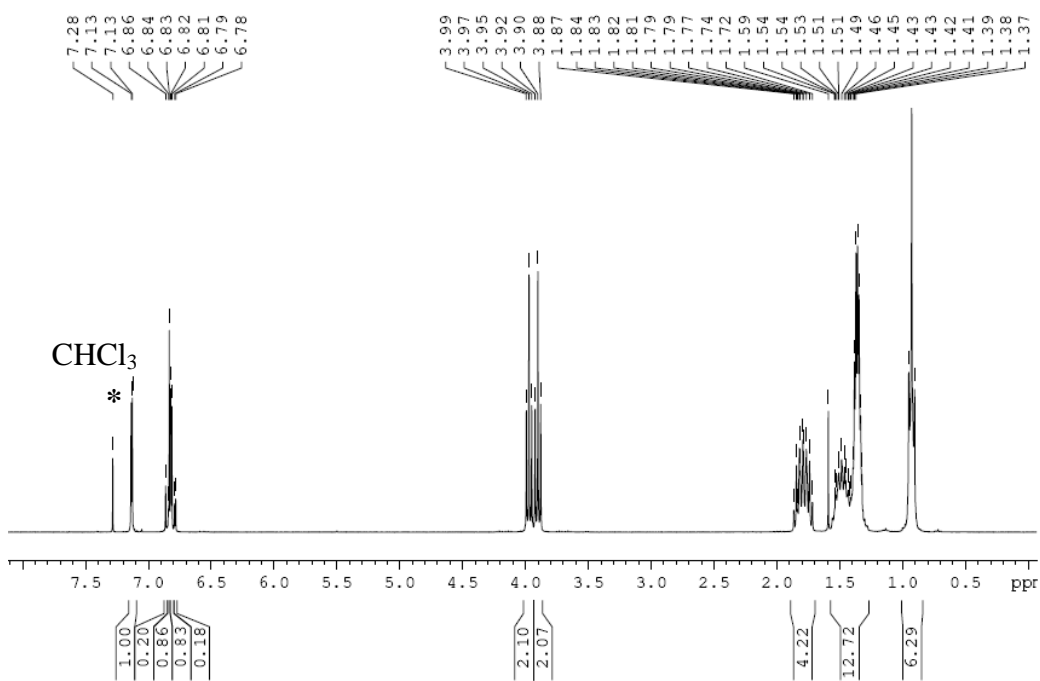
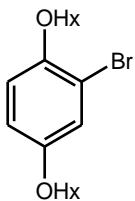


Figure 4 A.4 ¹H NMR (300 MHz, CDCl₃) of **6**.

2-Bromo-1,4-bis(hexyloxy) benzene (**6**)

Structure

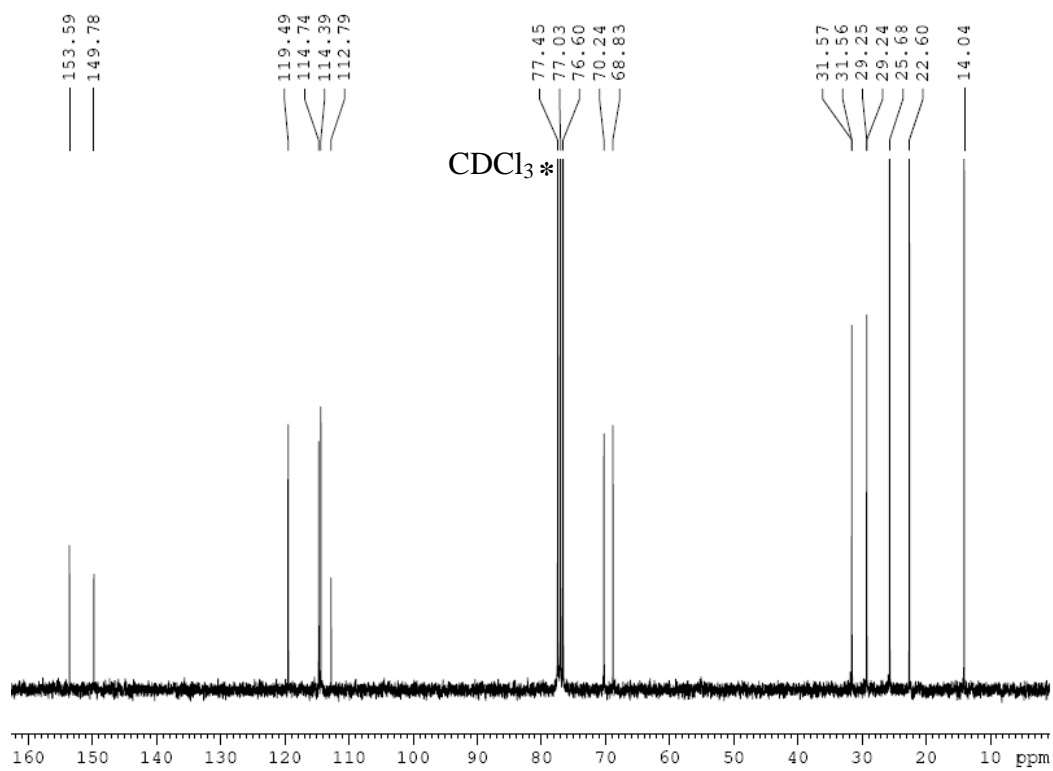
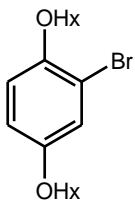


Figure 4 A.5 ¹³C NMR (75 MHz, CDCl₃) of **6**.

(2-(2,5-bis(hexyloxy) phenyl)ethynyl) trimethylsilane (**7**)

Structure

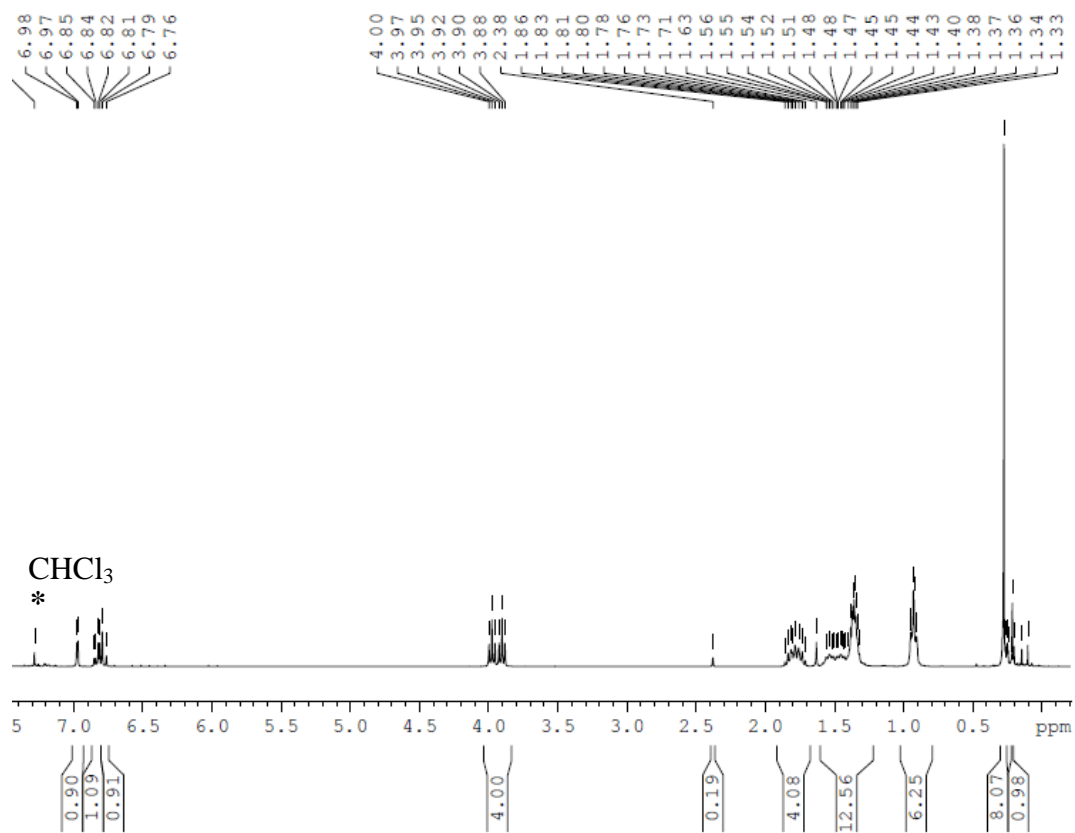
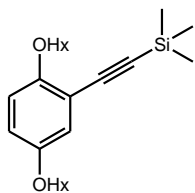


Figure 4 A.6 ¹H NMR (300 MHz, CDCl₃) of **7**.

(2-(2,5-bis(hexyloxy) phenyl)ethynyl) trimethylsilane (**7**)

Structure

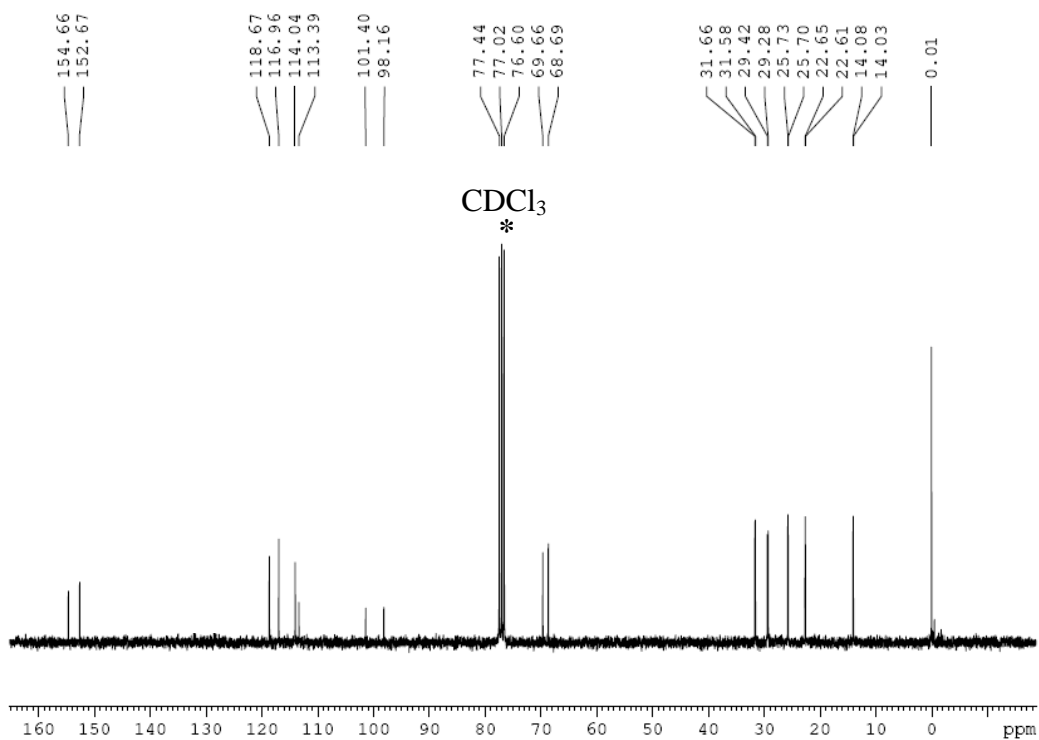
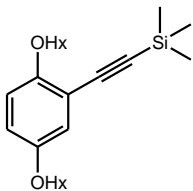


Figure 4 A.7 ^{13}C NMR (75 MHz, CDCl_3) of **7**.

2-ethynyl-1,4-bis(hexyloxy) benzene (**8**)

Structure

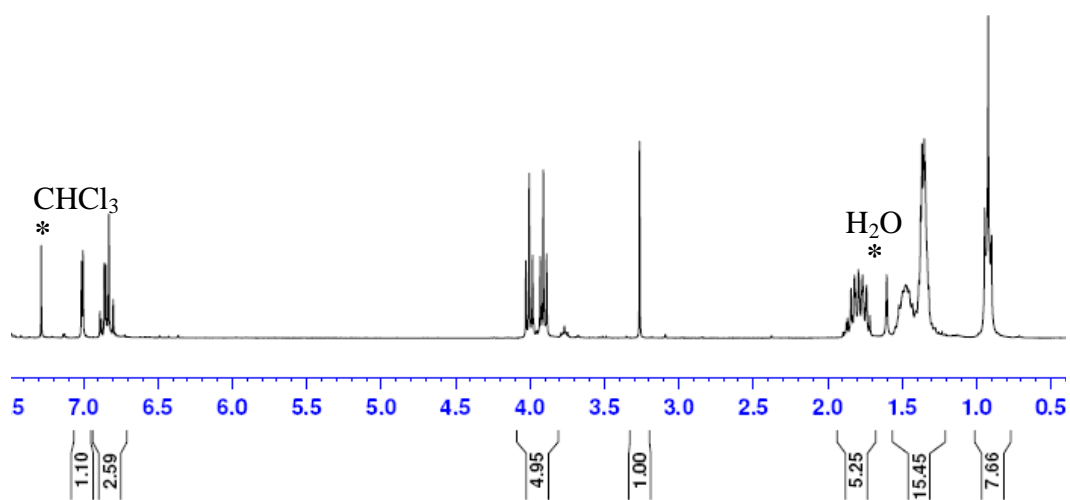
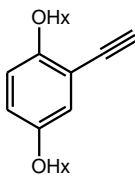


Figure 4 A.8 ¹H NMR (300 MHz, CDCl₃) of **8**.

2-ethynyl-1,4-bis(hexyloxy) benzene (**8**)

Structure

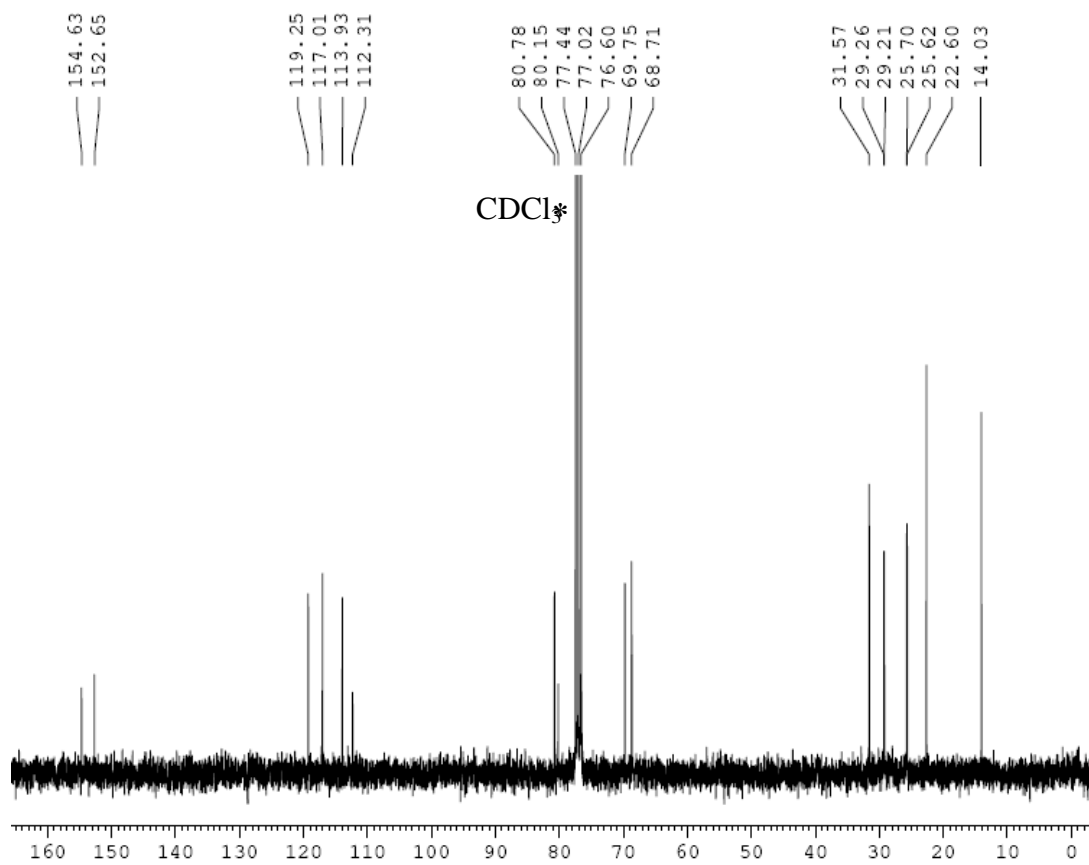
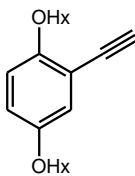


Figure 4 A.9 ^{13}C NMR (75 MHz, CDCl_3) of **8**.

Compound A

Structure

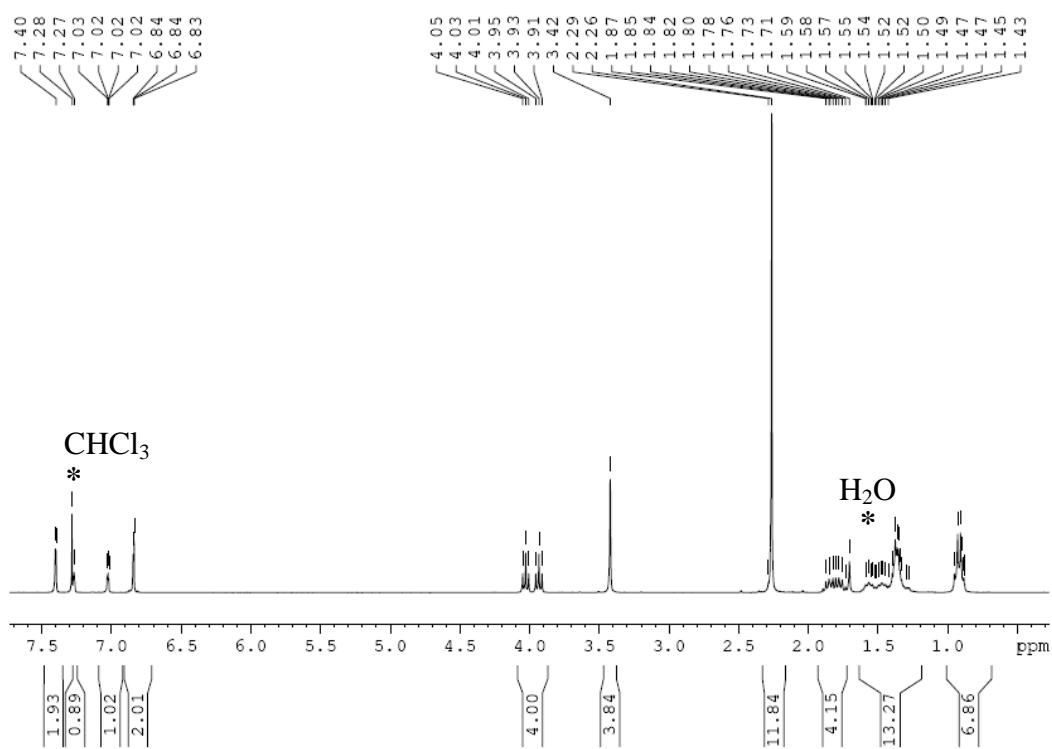
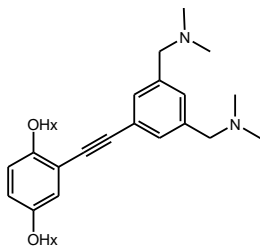


Figure 4 A.10 ¹H NMR (300 MHz, CDCl₃) of A.

Compound A

Structure

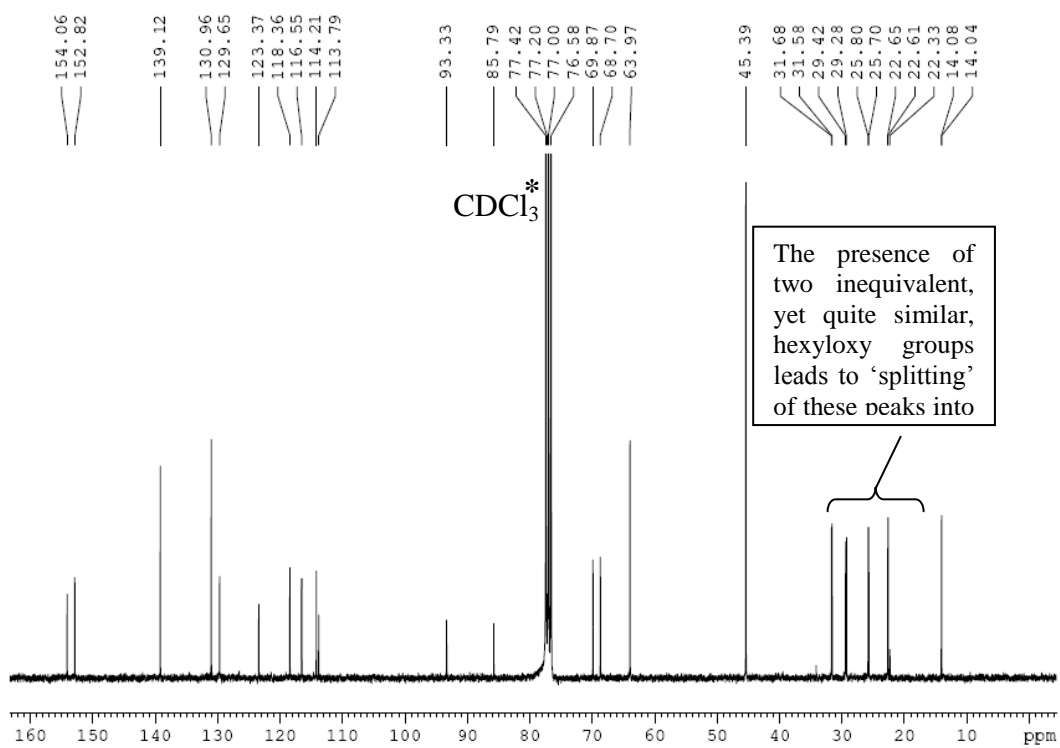
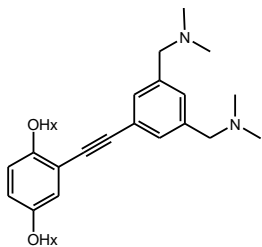


Figure 4 A.11 ¹³C NMR (75 MHz, CDCl₃) of A.

2,5-dibromo-1,4-bis(hexyloxy) benzene (**9**)

Structure

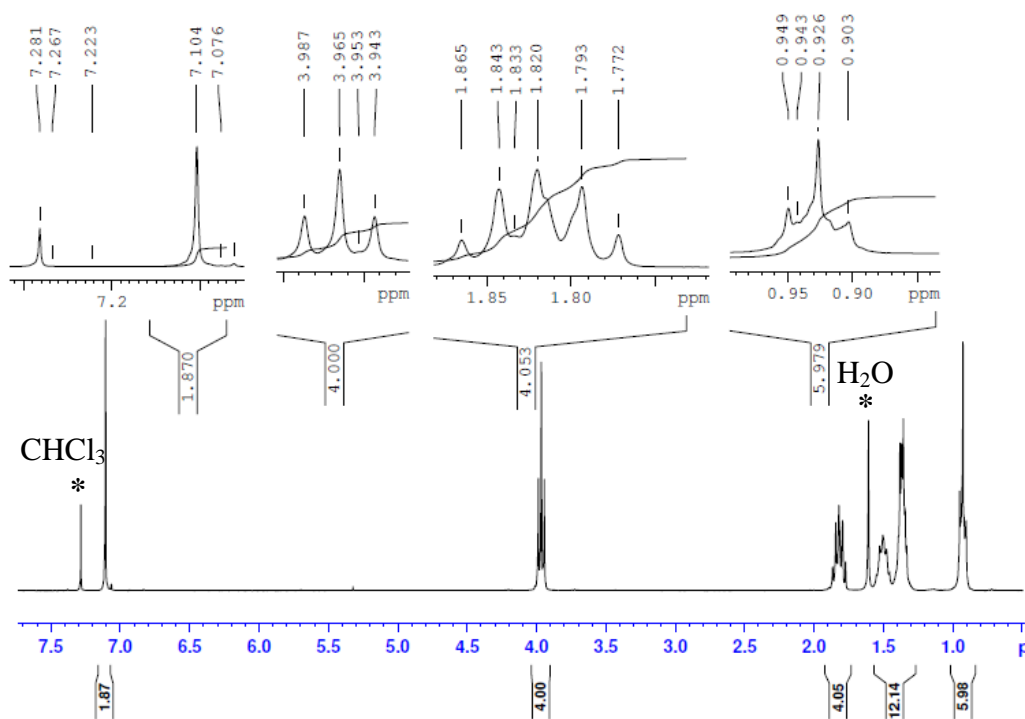
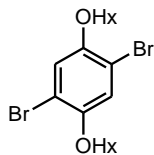


Figure 4 A.12 ¹H NMR (300 MHz, CDCl₃) of **9**.

2,5-dibromo-1,4-bis(hexyloxy) benzene (**9**)

Structure

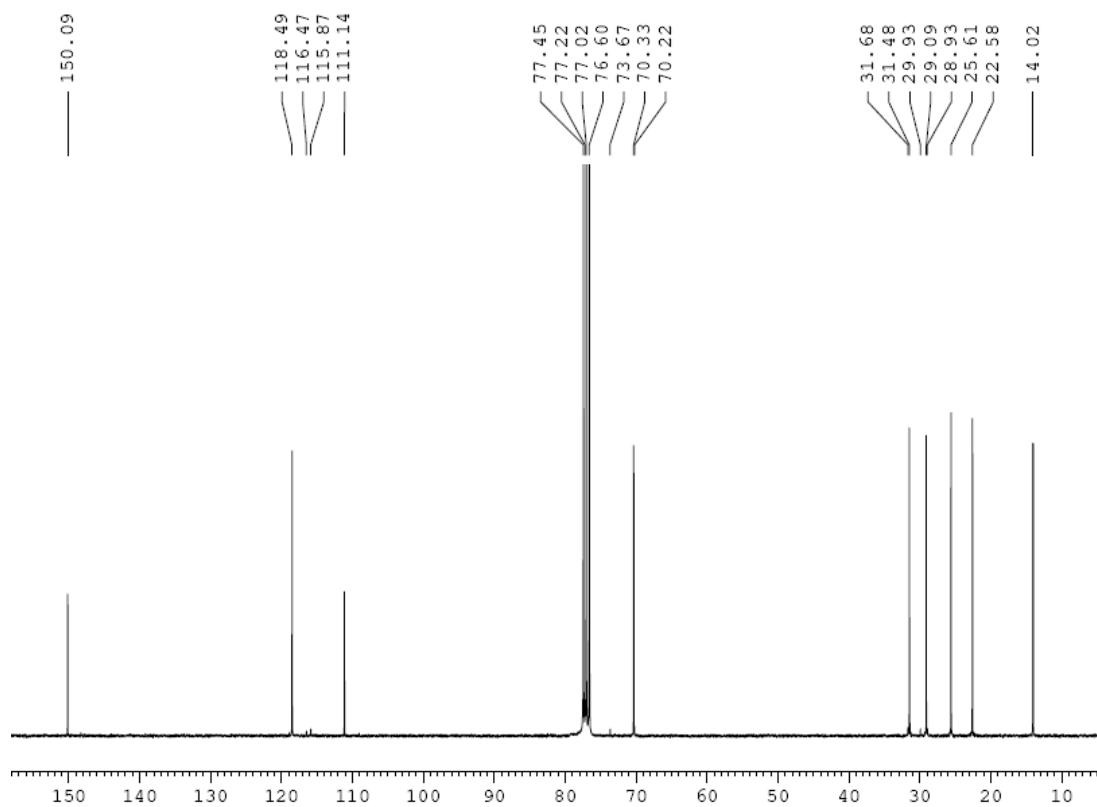
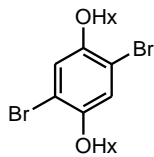


Figure 4 A.13 ^{13}C NMR (75 MHz, CDCl_3) of **9**.

1,4-bis(hexyloxy)-2,5-bis(2-(trimethylsilyl)ethynyl) benzene (**10**)

Structure

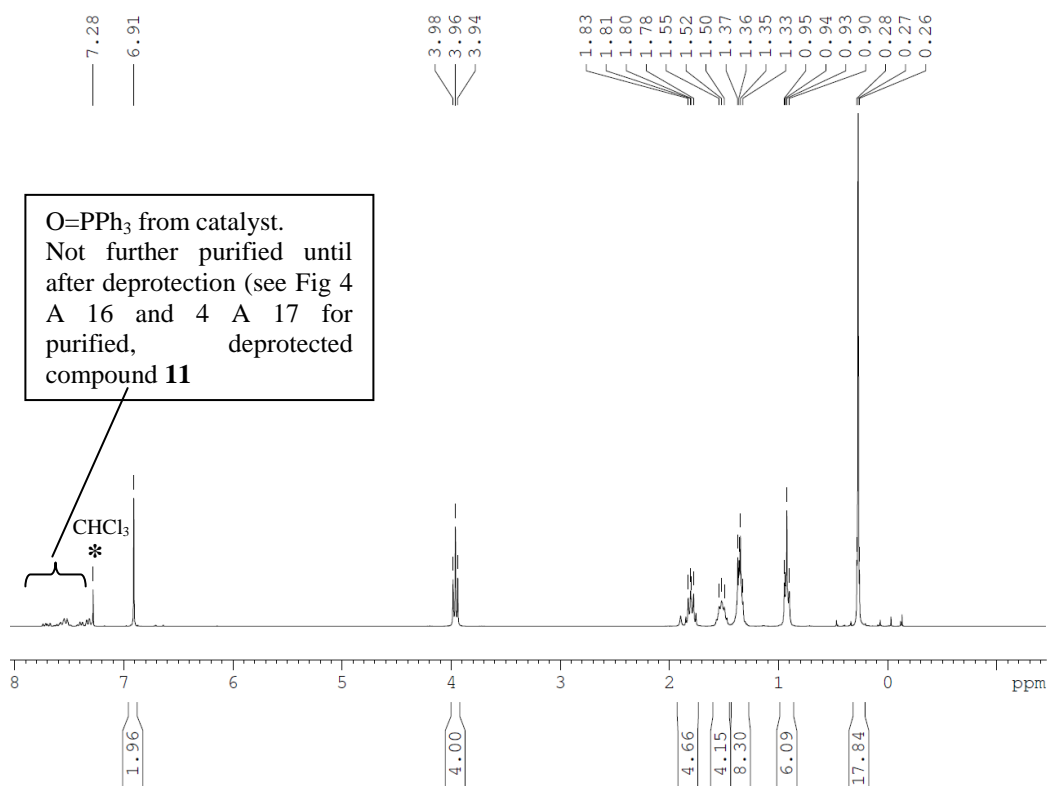
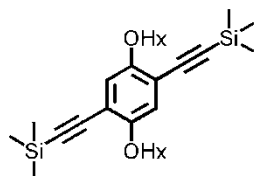


Figure 4 A.14 ¹H NMR (300 MHz, CDCl₃) of **10**.

1,4-bis(hexyloxy)-2,5-bis(2-(trimethylsilyl)ethynyl) benzene (**10**)

Structure

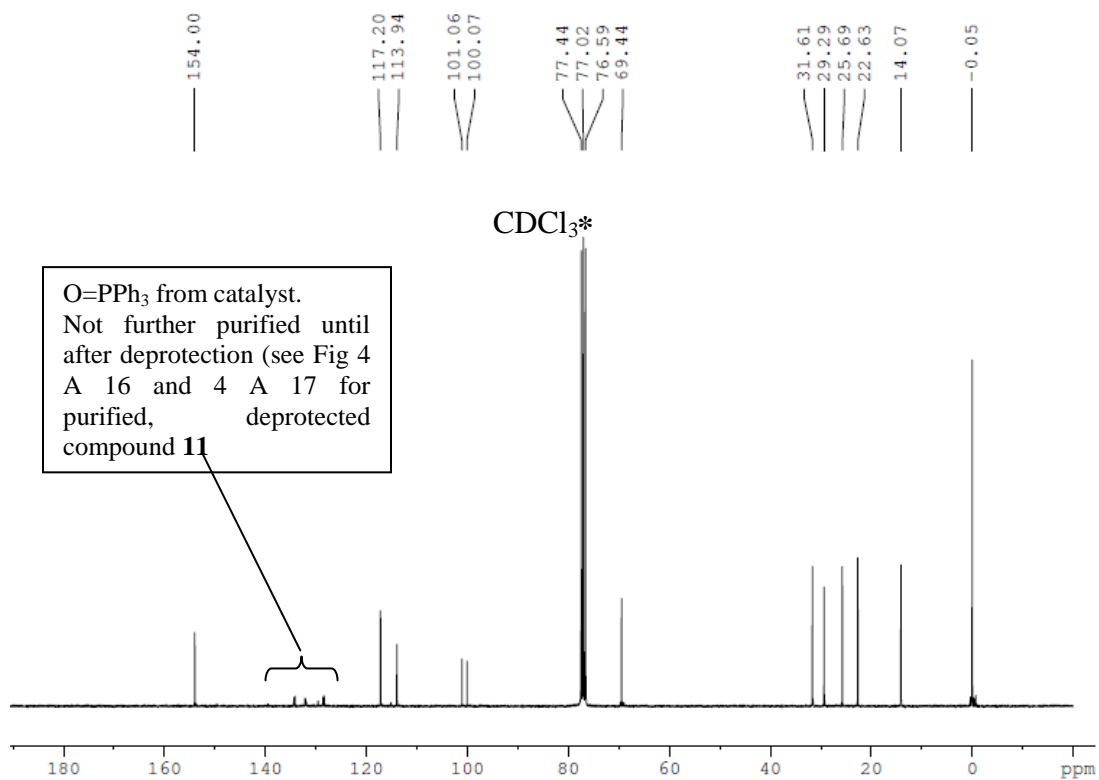
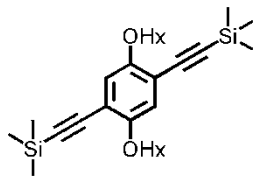


Figure 4 A 15 ¹³C NMR (75 MHz, CDCl₃) of **10**.

1,4-diethynyl-2,5-bis(hexyloxy) benzene (11)

Structure

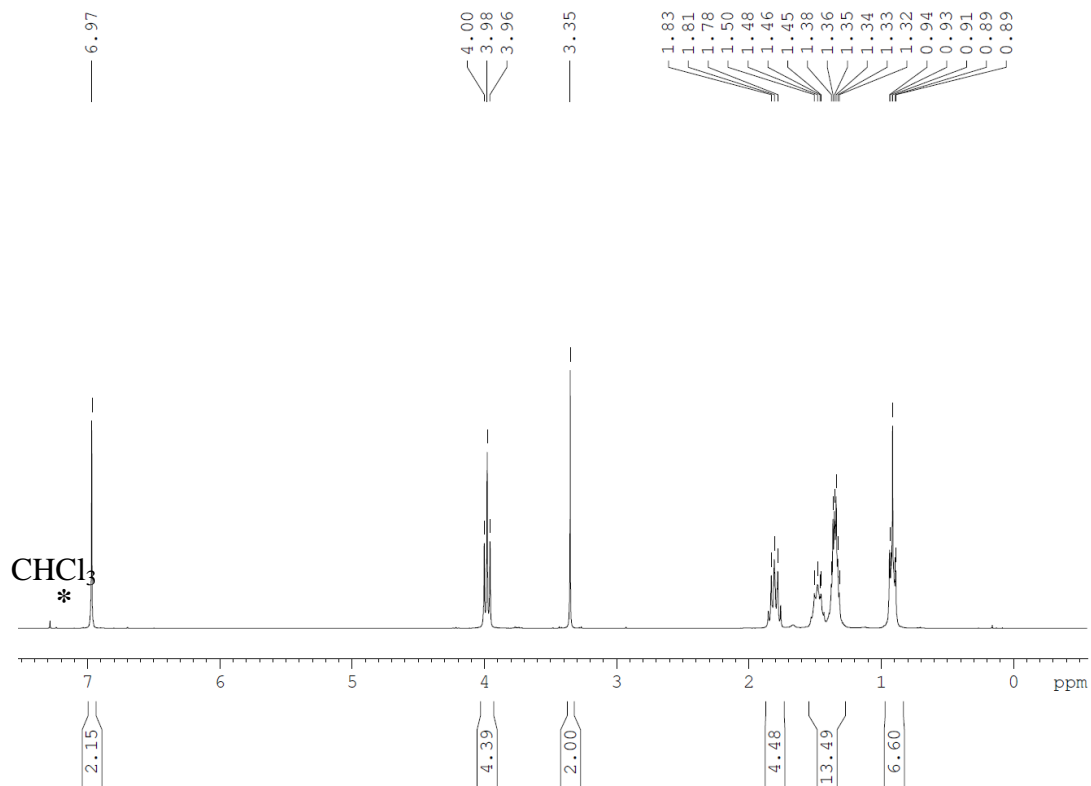
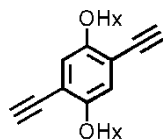


Figure 4 A.16 ^1H NMR (300 MHz, CDCl_3) of 11.

1,4-diethynyl-2,5-bis(hexyloxy) benzene (11)

Structure

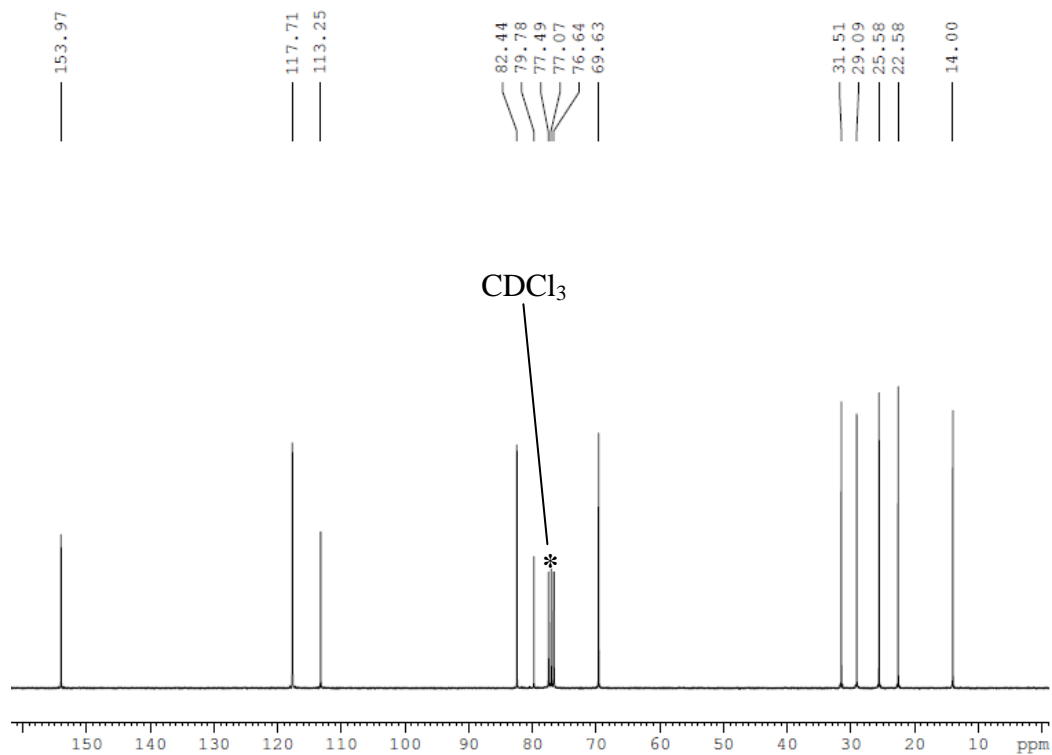
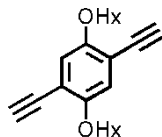


Figure 4 A.17 ^{13}C NMR (75 MHz, CDCl_3) of **11**.

Compound B

Structure

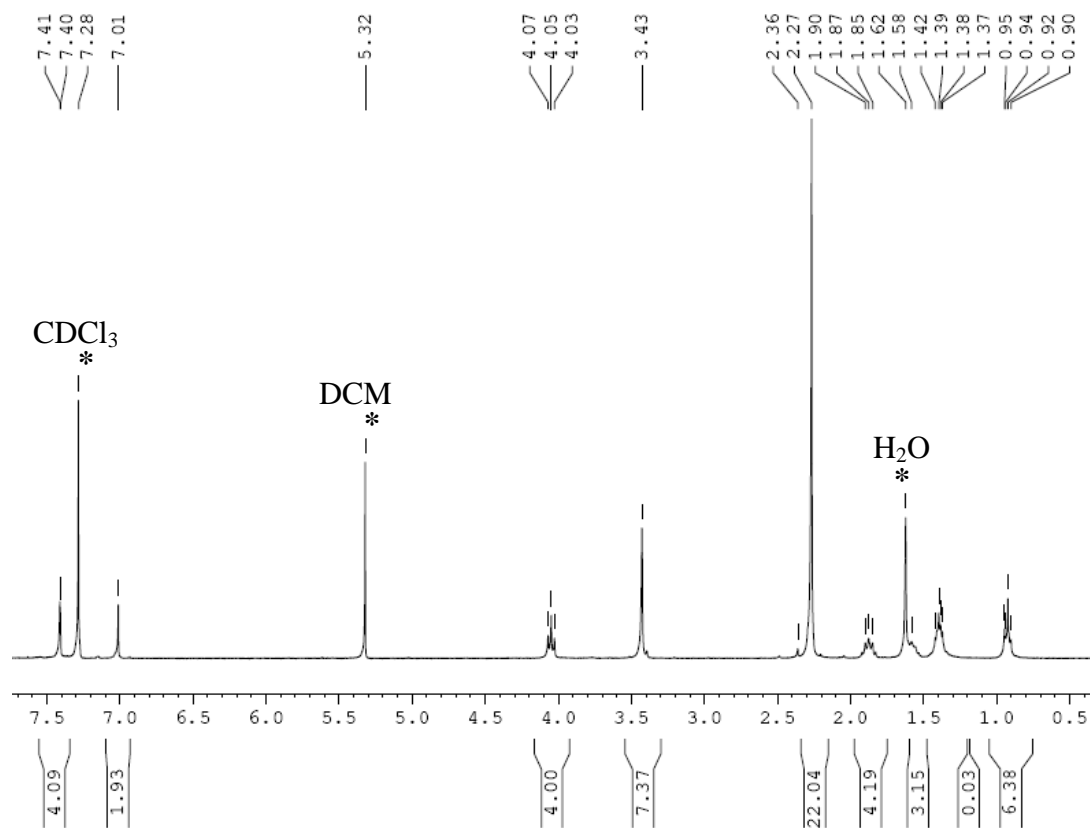
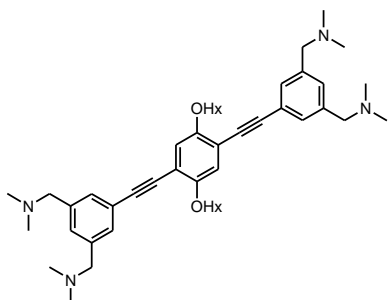


Figure 4 A.18 ¹H NMR (300 MHz, CDCl₃) of B.

Compound B

Structure

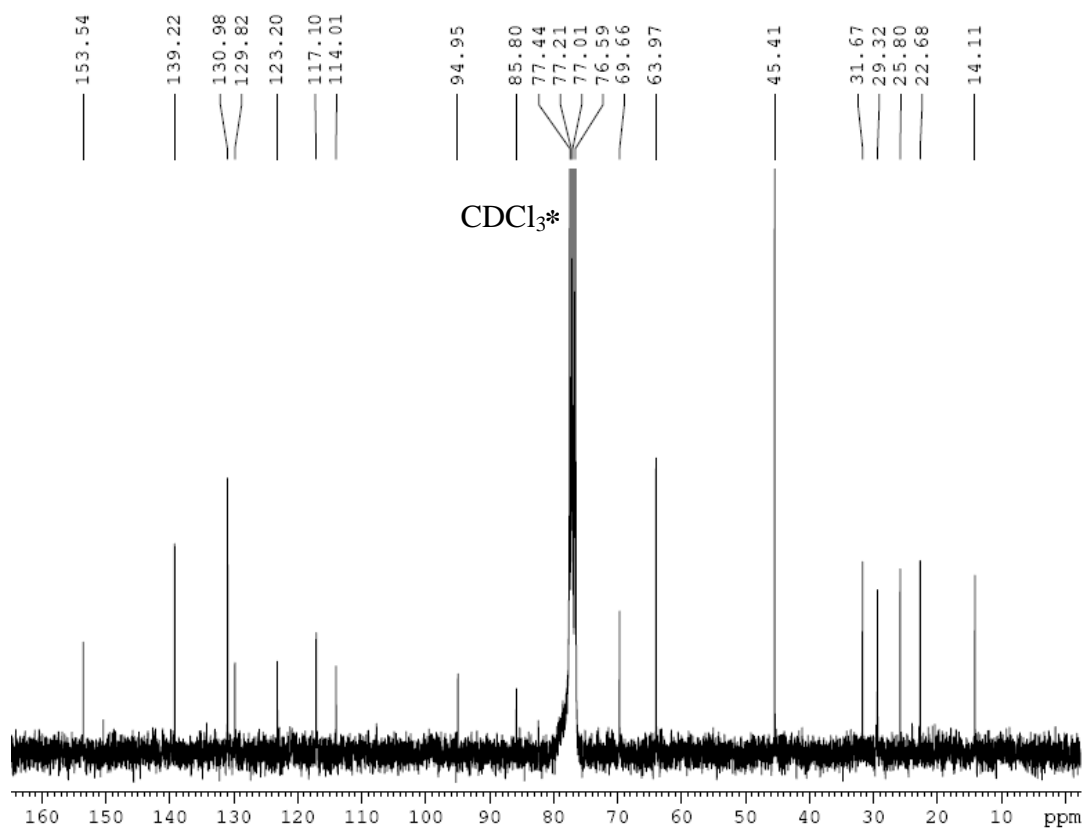
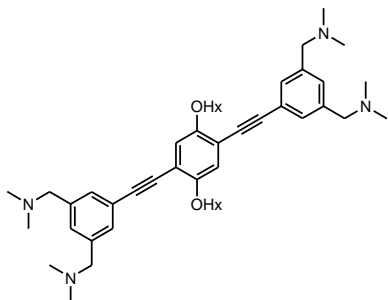


Figure 4 A.19 ¹³C NMR (75 MHz, CDCl₃) of B.

2-bromo-9,9-dihexyl-9-H-fluorene (**13**)

Structure

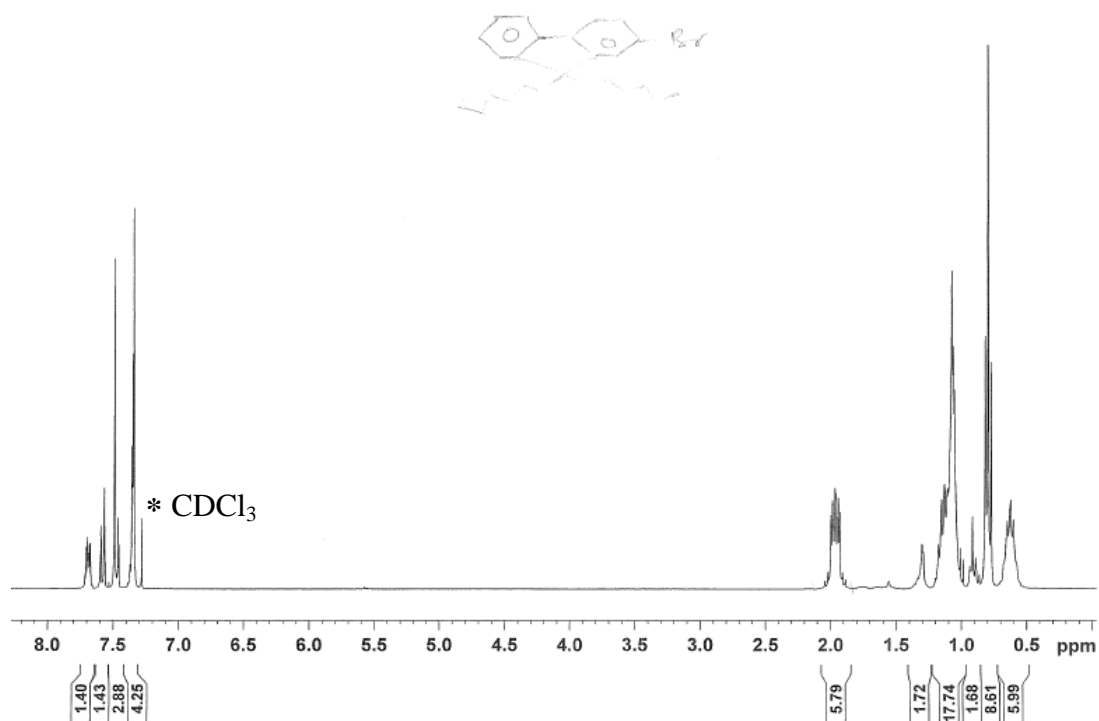
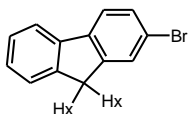


Figure 4 A.20 ¹H NMR (300 MHz, CDCl₃) of **13**.

2-bromo-9,9-dihexyl-9-H-fluorene (**13**)

Structure

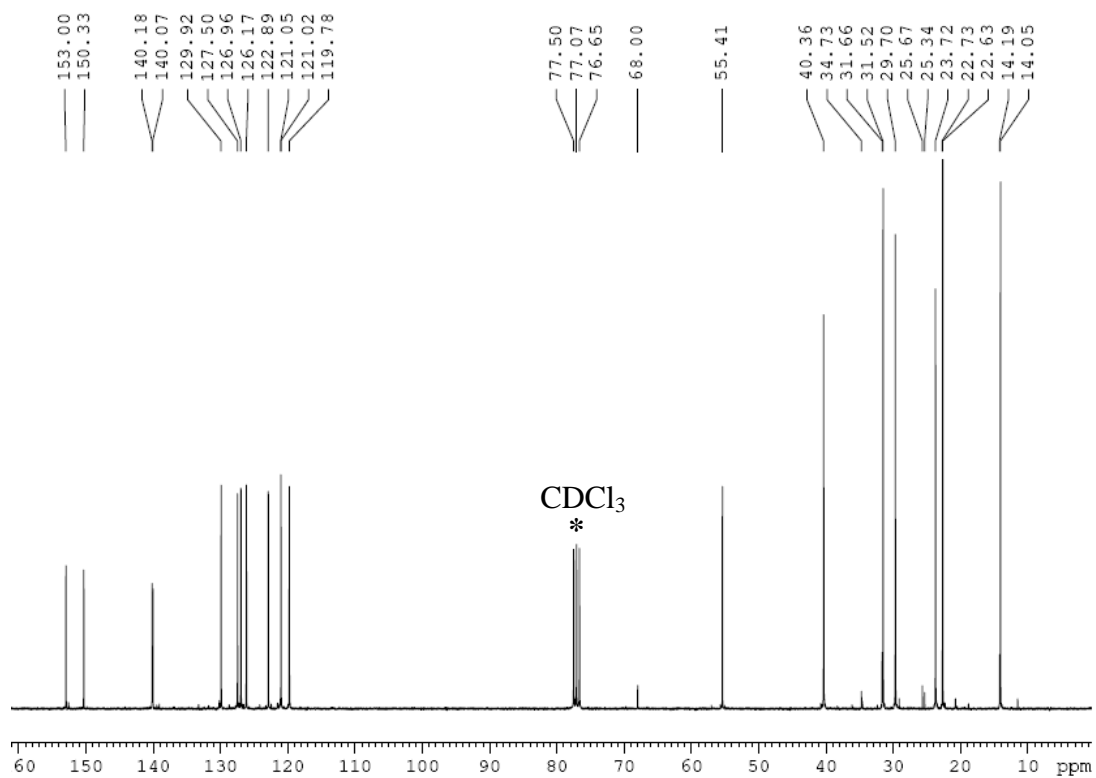
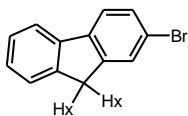


Figure 4 A.21 ¹³C NMR (75 MHz, CDCl₃) of **13**.

(2-(9,9-dihexyl-9-*H*-fluorene-2-yl) ethynyl)trimethylsilane (**14**)

Structure

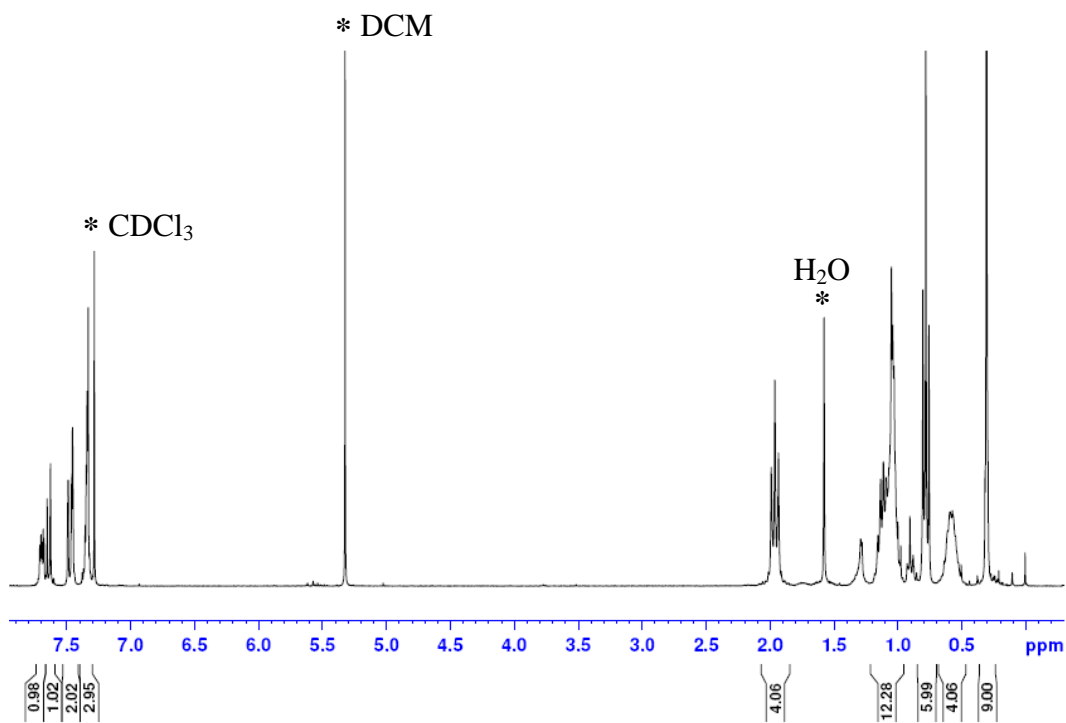
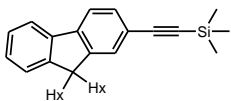


Figure 4 A.22 ¹H NMR (300 MHz, CDCl₃) of **14**.

(2-(9,9-dihexyl-9-*H*-fluorene-2-yl) ethynyl)trimethylsilane (**14**)

Structure

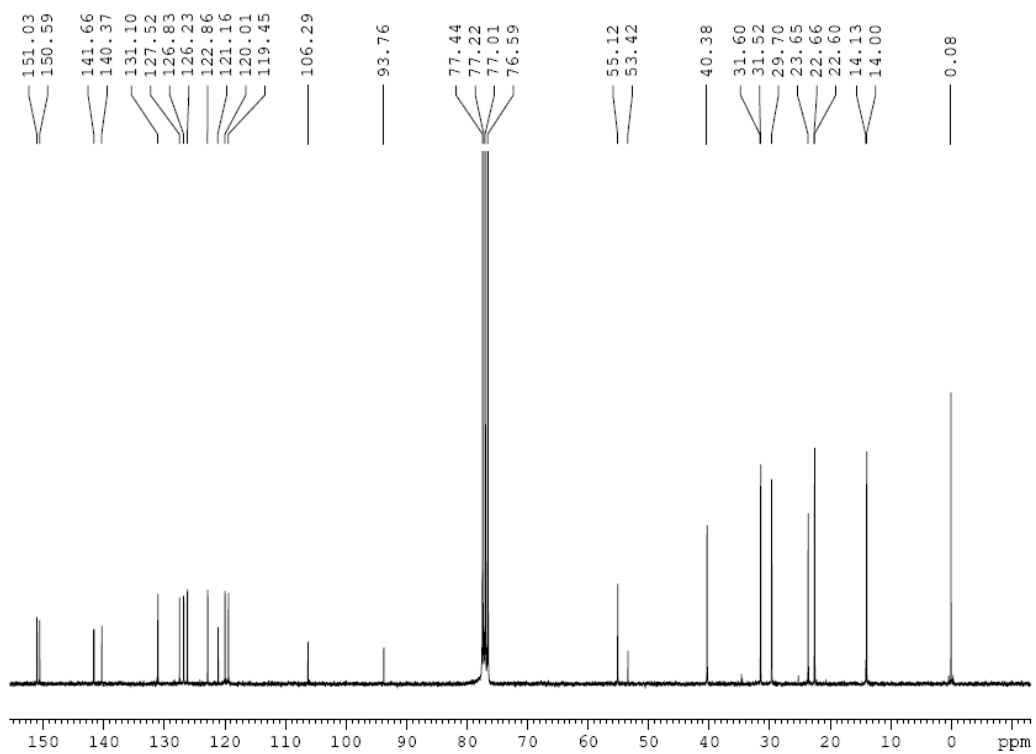
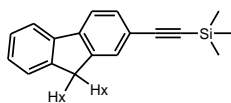


Figure 4 A.23 ^{13}C NMR (75 MHz, CDCl_3) of **14**.

2-ethynyl-9,9-dihexyl-9-*H*-fluorene (**15**)

Structure

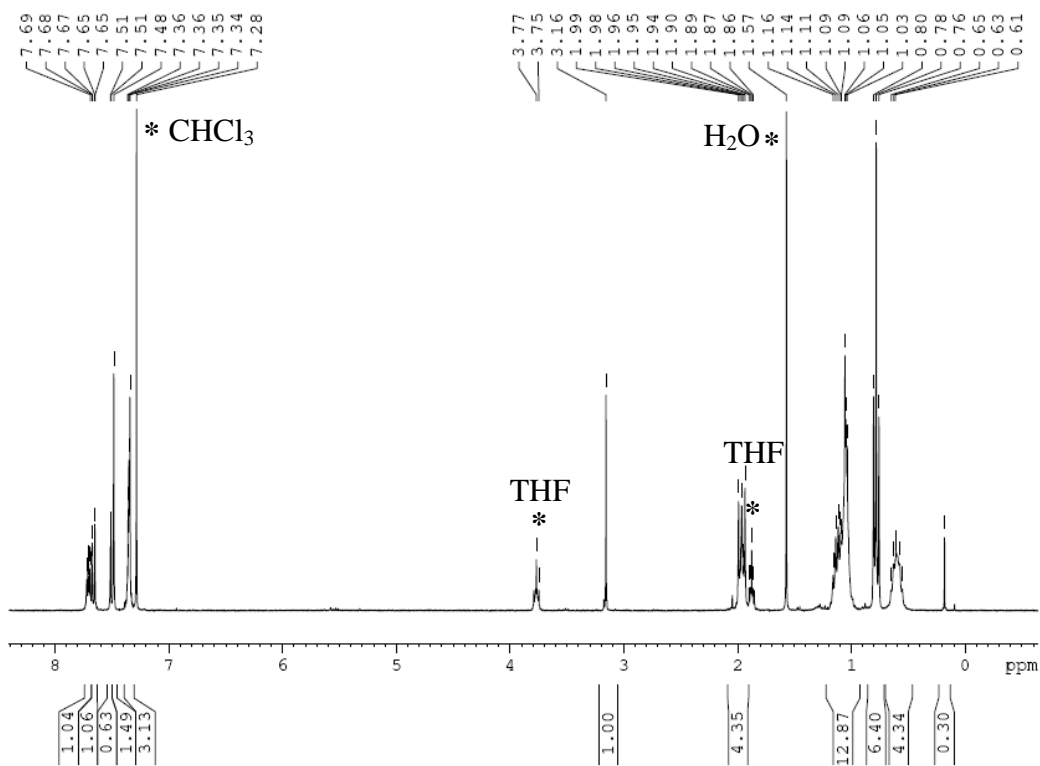
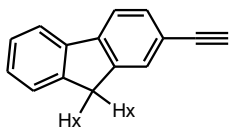


Figure 4 A.24 ¹H NMR (300 MHz, CDCl₃) of **15**.

2-ethynyl-9,9-dihexyl-9-*H*-fluorene (**15**)

Structure

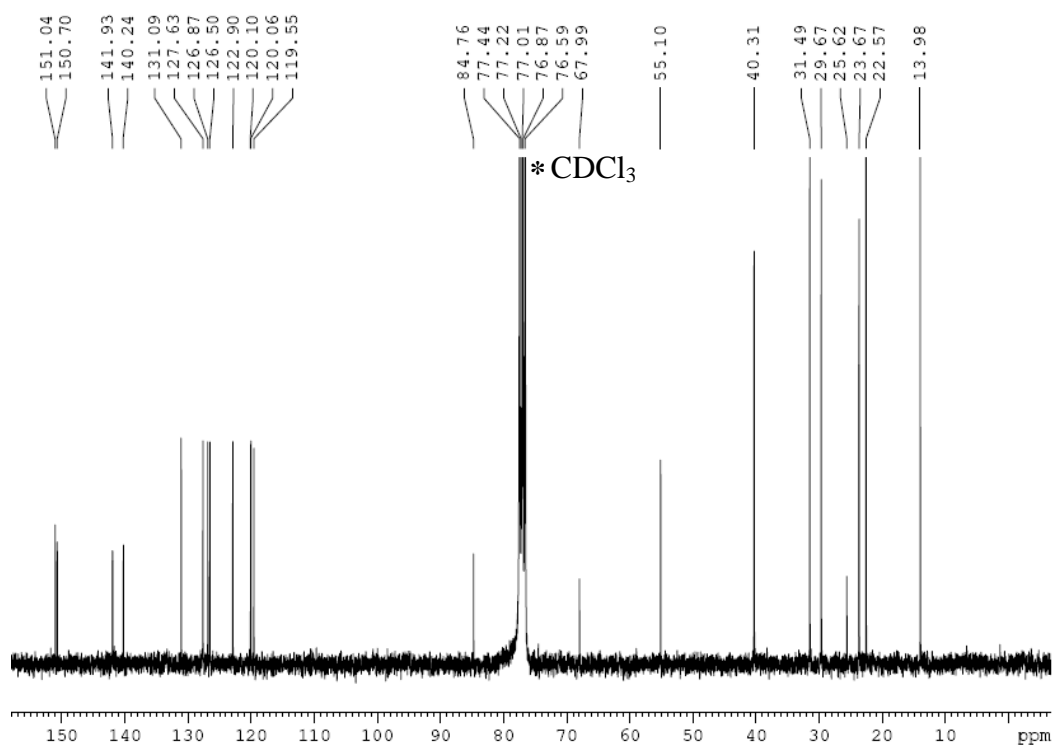
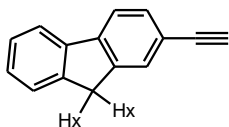


Figure 4 A.25 ^{13}C NMR (75 MHz, CDCl_3) of **15**.

Compound C

Structure

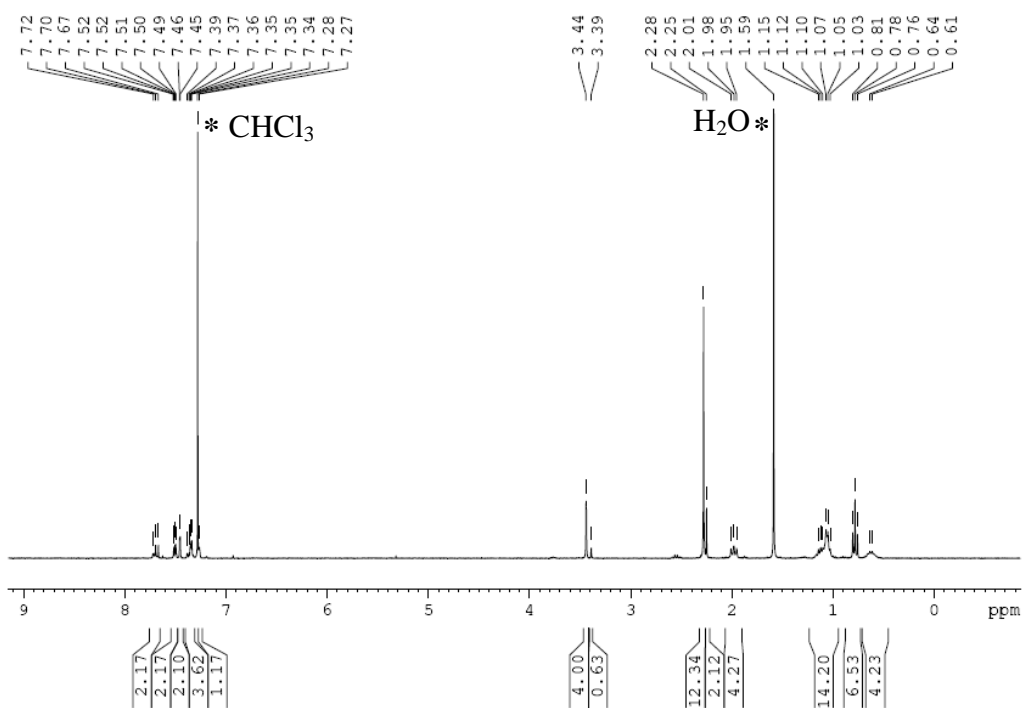
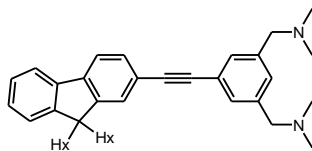


Figure 4 A.26 ¹H NMR (300 MHz, CDCl₃) of C.

Compound C

Structure

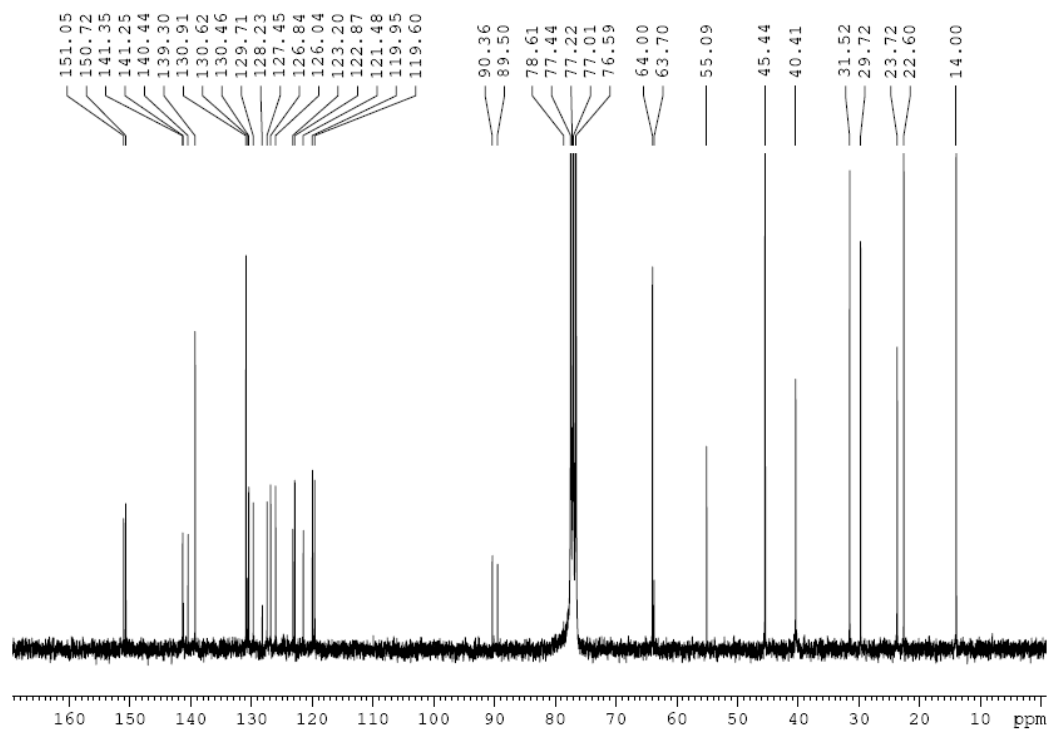
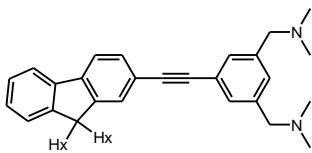


Figure 4 A.27 ¹³C NMR (75 MHz, CDCl₃) of C.

Compound **17**

Structure

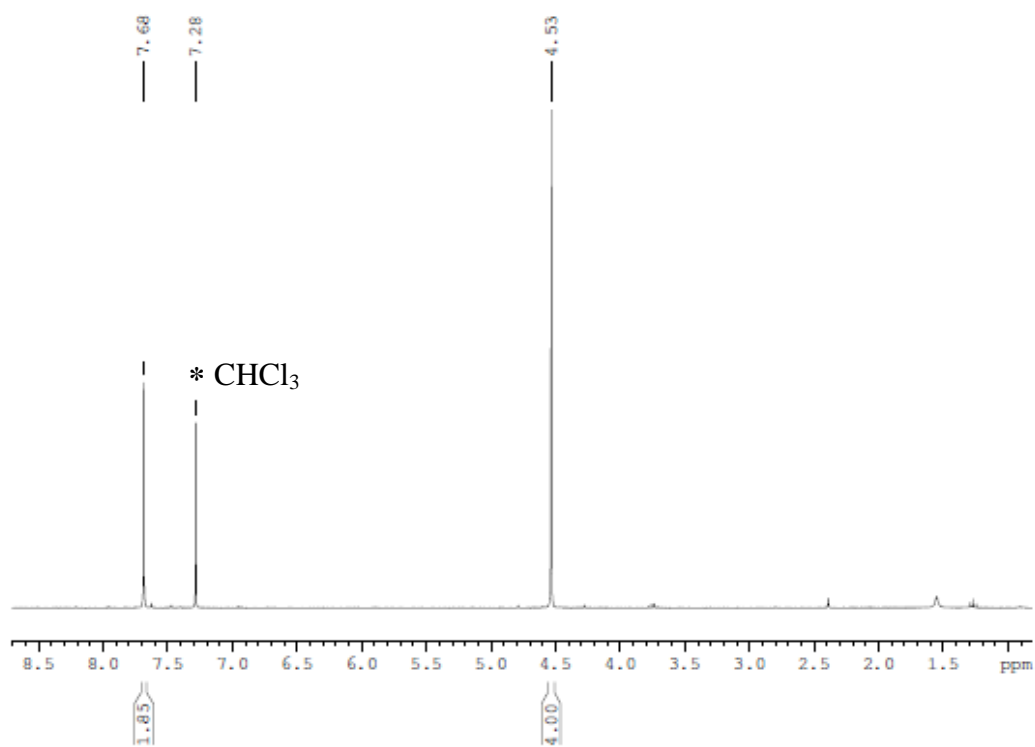
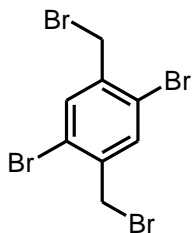


Figure 4 A.28 ¹H NMR (300 MHz, CDCl₃) of **17**.

4-hexyloxybenzaldehyde (**19**)

Structure

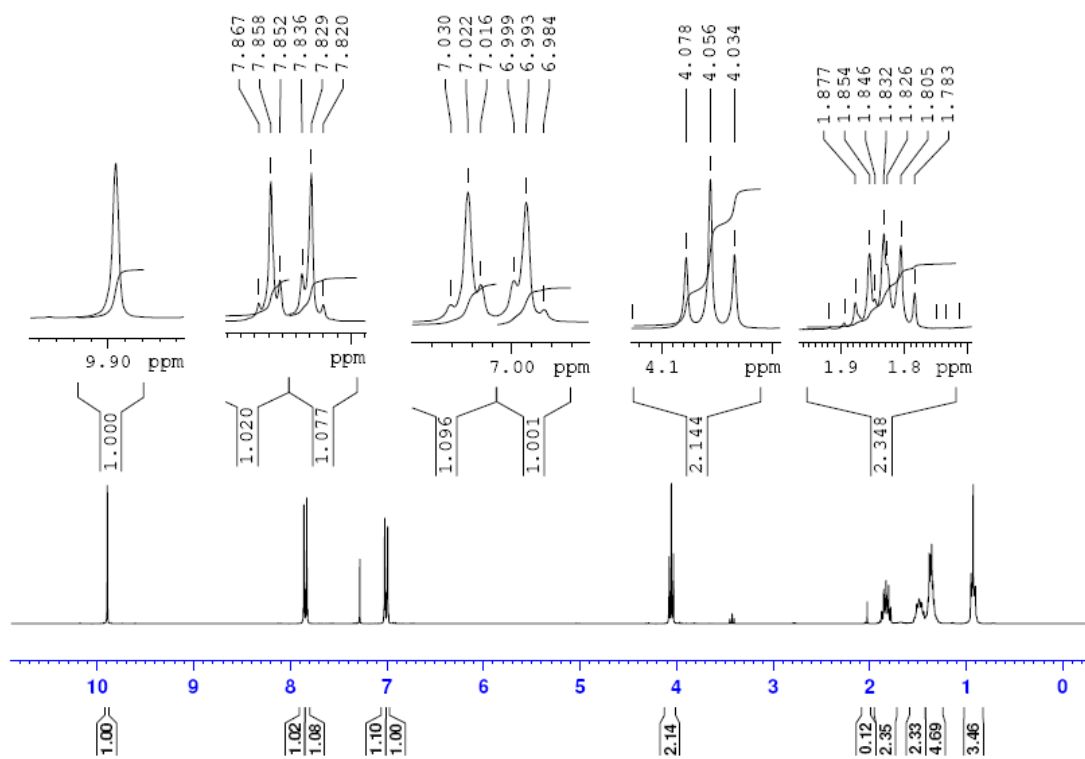
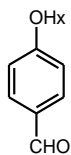


Figure 4 A.29 ¹H NMR (300 MHz, CDCl₃) of **19**.

Compound 20

Structure

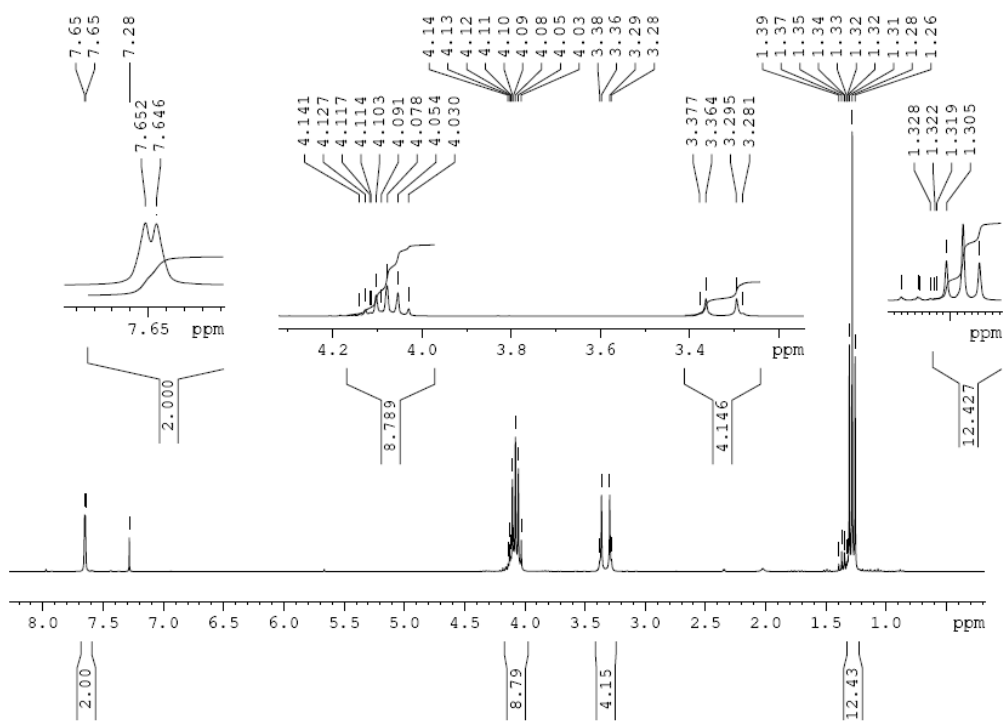
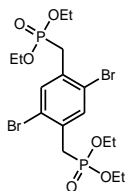


Figure 4 A.30 ¹H NMR (300 MHz, CDCl₃) of 20.

Compound 20

Structure

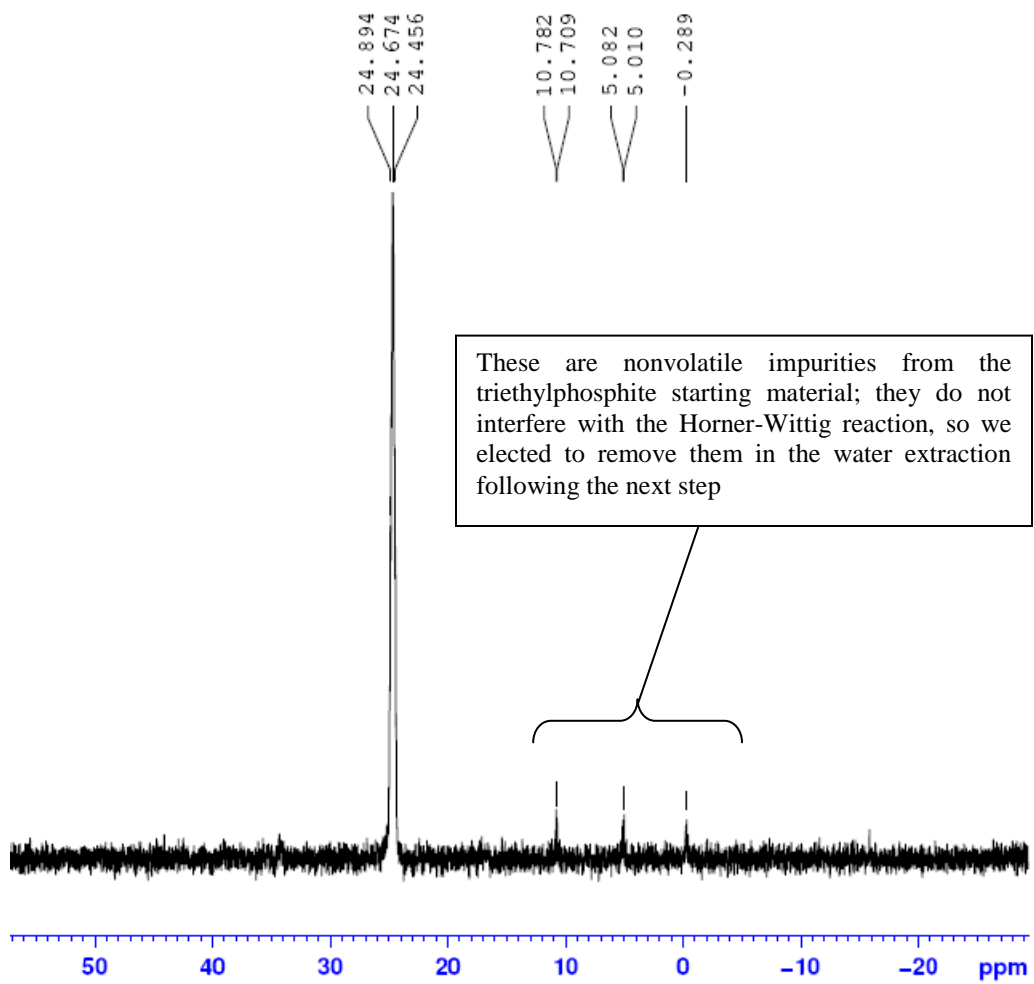
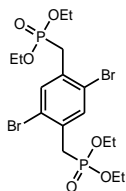


Figure 4 A.31 ^{31}P NMR (121 MHz, CDCl_3) of **20**.

Compound 21

Structure

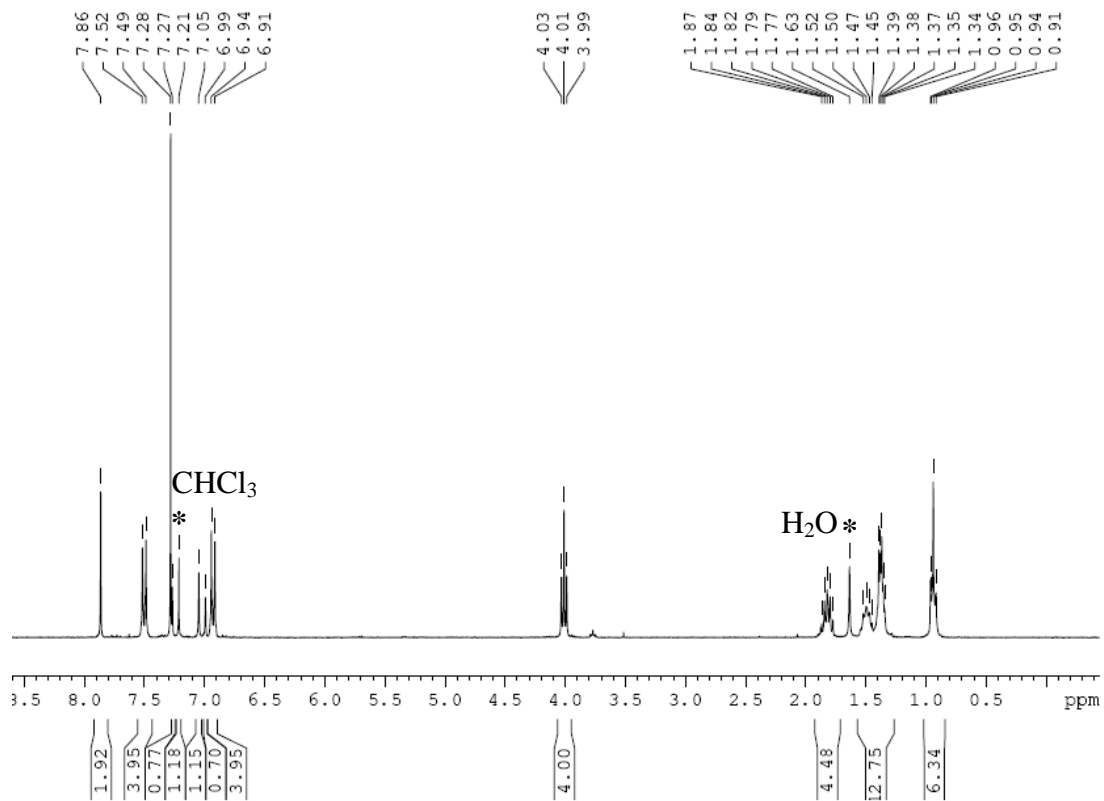
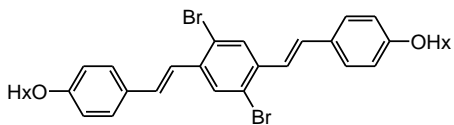


Figure 4 A.32 ¹H NMR (300 MHz, CDCl₃) of 21.

Compound 21

Structure

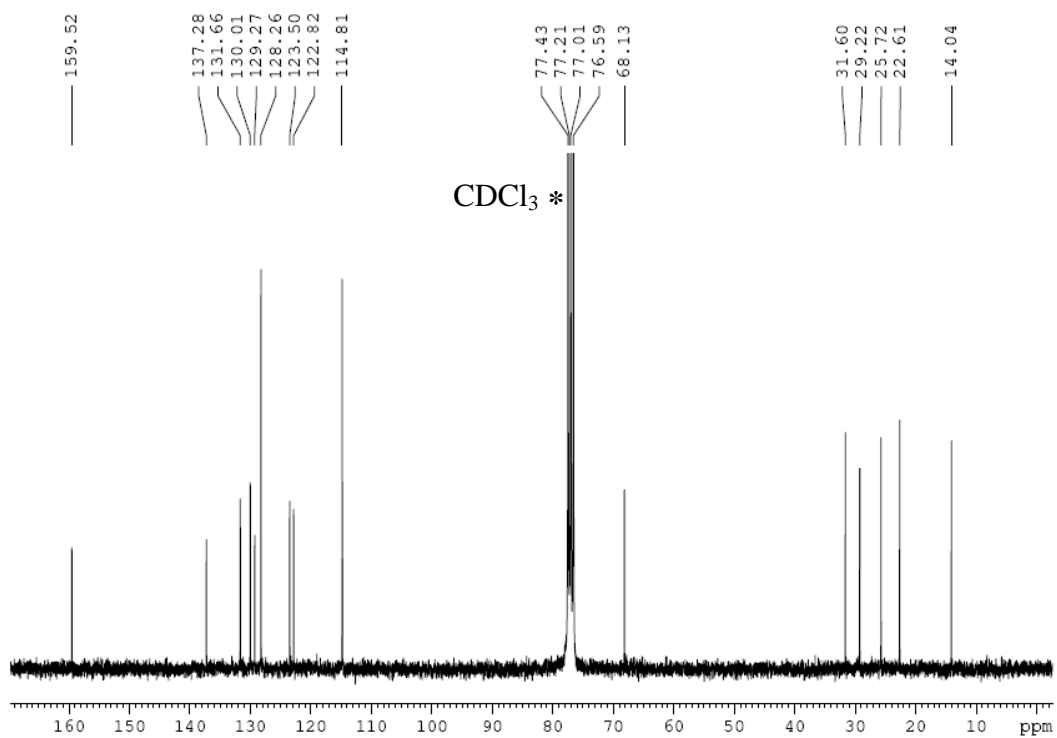
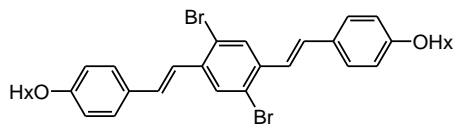


Figure 4 A.33 ^{13}C NMR (75 MHz, CDCl_3) of 21.

Compound 22

Structure

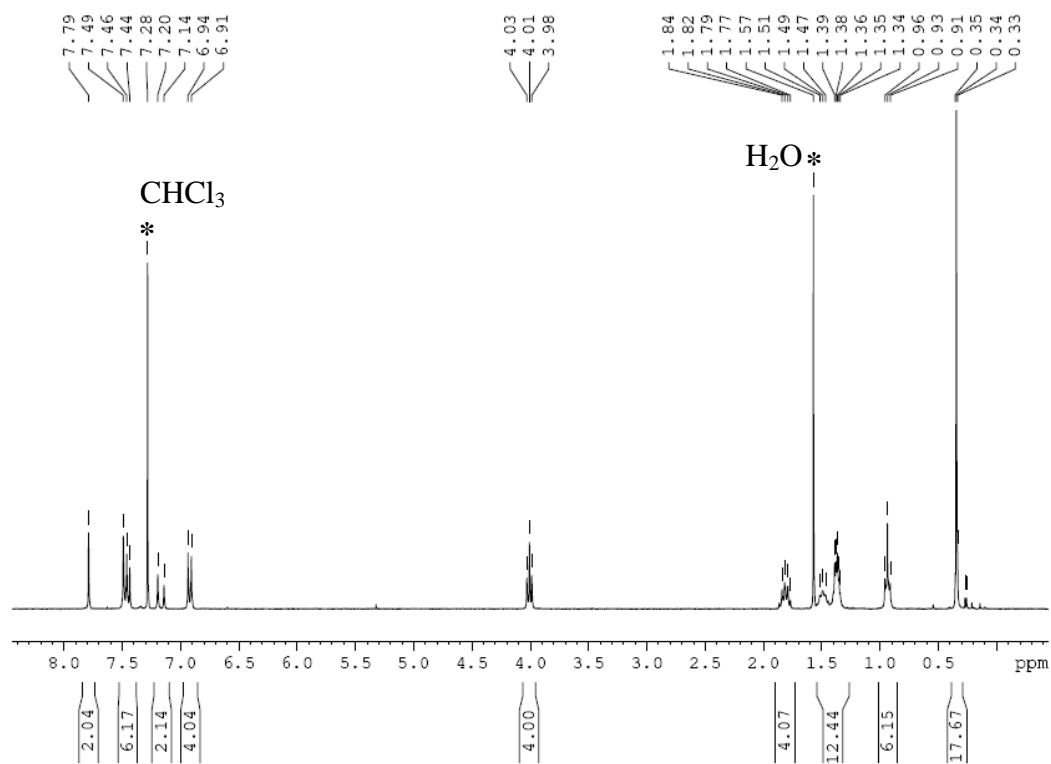
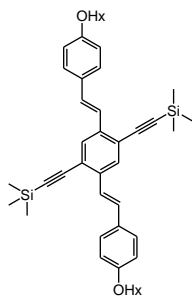


Figure 4 A.34 ¹H NMR (300 MHz, CDCl₃) of 22.

Compound 22

Structure

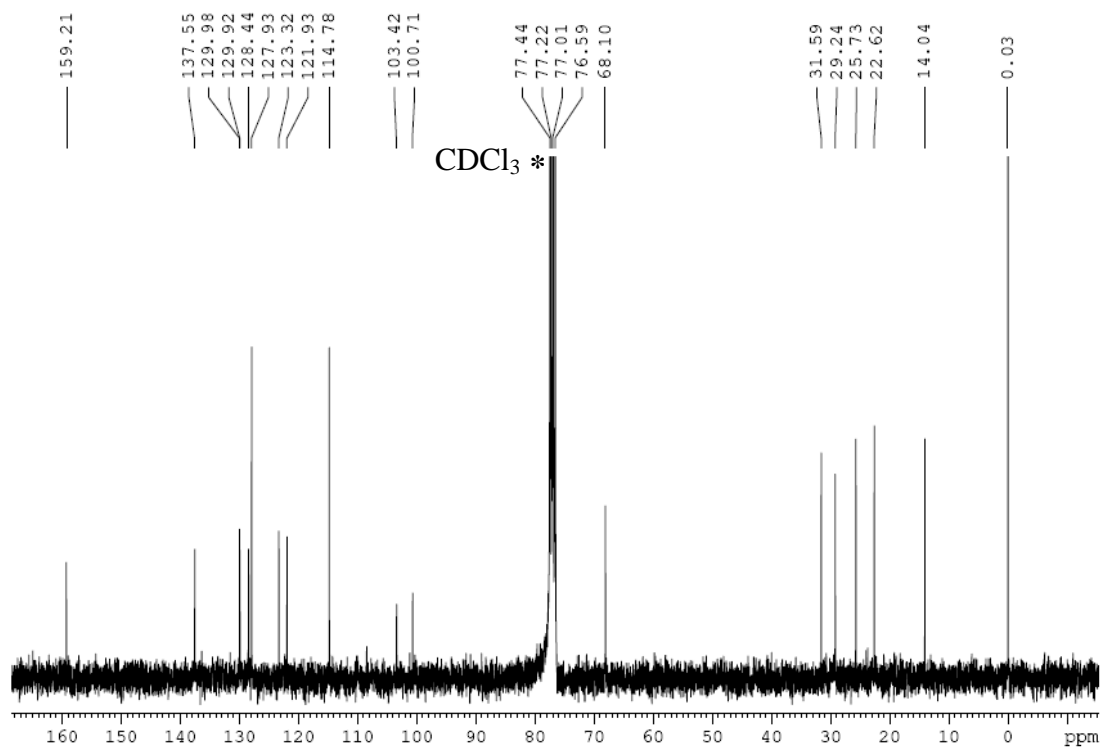
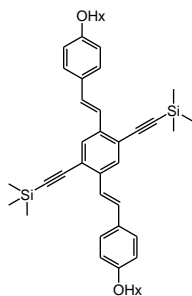
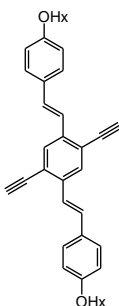


Figure 4 A.35 ^{13}C NMR (75 MHz, CDCl_3) of 22.

Compound 23

Structure



7.84
7.51
7.48
7.47
7.42
7.28
7.18
7.13
6.94
6.91

4.03
4.01
3.98
3.47

1.86
1.84
1.82
1.79
1.77
1.58
1.52
1.49
1.47
1.44
1.39
1.38
1.36
1.35
1.34
1.27
0.96
0.93
0.91

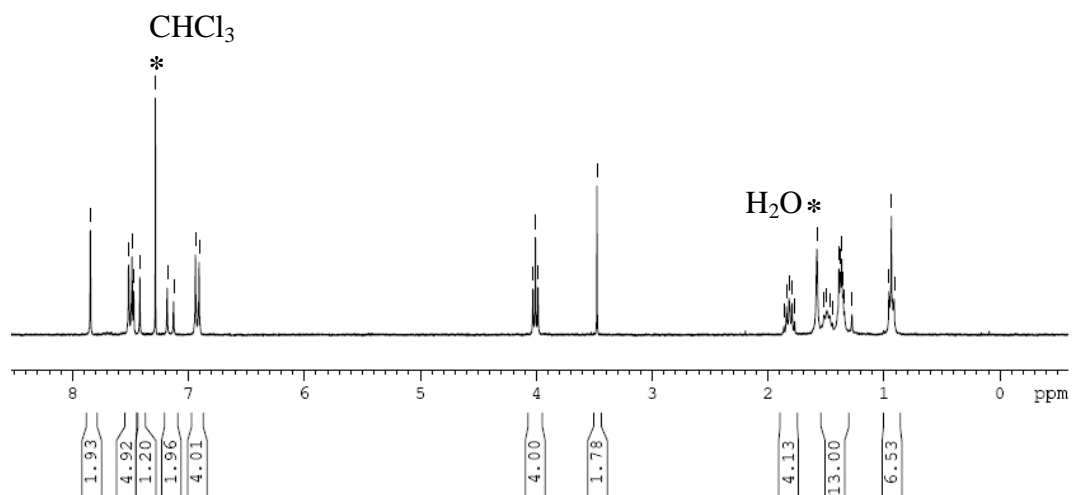


Figure 4 A.36 ¹H NMR (300 MHz, CDCl₃) of 23.

Compound D

Structure

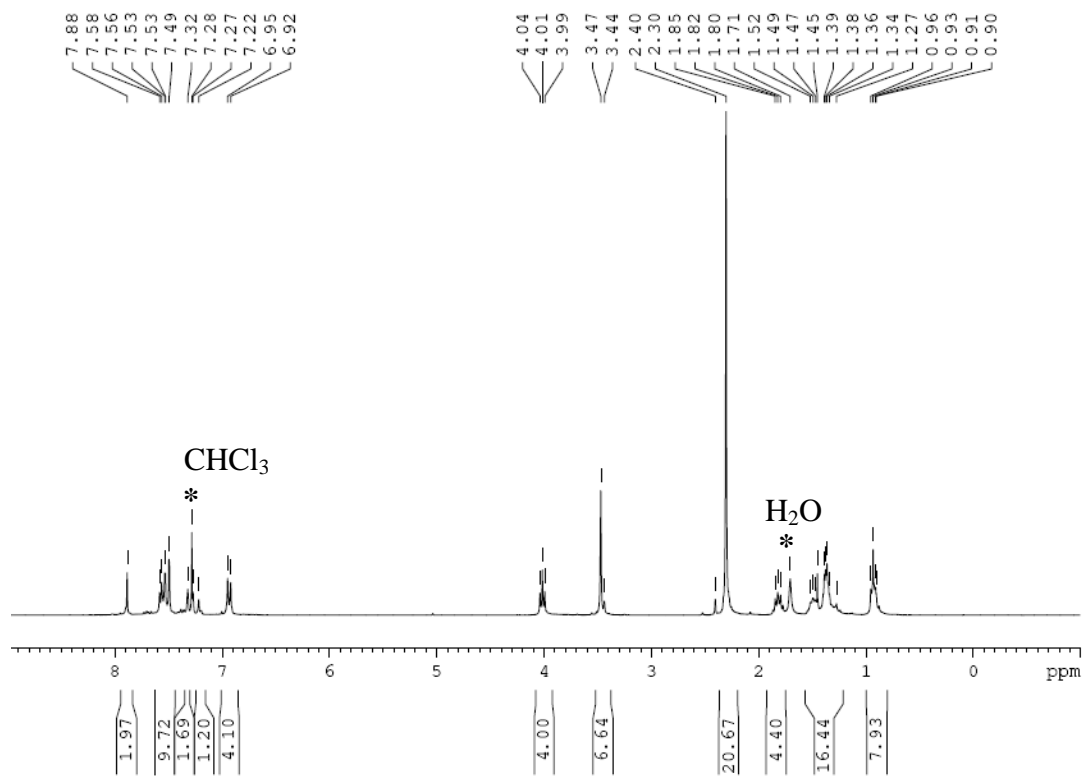
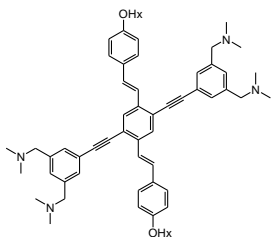


Figure 4 A.37 ¹H NMR (300 MHz, CDCl₃) of D.

Compound D

Structure

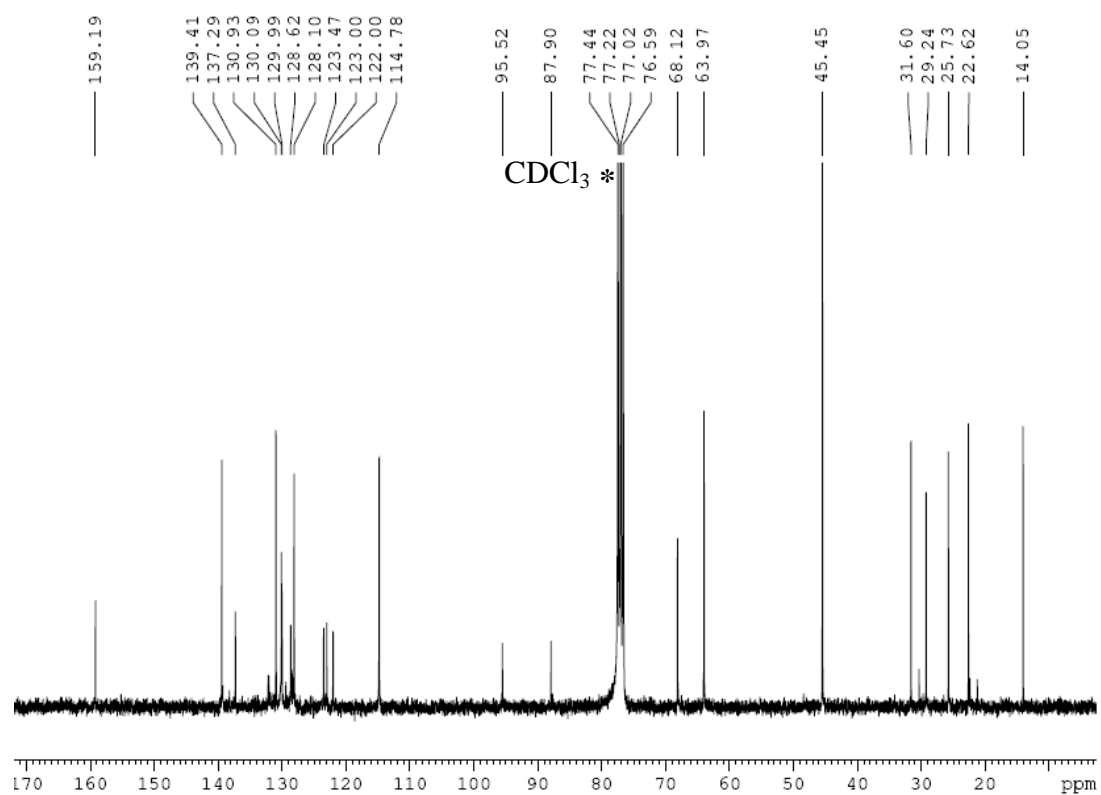
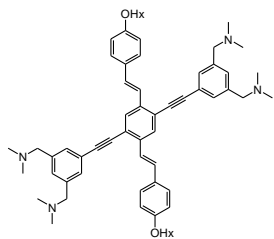


Figure 4 A.38 ^{13}C NMR (75 MHz, CDCl_3) of D.

Compound 25

Structure

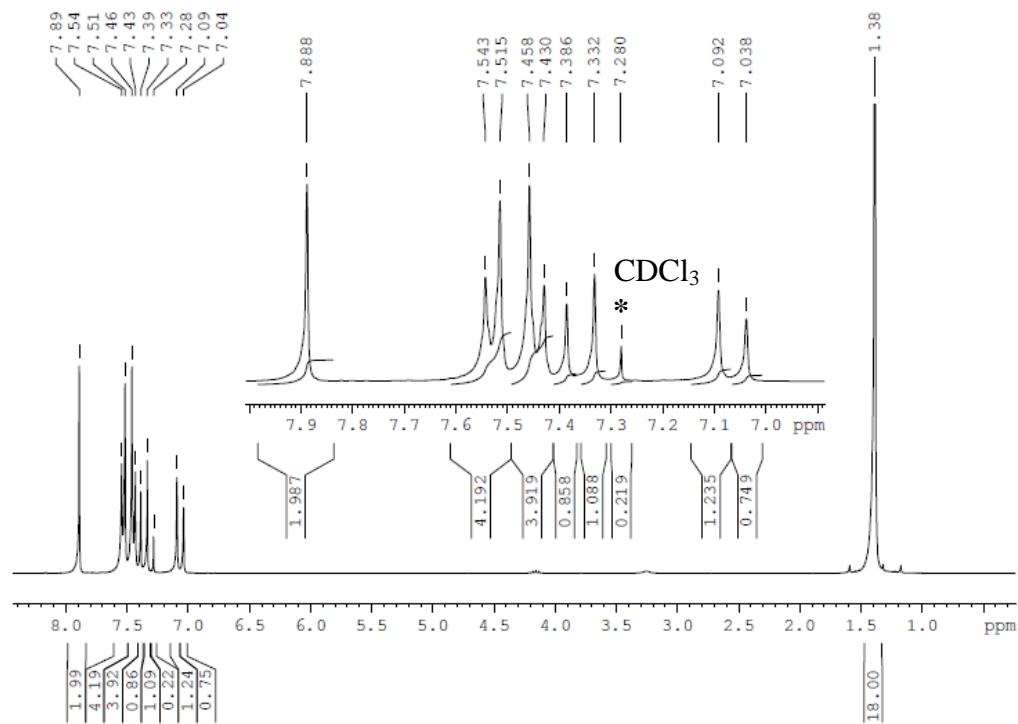
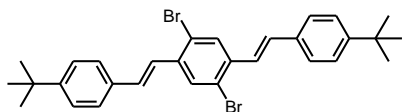


Figure 4 A.39 ¹H NMR (300 MHz, CDCl₃) of 25.

Compound 25

Structure

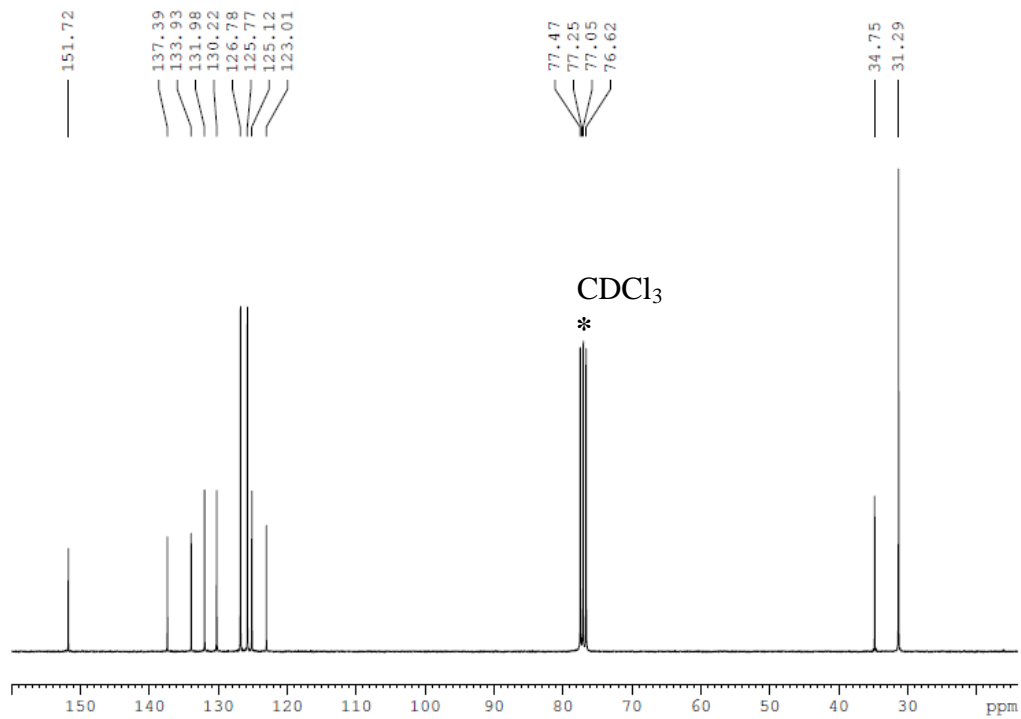
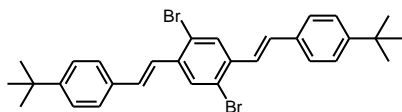


Figure 4 A.40 ¹³C NMR (75 MHz, CDCl₃) of 25.

Compound 26

Structure

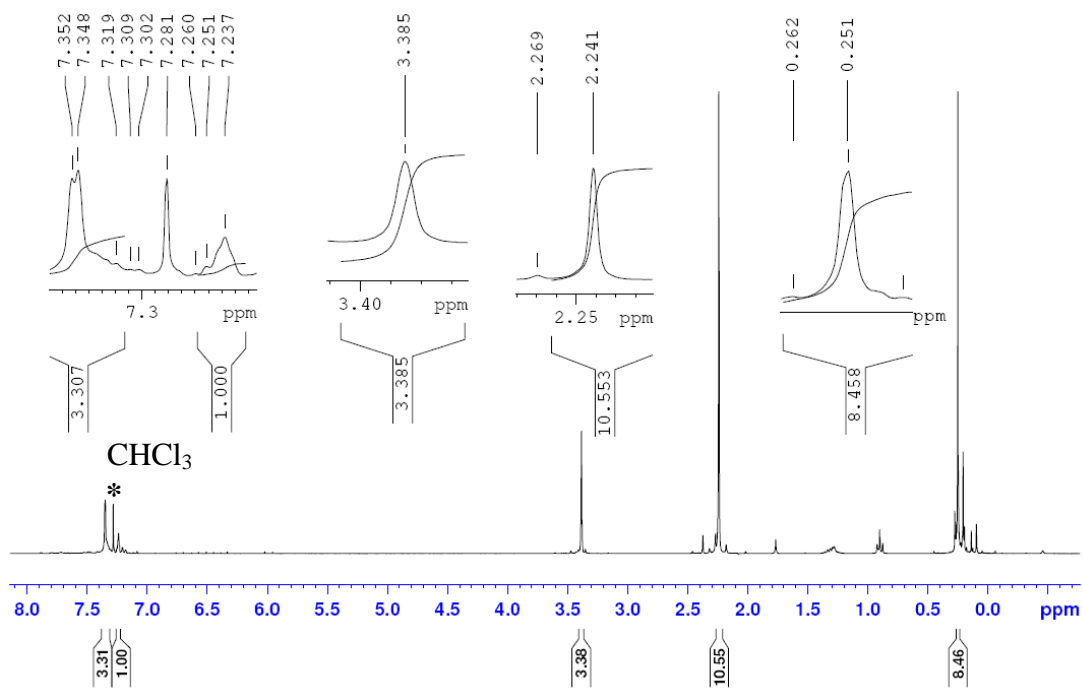
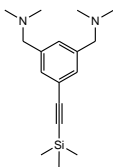
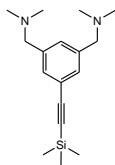


Figure 4 A.41 ^1H NMR (300 MHz, CDCl_3) of 26.

Compound 26

Structure



AM-1-122-sonogashira-TMSacetylene-hexane layer-CDCl₃-13C

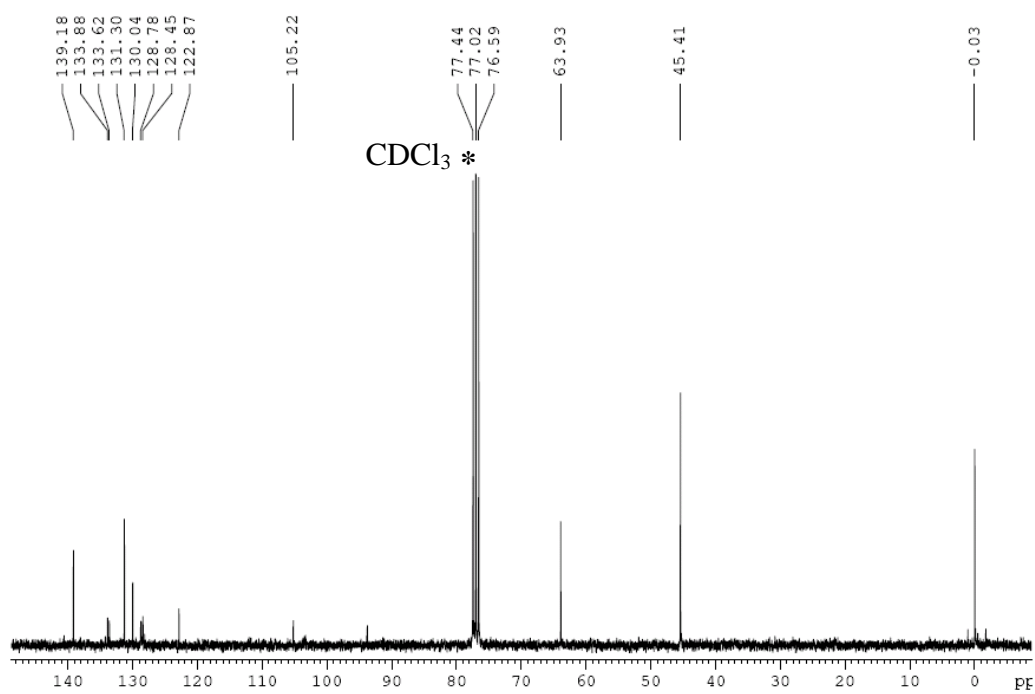


Figure 4 A.42 ¹³C NMR (75 MHz, CDCl₃) of 26.

Compound **27**

Structure

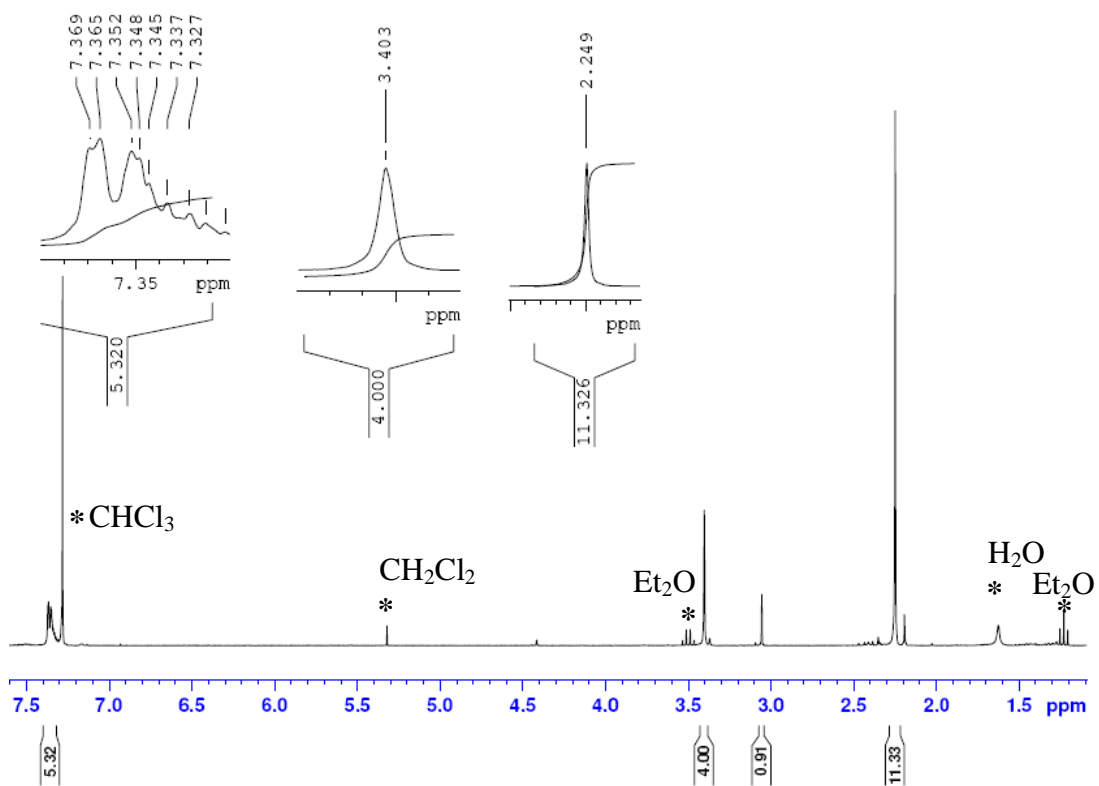
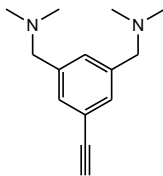


Figure 4 A.43 ^1H NMR (300 MHz, CDCl_3) of **27**.

Compound **27**

Structure

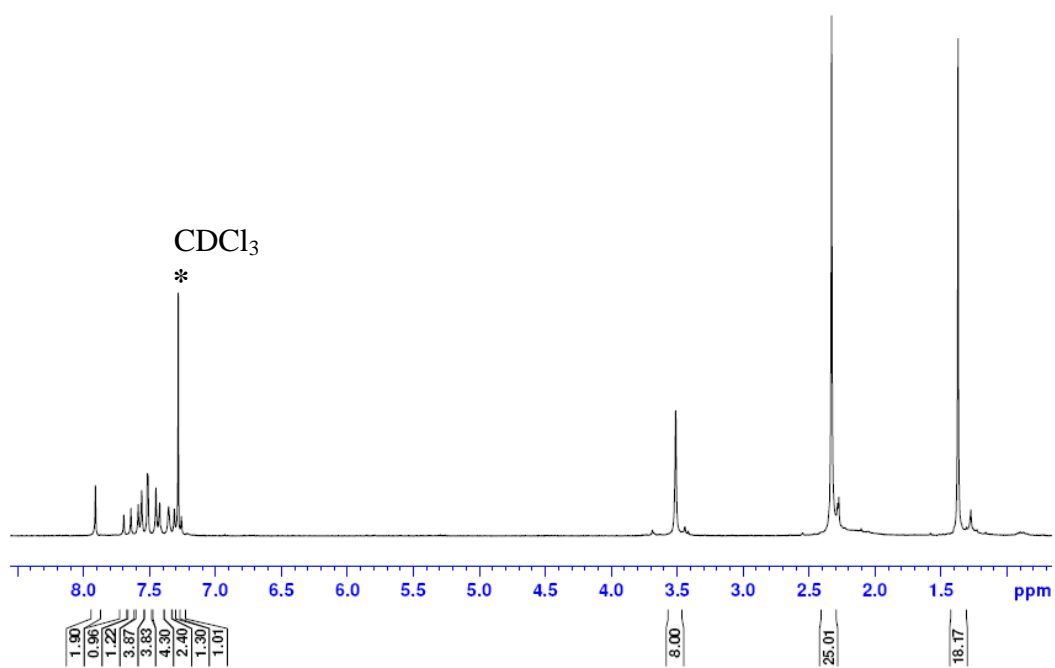
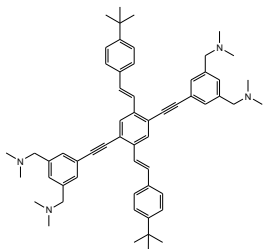


Figure 4 A.44 ¹H NMR (300 MHz, CDCl₃) of **E**.

Compound 27

Structure

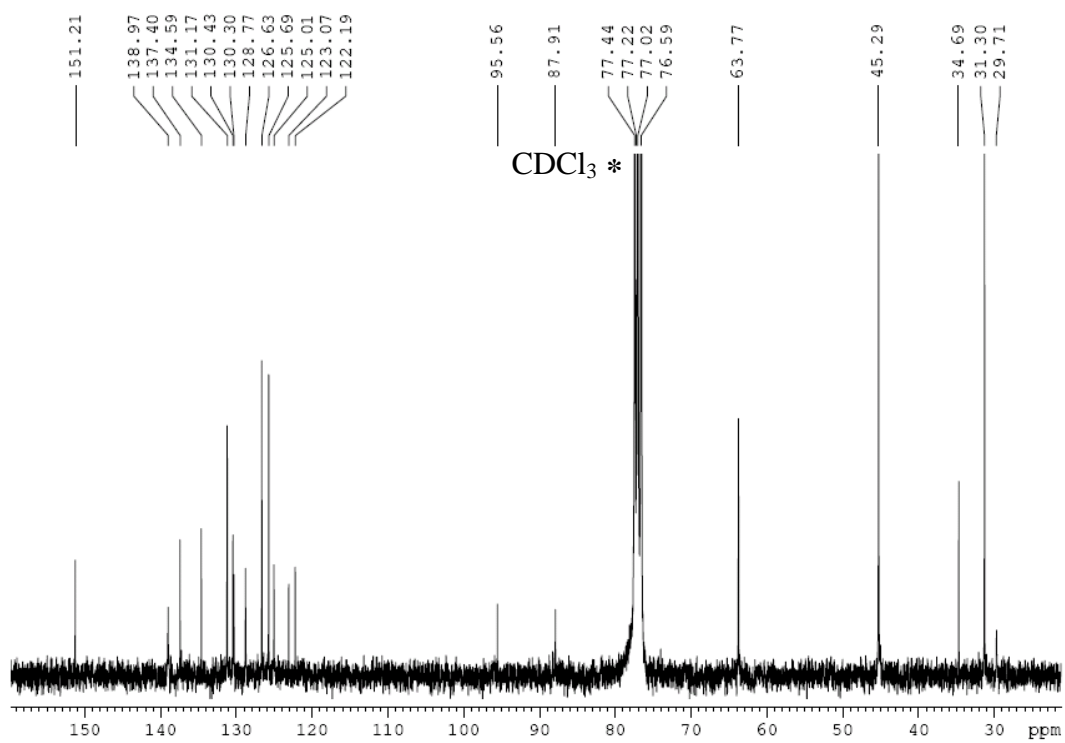
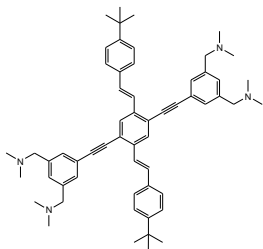


Figure 4 A.45 ^{13}C NMR (75 MHz, CDCl_3) of E.

Chapter 5

BIFUNCTIONAL CROSS-CONJUGATED LIGHT-HARVESTING PHOSPHINES AND PHOSPHINE DERIVATIVES: PHOSPHA-CRUCIFORMS[#]

5.1 Introduction

Optical properties of transition metal complexes have been of interest since the dawn of coordination chemistry, when Werner classified complexes on the basis of their color.^{1, 2} In more recent years, the role of light harvesting ligands in the photochemistry of transition metal complexes has been an ongoing area of interest, and chromophore-modified complexes have found use in diverse applications ranging from triplet emissive materials and light-emitting diodes (**LEDs**)³⁻⁸ to nonlinear optics (**NLO**)⁹⁻¹⁵ and photocatalysis.¹⁶⁻²⁰

Because of the interest in the photophysics of transition metal complexes and the widespread utility of phosphine ligands in coordination chemistry, it is surprising that there have been relatively few studies on transition metal complexes with visible absorbing / emitting phosphine ligands (though there are numerous phosphole complexes).

One reason for this may be the added synthetic challenges of phosphorus chemistry and the air sensitive, sometimes pyrophoric nature of intermediate compounds

[#] Adapted from Mangalum, A.; Smith, R. C. *Dalton Trans.*, **2010**, 39, 5145-5151, with permission.

used in the preparation of phosphines. Nonetheless, significant recent progress has been made in the development of phosphorus-containing small molecule chromophores²¹⁻²⁴ and π -conjugated polymers²⁵⁻²⁷ (**Figure 5.1A**), and this growing field has recently been comprehensively reviewed.²⁸

The development of phosphorus-containing chromophores provides intriguing possibilities for their utility as ligands. Some examples of the relatively limited number of fluorescent or visible-absorbing chromophore-modified phosphine complexes that have been studied are shown in (**Figure 5.1B**).^{23, 24, 29-32} Another interesting and potentially useful aspect of phosphorus-containing systems is that a variety of phosphine derivatives can be prepared with phosphorus in +3 or +5 oxidation states, allowing access to various interchromophore geometries about the phosphorus center, as well as a range of electronic perturbations on attached π -systems.^{23, 33}

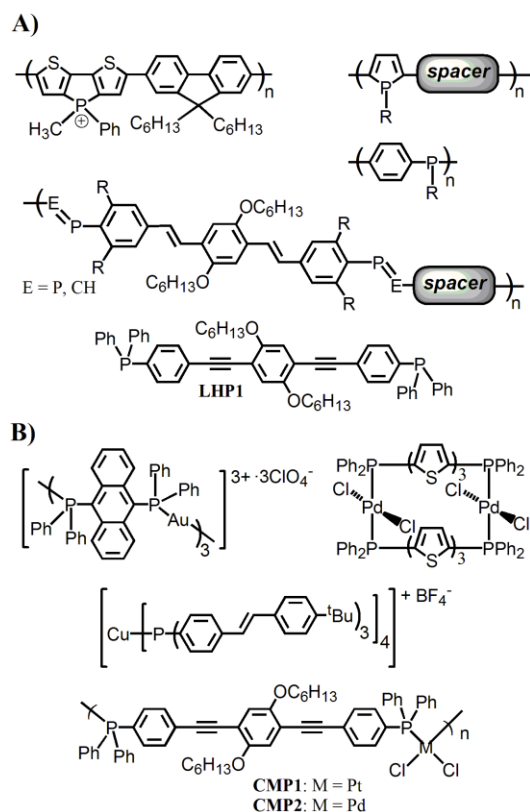


Figure 5.1 Phosphorous containing small molecule chromophores and π -conjugated polymers known in literature.

We recently reported luminescent metallopolymers polymerized through a light-harvesting diphosphine (**LHP1**, **Figure 5.1**) that displays visible-wavelength absorption and emission.²⁴ The light-harvesting phosphine used for polymerization was prepared using (4-iodophenyl)P(O)Ph₂ as a versatile precursor amenable to Pd-catalyzed coupling to various chromophores under mild conditions at room temperature. Following this work, we have become interested in light-harvesting phosphines with a variety of absorption and emission properties for the preparation of additional organophosphorus

species, photophysically interesting phosphine-metal complexes and emissive coordination polymers.

A relatively new class of photochemically interesting materials is comprised of materials featuring multiple π -systems that overlap at a central junction. Chromophores with such cross-conjugated branches,³⁴⁻³⁸ sometimes called cruciforms,³⁹⁻⁴³ are a class of molecules that can exhibit the unusual feature of having HOMOs and LUMOs that are geometrically separate. Some examples pertinent to the current study are shown in (Figure 5.2).

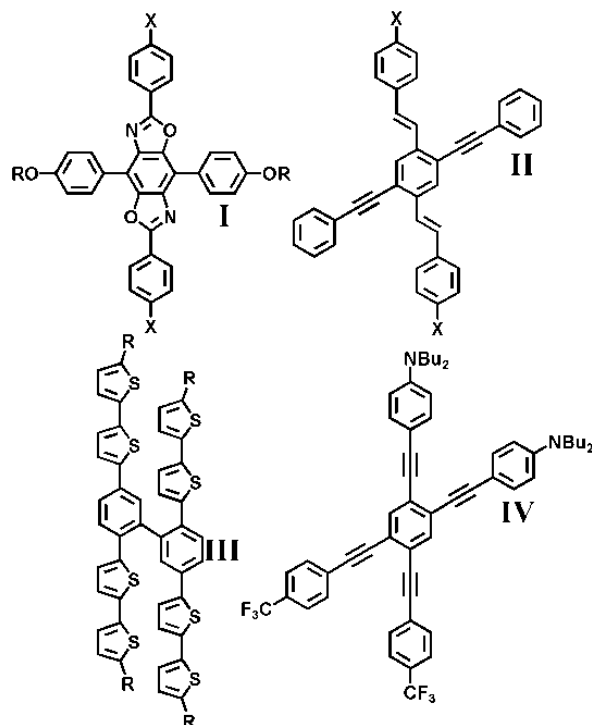


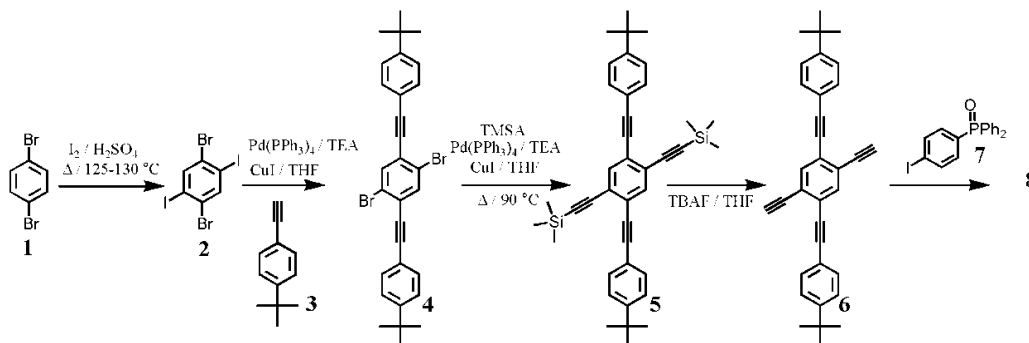
Figure 5.2 Cross conjugated materials such as cruciforms known in literature.

By appending stimuli-responsive functionalities to cross-conjugated constructs, the energy of one frontier orbital may be perturbed while that of the other remains fairly

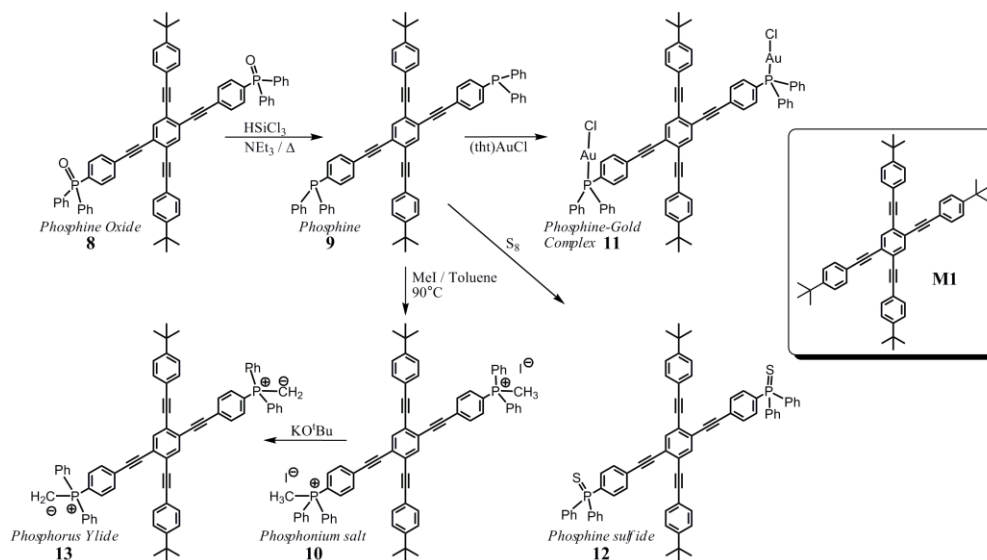
constant. Researchers have taken advantage of this property to rationally design sensors with anticipated responses characterized by a larger signal transduction relative to that observed from traditional π -conjugated chromophores. The particularly impressive success of cruciform-type molecules for metal-ion detection, coupled with our ongoing interest in unique light harvesting ligands for coordination control and materials assembly⁴⁴⁻⁴⁶ have lead us to explore cross-conjugated diphosphines.

Herein, we describe the preparation of phosphorus (III) and (V)-bearing cruciforms and a gold complex (**Schemes 5.1** and **5.2**), with accompanying photophysical characterization and density functional theory (**DFT**) calculations.

5.2 Synthesis and Characterization



Scheme 5.1 Synthesis of phosphine oxide **8** (structure provided in **Scheme 5.2**).



Scheme 5.2 Synthesis of compounds **9** - **13** and structure of phosphorus-free model **M1**.

5.2.1 Synthetic Characterization

The first *phospha*-cruciform, phosphine oxide **8**, was prepared from **7**²⁴ and the commercial precursors via the procedure outlined in **Scheme 5.1**, culminating in

Sonogashira-Miyaura type coupling of **6** and **7** to create the cross-conjugated cruciform architecture and install the phosphorus center.

With **8** in hand, transformation to other phosphorus-bearing species proceeded smoothly by classic methods (**Scheme 5.2**). Reduction of **8** to phosphine **9** was affected by the action of HSiCl_3 in toluene in 52% yield. Compound **9** was readily converted to phosphonium salt **10** by reaction with methyl iodide, to the gold complex **11** by reaction with $(\text{tht})\text{AuCl}$ (tht = tetrahydrothiophene), and to phosphine sulfide **12** via reaction with S_8 . All of these compounds were found to have good air stability in the solid state, though samples of phosphine **9** in solution were observed to slowly transform to oxide at rates comparable to PPh_3 (as gauged by ^{31}P NMR spectroscopy).

We attempted to convert phosphonium salt **10** to the phosphorus ylide by deprotonation with KO^tBu in THF. Although we were unable to isolate **13** in pure form due to its instability compared to the other *phospha*-cruciforms, the conversion of **12** to **13** was reasonably clean by phosphorus-31 NMR spectroscopy, with the resonance at 20.5 ppm attributed to the bis(ylide). The phosphorus-31 NMR resonances are summarized in (**Table 5.1**).

5.2.2 Density Functional Theory (DFT) Calculations

Because many of the stimuli-responsive properties of a cruciform derive from the geometric distribution of its HOMO and LUMO, materials **8**, **9** and **10** were examined by Density Functional Theory (**DFT**) calculations at the B3LYP-6-31G* level. The calculated HOMOs and LUMOs for **8**, **9**, and **10** are provided in (**Figure 5.3**).

The calculated HOMO-LUMO gaps (E_g) are in good agreement with the optical bandgap estimated by the red edge absorption onset in absorption spectra for **8** and **9**, though for phosphonium salt **10** the calculated bandgap (2.49 eV) was somewhat lower than the experimental optical bandgap (2.81 eV). This is probably due to the fact that calculations do not account for counterion effects or solvent effects, both of which are expected to be much more influential in the ionic **10** versus neutral compounds **8** and **9**.

The HOMO and LUMO become increasingly more geometrically distinct as the electron-withdrawing nature of the phosphorus functionality are increased from phosphine **9** to polar phosphine oxide **8** to cationic phosphonium **10**. The lack of significant HOMO - LUMO geometric separation in **9** is rather expected because the electronegativity of P and C are quite similar. Furthermore, the orbital size / energy mismatch between P and C leads to only limited n- π interaction.²⁵⁻²⁷ This is in contrast to nitrogen containing systems, such as polyaniline, in which the lone pair can engage in delocalization through an appended π -system.^{47, 48} The phosphorus-centered lone pair in **9** shows the greatest contribution to the HOMO-1 orbital (not shown in **Figure 5.3**).

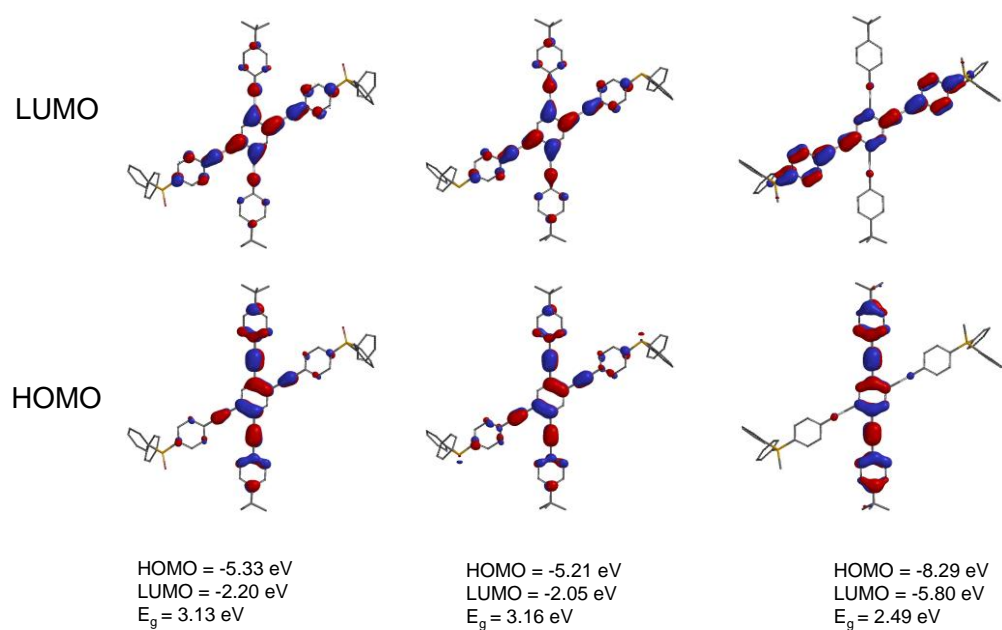


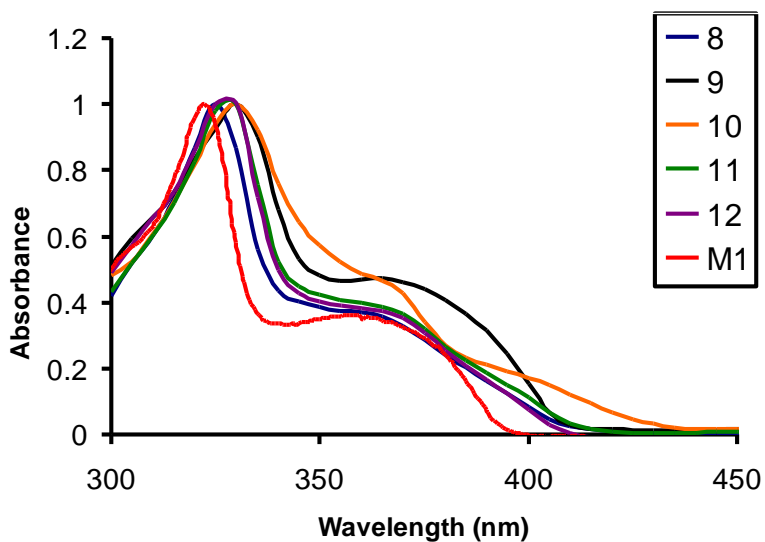
Figure 5.3 HOMO, LUMO and band gap (E_g) parameters from DFT calculations (B3LYP-6-31G* level) for compounds **8** (left), **9** (center) and **10** (right).

5.3 Photophysical Studies and Calculation

Normalised absorption (**Figure 5.4A**) and emission spectra (**Figure 5.4B**) for the series of compounds **8** - **12** are shown in **Figure 5.4** along with those for the model compound 1,2,4,5-tetrakis(2-(4-*tert*-butylphenyl)ethynyl)benzene (**M1**) for comparison. As noted previously, these spectral data are in line with the properties anticipated from DFT calculations.

Molar absorptivities of **8** - **12** are on the order of $10^5 - 10^6$, consistent with the anticipated π - π^* transitions. Absorption spectra for **8** - **12** each feature a $\lambda_{\pi-\pi^*}$ band at around 330 nm in addition to a shoulder to the red at around 350 - 400 nm. The shoulder is attributed to a charge transfer band between the π orbital on one of the in cross-conjugated segments and the π^* of the other π -conjugated segment, a feature observed in many tetraethynylbenzene derivatives.⁴⁹

(A)



(B)

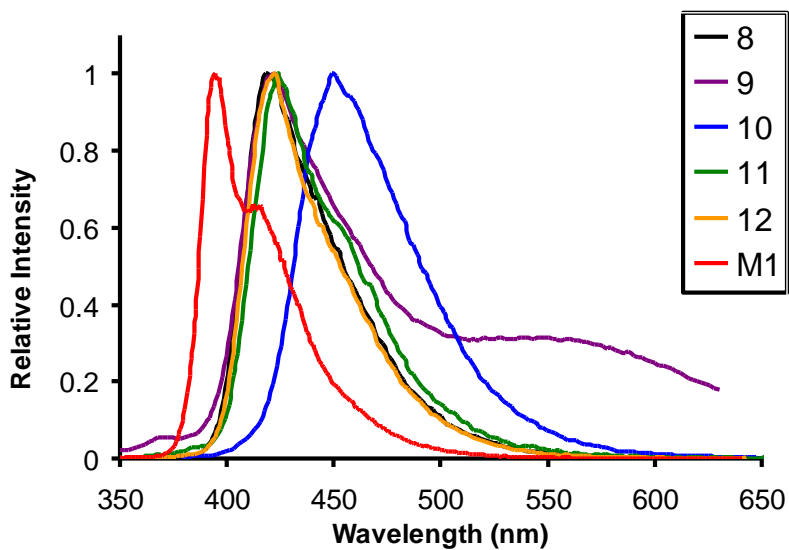


Figure 5.4 Absorption (A) and photoluminescence (B) spectra for compounds **8** - **12** and **M1** in dichloromethane. The trace for **9** is cut off before reaching baseline resolution because it overlaps the expected overtone peak at double the excitation wavelength at 660 nm ($\pi_{\text{ex}} = 330$ nm).

Table 5.1 Select properties of **8 - 13** and model **M1**.

	$\lambda_{\pi-\pi^*}$ (nm)	$\log \epsilon$	λ_{emit} (nm)	Φ	^{31}P NMR (ppm)
8	325.0	5.19	418.5	0.415	29.3
9	330.0	5.27	419.4	0.049	-4.3
10	330.0	5.12	449.4	0.217	22.6
11	330.0	5.33	423.3	0.294	33.7
12	325.0	4.99	422.5	0.405	43.7
13	320.0	NA	406.6	NA	20.5
M1	322.4	5.5	394.4	0.773	none

The absorption maxima of the higher energy band for phosphine-containing **8 - 12** are red-shifted to a small extent compared to **M1** due to the small extension of conjugation through the phosphorous centres²⁷ and the electron-withdrawing nature of many of the phosphorus derivatives.

Although the ylide **13** was not isolable in the solid state, the reaction solutions were examined by absorption spectroscopy and the data are summarized in **Table 5.1** (the extinction coefficient in **Table 5.1** was calculated assuming complete transformation of the phosphonium salt to the ylide). The ylide-containing solution did not exhibit appreciable fluorescence, but does exhibit a characteristic violet color. Although the ylide can be drawn in a resonance structure wherein there is a P – C double bond, the orbital makeup of phosphorus ylides suggests that this will not lead to any appreciable extension of p- π type conjugation.⁵⁰⁻⁵³

The change in the absorption features are likely promulgated through n- π interactions. The emission spectra of the series show a single band regardless of whether

excitation is provided into the $\pi-\pi^*$ band at ca. 330 nm or into the charge transfer band. All of the phosphorus-containing species **8** - **12** have emission maxima that are bathochromically shifted versus **M1** despite very similar absorption maxima. The larger Stokes shift in **8** - **12** versus **M1** reflects the polarizability and electron withdrawing nature of the phosphorus centers, as most dramatically illustrated by the considerably larger shift for cationic units present in **10** ($\lambda_{em} = 449$ nm), with its large Stokes shift of 119 nm.

The quantum yields are highest (40% and 41%, respectively) for the phosphine oxide (**8**) and gold complex **12**. The trend in photoluminescent quantum yields (Φ) for other phosphorus species mirror those reported for tris(styryl)phosphine and **LHP1** (**Figure 5.1**)²³ derivatives. Just as was observed for tris(stilbenyl) phosphorus species, the phosphine exhibits significantly lower Φ than the phosphonium or phosphine oxide analogues. This is attributable to the ability of the polarizable phosphorus lone pair to facilitate nonradiative decay processes.

The exceptionally low Φ of **9** allows the observation of a very weak ($\Phi < 0.01$) red-shifted emission feature in **Figure 5.4B** that may be attributable to some very weak triplet emission or emission from aggregates in solution. The latter would not be unexpected due to the limited solubility of the compounds, and it should be borne in mind that this emission band accounts for < 1% of the absorption intensity.

5.4 Conclusion

In summary, we have successfully synthesized and characterized six novel phosphorous-containing cross-conjugated cruciform systems and examined their photophysical properties. The presence of phosphorus centers on the tetraethynylbenzene core lead to a decrease in the bandgap and increased Stokes shifts versus the hydrocarbon model compound. DFT calculations and optical bandgap estimates indicate that band gap energies (E_g) for these materials are within the range of other materials that have found utility in organic optoelectronic applications.

Extensions of these molecules to the preparation of various luminescent charge-transfer polymers, polyelectrolytes and metallopolymers are currently being carried out in our lab.

5.5 Experimental Section

Reagents and General Methods

Reagents were obtained from Acros, Aldrich Chemical Co., TCI America, or Alfa Aesar and were used as received from the suppliers without further purification. All the solvents used were purified by passage through alumina column under a N₂ atmosphere employing an MBraun solvent purification system. All air sensitive manipulations were performed in an MBraun dry box or using standard Schlenk techniques under N₂ atmosphere. 1,4-dibromo-2,5-diiodobenzene (**2**)⁵⁴, 1,4-dibromo-2,5-bis(2-(4-*tert*-butylphenyl)ethynyl)benzene (**4**)⁵⁵, 1,4-bis(2-(4-*tert*-butylphenyl)ethynyl)-2,5-diethynylbenzene (**6**)⁵⁶ and 4-iodophenyl)diphenylphosphineoxide (**7**) were synthesized by modification of reported methods. All compounds were characterized by proton, carbon-13, and phosphorus-31 NMR spectra using a Bruker Avance 300 spectrometer operating at 300 MHz for proton, 75 MHz for carbon-13, and 121.5 MHz for phosphorus-31 nuclei. All spectra were collected at 25 °C and referenced to TMS or residual solvent peak for proton and carbon-13 and to 85% phosphoric acid for phosphorus-13.

General Spectroscopic Methods

Absorption spectra were recorded using Varian Cary 50 spectrophotometer and photoluminescence (**PL**) data were recorded using Varian Eclipse spectrofluorimeter in quartz cuvettes with a pathlength of 1 cm in DCM. Quantum yield (Φ) for all compounds were calculated relative to quinine bisulfate in 0.1 M H₂SO₄ (aq) ($\Phi = 0.546$).²⁴

Synthesis of 1,4-dibromo-2,5-diiodobenzene (2)

A solution of 1,4-dibromobenzene **1** (11.6 g, 49.2 mmol) and Iodine (48.0 g, 378 mmol) in 160 mL of concentrated sulfuric acid was stirred vigorously and heated at 130 °C for 6 h. The mixture was poured into ice-water followed by extraction with DCM (3 × 75 mL). The organic layer was collected, washed with sat. Na₂CO₃ solution (3 × 50 mL), dried over Na₂SO₄ and volatiles were removed under reduced pressure, yielding off white solid which was further washed with acetonitrile yielding pure compound. (7.00 g, 29.1 %). ¹H NMR (300 MHz, CDCl₃): δ = 8.06 (s, 2H, Aromatic).

Synthesis of 1,4-dibromo-2,5-bis(2-(4-tert-butylphenyl)ethynyl)benzene (4)

In the dry box, 1,4-dibromo-2,5-diiodobenzene **2** (1.00 g, 2.10 mmol) was dissolved in THF (50 mL) followed by the addition of Tetrakis(triphenylphosphine) palladium(0) (220 mg, 0.200 mmol) and copper iodide (40.0 mg, 0.200 mmol). In another vial, *t*-butylphenyl acetylene **3** (0.720 g, 4.50 mmol) was dissolved in diisopropyl amine (20 mL). This solution was added into the reaction mixture drop wise. Flask was taken out from the dry box and reaction mixture was stirred for 48 h at room temperature. Reaction mixture was passed through silica, silica was washed with DCM (100 mL) followed by extraction with sat. sodium bicarbonate solution (4 × 100 mL). Organic layer was collected and dried over sodium sulfate, volatiles were removed under reduced pressure. Residue was washed with pentane yielding off white solid (0.6 g, 65.0 %). ¹H NMR (300 MHz, CDCl₃): δ = 1.36 s, 18H, 6 × CH₃, 7.43 (dd, 4H, *J*₁ = 1.8 Hz, *J*₂ = 8.4 Hz, Aromatic), 7.55 (dd, 4H, *J*₁ = 2.1 Hz, *J*₂ = 8.7 Hz, Aromatic), 7.79 (s, 2H, Aromatic). ¹³C NMR (75.4 MHz, CDCl₃): δ = 31.1, 34.9, 86.3, 96.9, 119.3, 123.6, 125.5, 126.4, 131.5, 135.9, 152.5.

Synthesis of 1,4-bis(2-(4-tert-butylphenyl)ethynyl)-2,5-bis(2-(trimethylsilyl)ethynyl)benzene (5)

In the dry box, 1,4-dibromo-2,5-bis(2-(4-tert-butylphenyl)ethynyl)benzene **4** (1.00 g, 1.80 mmol) was dissolved in THF (50 mL) followed by the addition of Tetrakis(triphenylphosphine) palladium(0) (0.200 g, 0.200 mmol) and copper iodide (34.0 mg, 0.200 mmol) in the pressure flask. In another vial, trimethylsilyl acetylene (0.700 g, 7.20 mmol) was dissolved in diisopropyl amine (20 mL). This solution was added into the reaction mixture drop wise. Pressure flask was taken out from the dry box and reaction mixture was stirred for 48 h at 70 °C. Reaction mixture was passed through silica, silica was washed with DCM (100 mL) followed by extraction with sat. sodium bicarbonate solution (4 × 100 mL). Organic layer was collected and dried over sodium sulfate, volatiles were removed under reduced pressure. Residue was washed with pentane yielding light yellow solid (0.450 g, 44.0 %). ¹H NMR (300 MHz, CDCl₃): δ = 0.31 (s, 18H, 6 × Si-CH₃), 1.36 s, 18H, 6 × CH₃), 7.41 (d, 4H, *J* = 8.7 Hz, Aromatic), 7.51 (dd, 4H, *J*₁ = 1.8 Hz, *J*₂ = 8.4 Hz, Aromatic), 7.68 (s, 2H, Aromatic). ¹³C NMR (75.4 MHz, CDCl₃): δ = 0.0, 31.1, 34.8, 86.8, 95.5, 100.6, 102.4, 119.9, 125.1, 125.3, 125.4, 131.5, 135.4, 152.0.

Synthesis of 1,4-bis(2-(4-tert-butylphenyl)ethynyl)-2,5-diethynylbenzene (6)

A sample of 1,4-bis(2-(4-tert-butylphenyl)ethynyl)-2,5-bis(2-(trimethylsilyl)ethynyl)benzene **5** (0.440 g, 0.760 mmol) was dissolved in THF (30 ml) followed by the addition of tetrabutylammonium fluoride trihydrate (3.60 g, 11.4 mmol). Reaction mixture was stirred for 2 h at room temperature. and extracted with water (4 ×

100 mL). Organic layer was collected and dried over sodium sulfate, volatiles were removed under reduced pressure yielding green solid (0.320 g, 96.0 %). ^1H NMR (300 MHz, CDCl_3): δ = 1.35 s, 18H, $6 \times \text{CH}_3$), 3.45 (s, 2H, CCH), 7.42 (d, 4H, J = 8.4 Hz, Aromatic), 7.53 (dd, 4H, J_1 = 1.5 Hz, J_2 = 8.4 Hz, Aromatic), 7.7 (s, 2H, Aromatic). ^{13}C NMR (75.4 MHz, CDCl_3): δ = 0.0, 31.1, 34.8, 81.1, 82.9, 86.3, 95.8, 119.7, 124.4, 125.4, 125.8, 131.5, 135.5, 152.2.

Synthesis of (4-iodophenyl)diphenylphosphineoxide (7)

A solution of 1,4-diiodo benzene (5.00 g, 15.2 mmol) in dry THF (100 mL), under inert atmosphere, was cooled to $-78\text{ }^\circ\text{C}$ followed by the addition of n-BuLi (6.10 mL, 15.2 mmol) and stirred for 1 h at same temperature. Diphenylphosphine chloride (3.34 g, 15.2 mmol) dissolved in THF (5 mL) was added into the reaction mixture and stirred at room temperature for overnight. THF was removed under reduced pressure and residue was dissolved in DCM (50 mL) followed by addition of H_2O_2 (1.20 mL, 152 mmol). Reaction mixture was stirred for 24 h at room temperature. Reaction mixture was extracted with H_2O (3×100 mL). The organic layer was collected, dried over Na_2SO_4 and volatiles were removed under reduced pressure. The residue was dissolved in minimum amount of ether followed by addition of pentane (200 mL). While cooling white crystalline solid precipitated out. (3.00 g, 49.0 %). ^1H NMR (300 MHz, CDCl_3): δ = 7.86 - 7.37 (m, 14H, Aromatic). ^{31}P NMR (121.4 MHz, CDCl_3): δ = 29.33.

Synthesis of 1,4-bis(2-(4-tert-butylphenyl)ethynyl)-2,5-bis(2-(4-(diphenylphosphoryl)phenyl)ethynyl)benzene (8)

A sample of 1,4-bis(2-(4-tert-butylphenyl)ethynyl)-2,5-diethynyl benzene **6** (0.34 g, 0.78 mmol) and (4-iodophenyl)diphenylphosphineoxide **7** (0.85 g, 2.1 mmol) were degassed and taken into the dry box. Compound **7** was dissolved in THF (100 mL) followed by the addition of tetrakis(triphenylphosphine) palladium(0) (250 mg, 0.24 mmol) and copper iodide (45 mg, 0.24 mmol). In another vial, 1,4-bis(2-(4-tert-butylphenyl)ethynyl)-2,5-diethynylbenzene **6** was dissolved in diisopropyl amine (20 mL). This solution was added into the reaction mixture drop wise and stirred for 48 h at room temperature. DCM (100 mL) was added into the reaction mixture followed by extraction with sat. sodium bicarbonate solution (4 × 100 mL). Organic layer was collected and dried over sodium sulfate, volatiles were removed under reduced pressure. The residue was washed with acetonitrile to afford a yellow solid (0.35 g, 46 %). ¹H NMR (300 MHz, CDCl₃): δ = 1.34 (s, 18H, 6 × CH₃), 7.40 (d, 4H, *J* = 6.8 Hz, Aromatic), 7.54 – 7.48 (m, 12H, Aromatic), 7.60 – 7.57 (m, 4H, Aromatic), 7.74 – 7.66 (m, 16H, Aromatic), 7.78 (s, 2H, Aromatic). ¹³C NMR (75.4 MHz, CDCl₃): δ = 31.1, 34.9, 86.6, 90.0, 94.3, 96.1, 119.6, 125.0, 125.5, 125.6, 126.7, 126.7, 128.5, 128.7, 131.4, 131.5, 131.6, 132.0, 132.1, 132.1, 132.8, 133.5, 135.0, 152.3. ³¹P NMR (121.4 MHz, CDCl₃): δ = 29.3. HRMS (M+H)⁺: calc. for C₇₀H₅₇O₂P₂: 991.3834; found, 991.3837. UV-vis: λ_{max} 325 nm (ε = 160,000 M⁻¹ cm⁻¹).

Synthesis of 1,4-bis(2-(4-tert-butylphenyl)ethynyl)-2,5-bis(2-(4-(diphenylphosphino)phenyl)ethynyl)benzene (9)

Under nitrogen atmosphere, 1,4-bis(2-(4-tert-butylphenyl)ethynyl)-2,5-bis(2-(4-(diphenylphosphoryl)phenyl)ethynyl)benzene **8** (0.1 g, 0.1 mmol) was dissolved in 1:1

mixture of THF and toluene (30 mL) followed by addition of triethyl amine (1 mL). Trichlorosilane (1.34 mL, 3.00 mmol) was added into the reaction mixture and it was refluxed overnight. Degassed sodium bicarbonate solution (10 mL) was added in to it. Yellow precipitate was filtered off and organic layer was sat. sodium bicarbonate solution (3×50 mL). Organic layer was collected and dried over sodium sulfate, volatiles were removed under reduced pressure. Residue was dissolved in minimum amount of DCM followed by addition of pentane (20 mL) in to it. Yellow crystalline solid were obtained upon cooling (50 mg, 52.0 %). ^1H NMR (300 MHz, CDCl_3): $\delta = 1.34$ (s, 18H, $6 \times \text{CH}_3$), 7.39 - 7.27 (m, 28H, Aromatic), 7.56 – 7.49 (m, 8H, Aromatic), 7.76 (s, 2H, Aromatic). ^{13}C NMR (75.4 MHz, CDCl_3): $\delta = 31.1, 34.8, 86.8, 88.7, 95.1, 95.7, 119.8, 123.2, 125.1, 125.4, 125.4, 128.5, 128.6, 128.9, 131.4, 131.5, 131.6, 133.3, 133.5, 133.7, 134.0, 134.9, 136.5, 136.6, 138.5, 138.6, 152.3$. ^{31}P NMR (121.4 MHz, CDCl_3): $\delta = -4.3$. HRMS ($\text{M}+\text{H}$) $^+$: calc. for $\text{C}_{70}\text{H}_{57}\text{P}_2$, 959.3936; found, 959.3957. UV-vis: λ_{max} 330 nm ($\epsilon = 190,000 \text{ M}^{-1} \text{ cm}^{-1}$).

Synthesis of Phosphonium Salt (10)

Under nitrogen atmosphere, compound **9** (25.0 mg, 0.026 mmol) was dissolved in toluene (20 mL) followed by addition of methyl iodide (16.0 mg, 0.100 mmol). Reaction mixture was refluxed for 16 h. All the volatile was removed under reduced pressure yielding yellow solid (20.0 mg, 62.5 %). ^1H NMR (300 MHz, CDCl_3): $\delta = 1.33$ (s, 18H, $6 \times \text{CH}_3$), 3.35 (d, 6H, $J_{\text{HP}} = 12.0$ Hz), 7.43 (d, 4H, $J = 9.0$ Hz, Aromatic), 7.52 (d, 4H, $J = 9.0$ Hz, Aromatic), 7.67 – 7.84 (m, 30H, Aromatic). ^{13}C NMR (75.4 MHz, CDCl_3): $\delta = 31.1, 34.9, 86.2, 92.7, 93.2, 96.6, 118.2, 119.4, 124.7, 125.7, 125.8, 128.5, 128.7, 130.2,$

130.5, 130.7, 131.4, 132.0, 132.1, 133.1, 133.3, 133.3, 133.4, 133.5, 135.3, 135.6, 152.6. ^{31}P NMR (121.4 MHz, CDCl_3): $\delta = 22.6$. MS ($\text{M}-2\text{H}$) $^{2+}$: calc. for $\text{C}_{72}\text{H}_{62}\text{P}_2$, 988.4; found, 988.4. UV-vis: λ_{max} 330 nm ($\epsilon = 130,000 \text{ M}^{-1} \text{ cm}^{-1}$).

Synthesis of Phosphine Gold Complex (11)

Under nitrogen atmosphere, compound **9** (20.0 mg, 0.021 mmol) was dissolved in DCM (15 mL) followed by addition of (tht)AuCl (14.0 mg, 0.044 mmol). Reaction mixture was stirred for 16 h. All the volatile was removed under reduced pressure yielding yellow solid (26 mg, 89 %). ^1H NMR (300 MHz, CDCl_3): $\delta = 1.35$ (s, 18H, 6 \times CH_3), 7.42 (d, 4H, $J = 6.0$ Hz, Aromatic), 7.49 – 7.67 (m, 32H, Aromatic), 7.80 (s, 2H, Aromatic). ^{13}C NMR (75.4 MHz, CDCl_3): $\delta = 31.1, 34.9, 86.5, 90.6, 93.9, 96.2, 119.6, 124.9, 125.6, 125.6, 126.8, 126.9, 127.9, 128.6, 128.7, 129.3, 129.4, 131.4, 132.1, 132.1, 132.2, 132.2, 133.9, 134.1, 134.1, 134.2, 135.2, 152.5$. ^{31}P NMR (121.4 MHz, CDCl_3): $\delta = 33.7$. MALDI: calc. for $\text{C}_{70}\text{H}_{56}\text{Au}_2\text{Cl}_2\text{P}_2$ ($\text{M}+\text{H}$) $^+$, 1423.3; found, 1423.1. UV-vis: λ_{max} 330 nm ($\epsilon = 210,000 \text{ M}^{-1} \text{ cm}^{-1}$).

Synthesis of 1,4-bis(2-(4-tert-butylphenyl)ethynyl)2,5-bis(2-(4-diphenylphosphorothioyl)phenyl)ethynyl)benzene (12)

Under nitrogen atmosphere, compound **9** (15 mg, 0.016 mmol) was dissolved in dry THF (5 mL) followed by addition of S_8 (1.6 mg, 0.048 mmol). Reaction mixture was stirred for 16 h. All the volatiles were removed under reduced pressure. Residue was further dissolved in CHCl_3 in order to remove excess sulfur. This CHCl_3 was removed under pressure yielding yellow solid (11 mg, 69 %). ^1H NMR (300 MHz, CDCl_3): $\delta = 1.34$ (s, 18H, 6 \times CH_3), 7.41 - 7.38 (m, 4H, Aromatic), 7.57 – 7.46 (m, 16H, Aromatic),

7.66 – 7.62 (m, 4H, Aromatic), 7.80 – 7.71 (m, 13H, Aromatic). ^{13}C NMR (75.4 MHz, CDCl_3): δ = 31.2, 35.0, 86.6, 90.2, 94.4, 96.2, 119.7, 125.0, 125.6, 126.4, 128.6, 128.8, 131.5, 131.6, 131.7, 131.8, 132.0, 132.2, 132.4, 132.7, 133.1, 133.8, 135.1, 152.4. ^{31}P NMR (121.4 MHz, CDCl_3): δ = 43.7. HRMS ($\text{M}+\text{H}$) $^+$: calc. for $\text{C}_{70}\text{H}_{57}\text{Au}_2\text{Cl}_2\text{P}_2$, 1023.3377; found, 1023.3417. UV-vis: λ_{max} 330 nm (ϵ = 210,000 $\text{M}^{-1} \text{cm}^{-1}$).

Synthesis of Phosphorus Ylide (13)

Under nitrogen atmosphere, compound **10** (19.0 mg, 0.015 mmol) was dissolved in THF-d_8 (1 mL) followed by addition of potassium *tert*-butoxide until compound **10** completely dissolved in THF. Upon addition of the first portion of the base, an immediate color change from pale yellow to a light violet-brown color was observed. Consumption of **10** was complete within 30 min as determined by NMR spectroscopy. ^{31}P NMR (121.4 MHz, CDCl_3): δ = 20.5 (attributed to **13**); smaller resonances were present at δ = 25.0, 23.9, 13.6 and 11.2.

5.6 References

1. Werner, A., *Z. Anorg. Chem.* **1893**, 3, 267-342.
2. Kauffman, G. B., *J. Chem. Ed.* **1959**, 36, 521-527.
3. Chan, K. L.; Mak, C. S. K.; Evans, N. R.; Watkins, S. E.; Pascu, S. I.; Holmes, A. B.; Hayer, A.; Koehler, A.; Devi, L. S.; Friend, R. H., Synthesis of triplet emitters and hosts for electrophosphorescence. *Proceedings of SPIE-The International Society for Optical Engineering* **2005**, 5937, (Organic Light-Emitting Materials and Devices IX), 59370B/1-59370B/9.
4. Rothe, C.; King, S.; Monkman, A. P., Systematic study of the dynamics of triplet exciton transfer between conjugated host polymers and phosphorescent iridium (III) guest emitters. *Physical Review B: Condensed Matter and Materials Physics* **2006**, 73, (24), 245208/1-245208/9.
5. Evans, N. R.; Devi, L. S.; Mak, C. S. K.; Watkins, S. E.; Pascu, S. I.; Koehler, A.; Friend, R. H.; Williams, C. K.; Holmes, A. B., Triplet Energy Back Transfer in Conjugated Polymers with Pendant Phosphorescent Iridium Complexes. *Journal of the American Chemical Society* **2006**, 128, (20), 6647-6656.
6. Lamansky, S.; Djurovich, P.; Murphy, D.; Abdel-Razzaq, F.; Lee, H. E.; Adachi, C.; Burrows, P. E.; Forrest, S. R.; Thompson, M. E., Highly phosphorescent bis-cyclometalated iridium complexes: synthesis, photophysical characterization, and use in organic light emitting diodes. *J Am Chem Soc* **2001**, 123, (18), 4304-12.

7. Anzenbacher, P., Jr.; Montes, V. A.; Takizawa, S.-y., High-purity white light from a simple single dopant host-guest white organic light-emitting diode architecture. *Appl. Phys. Lett.* **2008**, 93, (16), 163302/1-163302/3.
8. Jiang, C.; Yang, W.; Peng, J.; Xiao, S.; Cao, Y., High-efficiency, saturated red-phosphorescent polymer light-emitting diodes based on conjugated and non-conjugated polymers doped with an Ir complex. *Advanced Materials (Weinheim, Germany)* **2004**, 16, (6), 537-541.
9. Lesley, G.; Yuan, Z.; Stringer, G.; Jobe, I. R.; Taylor, N. J.; Koch, L.; Scott, K.; Marder, T. B.; Williams, I. D.; Kurtz, S. K., Second-order optical nonlinearities in linear donor-acceptor substituted transition metal acetylides. *Special Publication - Royal Society of Chemistry* **1991**, 91, (Org. Mater. Non-linear Opt. 2), 197-203.
10. Dhenaut, C.; Ledoux, I.; Samuel, I. D. W.; Zyss, J.; Bourgault, M.; Le Bozec, H., Chiral metal complexes with large octupolar optical nonlinearities. *Nature (London)* **1995**, 374, (6520), 339-42.
11. Hurst, S. K.; Humphrey, M. G.; Isoshima, T.; Wostyn, K.; Asselberghs, I.; Clays, K.; Persoons, A.; Samoc, M.; Luther-Davies, B., Organometallic Complexes for Nonlinear Optics. 28. Dimensional Evolution of Quadratic and Cubic Optical Nonlinearities in Stilbenylethynylruthenium Complexes. *Organometallics* **2002**, 21, (10), 2024-2026.
12. Bidault, S.; Viau, L.; Maury, O.; Brasselet, S.; Zyss, J.; Ishow, E.; Nakatani, K.; Le Bozec, H., Optically tunable nonlinearities in polymers based on photoisomerizable

- metal-based coordination complexes. *Advanced Functional Materials* **2006**, 16, (17), 2252-2262.
13. Senechal-David, K.; Hemeryck, A.; Tancrez, N.; Toupet, L.; Williams, J. A. G.; Ledoux, I.; Zyss, J.; Boucekkine, A.; Guegan, J.-P.; Le Bozec, H.; Maury, O., Synthesis, Structural Studies, Theoretical Calculations, and Linear and Nonlinear Optical Properties of Terpyridyl Lanthanide Complexes: New Evidence for the Contribution of f Electrons to the NLO Activity. *Journal of the American Chemical Society* **2006**, 128, (37), 12243-12255.
14. Dalton, G. T.; Cifuentes, M. P.; Petrie, S.; Stranger, R.; Humphrey, M. G.; Samoc, M., Independent switching of cubic nonlinear optical properties in a ruthenium alkynyl cruciform complex by employing protic and electrochemical stimuli. *J. Am. Chem. Soc.* **2007**, 129, (39), 11882-11883.
15. Bidault, S.; Brasselet, S.; Zyss, J.; Maury, O.; Le Bozec, H., Role of spatial distortions on the quadratic nonlinear optical properties of octupolar organic and metallo-organic molecules. *Journal of Chemical Physics* **2007**, 126, (3), 034312/1-034312/13.
16. Esswein, A. J.; Nocera, D. G., Hydrogen Production by Molecular Photocatalysis. *Chem. Rev.* **2007**, 107, (10), 4022-4047.
17. Borgarello, E.; Kiwi, J.; Pelizzetti, E.; Visca, M.; Graetzel, M., Photochemical cleavage of water by photocatalysis. *Nature (London)* **1981**, 289, (5794), 158-60.

18. Sahai, R.; Baucom, D. A.; Rillema, D. P., Strongly luminescing ruthenium(II)/ruthenium(II) and ruthenium(II)/platinum(II) binuclear complexes. *Inorg. Chem.* **1986**, 25, (21), 3843-5.
19. Arachchige Shamindri, M.; Brown Jared, R.; Chang, E.; Jain, A.; Zigler David, F.; Rangan, K.; Brewer Karen, J., Design considerations for a system for photocatalytic hydrogen production from water employing mixed-metal photochemical molecular devices for photoinitiated electron collection. *Inorg Chem* **2009**, 48, (5), 1989-2000.
20. Du, P.; Schneider, J.; Li, F.; Zhao, W.; Patel, U.; Castellano, F. N.; Eisenberg, R., Bi- and Terpyridyl Platinum(II) Chloro Complexes: Molecular Catalysts for the Photogeneration of Hydrogen from Water or Simply Precursors for Colloidal Platinum? *J. Am. Chem. Soc.* **2008**, 130, (15), 5056-5058.
21. Durben, S.; Dienes, Y.; Baumgartner, T., Cationic Dithieno[3,2-b:2',3'-d]phospholes: A New Building Block for Luminescent, Conjugated Polyelectrolytes. *Org. Lett.* **2006**, 8, (25), 5893-5896.
22. Baumgartner, T.; Réau, R., Organophosphorus p-Conjugated Materials. *Chemical Reviews* **2006**, 106, 4681-4727, and references therein.
23. Smith, R. C.; Protasiewicz, J. D., Synthesis and luminescence properties of a series of tris(4-styrylphenyl)phosphorus-(III) and -(V) compounds and of a [Cu(PR₃)₄]BF₄ complex. *Dalton Transactions* **2003**, (24), 4738-4741.
24. Tennyson, E. G.; Smith, R. C., Visible-Absorbing Phosphines as Functional Elements of Luminescent Metallopolymers. *Inorg. Chem.* **2009**, 48, 11483-11485.

25. Jin, Z.; Lucht, B. L., Poly-p-phenylene phosphine/polyaniline alternating copolymers: Electronic delocalization through phosphorus. *Journal of the American Chemical Society* **2005**, 127, (15), 5586-5595.
26. Jin, Z.; Lucht, B. L., Transition metal mediated routes to poly(arylphosphine)s: investigation of novel phosphorus containing conjugated polymers. *Journal of Organometallic Chemistry* **2002**, 653, (1-2), 167-176.
27. Lucht, B. L.; St Onge, N. O., Synthesis and characterization of poly(p-phenylenephosphine)s. *Chemical Communications* **2000**, (21), 2097-2098.
28. Baumgartner, T.; Réau, R., Organophosphorus p-Conjugated Materials. *Chemical Reviews* **2006**, 106, 4681-4727.
29. Vidal, P.-L.; Divisia-Blohorn, B.; Bidan, G.; Hazemann, J.-L.; Kern, J.-M.; Sauvage, J.-P., p-Conjugated ligand polymers entwined around copper centers. *Chem. Eur. J.* **2000**, 6, (9), 1663-1673.
30. Clot, O.; Wolf, M. O.; Patrick, B. O., Electropolymerization of Pd(II) Complexes Containing Phosphinoterthiophene Ligands. *Journal of the American Chemical Society* **2001**, 123, (41), 9963-9973.
31. Clot, O.; Akahori, Y.; Moorlag, C.; Leznoff, D. B.; Wolf, M. O.; Batchelor, R. J.; Patrick, B. O.; Ishii, M., Model Complexes for Metalated Polythiophenes: Gold(I) and Palladium(II) Complexes of Bis(diphenylphosphino)oligothiophenes. *Inorganic Chemistry* **2003**, 42, (8), 2704-2713.
32. Yip, J. H. K.; Prabhavathy, J., A Luminescent Gold Ring That Flips Like Cyclohexane. *Angew. Chem. Int. Ed.* **2001**, 40, 2159-2162.

33. Yamaguchi, S.; Akiyama, S.; Tamao, K., The coordination number-photophysical properties relationship of trianthrylphosphorus compounds: doubly locked fluorescence of anthryl groups. *Journal of Organometallic Chemistry* **2002**, 646, (1-2), 277-281.
34. Klare, J. E.; Tulevski, G. S.; Sugo, K.; de Picciotto, A.; White, K. A.; Nuckolls, C., Cruciform pi-Systems for Molecular Electronics Applications. *J. Am. Chem. Soc.* **2003**, 125, (20), 6030-6031.
35. Tykwinski, R. R.; Schreiber, M.; Perez Carlon, R.; Diederich, F.; Gramlich, V., Donor/acceptor-substituted tetraethynylethenes. Systematic assembly of molecules for use as advanced materials. *Helv. Chim. Acta* **1996**, 79, (8), 2249-2281.
36. Spitler, E. L.; Shirtcliff, L. D.; Haley, M. M., Systematic Structure-Property Investigations and Ion-Sensing Studies of Pyridine-Derivatized Donor/Acceptor Tetrakis(arylethynyl)benzenes. *Journal of Organic Chemistry* **2007**, 72, (1), 86-96.
37. Samori, S.; Tojo, S.; Fujitsuka, M.; Spitler, E. L.; Haley, M. M.; Majima, T., Fine-Tuning of Radiolysis Induced Emission by Variable Substitution of Donor-/Acceptor-Substituted Tetrakis(arylethynyl)benzenes. *J. Org. Chem.* **2008**, 73, (9), 3551-3558.
38. Spitler, E. L.; Monson, J. M.; Haley, M. M., Structure-Property Relationships of Fluorinated Donor/Acceptor Tetrakis(phenylethynyl)benzenes and Bis(dehydrobenzoannuleno)benzenes. *J. Org. Chem.* **2008**, 73, (6), 2211-2223.
39. Pina, J.; Seixas de Melo, J.; Burrows, H. D.; Galbrecht, F.; Bilge, A.; Kudla, C. J.; Scherf, U., Excited State Properties of Oligophenyl and Oligothieryl Swivel Cruciforms. *J. Phys. Chem. B* **2008**, 112, (4), 1104-1111.

40. Bilge, A.; Zen, A.; Forster, M.; Li, H.; Galbrecht, F.; Nehls, B. S.; Farrell, T.; Neher, D.; Scherf, U., Swivel-cruciform oligothiophene dimers. *Journal of Materials Chemistry* **2006**, 16, (31), 3177-3182.
41. Wilson, J. N.; Hardcastle, K. I.; Josowicz, M.; Bunz, U. H. F., Synthesis and electronic properties of bis-styryl substituted trimeric aryeneethynylenes. Comparison of cruciforms with iso-cruciforms. *Tetrahedron* **2004**, 60, (34), 7157-7167.
42. Wilson, J. N.; Bunz, U. H. F., Switching of Intramolecular Charge Transfer in Cruciforms: Metal Ion Sensing. *Journal of the American Chemical Society* **2005**, 127, (12), 4124-4125.
43. Tolosa, J.; Zuccherro, A. J.; Bunz, U. H. F., Water-Soluble Cruciforms: Response to Protons and Selected Metal Ions. *J. Am. Chem. Soc.* **2008**, 130, 6498-6506.
44. Dennis, A. E.; Smith, R. C., "Turn-On" Fluorescent Sensor for the Selective Detection of Zinc Ion by a Sterically-Encumbered Bipyridyl-Based Receptor *Chemical Communications* **2007**, (44), 4641-4643.
45. He, S.; Iacono, S. T.; Budy, S. M.; Dennis, A. E.; Smith, D. W., Jr.; Smith, R. C., Photoluminescence and ion sensing properties of a bipyridyl chromophore-modified semifluorinated polymer and its metallopolymer derivatives. *J. Mater. Chem.* **2008**, 18, (17), 1970-1976.
46. He, S.; Dennis, A. E.; Smith, R. C., Steric Coordination Control of Interchain Interactions in Conducting Metallopolymer. *Macromolecular Rapid Communications* **2009**, 30, 2079-2083.

47. Yang, J.-S.; Chiou, S.-Y.; Liao, K.-L., Fluorescence Enhancement of trans-4-Aminostilbene by N-Phenyl Substitutions: The "Amino Conjugation Effect". *Journal of the American Chemical Society* **2002**, 124, (11), 2518-2527.
48. Ma, L.-H.; Chen, Z.-B.; Jiang, Y.-B., Intramolecular charge transfer with 4-(N-phenylamino)benzoic acid. The N-phenyl amino conjugation effect. *Chemical Physics Letters* **2003**, 372, (1,2), 104-113.
49. Marsden, J. A.; Miller, J. J.; Shirtcliff, L. D.; Haley, M. M., Structure-Property Relationships of Donor/Acceptor-Functionalized Tetrakis(phenylethynyl)benzenes and Bis(dehydrobenzoannuleno)benzenes. *J. Am. Chem. Soc.* **2005**, 127, 2464-2476.
50. Shah, S.; Yap, G. P. A.; Protasiewicz, J. D., Crystal structure of the phosphanylidene-^s₄-phosphorane DmpP:PMe₃ (Dmp = 2,6-Mes₂C₆H₃) and reactions with electrophiles. *Journal of Organometallic Chemistry* **2000**, 608, (1-2), 12-20.
51. Johnson, A. W., *Ylides and Imines of Phosphorus*. ed.; Wiley: New York, 1993; 'Vol.' p.
52. Gilheany, D. G., Ylides, phosphonium No d Orbitals but Walsh Diagrams and Maybe Banana Bonds: Chemical Bonding in Phosphines, Phosphine Oxides, and Phosphonium Ylides. *Chemical Reviews (Washington, DC, United States)* **1994**, 94, (5), 1339-74.
53. Mitchell, D. J.; Wolfe, S.; Schlegel, H. B., A theoretical study of the methylenesulfurane and methylenephosphorane hypersurfaces, geometries, tautomerization, and dissociation of sulfonium and phosphonium ylides. *Can. J. Chem.* **1981**, 59, (23), 3280-92.

54. Cui-Hua Wang, R.-R. H., Shuang Liang, Jia-Hua Chen, Zhen Yanga, Jian Pei, Linear C₂-symmetric polycyclic benzodithiophene: efficient, highly diversified approaches and the optical properties. *Tetrahedron Letters* **2005**, 46, 8153–8157.
55. Sanji, T.; Shiraishi, K.; Kashiwabara, T.; Tanaka, M., Base-Mediated Cyclization Reaction of 2-Alkynylphenylphosphine Oxides: Synthesis and Photophysical Properties of Benzo[b]phosphole Oxides. *Org. Lett.* **2008**, 10, (13), 2689-2692.
56. Dennis T.-Y. Bong; Eugene W. L. Chan; Rainer Diercks; Peter I. Dosa; Michael M. Haley; Adam J. Matzger; Ognjen . Miljani; K. Peter C. Vollhardt; Andrew D. Bond; Simon J. Teat; Stanger, A., Syntheses of Syn and Anti Doublebent [5]Phenylene. *Organic letters* **2004**, 6, (13), 2249-2252.

APPENDICES

Appendix 5 A

NMR Spectra

1,4-bis(2-(4-tert-butylphenyl)ethynyl)-2,5-bis(2-(4-(diphenylphosphoryl)phenyl)ethynyl)benzene (**8**)

Structure

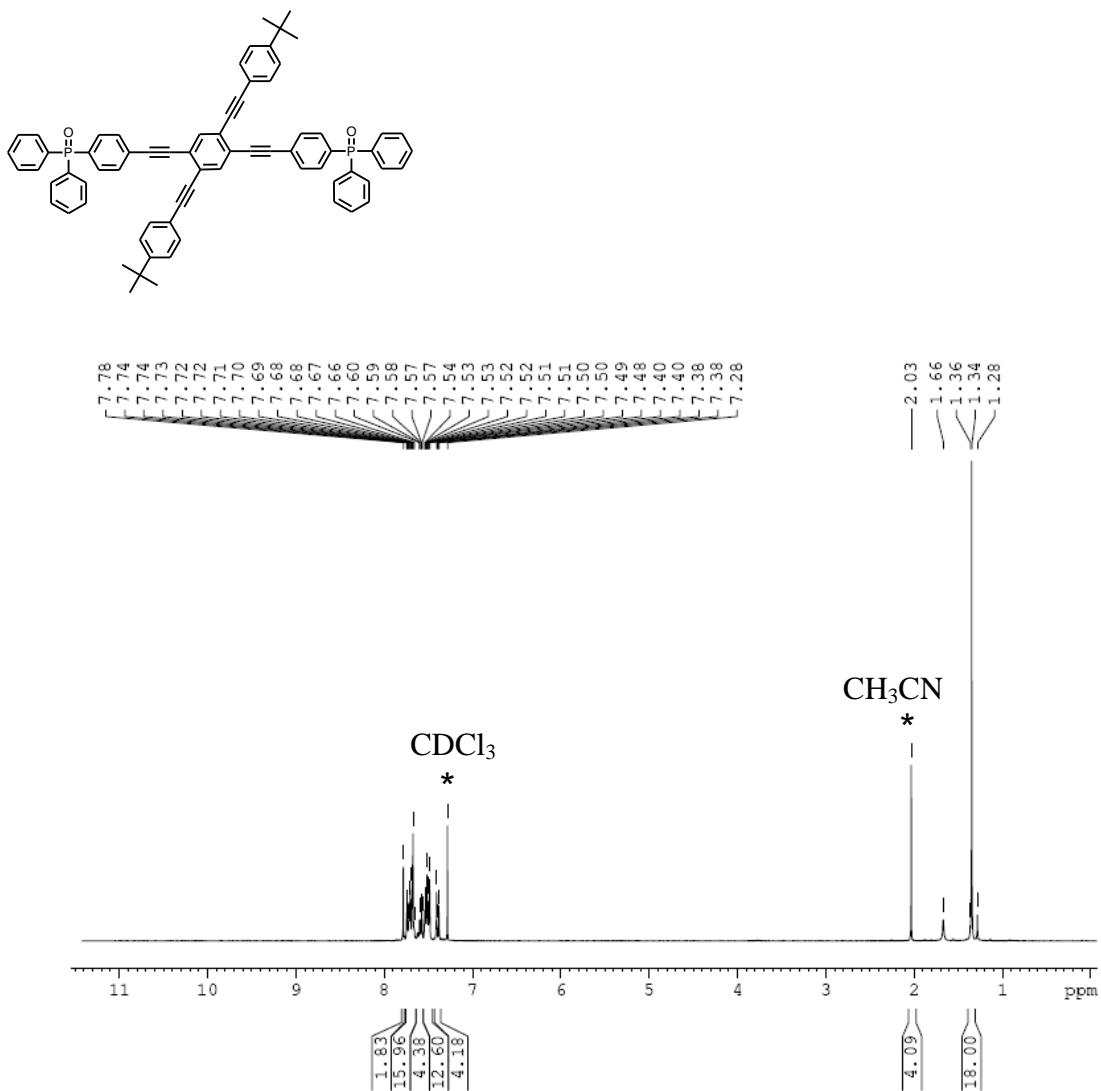


Figure 5 A.1 ¹H NMR (300 MHz, CDCl₃) of **8**.

1,4-bis(2-(4-tert-butylphenyl)ethynyl)-2,5-bis(2-(4-(diphenylphosphoryl)phenyl)ethynyl)benzene (**8**)

Structure

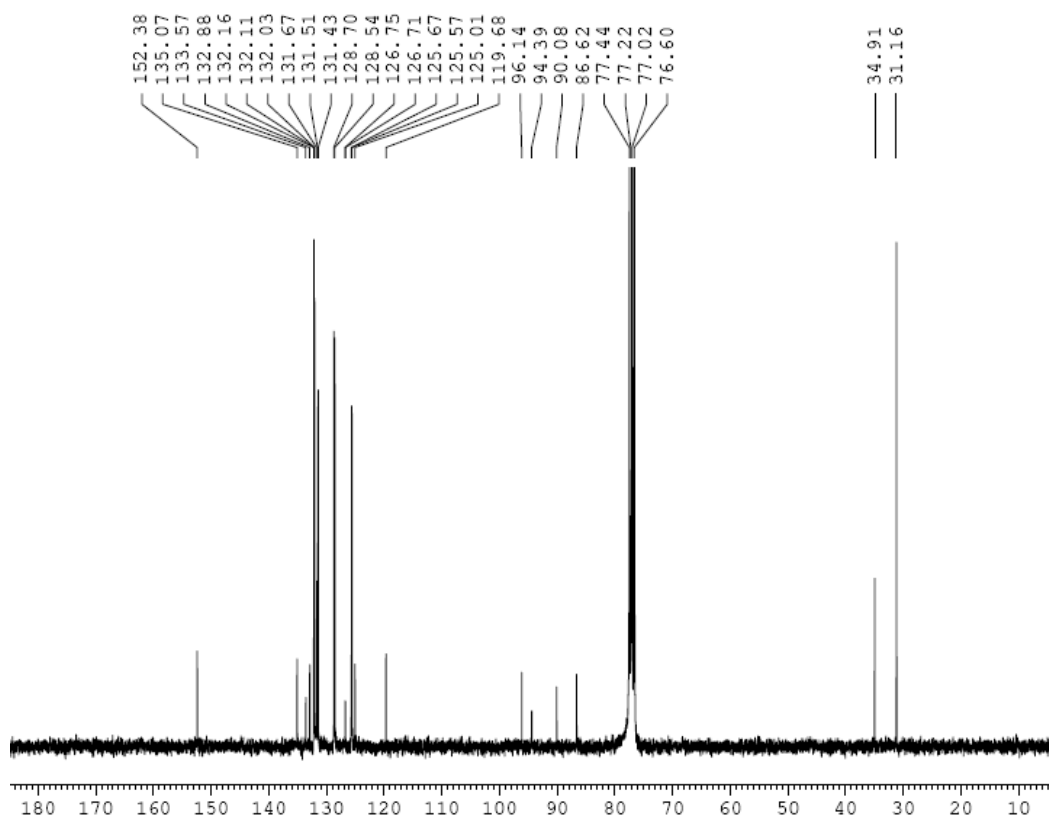
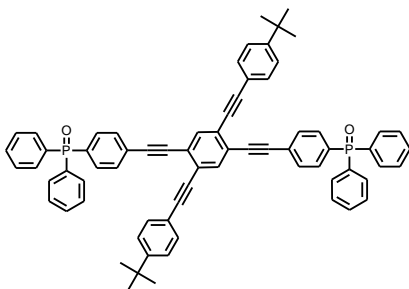


Figure 5 A.2 ^{13}C NMR (75 MHz, CDCl_3) of **8**.

1,4-bis(2-(4-tert-butylphenyl)ethynyl)-2,5-bis(2-(4-(diphenylphosphoryl)phenyl)ethynyl)
benzene (**8**)

Structure

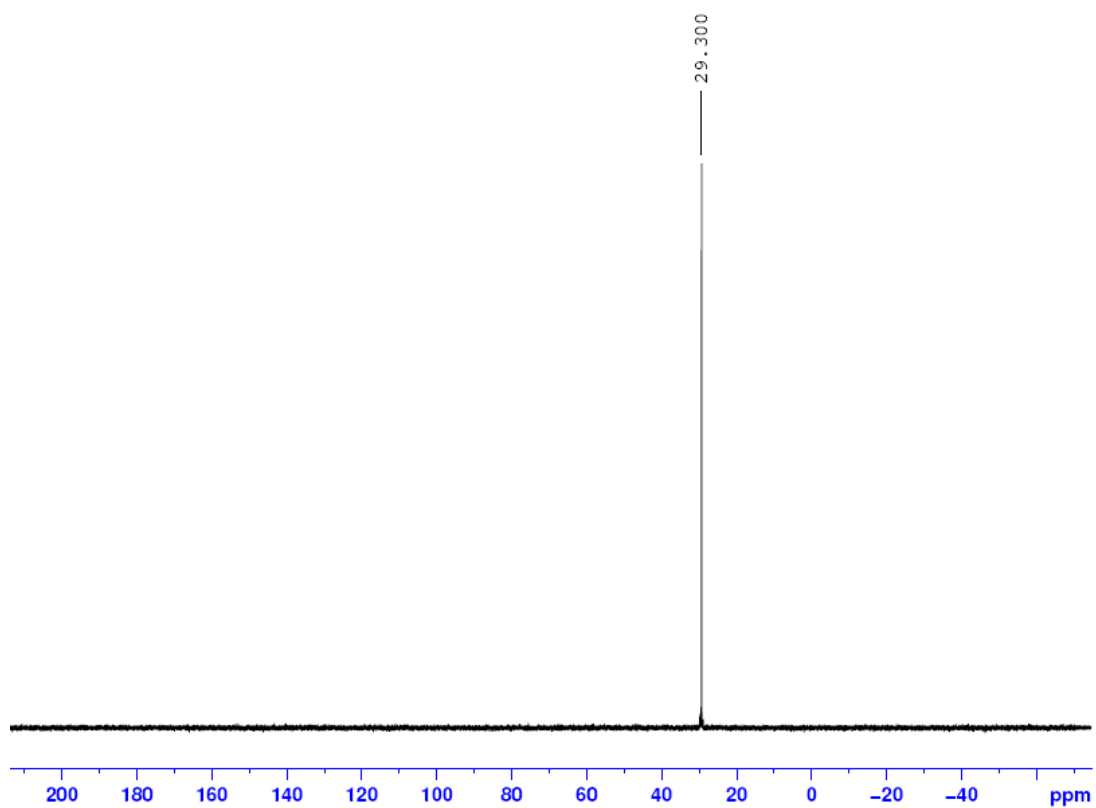
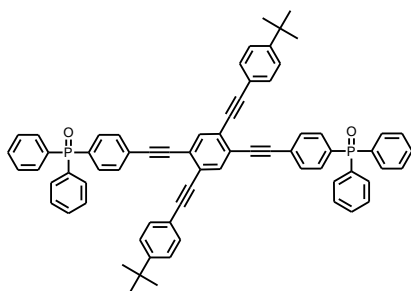


Figure 5 A.3 ^{31}P NMR (121 MHz, CDCl_3) of **8**.

1,4-bis(2-(4-tert-butylphenyl)ethynyl)-2,5-bis(2-(4-(diphenylphosphino) phenyl)ethynyl) benzene (**9**)

Structure

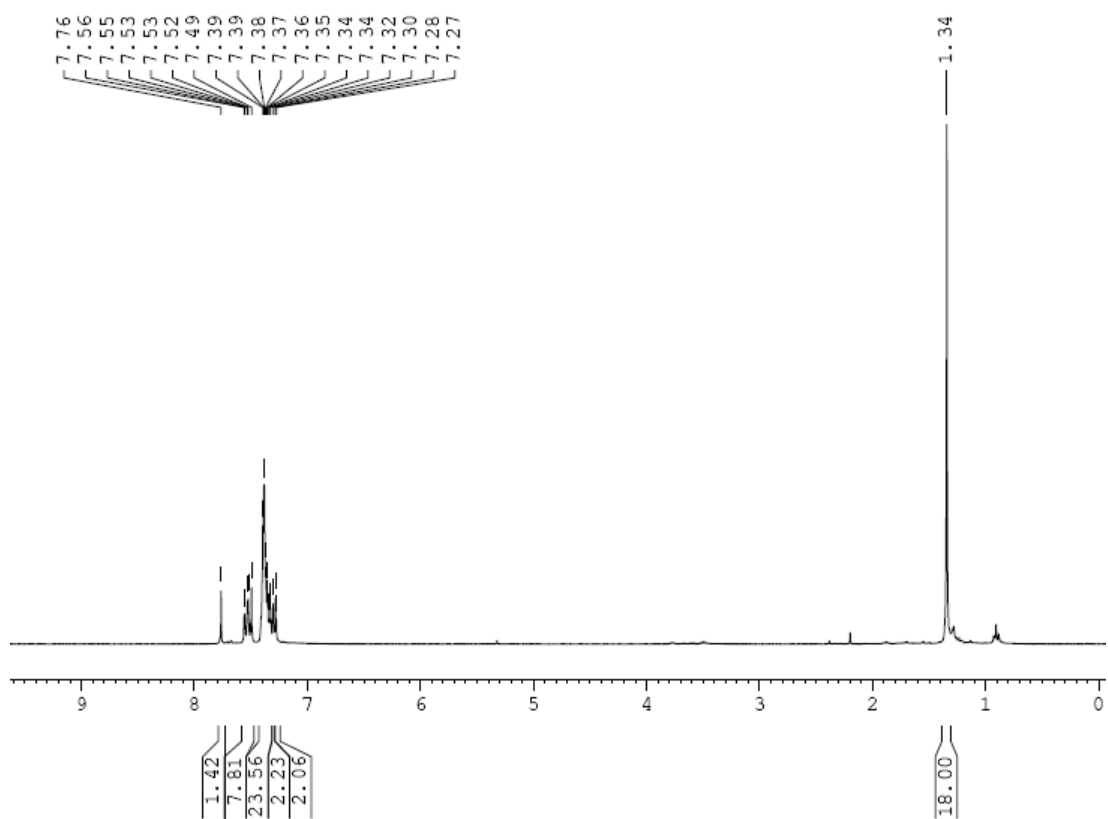
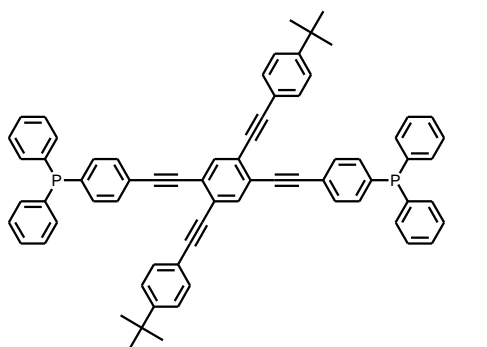


Figure 5 A.4 ¹H NMR (300 MHz, CDCl₃) of **9**.

1,4-bis(2-(4-tert-butylphenyl)ethynyl)-2,5-bis(2-(4-(diphenylphosphino) phenyl)ethynyl) benzene (**9**)

Structure

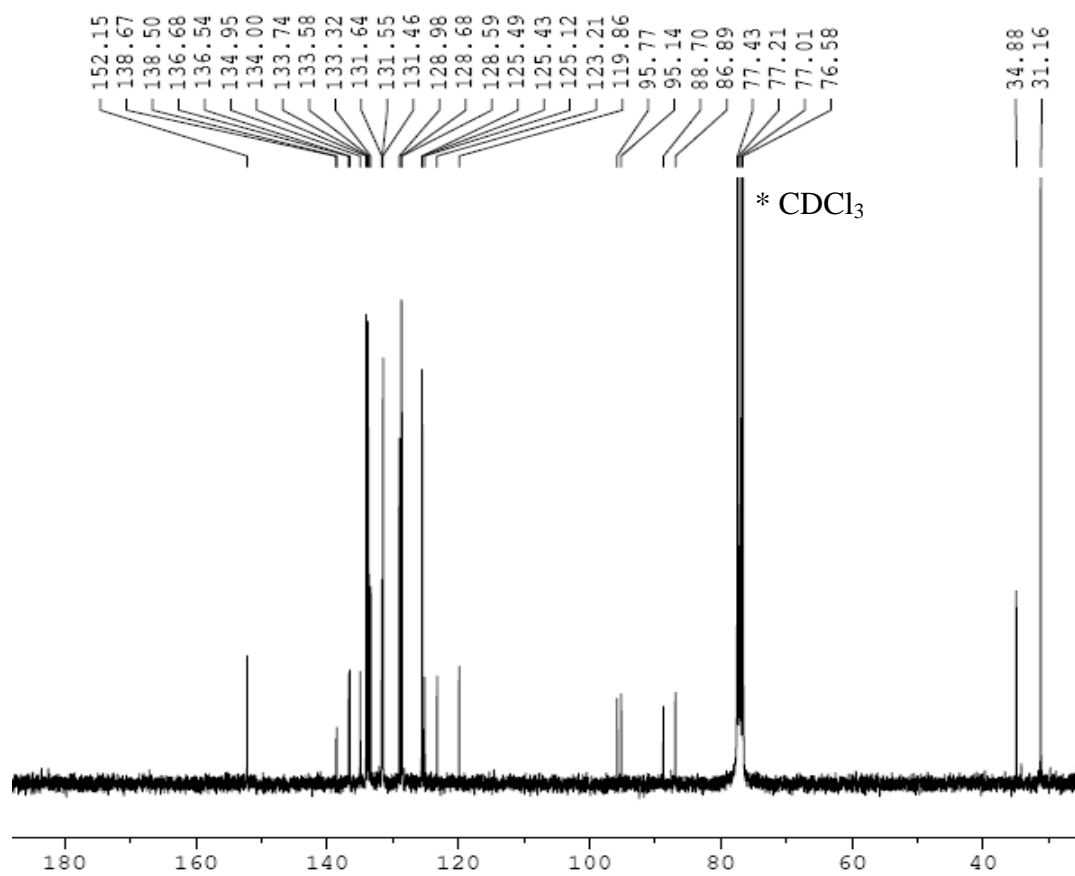
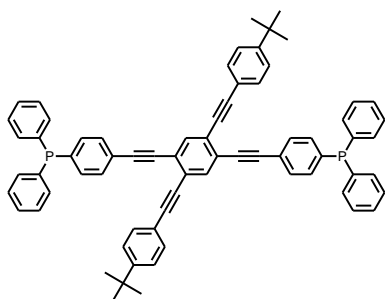


Figure 5 A.5 ^{13}C NMR (75 MHz, CDCl_3) of **9**.

1,4-bis(2-(4-tert-butylphenyl)ethynyl)-2,5-bis(2-(4-(diphenylphosphino) phenyl)ethynyl) benzene (**9**)

Structure

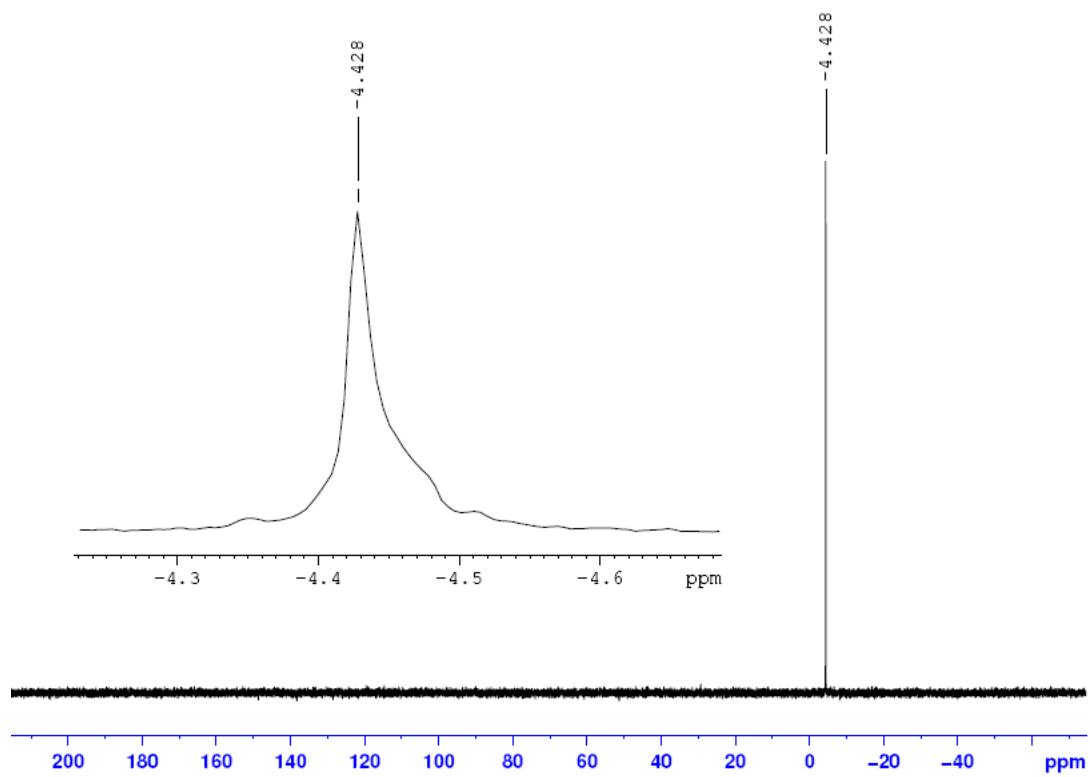
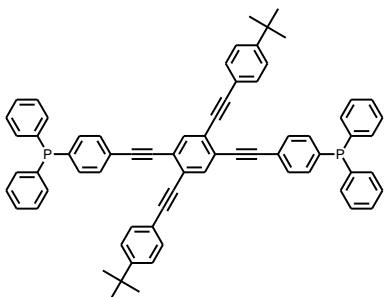


Figure 5 A.6 ^{31}P NMR (121 MHz, CDCl_3) of **9**.

Phosphonium Salt (**10**)

Structure

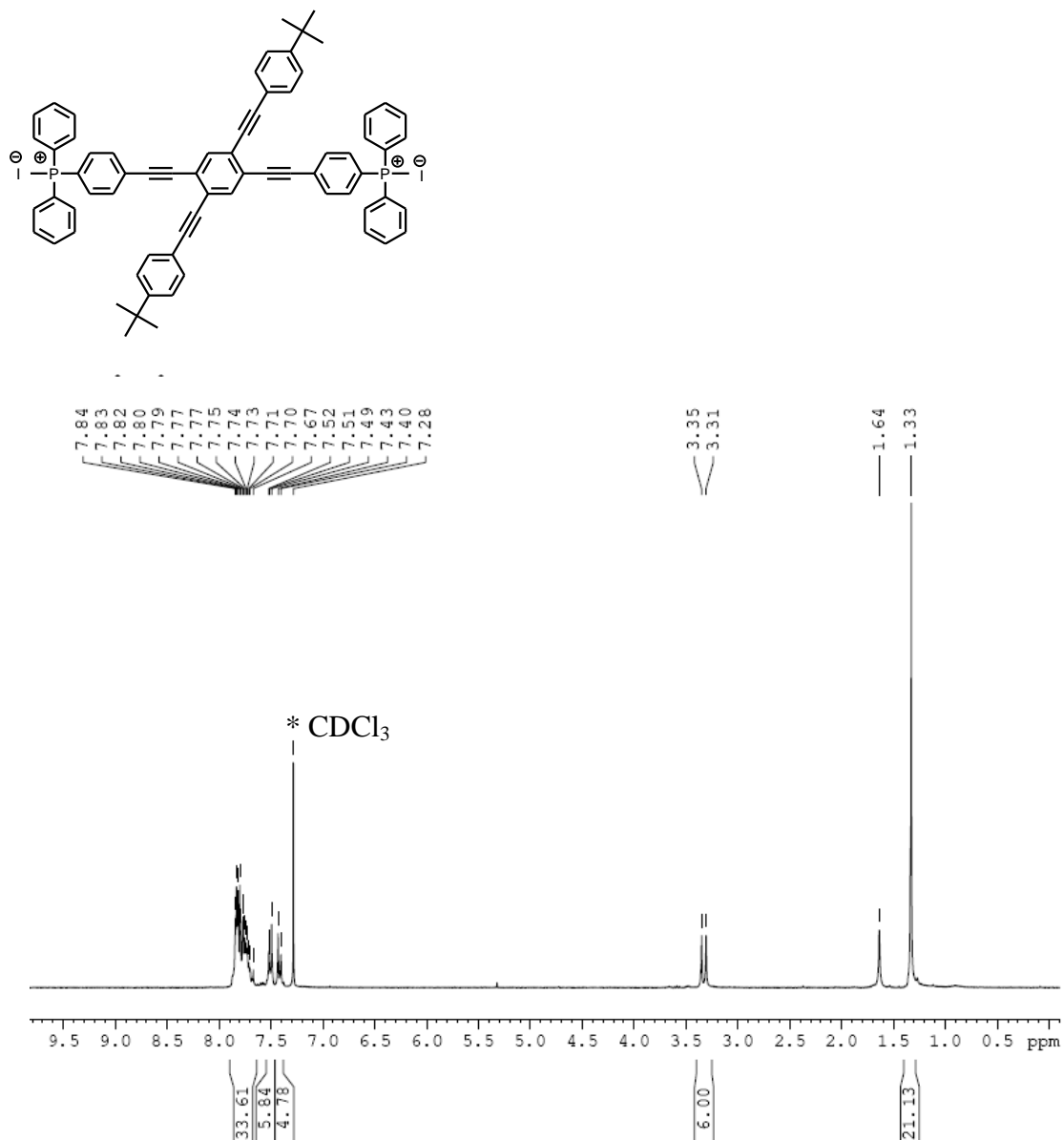


Figure 5 A.7 ¹H NMR (300 MHz, CDCl₃) of **10**.

Phosphonium Salt (**10**)

Structure

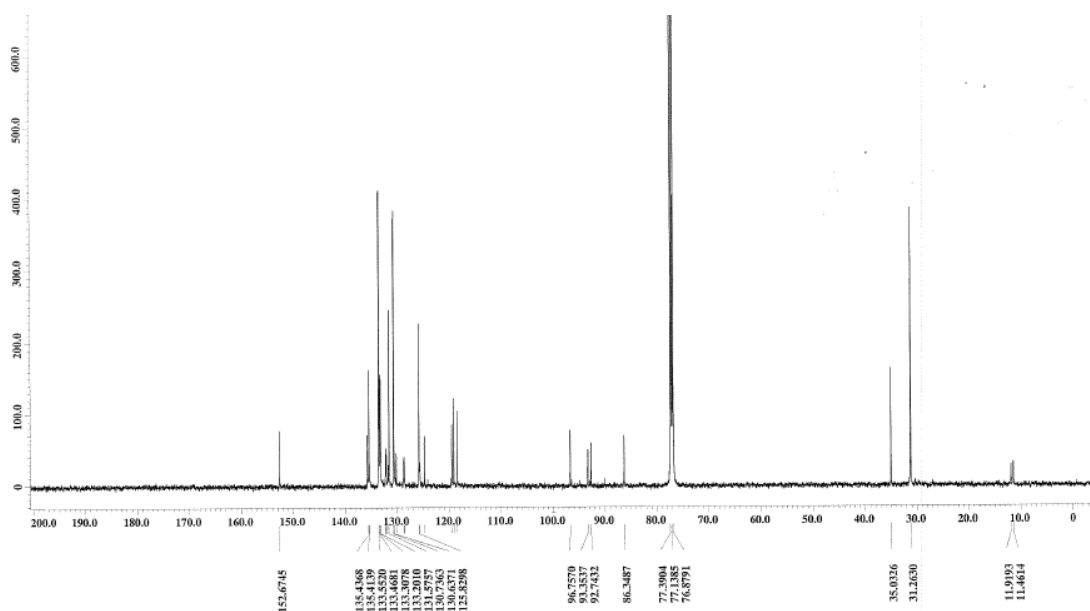
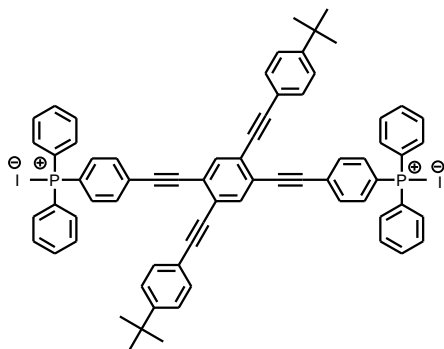


Figure 5 A.8 ^{13}C NMR (125 MHz, CDCl_3) of **10**.

Phosphonium Salt (**10**)

Structure

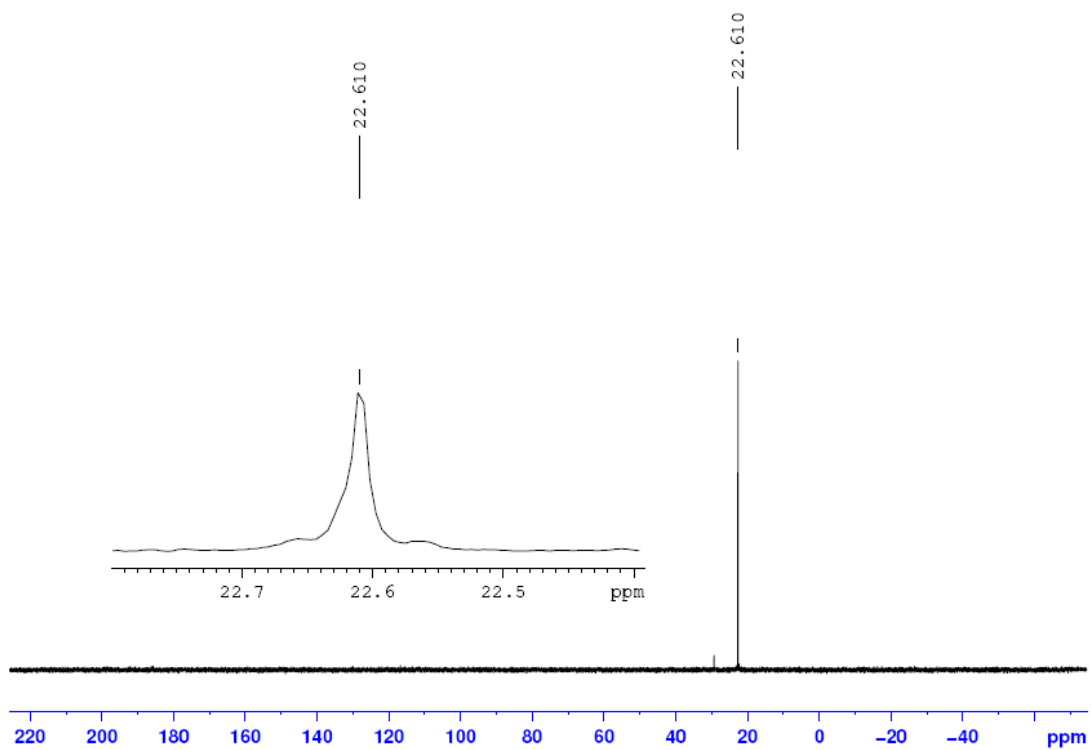
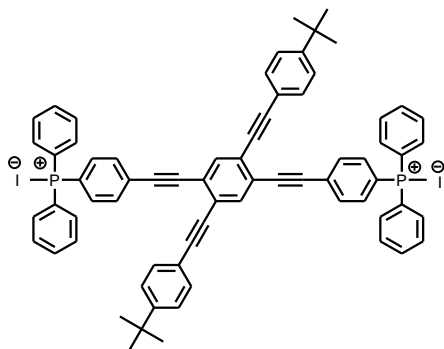


Figure 5 A.9 ^{31}P NMR (121 MHz, CDCl_3) of **10**.

Phosphine Gold Complex (**11**)

Structure

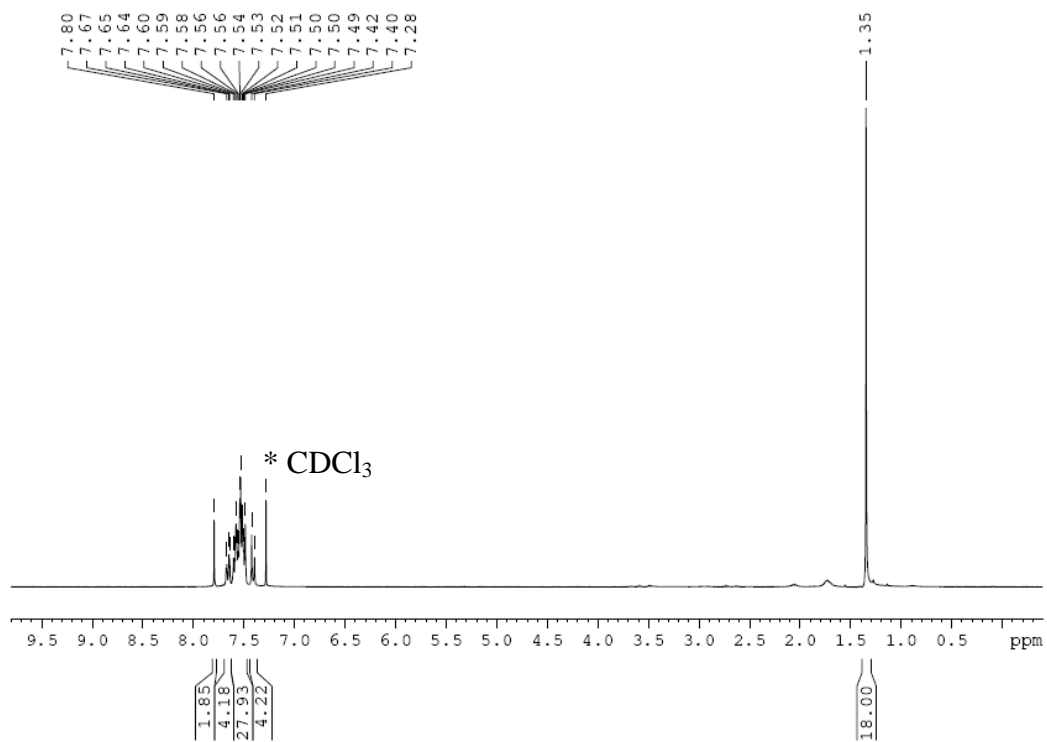
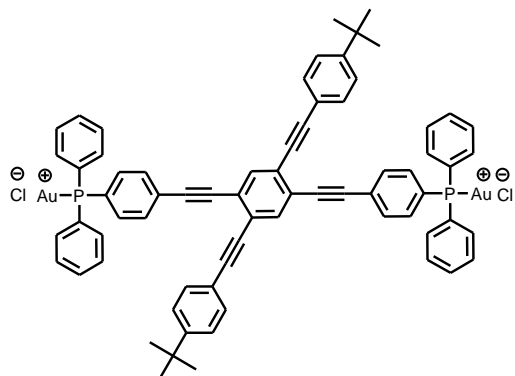


Figure 5 A.10 ¹H NMR (300 MHz, CDCl₃) of **11**.

Phosphine Gold Complex (**11**)

Structure

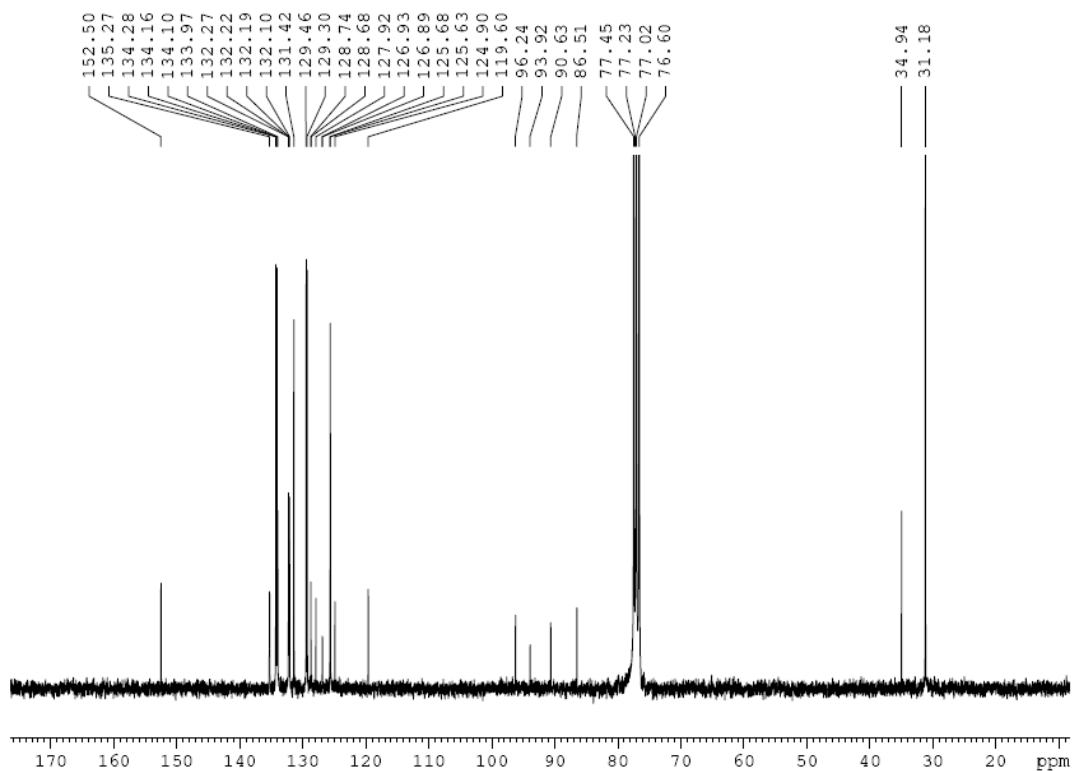
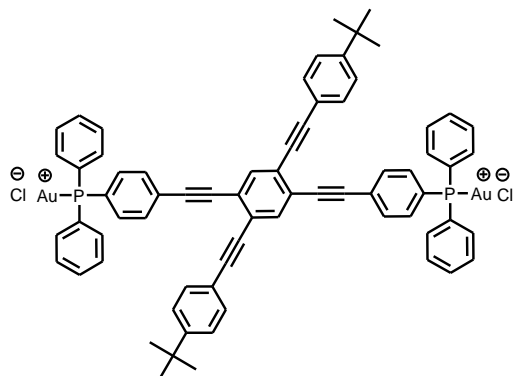


Figure 5 A.11 ^{13}C NMR (75 MHz, CDCl_3) of **11**.

Phosphine Gold Complex (**11**)

Structure

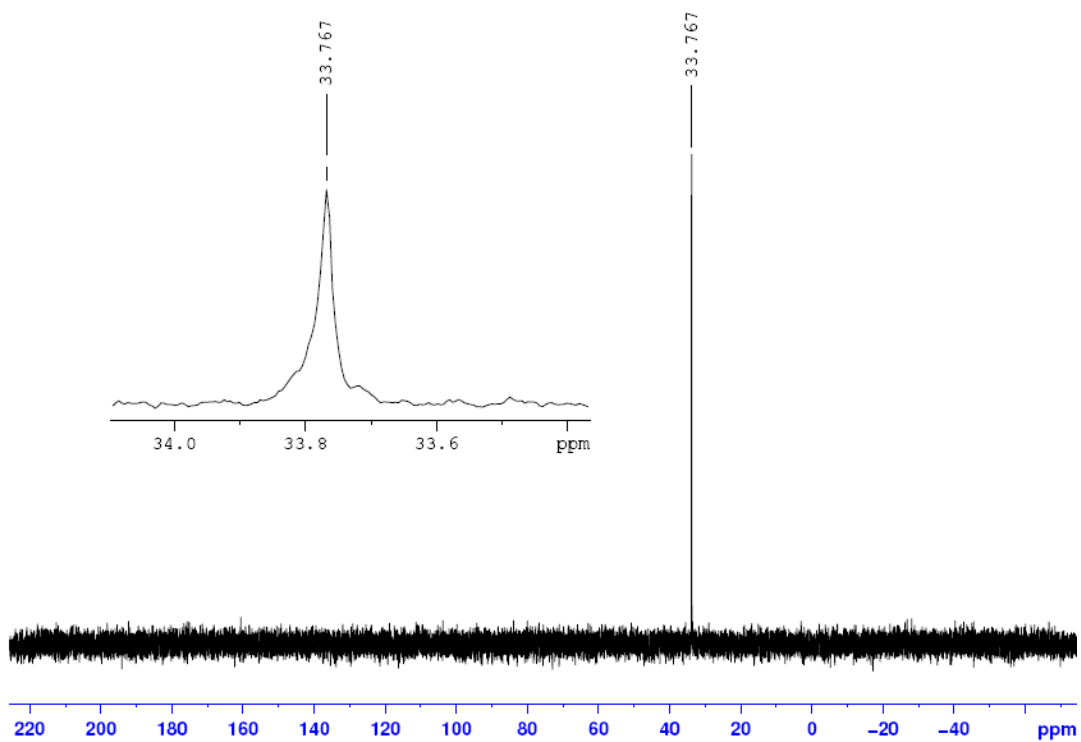
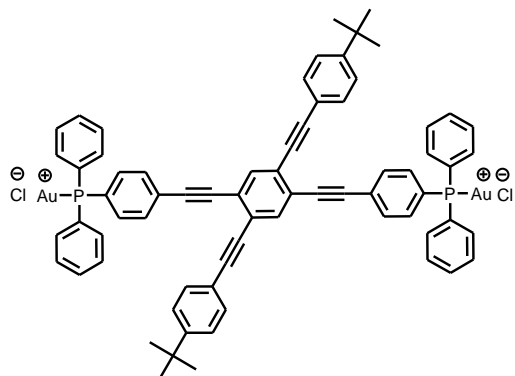


Figure 5 A.12 ^{31}P NMR (121 MHz, CDCl_3) of **11**.

1,4-bis(2-(4-tert-butylphenyl)ethynyl)2,5-bis(2-(4-diphenylphosphorothioyl)phenyl)ethynyl benzene (**12**)

Structure

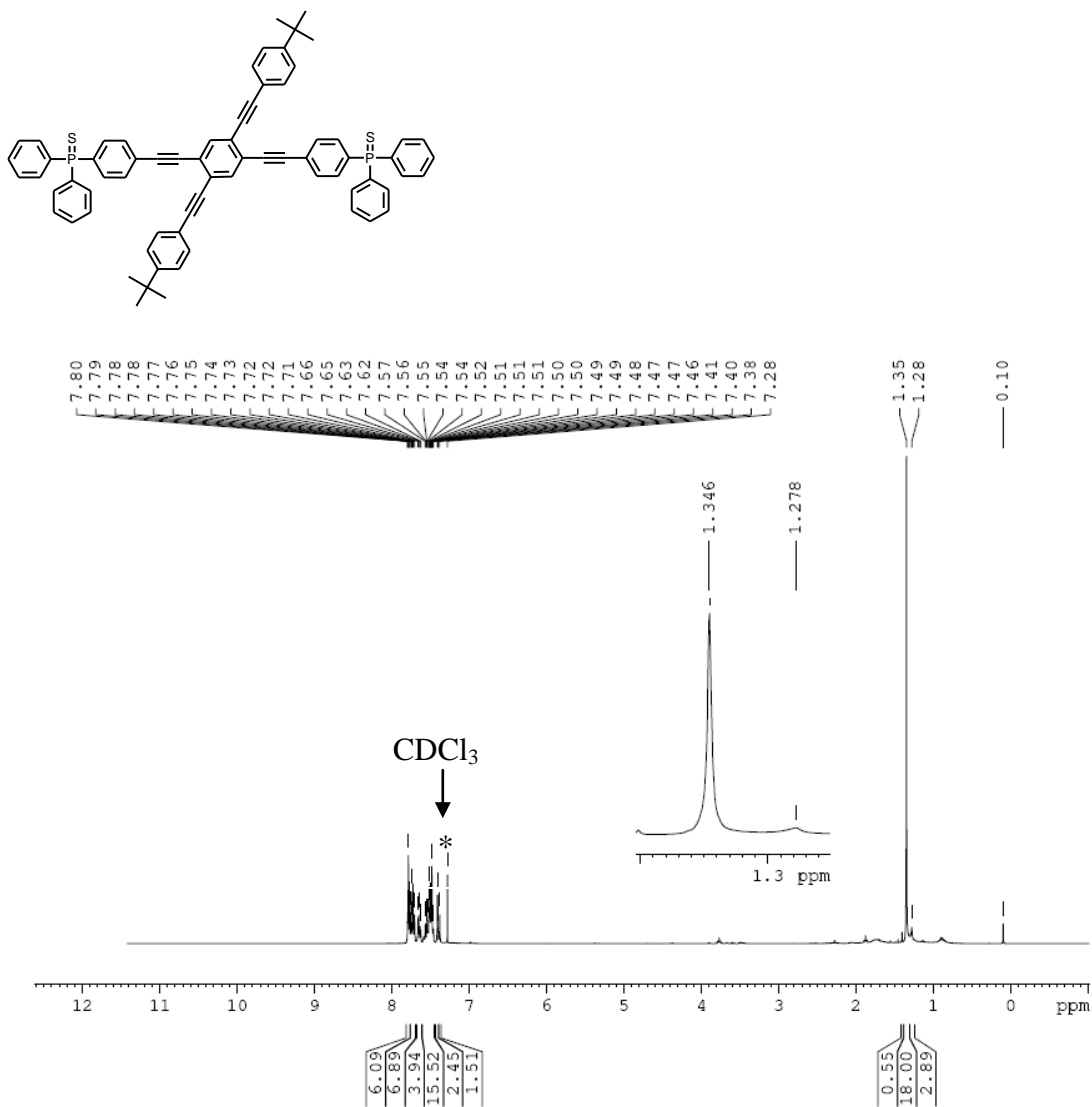


Figure 5 A.13 ¹H NMR (300 MHz, CDCl₃) of **12**.

1,4-bis(2-(4-tert-butylphenyl)ethynyl)2,5-bis(2-(4-diphenylphosphorothioyl)phenyl) ethynyl) benzene (**12**)

Structure

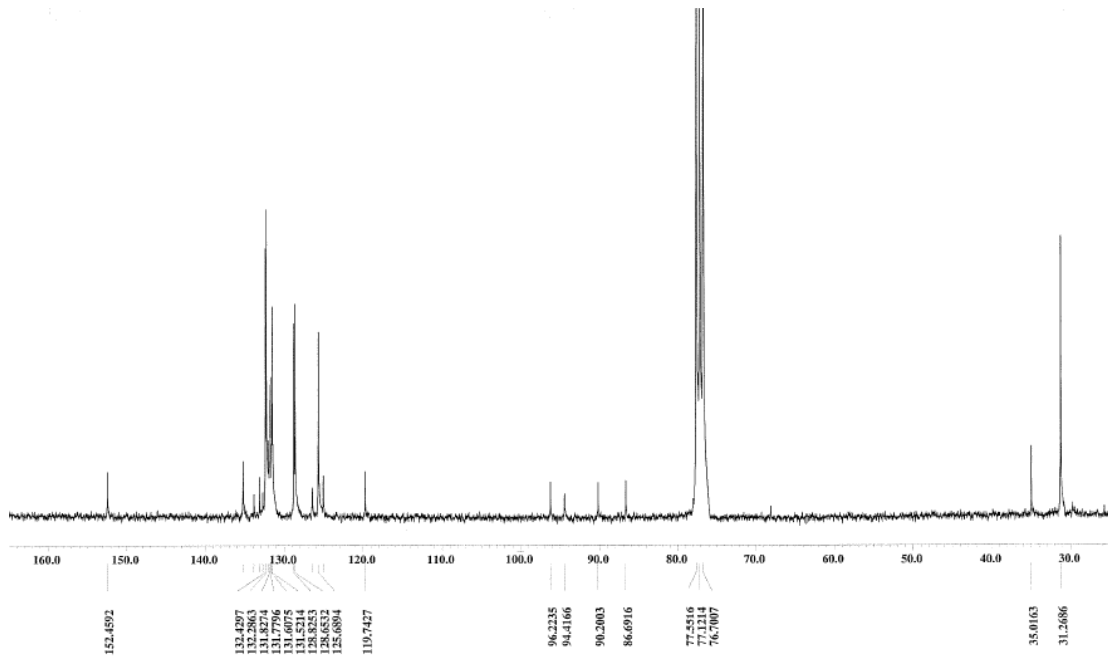
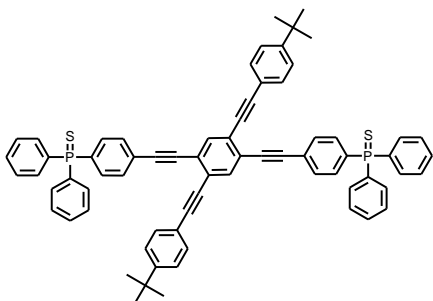


Figure 5 A.14 ^{13}C NMR (125 MHz, CDCl_3) of **12**.

1,4-bis(2-(4-tert-butylphenyl)ethynyl)2,5-bis(2-(4-diphenylphosphorothioyl)phenyl) ethynyl benzene (**12**)

Structure

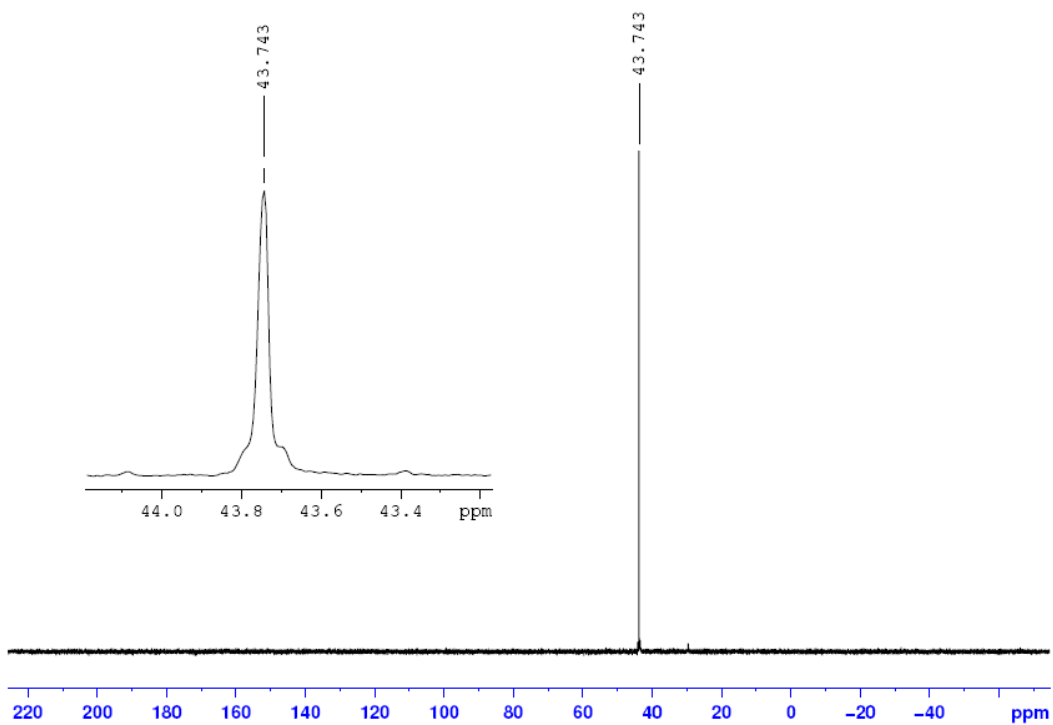
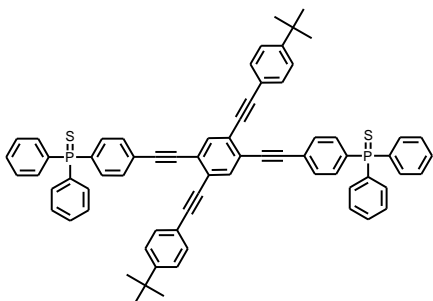


Figure 5 A.15 ^1P NMR (121 MHz, CDCl_3) of **12**.

CHAPTER SIX

INTERCHROMOPHORIC ORIENTATION SCAFFOLDING BY *m*- TERPHENYL OXACYCLOPHANES[#]

6.1 Introduction

Molecules featuring covalently-scaffolded interchromophore interactions^{1, 2} or that feature intramolecular charge-transfer (i.e., cruciforms)³⁻¹² have attracted considerable interest. Inter- π -system interactions between chromophores have important practical consequences because the optoelectronic performance of organic semiconducting polymers (CPs) is dictated by intermolecular morphology.^{1, 13-18} Developing rational design principles for organic electronics thus requires a deeper understanding of inter- π -system interactions, spurring a multitude of theoretical¹⁹⁻²² and experimental studies focused on scaffolded inter- π -system geometries.^{1, 23, 24}

Semiconducting and light-harvesting π -conjugating polymers (CPs) have been widely used in various photonic and electronic applications. Such materials are an integral part of device applications such as organic or polymer based light emitting devices (OLEDs / PLEDs) and organic photovoltaics (OPVs).²⁵⁻²⁷

OPVs are a prime concern especially in this era, when we are looking for the replacement of fuel sources to solve the energy crisis. Organic synthesis and bond

[#] Adapted in parts from: Mangalum, A.; Morgan, B. P.; Hanley, J. M.; Jecen, K. M.; McGill, C. J.; Robertson, G. A.; Smith, R. C. *Chem. Commun.*, **2010**, DOI 10.1039/c0cc00247j, with permission.

making reactions provide vast flexibility to synthesize **CPs** materials with different geometry in bulk in order to study the effect of orientation on their optical properties.

Optical properties of these materials depend on numerous factors such as inter / intra chromophoric interaction, geometry and its orientation in space.² Questions about charge carrier mobility, quantum yield, and how the excited states transfer energy, can be addressed by detailed study of such materials. In order to gain a better understanding about the functioning of such devices and their development, it is required to understand these interactions among π -conjugating materials.

Hence synthesizing scaffolds followed by covalently attaching chromophores on them in different spatial orientation is an important field of research. Cyclophane derivatives are widely used for this scaffolding of chromophore especially where two aryl rings engage in face-to-face²⁸ π -stacking.

6.1.1 Scaffolds for chromophores

(A) Cyclophane Core

First synthesized by Hart,²⁹ *m*-terphenyl scaffolded cappedophanes and cuppedophanes (**Figure 6.2**) can provide the required platform for chromophores which can be covalently attached in different orientation by using several well known coupling reactions such as Sonogashira, Heck, Stille and Suzuki.

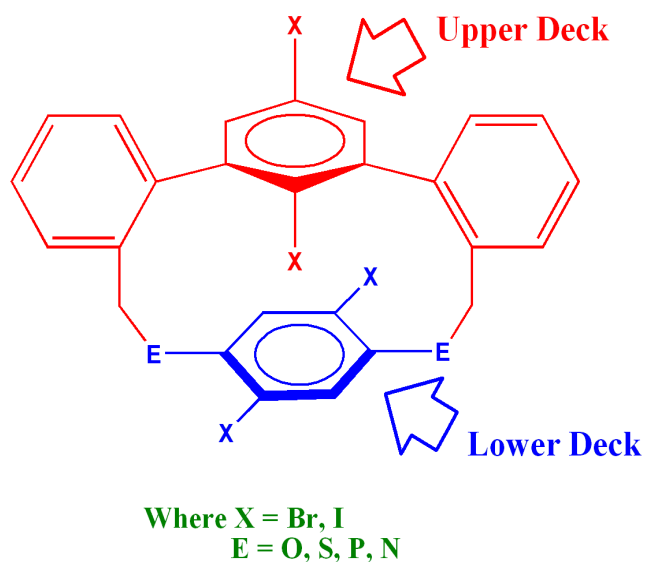


Figure 6.1 Generalized representation of cyclophane.

These cyclophanes can easily be synthesized by using a reactive group (e.g. CH_2Br) substituted terphenyl (**upper deck, Figure 6.1**) and a lower deck substituted with a good nucleophile (e.g. OH , SH , NH_2 or PR_2). The most striking feature of these cyclophane is the numerous possible functionalizable sites, which are shown in the general representation in **Figure 6.1**.^{30, 31} Here, X can be halides, generally bromide and iodide, which can serve as sites to append π -systems.

Also E in **Figure 6.1** can be replaced by oxygen, nitrogen, sulfur or phosphorous, and based on their electron donating or withdrawing ability, they can affect the electronic property of π -systems attached to the scaffold. Due to these functionality and possibility of transformation of cyclophane scaffold into π -system chromophores, such materials are an interesting platform for studying inter / intra chromophoric interaction.

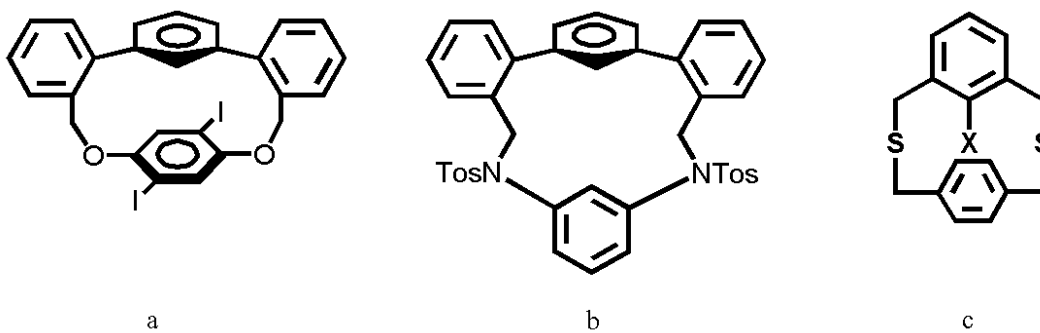


Figure 6.2 Representative *m*-terphenyl (a,b) and *m*-xylyl (c) cyclophanes.³⁰⁻³²

Smith *et al.* synthesized oxacyclophane (**Figure 6.2a**) and reported its orientation and bond distance in detail based on the X-ray crystallographic study. They found that two aryl rings are in face-to-face geometry and aryl centroid-to-centroid distance is 3.478 Å which is ideal for π -stacking in a scaffold.³²

(B) [2,2]paracyclophane Core

Bazan and co-workers have studied the [2,2]paracyclophane core substituted by various chromophores in detail in order to understand the effect of morphology, orientation, stacking, aggregation, and inter / intra chromophore interaction on the electronic and photonic properties.²

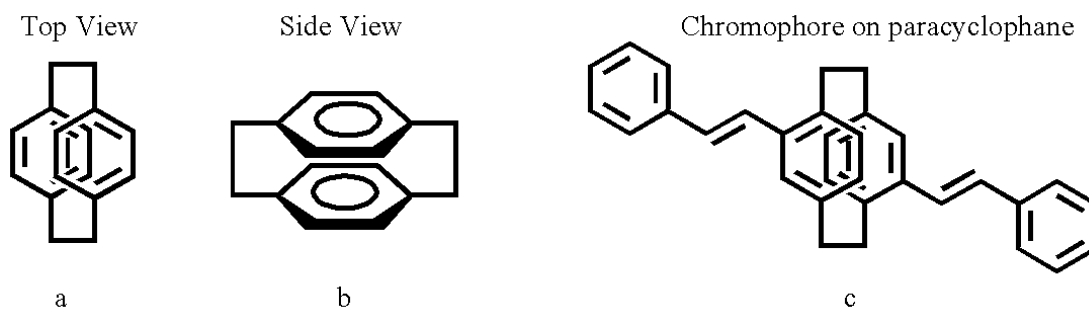


Figure 6.3 [2,2]paracyclophane with top (a) and side (b) view whereas (c) indicates one way in which chromophores can be attached to the paracyclophane.²

In [2,2]paracyclophanes (**Figure 6.3**), two benzene rings are held by two ethylene group linkage *para* to one another and the two rings are attached in parallel fashion *i.e.* face-to-face, with a distance between bridgehead carbons of 2.78 Å and 3.09 Å. Apart from the small molecule studies, paracyclophane have also been included in polymers to study the effects of orientation and inter / intra chromophore interactions. Lots of work has been done so far in this area and some of polymers are shown in **Figure 6.4**.^{2, 28, 33}

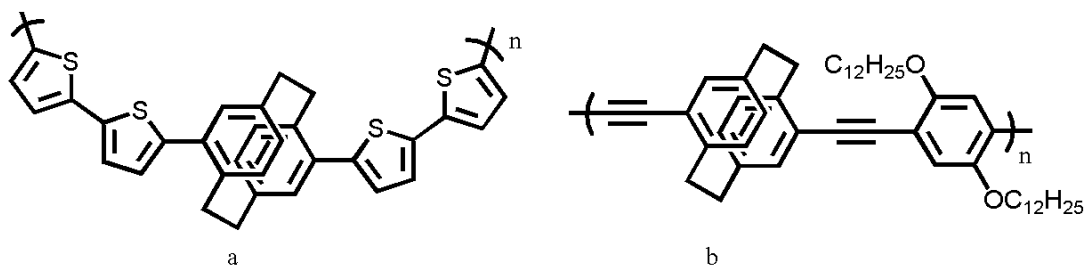


Figure 6.4 Inclusion of [2,2]paracyclophanes in polymeric systems.^{28, 33}

In this vein, we have designed a modular scaffold capable of replicating *multiple* types of inter- π -system orientations through the assembly of common building block

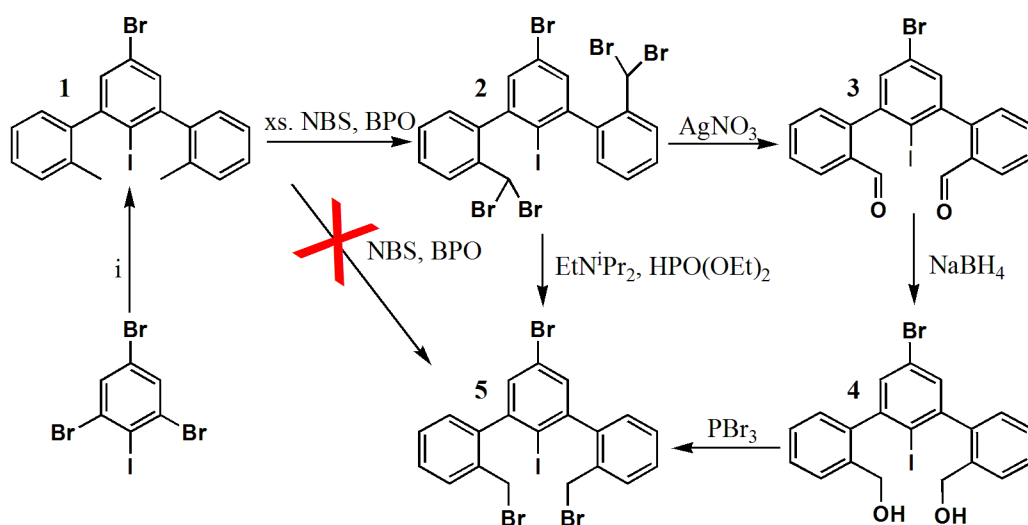
oxacyclophanes, followed by covalent attachment of *t*-butylphenylacetylene as chromophores on it by Sonogashira coupling. We are also trying to incorporate these oxacyclophanes in polymeric chain so that we can study their optical properties.

6.2 Synthesis and Characterization

Guided by *m*-terphenyl-scaffolded cappedophanes and cuppedophanes first reported by Hart,^{34, 35} we developed a π -conjugated polymer (**16**, **Scheme 6.3**) incorporating **CP1** cyclophane units (**Scheme 6.4**) with parallel aryl rings whose centroid-to-centroid distance (3.478 Å) was exceptionally suitable for π -stacking.³² This polymer proved useful in fluorescent detection of TNT. This successful study commenced our endeavor towards synthesizing variations on the oxacyclophane scaffold (**6**, **7**, **13**, **CP1**, and **CP2**).

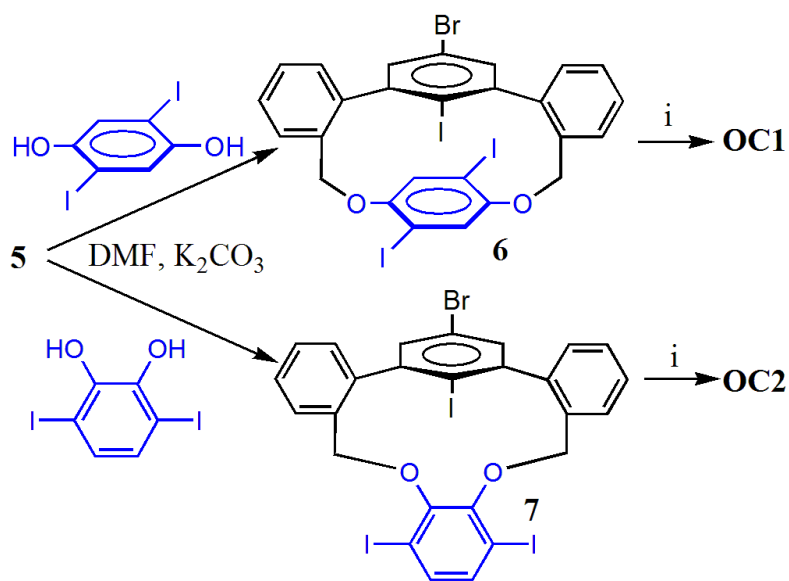
A key accomplishment was preparation of the tetrahalogenated oxacyclophanes **6** and **7** with different points of attachment of upper and lower deck (constitutional isomers) and their four-fold derivatization with chromophores **OC1** and **OC2** (**Scheme 6.2**). Compound **6** demonstrates parallel interactions between aryl rings, whereas **7** scaffolds orthogonal interactions.

Initial efforts to prepare **6** and **7** involved direct radical bromination of the benzylic sites in **1**³⁶ (**Scheme 6.1**). This route led to mixtures of bromomethyl- and dibromomethyl-substituted terphenyls.³⁷ The bis(dibromomethyl) derivative **2**, however, was cleanly produced using excess NBS, allowing access to **5** from **2** via conversion of **2** to aldehyde **3**, reduction to **4**, and finally treatment with PBr₃ to give **5** in 28% overall yield from **2** (**Scheme 6.1**). Significant improvements were accomplished by directly converting **2** to **5** by the action of diethylphosphite and EtNⁱPr₂,³⁸ yielding **5** in 60% yield from **2**.



Scheme 6.1 Routes to key precursor **5**; i. a) 10 equiv 2-tolylmagnesium bromide, Δ ; b) I_2 .
NBS = *N*-bromosuccinimide, BPO = benzoylperoxide.

Tetrahalogenated **6** (55%) and **7** (10%) were readily prepared via slow addition of a solution of **5** and 1,2-dihydroxy-3,6-diiodobenzene or 1,4-dihydroxy-2,5-diiodobenzene, respectively to a suspension of K_2CO_3 in DMF at 90 °C over 96 h (**Scheme 6.2**). Structures for the oxacyclophanes **6** and **7** were elucidated by a combination of 1D and 2D NMR spectroscopic techniques.³⁹ Chromophore incorporation into the scaffolds was readily accomplished by four-fold Sonogashira-Hagihara type coupling of the cores with 4-*t*-butylphenylacetylene to afford **OC1** (50%) and **OC2** (42%) (**Scheme 6.2**).



Scheme 6.2 Preparation of **6**, **7** and **OCs**; i) $[\text{Pd}(\text{PPh}_3)_4]$, CuI , (4-*t*-butylphenyl)acetylene, HN^iPr_2 , toluene, 90 °C.

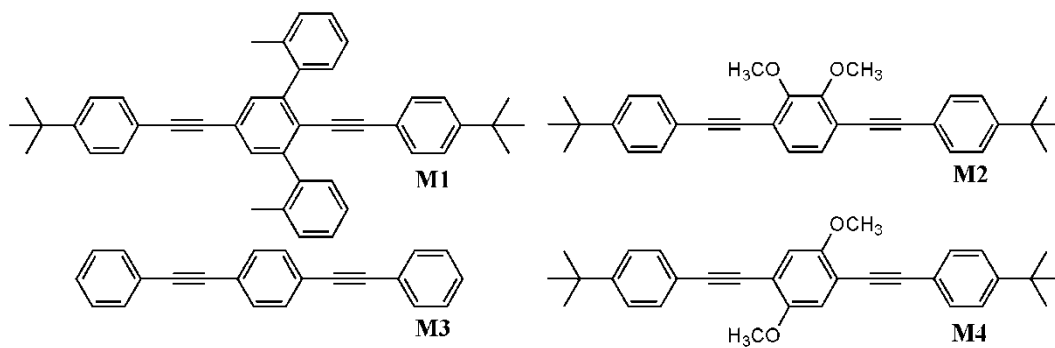
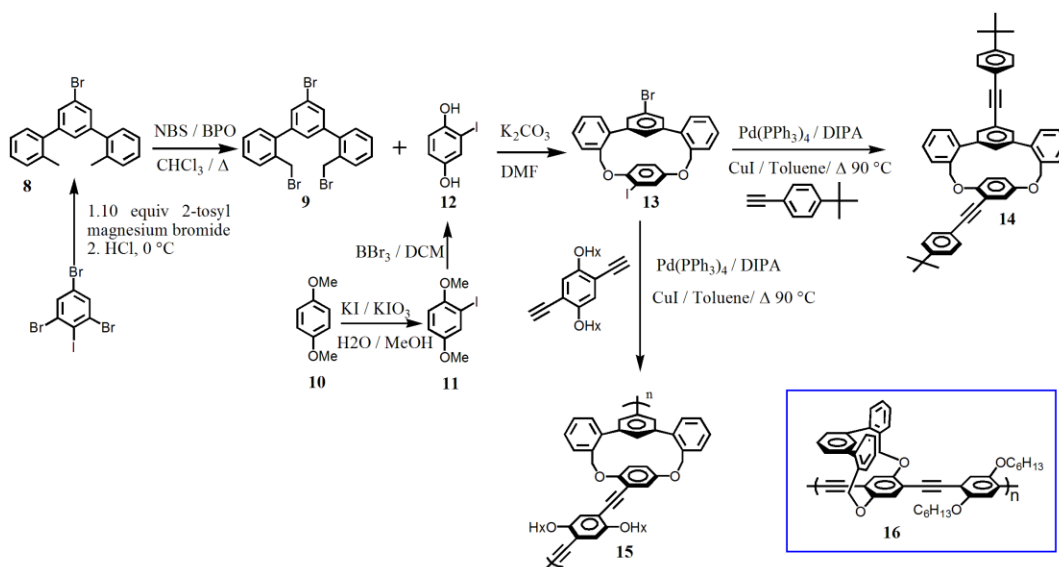


Figure 6.5 Unscaffolded model compounds for photophysical comparison.

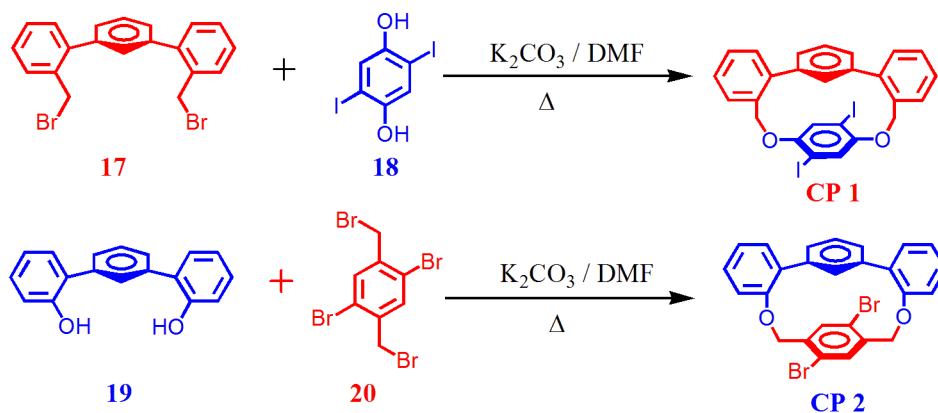
Compound **13** (Scheme 6.3) is a scaffold where only one halogen site is present on each deck in order to tether chromophores, where oxacyclophane scaffold provides a break in the π -system. Compound **13** (5%); which provides a scaffold to tether one chromophore each on upper and lower deck was synthesized by slow addition of a solution of compound **9** and **12** to a suspension of K_2CO_3 in DMF at $90\text{ }^\circ\text{C}$ over 96 h. Bromomethyl-substituted terphenyl **9** (28.7%) was synthesized from compound **8** by radical bromination of benzylic sites using NBS and BPO. Compound **12** (46%) was synthesized by selective iodination of 1,4-dimethoxybenzene **10** using KI and KIO_3 yielding **11** (58%) followed by deprotection of methoxy groups using tribromoborane. After having scaffold **13** in hand, two fold Sonogashira reaction yielded **14** (45%). Unit **13** was also incorporated into conjugated polymer **15** using 2,5-diethynyl-1,4-dihydroxybenzene as one of the monomer.



Scheme 6.3 Syntheses of 2-Way π system (monomer **14** and polymer **15**).

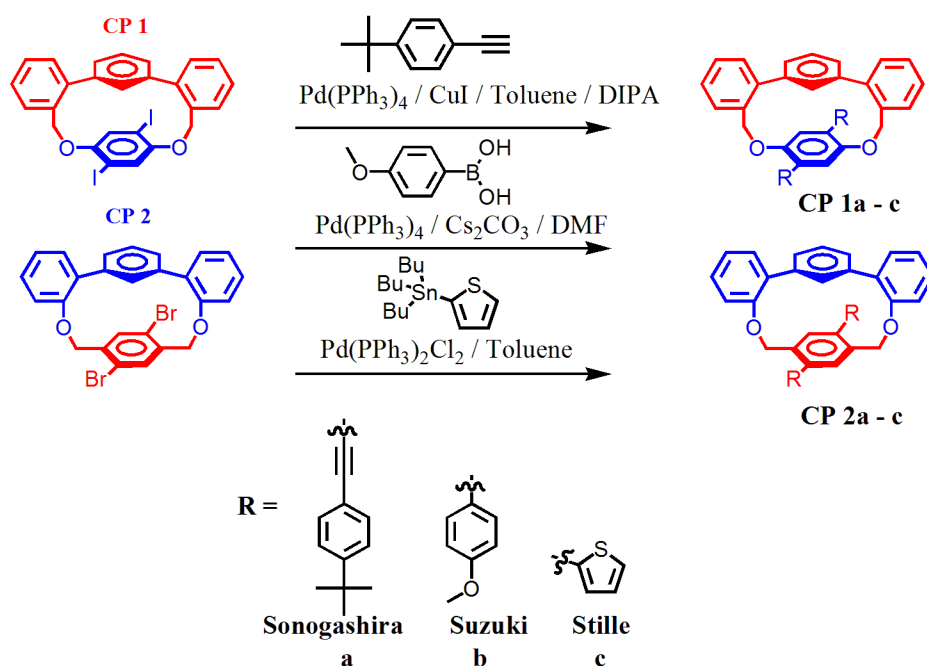
CP1 and **CP2** (Scheme 6.4) are almost similar except the position of electron donating atom *O*, which provides the electronic difference around the scaffold. Different chromophores such as *t*-butylphenylacetylene, thiophene and 4-methoxy phenyl chromophores were attached to **CP1** and **CP2** (Scheme 6.5) using commonly known C-C coupling reactions (Sonogashira, Stille and Suzuki reactions) and studied their optoelectronic properties.

In order to study the effect of electronic perturbation around chromophores, we synthesized two very similar oxacyclophane scaffolds **CP1** and **CP2** (Scheme 6.4) having sites to attach chromophores on lower deck only. These two scaffolds only differ in by the position of electron donating *O* atom, where in **CP1** oxygen is on lower deck and in **CP2** oxygen is attached to upper deck. **CP1** was synthesized by slow addition of a solution of compound **17** and **18** to a suspension of K_2CO_3 in DMF at 90 °C over 96 h while **CP2** (55.6%) was synthesized by using compound **19** and **20** following the same protocol.



Scheme 6.4 Syntheses of cyclophane 1 and 2 (**CP1** and **CP2**).

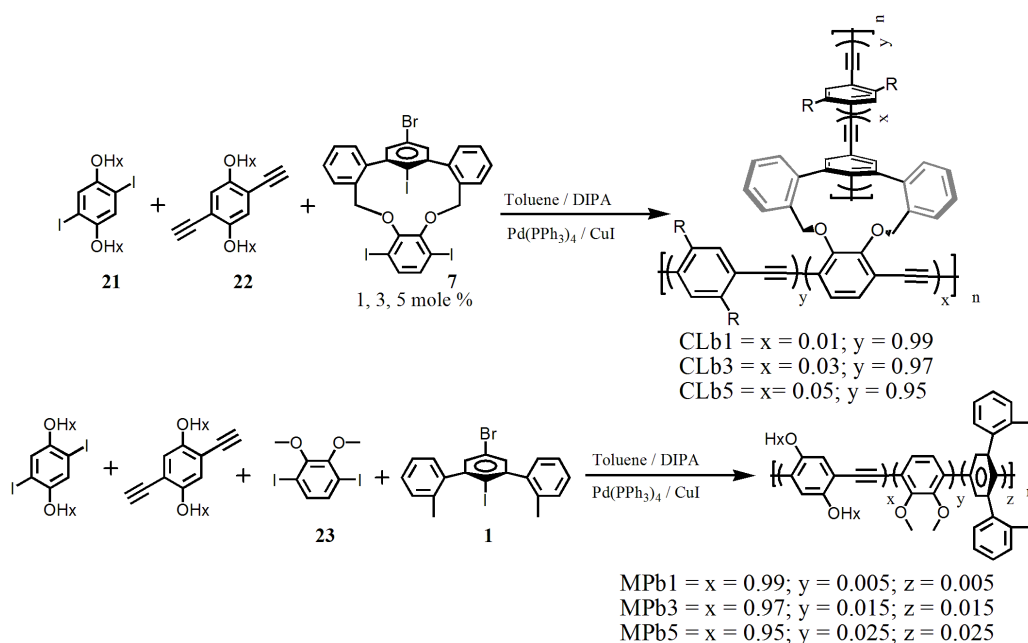
After having **CP1** and **CP2**, three different C-C coupling reactions were employed to attach different chromophores to these scaffolds. Two fold Sonogashira reaction was done to attach *t*-butylphenylacetylene yielding **CP1a** (27%) and **CP2a** (unable to fully purify). Two fold Suzuki reaction was done on **CP1** and **CP2** to attach 4-methoxy phenyl chromophore yielding **CP1b** (18%) and **CP2b** (17%) and similarly thiophene chromophore was attached by Stille reaction yielding **CP1c** (50%) and **CP2c** (37%) (**Scheme 6.5**).



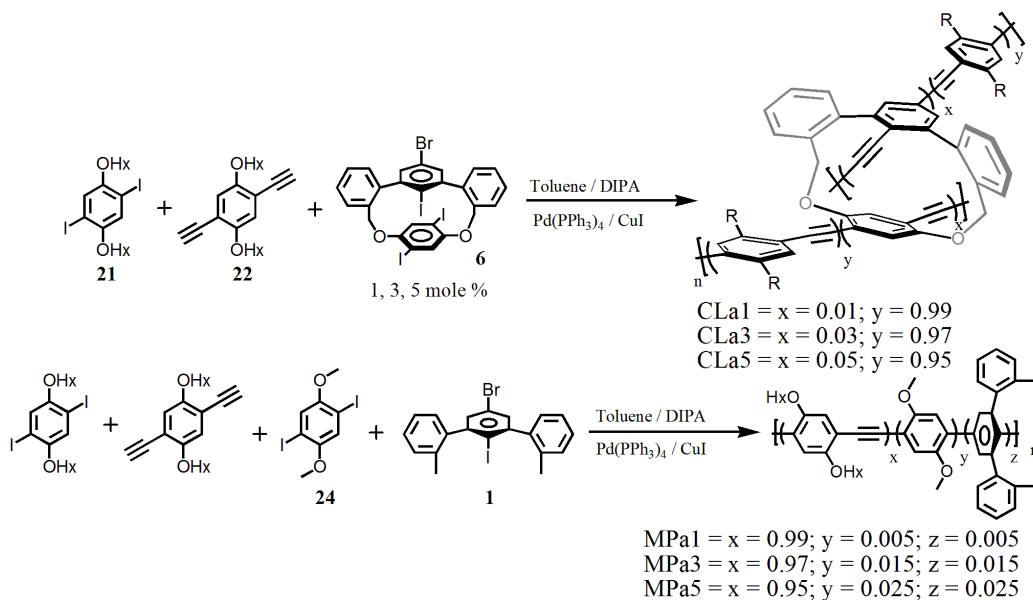
Scheme 6.5 Synthetic scheme for covalent attachment of chromophores on oxacyclophanes; (**CP1** and **CP2**). Details for all syntheses are provided in the experimental section **6.5**.

Tetrahalogenated oxacyclophane cores **6** and **7** (1, 3 and 5 mole %) were incorporated into a PPE polymer using Sonogashira reaction where these cores acts as a cross linking agent along the polymeric back bone. Also their model polymers; without the cross linking agent were synthesized keeping the composition of polymers similar to the cross linked polymers to study the effect of cross linking on photophysical properties over similar linear polymers.

The 1,2-cross linked polymers (**CLb1**, **CLb3** and **CLb5**) were synthesized by using monomers **21** and **22** with small amount of **7** as cross linking agent (**Scheme 6.6**) whereas linear model polymers (**MPb1**, **MPb3** and **MPb5**) have same monomers **21** and **22** along with compounds **1** and **23** in order to maintain the similar chemical composition. Similarly 1,4-cross linked polymers (**CLa1**, **CLa3** and **CLa5**) were synthesized by using monomers **21** and **22** with **6** as cross linking agent (**Scheme 6.7**) and their linear model polymers (**MPa1**, **MPa3** and **MPa5**) were prepared from monomers **21** and **22** along with compound **1** and **24**.



Scheme 6.6 Synthetic scheme for 1,2-cross linked polymer (**CLb1, 3 and 5**) and linear model polymers.



Scheme 6.7 Synthetic scheme for 1,4-cross linked polymer (**CLa1, 3 and 5**) and linear model polymers.

6.2.1 X-ray Characterization

The tetrahalogenated cores were also characterized by single crystal X-ray diffraction. The ORTEP drawings of the two cores (**Figure 6.6**) reveal that **6** holds upper and lower aryls in an offset π -stacking arrangement with a centroid-to-centroid distance of 3.623 Å. The relative positions of iodo and bromo substituents suggest that the axes of π -systems appended at these sites would be tilted at an angle (α) of 21° with respect to one another.

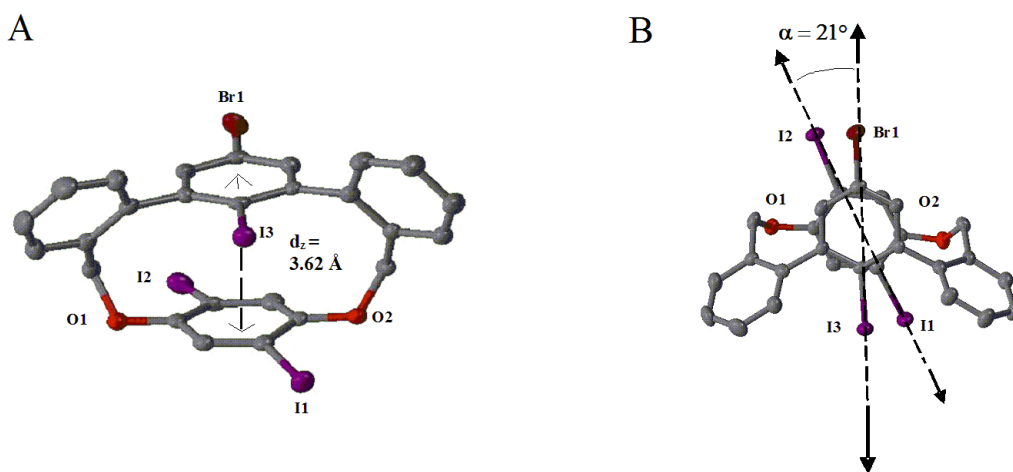


Figure 6.6 ORTEP drawing (50% ellipsoids) showing inter- π -system distance (**A**) and axial tilt angle as viewed looking down through the upper aryl ring (**B**) for compound **6**. H atoms are omitted for clarity and all the non-C atoms are labeled.

Table 6.1 Refinement detail for **6**.

Empirical formula	C ₂₆ H ₁₆ BrI ₃ O ₂
Formula weight (g/mol)	821.00
Temperature (K)	163 (2)
Wavelength (Å)	0.71073
Crystal system	Monoclinic
Space group	P2 ₁ /c
Unit cell dimensions	
<i>a</i> (Å)	10.633(2)
<i>b</i> (Å)	14.065(3)
<i>c</i> (Å)	32.946(7)
α (deg)	90.00
β (deg)	94.61(3)
γ (deg)	90.00
Volume (Å ³)	4911.3(17)
<i>Z</i>	8
Calculated density (Mg/m ³)	2.221
Absorption coefficient (mm ⁻¹)	5.467
<i>F</i> (000)	3056
Crystal size (mm)	0.41 × 0.12 × 0.07
Crystal color and shape	colourless plate
θ range for data collection (deg)	2.36 – 26.36
Limiting indices	-13 < <i>h</i> < 13 -11 < <i>k</i> < 17 -41 < <i>l</i> < 36
Reflections collected	34118
Independent reflections	9932
Completeness to θ	26.36 (99.1 %)
Max. transmission	0.6798
Min. transmission	0.2063
Refinement method	Full-matrix least-squares on <i>F</i> ²
Data / restraints / parameters	9932/0/577
Goodness of fit on <i>F</i> ²	1.113
Final R indices (<i>I</i> > 2σ(<i>I</i>))	
R1	0.0344
wR2	0.0729
R indices (all data)	
R1	0.0422
wR2	0.0771

In **7** (**Figure 6.7**) the upper and lower aryls are orthogonal (interplane angle = 89°) to one another with centroid-to-centroid distance of 5.577 \AA and α of 69° .

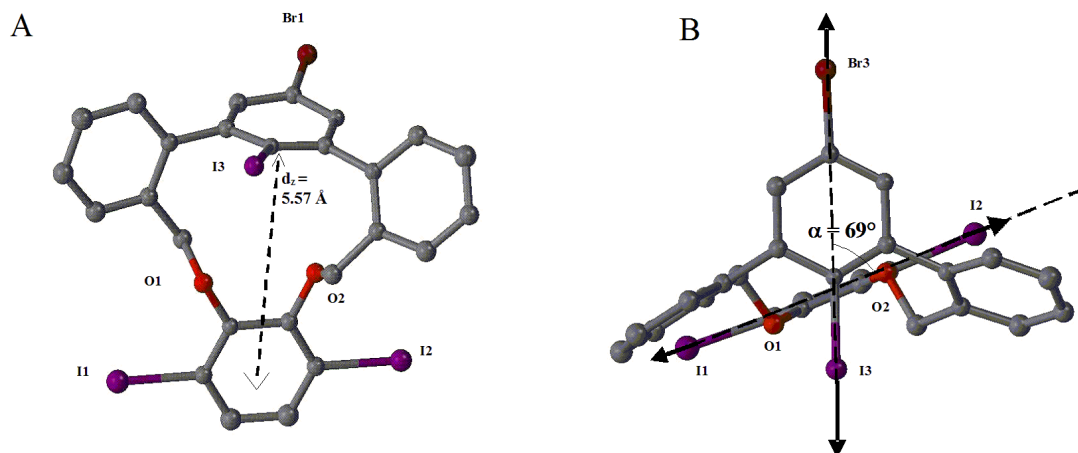


Figure 6.7 ORTEP drawing (50% ellipsoids) showing inter- π -system distance (**A**) and axial tilt angle as viewed looking down through the upper aryl ring (**B**) for compound **7**. H atoms are omitted for clarity and all the non-C atoms are labeled.

Table 6.2 Refinement detail for **7**.

Empirical formula	$C_{26}H_{16}BrI_3O_2$
Formula weight (g/mol)	821.00
Temperature (K)	153 (2)
Wavelength (Å)	0.71073
Crystal system	Monoclinic
Space group	$P2_{1/n}$
Unit cell dimensions	
<i>a</i> (Å)	7.6033(15)
<i>b</i> (Å)	19.178(4)
<i>c</i> (Å)	18.272(4)
<i>α</i> (deg)	90.00
<i>β</i> (deg)	100.12(3)
<i>γ</i> (deg)	90.00
Volume (Å ³)	2622.9(9)
<i>Z</i>	4
Calculated density (Mg/m ³)	2.079
Absorption coefficient (mm ⁻¹)	5.119
<i>F</i> (000)	1528
Crystal size (mm)	0.46 × 0.22 × 0.12
Crystal color and shape	colourless rod
θ range for data collection (deg)	2.26 – 25.10
Limiting indices	-9 < <i>h</i> < 8 0 < <i>k</i> < 22 0 < <i>l</i> < 21
Reflections collected	4651
Independent reflections	4651
Completeness to θ	25.10 (99.9 %)
Max. transmission	0.5787
Min. transmission	0.2017
Refinement method	Full-matrix least-squares on F^2
Data / restraints / parameters	4651/0/289
Goodness of fit on F^2	1.120
Final R indices ($I > 2\sigma(I)$)	
R1	0.0372
wR2	0.0907
R indices (all data)	
R1	0.0413
wR2	0.0937

Also 2-way- π -way core; compound **13** (**Figure 6.8**) was characterized by single crystal X-ray diffraction. Upper and lower deck aromatic ring is centroid-to-centroid distance of 3.553 Å. Bromine is substituted on upper and iodine on lower deck allows attaching chromophores on separate deck. Here we used *t*-butylphenylacetylene as a chromophore for both sites but such arrangement can also be used for attaching different chromophores (*i.e.*, donor or acceptor) on either deck.

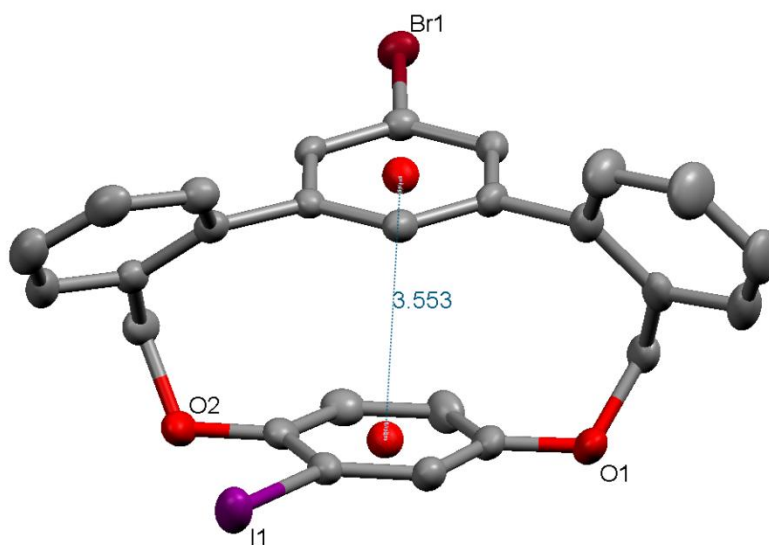


Figure 6.8 ORTEP drawing (50% ellipsoids) showing inter- π -system distance for compound **13**. H atoms are omitted for clarity and all the non-C atoms are labeled.

Table 6.3 Refinement detail for **13**.

Empirical formula	C ₂₆ H ₁₈ BrIO ₂
Formula weight (g/mol)	569.21
Temperature (K)	153 (2)
Wavelength (Å)	0.71073
Crystal system	Monoclinic
Space group	P2 ₁ /c
Unit cell dimensions	
<i>a</i> (Å)	17.725(4)
<i>b</i> (Å)	12.835(3)
<i>c</i> (Å)	9.831(2)
<i>α</i> (deg)	90.00
<i>β</i> (deg)	103.43(3)
<i>γ</i> (deg)	90.00
Volume (Å ³)	2175.4(8)
<i>Z</i>	4
Calculated density (Mg/m ³)	1.738
Absorption coefficient (mm ⁻¹)	3.329
<i>F</i> (000)	1112
Crystal size (mm)	0.48 × 0.43 × 0.43
Crystal color and shape	colorless chip
θ range for data collection (deg)	2.66 - 25.10
Limiting indices	-21 < <i>h</i> < 21 -12 < <i>k</i> < 15 -11 < <i>l</i> < 11
Reflections collected	17527
Independent reflections	3874
Completeness to θ	25.10 (99.8 %)
Max. transmission	0.3286
Min. transmission	0.2979
Refinement method	Full-matrix least-squares on <i>F</i> ²
Data / restraints / parameters	3874/0/271
Goodness of fit on <i>F</i> ²	1.144
Final R indices (<i>I</i> > 2σ(<i>I</i>))	
R1	0.0385
wR2	0.0991
R indices (all data)	
R1	0.0423
wR2	0.1030

In **CP1**; were oxygen is attached to lower deck (**Figure 6.9**) upper and lower aryls are almost parallel to one another with centroid-to-centroid distance of 3.477 Å.

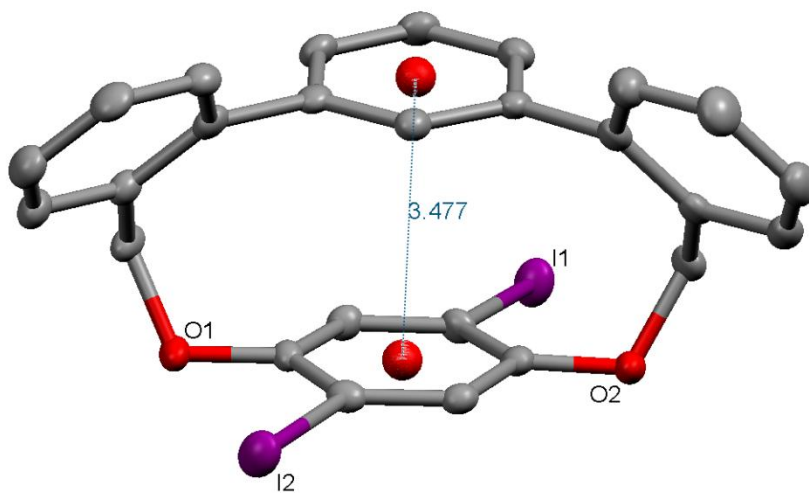


Figure 6.9 ORTEP drawing (50% ellipsoids) showing inter- π -system distance for compound **CP1**. H atoms are omitted for clarity and all the non-C atoms are labeled.

Table 6.4 Refinement detail for **CP1**.

Empirical formula	C ₂₆ H ₁₈ I ₂ O ₂
Formula weight (g/mol)	616.20
Temperature (K)	153 (2)
Wavelength (Å)	0.71073
Crystal system	Monoclinic
Space group	P2 ₁ /c
Unit cell dimensions	
<i>a</i> (Å)	13.146(3)
<i>b</i> (Å)	8.2785(17)
<i>c</i> (Å)	20.265(4)
<i>α</i> (deg)	90.00
<i>β</i> (deg)	103.91(3)
<i>γ</i> (deg)	90.00
Volume (Å ³)	2140.7(7)
<i>Z</i>	4
Calculated density (Mg/m ³)	1.912
Absorption coefficient (mm ⁻¹)	2.959
<i>F</i> (000)	1184
Crystal size (mm)	0.36 × 0.24 × 0.19
Crystal color and shape	colourless chip
θ range for data collection (deg)	2.93 - 25.10
Limiting indices	-15 < <i>h</i> < 15 -9 < <i>k</i> < 9 -24 < <i>l</i> < 21
Reflections collected	13664
Independent reflections	3772
Completeness to θ	25.10 (99.1 %)
Max. transmission	0.6033
Min. transmission	0.4156
Refinement method	Full-matrix least-squares on <i>F</i> ²
Data / restraints / parameters	3772/0/271
Goodness of fit on <i>F</i> ²	1.146
Final R indices (<i>I</i> > 2σ(<i>I</i>))	
R1	0.0334
wR2	0.0777
R indices (all data)	
R1	0.0364
wR2	0.0809

In **CP2**; where oxygen is attached to upper deck (**Figure 6.10**) upper and lower aryls are almost parallel to one another with centroid-to-centroid distance of 3.454 Å. Hence both **CP1** and **CP2** have almost similar centroid-to-centroid distance despite different point of attachment. **CP2** has smaller centroid-to-centroid distance due to presence of smaller bromine atom compared to **CP1** where halogens are iodine.

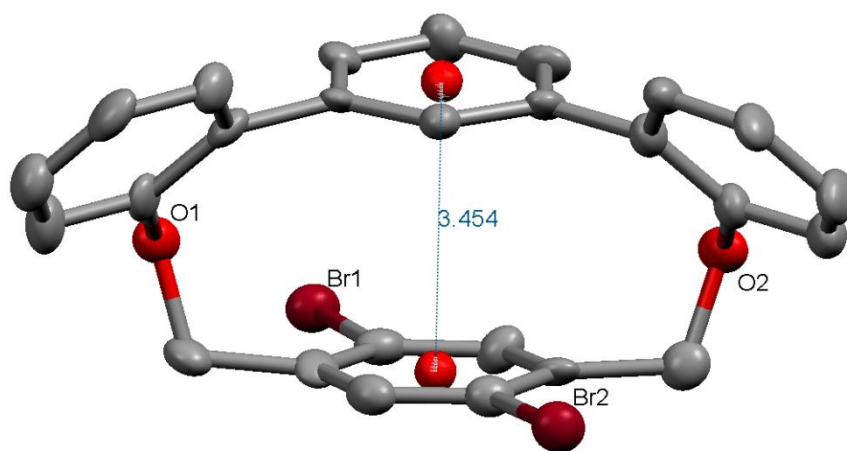


Figure 6.10 ORTEP drawing (50% ellipsoids) showing inter- π -system distance for compound **CP2**. H atoms are omitted for clarity and all the non-C atoms are labeled.

Table 6.5 Refinement detail for **CP2**.

Empirical formula	C ₂₆ H ₁₈ Br ₂ O ₂
Formula weight (g/mol)	522.22
Temperature (K)	153 (2)
Wavelength (Å)	0.71073
Crystal system	Orthorhombic
Space group	Fdd2
Unit cell dimensions	
<i>a</i> (Å)	23.488(5)
<i>b</i> (Å)	47.985(10)
<i>c</i> (Å)	7.3192(15)
<i>α</i> (deg)	90.00
<i>β</i> (deg)	90.00
<i>γ</i> (deg)	90.00
Volume (Å ³)	8249(3)
<i>Z</i>	16
Calculated density (Mg/m ³)	1.682
Absorption coefficient (mm ⁻¹)	3.952
<i>F</i> (000)	4160
Crystal size (mm)	0.20 × 0.20 × 0.20
Crystal color and shape	colorless chip
<i>θ</i> range for data collection (deg)	1.93 - 25.10
Limiting indices	-27 < <i>h</i> < 28 -45 < <i>k</i> < 56 -6 < <i>l</i> < 8
Reflections collected	7979
Independent reflections	2853
Completeness to <i>θ</i>	25.10 (99.3 %)
Refinement method	Full-matrix least-squares on <i>F</i> ²
Data / restraints / parameters	2853/1/271
Goodness of fit on <i>F</i> ²	1.089
Final R indices (<i>I</i> > 2σ(<i>I</i>))	
R1	0.0558
wR2	0.1379
R indices (all data)	
R1	0.0655
wR2	0.1509

In **CP2b** (**Figure 6.11**) upper and lower aryls are almost parallel to one another with centroid-to-centroid distance of 3.524 Å.

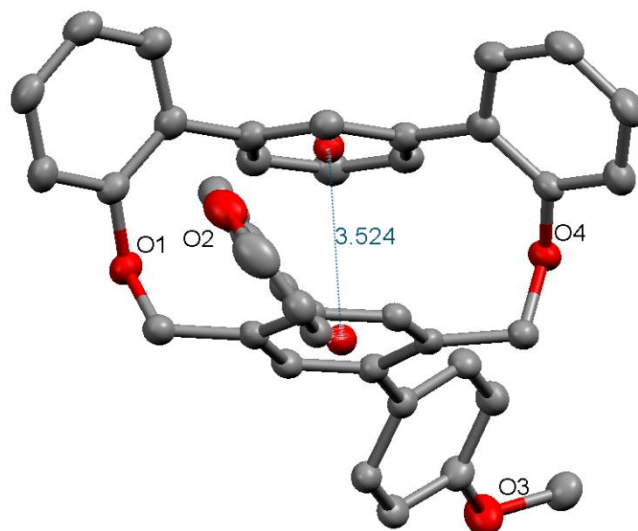


Figure 6.11 ORTEP drawing (50% ellipsoids) showing inter- π -system distance for compound **CP2b**. H atoms are omitted for clarity and all the non-C atoms are labeled.

Table 6.6 Refinement detail for **CP2b**.

Empirical formula	C ₄₀ H ₃₂ O ₄
Formula weight (g/mol)	576.66
Temperature (K)	153 (2)
Wavelength (Å)	0.71073
Crystal system	Monoclinic
Space group	P2 ₁ /c
Unit cell dimensions	
<i>a</i> (Å)	10.992(2)
<i>b</i> (Å)	13.240(3)
<i>c</i> (Å)	20.483(4)
<i>α</i> (deg)	90.00
<i>β</i> (deg)	90.77(3)
<i>γ</i> (deg)	90.00
Volume (Å ³)	2980.6(10)
<i>Z</i>	4
Calculated density (Mg/m ³)	1.285
Absorption coefficient (mm ⁻¹)	0.082
<i>F</i> (000)	1216
Crystal size (mm)	0.29 × 0.24 × 0.19
Crystal color and shape	yellow chip
θ range for data collection (deg)	2.60 - 25.10
Limiting indices	-13 < <i>h</i> < 12 -15 < <i>k</i> < 15 -24 < <i>l</i> < 24
Reflections collected	19601
Independent reflections	5294
Completeness to θ	25.10 (99.8 %)
Max. transmission	0.9846
Min. transmission	0.9767
Refinement method	Full-matrix least-squares on <i>F</i> ²
Data / restraints / parameters	5294/0/399
Goodness of fit on <i>F</i> ²	1.078
Final R indices (<i>I</i> > 2σ(<i>I</i>))	
R1	0.0567
wR2	0.1343
R indices (all data)	
R1	0.0856
wR2	0.1598

6.2.2 Density Functional Theory (DFT) Calculations

Optimized geometries (DFT at the B3LYP/6-31G(d) level) for the materials are shown in **Figure 6.12** confirming the aforementioned inter- π -system interactions in the cores. Because the relative orientation of the upper and lower π -systems dictates the interchromophore interaction, we believed that the systems supported by **OC1** and the **OC2** would exhibit radically different properties.

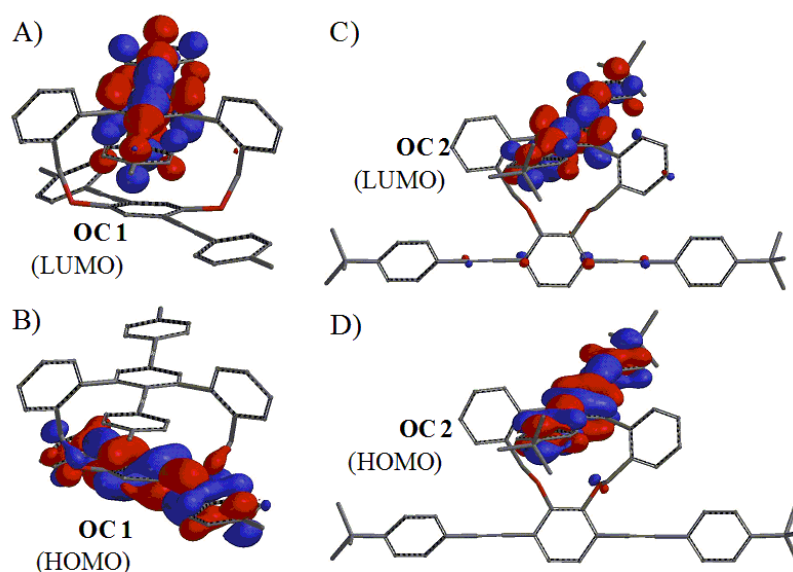
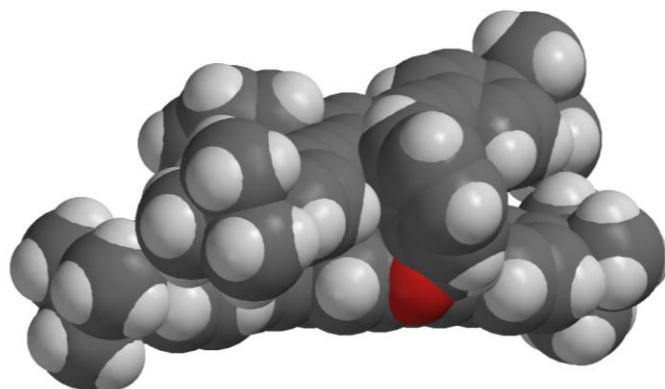


Figure 6.12 Calculated HOMO and LUMO distribution for **OC1** (A, B) and **OC2** (C, D) determined by DFT calculations at the B3LYP/6-31G(d) level.

The calculated centroid-to-centroid distance between aryls in **OC1** (3.86 Å) is within the range (3.77-4.50 Å) of π -stacking interactions that lead to notable photophysical effects in organic semiconducting polymer films.²⁰ The **OC2** is a reasonable model for orthogonal (“T-type”) interaction between aryls,⁴⁰ albeit with

longer centroid-to-centroid distance (5.39 Å) than typical (4.99-5.19 Å) for such interactions. Space-filling models (**Figure 6.13**) indicate that there is likely not enough free space between the central rings of upper and lower systems for inclusion of solvent or other guest molecules between them in either OC.

A)



B)

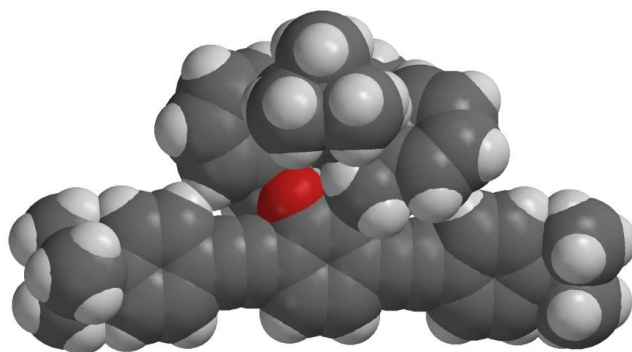


Figure 6.13 Space filling models of **OC1** (**A**) and **OC2** (**B**) shown in approximately the same orientation as in **Figure 6.6** and **6.7**. Geometries were calculated by semi empirical methods at the PM3 level of theory.

6.3 Photophysical Studies and Calculation

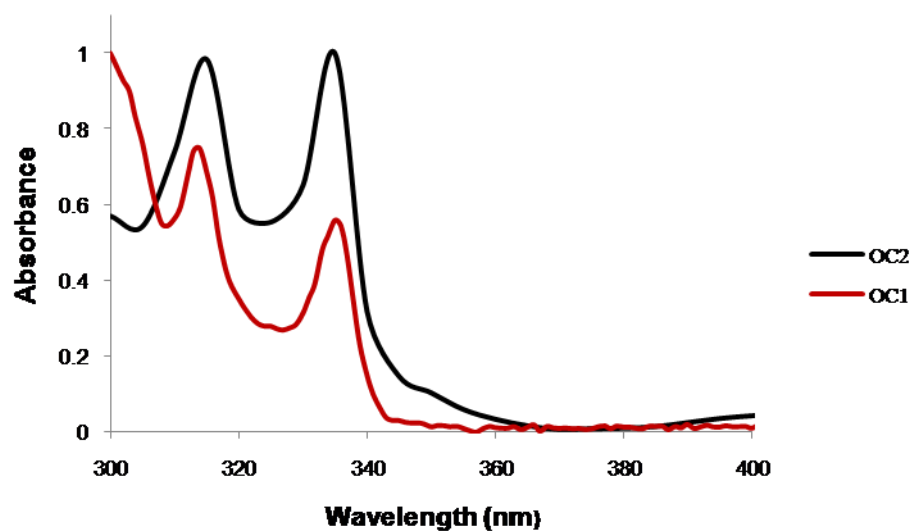
Photophysical properties of **OC1** and **OC2** (**Table 6.7**) were examined and compared to those of models (**Figure 6.5**) for both upper (**M1** and **M3**) or lower π -system (**CP1a**, **M2** and **M4**).

Table 6.7 Photophysical data for oxacyclophane materials and various upper and lower π -system models.

	$\lambda_{\pi-\pi^*}$ (nm)	log ϵ	λ_{emit} (nm)	Φ
OC2	335	4.56	429	0.52
OC1	335	4.79	420	0.012
CP1a	349	4.80	390	0.007
M1	335	4.91	362	0.58
M3	320	5.79	366	0.58
M2	330	5.05	360	0.40
M4	356	5.35	395	0.50

Because each OC features similar chromophores, their absorption spectra are expected to be quite similar barring some inter- π -system interaction in the ground state. Ground state effects typically require quite close proximity of two π -systems, such as that enforced by [2.2]paracyclophanes.^{2, 28, 33} At the distances inferred from optimized geometries of **OCs**, ground state perturbations are not likely, and NMR spectra show no sign of notable ground state inter- π -system interaction.

A)



B)

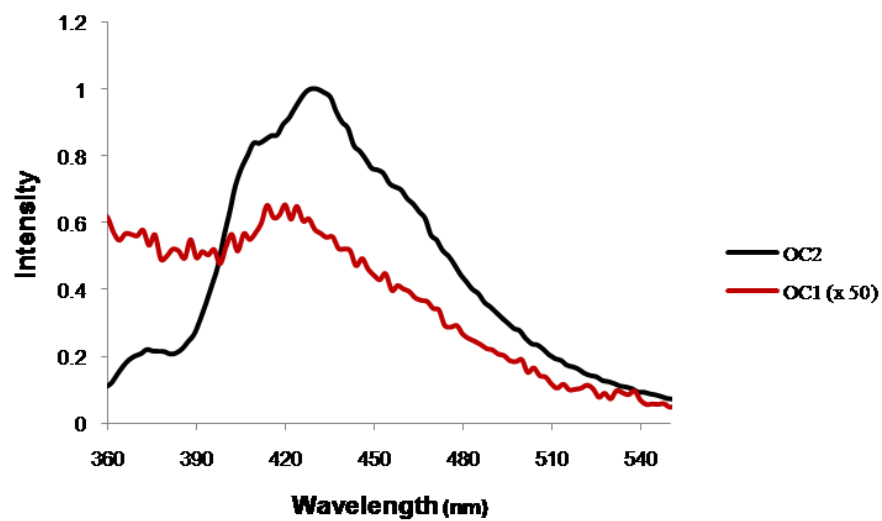
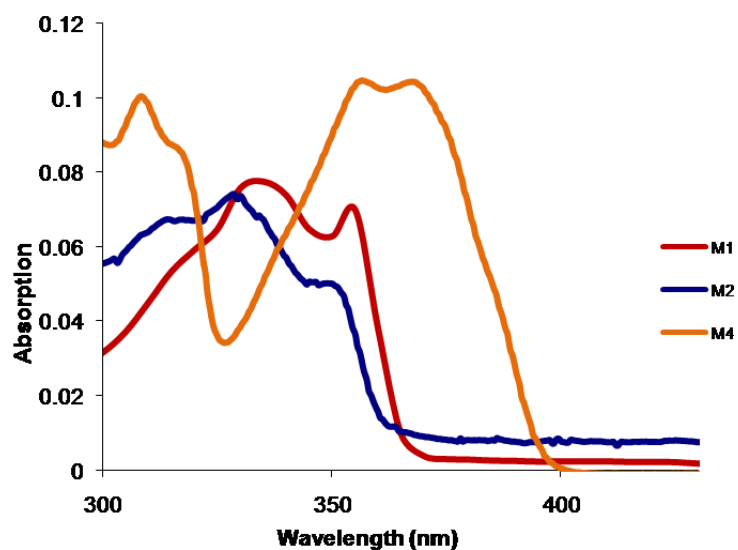


Figure 6.14 Normalized absorption (A, 5.9 μM for **OC1** and 5.2 μM for **OC2**) and emission spectra (B 0.59 μM for **OC1** and 0.52 μM for **OC2**) of **OC1** and **OC2**. All spectra were collected in THF.

Each absorption spectrum exhibits one π - π^* transition band with λ_{max} (335 nm for both) and ϵ values (**Table 6.7**) consistent with the chromophore units (a higher energy band attributable to the aryls attaching the two chromophores is also observed). **M2**, the model for the lower π -system of **OC2**, has a similar λ_{max} (330 nm) to that in **OC2**. **M4**, the model for the lower deck in **OC1**, however, has λ_{max} of 356 nm (**Figure 6.14**). The red shift for the transition in **M4** versus the similar unit in **OC1** is attributable to the constrained nature of the **OC1**. In **M4**, methoxy units act as strong electron donors, whereas the constrained geometry of **OC1** does not permit the planarization at oxygen necessary for the substituents to act as resonance donors.

A)



B)

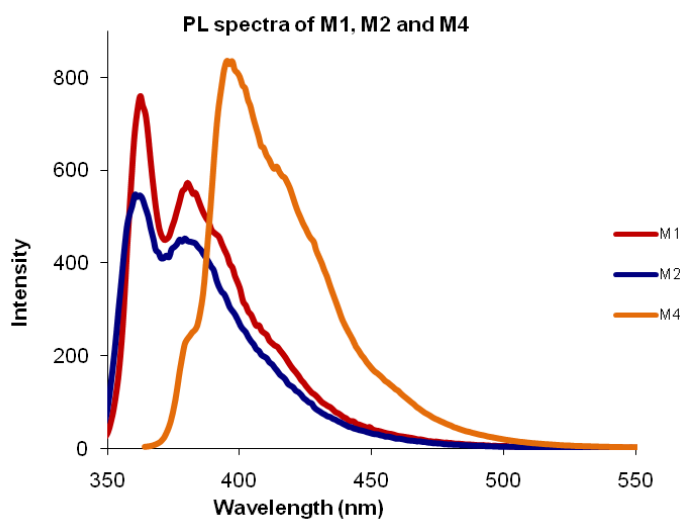


Figure 6.15 Absorption (A, 95 μM for **M1**, 66 μM for **M2** and 46 μM for **M4**) and emission spectra (B, 95 μM for **M1**, 66 μM for **M2** and 46 μM for **M4**,) of **M1**, **M2** and **M4**. All spectra were collected in THF.

Further support for this explanation comes from model **CP1a**, a model for **OC1** lacking the upper chromophore. Because **CP1a** lacks the upper chromophore, it is less constrained than **OC1**, but still more constrained than **M4**. Predictably, the λ_{max} for **CP1a** lies between values for **M4** and **OC1**. Both the **OCs** have the same upper chromophore, which we attempted to model with **M1**. **M1** has $\lambda_{\text{max}} = 335$ nm, the same value as observed in the **OCs** (**Figure 6.15**).

In contrast to the absorption spectra, significant differences should be manifest in the photoluminescence properties of **OC1** and **OC2**. Systems in which face-to-face inter- π -system interactions are operative (i.e., **OC1**) are predisposed to intramolecular energy / electron transfer (internal quenching rather than fluorescence) and may be expected to have low photoluminescence quantum yields (Φ). Systems in which π -systems are orthogonal (i.e., **OC2**), however, are not expected to undergo intermolecular energy / electron transfer processes, and should display higher Φ values.

The remarkably different Φ values for **OC2** (0.52) and **OC1** (0.012) unequivocally demonstrates the influence of the scaffolds on the fate of absorbed energy. DFT calculations suggest that the HOMO and LUMO are geometrically separate in **OC1**, reminiscent of cruciforms. These data suggest that internal energy transfer or internal self-quenching of fluorescence may be possible in **OC1**. Even the presence of the unmodified aryl in **CP1a** ($\Phi = 0.007$) is apparently sufficient for nonradiative quenching via intramolecular interaction, suggesting a vibrational relaxation mechanism is also viable. The exceedingly low quantum yield of **OC1** is particularly noteworthy when

compared to *any* of the models **M2** and **M4** and **M1** and **M3**, all of which have high quantum yields (0.40 - 0.58), similar to **OC2**.

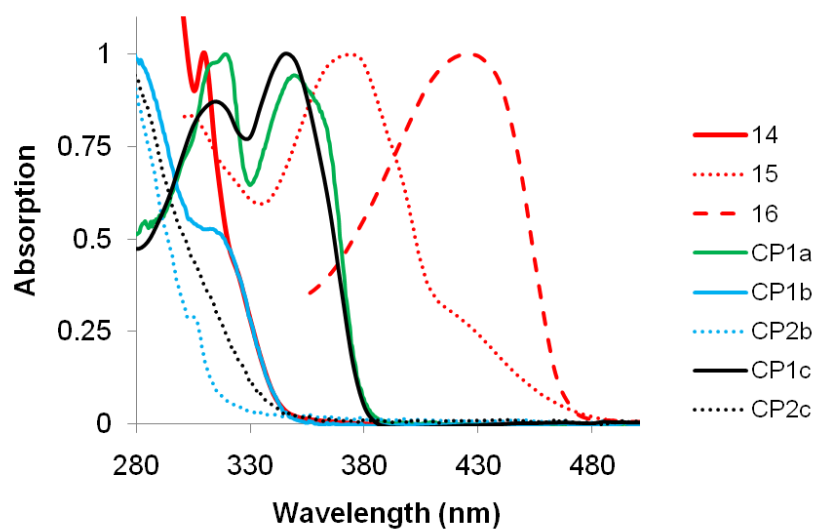
The successful study of chromophore appended on tetrahalogenated oxacyclophanes **6** and **7**, embarked the study of other possible variations on oxacyclophanes such as compound **13**, **CP1** and **CP2**. Also various chromophore attached on these oxacyclophanes were synthesized to study their optical properties. These oxacyclophanes provides appropriate geometric orientation which facilitate inter- π system interaction and the electronic perturbation atom around the chromophores due to the presence of electron donating atom *O* together has remarkable effect on their photophysical properties. Photophysical properties of the divided π -way monomer **14** and polymer **15** having a break in conjugation due to the oxacyclophane insertion (**Table 6.8**) were examined and compared with fully conjugated canopied polymer **16** (**Scheme 6.3**). Also photophysical properties of **CP1a**, **CP2a**, **CP1b**, **CP2b**, **CP1c** and **CP2c** (**Scheme 6.5**) having different chromophores appended on **CP1** and **CP2** were studied and select data is reported in **Table 6.8**.

Table 6.8 Photophysical data for oxacyclophane π -conjugated materials **14**, **15**, **CP1a**, **CP2a**, **CP1b**, **CP2b**, **CP1c** and **CP2c**.

	$\lambda_{\pi-\pi^*}$ (nm)	$\log \epsilon$	λ_{emit} (nm)	Φ
14	310	4.80	390	0.0070
15	374	4.27	407	0.57
16	427	4.60	462	0.57
CP1a	349	4.80	392	0.45
CP2a	N/A	N/A	N/A	N/A
CP1b	279	4.60	377	0.0050
CP2b	275	4.70	310	0.057
CP1c	345	4.44	403	0.28
CP2c	275	4.40	389	0.042

Compound **14** (**Figure 6.16**), a divided π -way monomer having *t*-butylphenylacetylene chromophore attached to each deck exhibits a π - π^* transition with λ_{max} at 310 nm. When this divided π -way core was incorporated into a polymer **15**, a red shift in absorption spectrum was observed with λ_{max} at 374 nm due to the increase in effective conjugation length. In comparison to fully conjugated canopied polymer **16**³² ($\lambda_{\text{max}} = 427$ nm), polymer **15** shows a blue shift which might be due the insertion of oxacyclophane into the polymeric backbone which leads to the break in the effective conjugation. Similar trend was observed in the photoluminescence profile of compound **14**, **15** and **16**.

(A)



(B)

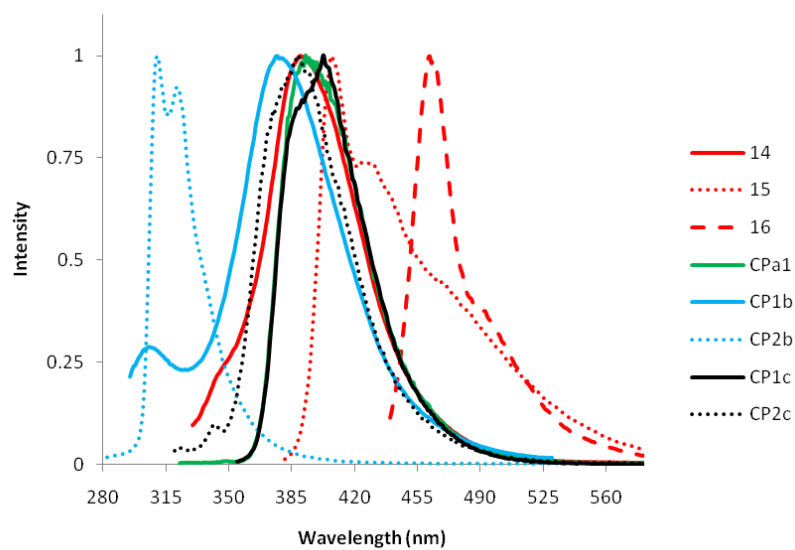


Figure 6.16 Normalized Absorption (A) and emission spectra (B) of **14**, **15**, **16**, **CP1a**, **CP1b**, **CP2b**, **CP1c** and **CP2c** in THF.

Monomer **14** has maximum emission (λ_{em}) at 390 nm and as expected polymer **15** observed a red shift with maximum emission (λ_{max}) at 407 nm whereas fully conjugated polymer **16** shows even more red shift in its photoluminescence spectrum with maximum emission (λ_{max}) at 462 nm. Furthermore quantum yield (Φ) **14** (0.007) is lowest in comparison to the polymers **15** (0.57) and **16** (0.57) which is also due the polymerization.

CP1a, were two *t*-butylphenylacetylene chromophores were tethered to the lower deck of **CP1** exhibits a π - π^* transition band with λ_{max} at 349 nm and maximum emission (λ_{em}) at 392 nm with decent quantum yield (0.45). Unfortunately, purification of **CP2b** was unsuccessful despite of repeated trial due to the similar retention factor R_f of compound and impurity on TLC chromatogram made impossible to study the effect of electronic perturbation around the chromophores on their optical properties.

Furthermore **CP1b**, were chromophores attached to the lower deck is 4-methoxy phenyl has maximum absorption (λ_{max}) at 279 nm and emission (λ_{em}) at 377 nm. In comparison to **CP1b**, **CP2b** exhibits a blue shift both in its absorption and photoluminescence profile with maximum absorption (λ_{max}) at 275 nm and emission (λ_{em}) at 310 nm. In **CP2b**, lone pair of O atom is next to the upper deck and separated by methylene group from the chromophore which make impossible for it to resonate with the π -system attributes this blue shift. Since **CP1b** and **CP2b** has short effective conjugation length which leads to the low quantum yield values, 0.005 and 0.057 respectively.

In case of **CP1c** and **CP2c**, thiophene is the chromophores appended on the lower deck of **CP1** and **CP2**. **CP1c** exhibits a π - π^* transition band with λ_{max} at 345 nm and

maximum emission (λ_{em}) at 403 nm with quantum yield (0.28). Since O is next to upper deck in **CP2c** which makes the π -system less electron rich leads to a blue shift both in its absorption and photoluminescence profile with maximum absorption (λ_{max}) at 275 nm and emission (λ_{em}) at 389 nm with diminished quantum yield (0.42).

In continuation to our oxacyclophanes work, the tetrahalogenated oxacyclophanes cores (**6** and **7**) were introduced into a polymeric backbone using 1,4-bis(hexyloxy)-2,5-diiodobenzene **21**, 1,4-diethynyl-2,5-bis(hexyloxy)benzene **22** as monomer units yielding cross linked **CLa** and **CLb** series polymers. Compound **6** and **7** has sites on both upper and lower deck to grow chain which also act as a cross linking agent. Also linear model polymers were synthesized, keeping the chemical composition similar to the above case. Photophysical properties of the all the cross linked and their linear model polymers were examined for both solution and film (**Figure 6.17** and **6.18**) and select photophysical data is reported in **Table 6.9**.

Table 6.9 Select photophysical data for cross linked and model polymers for solution and film.

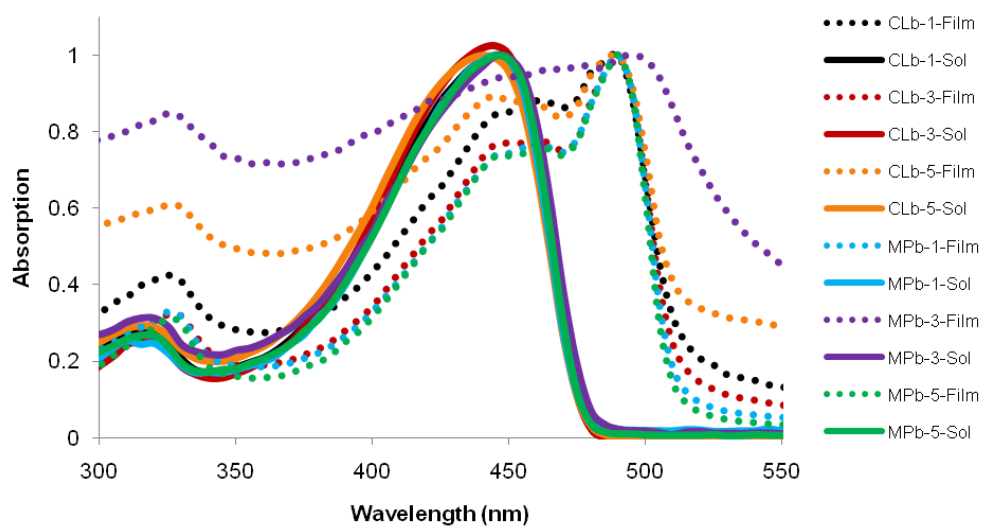
	Solution				Film		GPC		
	λ_{abs} (nm)	$\log \epsilon$	λ_{emit} (nm)	Φ	λ_{abs} (nm)	λ_{emit} (nm)	M_n	M_w	PDI
CLa1	440	4.28	473	0.31	490	568	15339	40340	2.6
CLa3	440	3.79	473	0.51	490	542	29720	78614	2.6
CLa5	445	4.47	473	0.52	485	583	52081	166295	3.1
CLb1	445	4.73	474	0.49	490	588			
CLb3	445	4.81	474	0.52	490	566			
CLb5	440	4.19	473	0.58	490	542			
MPa1	445	4.80	474	0.49	495	566	48822	144580	2.9
MPa3	445	4.77	473	0.63	490	571	61565	182033	2.9
MPa5	450	4.80	473	0.71	475	572	94526	225022	2.3
MPb1	445	4.97	473	0.51	490	547	69820	213371	3.0
MPb3	445	4.78	473	0.54	495	567	107008	262697	2.4
MPb5	445	4.82	474	0.62	490	547	37880	114414	3.0

Compound **CLa1**, **CLa3**, **CLa5**, **MPa1**, **MPa3** and **MPa5** have very similar absorption profile for both solution and film (**Figure 6.17 A**) with λ_{max} for π - π^* transition band at around 440 nm and 490 nm respectively with few exceptions. Similar absorption band is because of the same repeating monomer units used for polymerization which also leads to the conclusion that small amount of cross linking agent or their analogues has no effect on the their effective conjugation length. Also a red shift (~ 50

nm) was observed in the absorption profile for films than solution in all cases as due to the planarity attained by the film.

Similarly compounds discussed above have almost similar emission profile; for both solution and film (**Figure 6.17 B**) with λ_{em} at around 473 nm and 570 nm respectively (**Table 6.9**). Here also a red shift (~ 90 nm) was observed in the emission for films than solution due to the planarity attained by the film.

(A)



(B)

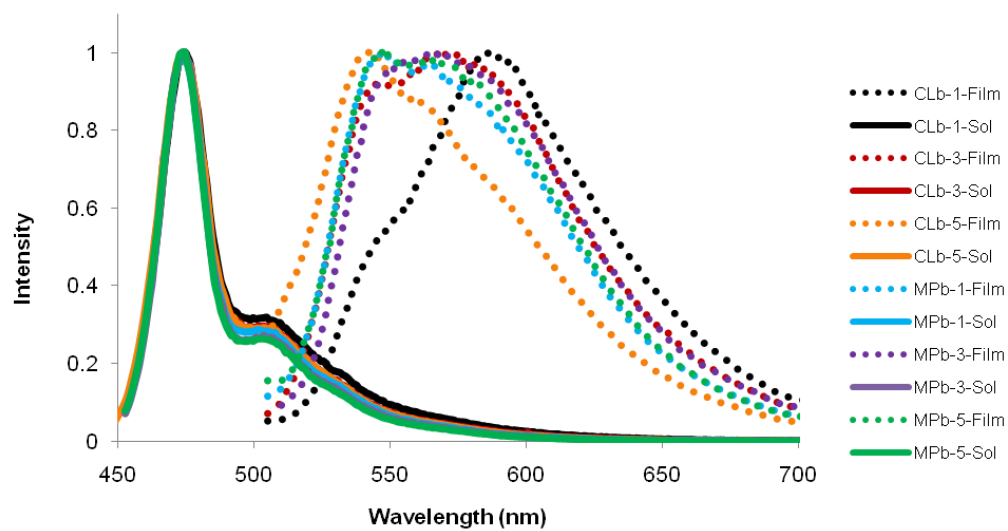
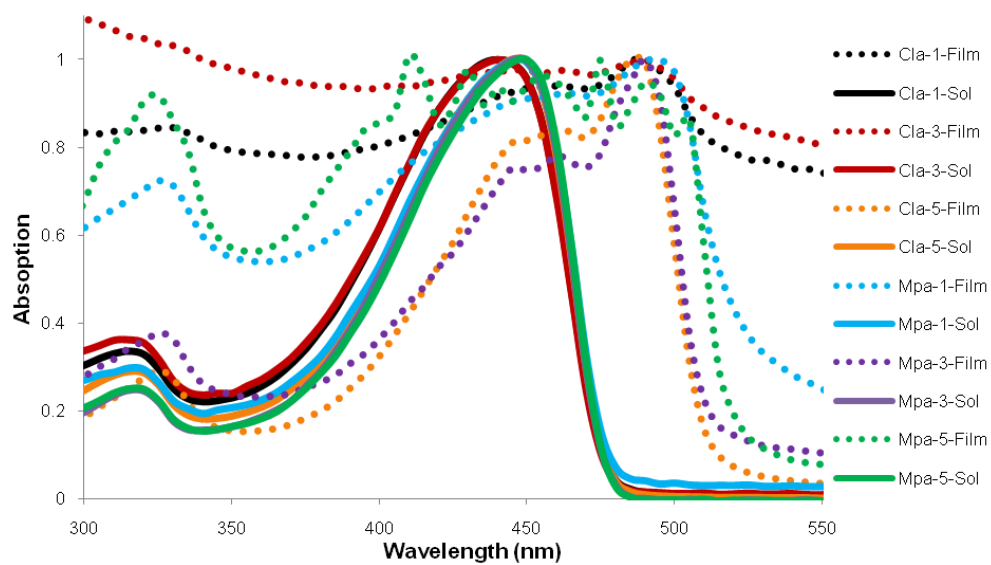


Figure 6.17 Normalized Absorption (A) and emission spectra (B) of **CLa1**, **CLa3**, **CLa5**, **MPa1**, **MPa3** and **MPa5** in THF.

Also in case of 1,2-cross linked and model polymers; we observed very similar photophysical data as compared to 1,4-series. Compounds **CLb1**, **CLb3**, **CLb5**, **MPb1**, **MPb3** and **MPb5** have very similar absorption profile for both solution and film (**Figure 6.18 A**) with λ_{max} for $\pi-\pi^*$ transition band at around 445 nm and 490 nm respectively with few exceptions. A red shift (~ 45 nm) was observed in the absorption profile for films than solution in all cases as due to the planarity attained by the film.

Similarly 1,2-cross linked and model polymers have almost similar emission profile; for both solution and film (**Figure 6.18 B**) with λ_{em} at around 474 nm and 560 nm respectively (**Table 6.9**).

(A)



(B)

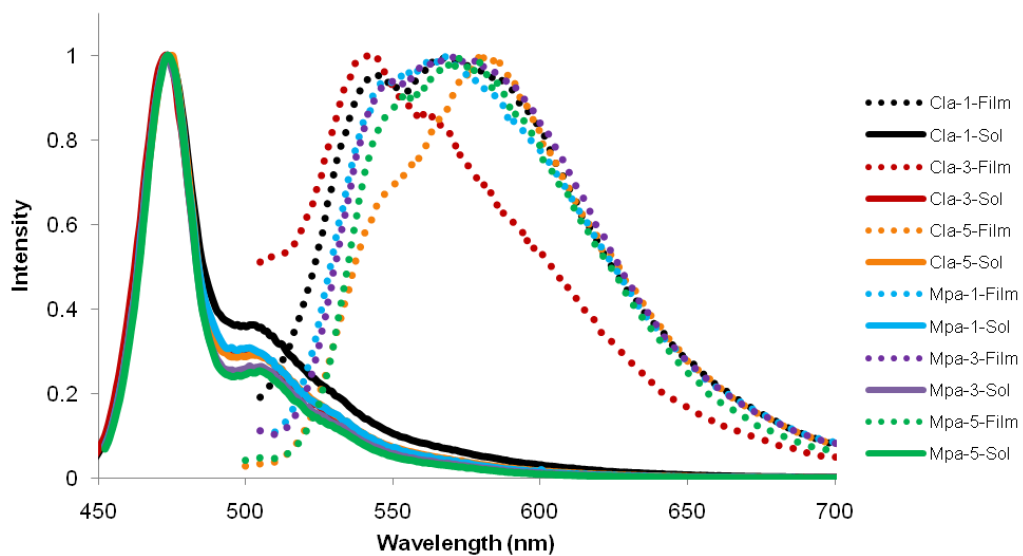


Figure 6.18 Normalized Absorption (A) and emission spectra (B) of **CLb1**, **CLb3**, **CLb5**, **MPb1**, **MPb3** and **MPb5** in THF.

6.4 Conclusion

In summary, synthetic routes have been developed to produce synthetically versatile tetrahalogenated *m*-terphenyl oxacyclophanes and to derivatize these scaffolds with up to four π -conjugated substituents. Also various other oxacyclophanes like 2-way- π -way core and **CP1** and **CP2** were synthesized and derivatized with various chromophores to study the effect of geometrical orientation and difference of electronic distribution around chromophores on their photophysical properties. The utility of the oxacyclophanes to scaffold π -conjugated systems in discrete geometries should have utility in the rational design of materials exhibiting energy / charge transfer or high photoluminescence. The simple attachment strategy and modularity of upper and lower components leads to facile elaboration of these materials to include additional and mixed chromophore systems and semiconducting π -conjugated polymers. Studies are underway to gain further insights into other inter- π -system influences that may be accessible with these scaffolds.

6.5 Experimental Section

Reagents and General Methods

All the reactions were performed under inert nitrogen atmosphere unless otherwise specified. Toluene was dried by passage through alumina columns under N₂. All other solvents and reagents were obtained from commercial sources and used without purification. Sonogashira, Suzuki and Stille reaction were carried out in MBraun dry box and synthesis of oxacyclophane using standard Schlenk techniques under an atmosphere of N₂. Compounds **1** and **8**,⁴¹ **11**,⁴² **17**, **18** and **CP1**,³² **19**,⁴³ **20**,⁴⁴ 1,4-bis(hexyloxy)-2,5-diiodobenzene **21**,⁴⁵ 1,4-diethynyl-2,5-bis(hexyloxy)benzene **22**,⁴⁶ 1,4-diiodo-2,3-dimethoxybenzene **23**,⁴⁷ 1,2-dihydroxy-3,6-diiodobenzene,⁴⁷ **12**, 1,4-diiodo-2,5-dimethoxybenzene **24**, and 1,4-dihydroxy-2,5-diiodobenzene,⁴⁸ 1,4-bis(2-(4-*t*-butylphenyl)ethynyl)-2,5-dimethoxybenzene (**M4**) and 1,4-bis(2-(4-*t*-butylphenyl)ethynyl)-2,3-dimethoxybenzene (**M2**)⁴⁹ were synthesized by adaptation / modification of the reported methods.

NMR spectra were acquired on a Bruker ARX spectrometer operating at 500 MHz for proton and 125 MHz for carbon-13 NMR, or on a Bruker Avance spectrometer operating at 300 MHz for proton and 75 MHz for carbon-13 NMR. Chemical shift are reported in ppm and referenced to tetramethylsilane or residual solvent signal. Glass backed sorbtech silica gel preparative TLC plates were used for preparative TLC purification, were pore diameter of the gel was 60Å. Gel was mixed with fluorescent indicator (UV254) of 500 µm thickness.

General Spectroscopic Methods

Absorption spectra were collected using a Varian Cary-50 Bio spectrophotometer and photoluminescence (PL) data were recorded using a Varian Eclipse spectrofluorimeter in Teflon-stopper-sealed Spectrosil cuvettes with a path length of 1 cm in dry, N₂-degassed THF. Quantum yields (Φ) were calculated relative to quinine bisulfate solution in 1 M H₂SO₄ (aq) ($\Phi = 0.546$).⁵⁰

Synthesis of 2

To a solution of **1** (6.35 g, 13.7 mmol) in 100 mL CHCl₃, *N*-bromosuccinimide (6.10 g, 34.2 mmol) and benzoyl peroxide (0.033 g, 0.01 mol) were added. The solution was heated to reflux under nitrogen for 5 d. The succinimide was removed by filtration and the filtrate was washed with water (3 × 100 mL). The filtrate was placed in a flask and product formed after approximately 1 h. 50 mL of acetonitrile was added to the flask and the product was filtered. To a solution of the product and 100 mL of benzene, another portion of *N*-bromosuccinimide (6.10 g, 34.2 mmol) and benzoyl peroxide (0.0330 g, 0.0100 mol) were added. After another 5 d of reflux under nitrogen, and additional amount of *N*-bromosuccinimide (12.2 g, 5.00 mol) and benzoyl peroxide (0.0330 g, 0.0100 mol) were added. The solution was heated to reflux under nitrogen for 2 d. The product was filtered and 10 mL of acetonitrile were added. The solid product that was filtered still exhibited a brown color indicative of bromine. The product was dissolved in 50 mL of dichloromethane and washed with aqueous Na₂SO₃ (50 mL of H₂O and 2 g Na₂SO₃) three times. The dichloromethane was evaporated, and the product was recrystallized in hexane to yield 2.78 g (26.0%) of **2** as a solid. For preparation of **3** or **5**,

we found that it was not necessary for compound **2** to be further purified, as mixed monobrominated (CH_2Br) and dibrominated (CHBr_2) sites are all smoothly converted to **3** or **5** in the subsequent steps. The NMR spectra for the material used in the next steps are shown in **appendix 6.A**, and indicate that the materials is >95% pure. (Chemical shifts of two isomers are reported without further assigning to syn- or anti-) ^1H NMR (CDCl_3 , 300 MHz): $\delta = 6.35$ (s, 1.2H), 6.42 (s, 0.8H), 7.08 - 7.11 (d, 0.8H, $J = 6$ Hz), 7.14 - 7.17 (d, 1.2H, $J = 6$ Hz) 7.43 - 7.48 (m, 2H), 7.53 (s, 2H), 7.56 - 7.62 (m, 2H), 8.10 - 8.13 (d, 2H, $J = 9$ Hz). ^{13}C NMR (CDCl_3 , 125 MHz): $\delta = 38.2, 38.3, 103.3, 104.2, 122.5, 129.2, 129.4, 129.6, 129.7, 129.9, 130.0, 131.8, 132.0, 139.0, 139.2, 146.8, 146.7, 146.8$.

Synthesis of 3

To a solution of **2** (2.00 g, 2.60 mmol) in a solution of THF (10 mL) and EtOH (absolute, 50 mmol), NaOAc (1.40 g, 6.60 mmol) and AgNO_3 (1.70 g, 15.0 mmol) was stirred at room temperature. The mixture rapidly forms a white precipitant. The solution was heated to reflux for 16 h and brought to room temperature. The solvent was evaporated after the removal of the solid by filtration. The resulting solid was dissolved in chloroform (30 mL) and 10 % hydrochloric acid (1 mL) was added. The reaction mixture stirred at room temperature for 18 h and was then washed with water (3×100 mL). The solvent was removed and enough diethyl ether was placed in flask to dissolve the product. The diethyl ether solution was pipetted into pentane, and the precipitate formed was filtered and dried. The product was recrystallized in hexane to yield 0.870 g (68.1%) of **3** as a solid. (Chemical shifts of two isomers are reported without further

assigning to syn- or anti-) ^1H NMR (CDCl_3 , 300 MHz): $\delta = 7.31 - 7.36$ (m, 3H), 7.51 - 7.73 (m, 5H), 8.04 - 8.06 (m, 2H), 9.90 (s, 1H), 9.93 (s, 1H). ^{13}C NMR (CDCl_3 , 125 MHz): $\delta = 104.1, 104.3, 122.3, 122.4, 128.3, 128.9, 129.1, 129.2, 130.4, 130.7, 132.0, 132.2, 133.2, 133.4, 133.8, 134.0, 146.0, 146.1, 146.2, 146.4, 190.7, 190.8$. HRMS calcd for $\text{C}_{20}\text{H}_{13}\text{BrIO}_2$ ($\text{M}+\text{H}$) $^+$: 490.9144, found: 489.9141.

Synthesis of 4

In the dry box, a solution of **3** (0.306 g, 0.623 mmol), methanol (2 mL), and THF (1.5 mL) was added drop by drop to NaBH_4 (0.470 g, 1.25 mmol) in THF (5 mL). The reaction mixture stirred 5 d in the dry box until a dark yellow solid had formed and the mixture was no longer able to stir. THF (3 mL) was added to solution and 15% hydrochloric acid (1 mL) was slowly added. The reaction mixture stirred for 1 h and the solvent was removed. Diethyl ether (20 mL) was added and washed with water (3×10 mL). The solvent was removed and the product was recrystallized in pentane to yield 0.298 g (96.5 %) of **4** as a white solid. A small amount (ca. 5%) of aldehyde **3** remained in the sample, as determined from aldehydic peak at ca. 9.9 ppm. This sample was used without further purification in the next step; however, note that this synthetic avenue was abandoned in favor of the more efficient route shown in **Scheme 6.1**. The material can be obtained in pure crystalline form by diffusion of pentane into a CH_2Cl_2 solution of **4**. For NMR data, chemical shifts of two isomers are reported without further assigning to syn- or anti-) ^1H NMR (CDCl_3 , 300 MHz): $\delta = 1.71$ (s, 2H), 4.26 - 4.66 (q, 4H, $J_1 = 12.5$ Hz, $J_2 = 47.0$ Hz), 7.16 - 7.19 (m, 2H), 7.38 - 7.43 (m, 4H), 7.47 - 7.51 (m, 2H), 7.58 - 7.63 (m, 2H). ^{13}C NMR (CDCl_3 , 125 MHz): $\delta = 63.1, 63.2, 104.4, 104.9, 122.1, 127.6, 127.7,$

127.8, 127.9, 128.8, 128.9, 129.2, 129.48 131.2, 131.4, 137.9, 137.9, 142.6 142.7, 148.1, 148.2.

Synthesis of 5 from 4

To a solution of **4** (0.298 g, 0.601 mmol), benzene (2 mL), and one drop of pyridine, slowly add solution of PBr₃ (0.0729 g, 0.270 mmol) and benzene (3 mL). Solution was stirred for 16 h and then reaction mixture was extracted three times with water (30 mL). All the volatile were removed under reduced pressure. Recrystallization from ethanol gave 0.164 g (43.0%) of **5** as an off-white solid.

Synthesis of 5 from 2

Solution of compound **2** (10.1 g, 15.6 mmol) in 50 mL of anhydrous THF was cooled to 0 °C in ice bath and stirred under nitrogen atmosphere. Diethyl phosphite (51.7 g, 374 mmol) was then added dropwise, followed by the addition of ethyldiisopropylamine (48.4 g, 374 mmol). After the reaction mixture was stirred at room temperature for 20 h, it was poured into 150 mL of water and extracted with diethyl ether (4 × 50 mL). The organic layer was washed with 100 mL of 1 M HCl followed by 100 mL of saturated aqueous sodium chloride solution. The organic layers were then collected, dried over Na₂SO₄ and all volatiles were removed under reduced pressure. Residue was washed with ethanol, yielding 5.41 g of **5** as an off white solid (55.0%). (Chemical shifts of two isomers are reported without further assigning to syn- or anti-) ¹H NMR (CDCl₃, 300 MHz): δ = 4.19 – 4.47 (m, 4H), 7.19 – 7.21 (m, 2H), 7.39 – 7.66 (m, 8H). ¹³C NMR (CDCl₃, 125 MHz): δ = 31.2, 31.3, 104.3, 104.7, 121.9, 122.0, 128.5,

128.6, 129.1, 129.2, 130.1, 130.2, 130.5, 130.6, 131.8, 131.9, 134.9, 135.0, 143.6, 143.7, 147.3, 147.3. HRMS calcd for C₂₀H₁₅Br₃I (M+H)⁺: 617.7690, found: 617.7687.

Synthesis of 1,2-dimethoxy-3,6-trimethylsilanebenzene

Veratrol was degassed and taken into dry box along pressure flask. In flask, veratrol (4.0 g, 29.0 mmol) was dissolved in 10 mL of hexane and 4 mL of tetramethylethylenediamine followed by the addition of *n*-BuLi (12.8 mL, 32.0 mmol) dropwise at room temperature. Reaction mixture was stirred for 28 hr followed by cooling it at -78 °C and chlorotrimethylsilane (4.5 mL, 35.6 mmol) was added dropwise into it. Reaction mixture was stirred for 5 h at room temperature. 100 mL of water was added into the reaction mixture and extracted with hexane (3 × 50 mL). Organic layer was collected, dried over Na₂SO₄ and removed under reduced pressure, yielding colorless oil (5.3 g, 86%). ¹H NMR (300 MHz, CDCl₃): δ = 0.32 (s, 9H, 3 × CH₃), 3.90 (s, 6H, 2 × O-CH₃), 6.99 (m, 2H, Aromatic), 7.09 (d, 1H; *J* = 9 Hz, Aromatic). ¹³C NMR (75.4 MHz, CDCl₃): δ = -0.3, 55.5, 60.5, 113.9, 120.8, 123.9, 126.2, 133.2, 151.8, 153.7.

Synthesis of 1,2-dimethoxy-3,6-ditrimethylsilanebenzene

1,2-dimethoxy-3-trimethylsilane benzene was degassed and taken into dry box along pressure flask. In flask, 1,2-dimethoxy-3-trimethylsilanebenzene (5.3 g, 25.2 mmol) was dissolved in 5 mL of tetramethylethylenediamine followed by the addition of *n*-BuLi (12.1 mL, 30.3 mmol) dropwise at room temperature. Reaction mixture was stirred for 25 h followed by cooling it at -78 °C and chlorotrimethylsilane (4.6 mL, 36.3 mmol) was added dropwise into it. Reaction mixture was stirred for 5 h at room

temperature. 100 mL of water was added into the reaction mixture and extracted with hexane (3 × 50 mL). Organic layer was collected, dried over Na₂SO₄ and removed under reduced pressure, yielding colorless oil (6.3 g, 89%). ¹H NMR (300 MHz, CDCl₃): δ = 0.32 (s, 18H, 6 × CH₃), 3.86 (s, 6H, 2 × O-CH₃), 7.14 (s, 2H, Aromatic). ¹³C NMR (75.4 MHz, CDCl₃): δ = -0.4, 59.5, 129.4, 135.9, 156.7.

Synthesis of 1,4-diiodo-2,3-dimethoxy benzene

1,2-dimethoxy-3,6-ditrimethylsilanebenzene (6.5 g, 23.0 mmol) was dissolved in 30 mL of DCM and solution was cooled to 0 °C. ICl (10.0 g, 60.0 mmol) was dissolved in 30 mL of DCM and added to the reaction mixture dropwise. Reaction mixture was allowed to stir for 45 min at room temperature and quenched by adding saturated solution of Na₂S₂O₃ (100 mL). Organic layer was collected, dried over Na₂SO₄ and removed under reduced pressure, yielding white solid (6.4 g, 76%). ¹H NMR (300 MHz, CDCl₃): δ = 3.89 (s, 6H, 2 × O-CH₃), 7.26 (s, 2H, Aromatic). ¹³C NMR (75.4 MHz, CDCl₃): δ = 60.6, 92.8, 135.4, 153.1.

Synthesis of 1,2-dihydroxy-3,6-diiodobenzene

1,4-diiodo-2,3-dimethoxy benzene (2.0 g, 5.1 mmol) was dissolved in 20 mL of DCM and solution was cooled to -78 °C. BBr₃ (30.8 mL, 30.8 mmol) was added into this solution dropwise and reaction was stirred for 14 h at room temperature. Reaction mixture was washed with water (3 × 50 mL) and organic layer was collected, dried over Na₂SO₄ and removed under reduced pressure. Crude residue was dissolved in minimum amount of DCM and 30 mL pentane was added into it, left for crystallization, yielding

white solid (0.90 g, 50%). ^1H NMR (300 MHz, CDCl_3): $\delta = 5.67$ (s, 2H, OH), 7.02 (s, 2H, Aromatic).

Synthesis of 2,5-Dimethoxy-1,4-diiodobenzene

In a flask, ICl (11.66 g, 71.80 mmol) was dissolved in 30 mL of methanol and cooled to 0 °C. 1,4-dimethoxy benzene (2.33 g, 179.6 mmol) was added into it and reaction mixture was refluxed for 4 h. Reaction mixture was cooled to room temperature and solid precipitate was filtered followed by washing by methanol (3 \times 20 mL), yielding white solid (6.71 g, 95.9%). ^1H NMR (300 MHz, CDCl_3): $\delta = 3.85$ (s, 6H, 2 \times O-CH₃), 7.22 (s, 2H, Aromatic).

Synthesis of 2,5-Diiodohydroquinone

2,5-Dimethoxy-1,4-diiodobenzene (5.00 g, 12.8 mmol) was dissolved in 50 mL of dichloromethane and cooled to -78 °C in acetone/dryice bath. 1 M borontribromide solution (38.4 mL, 38.4 mmol) was added dropwise through syringe. The reaction mixture was held at -78 °C for 30 min and then allowed to warm to room temperature overnight. Reaction mixture was added to ice cold H₂O white solid crashed out was filtered and collected. (2.6 g, 56%). ^1H NMR (300 MHz CDCl_3): $\delta = 7.15$ (s, 2 H), 9.82 (s, 2 H).

Synthesis of 6

In a 2 neck flask, under N₂, K₂CO₃ (2.20 g, 15.9 mmol) and DMF (60 mL) was stirred at 90 °C for 15 min. In a separate vial, **5** (346 mg, 0.560 mmol) and 1,4-dihydroxy-2,5-diiodobenzene (0.20 g, 0.55 mmol) was dissolved in DMF (10 mL). This solution was added into preheated flask dropwise via syringe pump for 4 days and

reaction mixture was stirred for next 3 days. DMF was removed under reduced pressure and residue was dissolved in minimum amount of CH₂Cl₂ and solution was filtered through silica. Silica was washed with CH₂Cl₂ (20 mL). CH₂Cl₂ was collected and removed under reduced pressure. Compound was further purified by prep TLC (95:5 hexane: ethylacetate), yielding white solid. (60 mg, 13%). ¹H NMR (300 MHz, CDCl₃): δ = 4.90 (d, 1H; *J* = 12 Hz, O-CH₂), 5.09 (d, 1H; *J* = 12 Hz, O-CH₂), 5.50 (d, 1H; *J* = 12 Hz, O-CH₂), 5.92 (d, 1H; *J* = 12 Hz, O-CH₂), 6.89 (s, 1H, Aromatic), 7.10 (s, 1H, Aromatic), 7.28 (b, 2H, Aromatic), 7.50 - 7.33 (m, 6H, Aromatic), 7.64 (m, 2H, Aromatic). ¹³C NMR (75 MHz, CDCl₃): δ = 71.3, 73.5, 87.3, 91.1, 108.6, 121.6, 128.1, 128.3, 128.8, 128.9, 129.0, 130.2, 130.7, 131.0, 132.9, 133.1, 133.2, 133.4, 133.5, 143.6, 147.6, 147.9, 152.4, 154.7. Elemental analysis calculated for C₂₆H₁₆OBr₃O₂: C, 38.04; H, 1.96. Found: C, 38.15; H, 1.84.

Synthesis of 7

In a 2 neck flask, under N₂, K₂CO₃ (2.20 g, 15.9 mmol) and DMF (60 mL) was stirred at 90 °C for 15 min. In a separate vial, **5** (346 mg, 0.560 mmol) and 1,2-dihydroxy-3,6-diiodobenzene (0.20 g, 0.56 mmol) was dissolved in DMF (10 mL). This solution was added into preheated flask dropwise via syringe pump for 4 days and reaction mixture was stirred for next 3 days. DMF was removed under reduced pressure and residue was dissolved in minimum amount of CH₂Cl₂ and solution was filtered through silica. Silica was washed with CH₂Cl₂ (20 mL). CH₂Cl₂ was collected and removed under reduced pressure. Compound was further purified by prep TLC (95:5 hexane: ethylacetate), yielding white solid. (50 mg, 10%). ¹H NMR (500 MHz, CDCl₃): δ

= 4.27 (d, 2H; $J = 10$ Hz, O-CH₂), 5.33 (d, 2H; $J = 10$ Hz, O-CH₂), 7.32 (s, 2H, Aromatic), 7.39 (s, 2H, Aromatic), 7.45 (dd, 2H; $J_1 = 9$ Hz, $J_2 = 2$ Hz, Aromatic), 7.55 – 7.49 (m, 4H, Aromatic), 7.72 (dd, 2H; $J_1 = 9$ Hz, $J_2 = 2$ Hz, Aromatic). ¹³C NMR (125 MHz, CDCl₃): $\delta = 75.9, 94.4, 102.4, 121.4, 128.5, 128.8, 129.0, 130.8, 130.9, 134.5, 136.6, 144.3, 148.3, 153.0$. HRMS calcd for C₂₆H₁₆BrI₃NaO₂ (M+Na)⁺: 842.7384, found: 842.7366.

Synthesis of OCI

In a pressure flask, **6** (20.0 mg, 0.024 mmol) was dissolved in 20 mL of toluene. Tetrakis(triphenylphosphine)palladium(0) (0.005 g, 0.004 mmol) and ~2 mg of copper iodide was added into the solution. In another vial, 4-*t*-butylphenylacetylene (60 mg, 0.38 mmol) was dissolved in diisopropyl amine (10 mL). This solution was added into the pressure flask drop wise. Pressure flask was capped and taken out from the dry box. Reaction mixture was stirred at room temperature for 3 h and then stirred for 48 h at 90 °C. 20 mL of CH₂Cl₂ was added to the reaction mixture and passed through silica. Silica was washed with CH₂Cl₂ (10 mL) and organic layer was extracted with sat. sodium bicarbonate solution (4 × 50 mL). Organic layer was collected and dried over sodium sulfate, volatiles were removed under reduced pressure. Preparative TLC (pentane) was done for purification, yielding white solid (12 mg, 50%). ¹H NMR (300 MHz, CDCl₃): $\delta = 1.36 - 1.34$ (m, 36H, 12 × CH₃), 5.72 (d, 2H; $J = 3$ Hz, O-CH₂), 5.96 (d, 2H; $J = 3$ Hz, O-CH₂), 7.44 – 7.35 (m, 13H, Aromatic), 7.50 – 7.47 (m, 10H, Aromatic), 7.68 (m, 4H, Aromatic). ¹³C NMR (75 MHz, CDCl₃): $\delta = 34.1, 34.6, 34.8, 34.9, 73.4, 81.5, 88.1, 90.7, 118.9, 119.5, 120.1, 120.2, 125.3, 125.3, 125.4, 125.8, 128.0, 128.3, 130.5, 131.3, 131.4,$

131.6, 132.2, 134.6, 151.4, 151.5, 151.6, 152.5. HRMS calcd for C₇₄H₆₉O₂ (M+H)⁺: 989.5298, found: 989.5292.

Synthesis of OC2

Compound **7** were degassed and taken into dry box along with pressure flask. In pressure flask, compound **7** (20.0 mg, 0.024 mmol) was dissolved in 20 mL of toluene. Tetrakis(triphenylphosphine) palladium(0) (0.005 g, 0.004 mmol) and ~2 mg of copper iodide was added into the solution. In another vial, 4-*t*-butylphenylacetylene (60 mg, 0.38 mmol) was dissolved in diisopropyl amine (10 mL). This solution was added into the pressure flask drop wise. Pressure flask was capped and taken out from the dry box. Reaction mixture was stirred at room temperature for 3 h and then stirred for 48 h at 90 °C. 20 mL of CH₂Cl₂ was added to the reaction mixture and passed through silica. Silica was washed with CH₂Cl₂ (10 mL) and organic layer was extracted with sat. sodium bicarbonate solution (4 × 50 mL). Organic layer was collected and dried over sodium sulfate, volatiles were removed under reduced pressure. Prep TLC (Pentane) was done for purification, yielding white solid (10 mg, 41%). ¹H NMR (300 MHz, CDCl₃): δ = 1.37 - 1.34 (m, 36H, 12 × CH₃), 5.73 (d, 2H; *J* = 3 Hz, O-CH₂), 5.96 (d, 2H; *J* = 3 Hz, O-CH₂), 7.42 – 7.37 (m, 20H, Aromatic), 7.44 (s, 2H, Aromatic), 7.51 – 7.47 (m, 16H, Aromatic), 7.71 (m, 4H, Aromatic). HRMS calcd for C₇₄H₆₉O₂ (M+H)⁺: 989.5298, found: 989.5294.

Synthesis of 1,4-bis(4-t-butylphenylethynyl)-2,6-bis(o-tolyl) benzene (MI)

Compound **1** was degassed and taken into dry box along with pressure flask. In pressure flask, compound **1** (0.95 g, 2.0 mmol) was dissolved in 5 mL of toluene. Tetrakis(triphenylphosphine) palladium(0) (0.047 mg, 0.041 mmol) and copper iodide

(0.0160 mg, 0.0818 mmol) was added into the solution. In another vial, *t*-butylphenylacetylene (1.3 g, 8.1 mmol) was dissolved in diisopropyl amine (5 mL). This solution was added into the pressure flask drop wise. Pressure flask was capped and taken out from the dry box. Reaction mixture was stirred for 48 h at 90 °C. Reaction mixture was passed through silica, followed by washing with 30 mL of ether. Organic layer was extracted with sat. sodium bicarbonate solution (4 × 100 mL). Organic layer was collected and dried over sodium sulfate, volatiles were removed under reduced pressure. Pure light yellow solid compound was obtained by using glass backed sorbtech silica gel preparative TLC plates, where pore diameter of the gel was 60 Å. The gel was mixed with a fluorescent indicator (UV254) of 500µm thickness. (R_f : 0.3, 10% ethylacetate:pentane). (0.30 g, 25%). ^1H NMR (300 MHz, CDCl_3): δ = 1.25 (s, 9H, 3 × CH_3), 1.35 (s, 9H, 3 × CH_3), 2.30 (s, 6H, 2 × CH_3), 6.70 (d, 2H; J = 6.0 Hz, Aromatic), 7.18 (d, 2H; J = 9.0 Hz, Aromatic), 7.35 (m, 12H, Aromatic), 7.50 (m, 4H, Aromatic). ^{13}C NMR (75 MHz, CDCl_3): δ = 20.0, 31.0, 31.1, 34.6, 34.8, 87.3, 88.6, 91.3, 97.0, 120.0, 120.2, 122.5, 125.0, 125.3, 125.4, 127.6, 129.6, 130.9, 131.0, 131.3, 136.4, 140.4, 144.4, 151.2, 151.7. HRMS (MALDI) calcd for $\text{C}_{44}\text{H}_{42}$ (M^+): 570.3287, found: 570.3134.

Synthesis of 1,4-bis(2-(4-tert-butylphenyl)ethynyl)-2,3-dimethoxybenzene (M2)

Under nitrogen, in pressure flask 1,4-diiodo-2,3-dimethoxy benzene (1.0 g, 2.6 mmol) was dissolved in 40 mL of toluene. Tetrakis(triphenylphosphine) palladium(0) (331.0 mg, 0.3 mmol) and copper iodide (60.0 mg, 0.3 mmol) was added into the solution. In separate vial, *t*-butyl phenyl acetylene (2.4 g, 15.4 mmol) was dissolved in triethylamine (20 mL) and added to the reaction mixture drop wise. Pressure flask was

capped and taken out from the dry box. Reaction mixture was stirred for 48 h at room temperature. Reaction mixture was passed through silica, followed by washing with 50 mL of DCM. Organic layer was extracted with sat. sodium bicarbonate solution (4 × 100 mL). Organic layer was collected and dried over sodium sulfate, volatiles were removed under reduced pressure. This crude material was washed with 20 mL of ether, yielding white solid. This white solid was filter and dried over vacuum (0.20 g, 18%). ¹H NMR (300 MHz, CDCl₃): δ = 1.35 (s, 18H, 6 × CH₃), 4.05 (s, 6H, 2 × O-CH₃), 7.21 (s, 2H, Aromatic), 7.42 (d, 4H; *J* = 8.4 Hz, Aromatic), 7.53 (d, 4H; *J* = 9 Hz, Aromatic).

Synthesis of 1,4-bis(2-(4-tert-butylphenyl)ethynyl)-2,5-dimethoxybenzene (M4)

M4 was synthesized following the protocol used for **M2**. ¹H NMR (300 MHz, CDCl₃): δ = 1.35 (s, 18H, 6 × CH₃), 3.92 (s, 6H, 2 × O-CH₃), 7.04 (s, 2H, Aromatic), 7.40 (d, 4H; *J* = 8.4 Hz, Aromatic), 7.54 (d, 4H; *J* = 8.4 Hz, Aromatic). ¹³C NMR (75.4 MHz, CDCl₃): δ = 31.1, 34.8, 56.5, 85.0, 95.1, 113.4, 115.7, 120.1, 125.3, 131.4, 151.6, 153.8.

Synthesis of 9

To a solution of **8** (13.2 g, 39.0 mmol) in 600 mL CHCl₃, *N*-bromosuccinimide (40.0 g, 226 mmol) and benzoyl peroxide (1.04 g, 4.00 mol) were added. The reaction mixture was refluxed overnight. After cooling to room temperature, the reaction mixture was washed with water (3 × 50 mL). The organic layer was collected and volatiles were removed under reduced pressure. The residue was washed with 20 mL of pentane yielding off white solid. (5.5 g, 28.7 %). ¹H NMR (500 MHz, CDCl₃): δ = 4.53 (s, 4H; 2 × CH₂), 7.33 – 7.31 (m, 2H; Aromatic), 7.44 – 7.38 (m, 4H; Aromatic), 7.49 (t, 1H; *J*_l =

1.5 Hz, $J_2 = 3.0$ Hz, Aromatic), 7.57 – 7.55 (m, 2H; Aromatic), 7.67 (d, 2H; $J = 1.5$ Hz, Aromatic).

Synthesis of 2-iodo-1,4-dimethoxy benzene (11)

In a round bottom flask, compound **10** (1.0 g, 7.3 mmol) was dissolved in 30 mL of H₂O and 5 mL of MeOH followed by the addition of KI (0.8 g, 4.8 mmol) and KIO₃ (0.52 g, 2.4 mmol). Aq. HCl solution (10%) was added dropwise to the reaction mixture over 45 min and continued to stirred over night. Saturated aq. sodium sulfite solution (50 mL) was added into the reaction mixture followed by DCM (50 mL) and extracted with H₂O (3 × 100 mL). Organic layer was collected, dried over anhydrous Na₂SO₄ and removed under reduced pressure. Residue was triturated with MeOH (20 mL), yielding colorless oil (1.1 g, 58%). ¹H NMR (300 MHz, CDCl₃): $\delta = 3.775$ (s, 3H; O-CH₃), 3.847 (s, 3H; O-CH₃), 6.791 (d, 1H; $J = 8.7$ Hz, Aromatic), 6.896 (m, 1H; Aromatic), 7.362 (d, 1H; $J = 2.7$ Hz, Aromatic). ¹³C NMR (75 MHz, CDCl₃): $\delta = 55.9, 57.0, 86.0, 111.6, 114.7, 124.8, 152.7, 154.2$.

Synthesis of 2-iodo-benzene-1,4-di-ol (12)

2-iodo-1,4-dimethoxy benzene **11** (1.10 g, 5.10 mmol) was dissolved in 20 mL of DCM and solution was cooled to -78 °C. BBr₃ (10.5 mL, 42.0 mmol) was added into the reaction mixture dropwise and reaction was stirred for 24 h at room temperature. Reaction mixture was poured on ice water and ethylacetate (50 mL) was added into it followed by washing with water (3 × 100 mL). Organic layer was collected, dried over Na₂SO₄ and removed under reduced pressure. Crude residue was triturated with pentane (20 mL), yielding off white solid (0.45 g, 46%). ¹H NMR (300 MHz, CDCl₃): $\delta = 6.80$

(m, 1H; Aromatic), 6.90 (d, 1H; $J = 9.0$ Hz, Aromatic), 7.19 (d, 1H; $J = 3.0$ Hz, Aromatic). ^{13}C NMR (125 MHz, CDCl_3): $\delta = 85.0, 115.2, 117.3, 124.3, 149.3, 149.6$.

Synthesis of 13

In a two neck flask, K_2CO_3 (7.70 g, 0.138 mol) and DMF (60 mL) was stirred at $90\text{ }^\circ\text{C}$ for 15 min under N_2 . In a separate vial, **9** (0.922 g, 1.86 mmol) and 2-iodobenzene-1,4-di-ol **12** (0.440 g, 1.86 mmol) was dissolved in DMF (10 mL). This solution was added into preheated flask dropwise via syringe pump for 3 d and reaction mixture was stirred for overnight. DMF was removed under reduced pressure and residue was dissolved in minimum amount of DCM and solution was filtered through silica. Silica was washed with DCM (20 mL). DCM was collected and removed under reduced pressure. Compound was further purified by prep TLC (95:5 hexane: ethylacetate), yielding white solid. (0.05 g, 5%). ^1H NMR (300 MHz, CDCl_3): $\delta = 5.18$ (b, 2H; O- CH_2), 5.64 (t, 2H; $J = 15.0$ Hz, O- CH_2), 6.44 (t, 1H; $J = 3.0$ Hz, Aromatic), 6.66 (s, 2H; Aromatic), 7.25 - 7.17 (m, 4H, Aromatic), 7.51 - 7.41 (m, 5H, Aromatic), 7.58 (b, 1H; Aromatic), 7.69 - 7.66 (m, 1H, Aromatic). ^{13}C NMR (75 MHz, CDCl_3): $\delta = 73.6, 74.4, 89.4, 120.1, 121.8, 128.7, 129.0, 129.1, 129.9, 130.4, 130.7, 132.4, 133.1, 140.9, 143.8, 153.6, 153.9$.

Synthesis of 14

Under nitrogen, compound **13** (0.090 g, 0.16 mmol) was dissolved in 20 mL of toluene. Tetrakis(triphenylphosphine) palladium(0) (0.0090 g, 0.0080 mmol) and copper iodide (0.0010 g, 0.0050 mmol) was added into the solution. In separate vial, 4-*t*-butylphenylacetylene (0.076 g, 0.48 mmol) was dissolved in diisopropylamine (10 mL)

and added into the reaction mixture drop wise. Reaction mixture was stirred for 36 h at 85 °C. Ether (20 mL) was added to the reaction mixture and organic layer was extracted with sat. sodium bicarbonate solution (4 × 50 mL). Organic layer was collected, dried over sodium sulfate and volatiles were removed under reduced pressure. Prep TLC (Pre soaked in TEA) in pentane was done for purification, yielding white solid (0.053 g, 45%). ¹H NMR (500 MHz, CDCl₃): δ = 1.319 (s, 9H; CH₃), 1.369 (s, 9H; CH₃), 5.80 – 4.90 (b, 4H; O-CH₂), 6.95 - 6.00 (b, 5H; Aromatic), 7.218 - 7.194 (m, 4H; Aromatic), 7.474 - 7.396 (m, 9H; Aromatic), 7.69 – 7.58 (b, 4H; Aromatic). ¹³C NMR (125 MHz, CDCl₃): δ = 31.2, 34.7, 34.8, 73.3, 73.5, 84.3, 84.4, 89.3, 120.1, 120.3, 120.3, 121.8, 122.5, 122.5, 124.3, 125.3, 128.3, 128.6, 128.7, 128.8, 128.9, 130.6, 130.7, 130.8, 131.2, 131.5, 132.2, 132.9, 133.7, 133.8, 141.1, 141.8, 142.0, 151.6. HRMS (M + 1): calc. for C₅₀H₄₅O₂, 677.3400; found, 677.3420. UV-vis: λ_{max} 310 nm (ε = 63346.6 M⁻¹ cm⁻¹).

Synthesis of 15

Under nitrogen, compound **13** (0.053 g, 0.094 mmol) was dissolved in 10 mL of toluene. Tetrakis(triphenylphosphine) palladium(0) (0.010 g, 0.0094 mmol) and copper iodide (0.0020 g, 0.0094 mmol) was added into the solution. In separate vial, 2,5-diethynyl-1,4-hexyloxy benzene (0.031 g, 0.094 mmol) was dissolved in diisopropylamine (5 mL) and added into the reaction mixture drop wise. Reaction mixture was stirred for 36 h at 85 °C. Ether (20 mL) was added to the reaction mixture and organic layer was extracted with sat. sodium bicarbonate solution (4 × 50 mL). Organic layer was collected, dried over sodium sulfate and volatiles were removed under reduced pressure. Residue was dissolved in minimum amount of DCM and

reprecipitated, yielding yellow solid (0.030 g). ^1H NMR (300 MHz, CDCl_3): δ = 0.90 - 0.89 (m, 8H), 1.52 - 1.21 (m, 17H), 1.79 - 1.66 (m, 6H), 4.04 - 3.84 (b, 2H), 5.67 - 5.04 (b, 2H), 6.84 - 6.21 (b, 3H), 7.89 - 7.17 (m, 11H).

Synthesis of CP2

To a solution of 1.00 g (3.81 mmol) of 1,1':3',1''-terphenyl-2,2''-diol in 50 mL of dry *N,N*-dimethylformamide (DMF) was added 1.61 g (3.81 mmol) of 1,4-dibromo-2,5-bis(bromomethyl)benzene. The resulting solution was then added dropwise over 6 days to a solution of 16.0 g (116 mmol) of anhydrous K_2CO_3 in 200 mL of anhydrous DMF preheated to 100 °C under nitrogen. The solution was then heated at 100 °C for 4 days followed by concentrating under reduced pressure to afford a dark brown residue. This was then passed through a short silica gel column using CH_2Cl_2 as the eluting solvent. The solution was concentrated under reduced pressure then washed with pentane to afford 1.11 g (55.6%) of **CP2** as a white solid. ^1H NMR (500 MHz, CDCl_3): δ 4.90 (d, 1H, J = 12.5 Hz), 5.14 (d, 1H, J = 12.0 Hz), 5.46 (d, 1H, J = 12.0 Hz), 5.71 (d, 1H, J = 12.0 Hz), 6.39 (s, 1H), 6.71 (s, 1H), 7.00 (s, 1H), 7.08 (d, 1H, J = 7.5 Hz), 7.16 (d, 1H, J = 7.5 Hz), 7.26 - 7.27 (m, 1H), 7.33 (t, 2H, J = 7.5 Hz), 7.46 - 7.51 (m, 4H), 7.62 - 7.67 (m, 2H) ppm

Synthesis of CP1a

In the dry box, compound **CP1** (0.10 g, 0.16 mmol) was dissolved in 10 mL of toluene. Tetrakis(triphenylphosphine) palladium(0) (0.017 g, 0.016 mmol) and copper iodide (0.0030 g, 0.016 mmol) was added into the solution. In separate vial, 4-*t*-butylphenylacetylene (0.15 g, 0.96 mmol) was dissolved in diisopropylamine (5 mL) and

added into the reaction mixture drop wise. Reaction mixture was stirred for 36 h at 85 °C. Ether (20 mL) was added to the reaction mixture and organic layer was extracted with sat. sodium bicarbonate solution (4 × 50 mL). Organic layer was collected, dried over sodium sulfate and volatiles were removed under reduced pressure. Prep TLC (Pre soaked in TEA) in pentane was done for purification, yielding white solid (0.030 g, 27%). ¹H NMR (300 MHz, CDCl₃): δ = 1.36 (s, 18H; CH₃), 6.29 – 5.08 (b, 4H; O-CH₂), 6.69 (t, 2H; *J* = 3.0 Hz, Aromatic), 7.13 (dd, 3H; *J*₁ = 3.0 Hz, *J*₂ = 9.0 Hz, Aromatic), 7.31 (m, 5H; Aromatic), 7.49 (m, 9H; Aromatic), 7.69 (d, 3H; *J* = 6.0 Hz, Aromatic). ¹³C NMR (75 MHz, CDCl₃): δ = 31.2, 34.8, 72.0, 74.7, 77.2, 84.5, 117.9, 120.2, 125.1, 125.6, 126.3, 128.1, 128.8, 130.9, 131.3, 132.6, 133.9, 141.5, 142.7, 151.6. HRMS (*M* + 1): calc. for C₅₀H₄₅O₂, 677.3420; found, 677.3420. UV-vis: λ_{max} 349 nm (ε = 69,616.5 M⁻¹ cm⁻¹).

Synthesis of CP2a

In the dry box, compound **CP2** (0.100 g, 0.191 mmol) was dissolved in 10 mL of toluene. Tetrakis(triphenylphosphine) palladium(0) (0.020 g, 0.0190 mmol) and copper iodide (0.00300 g, 0.0190 mmol) was added into the solution. In separate vial, 4-*t*-butylphenylacetylene (0.190 g, 1.20 mmol) was dissolved in diisopropylamine (5 mL) and added into the reaction mixture drop wise. Reaction mixture was stirred for 36 h at 85 °C. Ether (20 mL) was added to the reaction mixture and organic layer was extracted with sat. sodium bicarbonate solution (4 × 50 mL). Organic layer was collected, dried over sodium sulfate and volatiles were removed under reduced pressure. Prep TLC (Pre soaked in TEA) in pentane was done for purification but due to the same retention factor

(R_f) of compound and impurity, it was not possible to purify **CP2a**. HRMS ($M + 1$) (From impure sample): calc. for $C_{50}H_{45}O_2$, 677.3420; found, 677.3453.

Synthesis of CP1b

In the dry box, compound **CP1** (0.10 g, 0.16 mmol) was dissolved in 15 mL of DMF. Tetrakis(triphenylphosphine) palladium(0) (0.017 g, 0.016 mmol) and cesium carbonate (0.319 g, 0.980 mmol) was added into the solution followed by 4-methoxyphenylboronic acid (0.075 g, 0.490 mmol). Pressure flask was capped and taken out from the dry box and heated for 2 d at 110 °C. DMF was removed under reduced pressure and residue was dissolved in DCM (20 mL). Organic layer was collected and removed under reduced pressure. Prep TLC (Pre soaked in TEA) was done in 10% pentane ethylacetate solution, yielding white solid (0.017 g, 18%). 1H NMR (300 MHz, $CDCl_3$): δ = 3.90 (b, 6H; $2 \times O-CH_3$), 4.51 (b, 1H; $O-CH_2$), 5.06 (b, 2H; $O-CH_2$), 5.71 (b, 1H; $O-CH_2$), 7.99 – 6.60 (m, 22H; Aromatic). ^{13}C NMR (125 MHz, $CDCl_3$): δ = 55.3, 71.7, 74.4, 113.1, 113.7, 122.6, 123.7, 125.7, 126.4, 127.0, 128.1, 128.6, 130.2, 130.7, 131.9, 132.5, 134.0, 141.9, 142.6, 149.6, 152.5, 158.2. HRMS ($M + 1$): calc. for $C_{40}H_{33}O_4$, 577.2379; found, 577.2379. UV-vis: λ_{max} 279 nm ($\epsilon = 40,462 M^{-1} cm^{-1}$).

Synthesis of CP2b

In the dry box, compound **CP2** (0.10 g, 0.19 mmol) was dissolved in 15 mL of DMF. Tetrakis(triphenylphosphine) palladium(0) (0.021 g, 0.019 mmol) and cesium carbonate (0.39 g, 1.2 mmol) was added into the solution followed by 4-methoxyphenylboronic acid (0.091 g, 0.60 mmol). Pressure flask was capped and taken out from the dry box and heated for 2 d at 110 °C. DMF was removed under reduced pressure and

residue was dissolved in DCM (20 mL). Organic layer was collected and removed under reduced pressure. Prep TLC (Pre soaked in TEA) was done in 10% pentane ethylacetate solution, yielding white solid (0.019 g, 17%). ^1H NMR (300 MHz, CDCl_3): δ = 3.85 (s, 6H; $2 \times \text{O-CH}_3$), 4.86 (d, 2H; $J = 9.0$ Hz, O- CH_2), 5.16 (d, 2H; $J = 12.0$ Hz, O- CH_2), 6.75 (s, 1H; Aromatic), 6.79 (s, 2H; Aromatic), 6.87 (dd, 4H; $J_1 = 3.0$ Hz, $J_2 = 9.0$ Hz, Aromatic), 7.05 (dd, 5H; $J_1 = 3.0$ Hz, $J_2 = 9.0$ Hz, Aromatic), 7.31 – 7.13 (m, 10H; Aromatic). ^{13}C NMR (75 MHz, CDCl_3): δ = 55.2, 76.2, 77.2, 113.3, 123.2, 124.0, 126.2, 128.4, 129.1, 130.2, 130.6, 132.1, 132.3, 133.5, 136.7, 138.4, 139.4, 156.8, 158.5. UV-vis: λ_{max} 275 nm ($\epsilon = 50,867 \text{ M}^{-1} \text{ cm}^{-1}$).

Synthesis of CPIc

In the dry box, compound **CP1** (0.10 g, 0.16 mmol) and thiophene (2-tributylstannyl) (0.18 g, 0.48 mmol) was dissolved in 10 mL of toluene. Bis(triphenylphosphine)palladium(II) chloride (0.0056 g, 0.0081 mmol) was added into the solution. Pressure flask was capped and taken out from the dry box and heated for 2 d at 105 °C. Toluene was removed under reduced pressure and residue was dissolved in DCM (20 mL). Organic layer was collected and removed under reduced pressure. Prep TLC (Pre soaked in TEA) was done in 5% pentane ethylacetate solution, yielding white solid (0.043 g, 50%). ^1H NMR (300 MHz, CDCl_3): δ = 3.90 (b, 6H; $2 \times \text{O-CH}_3$), 4.51 (b, 1H; O- CH_2), 5.06 (b, 2H; O- CH_2), 5.71 (b, 1H; O- CH_2), 7.99 – 6.60 (m, 22H; Aromatic). ^{13}C NMR (125 MHz, CDCl_3): δ = 75.4, 76.2, 77.9, 123.6, 124.5, 124.6, 125.8, 126.0, 126.3, 126.4, 127.1, 127.3, 128.5, 128.6, 129.0, 129.3, 129.3, 130.3, 130.8, 130.9, 133.4, 133.5, 133.8, 135.2, 135.4, 135.9, 136.9, 137.0, 138.6, 140.1, 141.0, 156.8. HRMS ($\text{M} +$

1): calc. for $C_{34}H_{25}O_2S_2$, 529.1296; found, 529.1295. UV-vis: λ_{\max} 279 nm ($\epsilon = 28,235 \text{ M}^{-1} \text{ cm}^{-1}$).

Synthesis of CP2c

In the dry box, compound **CP2** (0.10 g, 0.19 mmol) and thiophene (2-tributylstannyl) (0.21 g, 0.57 mmol) was dissolved in 10 mL of toluene. Bis(triphenylphosphine)palladium(II) chloride (0.014 g, 0.0019 mmol) was added into the solution. Pressure flask was capped and taken out from the dry box and heated for 2 d at 105 °C. Toluene was removed under reduced pressure and residue was dissolved in DCM (20 mL). Organic layer was collected and removed under reduced pressure. Prep TLC (Pre soaked in TEA) was done in 5% pentane ethylacetate solution, yielding white solid (0.038 g, 37%). ^1H NMR (300 MHz, CDCl_3): $\delta = 3.90$ (b, 6H; $2 \times \text{O-CH}_3$), 4.51 (b, 1H; O- CH_2), 5.06 (b, 2H; O- CH_2), 5.71 (b, 1H; O- CH_2), 7.99 – 6.60 (m, 22H; Aromatic). ^{13}C NMR (125 MHz, CDCl_3): $\delta = 75.4, 76.1, 77.9, 123.5, 123.5, 123.5, 124.4, 124.6, 124.6, 125.8, 126.0, 126.2, 126.4, 127.1, 127.1, 127.2, 128.4, 128.6, 129.0, 129.2, 129.3, 129.3, 130.2, 130.2, 130.7, 130.7, 130.8, 133.1, 133.3, 133.4, 133.8.0, 135.5, 135.6, 136.0, 137.0, 137.1, 138.5, 138.6, 140.1, 141.0, 157.0$. HRMS ($\text{M} + 1$): calc. for $C_{34}H_{25}O_2S_2$, 529.1296; found, 529.1293. UV-vis: λ_{\max} 275 nm ($\epsilon = 27,977 \text{ M}^{-1} \text{ cm}^{-1}$)

Synthesis of CLaI

In the dry box, compound **21** (0.161 g, 0.303 mmol) and compound **6** (0.0025 g, 0.0030 mmol) were dissolved in 10 mL of toluene. Tetrakis(triphenylphosphine) palladium(0) (0.016 g, 0.015 mmol) and copper iodide (0.0030 g, 0.015 mmol) was added into the solution. In separate vial, compound **22** (0.100 g, 0.306 mmol) was

dissolved in diisopropylamine (5 mL) and added into the reaction mixture drop wise. Reaction mixture was stirred for 36 h at 80 °C. DCM (20 mL) was added to the reaction mixture and organic layer was extracted with sat. sodium bicarbonate solution (4 × 50 mL). Organic layer was collected, dried over sodium sulfate and volatiles were removed under reduced pressure. Residue was dissolved in minimum amount of DCM and reprecipitated in methanol (20 mL) as yellow powder (75 mg, 41%). ¹H NMR (300 MHz, CDCl₃): δ = 0.91 (brm, 16H; Aliphatic), 1.55 - 1.36 (brm, 38H; Aliphatic, overlap with water peak), 1.90 - 1.73 (brm, 9H; Aliphatic), 4.05 (brm, 8H; Aliphatic), 7.18 - 6.78 (brm, 4H; Aromatic), 8.15 - 7.49 (brm, 5H; Aromatic).

Synthesis of CLa3

In the dry box, compound **21** (0.157 g, 0.297 mmol) and compound **6** (0.00752 g, 0.00920 mmol) were dissolved in 10 mL of toluene. Tetrakis(triphenylphosphine) palladium(0) (0.016 g, 0.015 mmol) and copper iodide (0.0030 g, 0.015 mmol) was added into the solution. In separate vial, compound **22** (0.100 g, 0.306 mmol) was dissolved in diisopropylamine (5 mL) and added into the reaction mixture drop wise. Reaction mixture was stirred for 36 h at 80 °C. DCM (20 mL) was added to the reaction mixture and organic layer was extracted with sat. sodium bicarbonate solution (4 × 50 mL). Organic layer was collected, dried over sodium sulfate and volatiles were removed under reduced pressure. Residue was dissolved in minimum amount of DCM and reprecipitated in methanol (20 mL) as yellow powder (55 mg, 31%). ¹H NMR (300 MHz, CDCl₃): δ = 0.92 (brm, 21H; Aliphatic), 1.50 - 1.32 (brm, 33H; Aliphatic), 1.90 - 1.74

(brm, 13H; Aliphatic), 4.21 - 3.91 (brm, 8H; Aliphatic), 7.11 - 6.85 (brm, 4H; Aromatic), 7.98 - 7.68 (brm, 1H; Aromatic).

Synthesis of CLa5

In the dry box, compound **21** (0.154 g, 0.291 mmol) and compound **6** (0.0125 g, 0.0153 mmol) were dissolved in 10 mL of toluene. Tetrakis(triphenylphosphine) palladium(0) (0.016 g, 0.015 mmol) and copper iodide (0.0030 g, 0.015 mmol) was added into the solution. In separate vial, compound **22** (0.100 g, 0.306 mmol) was dissolved in diisopropylamine (5 mL) and added into the reaction mixture drop wise. Reaction mixture was stirred for 36 h at 80 °C. DCM (20 mL) was added to the reaction mixture and organic layer was extracted with sat. sodium bicarbonate solution (4 × 50 mL). Organic layer was collected, dried over sodium sulfate and volatiles were removed under reduced pressure. Residue was dissolved in minimum amount of DCM and reprecipitated in methanol (20 mL) as yellow powder (150 mg, 84%). ¹H NMR (300 MHz, CDCl₃): δ = 0.92 (brm, 17H; Aliphatic), 1.47 - 1.32 (brm, 26H; Aliphatic), 1.88 - 1.72 (brm, 12H; Aliphatic), 4.22 - 3.96 (brm, 8H; Aliphatic), 7.13 - 6.90 (brm, 4H; Aromatic), 7.23 - 7.13 (brm, 1H; Aromatic), 7.90 - 7.37 (brm, 2H; Aromatic).

Synthesis of CLb1

In the dry box, compound **21** (0.0803 g, 0.151 mmol) and compound **7** (0.00125 g, 0.00153 mmol) were dissolved in 10 mL of toluene. Tetrakis(triphenylphosphine) palladium(0) (0.00800 g, 0.00765 mmol) and copper iodide (0.00150 g, 0.00765 mmol) was added into the solution. In separate vial, compound **22** (0.050 g, 0.153 mmol) was dissolved in diisopropylamine (5 mL) and added into the reaction mixture drop wise.

Reaction mixture was stirred for 36 h at 80 °C. DCM (20 mL) was added to the reaction mixture and organic layer was extracted with sat. sodium bicarbonate solution (4 × 50 mL). Organic layer was collected, dried over sodium sulfate and volatiles were removed under reduced pressure. Residue was dissolved in minimum amount of DCM and reprecipitated in methanol (20 mL) as yellow powder (55 mg, 60%). ¹H NMR (300 MHz, CDCl₃): δ = 0.91 (brm, 16H; Aliphatic), 1.48 - 1.32 (brm, 23H; Aliphatic), 1.90 - 1.74 (brm, 10H; Aliphatic), 4.06 (brm, 8H; Aliphatic), 7.10 - 6.84 (brm, 4H; Aromatic), 7.25 - 7.10 (brm, 1H; Aromatic), 7.95 - 7.33 (brm, 2H; Aromatic).

Synthesis of CLb3

In the dry box, compound **21** (0.0787 g, 0.148 mmol) and compound **7** (0.00380 g, 0.00459 mmol) were dissolved in 10 mL of toluene. Tetrakis(triphenylphosphine) palladium(0) (0.00800 g, 0.00765 mmol) and copper iodide (0.00150 g, 0.00765 mmol) was added into the solution. In separate vial, compound **22** (0.050 g, 0.153 mmol) was dissolved in diisopropylamine (5 mL) and added into the reaction mixture drop wise. Reaction mixture was stirred for 36 h at 80 °C. DCM (20 mL) was added to the reaction mixture and organic layer was extracted with sat. sodium bicarbonate solution (4 × 50 mL). Organic layer was collected, dried over sodium sulfate and volatiles were removed under reduced pressure. Residue was dissolved in minimum amount of DCM and reprecipitated in methanol (20 mL) as yellow powder (50 mg, 55%). ¹H NMR (300 MHz, CDCl₃): δ = 0.91 (brm, 16H; Aliphatic), 1.47 - 1.32 (brm, 25H; Aliphatic), 1.88 - 1.71 (brm, 10H; Aliphatic), 4.17 - 4.3.98 (brm, 8H; Aliphatic), 7.10 - 6.75 (brm, 3H; Aromatic), 7.25 - 7.10 (brm, 1H; Aromatic), 7.89 - 7.36 (brm, 1H; Aromatic).

Synthesis of CLb5

In the dry box, compound **21** (0.0771 g, 0.145 mmol) and compound **7** (0.00630 g, 0.00765 mmol) were dissolved in 10 mL of toluene. Tetrakis(triphenylphosphine) palladium(0) (0.00800 g, 0.00765 mmol) and copper iodide (0.00150 g, 0.00765 mmol) was added into the solution. In separate vial, compound **22** (0.050 g, 0.153 mmol) was dissolved in diisopropylamine (5 mL) and added into the reaction mixture drop wise. Reaction mixture was stirred for 36 h at 80 °C. DCM (20 mL) was added to the reaction mixture and organic layer was extracted with sat. sodium bicarbonate solution (4 × 50 mL). Organic layer was collected, dried over sodium sulfate and volatiles were removed under reduced pressure. Residue was dissolved in minimum amount of DCM and reprecipitated in methanol (20 mL) as yellow powder (60 mg, 67%). ¹H NMR (300 MHz, CDCl₃): δ = 0.91 (brm, 14H; Aliphatic), 1.48 - 1.32 (brm, 21H; Aliphatic), 1.90 - 1.72 (brm, 9H; Aliphatic), 4.06 (brm, 8H; Aliphatic), 7.14 - 6.88 (brm, 3H; Aromatic), 7.83 - 7.33 (brm, 3H; Aromatic).

Synthesis of MPa1

In the dry box, compound **21** (160 mg, 0.303 mmol), compound **1** (0.708 mg, 0.00153 mmol) and compound **24** (0.596 mg, .00153 mmol) were dissolved in 10 mL of toluene. Tetrakis(triphenylphosphine) palladium(0) (16.0 mg, 0.0153 mmol) and copper iodide (3.00 mg, 0.0153 mmol) was added into the solution. In separate vial, compound **22** (100 mg, 0.306 mmol) was dissolved in diisopropylamine (5 mL) and added into the reaction mixture drop wise. Reaction mixture was stirred for 36 h at 80 °C. DCM (20 mL) was added to the reaction mixture and organic layer was extracted with sat. sodium

bicarbonate solution (4 × 50 mL). Organic layer was collected, dried over sodium sulfate and volatiles were removed under reduced pressure. Residue was dissolved in minimum amount of DCM and reprecipitated in methanol (20 mL) as yellow powder (130 mg, 71%). ¹H NMR (300 MHz, CDCl₃): δ = 0.92 (brm, 18H; Aliphatic), 1.51 - 1.32 (brm, 31H; Aliphatic), 1.88 - 1.74 (brm, 12H; Aliphatic), 4.17 - 4.04 (brm, 8H; Aliphatic), 7.25 - 6.83 (brm, 5H; Aromatic), 7.95 - 7.43 (brm, 2H; Aromatic).

Synthesis of MPa3

In the dry box, compound **21** (157 mg, 0.297 mmol), compound **1** (2.13 mg, 0.00460 mmol) and compound **24** (1.80 mg, .00460 mmol) were dissolved in 10 mL of toluene. Tetrakis(triphenylphosphine) palladium(0) (16.0 mg, 0.0153 mmol) and copper iodide (3.00 mg, 0.0153 mmol) was added into the solution. In separate vial, compound **22** (100 mg, 0.306 mmol) was dissolved in diisopropylamine (5 mL) and added into the reaction mixture drop wise. Reaction mixture was stirred for 36 h at 80 °C. DCM (20 mL) was added to the reaction mixture and organic layer was extracted with sat. sodium bicarbonate solution (4 × 50 mL). Organic layer was collected, dried over sodium sulfate and volatiles were removed under reduced pressure. Residue was dissolved in minimum amount of DCM and reprecipitated in methanol (20 mL) as yellow powder (140 mg, 78%). ¹H NMR (300 MHz, CDCl₃): δ = 0.92 (brm, 15H; Aliphatic), 1.48 - 1.32 (brm, 24H; Aliphatic), 1.93 - 1.72 (brm, 10H; Aliphatic), 4.14 - 4.04 (brm, 8H; Aliphatic), 7.12 - 6.77 (brm, 4H; Aromatic), 7.25 - 7.12 (brm, 1H; Aromatic), 7.93 - 7.44 (brm, 1H; Aromatic).

Synthesis of MPa5

In the dry box, compound **21** (154 mg, 0.290 mmol), compound **1** (3.54 mg, .00765 mmol), and compound **24** (2.98 mg, .00765 mmol) were dissolved in 10 mL of toluene. Tetrakis(triphenylphosphine) palladium(0) (16.0 mg, 0.0153 mmol) and copper iodide (3.00 mg, 0.0153 mmol) was added into the solution. In separate vial, compound **22** (100 mg, 0.306 mmol) was dissolved in diisopropylamine (5 mL) and added into the reaction mixture drop wise. Reaction mixture was stirred for 36 h at 80 °C. DCM (20 mL) was added to the reaction mixture and organic layer was extracted with sat. sodium bicarbonate solution (4 × 50 mL). Organic layer was collected, dried over sodium sulfate and volatiles were removed under reduced pressure. Residue was dissolved in minimum amount of DCM and reprecipitated in methanol (20 mL) as yellow powder (125 mg, 70%). ¹H NMR (300 MHz, CDCl₃): δ = 0.92 (brm, 19H; Aliphatic), 1.50 - 1.32 (brm, 31H; Aliphatic), 1.95 - 1.74 (brm, 13H; Aliphatic), 4.17 - 4.03 (brm, 8H; Aliphatic), 7.11 - 6.81 (brm, 3H; Aromatic), 7.25 - 7.12 (brm, 2H; Aromatic), 8.03 - 7.33 (brm, 3H; Aromatic).

Synthesis of MPbI

In the dry box, compound **21** (160 mg, 0.303 mmol), compound **1** (0.708 mg, .00153 mmol), and compound **23** (0.596 mg, .00153 mmol) were dissolved in 10 mL of toluene. Tetrakis(triphenylphosphine) palladium(0) (16.0 mg, 0.0153 mmol) and copper iodide (3.00 mg, 0.0153 mmol) was added into the solution. In separate vial, compound **22** (100 mg, 0.306 mmol) was dissolved in diisopropylamine (5 mL) and added into the reaction mixture drop wise. Reaction mixture was stirred for 36 h at 80 °C. DCM (20 mL) was added to the reaction mixture and organic layer was extracted with sat. sodium

bicarbonate solution (4 × 50 mL). Organic layer was collected, dried over sodium sulfate and volatiles were removed under reduced pressure. Residue was dissolved in minimum amount of DCM and reprecipitated in methanol (20 mL) as yellow powder (115 mg, 63%). ¹H NMR (300 MHz, CDCl₃): δ = 0.92 (brm, 19H; Aliphatic), 1.48 - 1.32 (brm, 31H; Aliphatic), 1.88 - 1.69 (brm, 15H; Aliphatic), 4.17 - 3.99 (brm, 8H; Aliphatic), 7.10 - 6.81 (brm, 3H; Aromatic), 7.25 - 7.10 (brm, 3H; Aromatic), 7.98 - 7.38 (brm, 3H; Aromatic).

Synthesis of MPb3

In the dry box, compound **21** (157 mg, 0.297 mmol), compound **1** (2.13 mg, 0.00460 mmol) and compound **23** (1.80 mg, .00460 mmol) were dissolved in 10 mL of toluene. Tetrakis(triphenylphosphine) palladium(0) (16.0 mg, 0.0153 mmol) and copper iodide (3.00 mg, 0.0153 mmol) was added into the solution. In separate vial, compound **22** (100 mg, 0.306 mmol) was dissolved in diisopropylamine (5 mL) and added into the reaction mixture drop wise. Reaction mixture was stirred for 36 h at 80 °C. DCM (20 mL) was added to the reaction mixture and organic layer was extracted with sat. sodium bicarbonate solution (4 × 50 mL). Organic layer was collected, dried over sodium sulfate and volatiles were removed under reduced pressure. Residue was dissolved in minimum amount of DCM and reprecipitated in methanol (20 mL) as yellow powder (145 mg, 81%). ¹H NMR (300 MHz, CDCl₃): δ = 0.92 (brm, 20H; Aliphatic), 1.50 - 1.32 (brm, 33H; Aliphatic), 1.94 - 1.70 (brm, 13H; Aliphatic), 4.17 - 4.04 (brm, 8H; Aliphatic), 7.08 - 6.89 (brm, 3H; Aromatic), 7.24 - 7.10 (brm, 2H; Aromatic), 7.75 - 7.32 (brm, 1H; Aromatic).

Synthesis of MPb5

In the dry box, compound **21** (154 mg, 0.290 mmol), compound **1** (3.54 mg, .00765 mmol), and compound **23** (2.98 mg, .00765 mmol) were dissolved in 10 mL of toluene. Tetrakis(triphenylphosphine) palladium(0) (16.0 mg, 0.0153 mmol) and copper iodide (3.00 mg, 0.0153 mmol) was added into the solution. In separate vial, compound **22** (100 mg, 0.306 mmol) was dissolved in diisopropylamine (5 mL) and added into the reaction mixture drop wise. Reaction mixture was stirred for 36 h at 80 °C. DCM (20 mL) was added to the reaction mixture and organic layer was extracted with sat. sodium bicarbonate solution (4 × 50 mL). Organic layer was collected, dried over sodium sulfate and volatiles were removed under reduced pressure. Residue was dissolved in minimum amount of DCM and reprecipitated in methanol (20 mL) as yellow powder (135 mg, 76%). ¹H NMR (300 MHz, CDCl₃): δ = 0.91 (brm, 31H; Aliphatic), 1.53 - 1.32 (brm, 51H; Aliphatic), 1.93 - 1.72 (brm, 20H; Aliphatic), 4.20 - 4.04 (brm, 14H; Aliphatic), 7.12 - 6.83 (brm, 5H; Aromatic), 7.23 - 7.13 (brm, 3H; Aromatic), 7.95 - 7.66 (brm, 3H; Aromatic).

6.6 Reference

1. Smith, R. C., Covalently Scaffolded Inter-p-System Orientations in p-Conjugated Polymers and Small Molecule Models. *Macromolecular Rapid Communications* **2009**, 30, 2067-2078.
2. Bazan, G. C., Novel Organic Materials through Control of Multichromophore Interactions. *Journal of Organic Chemistry* **2007**, 72, 8615-8635.
3. Klare, J. E.; Tulevski, G. S.; Sugo, K.; de Picciotto, A.; White, K. A.; Nuckolls, C., Cruciform pi-Systems for Molecular Electronics Applications. *J. Am. Chem. Soc.* **2003**, 125, (20), 6030-6031.
4. Tykwinski, R. R.; Schreiber, M.; Perez Carlon, R.; Diederich, F.; Gramlich, V., Donor/acceptor-substituted tetraethynylethenes. Systematic assembly of molecules for use as advanced materials. *Helv. Chim. Acta* **1996**, 79, (8), 2249-2281.
5. Spitler, E. L.; Shirtcliff, L. D.; Haley, M. M., Systematic Structure-Property Investigations and Ion-Sensing Studies of Pyridine-Derivatized Donor/Acceptor Tetrakis(arylethynyl)benzenes. *Journal of Organic Chemistry* **2007**, 72, (1), 86-96.
6. Samori, S.; Tojo, S.; Fujitsuka, M.; Spitler, E. L.; Haley, M. M.; Majima, T., Fine-Tuning of Radiolysis Induced Emission by Variable Substitution of Donor-/Acceptor-Substituted Tetrakis(arylethynyl)benzenes. *J. Org. Chem.* **2008**, 73, (9), 3551-3558.
7. Spitler, E. L.; Monson, J. M.; Haley, M. M., Structure-Property Relationships of Fluorinated Donor/Acceptor Tetrakis(phenylethynyl)benzenes and Bis(dehydrobenzoannuleno)benzenes. *J. Org. Chem.* **2008**, 73, (6), 2211-2223.

8. Pina, J.; Seixas de Melo, J.; Burrows, H. D.; Galbrecht, F.; Bilge, A.; Kudla, C. J.; Scherf, U., Excited State Properties of Oligophenyl and Oligothieryl Swivel Cruciforms. *J. Phys. Chem. B* **2008**, 112, (4), 1104-1111.
9. Bilge, A.; Zen, A.; Forster, M.; Li, H.; Galbrecht, F.; Nehls, B. S.; Farrell, T.; Neher, D.; Scherf, U., Swivel-cruciform oligothiophene dimers. *Journal of Materials Chemistry* **2006**, 16, (31), 3177-3182.
10. Wilson, J. N.; Hardcastle, K. I.; Josowicz, M.; Bunz, U. H. F., Synthesis and electronic properties of bis-styryl substituted trimeric aryleneethynylenes. Comparison of cruciforms with iso-cruciforms. *Tetrahedron* **2004**, 60, (34), 7157-7167.
11. Wilson, J. N.; Bunz, U. H. F., Switching of Intramolecular Charge Transfer in Cruciforms: Metal Ion Sensing. *Journal of the American Chemical Society* **2005**, 127, (12), 4124-4125.
12. Tolosa, J.; Zuccherro, A. J.; Bunz, U. H. F., Water-Soluble Cruciforms: Response to Protons and Selected Metal Ions. *J. Am. Chem. Soc.* **2008**, 130, 6498-6506.
13. He, S.; Dennis, A. E.; Smith, R. C., Steric Coordination Control of Interchain Interactions in Conducting Metallopolymers. *Macromolecular Rapid Communications* **2009**, 30, 2079-2083.
14. Osaka, I.; McCullough, R. D., Advances in Molecular Design and Synthesis of Regioregular Polythiophenes. *Acc. Chem. Res.* **2008**, 41, 1202-1214.
15. Mwaura, J. K.; Pinto, M. R.; Witker, D.; Ananthkrishnan, N.; Schanze, K. S.; Reynolds, J. R., Photovoltaic Cells Based on Sequentially Adsorbed Multilayers of

- Conjugated Poly(p-phenylene ethynylene)s and a Water-Soluble Fullerene Derivative. *Langmuir* **2005**, 21, (22), 10119-10126.
16. Kietzke, T.; Neher, D.; Kumke, M.; Montenegro, R.; Landfester, K.; Scherf, U., A Nanoparticle Approach To Control the Phase Separation in Polyfluorene Photovoltaic Devices. *Macromolecules* **2004**, 37, (13), 4882-4890.
17. Akbayir, C.; Bulut, F.; Farrell, T.; Goldschmidt, A.; Guentner, R.; Kam, A. P.; Miclea, P.; Scherf, U.; Seekamp, J.; Solovyev, V. G.; Torres, C. M. S., Nanostructured conjugated polymeric systems for photovoltaic applications. *Reviews on Advanced Materials Science* **2003**, 5, (3), 205-210.
18. Coakley, K. M.; McGehee, M. D., Conjugated Polymer Photovoltaic Cells. *Chemistry of Materials* **2004**, 16, (23), 4533-4542.
19. Roncali, J., Conjugated poly(thiophenes): synthesis, functionalization, and applications. *Chemical Reviews (Washington, DC, United States)* **1992**, 92, (4), 711-38.
20. Cornil, J.; Beljonne, D.; Calbert, J.-P.; Bredas, J.-L., Interchain interactions in organic pi-conjugated materials: impact on electronic structure, optical response, and charge transport. *Adv. Mater.* **2001**, 13, (14), 1053-1067.
21. Scherf, U.; List, E. J. W., Semiconducting polyfluorenes - towards reliable structure-property relationships. *Advanced Materials (Weinheim, Germany)* **2002**, 14, (7), 477-487.

22. Bredas, J.-L.; Beljonne, D.; Coropceanu, V.; Cornil, J., Charge-Transfer and Energy-Transfer Processes in p-Conjugated Oligomers and Polymers: A Molecular Picture. *Chemical Reviews (Washington, DC, United States)* **2004**, 104, (11), 4971-5003.
23. Knoblock, K. M.; Silvestri, C. J.; Collard, D. M., Stacked conjugated oligomers as molecular models to examine interchain interactions in conjugated materials. *J Am Chem Soc* **2006**, 128, (42), 13680-1.
24. Salhi, F.; Collard, D. M., p-Stacked conjugated polymers: the influence of paracyclophane p-stacks on the redox and optical properties of a new class of broken conjugated polythiophenes. *Advanced Materials (Weinheim, Germany)* **2003**, 15, (1), 81-85.
25. Kraft, A.; Grimsdale, A. C.; Holmes, A. B., Electroluminescent conjugated polymers-seeing polymers in a new light. *Angew. Chem., Int. Ed.* **1998**, 37, (4), 403-428.
26. Brabec, C. J.; Sariciftci, N. S.; Hummelen, J. C., Plastic solar cells. *Advanced Functional Materials* **2001**, 11, (1), 15-26.
27. Bunz, U. H. F., Poly(aryleneethynylene)s: Syntheses, Properties, Structures, and Applications. *Chemical Reviews (Washington, D. C.)* **2000**, 100, (4), 1605-1644.
28. Yasuhiro Morisaki; Chujo, Y., Through-Space Conjugated Polymers Based on Cyclophanes. *Angew. Chem. Int. Ed* **2006**, 45, 6430 – 6437.
29. Vinod, T. K.; Hart, H., Cupped- and cappedophanes, two new general classes of compounds with molecular cavities. *Journal of the American Chemical Society* **1988**, 110, (19), 6574-5.

30. Vinod, T. K.; Hart, H., Synthesis of two noninterconvertible conformers of a single host. Self-filled and vaulted cappedophanes. *Journal of the American Chemical Society* **1990**, 112, (8), 3250-2.
31. Vinod, T. K.; Hart, H., Cupped azacyclophanes based on a m-terphenyl framework: conformational features of their N-tosylamide precursors. *Journal of Organic Chemistry* **1990**, 55, (20), 5461-6.
32. Morgan, B. P.; Gilliard, R. J.; Loungani, R. S.; Smith, R. C., Poly(*p*-phenylene ethynylene) Incorporating Sterically Enshrouding *m*-Terphenyl Oxacyclophane Canopies. *Macromolecular Rapid Communications* **2009**, 30, 1399-1405.
33. Morisaki, Y.; Chujo, Y., Cyclophane-containing polymers. *Prog. Polym. Sci.* **2008**, 33, 346-364.
34. Vinod, T.; Hart, H., Synthesis of cuppedophanes and cappedophanes. Two new classes of cyclophanes with molecular cavities. *Journal of Organic Chemistry* **1990**, 55, (3), 881-90.
35. Vinod, T. K.; Hart, H., Cuppedo- and cappedophanes. *Topics in Current Chemistry* **1994**, 172, (Cyclophanes), 119-78.
36. Tsuji, K.; Sasaki, S.; Yoshifuji, M., Synthesis and redox properties of a diphosphene carrying a redox-active sterically protecting group. *Tetrahedron Letters* **1999**, 40, (16), 3203-3206.
37. Ma, L.; Woloszynek, R. A.; Chen, W.; Ren, T.; Protasiewicz, J. D., A New Twist on Pincer Ligands and Complexes. *Organometallics* **2006**, 25, (14), 3301-3304.

38. Liu, P.; Chen, Y.; Deng, J.; Tu, Y., An Efficient Method for the Preparation of Benzylic Bromides. *Synthesis* **2001**, 14, 2078-2080.
39. Techniques included ^1H and ^{13}C 1D spectra, ^1H - ^1H Correlation Spectroscopy (COSY), Heteronuclear Multiple Quantum Coherence (HMQC), Distortionless Enhancement by Polarization Transfer (DEPT) and Differential Nuclear Overhauser Effect (NOE). Spectra and full spectral assignments are provided in the ESI.
40. Jorgensen, W. L.; Severance, D. L., Aromatic-Aromatic Interactions: Free Energy Profiles for the Benzene Dimer in Water, Chloroform, and Liquid Benzene. *Journal of the American Chemical Society* **1990**, 112, 4768-4774.
41. Du, C. J. F.; Hart, H.; Ng, K. K. D., A one-pot synthesis of m-terphenyls, via a two-aryne sequence. *Journal of Organic Chemistry* **1986**, 51, (16), 3162-5.
42. Adimurthy, S.; Ramachandraiah, G.; Ghosh, P. K.; Bedekar, A. V., A new, environment friendly protocol for iodination of electron-rich aromatic compounds. **2003**, 44, (27), 5099-5101.
43. Grewal, R. S.; Hart, H.; Vinod, T. K., Oxacyclophanes based on a m-terphenyl framework. *Journal of Organic Chemistry* **1992**, 57, (9), 2721-2726.
44. Bonifacio, M. C.; Robertson, C. R.; Jung, J.-Y.; King, B. T., Polycyclic Aromatic Hydrocarbons by Ring-Closing Metathesis. *J. Org. Chem* **2005**, 70, 8522-8526.
45. Platera, M. J.; Sinclair, J. P.; Aiken, S.; Gelbrich, T.; Hursthouse, M. B., The CA.M lattice revisited. Gel formation from a linear bis-isocyanuric acid and 2-amino-4,6-bis-(4-tert-butylphenylamino)-1,3,5-triazine. *Tetrahedron* **2004**, 60, (30), 6385-6394.

46. Bong, D. T. Y.; Chan, E. W. L.; Diercks, R.; Dosa, P. I.; Haley, M. M.; Matzger, A. J.; Miljanic, O. S.; Vollhardt, K. P. C.; Bond, A. D.; Teat, S. J.; Stanger, A., Syntheses of Syn and Anti Doublebent [5]Phenylene. *Org. Lett.* **2004**, 6, (13), 2249-2252.
47. Zhu, Z.; Swager, T. M., Conjugated Polymers Containing 2,3-Dialkoxybenzene and Iptycene Building Blocks. *Organic Letters* **2001**, 3, (22), 3471-3474.
48. Ramey, M. B.; Hiller, J. A.; Rubner, M. F.; Tan, C.; Schanze, K. S.; Reynolds, J. R., Amplified Fluorescence Quenching and Electroluminescence of a Cationic Poly(*p*-phenylene-co-thiophene) Polyelectrolyte. *Macromolecules* **2005**, 38, (2), 234-243.
49. Victor, A. S.; Walter, H., Palladium-catalyzed synthesis of poly(*p*-phenyleneethynylene)s. *Macromolecular Chemistry and Physics* **1994**, 195, (1), 303-314.
50. *Handbook of Photochemistry*. 3rd ed.; CRC Press: Boca Raton, 2006; 'Vol.' p.

APPENDICES

Appendix 6 A

NMR Spectra

Compound 2

Structure

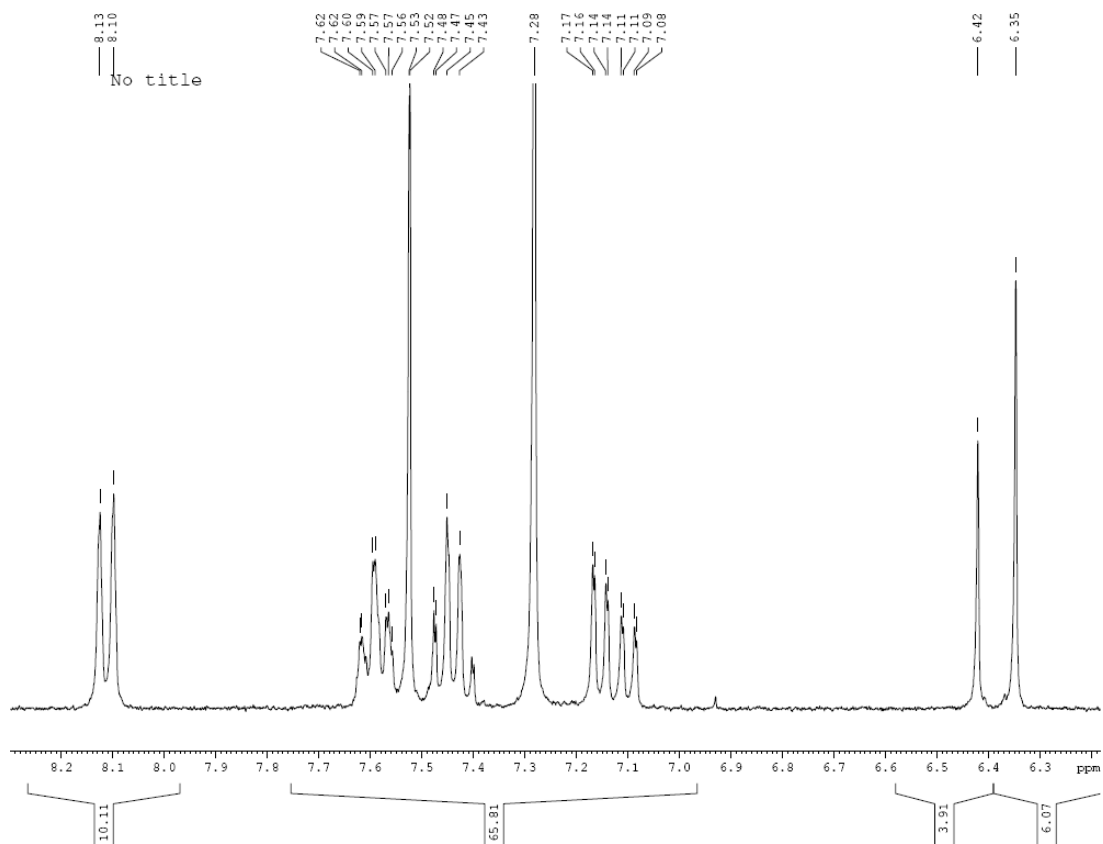
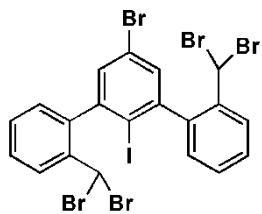
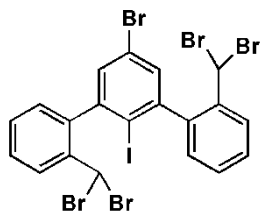


Figure 6 A.1 ^1H NMR (300 MHz, CDCl_3 no peaks other than a water peak from the NMR solvent appear outside this range) of **2**.

Compound 2

Structure



RCS-Am-JH-tetrabromo-terphenyl-13C

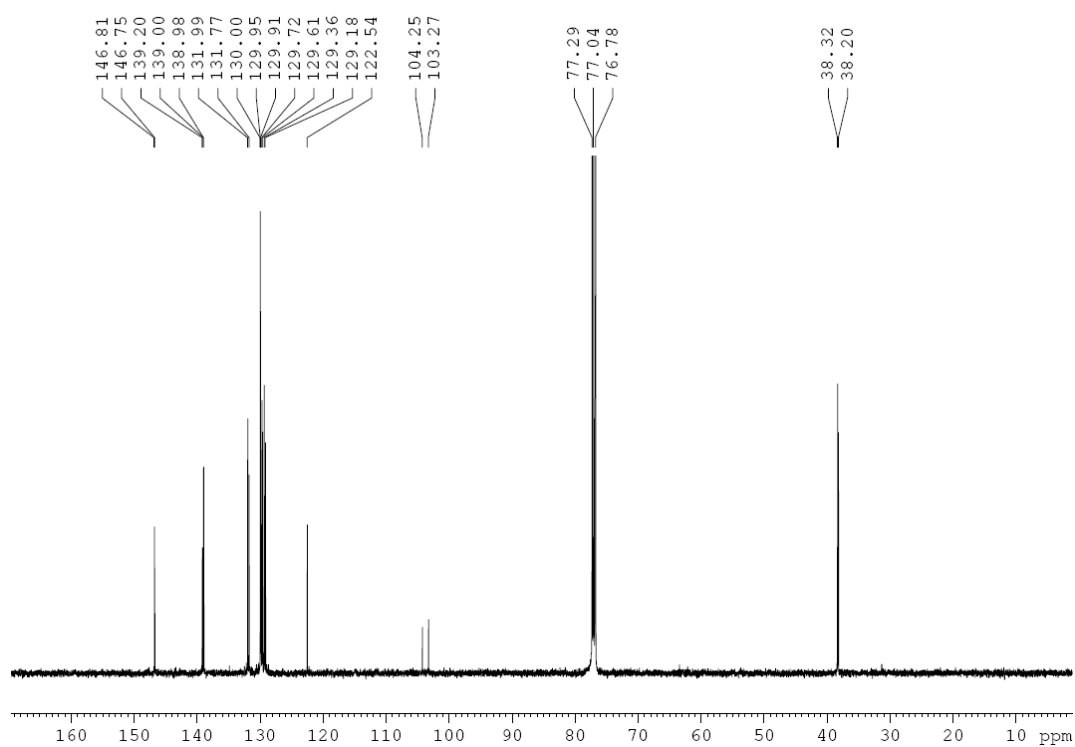


Figure 6 A.2 ^{13}C NMR (125 MHz, CDCl_3) of 2.

Compound 3

Structure

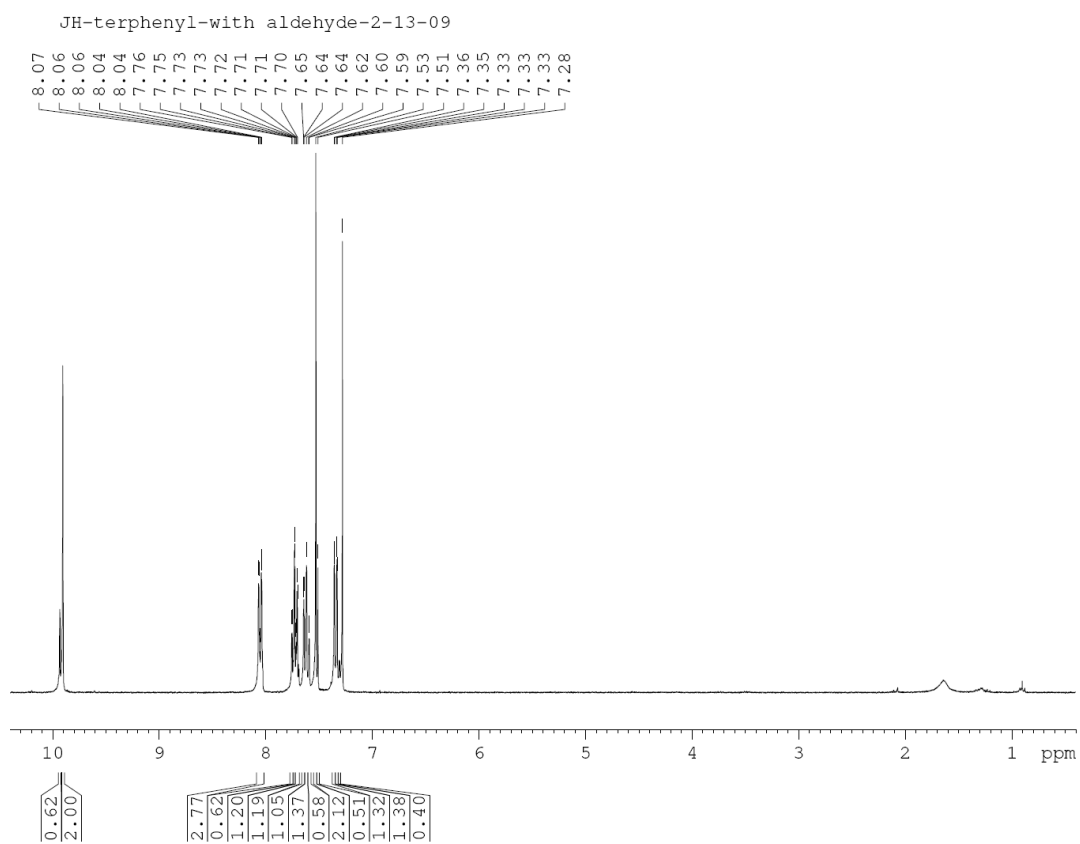
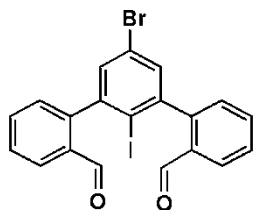
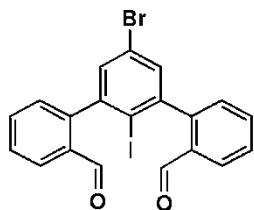


Figure 6 A.3 ^1H NMR (300 MHz, CDCl_3) of 3.

Compound 3

Structure



JH-terphenyl-with aldehyde-2-13-09-13C

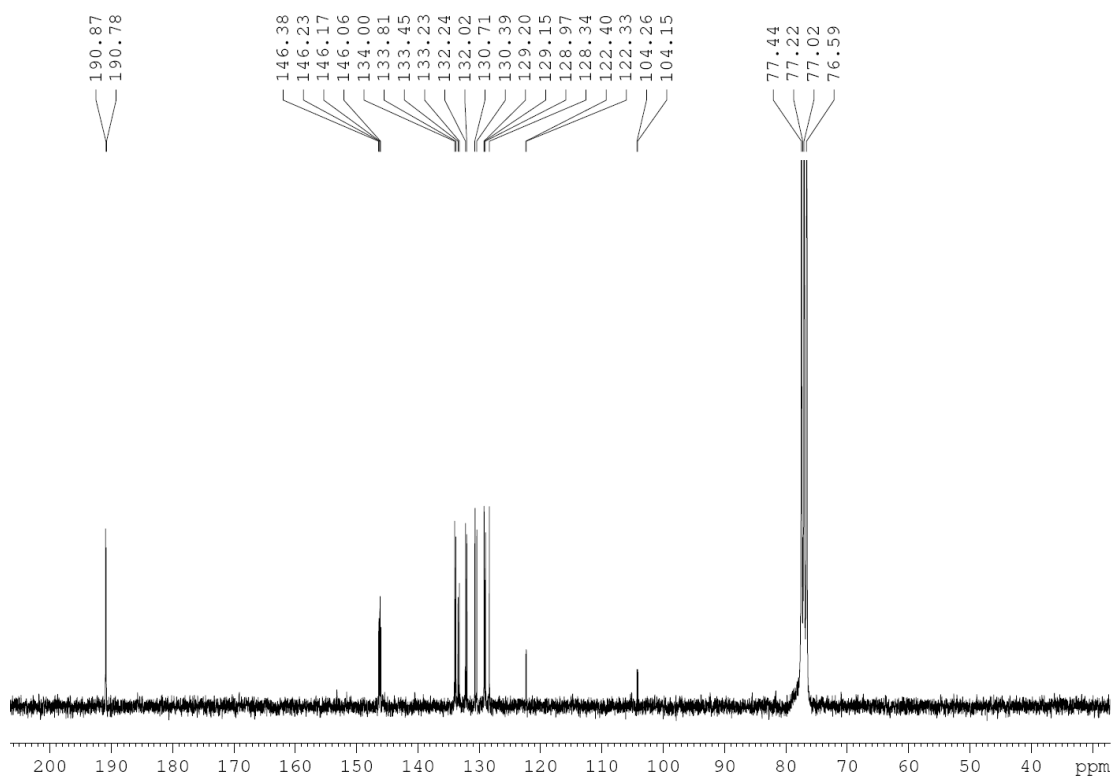


Figure 6 A.4 ^{13}C NMR (125 MHz, CDCl_3) of 3.

Compound 4

Structure

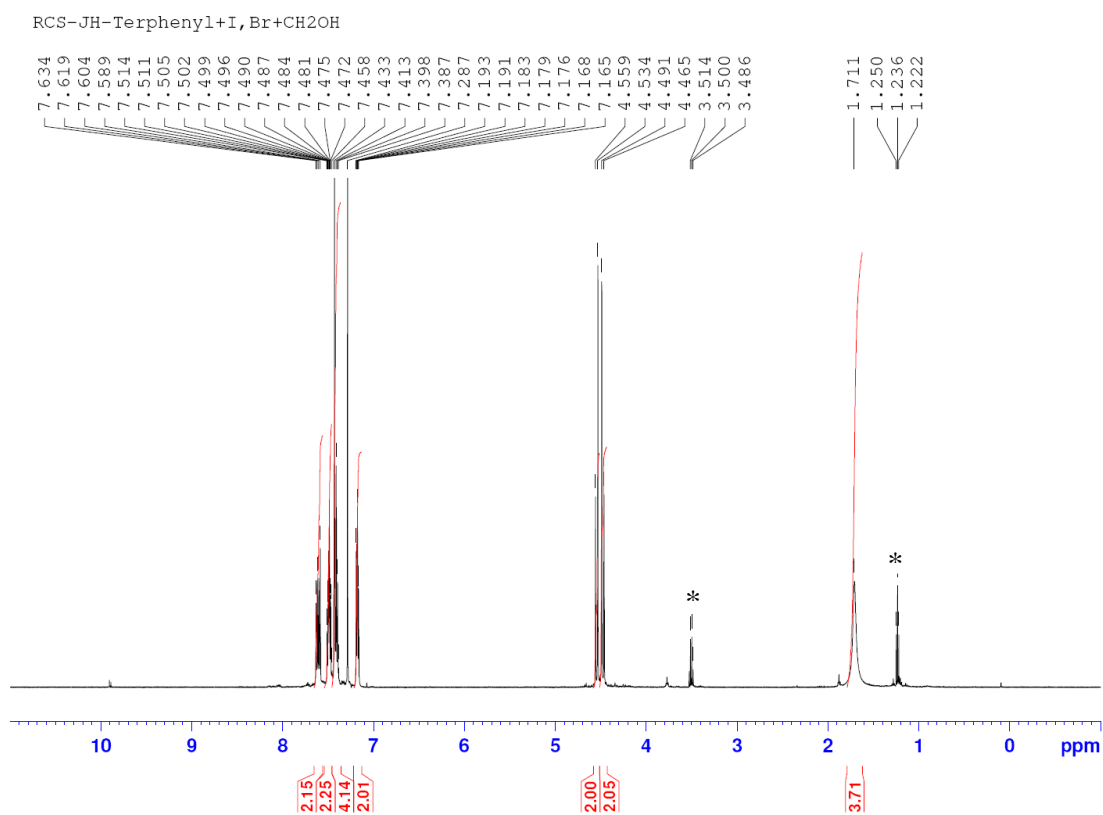
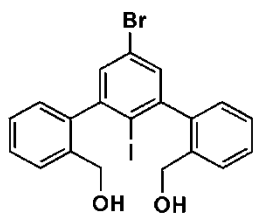
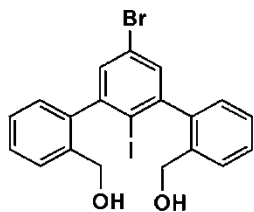


Figure 6 A.5 ^1H NMR (300 MHz, CDCl_3) of **4**. Peaks marked with an asterisk are attributable to diethyl ether.

Compound 4

Structure



RCS-JH-Terphenyl+I, Br+CH₂OH-13C

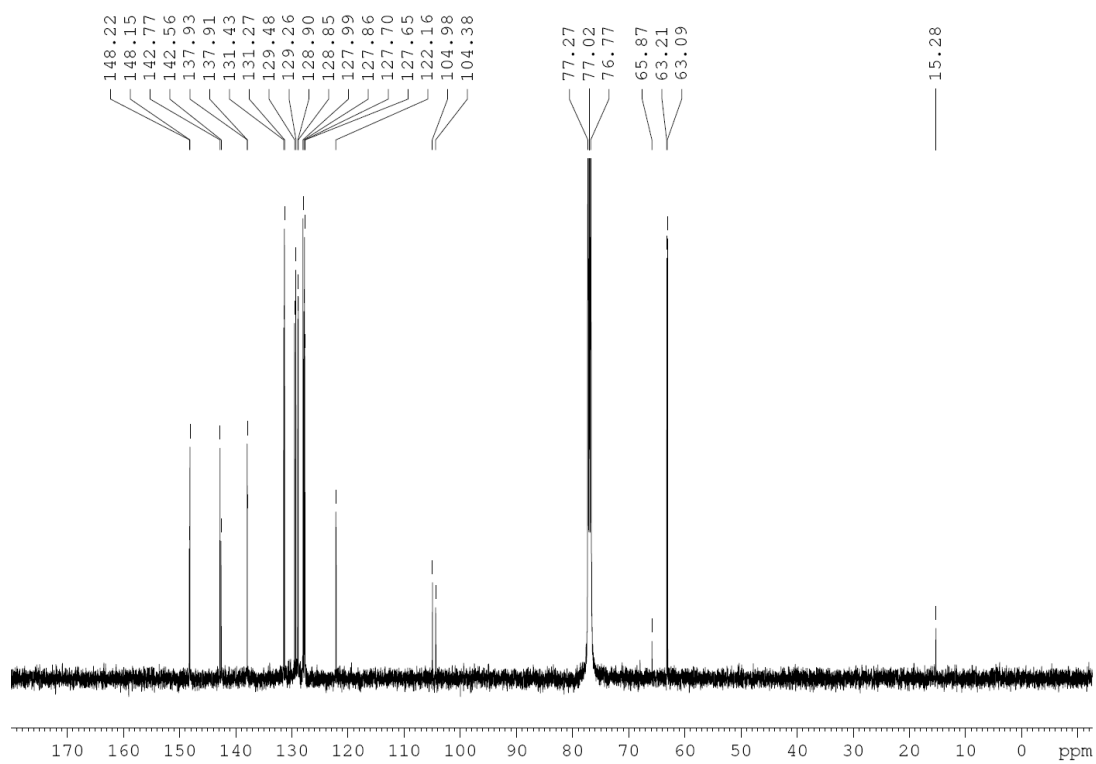


Figure 6 A.6 ¹³C NMR (125 MHz, CDCl₃) of **4**.

Compound 5

Structure

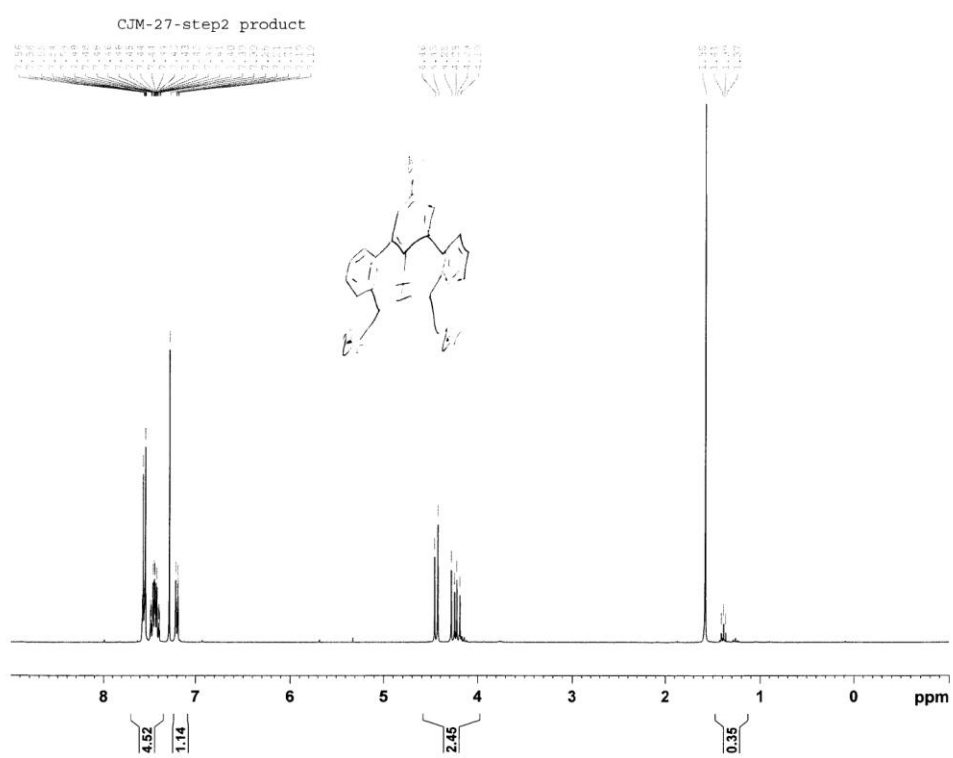
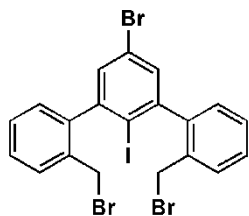


Figure 6 A.7 ^1H NMR (300 MHz, CDCl_3) of 5.

Compound 5

Structure

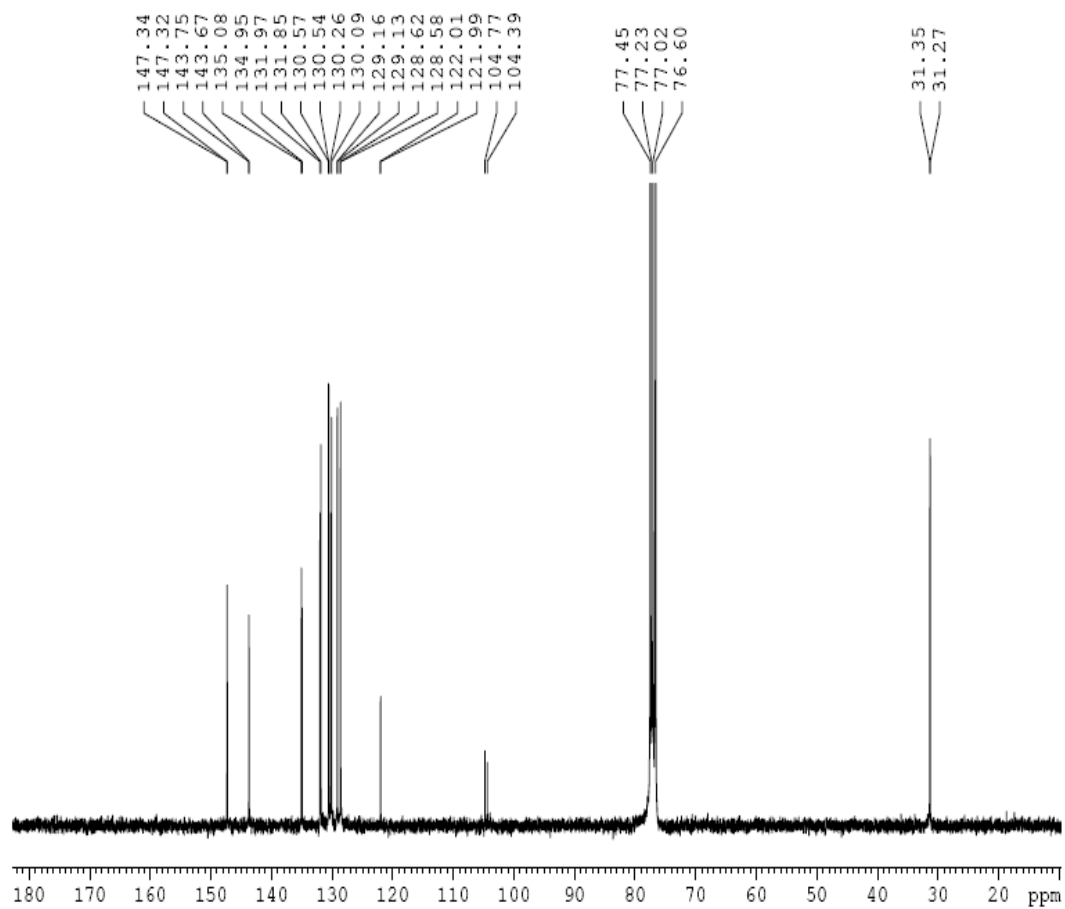
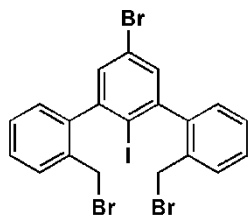


Figure 6 A.8 ^{13}C NMR (125 MHz, CDCl_3) of 5.

Compound 6

Structure

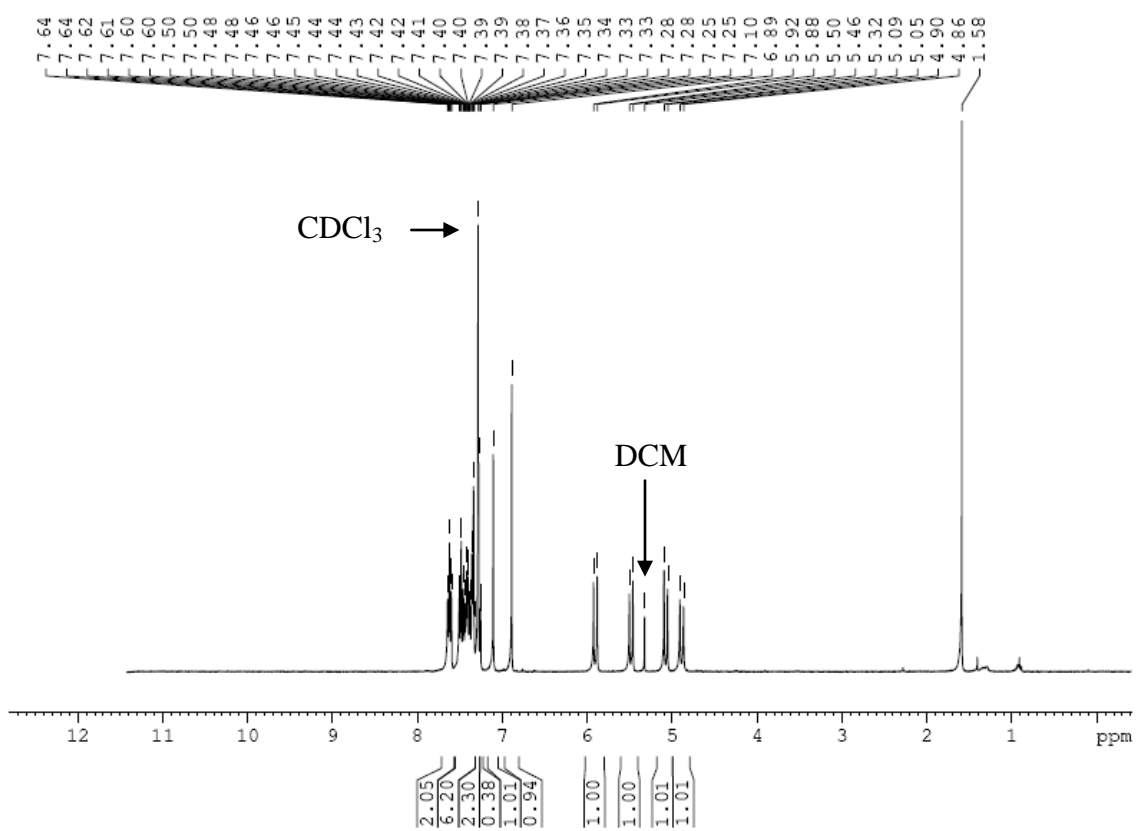
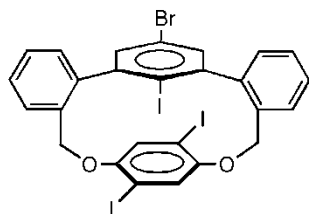


Figure 6 A.9 ¹H NMR (300 MHz, CDCl₃) of 6.

Compound 6

Structure

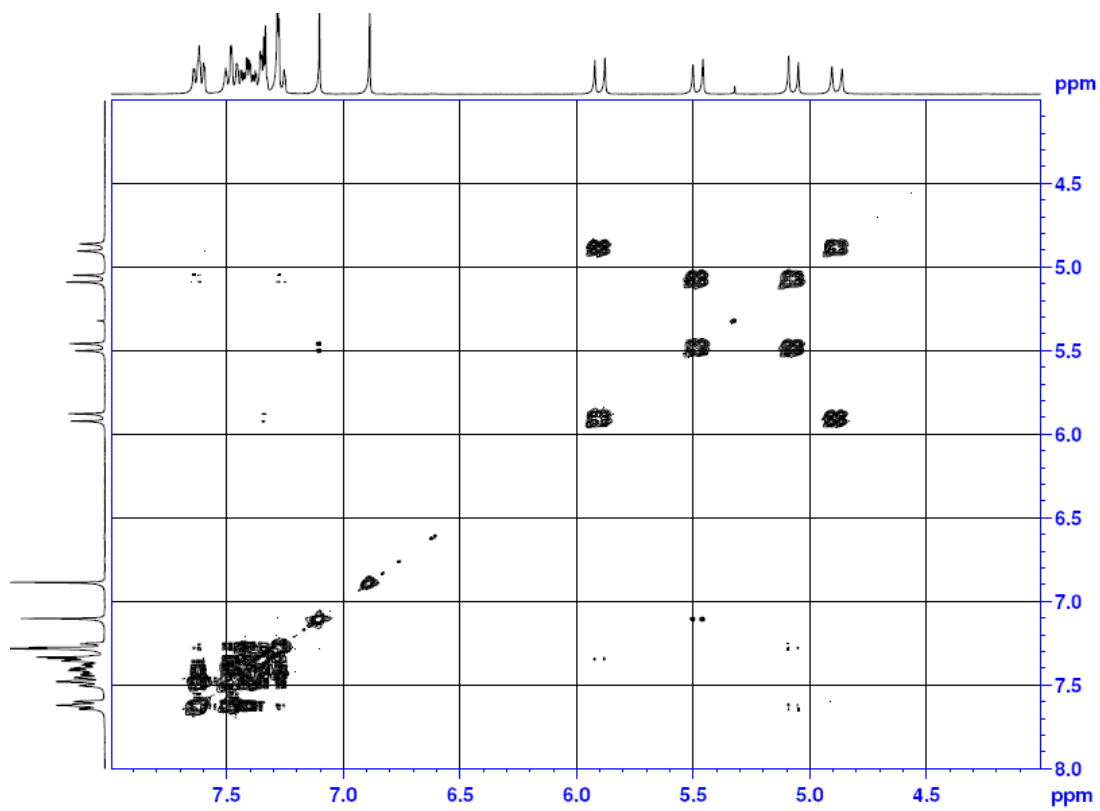
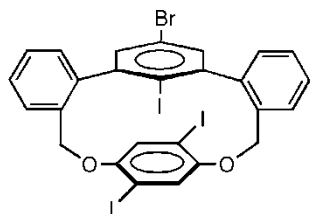


Figure 6 A.10 ^1H - ^1H COSY NMR (300 MHz, CDCl_3) of 6.

Compound 6

Structure

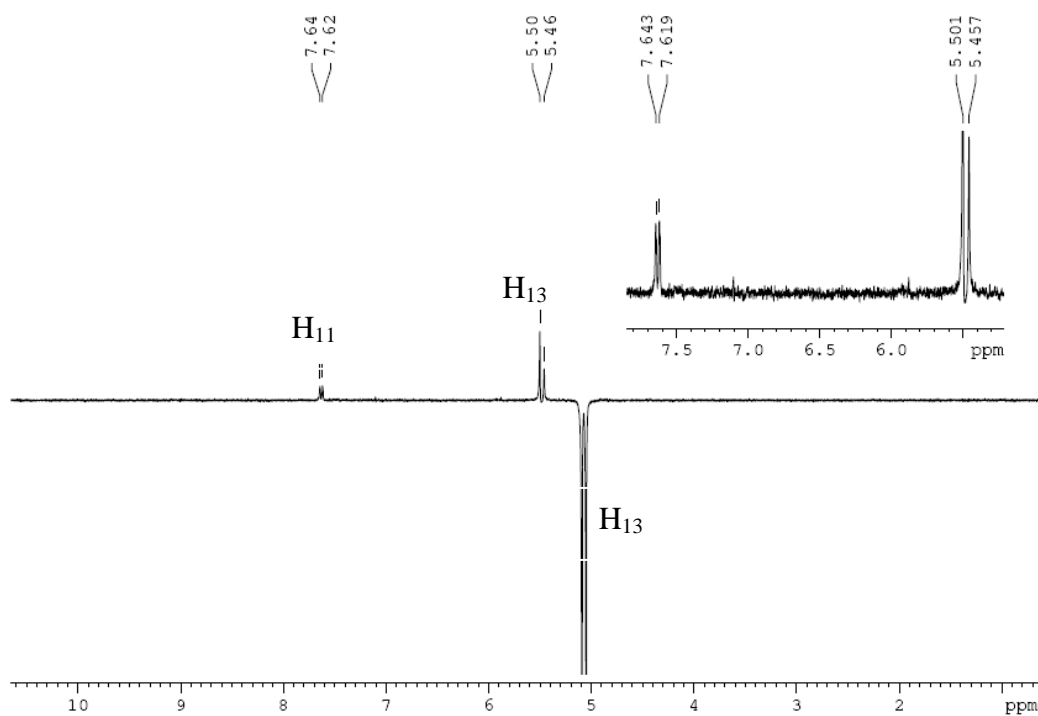
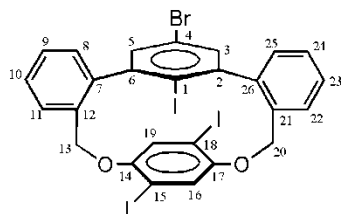


Figure 6 A.11 NOE spectra (300 MHz, CDCl₃) of **6** for proton resonating at 5.05 ppm.

Compound 6

Structure

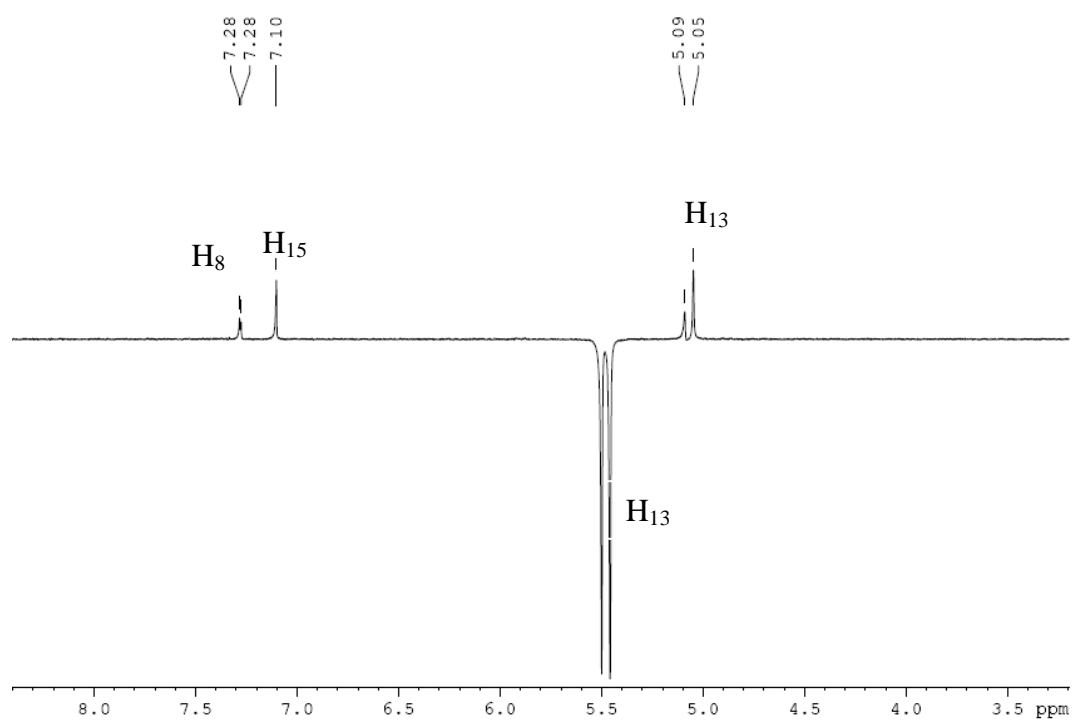
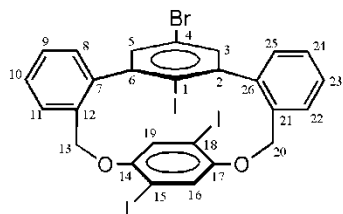


Figure 6 A.12 NOE spectra (300 MHz, CDCl₃) of **6** for proton resonating at 5.50 ppm.

Compound 6

Structure

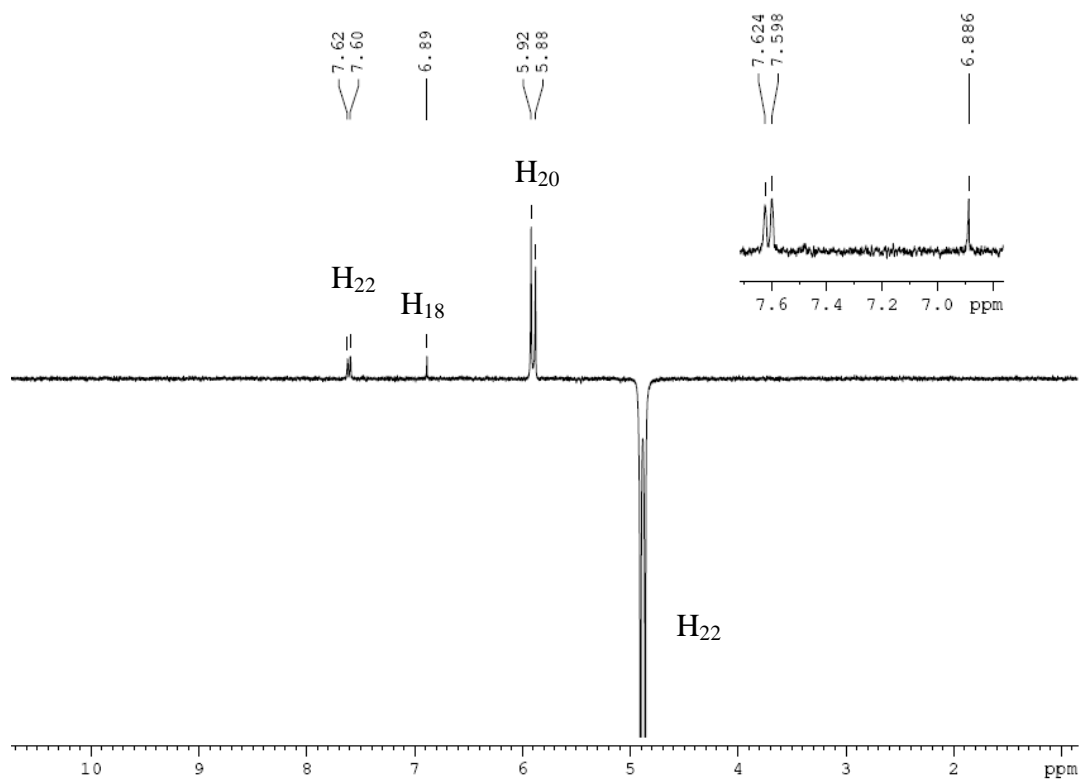
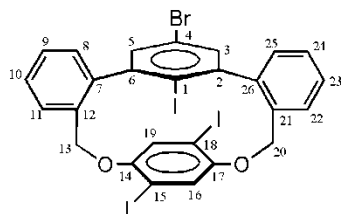


Figure 6 A.13 NOE spectra (300 MHz, CDCl₃) of **6** for proton resonating at 4.86 ppm.

Compound 6

Structure

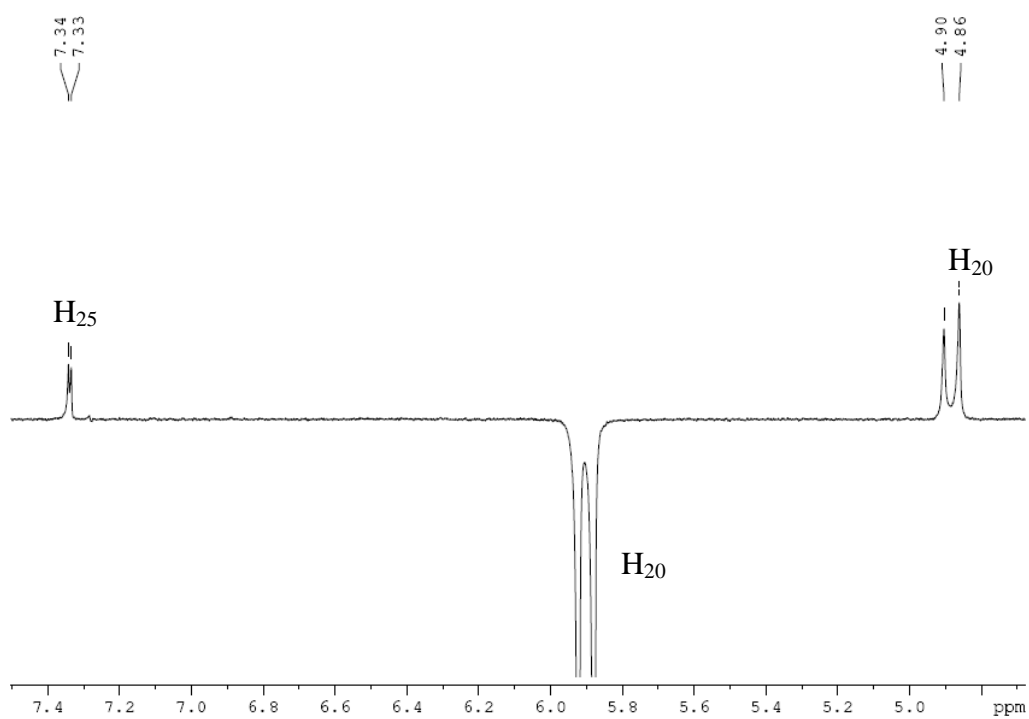
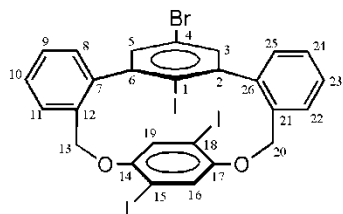


Figure 6 A.14 NOE spectra (300 MHz, CDCl₃) of **6** for proton resonating at 5.88 ppm.

Compound 6

Structure

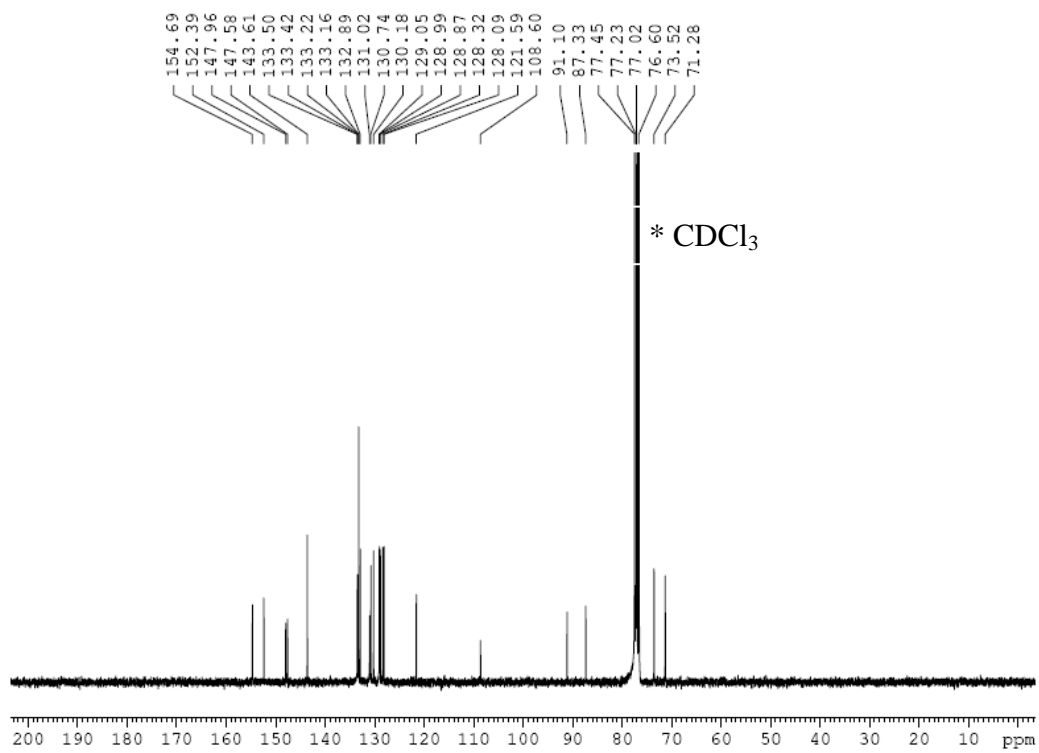
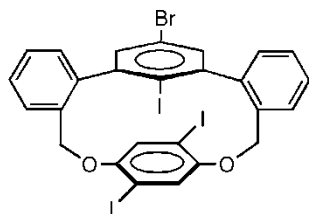


Figure 6 A.15 ¹³C NMR (75 MHz, CDCl₃) of 6.

Compound 6

Structure

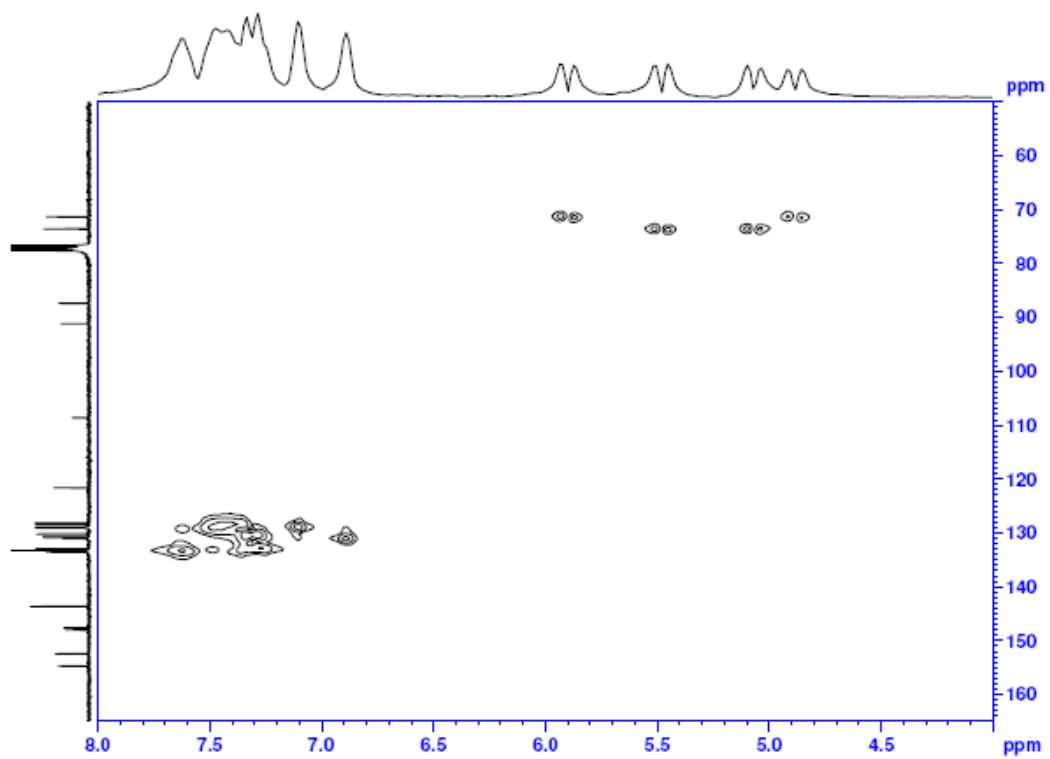
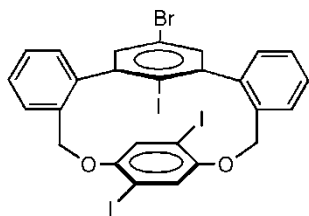


Figure 6 A.16 Heteronuclear Multiple Quantum Coherence (HMQC) spectra (300 MHz for ^1H , 75 MHz for ^{13}C , CDCl_3) of **6**.

Compound 6

Structure

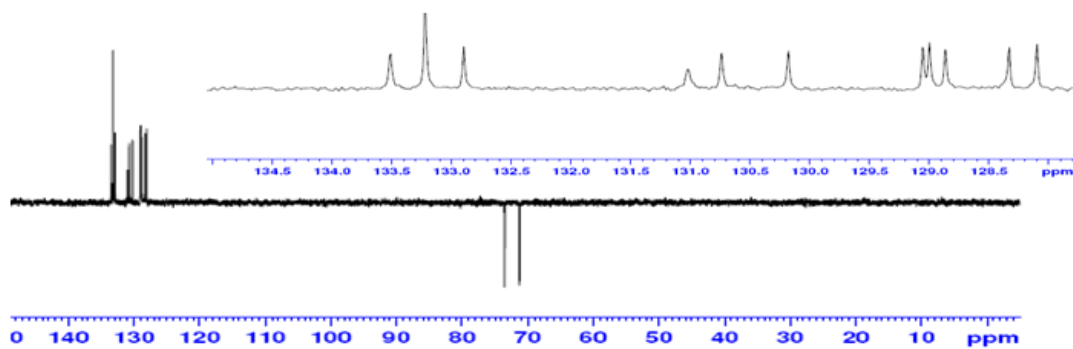
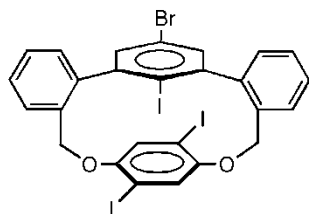


Figure 6 A.17 Distortionless Enhancement by Polarization Transfer (DEPT-135) spectra (75 MHz, CDCl₃) of **6**.

Compound 7

Structure

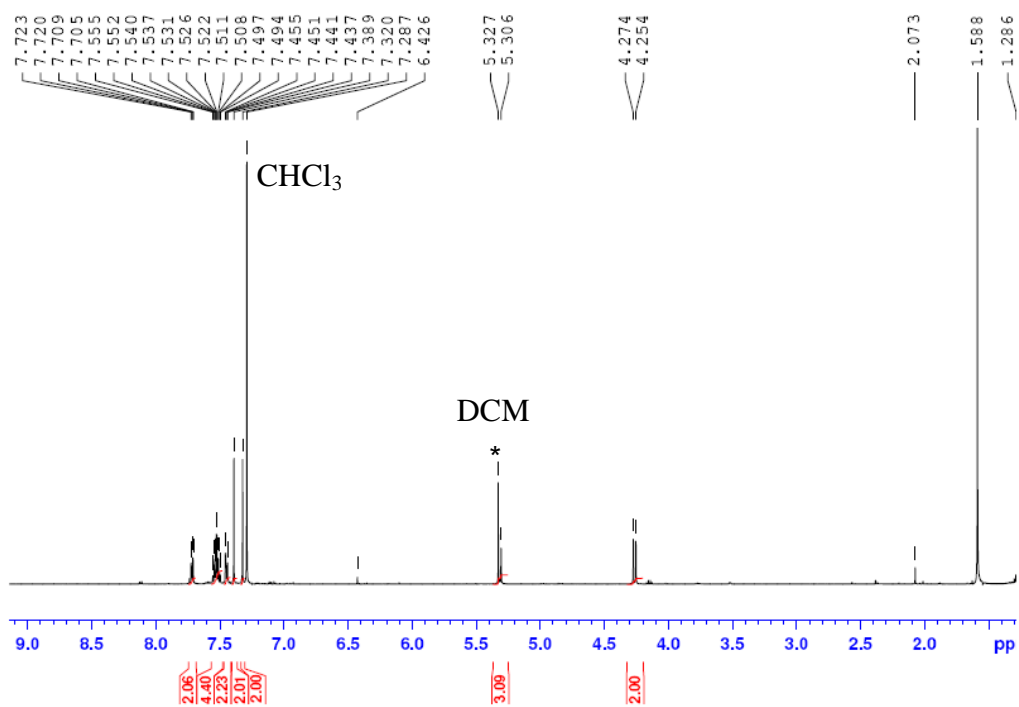
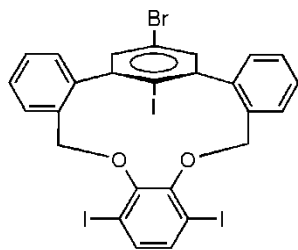


Figure 6 A.18 ¹H NMR (500 MHz, CDCl₃) of 7.

Compound 7

Structure

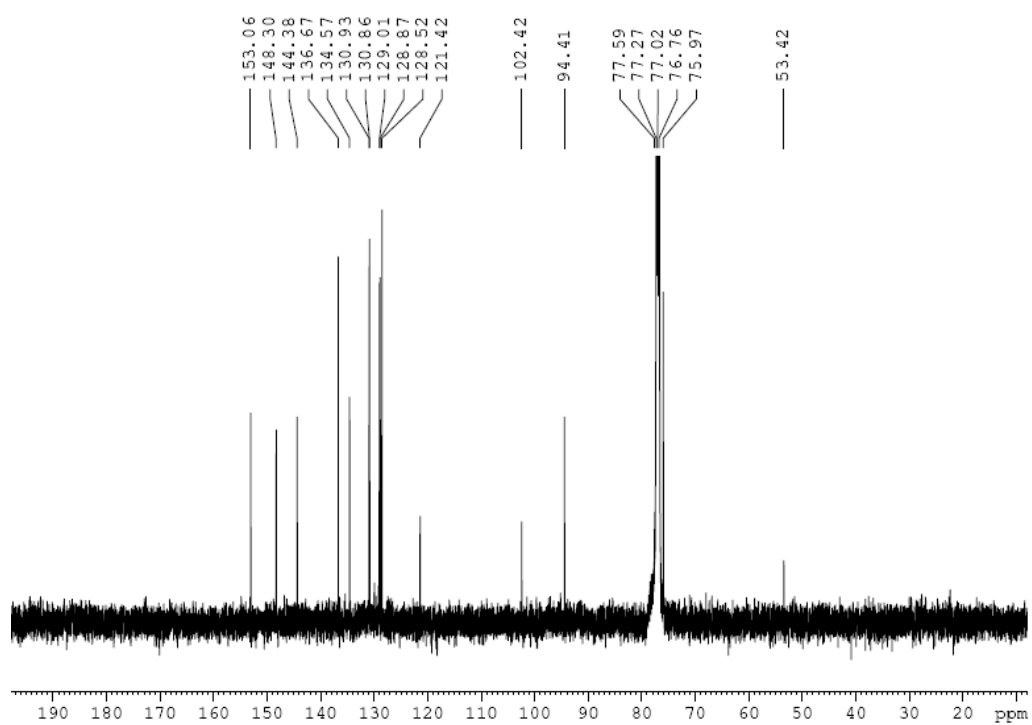
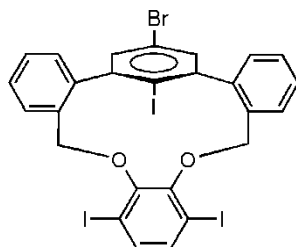


Figure 6 A.19 ¹³C NMR (125 MHz, CDCl₃) of 7.

Compound **OC1**

Structure

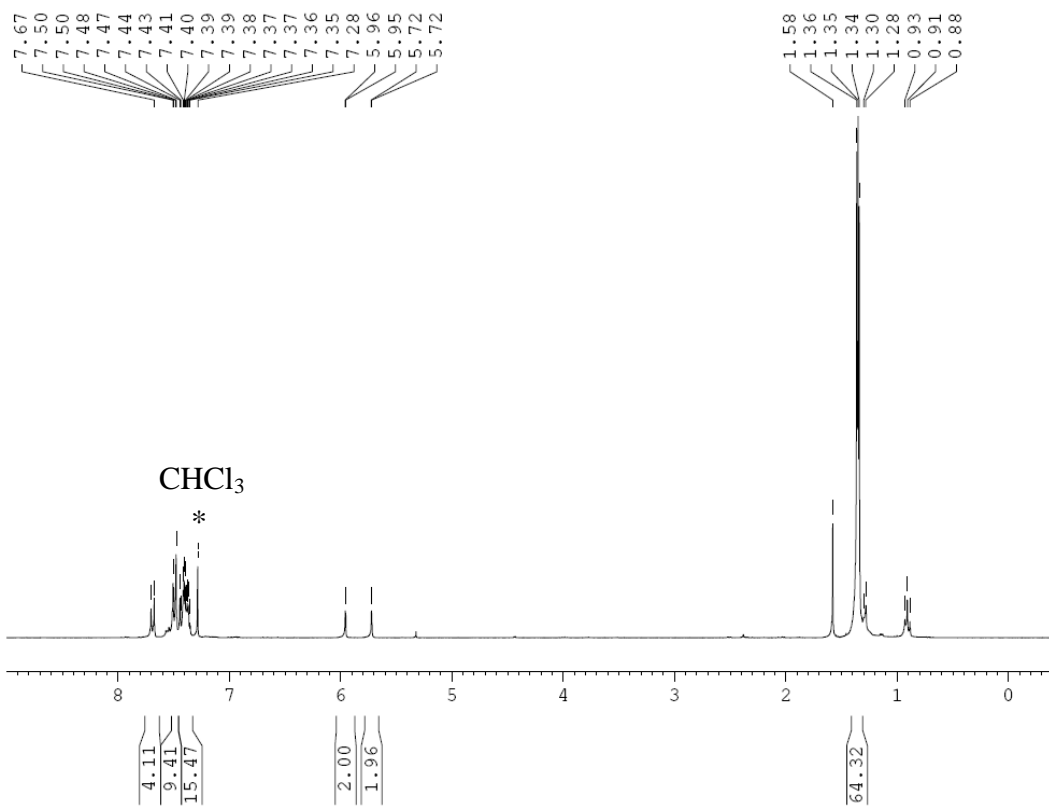
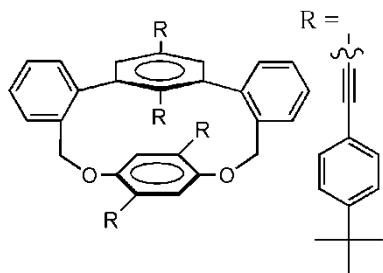


Figure 6 A.20 ¹H NMR (300 MHz, CDCl₃) of **OC1**.

Compound OC1

Structure

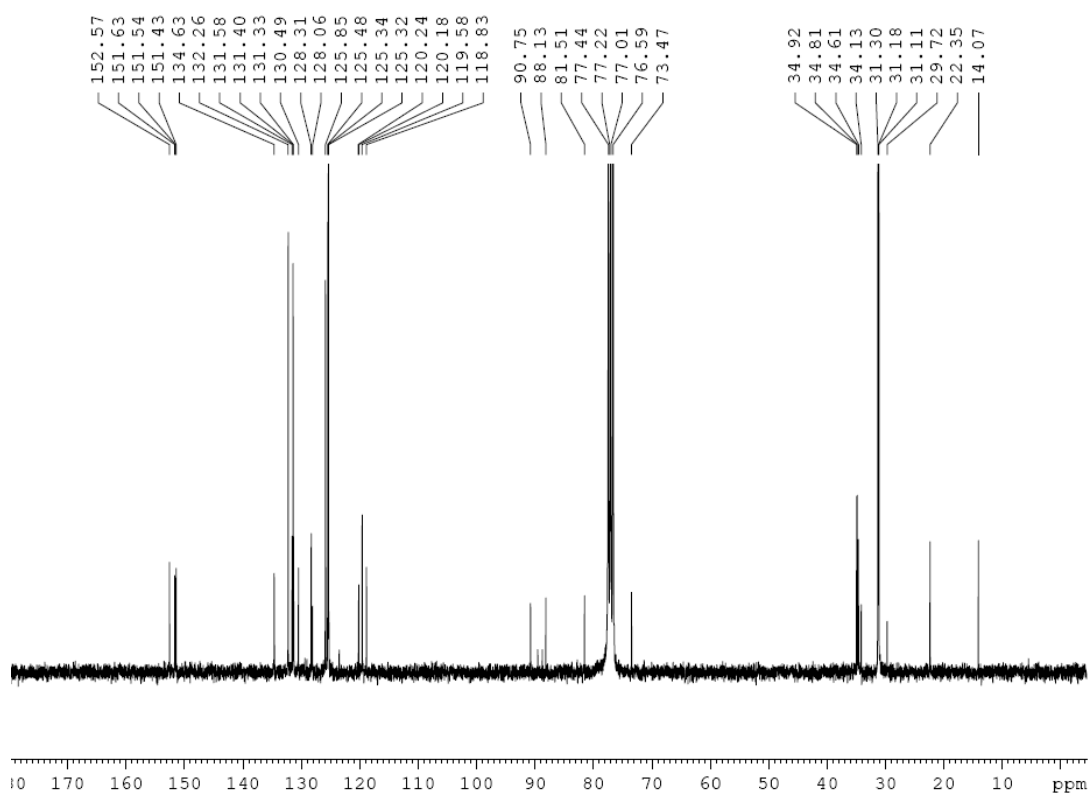
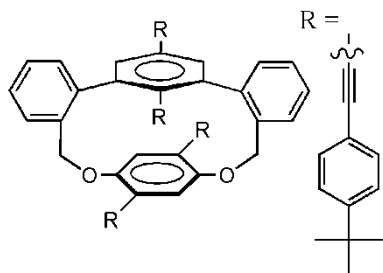


Figure 6 A.21 ^{13}C NMR (75 MHz, CDCl_3) of OC1.

Compound OC2

Structure

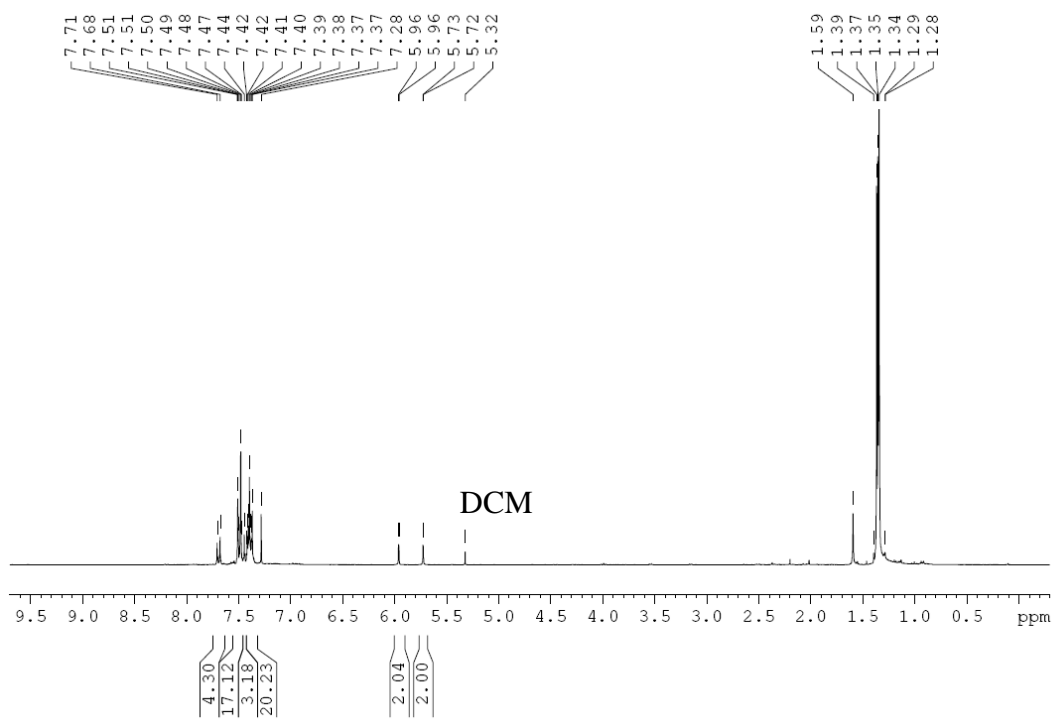
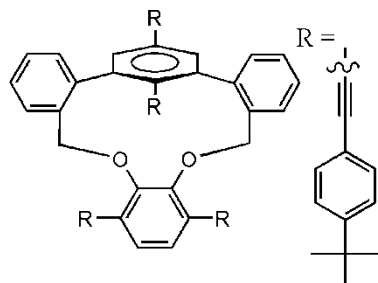


Figure 6 A.22 ^1H NMR (300 MHz, CDCl_3) of OC2.

Compound **M1**

Structure

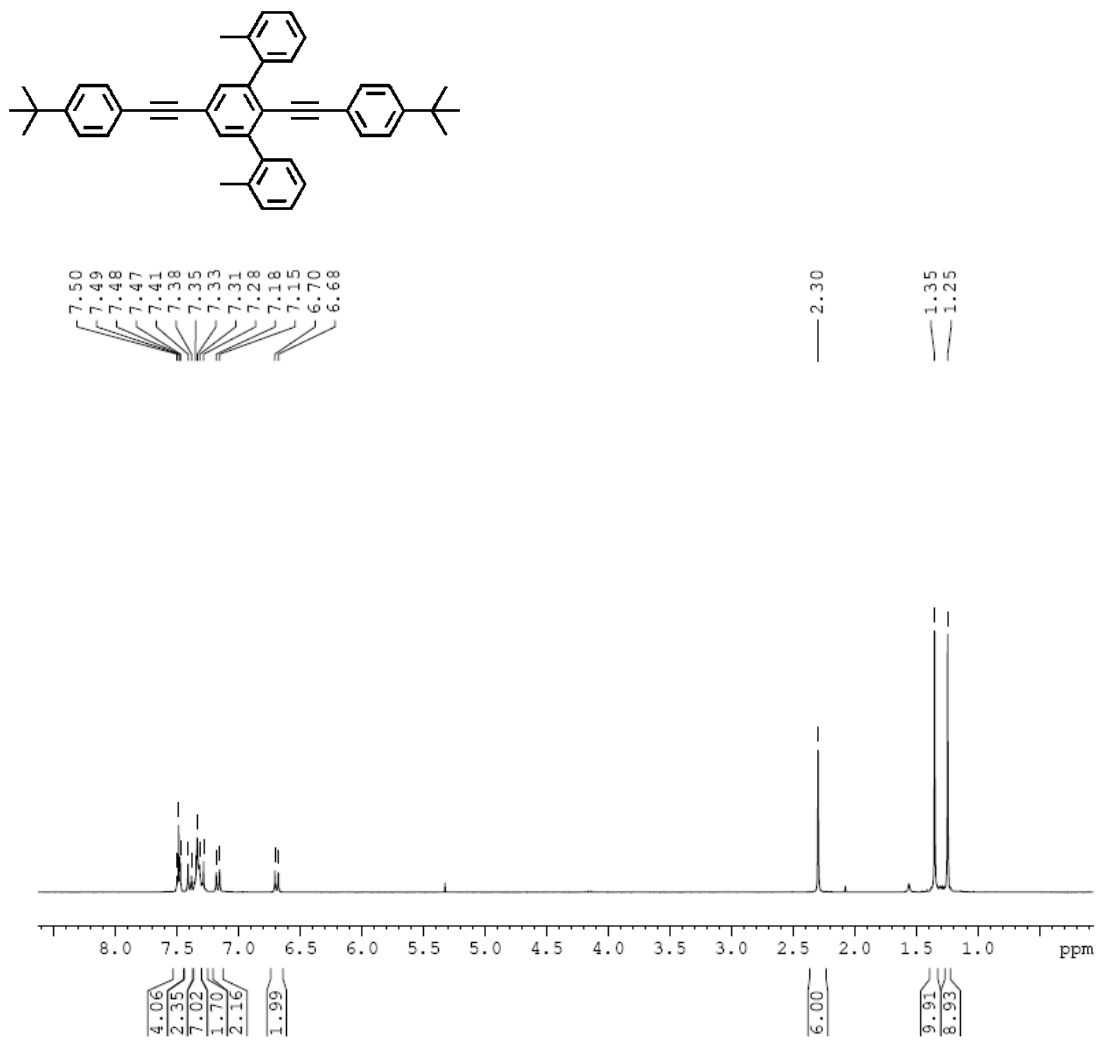


Figure 6 A.23 ^1H NMR (300 MHz, CDCl_3) of **M1**.

Compound M1

Structure

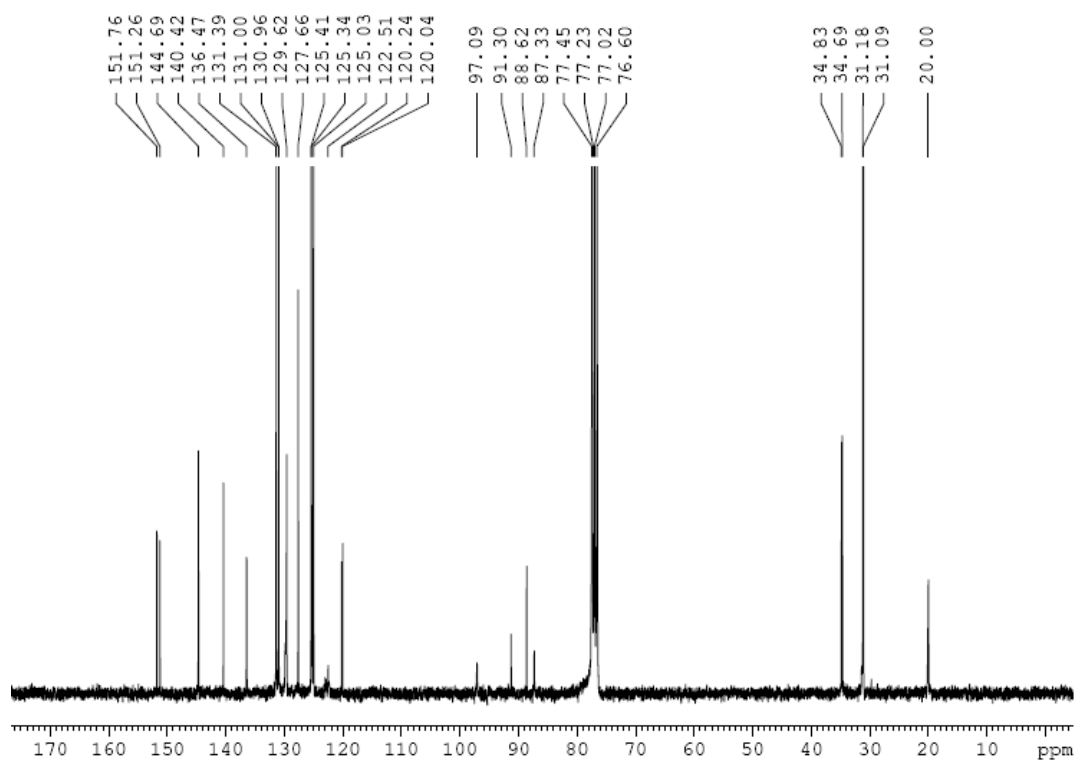
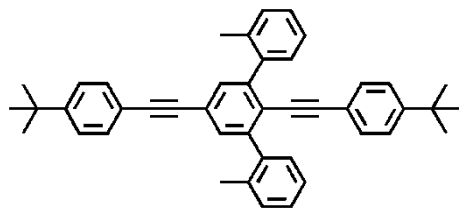


Figure 6 A.24 ¹³C NMR (75 MHz, CDCl₃) of M1.

Compound M2

Structure

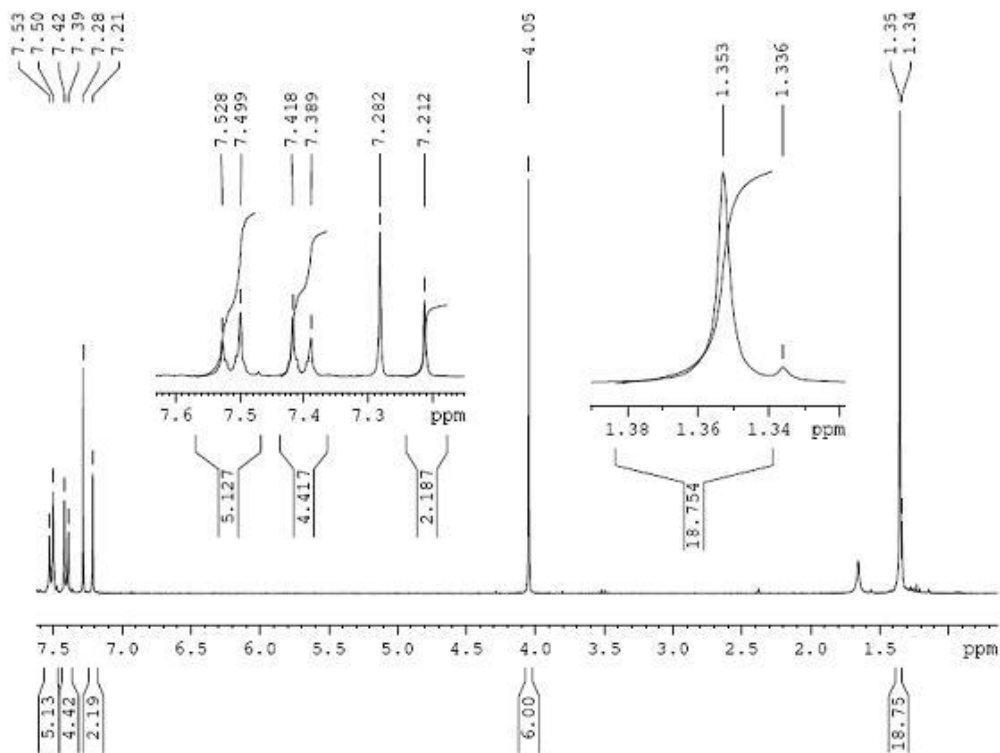
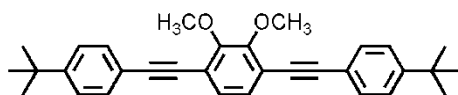


Figure 6 A.25 ¹H NMR (300 MHz, CDCl₃) of M2.

Compound M2

Structure

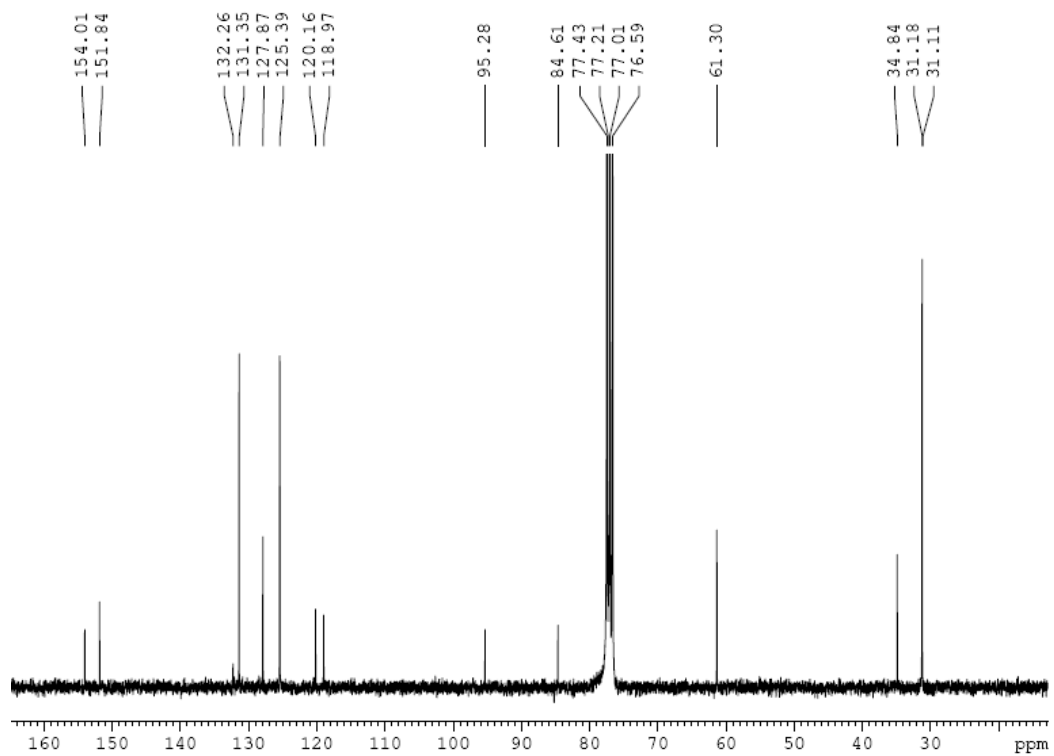
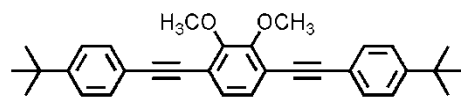


Figure 6 A.26 ¹³C NMR (75 MHz, CDCl₃) of M2.

Compound M4

Structure

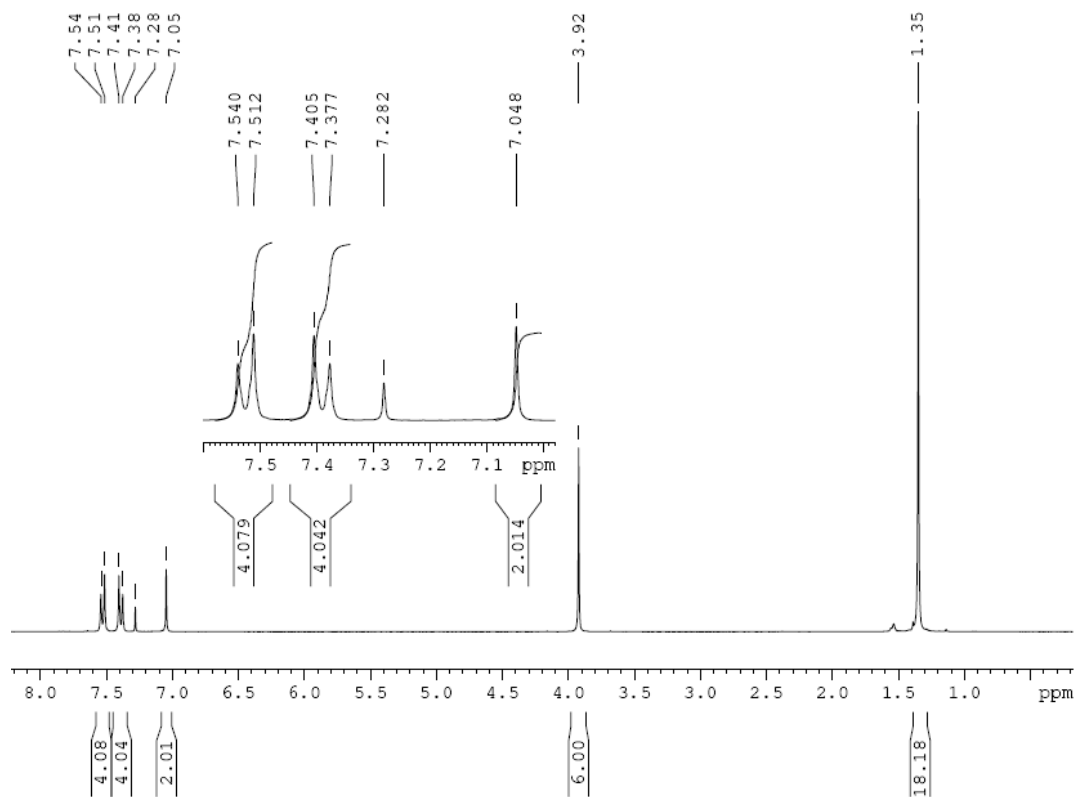
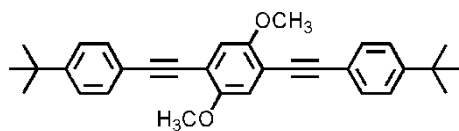


Figure 6 A.27 ^1H NMR (300 MHz, CDCl_3) of M4.

Compound M4

Structure

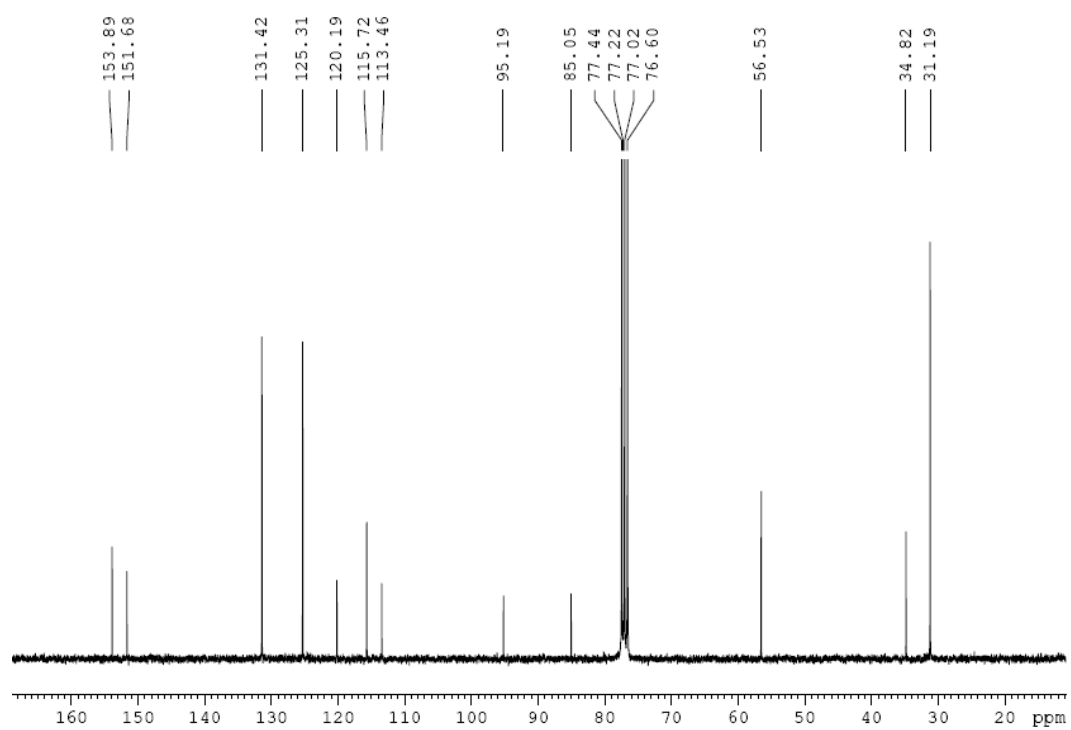
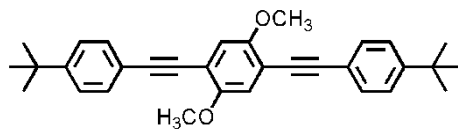


Figure 6 A.28 ¹³C NMR (75 MHz, CDCl₃) of M4.

Compound 9

Structure

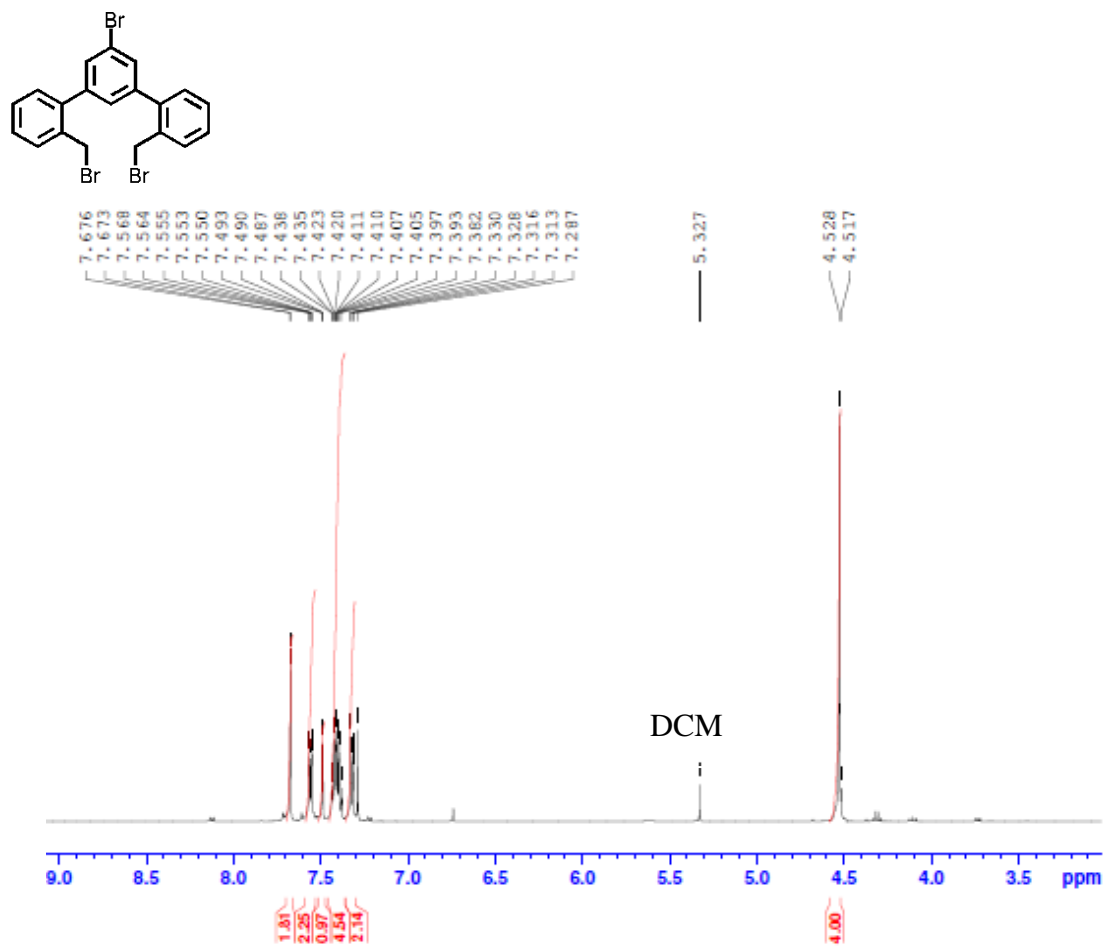


Figure 6 A.29 ¹H NMR (300 MHz, CDCl₃) of 9.

Compound 11

Structure

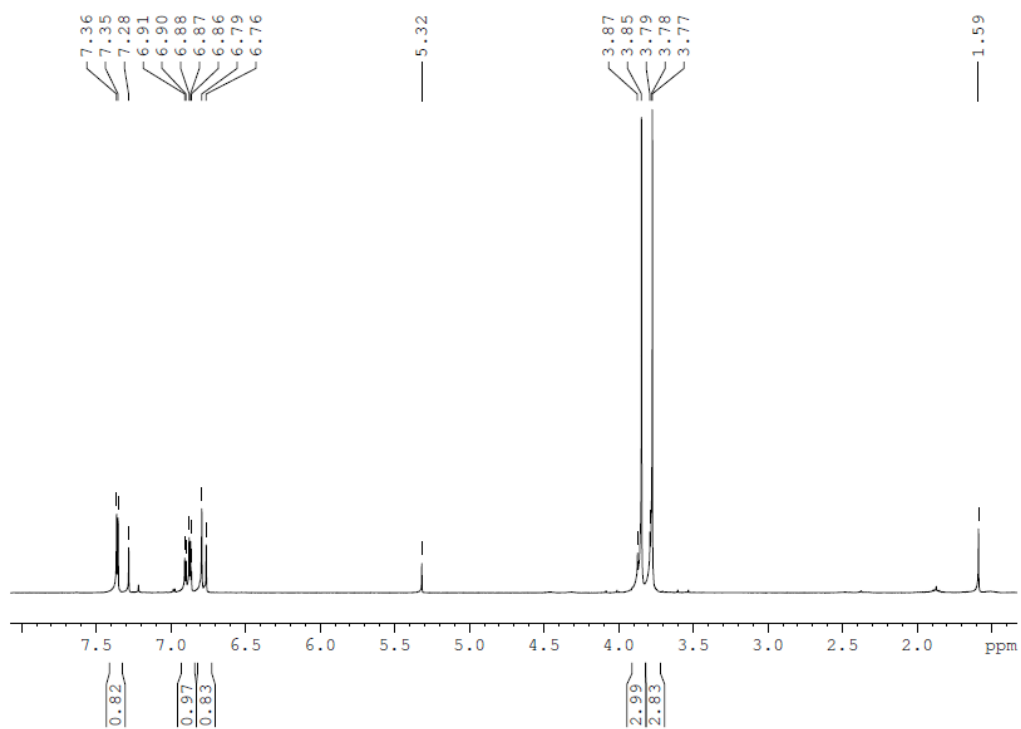
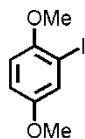


Figure 6 A.30 ¹H NMR (300 MHz, CDCl₃) of 11.

Compound **11**

Structure

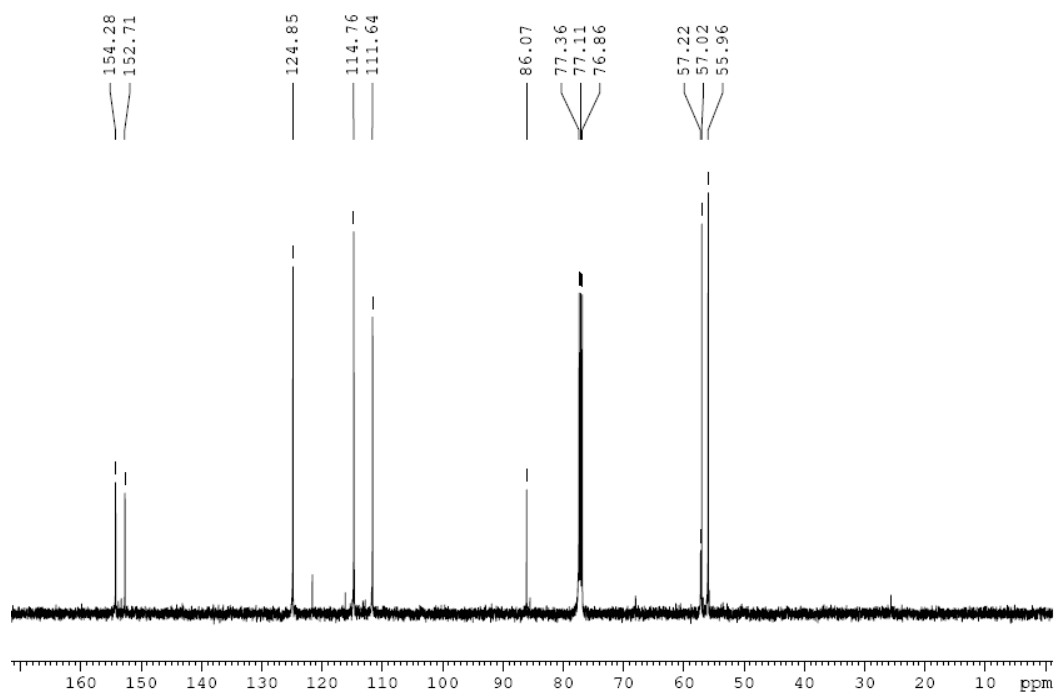
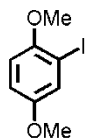


Figure 6 A.31 ^{13}C NMR (75 MHz, CDCl_3) of **11**.

Compound 12

Structure

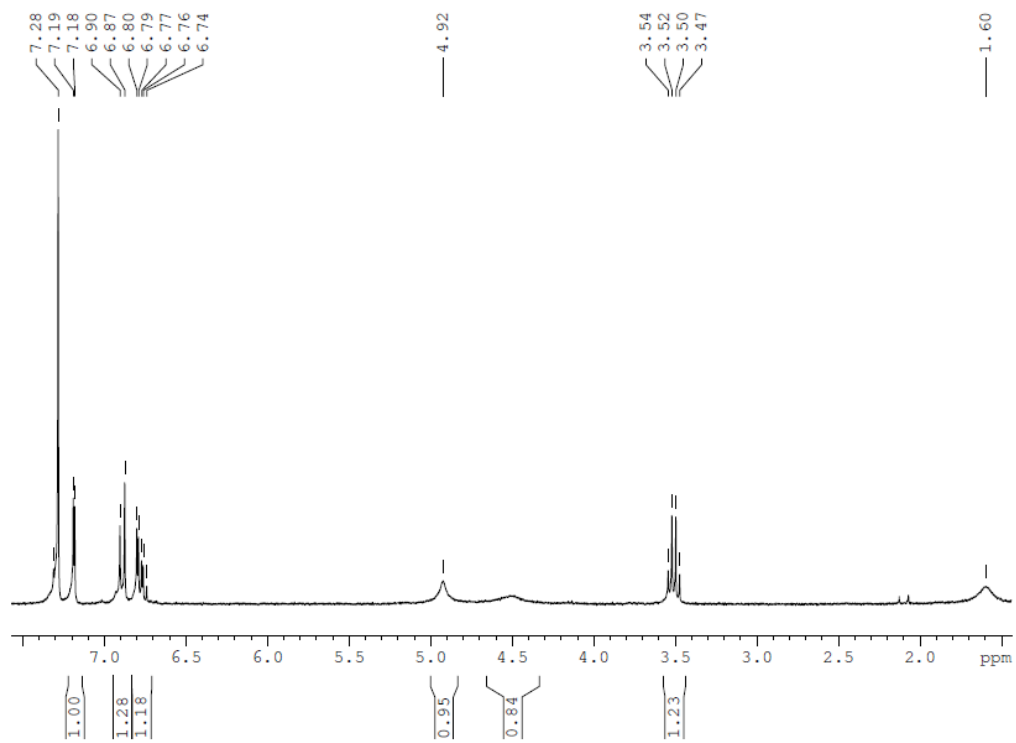
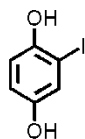


Figure 6 A.32 ^1H NMR (300 MHz, CDCl_3) of 12.

Compound **12**

Structure

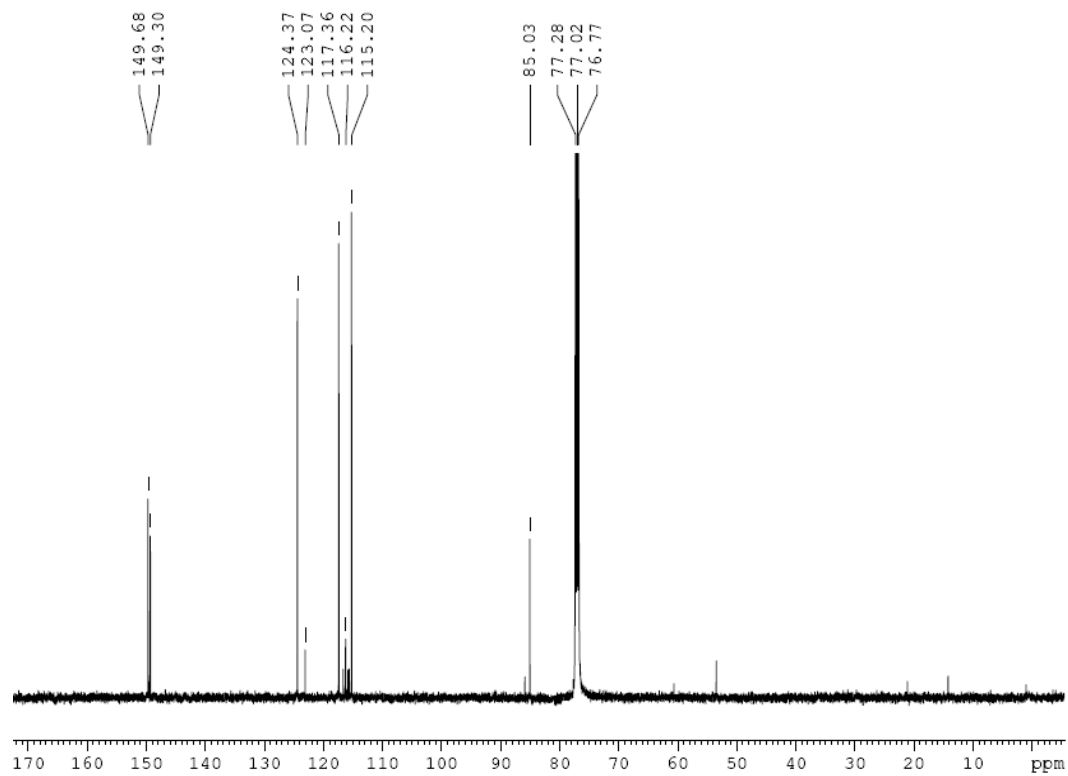
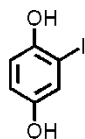


Figure 6 A.33 ^{13}C NMR (75 MHz, CDCl_3) of **12**.

Compound 13

Structure

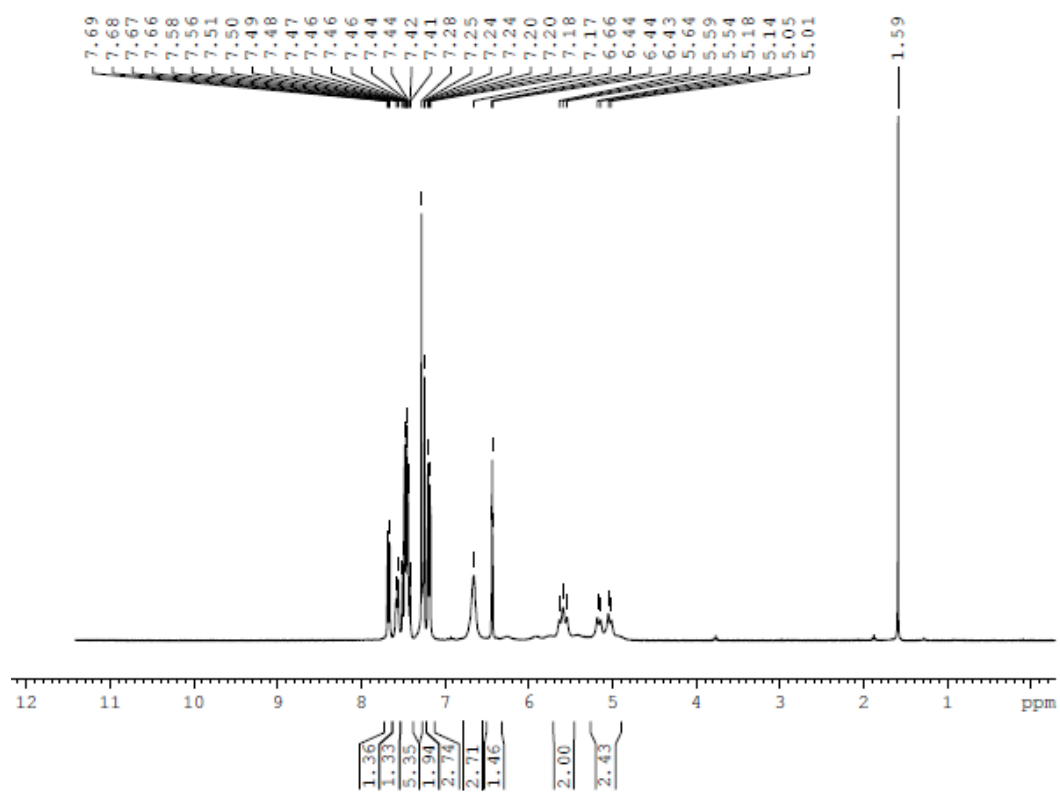
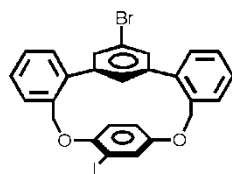


Figure 6 A.34 ^1H NMR (300 MHz, CDCl_3) of 13.

Compound 13

Structure

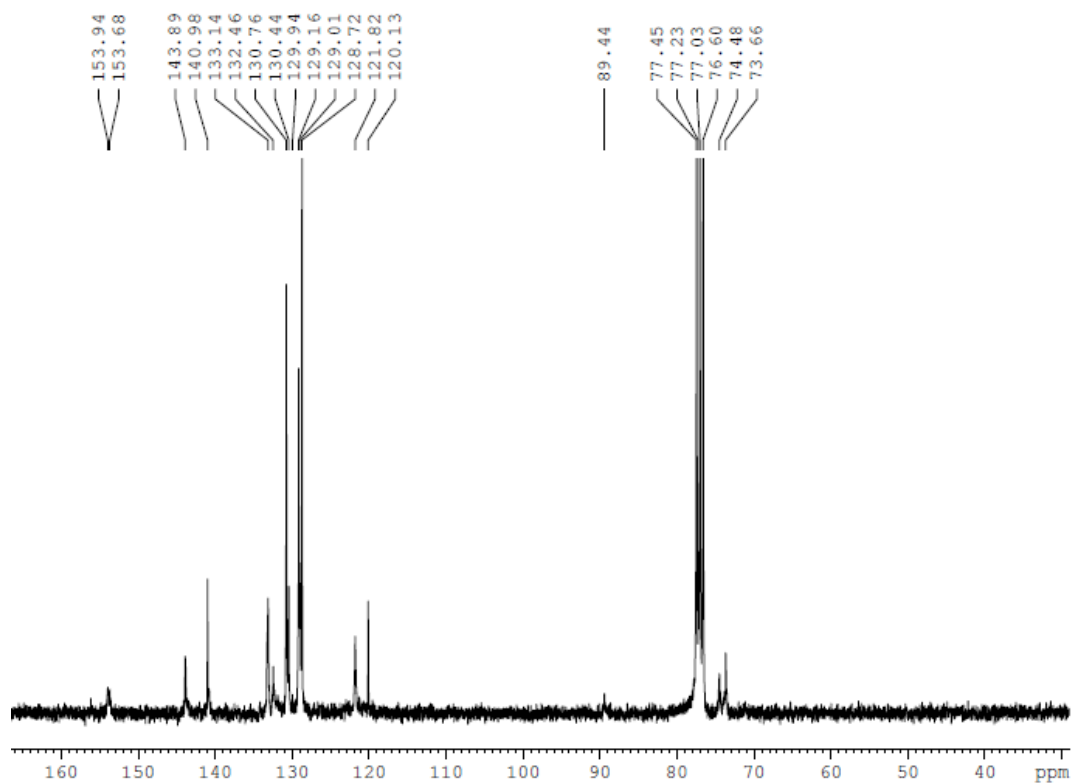
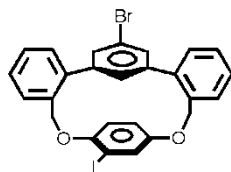


Figure 6 A.35 ^{13}C NMR (75 MHz, CDCl_3) of 13.

Compound **14**

Structure

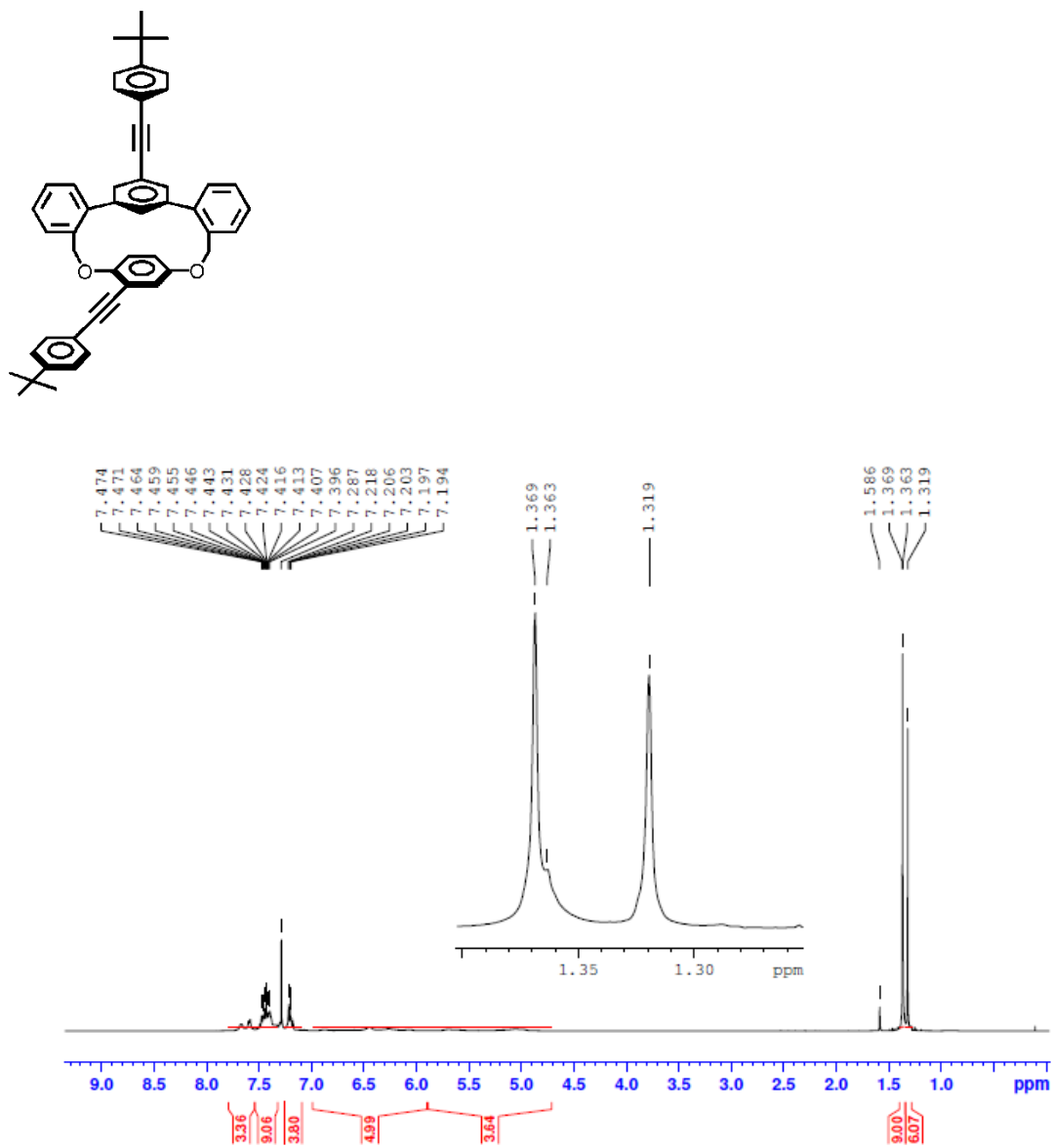


Figure 6 A.36 ^1H NMR (500 MHz, CDCl_3) of **14**.

Compound **14**

Structure

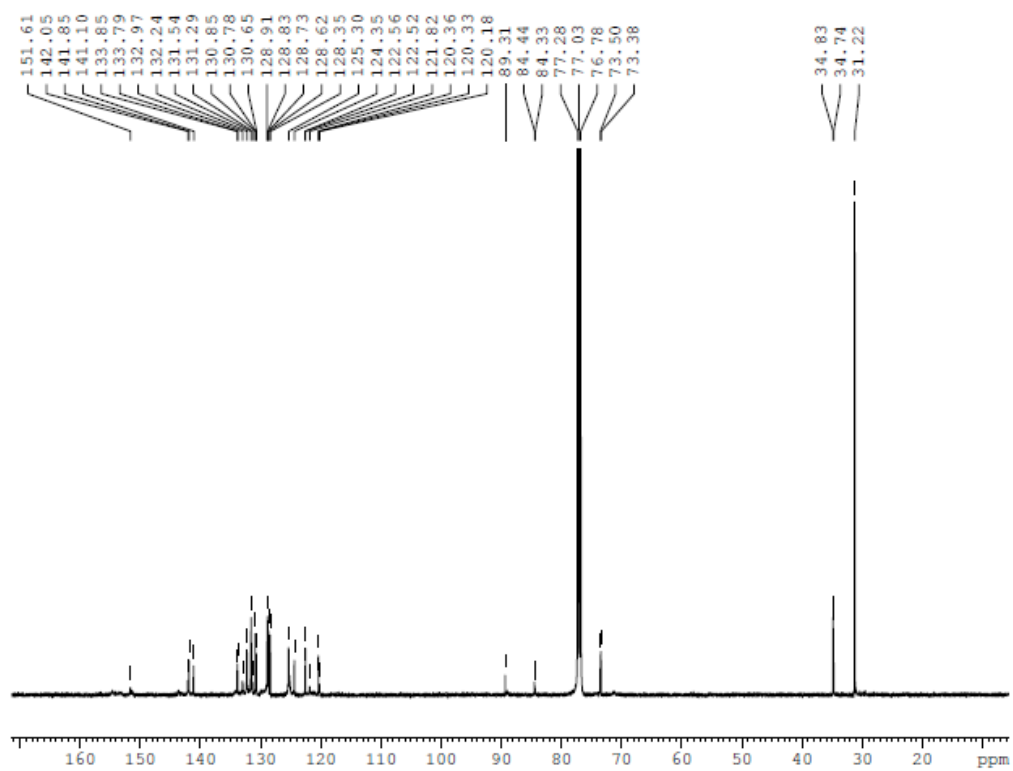
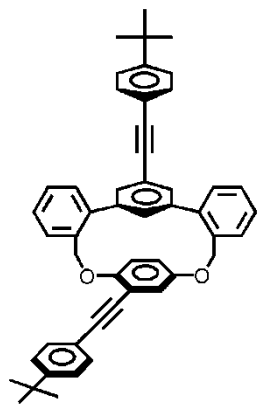


Figure 6 A.37 ^{13}C NMR (125 MHz, CDCl_3) of **14**.

Compound 15

Structure

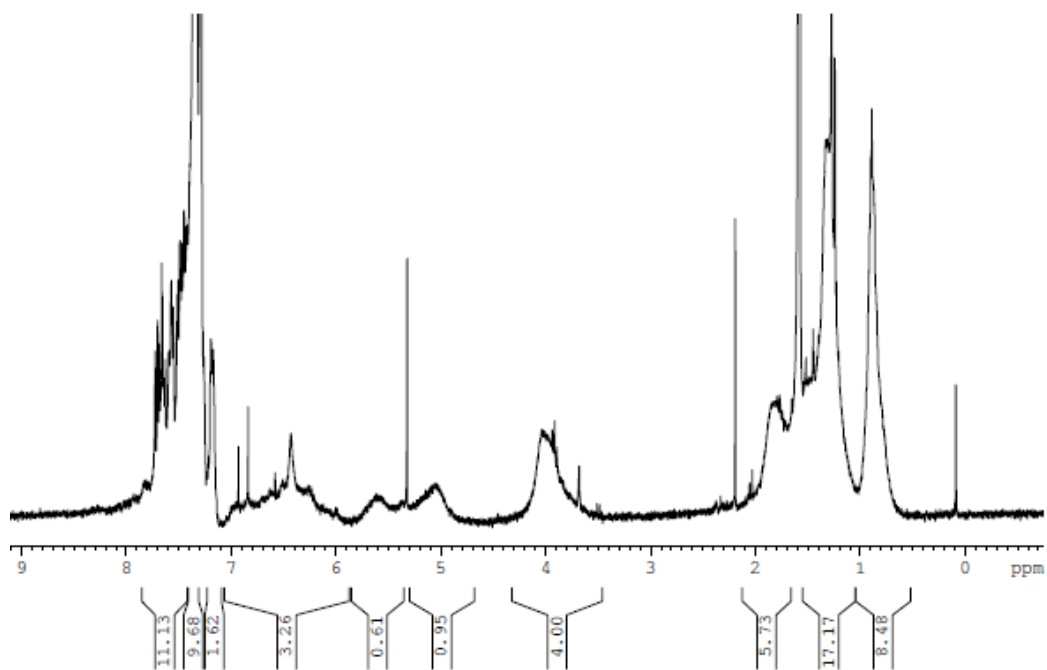
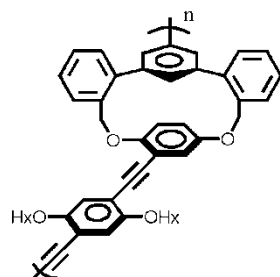


Figure 6 A.38 ^1H NMR (300 MHz, CDCl_3) of 15.

Compound **CP2**

Structure

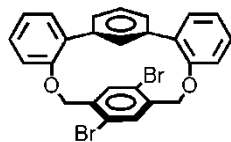


Figure 6 A.39 ^1H NMR (500 MHz, CDCl_3) of **CP2**.

Compound CP1a

Structure

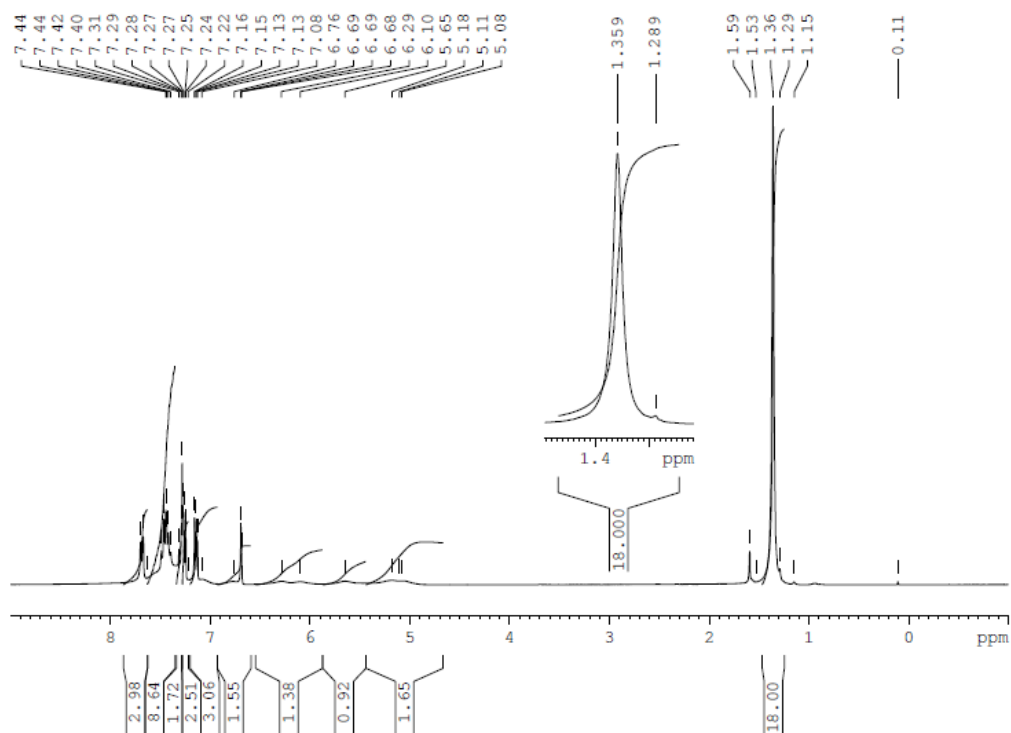
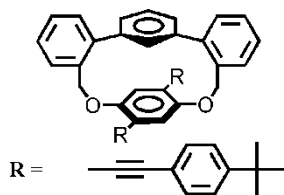


Figure 6 A.40 ^1H NMR (300 MHz, CDCl_3) of CP1a.

Compound CP1a

Structure

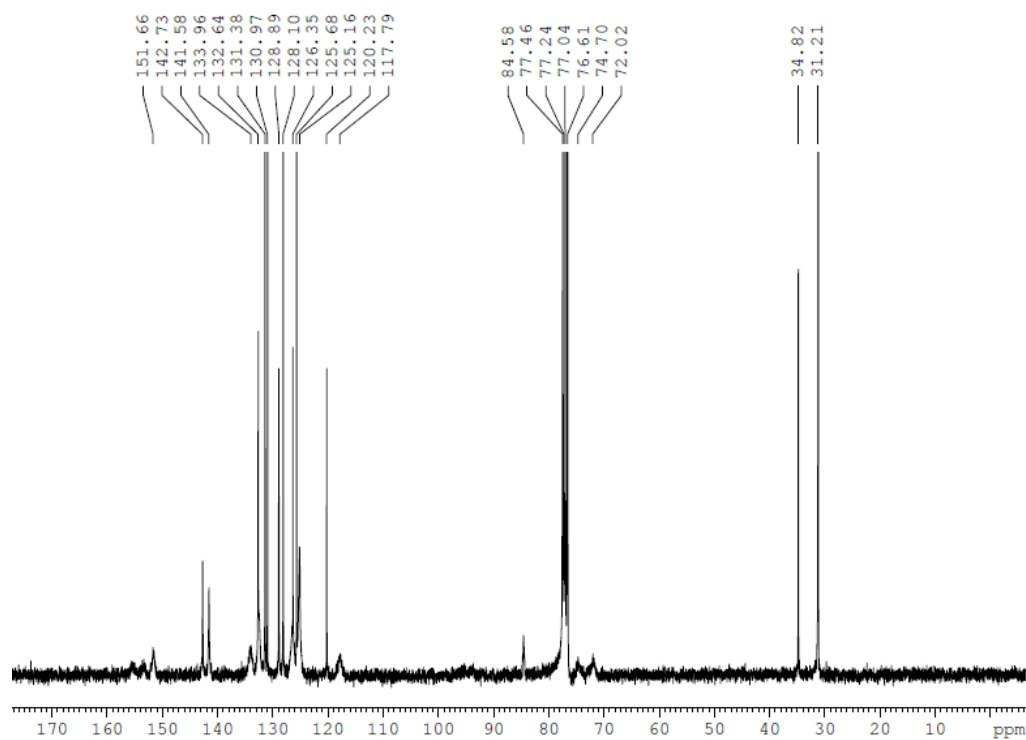
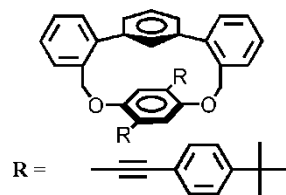


Figure 6 A.41 ^{13}C NMR (75 MHz, CDCl_3) of CP1a.

Compound CP1b

Structure

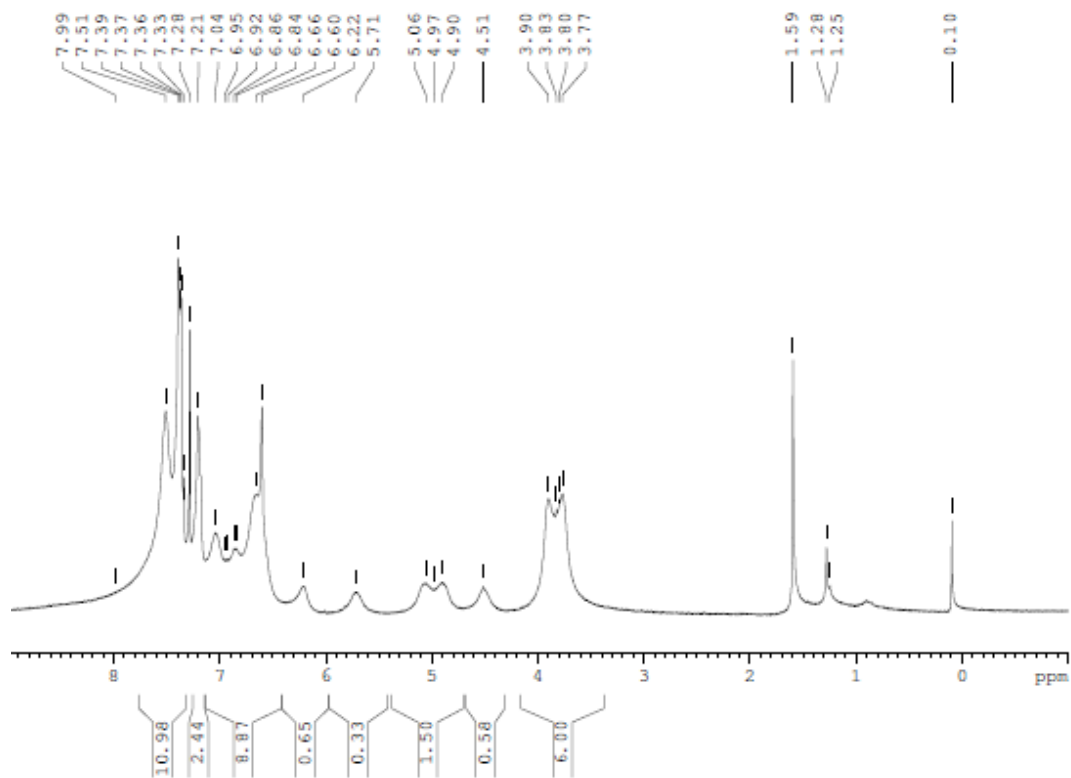
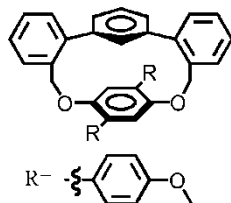


Figure 6 A.42 ^1H NMR (300 MHz, CDCl_3) of CP1b.

Compound CP1b

Structure

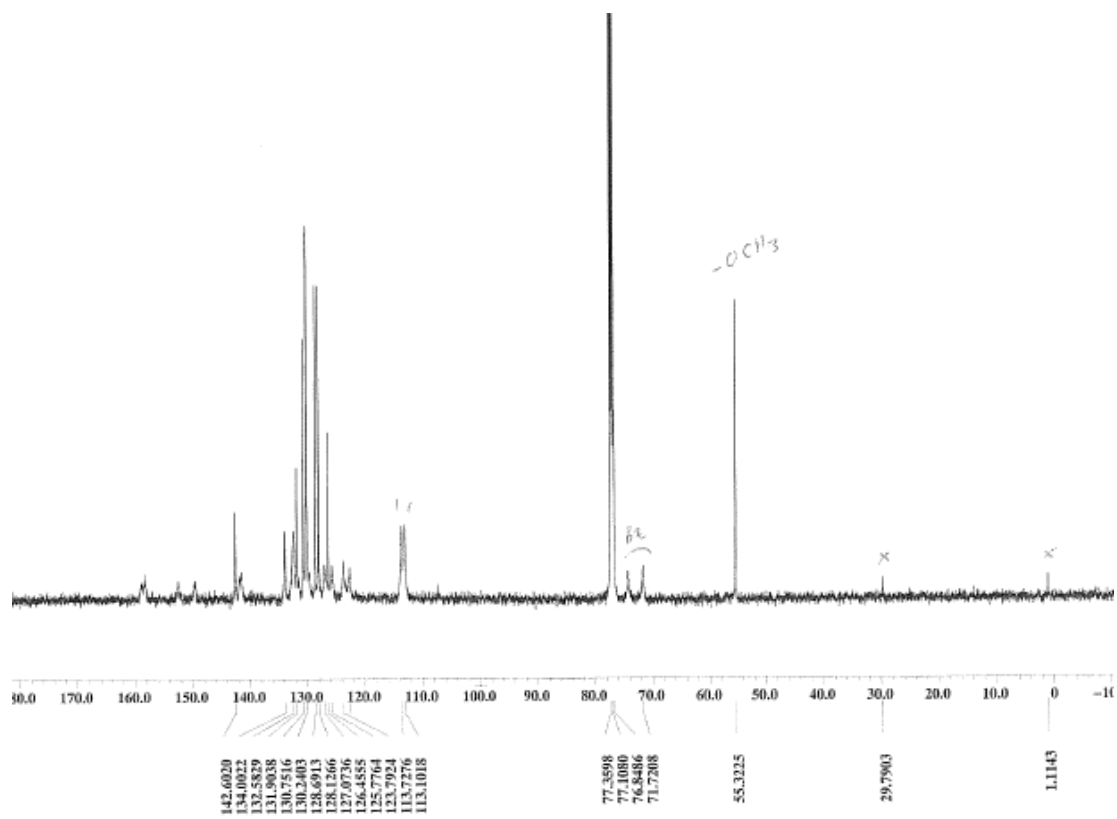
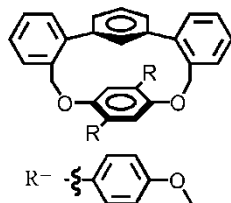


Figure 6 A.43 ^{13}C NMR (125 MHz, CDCl_3) of CP1b.

Compound **CP2b**

Structure

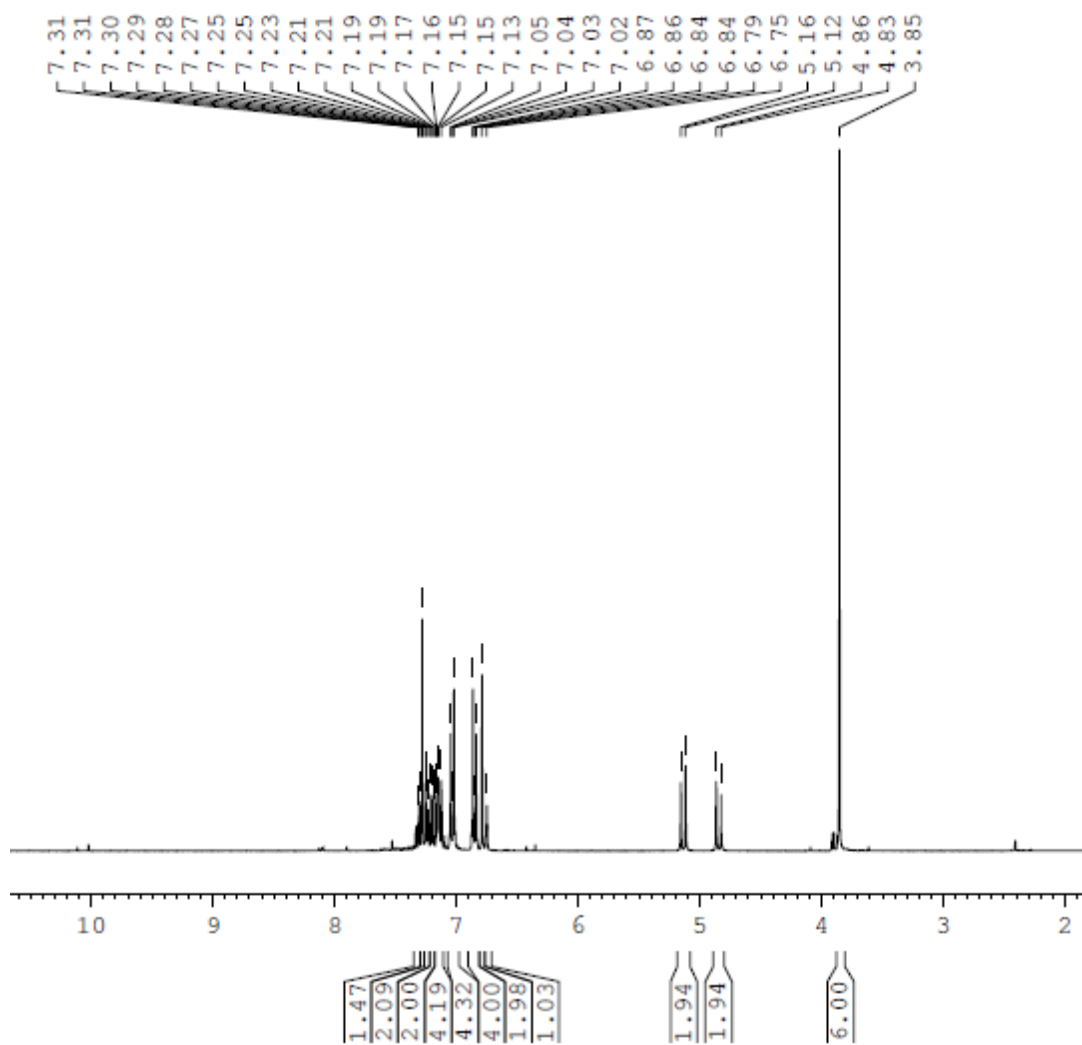
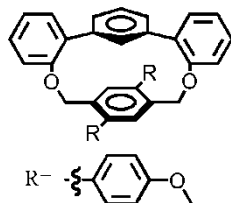


Figure 6 A.44 ^1H NMR (500 MHz, CDCl_3) of **CP2b**.

Compound CP2b

Structure

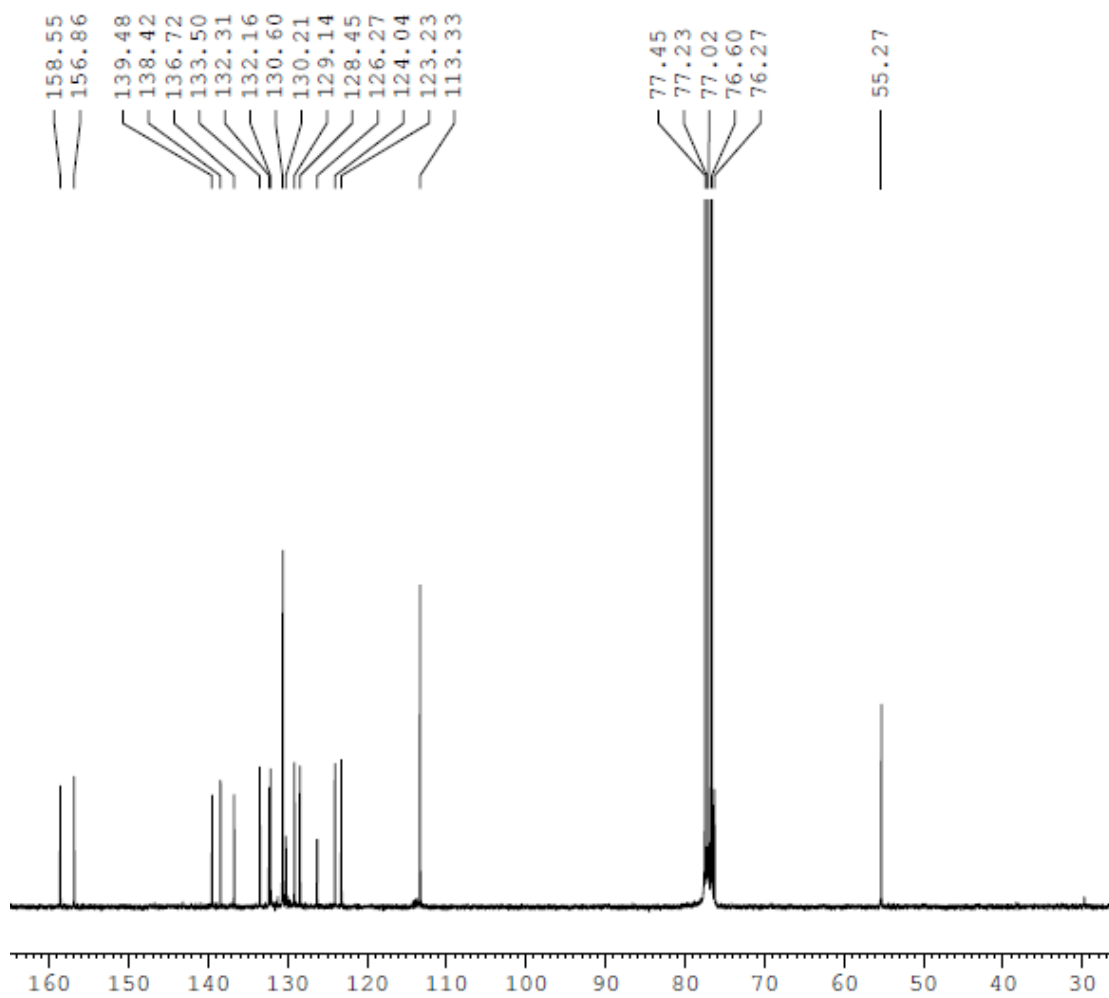
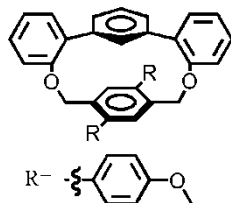


Figure 6 A.45 ^{13}C NMR (125 MHz, CDCl_3) of CP2b.

Compound CP1c

Structure

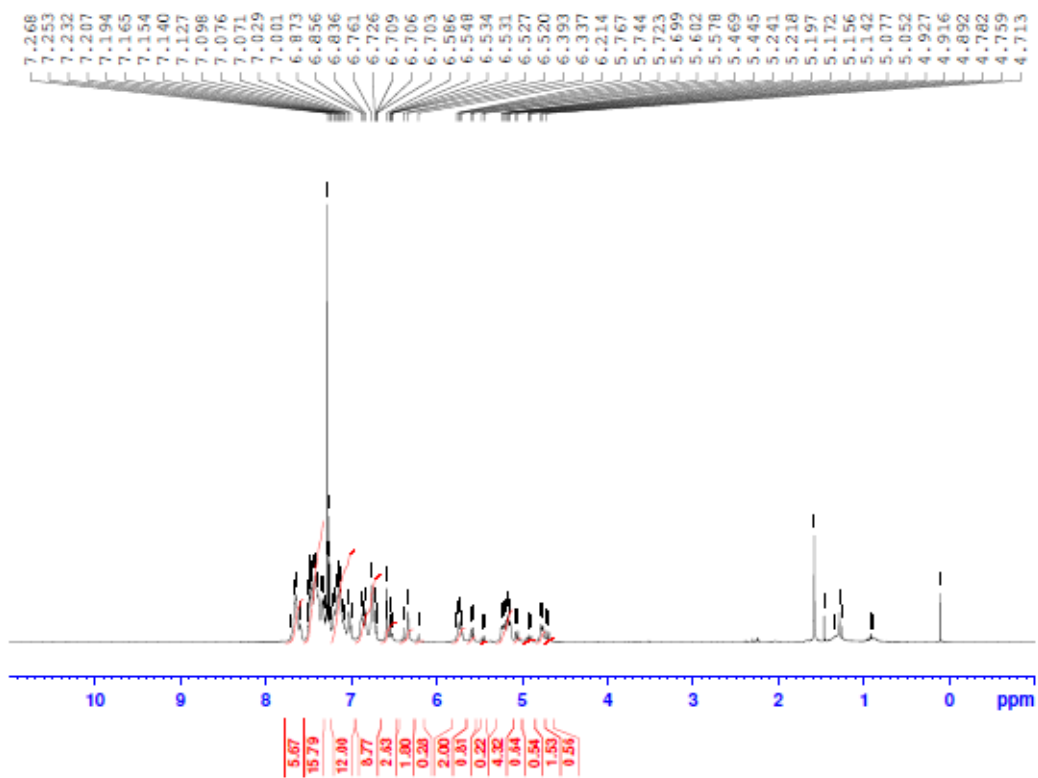
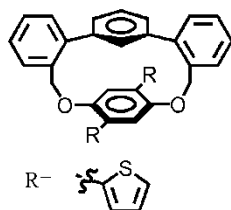


Figure 6 A.46 ^1H NMR (500 MHz, CDCl_3) of CP1c.

Compound CP1c

Structure

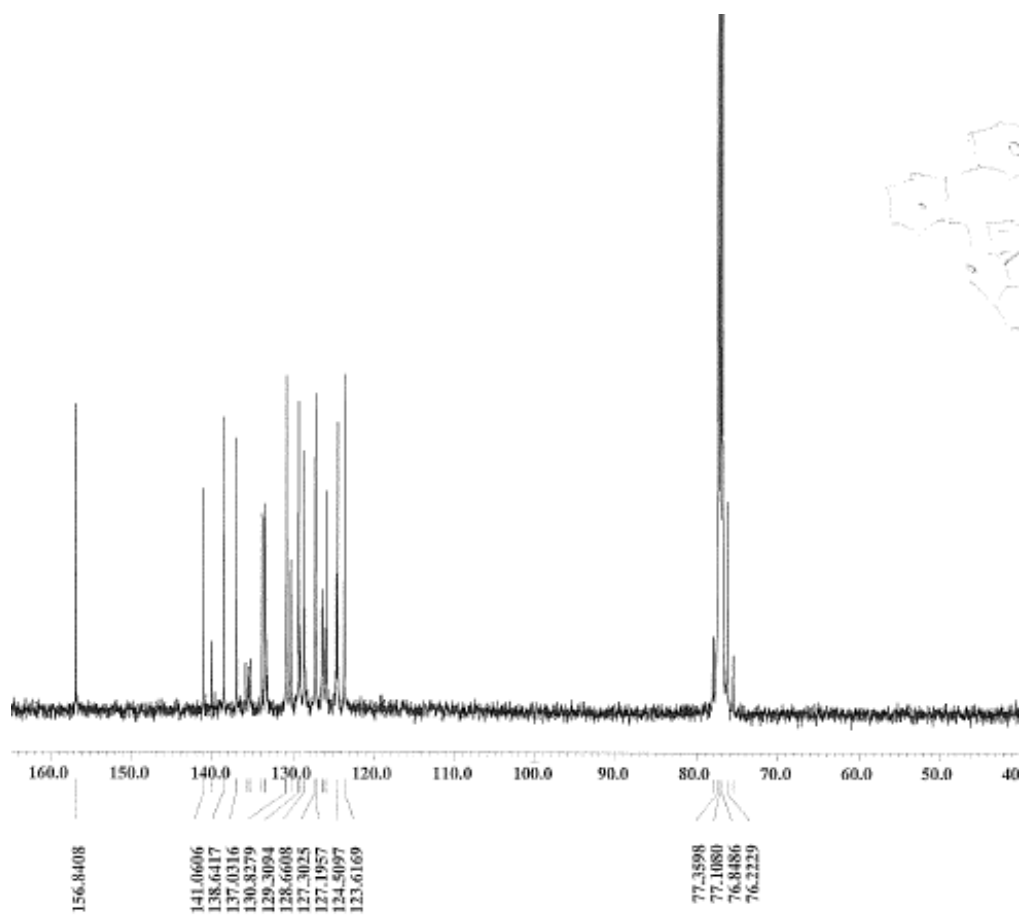
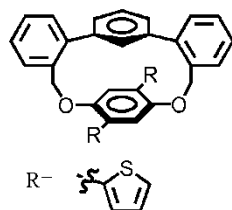


Figure 6 A.47 ^{13}C NMR (125 MHz, CDCl_3) of CP1c.

Compound CP2c

Structure

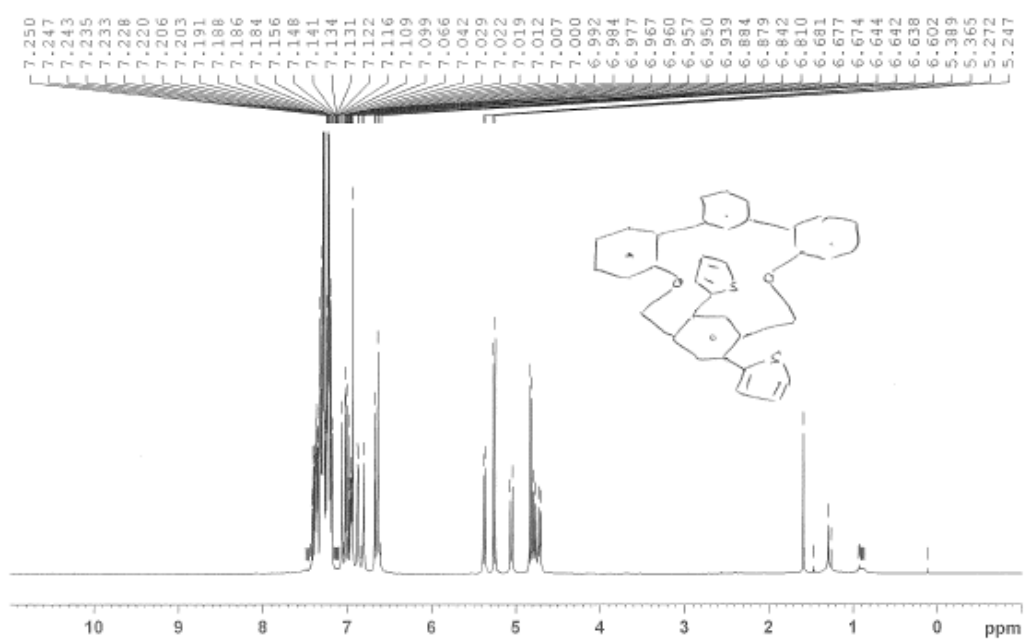
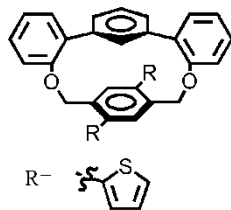


Figure 6 A.48 ^1H NMR (500 MHz, CDCl_3) of CP2c.

Compound **CP2c**

Structure

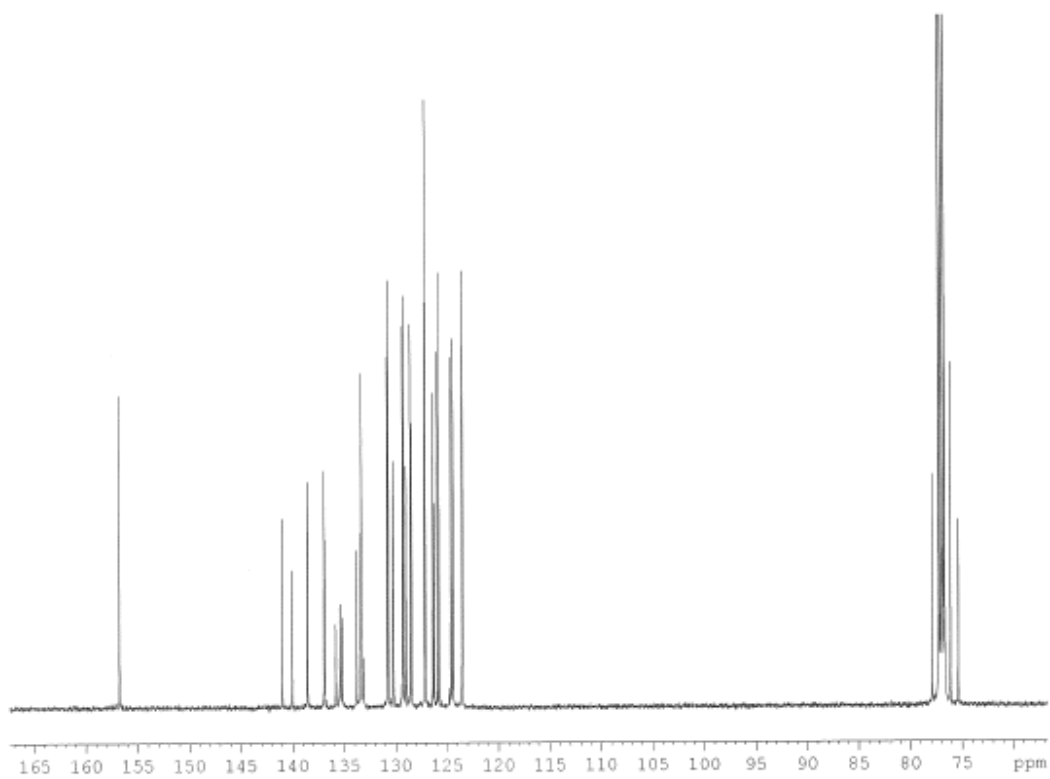
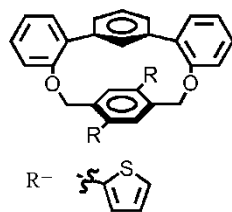


Figure 6 A.49 ^{13}C NMR (125 MHz, CDCl_3) of **CP2c**.

Compound **CLa1**

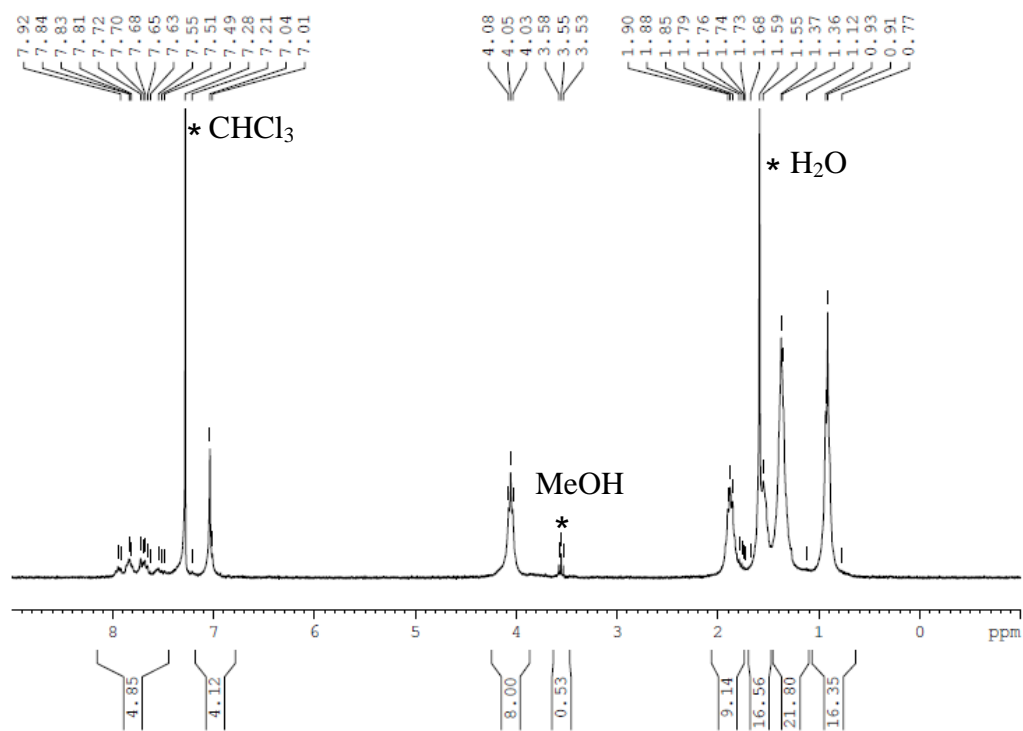


Figure 6 A.50 ¹H NMR (300 MHz, CDCl₃) of **CLa1**.

Compound **CLa3**

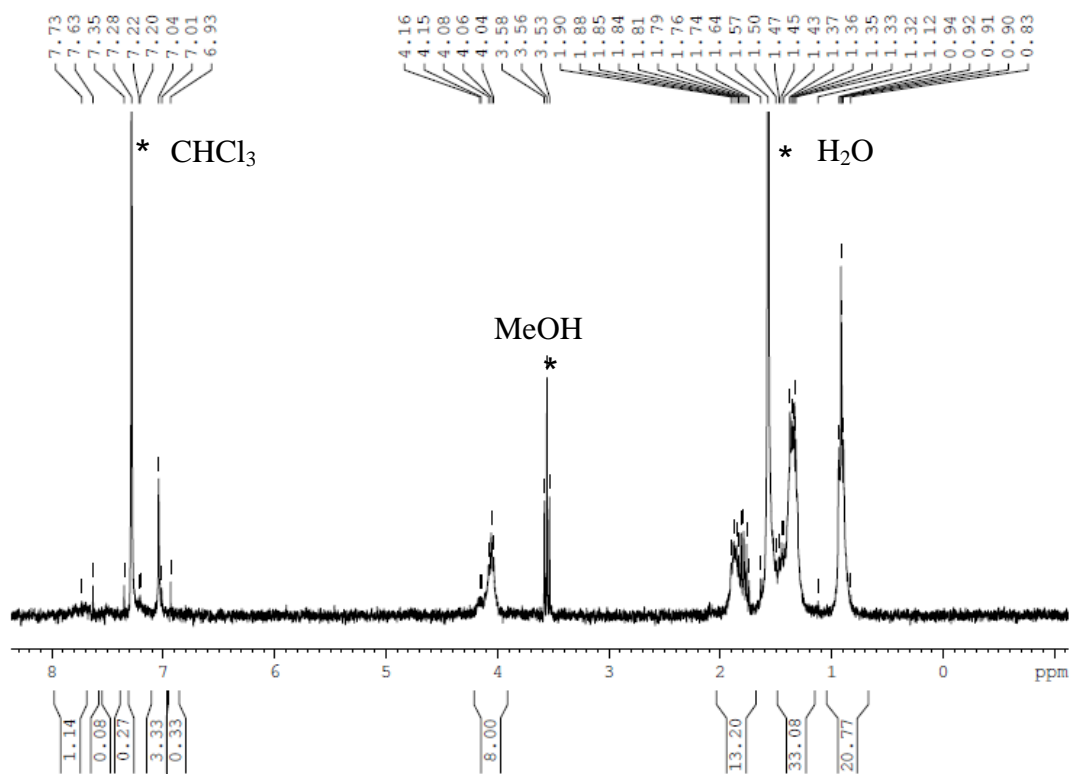


Figure 6 A.51 ¹H NMR (300 MHz, CDCl₃) of **CLa3**.

Compound **CLa5**

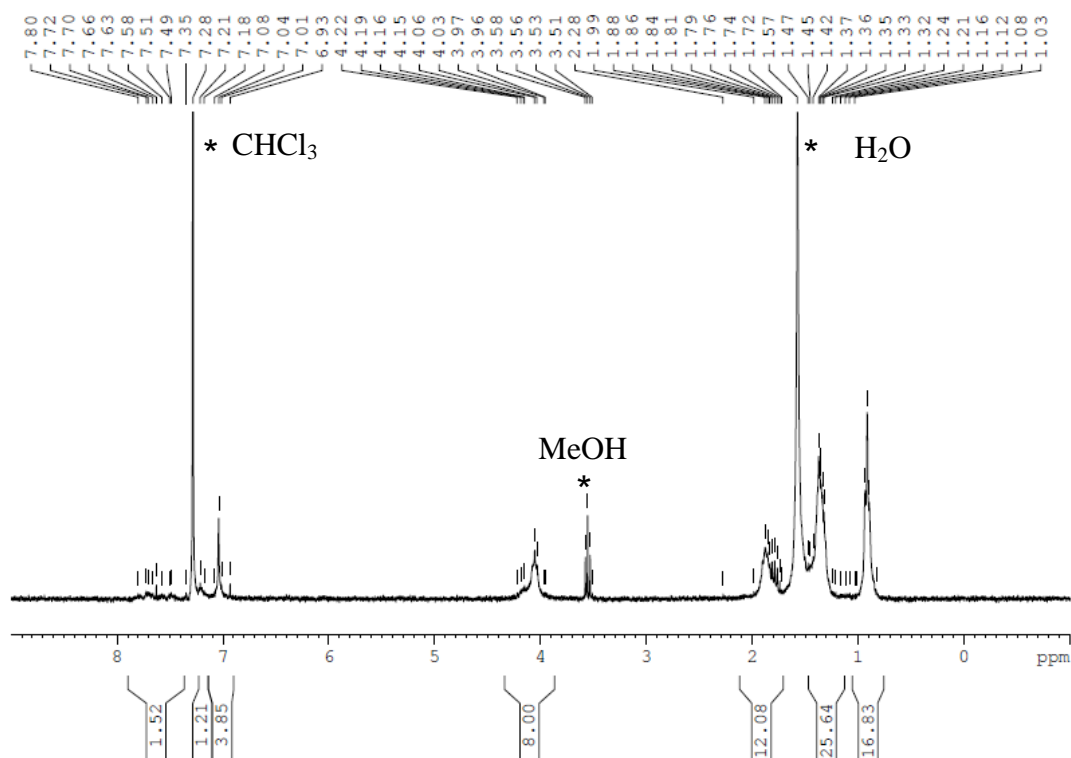


Figure 6 A.52 ¹H NMR (300 MHz, CDCl₃) of **CLa5**.

Compound **CLb1**

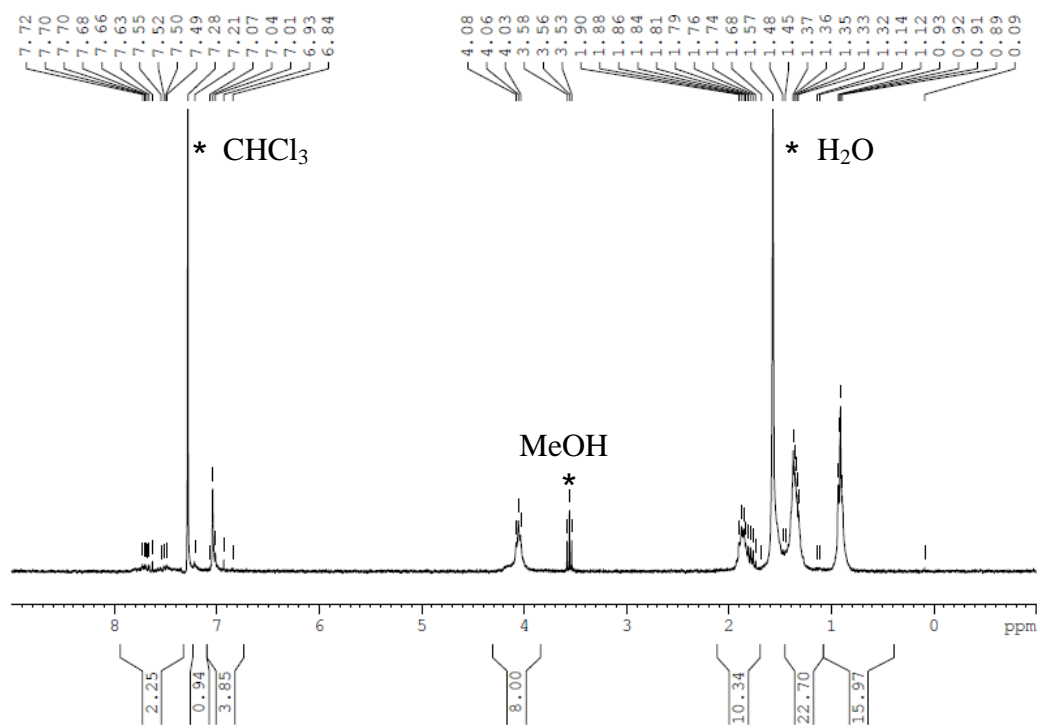


Figure 6 A.53 ¹H NMR (300 MHz, CDCl₃) of **CLb1**.

Compound **CLb3**

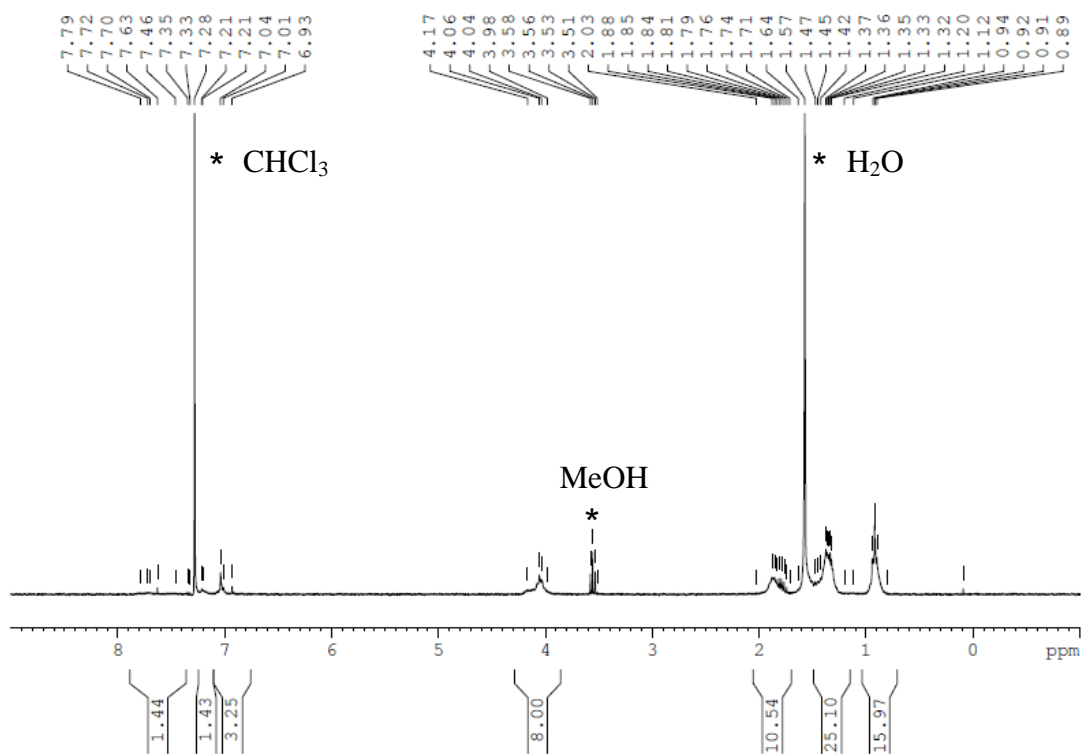


Figure 6 A.54 ¹H NMR (300 MHz, CDCl₃) of **CLb3**.

Compound **CLb5**

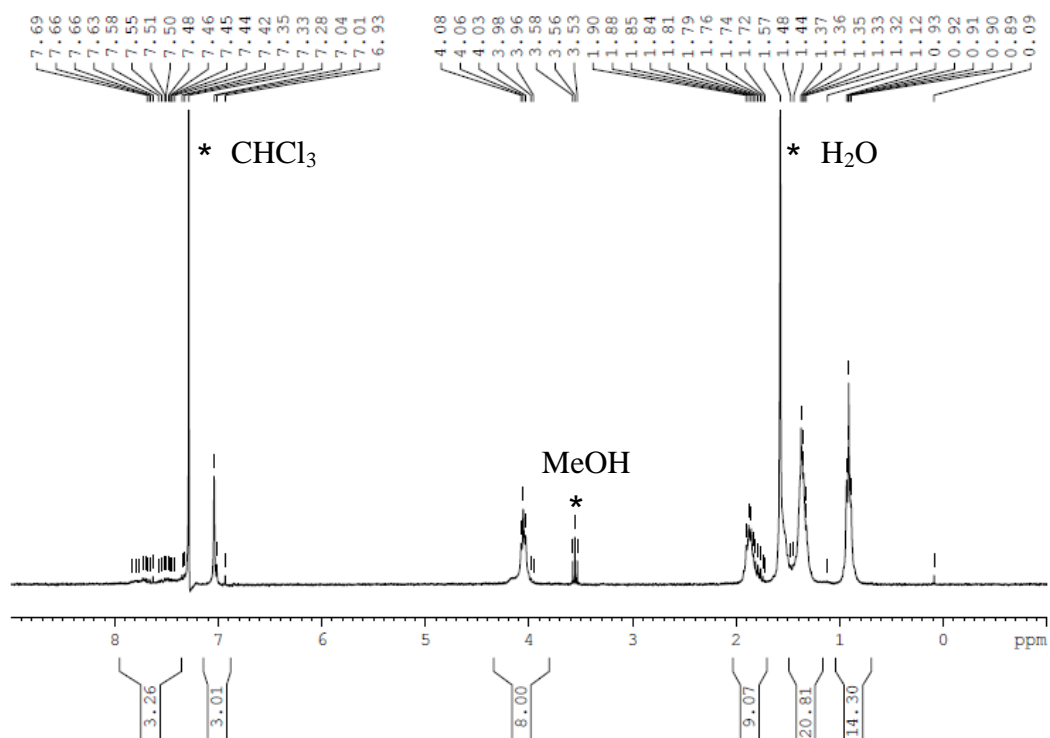


Figure 6 A.55 ¹H NMR (300 MHz, CDCl₃) of **CLb5**.

Compound **MPa1**

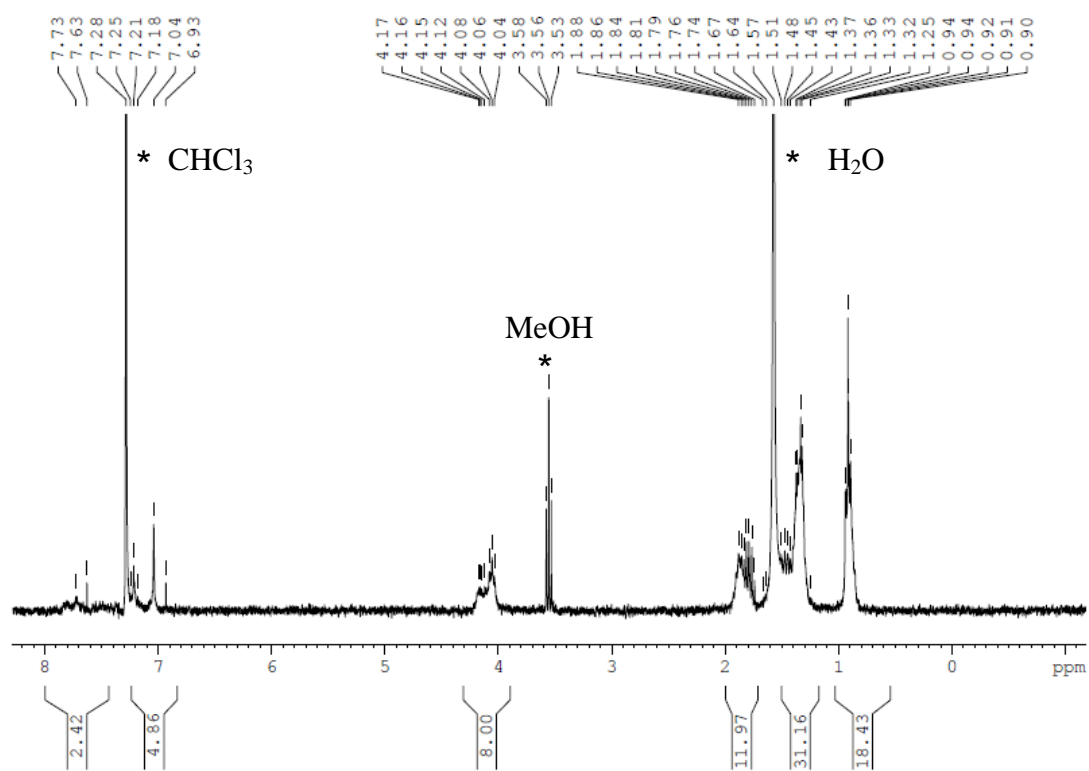


Figure 6 A.56 ¹H NMR (300 MHz, CDCl₃) of **MPa1**.

Compound **MPa3**

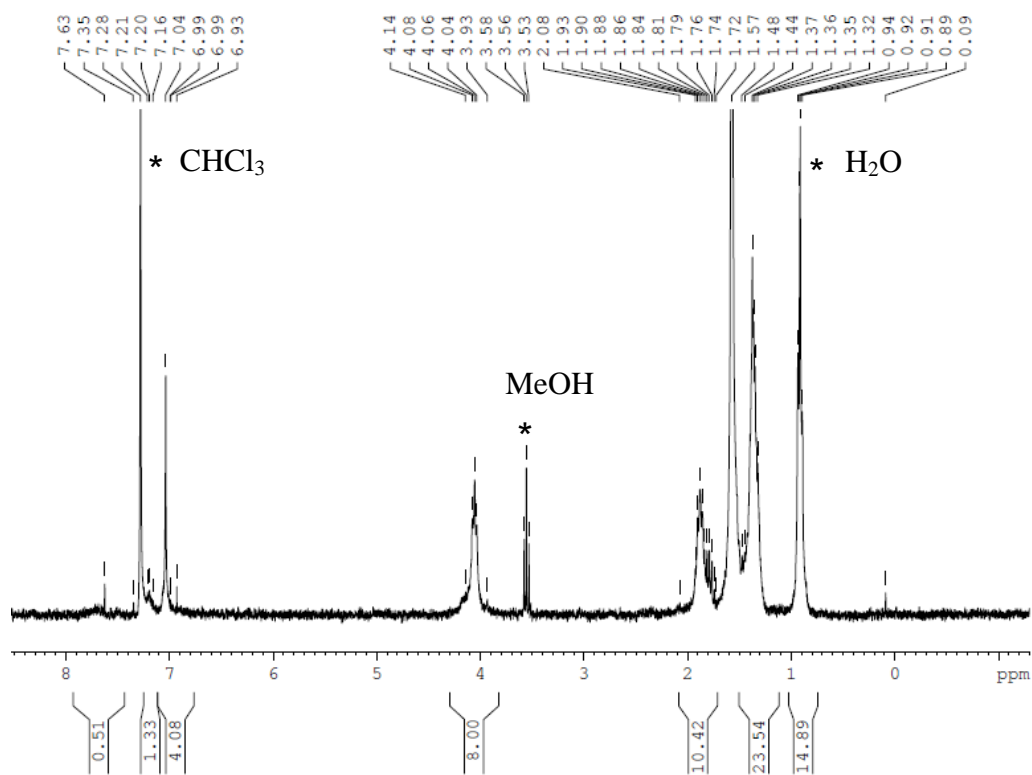


Figure 6 A.57 ¹H NMR (300 MHz, CDCl₃) of MPa3.

Compound **MPa5**

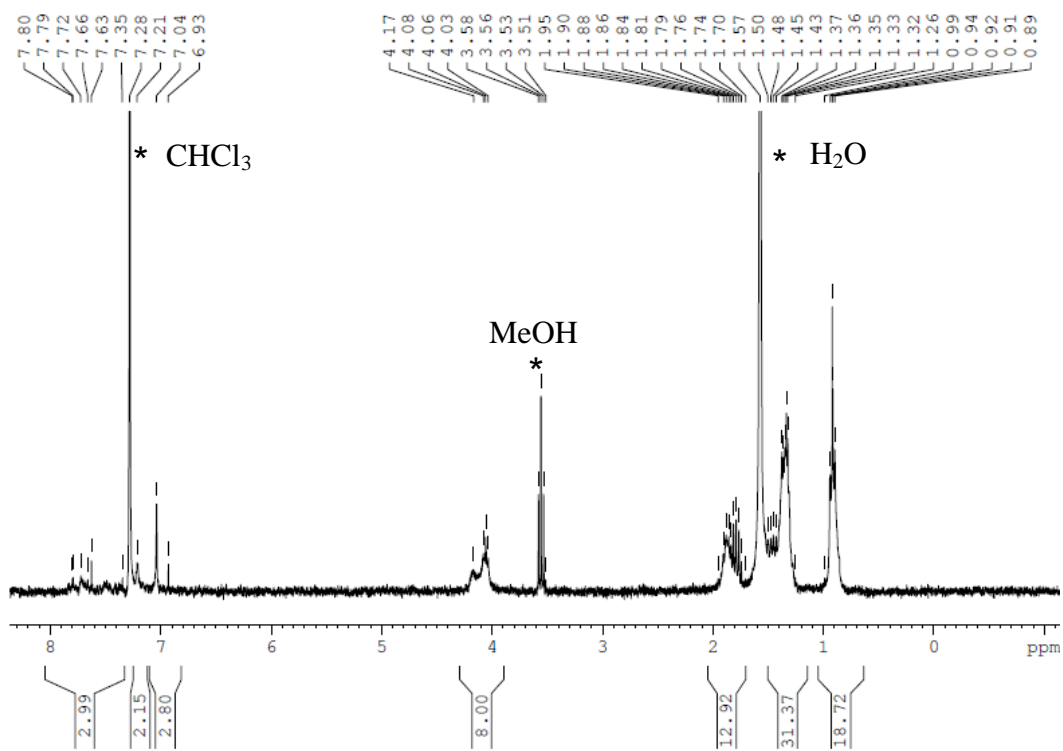


Figure 6 A.58 ¹H NMR (300 MHz, CDCl₃) of **MPa5**.

Compound **MPb1**

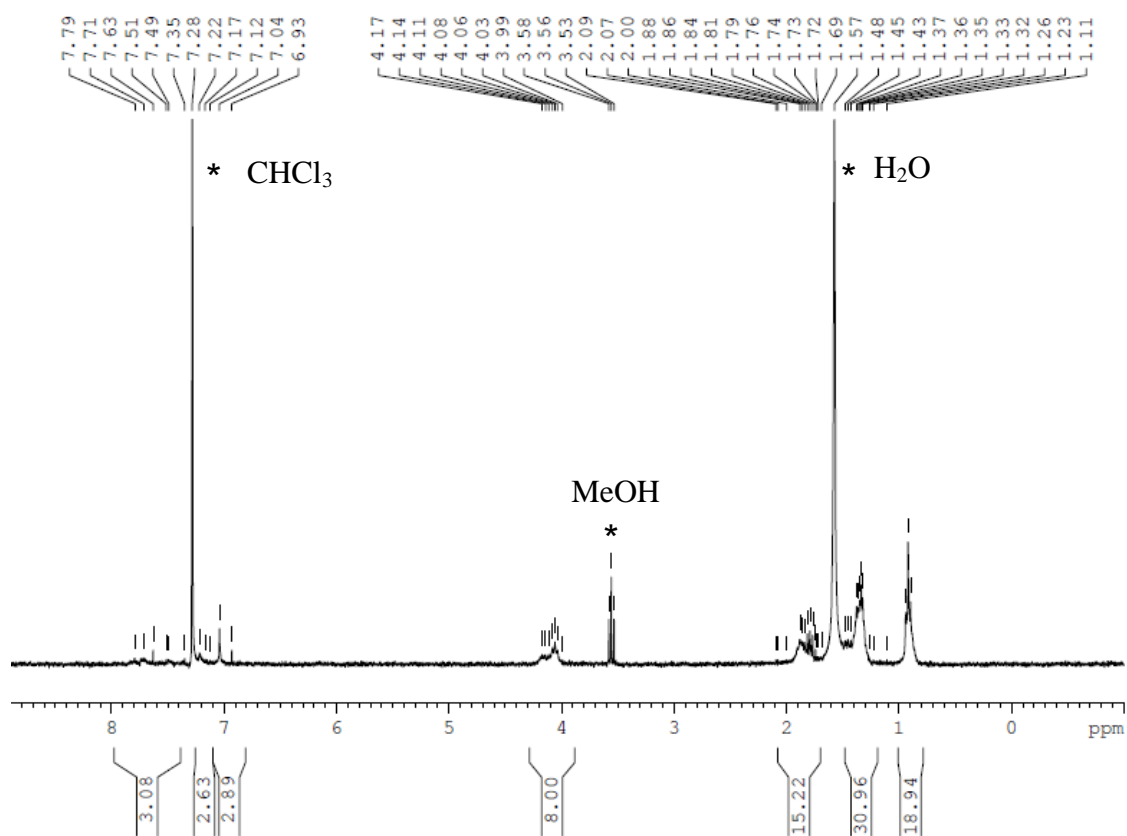


Figure 6 A.59 ¹H NMR (300 MHz, CDCl₃) of **MPb1**.

Compound **MPb3**

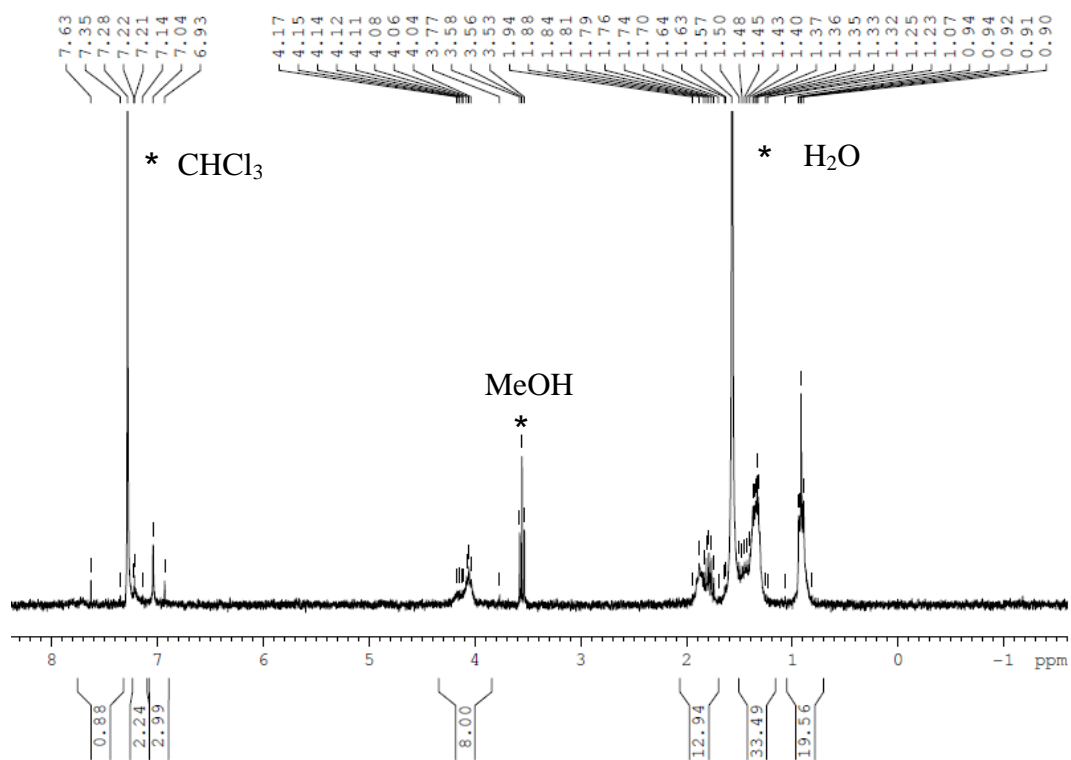


Figure 6 A.60 ¹H NMR (300 MHz, CDCl₃) of **MPb3**.

Compound **MPb5**

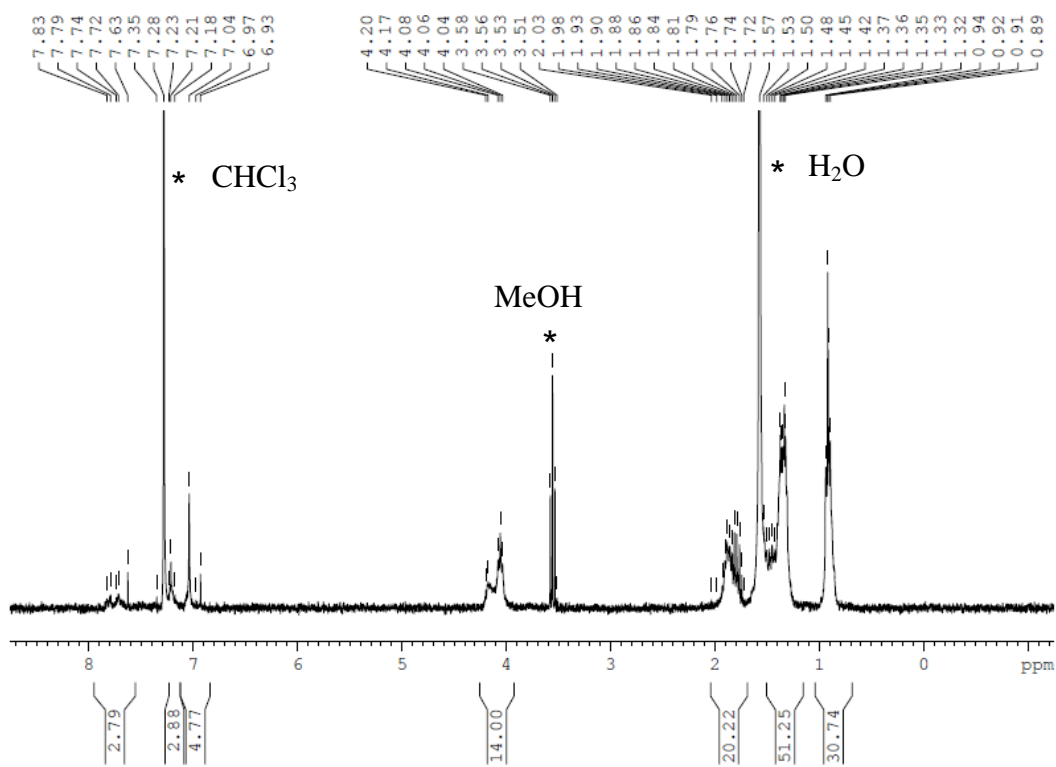


Figure 6 A.61 ¹H NMR (300 MHz, CDCl₃) of **MPb5**.

CHAPTER SEVEN

THE FINALE AND SCOPE

The primary focus of my research is to develop novel materials which can be employed as sensors for biological relevant molecules and ions and the synthesis of novel scaffolds to append chromophores on it to investigate the interchromophoric interactions in order to tune their photophysical properties.

As discussed in chapter two, *m*-xylene based hyperbranched polymers were synthesized and successfully studied as phosphate anion sensor. Their Co(III) complexes were used for the decomposition of phosphoester substrate at physiological pH which eventually enhanced the rate of hydrolysis of phosphoester by five orders of magnitude in comparison to the uncatalyzed reaction. Their zinc(II) complexes showed high affinity and selectivity for phosphates compared to other anions. Also the binding constants were calculated for the PG-bound enzyme models which are very different compared to their small monomer analogues.

As discussed in chapter three, *m*-terphenyl scaffold based ligands were synthesized and successfully tested as pyrophosphate anion sensor at physiological pH. This model showed selectivity for pyrophosphate over phosphate anion

A series of 1,3-bis(dimethylamino methyl)phenyl receptor containing cross-conjugated cruciform materials were synthesized and discussed in chapter four. Cruciforms, a very well known material for chemical sensing, have also been studied. The entire series of reported compounds observed photoluminescence response for Zn²⁺ or Cu²⁺ compared to other metal ions.

Synthesis and photophysical properties of six novel phosphacruciform systems and a model compound (without P) were discussed in detail in chapter five. Such molecules showed a decrease in the bandgap and increase in Stokes shift, due to the extension of conjugation (presence of P) on the tetraethynylbenzene core.

Synthesis of novel halogenated *m*-terphenyl-based oxacyclophane scaffolds for covalent attachment of chromophores using C-C coupling reaction is reported in chapter six. These materials allow one to study the controlled interchain interaction for both monomer and polymers.

The successful study of chromophore appended *m*-terphenyl based oxacyclophanes for controlled interchromophoric interaction and the effect of spatial orientation of chromophores on their optical properties opens a new avenue of research with numerous possible variations. So far our study is based on only one kind of chromophores attached on the scaffold.

Optoelectronic properties of conjugated system depend on donor and acceptor functional groups, hence it will be an interesting area of research to synthesize scaffolds featuring different (donor and acceptor) chromophores and how they affect optical properties of oxacyclophane-scaffolded systems. Transition metals like Pt can also be incorporated in to the oxacyclophanes containing monomer or polymer system to study triplet excited state or phosphorescent emissive material where oxacyclophane canopy influences π stacking to afford soluble, processable materials. This oxacyclophane scaffold allows us to tune the distance between the chromophores by utilizing different linker to connect upper and lower deck to study the effect of distance between the

chromophores on optoelectronic properties. Such electron rich conjugated materials are can be used for detection of electron deficient explosives materials such as TNT and RDX.

Conducting metallopolymers (**CMPs**) and monomers containing Pt-acetylides are very interesting phosphorescent emissive / electroluminescent materials to study which can potentially be used in **OLEDs** and **OPVs**. Also such materials can provide excellent insight as to the nature of the triplet excited state. To date, very few researches have studied the photophysical properties of Pt-acetylide where phosphines are directly attached to chromophores. Hence, the bifunctional cruciform phosphine can be an interesting scaffold to be introduced into a metallopolymers. Also it can be very easily transformed into cationic polyelectrolyte to study layer-by-layer.

REFERENCES

1. Techniques included ^1H and ^{13}C 1D spectra, 1H–1H Correlation Spectroscopy (COSY), Heteronuclear Multiple Quantum Coherence (HMQC), Distortionless Enhancement by Polarization Transfer (DEPT) and Differential Nuclear Overhauser Effect (NOE). Spectra and full spectral assignments are provided in the ESI. .
2. Superior examples include Strem Chemicals' Zinpyr-1 (cat. no. 07-0314) and Zinpyr-4 (07-0312).
3. *Handbook of Photochemistry*. 3rd ed.; CRC Press: Boca Raton, 2006; 'Vol.' p.
4. Adams, H.; Bradshaw, D.; Fenton, D. E., Dinuclear nickel(II) and zinc(II) complexes of 2,6-bis[*bis*(2-pyridylmethyl)amino]methyl]-4-methylphenol. *Inorganica Chimica Acta* **2002**, 332, 195-200.
5. Adimurthy, S.; Ramachandraiah, G.; Ghosh, P. K.; Bedekar, A. V., A new, environment friendly protocol for iodination of electron-rich aromatic compounds. **2003**, 44, (27), 5099-5101.
6. Aiet-Haddou, H.; Wiskur, S. L.; Lynch, V. M.; Anslyn, E. V., Achieving large color changes in response to the presence of amino acids: a molecular sensing ensemble with selectivity for aspartate. *Journal of the American Chemical Society* **2001**, 123, (45), 11296-11297.
7. Akbayir, C.; Bulut, F.; Farrell, T.; Goldschmidt, A.; Guentner, R.; Kam, A. P.; Miclea, P.; Scherf, U.; Seekamp, J.; Solovyev, V. G.; Torres, C. M. S.,

- Nanostructured conjugated polymeric systems for photovoltaic applications. *Reviews on Advanced Materials Science* **2003**, 5, (3), 205-210.
8. Akiyama, Y.; Nagahara, N.; Kitano, M.; Nakao, M. Gastrointestinal mucosa-adherent pharmaceutical composition. 9842311, 1998.
 9. Amendola, V.; Bonizzoni, M.; Esteban-Gomez, D.; Fabbrizzi, L.; Licchelli, M.; Sancenon, F.; Taglietti, A., Some guidelines for the design of anion receptors. *Coordination Chemistry Reviews* **2006**, 250, (11+12), 1451-1470.
 10. Anslyn, E. V., Supramolecular analytical chemistry. *Journal of Organic Chemistry* **2007**, 72, (3), 687-699.
 11. Anzenbacher, P., Jr.; Montes, V. A.; Takizawa, S.-y., High-purity white light from a simple single dopant host-guest white organic light-emitting diode architecture. *Appl. Phys. Lett.* **2008**, 93, (16), 163302/1-163302/3.
 12. Arachchige Shamindri, M.; Brown Jared, R.; Chang, E.; Jain, A.; Zigler David, F.; Rangan, K.; Brewer Karen, J., Design considerations for a system for photocatalytic hydrogen production from water employing mixed-metal photochemical molecular devices for photoinitiated electron collection. *Inorg Chem* **2009**, 48, (5), 1989-2000.
 13. Back, S.; Albrecht, M.; Spek, A. L.; Rheinwald, G.; Lang, H.; Koten, G. v., Toward Organometallic Polymers with High Directionality Containing Bis-ortho-Chelating Ligands. *Organometallics* **2001**, 20, (5), 1024-1027.
 14. Back, S.; Lutz, M.; Spek, A. L.; Lang, H.; Koten, G. v., Preparation and electrochemical behaviour of dinuclear platinum complexes containing NCN ligands (NCN=[C₆H₃(Me₂NCH₂)₂-2,6]-). The crystal structure of [C₆H₃(Me₂NCH₂)₂-

- 1,3-(C[6-point triple bond; length half of m-dash]C)-5]2. *Journal of Organometallic Chemistry* **2001**, 620, (1-2), 227-234.
15. Bauer-Siebenlist, B.; Meyer, F.; Farkas, E.; Vidovic, D.; Dechert, S., Effect of Zn...Zn separation on the hydrolytic activity of model dizinc phosphodiesterases. *Chemistry--A European Journal* **2005**, 11, (15), 4349-4360.
 16. Baumgartner, T.; Réau, R., Organophosphorus p-Conjugated Materials. *Chemical Reviews* **2006**, 106, 4681-4727, and references therein.
 17. Baumgartner, T.; Réau, R., Organophosphorus p-Conjugated Materials. *Chemical Reviews* **2006**, 106, 4681-4727.
 18. Bazan, G. C., Novel Organic Materials through Control of Multichromophore Interactions. *Journal of Organic Chemistry* **2007**, 72, 8615-8635.
 19. Benning, M. M.; Shim, H.; Raushel, F. M.; Holden, H. M., *Biochemistry* **2001**, 40, 2712.
 20. Berthiol, F.; Kondolff, I.; Doucet, H.; Santelli, M., Reaction of aryl di-, tri-, or tetrabromides with arylboronic acids or alkenes in the presence of a palladium-tetraphosphine catalyst. 689, (17), 2786-2798.
 21. Bidault, S.; Brasselet, S.; Zyss, J.; Maury, O.; Le Bozec, H., Role of spatial distortions on the quadratic nonlinear optical properties of octupolar organic and metallo-organic molecules. *Journal of Chemical Physics* **2007**, 126, (3), 034312/1-034312/13.
 22. Bidault, S.; Viau, L.; Maury, O.; Brasselet, S.; Zyss, J.; Ishow, E.; Nakatani, K.; Le Bozec, H., Optically tunable nonlinearities in polymers based on photoisomerizable

- metal-based coordination complexes. *Advanced Functional Materials* **2006**, 16, (17), 2252-2262.
23. Bilge, A.; Zen, A.; Forster, M.; Li, H.; Galbrecht, F.; Nehls, B. S.; Farrell, T.; Neher, D.; Scherf, U., Swivel-cruciform oligothiophene dimers. *Journal of Materials Chemistry* **2006**, 16, (31), 3177-3182.
24. Blum, J.; Zimmerman, M., Photocyclization of Substituted 1,4-Distyrylbenzenes to Dibenz[*a,h*] Anthracenes. *Tetrahedron* **1972**, 28, 275-280.
25. Boiocchi, M.; Bonizzoni, M.; Fabbrizzi, L.; Piovani, G.; Taglietti, A., A dimetallic cage with a long ellipsoidal cavity for the fluorescent detection of dicarboxylate anions in water. *Angewandte Chemie, International Edition* **2004**, 43, (29), 3847-3852.
26. Bong, D. T. Y.; Chan, E. W. L.; Diercks, R.; Dosa, P. I.; Haley, M. M.; Matzger, A. J.; Miljanic, O. S.; Vollhardt, K. P. C.; Bond, A. D.; Teat, S. J.; Stanger, A., Syntheses of Syn and Anti Doublebenz [5]Phenylene. *Org. Lett.* **2004**, 6, (13), 2249-2252.
27. Bonifacio, M. C.; Robertson, C. R.; Jung, J.-Y.; King, B. T., Polycyclic Aromatic Hydrocarbons by Ring-Closing Metathesis. *J. Org. Chem* **2005**, 70, 8522-8526.
28. Bonizzoni, M.; Fabbrizzi, L.; Piovani, G.; Taglietti, A., Fluorescent detection of glutamate with a dicopper(II) polyamine cage. *Tetrahedron* **2004**, 60, (49), 11159-11162.
29. Borgarello, E.; Kiwi, J.; Pelizzetti, E.; Visca, M.; Graetzel, M., Photochemical cleavage of water by photocatalysis. *Nature (London)* **1981**, 289, (5794), 158-60.

30. Bosman, A. W.; Janssen, H. M.; Meijer, E. W., About Dendrimers: Structure, Physical Properties, and Applications. *Chemical Reviews (Washington, D. C.)* **1999**, 99, (7), 1665-1688.
31. Brabec, C. J.; Sariciftci, N. S.; Hummelen, J. C., Plastic solar cells. *Advanced Functional Materials* **2001**, 11, (1), 15-26.
32. Bredas, J.-L.; Beljonne, D.; Coropceanu, V.; Cornil, J., Charge-Transfer and Energy-Transfer Processes in p-Conjugated Oligomers and Polymers: A Molecular Picture. *Chemical Reviews (Washington, DC, United States)* **2004**, 104, (11), 4971-5003.
33. Breslow, R.; Singh, S., Phosphate ester cleavage catalyzed by bifunctional zinc complexes: comments on the "p-nitrophenyl ester syndrome". *Bioorganic Chemistry* **1988**, 16, (4), 408-17.
34. Bunz, U. H. F., Poly(aryleneethynylene)s: Syntheses, Properties, Structures, and Applications. *Chemical Reviews (Washington, D. C.)* **2000**, 100, (4), 1605-1644.
35. Burdette, S. C.; Frederickson, C. J.; Bu, W.; Lippard, S. J., ZP4, an improved neuronal Zn²⁺ sensor of the zinpyr family. *Journal of the American Chemical Society* **2003**, 125, (7), 1778-1787.
36. Burdette, S. C.; Walkup, G. K.; Spingler, B.; Tsien, R. Y.; Lippard, S. J., Fluorescent Sensors for Zn²⁺ Based on a Fluorescein Platform: Synthesis, Properties and Intracellular Distribution. *Journal of the American Chemical Society* **2001**, 123, (32), 7831-7841.

37. Burnworth, M.; Rowan, S. J.; Weder, C., Fluorescent sensors for the detection of chemical warfare agents. *Chemistry--A European Journal* **2007**, 13, (28), 7828-7836.
38. Burroughes, J. H.; Bradley, D. D. C.; Brown, A. R.; Marks, R. N.; Mackay, K.; Friend, R. H.; Burns, P. L.; Holmes, A. B., Light-emitting diodes based on conjugated polymers. *Nature (London, United Kingdom)* **1990**, 347, (6293), 539-41.
39. Cain, F. W.; McNeill, G. P.; Tongue, T. Structured particulate systems for food items with improved mouthfeel and homogeneity. 1249180, 2002.
40. Carroll, R. L.; Christopher, B. G., The Genesis of Molecular Electronics. *Angewandte Chemie International Edition* **2002**, 41, (23), 4378-4400.
41. Chan, K. L.; Mak, C. S. K.; Evans, N. R.; Watkins, S. E.; Pascu, S. I.; Holmes, A. B.; Hayer, A.; Koehler, A.; Devi, L. S.; Friend, R. H., Synthesis of triplet emitters and hosts for electrophosphorescence. *Proceedings of SPIE-The International Society for Optical Engineering* **2005**, 5937, (Organic Light-Emitting Materials and Devices IX), 59370B/1-59370B/9.
42. Chang, C. J.; Jaworski, J.; Nolan, E. M.; Sheng, M.; Lippard, S. J., A tautomeric zinc sensor for ratiometric fluorescence imaging: Application to nitric oxide-induced release of intracellular zinc. *Proceedings of the National Academy of Sciences of the United States of America* **2004**, 101, (5), 1129-1134.
43. Cheng, Y.-J.; Yang, S.-H.; Hsu, C.-S., Synthesis of Conjugated Polymers for Organic Solar Cell Applications. *Chemical Reviews (Washington, D. C.)* **2009**, 109, (11), 5868-5923.

44. Clot, O.; Akahori, Y.; Moorlag, C.; Leznoff, D. B.; Wolf, M. O.; Batchelor, R. J.; Patrick, B. O.; Ishii, M., Model Complexes for Metalated Polythiophenes: Gold(I) and Palladium(II) Complexes of Bis(diphenylphosphino)oligothiophenes. *Inorganic Chemistry* **2003**, 42, (8), 2704-2713.
45. Clot, O.; Wolf, M. O.; Patrick, B. O., Electropolymerization of Pd(II) Complexes Containing Phosphinoterthiophene Ligands. *Journal of the American Chemical Society* **2001**, 123, (41), 9963-9973.
46. Coakley, K. M.; McGehee, M. D., Conjugated Polymer Photovoltaic Cells. *Chemistry of Materials* **2004**, 16, (23), 4533-4542.
47. Cody, J.; Fahrni, C. J., Fluorescence sensing based on cation-induced conformational switching: copper-selective modulation of the photoinduced intramolecular charge transfer of a donor-acceptor biphenyl fluorophore. *Tetrahedron* **2004**, 60, (49), 11099-11107.
48. Cornil, J.; Beljonne, D.; Calbert, J.-P.; Bredas, J.-L., Interchain interactions in organic pi-conjugated materials: impact on electronic structure, optical response, and charge transport. *Adv. Mater.* **2001**, 13, (14), 1053-1067.
49. Coulson, D. R., *Inorganic Synthesis*. ed.; 1990; 'Vol.' 28, p 107-109.
50. Crews, P.; Rodriguez, J.; Jaspars, M., *Organic Structure Analysis*. 2 ed.; Oxford University Press: New York, 2010; 'Vol.' p.
51. Croddy, E., "Urban terrorism: Chemical warfare in Japan". *Jane's Intelligence Rev.* **1995**, 7, 520-523.

52. Cui-Hua Wang, R.-R. H., Shuang Liang, Jia-Hua Chen, Zhen Yanga, Jian Pei, Linear C₂-symmetric polycyclic benzodithiophene: efficient, highly diversified approaches and the optical properties. *Tetrahedron Letters* **2005**, 46, 8153–8157.
53. Dai, Z.; Canary, J. W., Tailoring tripodal ligands for zinc sensing. *New J. Chem.* **2007**, 31, (10), 1708-1718.
54. Dalton, G. T.; Cifuentes, M. P.; Petrie, S.; Stranger, R.; Humphrey, M. G.; Samoc, M., Independent switching of cubic nonlinear optical properties in a ruthenium alkynyl cruciform complex by employing protic and electrochemical stimuli. *J. Am. Chem. Soc.* **2007**, 129, (39), 11882-11883.
55. de Boer, B.; Facchetti, A., Semiconducting Polymeric Materials. *Polymer Reviews* **2008**, 48, (3), 423 - 431.
56. Dennis, A. E.; Smith, R. C., “Turn-On” Fluorescent Sensor for the Selective Detection of Zinc Ion by a Sterically-Encumbered Bipyridyl-Based Receptor *Chemical Communications* **2007**, (44), 4641-4643.
57. Dennis T.-Y. Bong; Eugene W. L. Chan; Rainer Diercks; Peter I. Dosa; Michael M. Haley; Adam J. Matzger; Ognjen . Miljani; K. Peter C. Vollhardt; Andrew D. Bond; Simon J. Teat; Stanger, A., Syntheses of Syn and Anti Doublebent [5]Phenylene. *Organic letters* **2004**, 6, (13), 2249-2252.
58. Dhenaut, C.; Ledoux, I.; Samuel, I. D. W.; Zyss, J.; Bourgault, M.; Le Bozec, H., Chiral metal complexes with large octupolar optical nonlinearities. *Nature (London)* **1995**, 374, (6520), 339-42.

59. Du, C. J. F.; Hart, H.; Ng, K. K. D., A one-pot synthesis of m-terphenyls, via a two-aryne sequence. *Journal of Organic Chemistry* **1986**, 51, (16), 3162-5.
60. Du, P.; Schneider, J.; Li, F.; Zhao, W.; Patel, U.; Castellano, F. N.; Eisenberg, R., Bi- and Terpyridyl Platinum(II) Chloro Complexes: Molecular Catalysts for the Photogeneration of Hydrogen from Water or Simply Precursors for Colloidal Platinum? *J. Am. Chem. Soc.* **2008**, 130, (15), 5056-5058.
61. Durben, S.; Dienes, Y.; Baumgartner, T., Cationic Dithieno[3,2-b:2',3'-d]phospholes: A New Building Block for Luminescent, Conjugated Polyelectrolytes. *Org. Lett.* **2006**, 8, (25), 5893-5896.
62. Eggers, K.; Fyles, T. M.; Montoya-Pelaez, P. J., Synthesis and Characterization of Photoswitchable Lipids Containing Hemithioindigo Chromophores. *J. Org. Chem* **2001**, 66, 2966-2977.
63. Elangovan, A.; Kao, K.-M.; Yang, S.-W.; Chen, Y.-L.; Ho, T.-I.; Su, Y. O., Synthesis, Electronic Properties, and Electrochemiluminescence of Donor-Substituted Phenylethynylantrons. *J. Org. Chem* **2005**, 70, (11), 4460-4469.
64. Esswein, A. J.; Nocera, D. G., Hydrogen Production by Molecular Photocatalysis. *Chem. Rev.* **2007**, 107, (10), 4022-4047.
65. Evans, N. R.; Devi, L. S.; Mak, C. S. K.; Watkins, S. E.; Pascu, S. I.; Koehler, A.; Friend, R. H.; Williams, C. K.; Holmes, A. B., Triplet Energy Back Transfer in Conjugated Polymers with Pendant Phosphorescent Iridium Complexes. *Journal of the American Chemical Society* **2006**, 128, (20), 6647-6656.

66. Fabbrizzi, L.; Foti, F.; Taglietti, A., Metal-Containing Trifurcate Receptor that Recognizes and Senses Citrate in Water. *Organic Letters* **2005**, 7, (13), 2603-2606.
67. Fabbrizzi, L.; Licchelli, M.; Taglietti, A., The design of fluorescent sensors for anions: taking profit from the metal-ligand interaction and exploiting two distinct paradigms. *Dalton Transactions* **2003**, (18), 3471-3479.
68. Fabbrizzi, L.; Marcotte, N.; Stomeo, F.; Taglietti, A., Pyrophosphate detection in water by fluorescence competition assays: inducing selectivity through the choice of the indicator. *Angewandte Chemie, International Edition* **2002**, 41, (20), 3811-3814.
69. Fahrni, C. J.; O'Halloran, T. V., Aqueous Coordination Chemistry of Quinoline-Based Fluorescence Probes for the Biological Chemistry of Zinc. *Journal of the American Chemical Society* **1999**, 121, (49), 11448-11458.
70. Folmer-Andersen, J. F.; Lynch, V. M.; Anslyn, E. V., "Naked-eye" detection of histidine by regulation of CuII coordination modes. *Chemistry--A European Journal* **2005**, 11, (18), 5319-5326.
71. Friend, R. H.; Gymer, R. W.; Holmes, A. B.; Burroughes, J. H.; Marks, R. N.; Taliani, C.; Bradley, D. D. C.; Dos Santos, D. A.; Bredas, J. L.; Logdlund, M.; Salaneck, W. R., Electroluminescence in conjugated polymers. *Nature (London)* **1999**, 397, (6715), 121-128.
72. Fry, F. H.; Spiccia, L.; Jensen, P.; Moubaraki, B.; Murray, K. S.; Tiekink, E. R. T., Binuclear Copper(II) Complexes of Xylyl-Bridged Bis(1,4,7-triazacyclononane) Ligands. *Inorg. Chem.* **2003**, 42, 5594-5603.

73. Gilheany, D. G., Ylides, phosphonium No d Orbitals but Walsh Diagrams and Maybe Banana Bonds: Chemical Bonding in Phosphines, Phosphine Oxides, and Phosphonium Ylides. *Chemical Reviews (Washington, DC, United States)* **1994**, 94, (5), 1339-74.
74. Goldsmith, C. R.; Jaworski, J.; Sheng, M.; Lippard, S. J., Selective Labeling of Extracellular Proteins Containing Polyhistidine Sequences by a Fluorescein-Nitrilotriacetic Acid Conjugate. *Journal of the American Chemical Society* **2006**, 128, (2), 418-419.
75. Gorman, C., Metallodendrimers. Structural diversity and functional behavior. *Advanced Materials (Weinheim, Germany)* **1998**, 10, (4), 295-309.
76. Grewal, R. S.; Hart, H.; Vinod, T. K., Oxacyclophanes based on a m-terphenyl framework. *Journal of Organic Chemistry* **1992**, 57, (9), 2721-2726.
77. Grimsdale Andrew, C.; Chan, K. L.; Martin, R. E.; Jokisz, P. G.; Holmes Andrew, B., Synthesis of Light-Emitting Conjugated Polymers for Applications in Electroluminescent Devices. *Chemical Reviews (Washington, D. C.)* **2009**, 109, (3), 897-1091.
78. Guillou, V.; Morançais, J.-L. Foaming cosmetic cream for cleansing skin and hair. 1166747, 2002.
79. Hammond, P. R., The effect of experimental errors on Benesi-Hildebrand plots and on the inherent accuracy of the equation. *Journal of the Chemical Society* **1964**, (Jan.), 479-84.

80. Han, M. S.; Kim, D. H., Naked-eye detection of phosphate ions in water at physiological pH. A remarkably selective and easy-to-assemble colorimetric phosphate-sensing probe. *Angewandte Chemie, International Edition* **2002**, 41, (20), 3809-3811.
81. Hanshaw, R. G.; Hilkert, S. M.; Jiang, H.; Smith, B. D., An indicator displacement system for fluorescent detection of phosphate oxyanions under physiological conditions. *Tetrahedron Letters* **2004**, 45, (47), 8721-8724.
82. Hanshaw, R. G.; Lakshmi, C.; Lambert, T. N.; Johnson, J. R.; Smith, B. D., Fluorescent detection of apoptotic cells by using zinc coordination complexes with a selective affinity for membrane surfaces enriched with phosphatidylserine. *ChemBioChem* **2005**, 6, (12), 2214-2220.
83. Hanshaw, R. G.; Smith, B. D., New reagents for phosphatidylserine recognition and detection of apoptosis. *Bioorganic & Medicinal Chemistry* **2005**, 13, (17), 5035-5042.
84. He, S.; Dennis, A. E.; Smith, R. C., Steric Coordination Control of Interchain Interactions in Conducting Metallopolymers. *Macromolecular Rapid Communications* **2009**, 30, 2079-2083.
85. He, S.; Iacono, S. T.; Budy, S. M.; Dennis, A. E.; Smith, D. W., Jr.; Smith, R. C., Photoluminescence and ion sensing properties of a bipyridyl chromophore-modified semifluorinated polymer and its metallopolymer derivatives. *J. Mater. Chem.* **2008**, 18, (17), 1970-1976.

86. Heeger, A. J., Semiconducting and Metallic Polymers: The Fourth Generation of Polymeric Materials (Nobel Lecture)13. *Angewandte Chemie International Edition* **2001**, 40, (14), 2591-2611.
87. Henary, M. M.; Wu, Y.; Fahrni, C. J., Zinc(II)-selective ratiometric fluorescent sensors based on inhibition of excited-state intramolecular proton transfer. *Chemistry--A European Journal* **2004**, 10, (12), 3015-3025.
88. Hilderbrand, S. A.; Lim, M. H.; Lippard, S. J., Dirhodium tetracarboxylate scaffolds as reversible fluorescence-based nitric oxide sensors. *Journal of the American Chemical Society* **2004**, 126, (15), 4972-4978.
89. Holliday, B. J.; Swager, T. M., Conducting metallopolymers: the roles of molecular architecture and redox matching. *Chem. Commun.* **2005**, (1), 23-36.
90. Hortalá, M. A.; Fabbrizzi, L.; Marcotte, N.; Stomeo, F.; Taglietti, A., Designing the selectivity of the fluorescent detection of amino acids: A chemosensing ensemble for histidine. *Journal of the American Chemical Society* **2003**, 125, (1), 20-21.
91. Horton, H. R.; Moran, L. A.; Scrimgeour, K. G.; Perry, M. D.; Rawn, J. D., *Principles of Biochemistry*. 4 ed.; Pearson Prentice Hall, : Upper Saddle River, NJ, 2006; 'Vol.' p.
92. Hovestad, N. J.; Eggeling, E. B.; Heidbuchel, H. J.; Jastrzebski, J. T. B. H.; Kragl, U.; Keim, W.; Vogt, D.; Van Koten, G., Selective hydrovinylation of styrene in a membrane reactor: use of carbosilane dendrimers with hemilabile P,O ligands. *Angewandte Chemie, International Edition* **1999**, 38, (11), 1655-1658.

93. http://www.eia.doe.gov/cneaf/alternate/page/renew_energy_consump/images/fig1_09_small.jpg, r. J., 2010).
94. Huck, W. T. S.; Snellink-Ruel, B. H. M.; Lichtenbelt, J. W. T.; van Veggel, F. C. J. M.; Reinhoudt, D. N., Self-assembly of hyperbranched spheres; correlation between monomeric synthon and sphere size. *Chemical Communications (Cambridge)* **1997**, (1), 9-10.
95. Hurst, S. K.; Humphrey, M. G.; Isoshima, T.; Wostyn, K.; Asselberghs, I.; Clays, K.; Persoons, A.; Samoc, M.; Luther-Davies, B., Organometallic Complexes for Nonlinear Optics. 28. Dimensional Evolution of Quadratic and Cubic Optical Nonlinearities in Stilbenylethynylruthenium Complexes. *Organometallics* **2002**, 21, (10), 2024-2026.
96. Jacobson, M. Z., Review of solutions to global warming, air pollution, and energy security *Energy & Environmental Science* **2009**, 2, (2), 148-173.
97. James, S. L.; Verspui, G.; Spek, A. L.; van Koten, G., Organometallic polymers: an infinite organoplatinum chain in the solid state formed by (CCHClPt) hydrogen bonds. *Chemical Communications (Cambridge)* **1996**, (11), 1309-1310.
98. Jang, Y. J.; Jun, E. J.; Lee, Y. J.; Kim, Y. S.; Kim, J. S.; Yoon, J., Highly Effective Fluorescent and Colorimetric Sensors for Pyrophosphate over H₂PO₄⁻ in 100% Aqueous Solution. *Journal of Organic Chemistry* **2005**, 70, (23), 9603-9606.
99. Jiang, C.; Yang, W.; Peng, J.; Xiao, S.; Cao, Y., High-efficiency, saturated red-phosphorescent polymer light-emitting diodes based on conjugated and non-

- conjugated polymers doped with an Ir complex. *Advanced Materials (Weinheim, Germany)* **2004**, 16, (6), 537-541.
100. Jin, Z.; Lucht, B. L., Transition metal mediated routes to poly(arylphosphine)s: investigation of novel phosphorus containing conjugated polymers. *Journal of Organometallic Chemistry* **2002**, 653, (1-2), 167-176.
101. Jin, Z.; Lucht, B. L., Poly-p-phenylene phosphine/polyaniline alternating copolymers: Electronic delocalization through phosphorus. *Journal of the American Chemical Society* **2005**, 127, (15), 5586-5595.
102. Johnson, A. W., *Ylides and Imines of Phosphorus*. ed.; Wiley: New York, 1993; 'Vol.' p.
103. Jorgensen, W. L.; Severance, D. L., Aromatic-Aromatic Interactions: Free Energy Profiles for the Benzene Dimer in Water, Chloroform, and Liquid Benzene. *Journal of the American Chemical Society* **1990**, 112, 4768-4774.
104. Kauffman, G. B., *J. Chem. Ed.* **1959**, 36, 521-527.
105. Kietzke, T.; Neher, D.; Kumke, M.; Montenegro, R.; Landfester, K.; Scherf, U., A Nanoparticle Approach To Control the Phase Separation in Polyfluorene Photovoltaic Devices. *Macromolecules* **2004**, 37, (13), 4882-4890.
106. Kim, I.-B.; Dunkhorst, A.; Gilbert, J.; Bunz Uwe, H. F., Sensing of Lead Ions by a Carboxylate-Substituted PPE: Multivalency Effects. *Macromolecules* **2005**, 38, (11), 4560-4562.

107. Kim, J.; McQuade, D. T.; McHugh, S. K.; Swager, T. M., Ion-specific aggregation in conjugated polymers: highly sensitive and selective fluorescent ion chemosensors. *Angewandte Chemie, International Edition* **2000**, 39, (21), 3868-3872.
108. Kim, S. K.; Lee, D. H.; Hong, J.-I.; Yoon, J., *Acc. Chem. Res.* **2008**.
109. Kirby, A. J.; Jencks, W. P., *J. Am. Chem. Soc.* **1965**, 87, 3209.
110. Klare, J. E.; Tulevski, G. S.; Sugo, K.; de Picciotto, A.; White, K. A.; Nuckolls, C., Cruciform pi-Systems for Molecular Electronics Applications. *J. Am. Chem. Soc.* **2003**, 125, (20), 6030-6031.
111. Knapton, D.; Burnworth, M.; Rowan, S. J.; Weder, C., Fluorescent organometallic sensors for the detection of chemical-warfare-agent mimics. *Angewandte Chemie, International Edition in English* **2006**, 45, (35), 5825-5829.
112. Knoblock, K. M.; Silvestri, C. J.; Collard, D. M., Stacked conjugated oligomers as molecular models to examine interchain interactions in conjugated materials. *J Am Chem Soc* **2006**, 128, (42), 13680-1.
113. Kraft, A.; Grimsdale, A. C.; Holmes, A. B., Electroluminescent conjugated polymers-seeing polymers in a new light. *Angew. Chem., Int. Ed.* **1998**, 37, (4), 403-428.
114. Kraft, A.; Grimsdale, A. C.; Holmes, A. B., Electroluminescent Conjugated Polymers-Seeing Polymers in a New Light. *Angew. Chem. Int. Ed* **1998**, 37, 402-428.

115. Kristina Kurz; Gobel, M. W., Hydrolytical cleavage of TAR-RNA, the trans-activation responsive region of HIV-1, by a bis(guanidinium) catalyst attached to arginine. *Helv. Chim. Acta* **1996**, 79, 1967-1979.
116. Lamansky, S.; Djurovich, P.; Murphy, D.; Abdel-Razzaq, F.; Lee, H. E.; Adachi, C.; Burrows, P. E.; Forrest, S. R.; Thompson, M. E., Highly phosphorescent bis-cyclometalated iridium complexes: synthesis, photophysical characterization, and use in organic light emitting diodes. *J Am Chem Soc* **2001**, 123, (18), 4304-12.
117. Lavigne, J. J.; Anslyn, E. V., Teaching old indicators new tricks: a colorimetric chemosensing ensemble for tartrate/malate in beverages. *Angewandte Chemie, International Edition* **1999**, 38, (24), 3666-3669.
118. Lee, D. H.; Im, J. H.; Son, S. U.; Chung, Y. K.; Hong, J.-I., An azophenol-based chromogenic pyrophosphate sensor in water. *Journal of the American Chemical Society* **2003**, 125, (26), 7752-7753.
119. Lee, H. N.; Swamy, K. M. K.; Kim, S. K.; Kwon, J.-Y.; Kim, Y.; Kim, S.-J.; Yoon, Y. J.; Yoon, J., Simple but Effective Way to Sense Pyrophosphate and Inorganic Phosphate by Fluorescence Changes. *Organic Letters* **2007**, 9, (2), 243-246.
120. Leevy, W. M.; Gammon, S. T.; Jiang, H.; Johnson, J. R.; Maxwell, D. J.; Jackson, E. N.; Marquez, M.; Piwnica-Worms, D.; Smith, B. D., Optical Imaging of Bacterial Infection in Living Mice Using a Fluorescent Near-Infrared Molecular Probe. *Journal of the American Chemical Society* **2006**, 128, (51), 16476-16477.

121. Leevy, W. M.; Johnson, J. R.; Lakshmi, C.; Morris, J.; Marquez, M.; Smith, B. D., Selective recognition of bacterial membranes by zinc(II)-coordination complexes. *Chemical Communications (Cambridge, United Kingdom)* **2006**, (15), 1595-1597.
122. Lejeune, K. E.; Mesiano, A. J.; Bower, S. B.; Grimsley, J. K.; Wild, J. R.; Russell, A. J., Dramatically stabilized phosphotriesterase-polymers for nerve agent degradation. *Biotechnology and Bioengineering* **1997**, 54, (2), 105-114.
123. LeJeune, K. E.; Wild, J. R.; Russell, A. J., Nerve agents degraded by enzymic foams. *Nature (London)* **1998**, 395, (6697), 27-28.
124. Lesley, G.; Yuan, Z.; Stringer, G.; Jobe, I. R.; Taylor, N. J.; Koch, L.; Scott, K.; Marder, T. B.; Williams, I. D.; Kurtz, S. K., Second-order optical nonlinearities in linear donor-acceptor substituted transition metal acetylides. *Special Publication - Royal Society of Chemistry* **1991**, 91, (Org. Mater. Non-linear Opt. 2), 197-203.
125. Lewis, E. A.; Tolman, W. B., Reactivity of Dioxygen-Copper Systems. *Chemical Reviews (Washington, DC, United States)* **2004**, 104, (2), 1047-1076.
126. Li Liu; Wong, W.-Y.; Lam, Y.-W.; Tam, W.-Y., Exploring a series of monoethynylfluorenes as alkynylating reagents for mercuric ion: Synthesis, spectroscopy, photophysics and potential use in mercury speciation. *Inorganica Chimica Acta* **2007**, 360, 109-121.
127. Lim, M. H.; Lippard, S. J., Fluorescence-Based Nitric Oxide Detection by Ruthenium Porphyrin Fluorophore Complexes. *Inorganic Chemistry* **2004**, 43, (20), 6366-6370.

128. Lim, M. H.; Xu, D.; Lippard, S. J., Visualization of nitric oxide in living cells by a copper-based fluorescent probe. *Nature Chemical Biology* **2006**, *2*, (7), 375-380.
129. Lippard, S. J.; Berg, J. M., *Principles of Bioinorganic Chemistry*. ed.; University Science Books: Mill Valley, CA, 1994; 'Vol.' p 450.
130. Lipscomb, W. N.; Strater, N., Recent Advances in Zinc Enzymology. *Chemical Reviews (Washington, D. C.)* **1996**, *96*, (7), 2375-2434.
131. Liu, B.; Bazan Guillermo, C., Synthesis of cationic conjugated polymers for use in label-free DNA microarrays. *Nature Protocols* **2006**, *1*, (4), 1698-1702.
132. Liu, M. S.; Jiang, X.; Liu, S.; Herguth, P.; Jen, A., K.-Y., Effect of Cyano Substituents on Electron Affinity and Electron-Transporting Properties of Conjugated Polymers. *Macromolecules* **2002**, *35*, (9), 3532-3538.
133. Liu, P.; Chen, Y.; Deng, J.; Tu, Y., An Efficient Method for the Preparation of Benzylic Bromides. *Synthesis* **2001**, *14*, 2078-2080.
134. Lucht, B. L.; St Onge, N. O., Synthesis and characterization of poly(p-phenylenephosphine)s. *Chemical Communications* **2000**, (21), 2097-2098.
135. Ma, L.; Woloszynek, R. A.; Chen, W.; Ren, T.; Protasiewicz, J. D., A New Twist on Pincer Ligands and Complexes. *Organometallics* **2006**, *25*, (14), 3301-3304.
136. Ma, L.-H.; Chen, Z.-B.; Jiang, Y.-B., Intramolecular charge transfer with 4-(N-phenylamino)benzoic acid. The N-phenyl amino conjugation effect. *Chemical Physics Letters* **2003**, *372*, (1,2), 104-113.

137. MacDiarmid, A. G., "Synthetic Metals": A Novel Role for Organic Polymers (Nobel Lecture). *Angewandte Chemie International Edition* **2001**, 40, (14), 2581-2590.
138. Mangalum, A.; Smith, R. C., Bifunctional cross-conjugated luminescent phosphines and phosphine derivatives: phospho-cruciforms. *Dalton Trans.* **2010**, 39, 5145-5151.
139. Marsden, J. A.; Miller, J. J.; Shirtcliff, L. D.; Haley, M. M., Structure-Property Relationships of Donor/Acceptor-Functionalized Tetrakis(phenylethynyl)benzenes and Bis(dehydrobenzoannuleno)benzenes. *J. Am. Chem. Soc.* **2005**, 127, 2464-2476.
140. Matsufuji, K.; Shiraishi, H.; Miyasato, Y.; Shiga, T.; Ohba, M.; Yokoyama, T.; Okawa, H., m-Hydroxo-m-phenolato dinuclear zinc(II) and nickel(II) complexes derived from dinucleating compartmental ligands of "end-off" type: synthesis, structures, and properties. *Bulletin of the Chemical Society of Japan* **2005**, 78, (5), 851-858.
141. McCarty, D. J.; Solomon, S. D.; Warnock, M. L.; Paloyan, E., Inorganic pyrophosphate concentrations in the synovial fluid of arthritic patients. *J. Lab. Clin. Med.* **1971**, 78, (2), 216-29.
142. McCleskey, S. C.; Floriano, P. N.; Wiskur, S. L.; Anslyn, E. V.; McDevitt, J. T., Citrate and calcium determination in flavored vodkas using artificial neural networks. *Tetrahedron* **2003**, 59, (50), 10089-10092.
143. Mitchell, D. J.; Wolfe, S.; Schlegel, H. B., A theoretical study of the methylenesulfurane and methylenephosphorane hypersurfaces, geometries,

- tautomerization, and dissociation of sulfonium and phosphonium ylides. *Can. J. Chem.* **1981**, 59, (23), 3280-92.
144. Miyakoshi, R.; Shiono, K.; Yokoyama, A.; Yokozawa, T., Catalyst-Transfer Polycondensation for the Synthesis of Poly(p-phenylene) with Controlled Molecular Weight and Low Polydispersity. *J. Am. Chem. Soc.* **2006**, 128, 16012-16013.
145. Morgan, B. P.; Gilliard, R. J.; Loungani, R. S.; Smith, R. C., Poly(p-phenylene ethynylene) Incorporating Sterically Enshrouding *m*-Terphenyl Oxacyclophane Canopies. *Macromolecular Rapid Communications* **2009**, 30, 1399-1405.
146. Morgan, B. P.; He, S.; Smith, R. C., Dizinc Enzyme Model / Complexometric Indicator Pairs in Indicator Displacement Assays for Inorganic Phosphates under Physiological Conditions. *Inorganic Chemistry* **2007**, 46, 9262-9266.
147. Morisaki, Y.; Chujo, Y., Cyclophane-containing polymers. *Prog. Polym. Sci.* **2008**, 33, 346-364.
148. Murphy, A. R.; Frechet, J. M. J., Organic Semiconducting Oligomers for Use in Thin Film Transistors. **2007**, 107, (4), 1066-1096.
149. Mwaura, J. K.; Pinto, M. R.; Witker, D.; Ananthakrishnan, N.; Schanze, K. S.; Reynolds, J. R., Photovoltaic Cells Based on Sequentially Adsorbed Multilayers of Conjugated Poly(p-phenylene ethynylene)s and a Water-Soluble Fullerene Derivative. *Langmuir* **2005**, 21, (22), 10119-10126.
150. Nguyen, B. T.; Anslyn, E. V., Indicator-displacement assays. *Coordination Chemistry Reviews* **2006**, 250, (23+24), 3118-3127.

151. Nguyen, B. T.; Wiskur, S. L.; Anslyn, E. V., Using Indicator-Displacement Assays in Test Strips and To Follow Reaction Kinetics. *Organic Letters* **2004**, 6, (15), 2499-2501.
152. Nolan, E. M.; Jaworski, J.; Okamoto, K.; Hayashi, Y.; Sheng, M.; Lippard, S. J., QZ1 and QZ2: Rapid, Reversible Quinoline-Derivatized Fluoresceins for Sensing Biological Zn(II). *Journal of the American Chemical Society* **2005**, 127, (48), 16812-16823.
153. Nolan, E. M.; Ryu, J. W.; Jaworski, J.; Feazell, R. P.; Sheng, M.; Lippard, S. J., Zinspy Sensors with Enhanced Dynamic Range for Imaging Neuronal Cell Zinc Uptake and Mobilization. *Journal of the American Chemical Society* **2006**, 128, (48), 15517-15528.
154. O'Neil, E. J.; Smith, B. D., Anion recognition using dimetallic coordination complexes. *Coordination Chemistry Reviews* **2006**, 250, (23+24), 3068-3080.
155. Osaka, I.; McCullough, R. D., Advances in Molecular Design and Synthesis of Regioregular Polythiophenes. *Acc. Chem. Res.* **2008**, 41, 1202-1214.
156. Patel, M. V.; Chen, F.-J. Pharmaceutical compositions and methods for improved delivery of hydrophobic therapeutic agents. 2000050007, 2000.
157. Patil, A. O.; Heeger, A. J.; Wudl, F., Optical properties of conducting polymers. **1988**, 88, (1), 183-200.
158. Patrick, M.; Hamilton, E.; Hornby, J.; Doherty, M., Synovial fluid pyrophosphate and nucleoside triphosphate pyrophosphatase: comparison between normal and

- diseased and between inflamed and non-inflamed joints. *Ann. Rheum. Dis.* **1991**, 50, (4), 214-8.
159. Piatek, A. M.; Bomble, Y. J.; Wiskur, S. L.; Anslyn, E. V., Threshold detection using indicator-displacement assays: An application in the analysis of malate in Pinot Noir grapes. *Journal of the American Chemical Society* **2004**, 126, (19), 6072-6077.
160. Pina, J.; Seixas de Melo, J.; Burrows, H. D.; Galbrecht, F.; Bilge, A.; Kudla, C. J.; Scherf, U., Excited State Properties of Oligophenyl and Oligothieryl Swivel Cruciforms. *J. Phys. Chem. B* **2008**, 112, (4), 1104-1111.
161. Platera, M. J.; Sinclair, J. P.; Aiken, S.; Gelbrich, T.; Hursthouse, M. B., The CA.M lattice revisited. Gel formation from a linear bis-isocyanuric acid and 2-amino-4,6-bis-(4-tert-butylphenylamino)-1,3,5-triazine. *Tetrahedron* **2004**, 60, (30), 6385-6394.
162. Que, L., Jr.; Tolman, W. B., Bis(m-oxo)dimetal "diamond" cores in copper and iron complexes relevant to biocatalysis. *Angewandte Chemie, International Edition* **2002**, 41, (7), 1114-1137.
163. Ramey, M. B.; Hiller, J. A.; Rubner, M. F.; Tan, C.; Schanze, K. S.; Reynolds, J. R., Amplified Fluorescence Quenching and Electroluminescence of a Cationic Poly(p-phenylene-co-thiophene) Polyelectrolyte. *Macromolecules* **2005**, 38, (2), 234-243.
164. Roncali, J., Conjugated poly(thiophenes): synthesis, functionalization, and applications. *Chemical Reviews (Washington, DC, United States)* **1992**, 92, (4), 711-38.

165. Rosenthal, A. K., Update in calcium deposition diseases. *Current Opinion in Rheumatology* **2007**, 19, (2), 158-162.
166. Rothe, C.; King, S.; Monkman, A. P., Systematic study of the dynamics of triplet exciton transfer between conjugated host polymers and phosphorescent iridium (III) guest emitters. *Physical Review B: Condensed Matter and Materials Physics* **2006**, 73, (24), 245208/1-245208/9.
167. Royo, S.; Martínez-Máñez, R.; Sancenón, F.; Costero, A. M.; Parra, M.; Gil, S., Chromogenic and fluorogenic reagents for chemical warfare nerve agents' detection. *Chemical Communications* **2007**, 4839 - 4847.
168. Saednya, A.; Hart, H., Two efficient routes to meta-terphenyls from 1,3-dichlorobenzenes. *Synthesis* **1996**, (12), 1455-1458.
169. Sahai, R.; Baucom, D. A.; Rillema, D. P., Strongly luminescing ruthenium(II)/ruthenium(II) and ruthenium(II)/platinum(II) binuclear complexes. *Inorg. Chem.* **1986**, 25, (21), 3843-5.
170. Sakai, T.; Satou, T.; Kaikawa, T.; Takimiya, K.; Otsubo, T.; Aso, Y., Syntheses, Structures, Spectroscopic Properties, and pi-Dimeric Interactions of [n.n]Quinquethiophenophanes. *J. Am. Chem. Soc.* **2005**, 127, (22), 8082-8089.
171. Salhi, F.; Collard, D. M., p-Stacked conjugated polymers: the influence of paracyclophane p-stacks on the redox and optical properties of a new class of broken conjugated polythiophenes. *Advanced Materials (Weinheim, Germany)* **2003**, 15, (1), 81-85.

172. Samori, S.; Tojo, S.; Fujitsuka, M.; Spitler, E. L.; Haley, M. M.; Majima, T., Fine-Tuning of Radiolysis Induced Emission by Variable Substitution of Donor-/Acceptor-Substituted Tetrakis(arylethynyl)benzenes. *J. Org. Chem.* **2008**, 73, (9), 3551-3558.
173. Sanji, T.; Shiraishi, K.; Kashiwabara, T.; Tanaka, M., Base-Mediated Cyclization Reaction of 2-Alkynylphenylphosphine Oxides: Synthesis and Photophysical Properties of Benzo[b]phosphole Oxides. *Org. Lett.* **2008**, 10, (13), 2689-2692.
174. Sariciftci, N. S.; Smilowitz, L.; Heeger Alan, J.; Wudl, F., Photoinduced Electron Transfer from a Conducting Polymer to Buckminsterfullerene *Science* **1992**, 258, (5087), 1474-1476.
175. Scherf, U.; List, E. J. W., Semiconducting polyfluorenes - towards reliable structure-property relationships. *Advanced Materials (Weinheim, Germany)* **2002**, 14, (7), 477-487.
176. Senechal-David, K.; Hemeryck, A.; Tancrez, N.; Toupet, L.; Williams, J. A. G.; Ledoux, I.; Zyss, J.; Boucekkine, A.; Guegan, J.-P.; Le Bozec, H.; Maury, O., Synthesis, Structural Studies, Theoretical Calculations, and Linear and Nonlinear Optical Properties of Terpyridyl Lanthanide Complexes: New Evidence for the Contribution of f Electrons to the NLO Activity. *Journal of the American Chemical Society* **2006**, 128, (37), 12243-12255.
177. Seo, J. S.; Sung, N.-D.; Hynes, R. C.; Chin, J., Structure and Reactivity of a Dinuclear Cobalt(III) Complex with a Bridging Phosphate Monoester. *Inorganic Chemistry* **1996**, 35, (26), 7472-7473.

178. Shah, S.; Yap, G. P. A.; Protasiewicz, J. D., Crystal structure of the phosphanylidene-s⁴-phosphorane DmpP:PMe₃ (Dmp = 2,6-Mes₂C₆H₃) and reactions with electrophiles. *Journal of Organometallic Chemistry* **2000**, 608, (1-2), 12-20.
179. Shiraishi, H.; Jikido, R.; Matsufuji, K.; Nakanishi, T.; Shiga, T.; Ohba, M.; Sakai, K.; Kitagawa, H.; Okawa, H., Dinuclear Mn(II), Ni(II), and Zn(II) complexes bridged by bis(p-nitrophenyl) phosphate ion: Relevance to bimetallic phosphodiesterase. *Bulletin of the Chemical Society of Japan* **2005**, 78, (6), 1072-1076.
180. Shirakawa, H., The Discovery of Polyacetylene Film: The Dawning of an Era of Conducting Polymers (Nobel Lecture)13. *Angewandte Chemie International Edition* **2001**, 40, (14), 2574-2580.
181. Shirakawa, H.; Louis, E. J.; MacDiarmid, A. G.; Chiang, C. K.; Heeger, A. J., Synthesis of electrically conducting organic polymers: halogen derivatives of polyacetylene, (CH)_x. *Journal of the Chemical Society, Chemical Communications* **1977**, (16), 578-80.
182. Shirakawa, H.; McDiarmid, A.; Heeger, A. J., Twenty-five years of conducting polymers. *Chemical Communications* **2003**, (1), 1-4.
183. Shirota, Y.; Kageyama, H., Charge Carrier Transporting Molecular Materials and Their Applications in Devices. *Chemical Reviews (Washington, D. C.)* **2007**, 107, (4), 953-1010.
184. Slagt, M. Q.; Stiriba, S.-E.; Kautz, H.; Gebbink, R. J. M. K.; Frey, H.; Van Koten, G., Optically Active Hyperbranched Polyglycerol as Scaffold for Covalent and

- Noncovalent Immobilization of Platinum(II) NCN-Pincer Complexes. Catalytic Application and Recovery. *Organometallics* **2004**, 23, (7), 1525-1532.
185. Slagt, M. Q.; Stiriba, S.-E.; Klein Gebbink, R. J. M.; Kautz, H.; Frey, H.; van Koten, G., Encapsulation of Hydrophilic Pincer-Platinum(II) Complexes in Amphiphilic Hyperbranched Polyglycerol Nanocapsules. *Macromolecules* **2002**, 35, (15), 5734-5737.
186. Smith, R. C., Covalently Scaffolded Inter-p-System Orientations in p-Conjugated Polymers and Small Molecule Models. *Macromolecular Rapid Communications* **2009**, 30, 2067-2078.
187. Smith, R. C.; Protasiewicz, J. D., Synthesis and luminescence properties of a series of tris(4-styrylphenyl)phosphorus-(III) and -(V) compounds and of a [Cu(PR₃)₄]BF₄ complex. *Dalton Transactions* **2003**, (24), 4738-4741.
188. Smith, R. C.; Protasiewicz, J. D., A Trans-Spanning Diphosphine Ligand Based on a m-Terphenyl Scaffold and Its Palladium and Nickel Complexes. *Organometallics* **2004**, 23, (18), 4215-4222.
189. Song, C.; Swager, T. M., π -Dimer Formation as the Driving Force for Calix[4]arene-Based Molecular Actuators. *Org. Lett.* **2008**, 10, 3575-3578.
190. Spitler, E. L.; Monson, J. M.; Haley, M. M., Structure-Property Relationships of Fluorinated Donor/Acceptor Tetrakis(phenylethynyl)benzenes and Bis(dehydrobenzoannuleno)benzenes. *J. Org. Chem.* **2008**, 73, (6), 2211-2223.

191. Spitler, E. L.; Shirlcliff, L. D.; Haley, M. M., Systematic Structure-Property Investigations and Ion-Sensing Studies of Pyridine-Derivatized Donor/Acceptor Tetrakis(arylethynyl)benzenes. *Journal of Organic Chemistry* **2007**, 72, (1), 86-96.
192. Steenwinkel, P.; James, L. S.; Grove, D. M.; Veldman, N.; Spek, A. L.; van Koten, G., New ruthenium(II) complexes of functionalized monoanionic aryldiamine N,C,N'-terdentate ligands: syntheses of [RuII{2,6-(Me₂NCH₂)₂-4-RC₆H₂}(terpy)]⁺Cl⁻; X-ray structure of a dimeric organolithium compound, [Li{2,6-(Me₂NCH₂)₂-4-Ph-C₆H₂}]₂. *Chemistry--A European Journal* **1996**, 2, (11), 1440-1445.
193. Stiriba, S.-E.; Slagt, M. Q.; Kautz, H.; Gebbink, R. J. M. K.; Thomann, R.; Frey, H.; Van Koten, G., Synthesis and supramolecular association of immobilized NCN-pincer platinum(II) complexes on hyperbranched polyglycerol supports. *Chemistry--A European Journal* **2004**, 10, (5), 1267-1273.
194. Sunder, A.; Heinemann, J.; Frey, H., Controlling the growth of polymer trees: concepts and perspectives for hyperbranched polymers. *Chemistry--A European Journal* **2000**, 6, (14), 2499-2506.
195. Sunder, A.; Mulhaupt, R. Method for producing highly branched glycidol-based polyols. 99-EP9773 2000037532, 19991210., 2000.
196. Suzuki, M.; Kanatomi, H.; Murase, I., Synthesis and properties of a binuclear cobalt(II) oxygen adduct with 2,6-bis[bis(2-pyridylmethyl)aminomethyl]-4-methylphenol. *Chemistry Letters* **1981**, (12), 1745-8.
197. Takita, R.; Song, C.; Swager, T. M., π -Dimer Formation in an Oligothiophene Tweezer Molecule. *Org. Lett.* **2008**, 10, 5003-5005.

198. Tao, K. W. C.; Yu, P.; Roberts, R. L. High molecular weight, lipophilic, orally ingestible bioactive agents in formulations having improved bioavailability. 2003013566, 2003.
199. Tennyson, E. G.; Smith, R. C., Visible-Absorbing Phosphines as Functional Elements of Luminescent Metallopolymers. *Inorg. Chem.* **2009**, 48, 11483-11485.
200. Teta, N. L.; Brown, D.; Glass, M. Enzyme-containing polymeric sensors. 6913928, 2005.
201. Thomas, S. W., III; Joly, G. D.; Swager, T. M., Chemical Sensors Based on Amplifying Fluorescent Conjugated Polymers. *Chemical Reviews (Washington, DC, United States)* **2007**, 107, (4), 1339-1386.
202. Tobey, S. L.; Anslyn, E. V., Determination of inorganic phosphate in serum and saliva using a synthetic receptor. *Organic Letters* **2003**, 5, (12), 2029-2031.
203. Tolman, W. B.; Que, L., Jr., Sterically hindered benzoates: a synthetic strategy for modeling dioxygen activation at diiron active sites in proteins. *Journal of the Chemical Society, Dalton Transactions* **2002**, (5), 653-660.
204. Tolosa, J.; Zuccherro, A. J.; Bunz, U. H. F., Water-Soluble Cruciforms: Response to Protons and Selected Metal Ions. *J. Am. Chem. Soc.* **2008**, 130, 6498-6506.
205. Tomalia, D. A.; Durst, H. D., Genealogically directed synthesis: starburst/cascade dendrimers and hyperbranched structures. *Topics in Current Chemistry* **1993**, 165, (Supramolecular Chemistry I), 193-313.

206. Tshuva, E. Y.; Lippard, S. J., Synthetic Models for Non-Heme Carboxylate-Bridged Diiron Metalloproteins: Strategies and Tactics. *Chemical Reviews (Washington, DC, United States)* **2004**, 104, (2), 987-1011.
207. Tsien, R. Y., *Biochemistry* **1980**, 19, 2396.
208. Tsuji, K.; Sasaki, S.; Yoshifuji, M., Synthesis and redox properties of a diphosphene carrying a redox-active sterically protecting group. *Tetrahedron Letters* **1999**, 40, (16), 3203-3206.
209. Tykwinski, R. R.; Schreiber, M.; Perez Carlon, R.; Diederich, F.; Gramlich, V., Donor/acceptor-substituted tetraethynylethenes. Systematic assembly of molecules for use as advanced materials. *Helv. Chim. Acta* **1996**, 79, (8), 2249-2281.
210. Valenty, V. B. Thickening agents for nitrocellulose-free aqueous nail polish compositions with good adhesion. 5747018, 1998.
211. Vedejs, E.; Peterson, M. J., *Top. Stereochem.* **1994**, 21, 1-157.
212. Victor, A. S.; Walter, H., Palladium-catalyzed synthesis of poly(*p*-phenyleneethynylene)s. *Macromolecular Chemistry and Physics* **1994**, 195, (1), 303-314.
213. Vidal, P.-L.; Divisia-Blohorn, B.; Bidan, G.; Hazemann, J.-L.; Kern, J.-M.; Sauvage, J.-P., *p*-Conjugated ligand polymers entwined around copper centers. *Chem. Eur. J.* **2000**, 6, (9), 1663-1673.
214. Vinod, T.; Hart, H., Synthesis of cuppedophanes and cappedophanes. Two new classes of cyclophanes with molecular cavities. *Journal of Organic Chemistry* **1990**, 55, (3), 881-90.

215. Vinod, T. K.; Hart, H., Cupped- and cappedophanes, two new general classes of compounds with molecular cavities. *Journal of the American Chemical Society* **1988**, 110, (19), 6574-5.
216. Vinod, T. K.; Hart, H., Cupped azacyclophanes based on a m-terphenyl framework: conformational features of their N-tosylamide precursors. *Journal of Organic Chemistry* **1990**, 55, (20), 5461-6.
217. Vinod, T. K.; Hart, H., Synthesis of two noninterconvertible conformers of a single host. Self-filled and vaulted cappedophanes. *Journal of the American Chemical Society* **1990**, 112, (8), 3250-2.
218. Vinod, T. K.; Hart, H., Cuppedo- and cappedophanes. *Topics in Current Chemistry* **1994**, 172, (Cyclophanes), 119-78.
219. Vulfson, E. N.; Law, B. A. Modified food products and beverages, and additives for food and beverages. 2000041491, 2000.
220. Walkup, G. K.; Burdette, S. C.; Lippard, S. J.; Tsien, R. Y., A New Cell-Permeable Fluorescent Probe for Zn²⁺. *Journal of the American Chemical Society* **2000**, 122, (23), 5644-5645.
221. Wang, W.; Xu, J.; Lai, Y.-H., Alternating Conjugated and Transannular Chromophores: Tunable Property of Fluorene-Paracyclophane Copolymers via Transannular p-p Interaction. *Organic Letters* **2003**, 5, (16), 2765-2768.
222. Werner, A., *Z. Anorg. Chem.* **1893**, 3, 267-342.

223. Weston, J., Mode of Action of Bi- and Trinuclear Zinc Hydrolases and Their Synthetic Analogues. *Chemical Reviews (Washington, DC, United States)* **2005**, 105, (6), 2151-2174.
224. Wilson, J. N.; Bunz, U. H. F., Switching of Intramolecular Charge Transfer in Cruciforms: Metal Ion Sensing. *Journal of the American Chemical Society* **2005**, 127, (12), 4124-4125.
225. Wilson, J. N.; Hardcastle, K. I.; Josowicz, M.; Bunz, U. H. F., Synthesis and electronic properties of bis-styryl substituted trimeric aryleneethynylenes. Comparison of cruciforms with iso-cruciforms. *Tetrahedron* **2004**, 60, (34), 7157-7167.
226. Wilson, J. S.; Chawdhury, N.; Al-Mandhary, M. R.; Younus, M.; Khan, M. S.; Raithby, P. R.; Kohler, A.; Friend, R. H., The energy gap law for triplet states in Pt-containing conjugated polymers and monomers. *J Am Chem Soc FIELD Full Journal Title: Journal of the American Chemical Society* **2001**, 123, (38), 9412-7.
227. Wiskur, S. L.; Ait-Haddou, H.; Lavigne, J. J.; Anslyn, E. V., Teaching old indicators new tricks. *Accounts of Chemical Research* **2001**, 34, (12), 963-972.
228. Wiskur, S. L.; Anslyn, E. V., Using a Synthetic Receptor to Create an Optical-Sensing Ensemble for a Class of Analytes: A Colorimetric Assay for the Aging of Scotch. *Journal of the American Chemical Society* **2001**, 123, (41), 10109-10110.
229. Wiskur, S. L.; Lavigne, J. J.; Metzger, A.; Tobey, S. L.; Lynch, V.; Anslyn, E. V., Thermodynamic analysis of receptors based on guanidinium/boronic acid groups for the complexation of carboxylates, α -hydroxycarboxylates, and diols: Driving force

- for binding and cooperativity. *Chemistry--A European Journal* **2004**, 10, (15), 3792-3804.
230. Wu, C.-J. J.; Xue, C.; Kuo, Y.-M.; Luo, F.-T., Preparation and photoluminescence of p-terphenyl derivatives containing cyano groups. *Tetrahedron* **2005**, 61, 4735-4741.
231. Wu, F.; Tian, W.; Sun, J.; Shen, J.; Pan, X.; Su, Z., Study on the electronic structure of phenylene vinylene dimers with different substituents. *Materials Science & Engineering, B: Solid-State Materials for Advanced Technology* **2001**, 85, (2-3), 165-168.
232. Yamaguchi, S.; Akiyama, S.; Tamao, K., The coordination number-photophysical properties relationship of trianthrylphosphorus compounds: doubly locked fluorescence of anthryl groups. *Journal of Organometallic Chemistry* **2002**, 646, (1-2), 277-281.
233. Yang, J.-S.; Chiou, S.-Y.; Liao, K.-L., Fluorescence Enhancement of trans-4-Aminostilbene by N-Phenyl Substitutions: The "Amino Conjugation Effect". *Journal of the American Chemical Society* **2002**, 124, (11), 2518-2527.
234. Yang, Y.-C., Chemical Detoxification of Nerve Agent VX. *Acc. Chem. Res.* **1999**, 32, 109-115.
235. Yang, Y.-C.; Baker, J. A.; Ward, J. R., Decontamination of Chemical Warfare Agents. *Chem. Rev.* **1992**, 92, 1729-1743.
236. Yasuhiro Morisaki; Chujo, Y., Through-Space Conjugated Polymers Based on Cyclophanes. *Angew. Chem. Int. Ed* **2006**, 45, 6430 – 6437.

237. Yip, J. H. K.; Prabhavathy, J., A Luminescent Gold Ring That Flips Like Cyclohexane. *Angew. Chem. Int. Ed.* **2001**, 40, 2159-2162.
238. Zacharias, D. A.; Baird, G. S.; Tsien, R. Y., Recent advances in technology for measuring and manipulating cell signals. *Current Opinion in Neurobiology* **2000**, 10, (3), 416-421.
239. Zeng, F.; Zimmerman, S. C., Dendrimers in supramolecular chemistry: from molecular recognition to self-assembly. *Chemical Reviews (Washington, D. C.)* **1997**, 97, (5), 1681-1712.
240. Zhang, J.; Campbell, R. E.; Ting, A. Y.; Tsien, R. Y., Creating New Fluorescent Probes for Cell Biology. *Nature Reviews Molecular Cell Biology* **2002**, 3, (12), 906-918.
241. Zhang, L.; Clark, R. J.; Zhu, L., A heteroditopic fluoroionophoric platform for constructing fluorescent probes with large dynamic ranges for zinc ions. *Chem. Eur. J.* **2008**, 14, (9), 2894-2903.
242. Zhang, W.-W.; Yu, Y.-G.; Lu, Z.-D.; Mao, W.-L.; Li, Y.-Z.; Meng, Q.-J., Ferrocene⁺Phenothiazine Conjugated Molecules: Synthesis, Structural Characterization, Electronic Properties, and DFT-TDDFT Computational Study. *Organometallics* **2007**, 26, (4), 865-873.
243. Zhao, X.; Cardolaccia, T.; Farley, R. T.; Abboud, K. A.; Schanze, K. S., A platinum acetylide polymer with sterically demanding substituents: Effect of aggregation on the triplet excited state. *Inorganic Chemistry* **2005**, 44, (8), 2619-2627.

244. Zhou, C.-Z.; Liu, T.; Xu, J.-M.; Chen, Z.-K., Synthesis, Characterization, and Physical Properties of Monodisperse Oligo(p-phenyleneethynylene)s. *Macromolecules* **2003**, 36, 1457-1464.
245. Zhu, S. S.; Carroll, P. J.; Swager, T. M., Conducting Polymetallorotaxanes: A Supramolecular Approach to Transition Metal Ion Sensors. *Journal of the American Chemical Society* **1996**, 118, (36), 8713-8714.
246. Zhu, Z.; Swager, T. M., Conjugated Polymers Containing 2,3-Dialkoxybenzene and Iptycene Building Blocks. *Organic Letters* **2001**, 3, (22), 3471-3474.
247. Zuccherro, A. J.; McGrier, P. L.; Bunz, U. H. F., Cross-Conjugated Cruciform Fluorophores. *Acc. Chem. Res.* **2010**, 43, (3), 397-408.
248. Zuccherro, A. J.; Wilson, J. N.; Bunz, U. H. F., Cruciforms as functional fluorophores: Response to protons and selected metal ions. *Journal of the American Chemical Society* **2006**, 128, (36), 11872-11881.